An Investigation of the Prognostic Value of Pathological and Genomic Factors in Pancreatic Ductal Adenocarcinoma

Nigel Balfour Jamieson

MBChB, B Med Sci (Hons), MRCS (Glas)

A thesis submitted to the University of Glasgow in fulfilment of the requirements for the Degree of Doctor of Philosophy

March 2012

University of Glasgow Department of Medical Oncology and Department of Surgery

Abstract

Introduction

Improving the survival of patients with pancreatic ductal adenocarcinoma (PDAC) remains an oncological and surgical challenge. PDAC pathogenesis is underlined by numerous molecular aberrations occurring at a genetic and epigenetic level, however their spectrum of occurrence and clinical impact has not yet been fully elucidated. The majority of patients present with locally advanced or metastatic disease and even the 15-20% of patients who undergo resection for cure have a median survival limited to 18-24 months. Surgical treatment carries a high morbidity and identification of patients expected to have a poor prognosis could assist in the decision making process.

Advances in the selection algorithms for therapy are mandatory if improvement in outcome and quality of life for these patients is to be achieved. Potentially the identification of pathological and molecular markers of poor prognosis could stratify outcome following resection as well as provide insight into the biological behaviour of these tumours resulting in novel therapeutic targets.

It is hypothesised that enhancements to the pathological staging criteria and detailed molecular characterisation at a protein, gene, microRNA and copy number aberration level have the potential to improve PDAC characterisation resulting in improved stratification of survival following resection with potential to select treatment more appropriately.

The overall aim of the thesis was to examine the prognostic impact of a selection of pathological, molecular and genomic factors in patients with PDAC undergoing resection with curative intent so as to potentially enhance outcome stratification.

Chapter 3

Resection margin involvement is a contentious issue associated with the management of PDAC. It is hypothesised that not all involved margins have equal prognostic influence. The aim of this chapter was to assess the frequency and prognostic impact of resection margin involvement, and furthermore to determine the prognostic influence of tumour involvement at individual margins. Following re-evaluation of the traditional pathological staging system and pathology resections from 148 patients with PDAC, tumour was identified at or within 1 mm of a margin in 74% of specimens. Resection margin involvement was associated with poor overall survival independent of other pathological factors. Furthermore transection (pancreatic body and medial) margin involvement conferred a poorer prognosis than mobilisation (anterior and posterior) margin involvement. It may therefore be both appropriate and better practice to regard these novel definitions as separate categories. There was no significant difference in survival of the mobilisation margin involved group compared to the resection margin negative group. These data have implications for patient outcome

stratification and may impact upon adjuvant therapy allocation within the setting of future randomised controlled trials.

Chapter 4

Peripancreatic fat invasion is currently a component of the pathological staging criteria. It is hypothesised that invasion of tumour into the fat surrounding the pancreas may be a more powerful prognostic factor than is currently presumed. Therefore the aim of this chapter was to investigate firstly the influence of peripancreatic fat invasion on survival following resection and secondly the impact of clinicopathological factors including peripancreatic fat invasion on the pattern of recurrence. Following re-evaluation of the pathology specimens for 189 patients with PDAC, histological peripancreatic fat invasion was evident in 51 (27%) patients and was associated with lymph node metastases and larger tumour size. It was identified that peripancreatic fat invasion provided prognostic information independent of tumour stage, grade and lymph node status following resection and subsequently may be a more important pathological factor than is currently acknowledged. Additionally, the presence of peripancreatic fat invasion appeared to be associated with locoregional disease as the primary site of recurrence. These data may have implications for the pathological staging of PDAC and the stratification of patients within adjuvant therapy trials.

Chapter 5

Molecular signalling pathways are notably deranged in pancreatic cancer and it is hypothesised that assessment of these aberrations could potentially stratify outcome, identifying patients with particularly deleterious outcome following resection. The aim of this chapter was to investigate the relationship of candidate protein biomarker expression with overall survival in a large PDAC tissue microarray cohort using immunohistochemistry. A systematic review of the prognostic marker literature identified candidate biomarker proteins along with a selection of other targets that were evaluated in a tissue microarray cohort of 119 patients along with traditional prognostic factors. These protein markers were categorised according to their functional role in cancer. It was established that a number of protein markers were associated with clinicopathological status and independently with overall survival following resection including Lkb1, p21, Cox-2, pAkt, β-catenin, GSK3β and E-cadherin. Furthermore, these data were integrated by hierarchical clustering to create a multimarker prognostic protein expression signature.

Chapter 6

PDAC is associated with an abnormal pattern of gene expression compared to normal pancreatic tissue. It was hypothesised that patient outcome can be stratified according to the gene expression signature of the tumour. The aim of this chapter was to assess the gene expression profiles associated with pancreatic cancer compared to normal tissue using gene

expression microarray analysis in 48 patients undergoing pancreatic cancer resection for which fresh frozen tissue was prospectively collected. Gene expression signatures associated with clinicopathological states including lymph node status, tumour grade and resection margin status were subsequently developed. In an attempt to further define important molecular signalling pathways that are associated with prognosis in pancreatic cancer, the development of an unbiased gene expression signature was performed. A 107-gene survival profile was identified, which clustered the 48 patient cohort into long- or short-survival groups. In multivariate analysis tumour stage, lymph node status and the 107-gene survival profile yielded independent prognostic value. The prognostic utility of this signature was successfully validated in data available from two independent pancreatic cancer microarray studies. The independent prognostic significance of a component of the gene survival profile, CLIC3, was subsequently validated at the protein level in the 119 patient tissue microarray cohort. Furthermore, a recently described gene expression signature from an independent study successfully stratified patient outcome in this cohort providing further evidence of the prognostic utility of gene expression signatures in PDAC.

Chapter 7

MicroRNAs, small non-coding RNA sequences, are increasingly associated with malignancy including pancreatic cancer. It is hypothesised that PDAC microRNA expression patterns could stratify patient outcome following resection. The aim of this chapter was to investigate the genome wide microRNA expression profile in the 48 patient PDAC cohort and corresponding normal tissues and to correlate this molecular signature with clinicopathological variables including survival. MicroRNA microarray expression profiling of fresh frozen tumour specimens was performed. The PDAC microRNA signature generated was reassuringly similar to previous profiling studies. Furthermore, microRNAs were identified that associated with clinicopathological factors including lymph node involvement, tumour grade, tumour stage and overall survival following resection. Aberrant expression of a number of microRNAs independently associated with reduced survival including over-expression of miR-21 and under-expression of miR-34a along with miR-30d. Successful validation of the expression of miR-21 and miR-34a in a separate cohort of 24 patients provided valuable insight into the role played by these microRNAs in pancreatic cancer.

Chapter 8

Copy number aberrations are recognised to have an established role in pancreatic cancer tumourigenesis. It is postulated that chromosomal regions as well as the frequency of copy number change in PDACs may have prognostic implications for patients. The aim of this

chapter was to undertake a detailed analysis using array comparative genomic hybridisation of chromosomal imbalances in a cohort of 45 resected PDACs. Copy number change was examined in fresh frozen tumour tissue and correlated with clinicopathological factors including tumour stage, lymph nodes status and venous invasion. The genomic identification of significant targets in cancer algorithm methodology was used for the first time in PDAC, subsequently novel areas of copy number aberration were identified. Furthermore, a high rate of copy number aberration was identified as being associated with poor outcome and a number of novel chromosomal loci that correlate with outcome following resection, including 1p36.1 and 7q34, were also identified.

Chapter 9

The integration of high-throughput genomic technologies has the potential to improve understanding of PDAC tumour biology. It was proposed that key molecular features of PDAC not identified by analysis of the individual data sets from the previous chapters could be realised by the integration of the findings. The aim of this chapter was to identify potentially important regulator genes contributing to pancreatic tumourigenesis by integrating the data from chapter 6, 7 and 8. This successfully identified numerous genes for which expression and copy number correlated, providing a list of potential targets for future investigation and validation including mTOR, HNF4A, N-Cor, FBI-1 and SIRT2. mTOR protein expression was subsequently validated within the tissue microarray cohort and found to correlate with overall survival supporting an important role in pancreatic cancer biology. Finally, the integration of microRNA data with other genomic and protein expression data was investigated. This highlighted regulatory influences and targets of miR-21 and miR-34a in human PDAC. In particular miR-21 expression was found to correlate with expression of the downstream targets PTEN and Bcl-2, with miR-34a correlated with p53 protein expression while copy number loss was evident in the miR-34a loci.

In this work a combination of enhanced pathological staging criteria along with the correlation of molecular marker expression and genomic profiling signatures with clinical outcome data has yielded interesting results in patients undergoing resection for pancreatic cancer that allowed detailed disease characterisation and subsequent clinically relevant outcome stratification. Further work is required to confirm the potential value of these factors in the individualisation and targeting of therapy for such patients, develop their incorporation into current staging systems as well as to perform mechanistic validation of novel targets.

Table of contents

List of tables

List of figures

List of publications

Publications directly resulting from the thesis

Jamieson NB, Foulis AK, Oien KA, Going JJ, Glen P, Dickson EJ, Imrie CW, McKay CJ, Carter R. (2010) Positive mobilisation margins alone do not influence survival following pancreatico-duodenectomy for pancreatic ductal adenocarcinoma. *Ann. Surg*., 251(6): 1003-10.

Jamieson NB, Foulis AK, Oien KA, Dickson EJ, Imrie CW, Carter R, McKay CJ. (2010) Peripancreatic fat invasion is an independent predictor of poor outcome following pancreaticoduodenectomy for pancreatic ductal adenocarcinoma *J.Gastrointest. Surg*., 15:512-524.

Jamieson NB, Carter R, McKay CJ, Oien KA. (2011) Tissue biomarkers for prognosis in pancreatic ductal adenocarcinoma: a systematic review and meta-analysis. *Clin. Cancer. Res*., 17:3316-3331.

Steele CW, Oien KA, McKay CJ, **Jamieson NB**. (2011) Clinical potential of microRNAs in pancreatic ductal adenocarcinoma. *Pancreas,* 40:1165-71.

Jamieson NB, Dickson EJ, Carter R, Evans TR, McKay CJ, Oien KA. (2012) MicroRNA molecular profiles associated with diagnosis, clinicopathological criteria, and overall survival in patients with resectable pancreatic ductal adenocarcinoma. *Clin. Cancer. Res*., 18:534-45.

Publications indirectly resulting from the thesis

Morton JP, Timpson P, Karim SA, Ridgway RA, Athineos D, Doyle B, **Jamieson NB,** Oien KA, Lowy AM, Brunton VG, Frame MC, Evans TR, Sansom OJ. (2010) Mutant p53 drives metastasis and overcomes growth arrest/senescence in pancreatic cancer. *Proc. Natl. Acad. Sci. U S A*., 107: 246-251.

Morton JP, **Jamieson NB**, Karim SA, Athineos D, Ridgway RA, Nixon C, McKay CJ, Carter R, Brunton VG, Frame MC, Ashworth A, Oien KA, Evans TR, Sansom OJ. (2010) LKB1 haploinsufficiency cooperates with kras to promote pancreatic cancer through suppression of p21-dependent growth arrest. *Gastroenterology*, 139: 586-97.

Kennedy AL, Morton JP, Manoharan I, Nelson DM, **Jamieson NB**, Pawlikowski JS, McBryan T, Doyle B, Oien KA, Enders GH, Zhang R, Sansom OJ, Adams PD. (2011) Activation of the PIK3CA/AKT pathway suppresses senescence induced by an activated RAS oncogene to promote tumourigenesis. *Mol. Cell.,* 42:36-49.

Jamieson NB, Denley SM, Logue J, McKenzie DJ, Foulis AK, Dickson EJ, Imrie CW, Carter R, McKay CJ, McMillan, DC. (2010) A prospective comparison of the prognostic value of tumour and patient related factors in patients undergoing potentially curative surgery for pancreatic ductal adenocarcinoma. *Ann. Surg. Oncol.,* 18:2318-28.

Acknowledgements

I would like to thank Colin McKay (CJM) and Karin Oien (KO) for the opportunity to work on what has been a tremendous project and for their supervision over the last three years. Thanks also to my adviser Hing Leung for his support. I am grateful to Professor Paul Horgan for giving up his time to review the thesis in detail.

Special thanks also to Ross Carter (CRC) who although not acknowledged as a supervisor has provided research ideas, technical assistance and encouragement to ensure that I submitted on time. Euan Dickson (EJD) has also provided support and encouragement to perform to the highest standard. Furthermore Professor Clem Imrie (CWI) has provided continual support and encouragement. Furthermore, Professor Donny McMillan has supported my research interests over many years.

I would also like to thank members of the Beatson group including Professor Nicol Keith, Clare Cairney, Stacey Hoare and Alan Bilsland. Professor Owen Sansom and Jen Morton as well as Professor Jeff Evans have been valuable colleagues and collaborators. I hope to continue this in future translational projects.

The staff of the GRI Department of Pathology in particular Alan Foulis (AKF) and James Going (JJG). For technical help and collaboration thanks to: Ian Downie (ID) for immunohistochemistry; Jane Hair (JH) and all BioBank staff for access to tissue resources; Alex King (AK) for help and advice with tissue microarrays; Maura Faquharson (MF) for PCR advice.

Special thanks to my girlfriend Julie who has supported throughout this work.

This research was funded and made possible by the Scottish Government, Chief Scientist Office (CSO) that provided me with a Clinical PhD Fellowship.

Author's Declaration

I am the sole author of this thesis. All of the references have been reviewed by myself in the preparation of this manuscript. Except where otherwise stated, the work presented in this thesis was performed by myself. The thesis has not been previously submitted for a degree or diploma at this or any other institution.

Nigel B Jamieson

March 2012

Definitions/abbreviations

5FU	5-fluorouracil
aCGH	array comparative genomic hybridisation
ADM	acinar-ductal-metaplasia
ATDC	ataxia telangiectasia group D-associated
AJCC	American Joint Committee on Cancer
APC	adenomatous polyposis coli
AQP	aquaporin
AMPK	adenosine monophosphate-activated protein kinase
BAC	bacterial artificial chromosome
BCL	B-cell lymphoma
BRCA2	Breast Cancer 2 susceptibility protein
BRB	Biometric Research Branch
BSA	bovine serum albumin
CA19-9	carbohydrate antigen 19-9
CAC	centroacinar cells
CBS	circular binary segmentation
cDNA	complementary deoxyribonucleic acid
CGH	comparative genomic hybridisation
CI	confidence interval
CLIC3	chloride ion transporter 3
CN	copy number
CNA	copy number aberration
CT	computerised tomography
CP	chronic pancreatitis
Cy3	cyanine 3-deoxyribonucleotide
Cy5	cyanine 5-deoxyribonucleotide
CDK	cyclin dependent kinase
CSC	cancer stem cells
DAB	diaminobenzidine
DEPC	diethylpyrocarbonate
dH20	de-ionised and distilled water
DMNT	DNA methyltransferase
DMSO	dimethyl sulfoxide
DNA	deoxyribonucleic acid
DUSP	dual specificity phosphatases
EDTA	ethyleneidiaminetetracetic acid
EGF	epidermal growth factor
EMT	Epithelial-Mesenchymal Transition
ERCP	endoscopic retrograde cholangiopancreaticography
ERK	extracellular signal-regulated kinase
ESPAC	European Study of Pancreatic and Ampullary Cancer
EUS	endoscopic ultrasound
FAP	Familial Adenomatous Polyposis
FAMMs	Familial Atypical Multiple Mole syndrome
FASL	fas ligand
FDR	false discovery rate
FGF	fibroblast growth factor
FFPE	fresh frozen paraffin embedded
FNA	fine needle aspiration
GAPDH	glyceraldehyde 3-phosphate dehydrogenase
GISTIC	Genomic Identification of Significant Targets in Cancer
GO	gene ontology
GRI	Glasgow Royal Infirmary
GSK3β	glycogen synthase kinase 3β
GTP	guanosine 5'-triphosphate
Hh	hedgehog
HOP	head of pancreas
HNPCC	hereditary nonpolyposis colorectal cancer
HR	hazard ratio
H&E	haematoxylin and eosin
ICCC	intra-class correlation coefficient
IHC	immunohistochemistry
IMV	inferior mesenteric vein

IPMN	intraductal papillary mucinous neoplasia
IVC	inferior vena cava
JNK	c-jun N-terminal kinase
KEGG	Kyoto Encyclopedia of Genes and Genomes
LOOCV	leave-one-out cross-validation
LNR	lymph node ratio
LKB1	liver kinase B1
MAPK	mitogen activated phosphorylated kinase
MCN	mucinous cystic neoplasm
MEN1	multiple endocrine neoplasia 1
MMP	matrix metalloproteinase
MSI	microsatellite instability
MRI	magnetic resonance imaging
MRCP	magnetic resonance cholangiopancreaticography
miRNA	microribonucleic acid
mRNA	messenger ribonucleic acid
mTOR	mammalian target of rapamycin
NSCLC	non-small cell lung cancer
OD	optical density
PanIN	pancreatic intraepithelial neoplasia
PD	pancreaticoduodenectomy
PDAC	pancreatic ductal adenocarcinoma
PET	positron emission tomography
PI3K	phosphatidylinositol 3-kinase
PITX1	Pituitary homeobox 1
PJS	Peutz-Jeghers syndrome
Pol II	polymerase II
PSCA	prostate stem cell antigen
PTEN	phosphatase and tensin homolog
QM	quasi-mesenchymal
R0	resection margin negative
R1	resection margin positive
Rb	retinoblastoma gene
RCPath	British Royal College of Pathologists
REMARK	REporting recommendations for tumour MARKer prognostic studies
RIN	RNA integrity number
RISC	RNA-inducing silencing complex
RNA	ribonucleic acid
RT-PCR	reverse transcription polymerase chain reaction
SAM	significance analysis of microarrays
SD	standard deviation
SE	standard error
SELENBP1	selenium binding protein 1
SMA	superior mesenteric artery
SMV	superior mesenteric vein
STK	serine threonine kinase
SAGE	serial analysis of genes
SPINK1	serine peptidase inhibitor kazal-type 1
SUFU	suppressor of fused
TBS	tris buffered saline
TGFβ	transforming growth factor β
TGM2	transglutaminase 2
TMA	tissue microarray
TNM	Tumour Node Metastasis
TNF	tumour necrosis factor
TSG	tumour suppressor gene
UICC	International Union Against Cancer
VEGF	vascular endothelial growth factor
VHL	von Hippel-Lindau
XPO5	exportin 5

Units

°C	degree Celsius
g	gram
g	gravity
K	thousand
L	litre
M	molar
m	milli
m	meter
n	nano
nt	nucleotides
p	pico
rpm	revolutions per minute
µ	micro
U	unit

1 Introduction

1.1 Pancreatic ductal adenocarcinoma: a surgical and oncological challenge

Predicting the outcome of patients with pancreatic ductal adenocarcinoma (PDAC) remains an oncological and surgical challenge. The majority of patients present with locally advanced or metastatic disease and have a median survival of 6-8 months irrespective of treatment modality (1). In selected patients (15%) with localised PDAC, surgical resection remains the only treatment potentially offering long-time survival (2), however, 5-year survival rates remain low. Stratification and, ultimately, individualisation of therapy for cancer are currently major oncological challenges. While a number of clinicopathological factors have been identified to aid prognosis following pancreaticoduodenectomy (PD), all require post-operative pathological specimen assessment. In PDAC (3) as in other cancers (4, 5), tumours with identical clinicopathological parameters have markedly different mRNA expression profiles, and tumour subgroups classified by gene expression can have disparate outcomes. Therefore an urgent need exists to identify prognostic biomarkers for use in the management of operable PDAC, with a particular requirement for markers that can be determined preoperatively potentially augmenting the current staging criteria, which relies wholly on imaging modalities. The ultimate aim being enhanced patient selection for PD, with the most aggressive therapies focused on those most likely to benefit.

1.1.1 Epidemiology and aetiology of pancreatic cancer

PDAC is the 10th commonest cancer diagnosis in the UK associated with 8,085 new cases in 2008, with similar numbers in men and women (6). Comparison between the 1997-1999 and 2006-2008 periods demonstrates the incidence of pancreatic cancer in UK men appears to have risen, from 10.5 to 10.6 cases/100,000 (1% rise). For women this rate appears static at 8.2 cases/100,000. It ranks as the 5th most common cause of cancer related mortality in 2008 (7,781 deaths), with a UK 5-year overall survival rate of 2% in men and 3% in women, the poorest survival figures for any cancer.

As the majority of patients present with incurable disease, identification and evasion of controllable contributors has become particularly important for those at greatest risk. These risk factors can be divided into those that are potentially modifiable and those that are not. Although most do not directly cause the disease, level of exposure often influences cancer development.

1.1.1.1 Non-modifiable risk factors

Pancreatic cancer is generally a disease of the elderly, rare before the age of 40, with 80% diagnosed between 60 and 80 years (median 73 years). Further non-modifiable risk factors include male gender, family history of chronic pancreatitis (CP) (7), non-O blood group (8) and African-American ethnicity. Evidence for the latter appears to be conflicting, and

potentially confounded by environmental factors, incidence of diabetes and differing mutation rates (9).

Increased risk is seen in relatives of PDAC patients, and it is estimated that 10% of PDAC cases are associated with an inherited predisposition based on familial clustering (10). Patients with familial disease have more precancerous lesions than those with sporadic pancreatic tumours (11) and an increased risk of extra-pancreatic cancers (12). This 'familial pancreatic cancer' appears to be distinct from definite syndromes associated with an increased risk of developing PDAC discussed later in this chapter. In those families with three or more relatives affected, unaffected first-degree relatives were 57 times more likely to develop pancreatic cancer, suggesting an as yet undefined genetic risk factor (7).

Hereditary pancreatitis is an autosomal dominant disorder accounting for 5% of pancreatitis resulting from a mutation in the cationic trypsinogen gene PRSS1 (13) or the serine peptidase inhibitor kazal-type 1 (SPINK1) (14) and carries a lifetime risk of 25-40% by age 60 of PDAC development, increasing to 75% with paternal transmission of hereditary pancreatitis.

A mutual association between pancreatic cancer and diabetes mellitus has been long been monitored. However, the linkage is complicated by the fact while long-term diabetes is considered a risk factor, newly developed diabetes is an early manifestation (15). Meta-analysis data suggests an overall two-fold relative risk for developing PDAC (16). Of note metformin potentially may decrease pancreatic cancer risk (17).

A number of studies have associated previous gastric surgery with pancreatic cancer risk, with the mechanism postulated to result from hypoacidity leading to excess N-nitroso carcinogens in gastric juice (18). Similarly, *H. pylori* infection has been proposed as a risk factor but the evidence is not strong (19). Further conditions associated with pancreatic cancer risk include ataxia telangiectasia (20) and pernicious anaemia.

1.1.1.2 Modifiable risk factors

While multifactorial interactions appear to underlie this disease, cigarette smoking dominates and remains the most consistently reported modifiable risk factor (21). The carcinogenic effect of tobacco on pancreatic tissue may be explained by the direct action of N-nitrosamines or their secretion into bile and subsequent reflux into the pancreatic duct. The relative risk of PDAC development was shown to be 2.5 fold in current smokers, 1.6 fold for previous smokers, when compared to those with no history, with a dose dependent increase in risk also evident (22). The effect of smoking cessation has been assessed, with risk of former smokers decreasing precipitously, approaching that of those with no smoking history after 10 years (22). It is estimated that up to 20% of PDACs are attributable to cigarette smoking, with such cancers harbouring more genetic aberrations (23).

The evidence for alcohol consumption resulting in pancreatic cancer development is confounded by alcohol excess often being accompanied by cigarette smoking. A retrospective cohort study of 200,000 patients with a heavy alcohol intake demonstrated only a modest 40% increased risk of pancreatic cancer development when compared to a reference population (24). Unfortunately, smoking data was deficient, though following adjustment for the population-smoking rate it was felt that excess risk among alcoholics could conceivably be attributed to confounding by smoking.

The role of alcohol is made more complex as it contributes risk to CP development. Two large retrospective analyses of risk of pancreatic cancer among patients with CP suggest an increased relative risk between 2.0 and 18.5, however, both were limited by poor definition of CP and reliance on patient registry data (25, 26). A prospective, single centre trial observing 373 patients with stringent CP diagnostic criteria demonstrated an increased risk of developing pancreatic cancer (27). However, this study was limited by only four cases of PDAC therefore limiting the conclusions that can be drawn from this CP data. Further modifiable risk has been attributed to obesity in men and women (28). Additionally a diet high in saturated fat and red meat (29) while low in folate and methiathione increases risk (30).

1.1.2 Pancreas anatomy and physiology

The pancreas, an organ of endodermal derivation, is the key regulator of protein and carbohydrate digestion and glucose homeostasis. The exocrine pancreas is composed of a branching network of acinar and duct cells that produce and deliver digestive zymogens into the gastrointestinal tract. The acinar cells that are organised in functional units along the duct network synthesise and secrete zymogens into the ductal lumen. Within the acinar units near the ducts are centroacinar cells (CAC). The endocrine pancreas, which regulates metabolism and glucose homeostasis through hormone secretion, is composed of specialised endocrine cell types gathered into the islets of Langerhans.

1.1.3 Pancreatic pathology

There is a spectrum of pancreatic malignancies that have histological and molecular features that recall the characteristics of the various normal cellular constituents. These multiple tumour types and hallmark features are summarised in Table 1.1. PDAC, whose nomenclature derives from histological resemblance to ductal cells, is the most common neoplasm accounting for 85% of pancreatic tumours.

Table 1.1 Pancreatic tumours and associated genetic alterations

Pancreatic neoplasm	Histological features	Common genetic alterations
Ductal adenocarcinoma	Ductal morphology, stromal reaction, desmoplasia	KRAS, $p16^{INK4a}$, TP53, SMAD4 (31)
Variants of ductal adenocarcinoma		
Medullary carcinoma	Poorly differentiated, intratumoural lymphocytes	hMLH1, hMLH2 (32)
Colloid (mucinous noncystic) carcinoma	Mucin pools	MUC2 overexpression (33)
Acinar cell carcinoma	Zygomen granules	APC/β-catenin (34)
Pancreatoblastoma	Squamoid nests, multilineage differentiation	APC/β-catenin (34)
Solid pseudopapillary neoplasm	"Pseudo" papillae, solid and cystic areas, hyaline globules	APC/β-catenin, CD10 (35)

APC – adenomatous polyposis coli gene

1.1.4 Pathophysiology of developing pancreatic neoplasms

Clinical and histopathological studies have identified three potential PDAC precursor lesions: pancreatic intraepithelial neoplasia (PanIN), mucinous cystic neoplasm (MCN) and intraductal papillary mucinous neoplasm (IPMN) (36). Of these, the most common and well studied is PanIN, found in small calibre pancreatic ducts and seen in up to 30% of specimens. PanINs show a spectrum of divergent morphological alterations relative to normal ducts representing graded stages of increasingly dysplastic growth (36). PanINs are graded in stages 1 to 3, with the early lesions PanIN-1A, then 1B (hyperplasia) characterised by a columnar, mucinous epithelium with increasing architectural disorganisation and nuclear atypia through to PanIN-2 then to PanIN-3 or carcinoma in situ (Figure 1.1B). There is evidence that high-grade PanINs ultimately transform into frank PDAC with evidence of areas of invasion beyond the basement membrane. Several molecular profiling studies have subsequently reinforced the PanIN-to-PDAC progression model through documentation of an increasing number of gene alterations in higher grade PanIN (37). The progression from stage PanIN1b to 2 was highlighted as being the source of most frequent aberrations suggesting this stage is the true preneoplastic phase (38). PanINs may provide an opportunity for the identification of novel early disease markers, however detection of these lesions is clearly problematic.

Figure 1.1 Routes to pancreatic ductal adenocarcinoma development

A) *Potential routes for PDAC development. Distinct pancreatic cell lineages may progress to different preneoplastic lesions by KRAS-induced ductal reprogramming.*

B) *Genetic progression model of pancreatic adenocarcinoma. The progression from histologically normal epithelium to low-grade pancreatic intraepithelial neoplasia (PanIN), to high-grade PanIN, to invasive carcinoma (left to right) appear to associate with the accumulation of genetic alterations. On the basis of their temporal appearance, the molecular abnormalities can be classified as early (KRAS, telomere shortening), intermediate (CDKN2A, CDKN1A, CCDN1 - cell cycle progression), or late (SMAD4/TGFβ signalling, BCL-2 – apoptosis, CTNNB1, CDH1, GSK3β – cell-adhesion and invasion, TP53 and BRCA2 - DNA damage repair, Notch and hedgehog signalling – embryonic pathways). These signature genomic alterations are accompanied by a multitude of expression abnormalities. Note this progression model is specific for PanINs; other recognised precursor lesions (IPMN and MCN) are likely to harbour a distinct compendium of genetic alterations in their path to invasive cancer (Central diagram modified from Reference 36).*

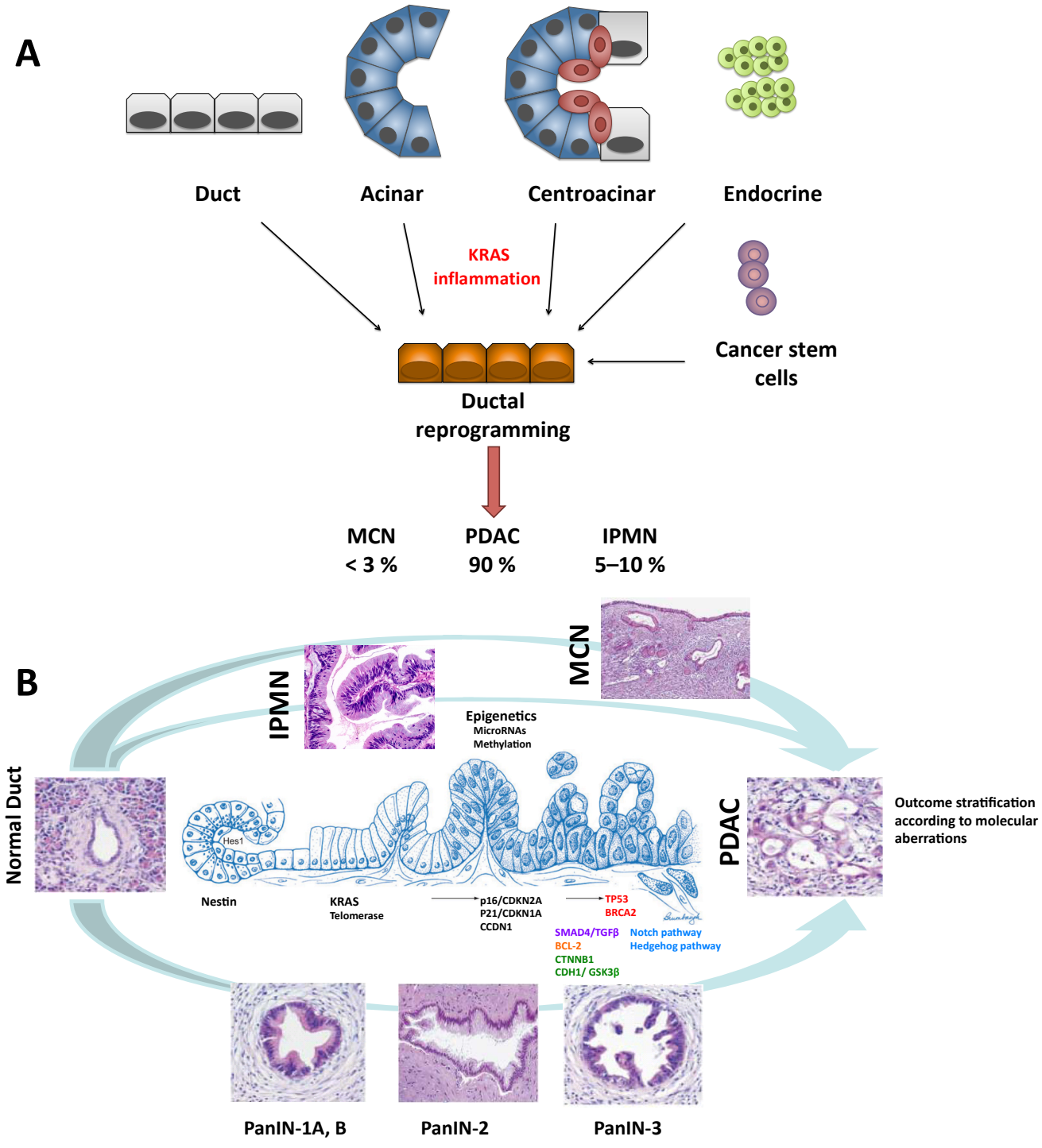

1.1.5 Cellular origin of PDAC

Although not fully defined, significant progress has been made in defining the specific population within the cancer that is able to initiate new tumours (Figure 1.1A). Recently the concept of cancer stem cells (CSC) has been applied to PDAC. This concept states that a small subpopulation of tumour cells, form the basis of tumour development with self-renewal properties and ability to replenish the tumour. Normal stem cells undergo asymmetric cell division, with one daughter cell retaining self-renewal capacity and the other differentiating into a transit-amplifying cell. A CSC population in PDAC has been proposed measuring < 1% of the bulk population, characterised by CD44, CD34 and epithelial-specific antigen (39). Potentially, CSCs may harbour resistance to chemo-therapeutics, a feature that has already been shown in pancreatic CSCs (40). While this concept is established in haematopoietic malignancy, in PDAC it may be that a facultative 'stem cell' population exists in the pancreas that, under certain conditions, is recruited, acquiring stem cell like properties by de-differentiation. Recent evidence emerging is challenging the ductal system as the solitary site of PDAC origin. The centroacinar-acinar compartment may be a potential candidate, located at the acinar-ductal junction. Adenocarcinoma may develop through a process of acinar-ductal-metaplasia (ADM) or through expansion of the centroacinar cells accompanied by apoptosis of the acinar cells (41), with persistence of embryonic gene expression (42).

1.1.6 Tumour site and clinical presentation

Distribution is such that approximately 65% of PDACs are located in the head of the pancreas (HOP), 15% body, 10% tail with 10% multifocal. Early stage disease is clinically silent, becoming apparent following local invasion or distant metastases. Pancreatic cancer patients who undergo abdominal computerised tomography (CT) scanning for other reasons prior to diagnosis are often noted in retrospect to have had subtle abnormalities for up to 1 year before symptoms develop (43), potentially providing an opportunity for early detection and treatment.

Tumours of the HOP tend to present earlier with obstructive jaundice, abdominal and back pain and weight loss. The latter can be the result of anorexia, cachexia and maldigestion secondary to pancreatic duct obstruction. Rarely, duct obstruction results in presentation with acute pancreatitis. Deep and superficial venous thrombosis may also herald this malignant disease. At diagnosis, diabetes is present in approximately 25% of patients, with 40% displaying impaired glucose tolerance (15). Potentially, new-onset diabetes in patients older than 50 may serve as high-risk screening group for the targeting of novel diagnostic biomarkers. Tumours of the body and tail tend to present late and are associated with an even worse prognosis. PDAC must be distinguished from carcinomas of the intrapancreatic bile duct, ampulla of Vater or duodenal mucosa as these tumours have a varying prognosis.

1.1.7 Diagnosis of pancreatic cancer

1.1.7.1 Non-invasive imaging techniques

Transabdominal ultrasound, an initial investigation, may detect tumours > 2 cm in size, biliary tract and main pancreatic duct dilatation or possible extrapancreatic spread, with a diagnostic accuracy of approximately 75% (44). Ultrasound is of limited value in early disease, if the bile duct is non-dilated or in obese patients. Therefore, contrast-enhanced multi-detector CT scan is currently considered the single most useful imaging modality (pancreas protocol CT−1 mm images) achieving diagnosis in approximately 97% (45). It has been reported that the accuracy for predicting an unresectable lesion is 90%, but the accuracy of predicting a resectable lesion is less at 80–85% (45, 46). The resolution of CT scans has reduced the need for staging laparoscopy, however understaging of disease can occur due to small hepatic and peritoneal metastases (< 1 cm). Magnetic resonance imaging (MRI) produces similar results to contrast-enhanced multi-slice CT and may be useful for patients unable to receive intravenous contrast (47). Positron emission tomography (PET) appears not to be useful in differentiating inflammatory conditions from pancreatic tumours accurately and the sensitivity is approximately 70–85% with specificity of approximately 65–80% (48). Therefore, CT-PET scanning appears to add little to the use of CT alone (49) although a multi-centre UK trial is currently underway.

1.1.7.2 Invasive imaging techniques

Endoscopic ultrasonography (EUS) offers no clear advantage over CT in the staging of PDAC but appears to be better for the detection of early pancreatic tumours as small as 2–3 mm (50). The addition of fine needle aspiration (FNA) cytology to EUS has been reported to improve accuracy for identifying malignancy in lesions identified on EUS and not seen on CT (50). The sensitivity and specificity of endoscopic retrograde cholangiopancreatography (ERCP) alone are approximately 70–82% and 88–94%, respectively, in symptomatic patients or those with suspected pancreatic cancer, but should no longer be used as a pure imaging modality with magnetic resonance cholangiopancreatography (MRCP) and EUS being widely available

1.1.7.3 Diagnostic biopsy

Percutaneous FNA cytology has a sensitivity and specificity of approximately 69% and 100%, respectively, for tissue diagnosis, but concerns remain regarding the risk of intraperitoneal seeding, with an incidence approaching 16% (51). The diagnostic accuracy of EUS-FNA carries a sensitivity and specificity of approximately 90% and close to 100%, respectively, but requires an expert team with a cytologist available to examine the tissue specimens in the EUS suite, repeating the procedure until the diagnosis is conclusive (52).

The incidence of carcinomatosis has been reported to be less after EUS-guided biopsy than percutaneous biopsy (51). EUS-guided biopsy is currently the preferred procedure for cytological confirmation in advanced pancreatic cancer before chemotherapy or to diagnose small, uncharacterised lesions. However, a biopsy specimen is not always needed for resection when the suspicion of malignancy is high, as a negative biopsy result may not preclude resection where radiology and clinical presentation strongly suggest malignancy.

1.1.7.4 Tumour markers

The most commonly used serum marker, carbohydrate antigen 19-9 (CA19-9) has a sensitivity of 70–90%, specificity of approximately 90% and appears to be superior to other markers including CA-50 and carcinoembryonic antigen. It has been reported that levels of more than 100–200 U/mL predict unresectability and survival (53). False positives are associated with obstructive jaundice and CP. CA19-9 may be useful in assessing response to treatment in advanced cases, identifying early recurrence in resected cases and serve as a preoperative staging aid. New serum markers including osteopontin (54) have been evaluated, but have yet to impact clinical management.

1.1.8 Principles of staging and management for resectable pancreatic cancer

Patients with pancreatic cancer are best managed within a multidisciplinary environment. PDAC is a heterogeneous disease at the molecular, pathological and clinical level, consequently a patient's response to treatment and outcome will depend on numerous factors including cancer biology, performance status and extent of disease progression. Patients require a thorough preoperative cardiorespiratory fitness assessment and for the tumour to be staged for resectability according to factors set out in Table 1.2.

Table 1.2 Indicators of resectability in pancreatic cancer

Factors contraindicating resection	Factors not contraindicating resection
Liver, peritoneal or other metastasis	Continuous invasion of duodenum, stomach or colon
Distant lymph node involvement	Lymph node metastasis within the operative field
Major venous encasement > 2 cm in length, > 50% circumference involvement	Para-aortic lymph node involvement
Severe comorbid illness	Venous impingement or minimal invasion of superior mesenteric and hepatic portal veins
Cirrhosis with portal hypertension	Gastroduodenal artery encasement
Superior mesenteric, coeliac or hepatic artery encasement	Age of patient

Table adapted from Reference (55)

1.1.8.1 Surgical techniques

The standard operation for PDAC is PD (56). With various options available for pancreatic reconstruction, the benefit of pancreaticogastrostomy over pancreaticojejunostomy remains unclear (57). The pylorus-preserving PD is the most commonly used approach, which appears as effective from an oncological perspective as a classical PD (58). There appears to be no role for total pancreatectomy unless there is no alternative to achieving clear margins

(59). An extended radical lymphadenopathy was associated with significantly increased morbidity without any survival benefit in a randomised trial (60). Postoperative morbidity remains high at 40% even in high-volume tertiary referral centres (61). Independent negative risk factors reported are age > 70 years, extended resection and main pancreatic duct diameter < 3 mm (62). Portal or superior mesenteric vein (SMV) resection is appropriate if it enables an R0 resection and can be carried out without increasing morbidity (63). Preoperative biliary drainage is considered mandatory in the setting of cholangitis or severe liver dysfunction. Otherwise, routine preoperative drainage might not be necessary, with recent study findings suggesting worse outcome for those undergoing routine preoperative drainage versus surgical resection alone (64). The potential complications associated with surgery result in many candidates not undergoing surgical resection because of associated comorbidity (65).

1.1.8.2 Adjuvant therapy

The basis of offering adjuvant chemotherapy to those resected with curative intent, has been established as a result of randomised control trials (GITSG, CONKO-001 and RTOG-9704) (66-68) and retrospective analysis (69, 70). The GITSG trial, demonstrated 5-FU augmented chemoradiation appeared to be superior to observation alone (66). The addition of radiation to adjuvant chemotherapy remains unproven, with the first European Study of Pancreatic Cancer (ESPAC-1) demonstrating that while adjuvant 5-FU afforded significant benefit over non-treatment, adjuvant chemoradiation failed to increase survival, although this trial had limitations in terms of variability of radiation regimen delivered (71). The RTOG-9704 trail compared gemcitabine with 5-FU before and after 5-FU-based chemoradiation, however little difference was noted (68). Gemcitabine appeared superior to observation in CONKO-001 trial, with a modest survival benefit of 2.6 months. In ESPAC-3 there appeared to be no difference in outcome noted when gemcitabine was compared with 5-FU, although the former was associated with fewer complications (72). Certainly adjuvant chemotherapy (in the form of gemcitabine) would appear to be of benefit, however for chemoradiotherapy the evidence is weaker though it may be of benefit in some patients.

1.1.8.3 Neoadjuvant therapy

In an effort to improve the dismal outcome associated with even localised disease, efforts have focused towards neoadjuvant therapy (73). As yet no randomised controlled trials support neoadjuvant over adjuvant therapy, however, meta-analysis suggests the proportion of patients who can have resection is similar regardless of whether neoadjuvant therapy is given or not (74). This approach has the benefit of selecting out those patients who might not tolerate the stress of surgery or who might develop metastatic disease early in the treatment course and so avoid resection. It has the potential to downstage borderline

resectable disease (74), and has resulted in extended survival for a 'super-selected' cohort (75). A further potential advantage is that post-operative complications do not delay systemic therapy administration.

1.1.8.4 Borderline resectable disease

Despite the accuracy of imaging modalities, a wide range of tumour-vessel involvement relationships exist, from minimal tumour abutment of the superior mesenteric artery (SMA) to complete encasement with associated SMV occlusion. Tumours that demonstrate arterial abutment (tumour-vessel involvement of 180° or less) may be considered for surgery as part of a multimodality approach that includes neoadjuvant chemotherapy (76). Even short-segment occlusion of the portal/ SMV confluence does not contraindicate resection, as long as a suitable vein exists proximally and distally to facilitate reconstruction (77).

1.2 Prognostic factors in PDAC

1.2.1 Biomarkers and prognosis in cancer

A biomarker has been defined as 'a characteristic that is objectively measured and evaluated as an indicator of normal biological, pathogenic processes or pharmacologic responses to a therapeutic intervention' (78). These biological measurements may be used for a diverse range of medical purposes including diagnostic, prognostic or predictive end points. Effective development and validation of biomarkers depends critically on the intended use of the biomarker. One fundamental distinction that must be made in oncology is between predictive and prognostic markers. A prognostic factor is a marker showing a statistically significant association with outcome after a specific therapy. Standard, classical clinical examples include advanced stage of disease or tumour size, both associated with a poor outcome in multiple cancers. They can be more complex, such as abnormal levels of proteins, for example in patients with neuroblastoma amplification of N-Myc is associated with poor prognosis (79). A predictive marker, on the other hand, shows a statistically significant interaction with the benefit from being assigned to a treatment; e.g., defines patient subsets that are responsive to a specific therapy.

1.2.2 Pancreatic cancer a surgical dilemma: improving patient selection for pancreaticoduodenectomy

While only 15% of patients with PDAC are eligible for resection at the time of presentation, of those resected, 30% who undergo resection die within one year from progressive disease. Certainly current staging is unable to reliably select this poor survival cohort; however, preoperatively determined biomarkers have the potential to enhance the selection algorithm so as to avoid the potential morbidity and mortality associated with radical resection.

1.2.3 Pathological prognostic factors in PDAC

1.2.3.1 TNM staging

The current staging system of the Union for International Cancer Control (UICC) defines pancreatic exocrine malignancies in terms of the size and anatomic extent of the primary tumour (T), the presence or absence of lymph node metastases (N) and presence of distant metastases (M) (80). The T1 and T2 designations describe tumours confined to the pancreas while T3 and T4 indicate extrapancreatic extension of the primary, with the latter being those with extension to the coeliac axis or SMA. A recent change in the TNM staging is that a neoplasm invading the portal or SMV is now deemed T3 disease if still resectable. Following resection various pathological variables are recognised as impacting upon survival as discussed below.

1.2.3.2 Tumour grade

Histological grading of PDAC into well, moderate and poorly differentiated states according to established criteria (81) appears to have independent prognostic value (61, 82, 83).

1.2.3.3 Lymph node status

Multivariate analysis has confirmed lymph node involvement to be an independent prognostic factor (61), however, evaluation of lymph node ratio (LNR) defined as the number of lymph nodes with evidence of metastatic disease among the total number of lymph nodes examined would appear to increasingly important in cancer staging. In PDAC it has potentially yielded further prognostic information amongst the lymph node positive cohort (84), but has yet to be incorporated within the staging system, principally as the definition for ratio cut-offs vary between studies.

1.2.3.4 Perineural invasion

A characteristic of PDAC is that there appears to be a strong association between intrapancreatic neural invasion and extrapancreatic plexus invasion (85), which is a major contributor to local recurrence. Although the reported rate varies, there is evidence supporting the role of perineural invasion as a significant prognostic factor (2, 86).

1.2.3.5 Intratumoural vascular invasion

Intratumoural vascular invasion is also a route of pancreatic cancer spread that has been shown to associate with poor outcome following surgical resection (2, 87, 88). The histopathologic characteristics of vascular invasion are poorly defined but it would appear to occur in approximately 50% of resected specimens (2, 88).

1.2.3.6 Vascular invasion

While radiological evidence of tumour extension into the coeliac axis is a surgical contraindication to surgery, SMA resection is possible (89). Resection of involved venous structures is also possible, with involvement diagnosed when a vein wall segment is attached to the specimen that is clearly infiltrated by tumour on histological examination. Often,

however, there is no histological evidence of invasion of the resected vessel wall, and the vessel tethering is the result of inflammatory changes. Controversy still exists as to whether microscopic tumour infiltration of the vessel wall influences survival (89, 90).

1.2.3.7 Tumour size

Tumour size in usually an independent prognostic factor for PDAC (61, 91), with tumours < 2 cm, although rare, having better survival, however, nodal metastasis, SMV and resection margin involvement are seen in such small tumours (92). Therefore, they do not necessarily represent biologically early stage disease.

1.2.3.8 Resection margin involvement: frequency and prognosis

The rate of margin positivity following PD for PDAC is currently a topic of debate with the reported rate ranging from 10–84% (61, 93, 94). Clearly the definition of margin positivity (R1) is vital, with R1 status being defined by the UICC classification as microscopic tumour at the edges of the surgical specimen (80), while the British Royal College of Pathologists (RCPath) (95) regards the presence of tumour ≤ 1mm from a circumferential margin or surface of the pancreatic resection specimen, whether by direct invasion or by tumour within a lymph node, as an involved margin. Additionally, this degree of rate variation may be partly explained by under-reporting of R1 resections as a result of non-standardised pathology reporting. Indeed, it appears that the ability of R1 status to predict outcome correlates with greater frequency of R1 positivity. Certainly, the development of protocol driven reporting of pathological examination of specimens by Verbeke and co-workers has been integral to increasing R1 rates (93, 96), which then correlate more accurately with patient survival.

1.2.3.9 The prognostic value of local tumour invasion and influence on recurrence

The extension of the tumour beyond the pancreas to the surrounding tissues including the duodenum (and ampulla), the biliary tract and the peripancreatic fat promotes a tumour from T2 to T3 status. T stage correlates well with prognosis (97), and peripancreatic tissue invasion has been reported in up to 90% of resections, subsequently correlating with poor prognosis (88). There has been no specific study of the prognostic influence of peripancreatic fat invasion.

1.2.3.10 Predictors of site of recurrence

Almost all patients develop metastatic disease, most commonly of the liver and peritoneum but also the lungs, and this may occur with or without local recurrence. Despite the limited survival benefit associated with resection, further management challenges result from a high local failure rate that can reach 80% (98, 99). Adjuvant chemoradiotherapy has been proposed as a means to reduce the risk of local recurrence towards 20% (100, 101). However, evidence is lacking to support the routine use of chemoradiation. The main

outcome measure following PD for PDAC remains overall survival, with minimal data describing the pattern of recurrence (94, 98, 99, 102). To date, limited variables (resection margin status) have been compared to pattern of failure (94, 103), with no consideration made of association between the pattern of failure and the presence of venous, perineural or peripancreatic invasion, and furthermore, there has been limited investigation of the role molecular factors in the pattern of failure.

1.3 Molecular biology of pancreatic cancer

1.3.1 Molecular genetics and signalling pathway aberrations of PDAC

Pancreatic cancer is a disease of specific inherited and somatic mutations as sequenced in Figure 1.1B. The molecular characteristics of PDAC as presented in Figure 1.1B are described in the subsequent sections including; KRAS signalling, cell cycle progression G1/S phase, cell-adhesion and invasion, transforming growth factor β (TGFβ) signalling, DNA damage repair and embryonic signalling pathway (Figure 1.2). Further important molecular concepts that have recently been applied to PDAC tumour biology including senescence and epithelial-mesenchymal transition (EMT) are also discussed below.

Figure 1.2 Aberrant signalling pathways in pancreatic cancer

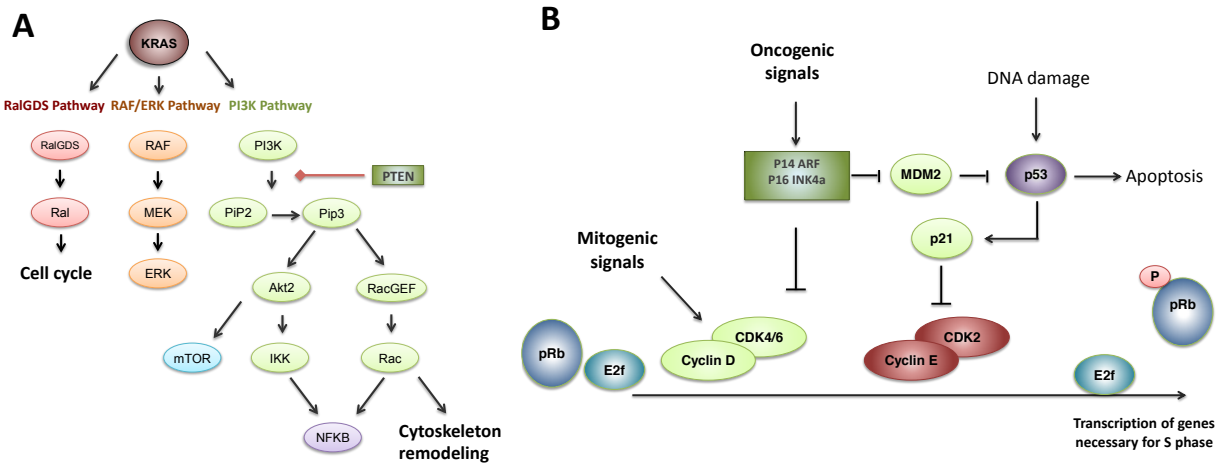

A) Ras signalling network. Ras uses a multitude of downstream effectors. The three major signalling cascades that have been implicated in PDAC progression are depicted: Raf/ Map Kinase (ERK), PI3K pathway and RalGDS pathway.

B) Mitogenic signals give rise to increased levels of cyclin D and consequently formation of active cyclin D/ cyclin-dependent kinase 4 or 6 (CDK4/6) complexes leads to the phosphorylation of retinoblastoma (Rb), facilitating the transcription of E2F-reglated genes (including cyclin E) required for the S-phase. The TSG p16 inhibits this process by binding to CDK4/CDK6, thus preventing the formation of active cyclin D-CDK4/CDK6 complexes. p53, is activated in response to DNA damage or other cellular stress. MDM2, a p53 inducible gene keeps p53 levels low. Rb-dependent cell cycle arrest by p53, induces the transcription of p21 CIP1, which inhibits cyclin E-CDK2 or leads to apoptosis.

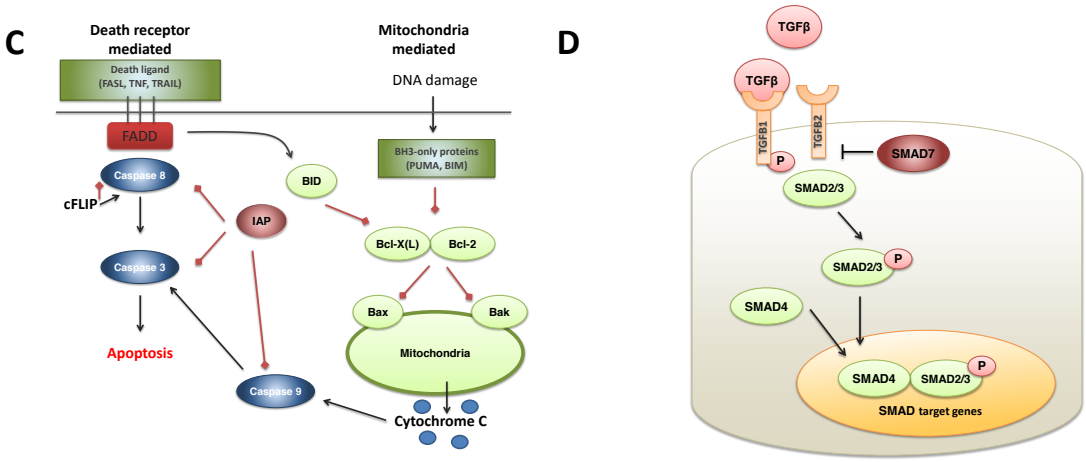

C) Apoptosis signalling. *On the left the death receptor pathway is activated by binding of death receptor ligands like FAS ligand (FASL), tumour-necrosis factor (TNF), or TRAIL to the death receptor. This initiates formation of multiprotein death-inducing signalling complex (DISC) including the adaptor protein FADD. Conformational changes trigger catalytic activity of caspase 8 which in turn can activate caspase 3, the key executioner of apoptosis. cFLIP can either inhibit or potentiate binding of caspase 8 to FADD depending on its concentration. IAP inhibits caspase activity. In the mitochondrial (intrinsic) pathway proapoptotic BH-3 only proteins are activated by DNA damage. These proteins interact and inhibit antiapoptotic BCL2 or* BCL_{XL}. *As a consequence, BAX and BAK induce mitochondrial permeabilisation with release of cytochrome C, which activates caspase 9 then caspase 3. Crosstalk between the pathways is mediated by truncated BID produced by caspase 8 cleavage. This can inhibit BCL2 and* BCL_{XL} *and activates BAX and BAK.*

D) TGFβ signalling pathway. *Upon binding of the dimeric TGFβ, the serine/threonine receptor assembles as a heterotetramer consisting of the TGFβ receptor I (TGFβRI) and TGFβ receptor II (TGFβRII) subunits. TGFβRII phosphorylates and activates TGFβRI which in turn phosphorylates and activates receptor bound SMAD proteins (SMAD2 or 3). Activated SMAD2/3 forms a complex with SMAD4 and transports it to the nucleus where it influences SMAD target gene transcription. SMAD7 can inhibit TGFβ signalling through inhibition of TGFβR1 phosphorylation.*

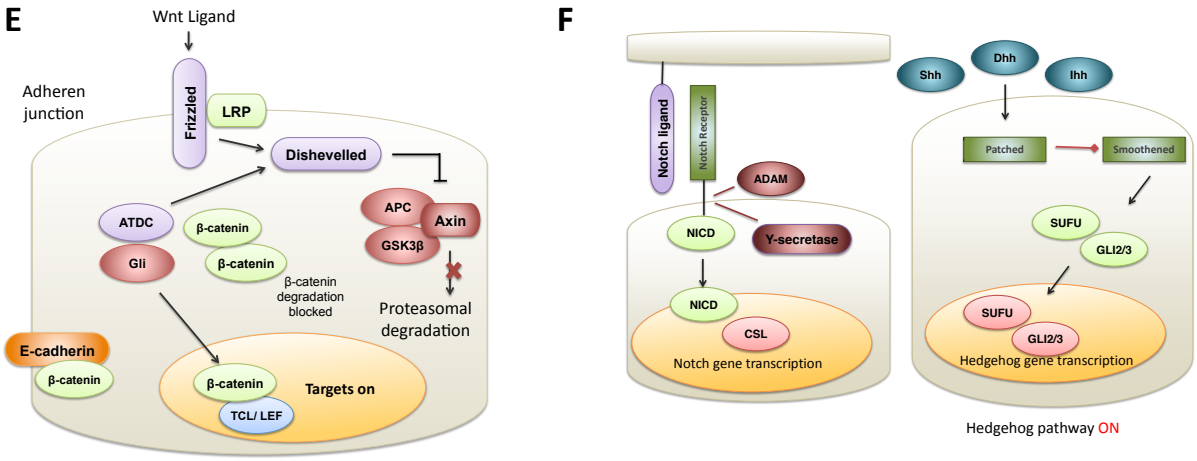

E) Deregulated Wnt-β-catenin pathway activation in PDAC. *Accumulated β-catenin can translocate into the nucleus and activate target genes in concert with TCF/LEF co-factors. Presently, the dominant mechanism of persistent β-catenin accumulation and activity in PDAC is unclear. There is evidence for both autocrine (owing to epithelial-derived Wnt ligands) and cell-autonomous activation (through Gli signalling and ataxia telangiectasia group D-associated [ATDC], which activates Dishevelled). The extracellular matrix may contribute to the promotion of β-catenin accumulation.*

F) Embryonic signalling pathways. *Upon Notch ligand binding, ADAM performs the first cleavage followed by the second cleavage performed by γ-secretase. This releases the Notch intracellular domain (NICD) that results in gene transcription. The Patched receptor normally represses the smoothened receptor. Intracellularly, the hedgehog inhibitor suppressor of fused (SUFU) binds the GLI family zinc finger transcription factors GLI2/3 thereby inducing proteasomal cleavage resulting in repressor forms of GLI2/3. Hedgehog ligand binding to Patched, abrogates the inhibition on Smoothened. Smoothened inhibits proteasomal cleavage of GLI2/3 and thereby facilitates transcriptional activity.*

1.3.1.1 KRAS signalling

KRAS is a member of the RAS superfamily of GTPases that mediate a variety of cellular functions including proliferation, differentiation and survival. Mutations of the KRAS gene (chromosome 12p) have been report in approximately 30% of early pancreatic neoplasms. In PDAC the gene is almost always activated by a point mutation in codon 12 (glycine to aspartate, $KRAS^{G12D}$), of the GTP binding domain, leading to constitutively active Ras protein (104). This molecular switch remains in the 'on' position sending its potent oncogenic stimulating signal. The high frequency of mutation at an early point in development is consistent with an important role for KRAS mutation in PDAC tumourigenesis. Direct evidence that activating KRAS mutations can induce PDAC is provided by murine models expressing constitutively active KRAS in the pancreas that develop PanIN lesions that progress to invasive PDAC (105). Progression subsequently occurs if these mice are crossed with an appropriate tumour suppressor background. KRAS has three principal downstream pathways, all of which are implicated in PDAC tumourigenesis: 1) the RAF/ERK pathway, 2) phosphatidylinositol 3-kinase (PI3K) pathway and 3) RalGDS pathway (Figure 1.2A)

The three foremost mitogen activated phosphorylated kinases (MAPKs) include: extracellular signal-regulated kinase (ERK), c-Jun N-terminal Kinase (JNK) and p38. For PDAC the ERK pathway is the most significant consisting of the Raf protein that phosphorylates MEK, resulting in ERK phosphorylation with subsequent gene transcription. Of the tumours with wild-type KRAS, a mutation in the BRAF oncogene (chromosome 7q) is present in ~5% of all PDACs, with Raf, the protein product, a downstream target in the Ras signalling pathway, hence the mutually exclusive nature of KRAS and BRAF mutations in PDAC (106). RAF mutations occur mainly in the medullary PDAC subtype, characterised by a lack of KRAS mutation (106). The KRAS and JNK pathways interact with phosphorylation of JNK partly accountable for induction of angiogenesis through KRAS.

The PI3K pathway has been implicated in PDAC by several evidence strands: repressed phosphatase and tensin homolog (PTEN) (a PI3K inhibitor) being present in some PDACs (107); conditional knockout of PTEN in the mouse pancreas results in PDAC (42); activation of the PI3K pathway maintains KRAS initiated xenograft tumours; the downstream effector of PI3K, AKT2 is amplified in 10-20% of PDAC (108), while PI3K/Akt signalling is activated in approximately 60% of pancreatic cancers (109); inhibition of mammalian target of rapamycin (mTOR), another downstream effector in PI3K pathways inhibits PDAC xenograft growth (110).

The RalGDS pathway, which can activate the RAL exchange factor enhancing cellular transformation (111), has been implicated in PDAC progression downstream of KRAS.

The NFκB pathway can be activated by multiple factors, notably proinflammatory signals including oncogenic KRAS signalling (112). Although absent from the normal pancreas, constitutive activity is common in PDAC and may influence anti-apoptotic and angiogenic pathways (113).

1.3.1.2 Cell cycle progression G1/S phase

The progression through G1/S-phase appears to play an important function in enabling unrestrained cancer cell progression. The tumour suppressor gene (TSG) CDKN2A gene (chromosome 9p21) is inactivated in approximately 90% of PDACs (114) by either homozygous deletion or an intragenic mutation in combination with loss of heterogeneity of the remaining wild type allele. Promoter hypermethylation is the cause for loss of CDKN2A in the remaining cases (114). The protein product p16, inhibits phosphorylation of retinoblastoma (Rb), thereby preventing G1/S transition and acting as a cell-cycle progression inhibitor (Figure 1.2B). Loss subsequently results in uncontrolled G1/S transition and unregulated cell division with associated tumour progression (115). CDNK2A mutations appear to act synergistically with KRAS in PDAC, hastening development (116).

1.3.1.3 Apoptosis

Programmed cell death or apoptosis, is a vital component of cancer development as resistance leads to cancer cell survival (Figure 1.2C). Contribution to PDAC tumourigenesis is however poorly defined. Two pathways can activate apoptosis: firstly by the death receptor pathway requiring binding of the ligands FASL, TRAIL and TNF to the death receptor. Secondly, the mitochondrial pathway in which a balance exists between proapoptotic (e.g. Bid, Bim, PUMA) and antiapoptotic (B-cell lymphoma 2 [Bcl-2], BCL_{XL}). Both mechanisms are perturbed in PDAC resulting in a tumour less receptive to pro-apoptotic stimuli. The death receptor pathway can be inhibited by the high expression of the inhibitors of apoptosis specifically survivin, overexpressed in up to 85% of PanIN III lesions (117).

At the level of the mitochondria, deregulated expression of Bcl-2 results in apoptotic resistance in PDAC. Anti-apoptotic genes Bcl-2, Bcl_{XL} and Mcl-1 are expressed to varying degrees and repression was shown to enhance apoptosis in PDAC (118). Conversely, the pro-apoptotic Bax protein is reduced in 50% of PDAC (119).

1.3.1.4 SMAD4/TGFβ signalling

The TGFβ pathway is associated with cell proliferation, differentiation, apoptosis and angiogenesis (120) and has been strongly linked to PDAC tumourigenesis. Binding of a TGFβ ligand to the TGFβII receptor leads to phosphorylation and activation of the TGFβI receptor resulting in signal transduction of the SMAD protein family (SMAD 1-3, 5, 8), allowing that protein to integrate with SMAD4 (Figure 1.2D). The latter assists the regulator

SMAD complex in nuclear transfer with induction of transcription of the gene target. SMAD7 is the only characterised inhibitory SMAD acting via inhibition of the TGFβ receptor phosphorylation. TGFβ influences cellular proliferation through inhibition of the G1/S transition, via cyclin kinase inhibitors including p15, p21 and p27 (121). Additionally TGFβ signalling represses c-Myc expression, a powerful promoter of cell cycle progression.

SMAD4 is the most commonly affected protein in the TGFβ pathway, with 90% of PDACs demonstrating loss of heterozygosity at the SMAD4 locus and 50% showing further inactivation of the remaining allele (122). Loss of SMAD4 has important effects on the tumour microenvironment and potentiation of invasion (123). The late loss of SMAD4 in PanIN lesions suggests that SMAD4 is necessary for PDAC maintenance. Furthermore, increased expression of the inhibitory SMADs has been observed (124). In many epithelial tissues, TGFβ exerts a growth inhibitory effect preventing cancer initiation, however it can promote fibroblast proliferation in breast cancer resulting in dedifferentiation and an aggressive phenotype (125). How SMAD4 mutations affect the balance remains to be elucidated but one study has shown that SMAD4 deficiency abolishes TGFβ mediated cell-cycle arrest but not TGFβ induced EMT, thereby shifting the balance of TGFβ signalling towards a more aggressive phenotype (126).

1.3.1.5 Cell adhesion and invasion

A reduction in cell-to-cell adhesion and interaction plays an important role in carcinogenesis. The ability of cells to detach and metastasise in healthy pancreatic tissue is limited by anchoring attachments via multiple connections usually facilitated by junctions resulting from E-cadherin and catenins (127). E-cadherin is important for cell-to-cell cohesion, recognition and epithelial polarity. The extracellular domain of E-cadherin binds to other cadherins of neighbouring cells, while the intracellular cytoplasmic tail interacts with β-catenin, p120 catenin and Hakai protein, with resulting regulation of β-catenin signalling in the Wnt pathway (127). Free cytosolic β-catenin is also regulated by catenin destruction complexes including APC, Axin and Glycogen synthase kinase 3β (GSK3β) (Figure 1.2E).

E-cadherin appears to suppress invasion, either by mediating direct tumour cell interaction or via its intracellular domain and β-catenin (128). Increased expression of β-catenin leads to nuclear translocation and induction of target genes. Reduced expression of E-cadherin, α- and β-catenins was demonstrated respectively in up to 60%, 40% and 60% of PDAC specimens (129).

GSK3β can promote cell survival or apoptosis via activation of the intrinsic apoptosis pathway. Active GSK3β phosphorylates β-catenin, priming it for proteasome-mediated degradation (130), with GSK3β inhibition leading to β-catenin stabilisation resulting in

nuclear translocation, heterodimerisation, transcription of target genes and cell survival (131). There is limited information regarding the influence of GSK3β expression in human PDAC, or association with clinicopathological factors.

1.3.1.6 DNA damage repair

DNA damage control genes are responsible for maintaining DNA integrity. The TSG TP53 gene (chromosome 17p) plays a vital role appearing in late stage PanINs. The frequent elimination of TP53 in PDAC (up to 40%), may account for the characteristic genomic instability, providing malignant cells with a survival advantage (132). Germline BRCA2 gene mutations, integral to cross-linking DNA repair (133), are accountable for approximately 10% of familial pancreatic cancer; yet even in sporadic cases its frequency is up to 7% (134).

The mismatch repair family of genes target base substitutions and insertion-deletion mismatches occurring following replication. Aberrations of MLH1, MSH2 and PMS2 eventually lead to microsatellite instability (MSI) enhancing genomic vulnerability to further genetic errors. Although the incidence of pancreatic tumours with MSI is rare compared to other GI tract malignancies (~5%), medullary type pancreatic carcinomas have a distinct appearance similar to those occurring in the colon, and have a more favourable prognosis than classical PDAC (32).

1.3.1.7 Embryonic pathways

As embryogenesis shares many characteristics with carcinogenesis, different embryonic pathways are though to be involved in tumour development notably: Hedgehog (Hh), Notch and Wnt. The Hh signalling cascade plays an important role in GI tract development. Although absent from the developing pancreas, it is re-activated during tumourigenesis in 70% of PDACs (135). Hh binding to its transmembrane receptor patched disinhibits the tonical inactivation of Smoothened, the cellular binding partner of Patched, resulting in signal transmission. Targets of the Hh pathway include Wnt proteins, Cyclin D1 and TGFβ assisted by GLI transcription factors (136). While the role of Hh signalling in PDAC requires clarification, inhibition by cyclopamine enhances survival in a murine pancreatic cancer model (137). Hh signalling also appears to have a role in PDAC stem-cell viability (138).

The Notch signalling pathway is activated by the binding of Notch ligands to one of four Notch receptors resulting in proteolytic degradation with nuclear translocation. The Notch pathway plays a vital role in pancreatic embryonic development, but following pancreatic formation, signalling is limited to CACs (139), however appears reactivated in PanIN lesions (140). Up-regulation of the Notch pathway has been demonstrated in PDAC, with inhibition resulting in decreased tumour growth and accelerated apoptosis (140). Although

ectopic expression of Notch is not sufficient to induce PDAC in mouse progenitor cells (141), evidence suggests that Notch may well interact with KRAS to initiate PDAC (142).

The third embryonic pathway, Wnt, shows increased activity in approximately 30-65% of PDACs, with increased Wnt-target expression correlating with poorer differentiation (143). Activation of the Wnt signalling cascade occurs through interactions with Hh, NFκB, TGFβ and Notch pathways (144) resulting in transcription of various target genes including Cyclin D1, matrix metalloproteinase 7 (MMP7) and c-Myc.

1.3.1.8 Senescence

Senescence has been proposed as a barrier to tumourigenesis in multiple cancer types. It has been suggested that cellular senescence is a key tumour suppressor pathway downstream of Ras signalling. Potentially, senescence in the context of the PanIN framework would be present at the early stages along with KRAS mutations, but prior to the development of mutations that allow the evasion of senescence. Cellular senescence is associated with senescence associated β-galactosidase and induction of cell cycle regulators including p16, p53 and its target p21 which is known to play a role in senescence/growth arrest (145). The initial reports in the pancreas suggest widespread evidence of senescence in response to endogenous expression of $KRAS^{G12V}$, as assessed by p16 and p15 and Dec1 (146). Certainly the role that senescence plays in PDAC tumourigenesis is a focus of much interest.

1.3.1.9 Epithelial mesenchymal transition in pancreatic cancer

EMT may be viewed as an initiating step in metastatic spread. The dissociation of cells from the epithelial layer necessitates the deregulation of cell-to-cell contacts and the acquisition of migratory abilities. A characteristic feature of EMT in PDAC is the switch of the epithelial-specific junction protein E-cadherin to mesenchymal N-cadherin along with up-regulation of S100A4 and vimentin. Various factors can potentially trigger EMT including TGFβ, epidermal growth factor (EGF) and fibroblast growth factor (FGF) (147). Loss or reduced E-cadherin expression can be caused by somatic mutations, chromosomal deletions or furthermore the transcriptional factors Snail and Slug (zinc finger proteins) have been described as direct repressors of the E-cadherin promoter (148). Twist, a helix-loop-helix transcriptional factor is also potentially capable of suppressing E-cadherin in pancreatic cancer increasing the capability to invade and metastasise (149, 150).

1.3.1.10 Genetic susceptibility

As previously mentioned approximately 5–10% of PDAC patients have a positive family history of disease. An afflicted first-degree relative doubles the risk of development of PDAC with the risk increasing with number of affected relatives, implicating a hereditary component. Some cases will arise in the setting of a familial cancer syndrome; however, for most the genetic basis of the familial aggregation is not apparent (151). Five principal

hereditary syndromes are described which increase the risk of PDAC development. The Familial Atypical Multiple Mole syndrome (FAMMs) is the result of a CDKN2A germline mutation, carrying a 20–34 fold risk (152) especially when affecting a specific 19-base pair deletion (153).

Peutz-Jeghers syndrome (PJS) is the result of mutation in the STK11/ liver kinase B1 (LKB1) gene (154), a serine threonine kinase affecting multiple pathways in particular cell polarity and metabolism. It is associated with a 132-fold increased risk of PDAC development with a 30–60% lifetime risk by age 70 (155). Restoration of silenced LKB1 in PDAC cells induces apoptosis *in vitro* (156). Furthermore, LKB1 gene inactivation has been observed in IPMNs (157). Lkb1 activates a number of downstream kinases, including the AMP-activated protein kinase (AMPK), which responds to energy stress by negatively regulating the mTOR kinase (158). Lkb1 is also able to regulate cell growth and apoptosis, potentially through interaction with p53 (159). Ectopic expression of Lkb1 in cells lacking the endogenous protein induces p21 expression and cell cycle arrest in a p53-dependent manner, and chromatin immunoprecipitation analysis has revealed that Lkb1 is recruited to the p21 promoter by p53 (159). Lkb1 deficiency has also been shown to prevent culture-induced senescence although, paradoxically, it renders cells resistant to subsequent transformation by H-Ras (160).

The hereditary cancer susceptibility disorder, Falconi anaemia has a number of pathway components. The BRCA2 protein interacts with different genes in the pathway, including FANCC, FANCG and more recently PALB2 (161). Mutation in the DNA mismatch repair gene family results in Lynch syndrome, however, the exact role in PDAC development along with risk, requires further elucidation (162).

Table 1.3 Genetic syndromes associated with familial pancreatic cancer

Cancer syndrome	Gene mutation	Pancreatic cancer lifetime risk	Relative risk	Histologic feature of neoplasm	Extrapancreatic cancer
Familial pancreatic cancer (10)	BRCA in up to 20%	Variable risk – up to 50%	10 fold	Ductal	Unknown
Family X (163)	Palladin	Family X affected subjects carry the P239S variant	Risk may have been over-estimated	Ductal	None
FAMMM (152)	CDKN2A	17% - p16 Leiden mutation	13-22 fold	Ductal	Melanoma
Familial breast and ovarian cancer syndrome (161)	BRCA1, BRCA2, FANCC, FANCG, PALB2	Pedigree dependent	6-10 fold	Ductal	Breast, ovary, prostate
Peutz-Jeghers syndrome (155)	STK1/LKB1	36%	132 fold	Ductal, IPMN	Small intestine, colorectal, oesophagus, stomach, lung, breast, ovary, uterus
Hereditary pancreatitis (13)	PRSS1 in up to 80%	35%	26-60 fold	Ductal	None
von Hippel-Lindau disease (164)	VHL	Approx 5%	Not known	Ductal, neuroendocrine Pancreatic serous cystadenoma	Renal, haemangioblastoma
Ataxia telangiectasia (20)	ATM	Rare	Not known	Ductal	Lymphoma, breast, ovarian, stomach, melanoma
Li-Fraumeni syndrome (165)	TP53	5%	Not known	Ductal	Breast, brain, sarcoma
Cystic fibrosis (166)	CFTR	5%	5-6 fold	Ductal	Unknown
FAP (164)	APC	Unsure	4 fold	IPMN, ductal, pancreatoblastoma	Colorectal, small intestine, stomach
HNPCC (162)	MLH1, MSH2	5%	8-9 fold	Medullary	Colorectal, small intestine, endometrium

FAMMM – Familial atypical multiple mole melanoma, FAP – Familial adenomatous polyposis, HNPCC – Hereditary nonpolyposis colorectal cancer syndrome, IPMN – intraductal papillary mucinous neoplasm, VHL – von Hippel-Lindau

1.3.1.11 Experience from the study of animal models

The development of genetically engineered animal models of pancreatic cancer have enhanced comprehension of transcription factor activity in the developing pancreas and elucidated the sequence of genetic alteration in PDAC development. Targeted expression of oncogenic KRAS to pancreatic progenitor cells in mice resulted in the generation of progressive PanIN lesions, with subsequent low frequency progression to invasive adenocarcinoma (167). Pancreatic cancer development was accelerated by the inclusion of mutations in CDK2NA or TP53 (168), supporting the concept of KRAS initiating PanIN formation while key TSGs limit onward malignant conversion.

1.3.2 Prognostic influence of molecular pathways in PDAC

As discussed, there are a variety of molecular signalling abnormalities in PDAC. Despite a number of studies, no biomarker has found clinical use within a PDAC management algorithm. A summary of studies evaluating prognostic markers using immuno-histochemistry (IHC) is found in Table 11.1, presenting the strength of evidence for each protein in terms of frequency, multivariate analysis and direction of prognostic influence.

1.3.3 Gene expression abnormalities in pancreatic cancer

A gene expression signature is a biomarker in which the expression levels of multiple genes are combined in a defined manner to provide either a continuous score or a categorical classifier and have found utility as prognostic or predictive tools. The initial studies in cancer developed breast carcinoma portraits, profiling gene expression using unsupervised clustering of microarray data. An influential study identified four distinct subtypes, two of which where previously unknown (169). Subsequently, gene expression microarray profiling has been applied to other tumours including colon (170). Usually performed on oligonucleotide and complementary DNA (cDNA) microarrays, structures with several thousand gene specific nucleic acids placed by spotting or direct synthesis (171). The principles underlying microarray experimentation are shown in Figure 2.3.

1.3.3.1 Prognostic genomic signatures

Outcome prediction utilising gene expression signatures then developed, with the newly identified basal like type of breast carcinoma associated with poor prognosis (172). Subsequently a 70-gene set, able to predict metastasis development in young patients with breast carcinoma, was developed and subsequently validated in 295 early stage breast cancer patients (173). This signature predicted outcome more accurately than standard parameters (5). In a further breast cancer cohort, a gene set was described that identified distant recurrence within 5 years and subsequently has undergone extensive validation (174).

1.3.3.2 Gene expression profiling of pancreatic ductal adenocarcinoma

Potential exists for a variety of novel aberrations to exist that drive the pathological features of PDAC. Several studies have elucidated gene expression changes in PDAC utilising representational difference analysis, serial analysis of genes and microarrays (175-177). Eight studies using DNA microarray technology (175, 178-184) have generated large sets of new cancer genes dysregulated at the mRNA level. Logsdon and co-workers identified genes differentially expressed between PDAC and CP, revealing that many deregulated genes were common in both situations in comparison to normal ductal tissue, with the highest fold change evident in the PDAC tissue (180). A selection of the genes identified as overexpressed in PDAC from multiple profiling studies are listed in Table 1.4.

Repositories of gene expression data exist as the Pancreatic Expression Database (185) (www.pancreasexpression.org) and the Oncomine database (www.oncomine.org) which contains six studies including 134 samples (38, 179, 180, 186-188). The Pancreatic Expression Database was used to generate a list of differentially expressed genes for PDAC versus normal ductal tissue and for PDAC versus CP. 132 genes were selected in total, 33 of which were expressed in at least five studies. From the Oncomine repository the 20 most highly over- and under-expressed genes were selected. The two lists shared seven components: CLPS, CPA2, THBS2, FN1, S100P, PNLIPRP1 and AMY1A.

Table 1.4 Selection of aberrantly genes identified by PDAC expression profiling

Aberrantly expressed genes in PDAC		
Gene Symbol	**Method**	**Study source**
CEACAM5	DNA microarray	(179, 180, 184, 189)
ITGA2	DNA microarray	(179, 180, 189, 190)
MMP11	DNA microarray	(188)
MSLN	DNA microarray	(176) (180, 189, 191)
MUC5AC	DNA microarray	(175, 179, 184, 189)
S100P	DNA microarray	(179, 180, 184, 189, 192, 193)
S100A11	DNA microarray	(179, 180, 184, 189)
SFN	DNA microarray	(179, 180, 184, 189)
SPARC	DNA microarray	(181, 184, 189, 193)
TFF2	DNA microarray	(179, 191)

1.3.4 Epigenetics of pancreatic ductal adenocarcinoma

Epigenetics is defined as heritable changes in gene expression without accompanying changes in DNA sequence. The main epigenetic mechanisms that may affect gene expression include DNA methylation, histone modification and microRNA (miRNA) expression.

1.3.4.1 DNA methylation

DNA methylation is the covalent binding of a methyl group (CH_3-) to cytosine residues, a process catalyzed and maintained by the DNA methyltransferases (DMNTs). Approximately 80% of PDAC overexpress dnmt1 protein (194). A major pattern of DNA methylation occurs in CpG islands, stretches of DNA with a high CG nucleotide content (> 50%), frequently located near transcriptional start sites of genes. Aberrant hypermethylation of promoter CpG islands is tightly associated with gene silencing and may be associated with loss of TSG function (195).

An increasing number of important genes undergo aberrant promoter CpG island hypermethylation in a subset of PDACs including CDKN2A (114). MLH1 undergoes DNA methylation in PDAC and is associated with microsatellite instability in medullary carcinomas (32). The CDH1 gene that encodes E-cadherin, is hypermethylated in a small proportion (196), while other targets that undergo methylation and subsequent gene silencing include RUNX3 (197) and SOCS-1 (198).

Hypomethylation can result in loss of regulation and promotion of gene and protein expression. S100A4 (199), CLDN4 and prostate stem cell antigen (PSCA) (200) are frequently hypomethylated genes overexpressed in PDAC cells.

1.3.5 MicroRNA expression abnormalities in PDAC

miRNAs are a class of single stranded, evolutionary conserved, noncoding RNA molecules, 19 to 25 nucleotides (nts) long that regulate gene expression by binding to sequences in the 3'untranslated region of an expressed mRNA (201). miRNAs are first transcribed into long primary miRNAs (Figure 1.3) (202). A Drosha RNase III endonuclease, in complex with the double-stranded RNA-binding domain protein DGCR8, cleaves the primary miRNA leaving a hairpin loop structure ~70 nt in length known as precursor miRNA. This is exported from

the nucleus to the cytoplasm by Exportin-5 (203). These small RNAs exert their functionality via sequence-specific regulation of post-transcriptional gene expression by targeting mRNAs for cleavage or translational repression (204). The RNA-induced silencing complex (RISC) is guided to the mRNA target site by the miRNA strand. Perfect or near-perfect complementarity binding to the target site can induce gene silencing via the RNA interference pathway (205); causing cleavage of the mRNA transcript and degradation of the target mRNA. Predominantly, however, the miRNA-mRNA interaction is imperfect, resulting in translational repression and subsequent reduction of steady state protein levels of targeted genes (206), meaning that each miRNA can regulate a broad set of targets.

1.3.5.1 MicroRNAs and cancer

Recent reports have evidenced a role for miRNAs in the regulation of crucial processes including cell proliferation, apoptosis, development, inflammation (207) and recently have been linked to cancer. Deletions, local amplifications and chromosomal break points in regions harboring miRNA sequences, suggest a direct role in many aspects of tumour biology, including oncogenesis, progression, metastasis and angiogenesis (201). Indeed more than 50% of miRNAs are localised within genomic regions associated with cancer or fragile sites.

Calin and co-workers originally showed that miR-15a and miR-16-1 are down-regulated or deleted in most patients with chronic lymphocytic leukemia. The gene coding for these two miRNAs is located at chromosome 13q14, a region deleted in 65% of cases (208). miRNAs influence various cancers with miR-21, miR-143 and miR-145 in colorectal (209), miR-221 in thyroid (210) and miR-21 in breast cancer (211). Many have been demonstrated to act either as TSGs or oncogenes according to the mRNA target and are proven to accelerate the oncogenic process (212). miRNAs themselves can act as TSGs when down-regulated e.g. miR-15a (213) or as oncogenes when overexpressed e.g. miR-21 (214).

1.3.5.2 Clinical applications of microRNAs in cancer

The central involvement of miRNAs in cancer development and progression suggests potential diagnostic and prognostic utility. miRNA profiling studies have differentiated between normal and tumour cells, between different tumour subtypes and proven utility of miRNAs for diagnosis (215-217). Notably, miRNA profiling of 217 targets has been demonstrated to classify cancer types more effectively than 16,000 mRNA probes (215). Furthermore, prognostic miRNA signatures have been reported in non-small cell lung cancer (NSCLC) (218) and chronic lymphocytic leukemia (216).

1.3.5.3 MicroRNA expression profiling in PDAC

Attempts to determine the role of miRNAs for pancreatic cancer diagnosis have focused on both individual miRNAs and miRNA expression signatures. Analysis suggests that PDAC

has a unique miRNA signature that could help differentiate pancreatic cancer from other tumours. Initial studies profiling a large number of tumour types did not achieve a pancreatic cancer specific signature (215, 217), but did identify that miR-21, miR-191 and miR-17-5p were significantly overexpressed. miR-216 has been identified as pancreas specific and is regularly down-regulated in PDAC compared to normal pancreatic tissue.

In order for miRNA expression data to be interpreted successfully and to be clinically relevant, it is vital to establish the profile of the specific tissues, in particular normal pancreas, CP and PDAC. Studies have succeeded in profiling miRNA expression of the three principal groups, however, expression profiles of normal pancreas could be further compartmentalised into acinar, islet, stromal and ductal tissue but as yet these data are not complete. Authors, focused solely on the miRNAome in PDAC, performed hierarchical clustering based on reverse-transcription polymerase chain reaction (RT-PCR) measured expression of 222 miRNA precursors in cancer, adjacent normal tissue and CP samples (219). They reported aberrant expression of > 100 miRNAs many differentially expressed in cancer. Localisation revealed that miR-221, miR-376 and miR-301 were expressed in tumour but not in stroma or normal ducts.

A study based on a 377 miRNA microarray format was used to investigate the PDAC miRNAome using PDAC-derived cell lines, normal pancreas, PDAC and CP specimens (220). They identified miR-216 and miR-217 over-expression and lack of miR-133 as being specific for pancreatic tissue, while PDAC specimens showed a significantly altered miRNA profile. Using a semi-quantitative RT-PCR index including miR-217 and miR-196a, normal pancreas, CP and PDAC tissue were differentiated, highlighting the diagnostic utility of miRNA profiling in pancreatic disease.

The results of these studies suggest that variability of individual miRNAs with tumour type makes the use of a single miRNA biomarker unrealistic. Therefore a combination will be a more successful method in PDAC detection and prognostication. A summary of the miRNAs so far established as yielding prognostic value in PDAC is presented in Table 1.5.

Table 1.5 MicroRNAs associated with prognosis in PDAC following resection

MiRNA	Cohort	Authors (Ref)
miR-21	Post-resection and metastatic disease Adjuvant therapy	Giovannetti et al (221) Hwang et al (222)
miR-155, miR-203, miR-210, miR-222	Post-resection	Greither et al (223)
miR-203	Post-resection	Ikenaga et al (224)
miR-196a-2, miR-219	Post-resection	Bloomston et al (225)
miR-200c	Post-resection	Yu J et al (226)

Figure 1.3 Illustrative overview of microRNA generation in pancreatic cancer

RNA polymerase II (Pol II) produces a 500-3000 nucleotide transcript, called the primary microRNA (miRNA) or Pri-miRNA that is then cropped to form a pre-miRNA hairpin by a multi-protein complex that includes DROSHA. This double-stranded hairpin structure is exported from the nucleus by RNA GTPase and exportin 5 (XPO5). Finally, the pre-miRNA is cleaved by DICER1 to produce two miRNA strands, a mature miRNA sequence, approximately 20nt in length and its short-lived complementary sequence, which is denoted miR. The thermodynamic stability of the miRNA duplex termini and the identity of the nucleotides in the 3' overhang determine which of the strands is incorporated into the RNA-inducing silencing complex (RISC). miRNAs in green have been shown to be down regulated in PDAC, while for those in red there is evidence to suggest they are up-regulated. Established targets for these miRNAs are shown opposite the controlling miRNA.*

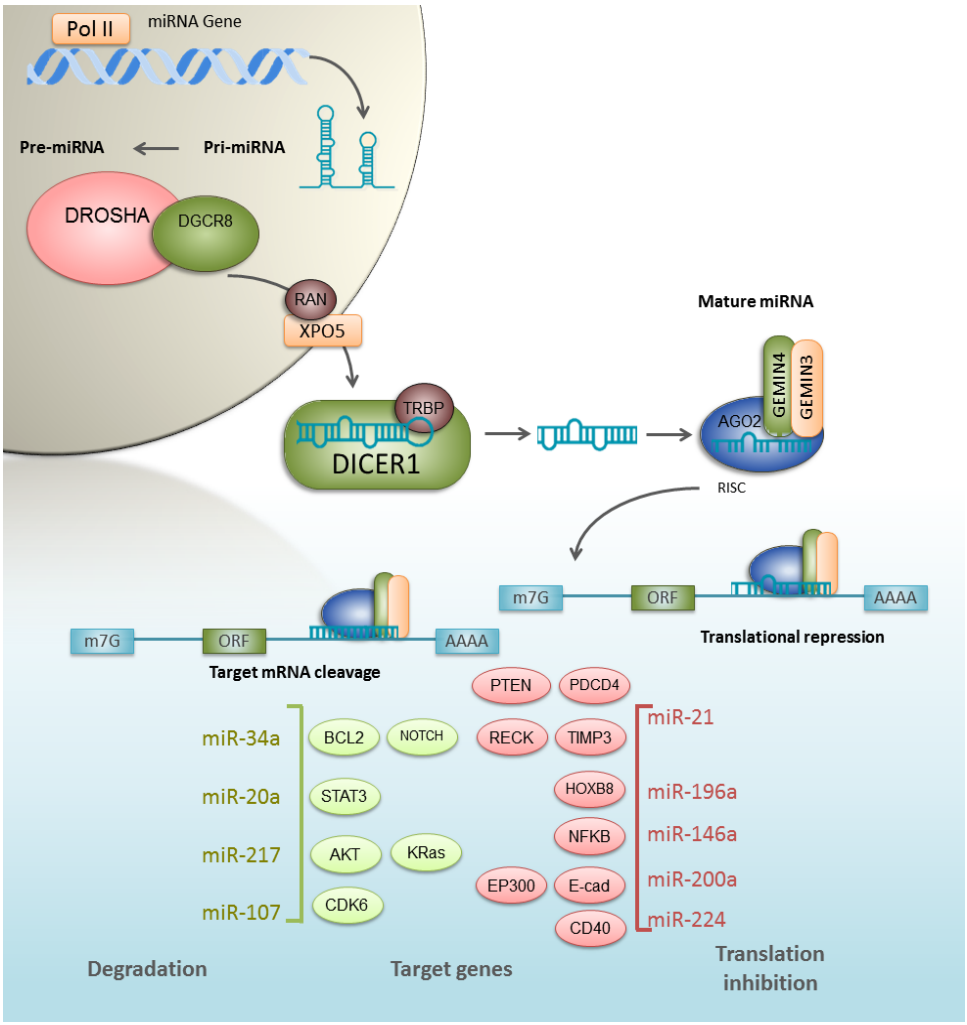

1.3.6 Chromosomal and cytogenetic aberrations in PDAC

In addition to mutations in molecular signalling cascades, chromosomal aberration has long been known to play a critical role in human cancer pathogenesis (227) and is another mechanism leading to gene dysregulation in PDAC. The identification of regions of genomic gains and losses has resulted in the discovery of novel oncogenes and TSGs (228).

PDAC cells show significant genomic instability, principally telomere abnormalities. Telomere shortening is encountered in virtually all precursor lesions and invasive pancreatic tumours (229). Telomerase, the gene that maintains telomere length, has low expression during early pancreatic tumourigenesis with prominent reactivation in invasive tumour. It is thought to restore genomic stability allowing effective tumour progression by preventing the accrual of lethal chromosomal damage (230). Chronologically, telomere shortening precedes loss of p53 function and it is possible that the chromosomal abnormality of short telomeres activates p53-mediated suppressor pathways. While its molecular basis is not clear there is evidence that mutation in genes controlling the kinetochore and centrosome formation and mitotic spindle checkpoint can lead to precursor lesions in PDAC (231).

Conventional chromosome analysis carried out on low passage cells derived from primary tumours or metastases, has provided important insight into common PDAC chromosomal abnormalities. The most commonly reported alterations have been chromosome copy number changes affecting chromosome number. Overall chromosome losses have been observed more frequently than gains by conventional cytogenetic techniques, the most common being chromosome 18 (30% of tumours), with frequent losses affecting chromosome 6 (44%), 22 (42%), 17 (56%) and 21 (42%) and extra copies of whole chromosomes 2, 7 and 20 (232).

1.3.6.1 Comparative genomic hybridisation

Comparative genomic hybridisation (CGH) identifies and maps DNA copy number alteration across the whole genome in a single hybridisation, without need for the sample to be mitotically active and without knowledge of the sample's genetic makeup. The chromosomal origin of these gains and losses of genetic material can be identified and mapped to specific chromosome bands. CGH has been widely used for the analysis of PDAC revealing chromosomal abnormalities in almost 100% of PDAC cell lines and in 67-100% of primary tumours. The slightly lower frequency of aberrations in primary tumours is partly explained by the presence of normal cell contamination so typical of PDAC (233).

The introduction of array-based CGH (aCGH) provided a high-resolution approach to detect copy number aberration (CNA), with the hybridisation targets being spotted DNA fragments, typically genomic bacterial artificial chromosome (BAC) clones, cDNA clones or oligonucleotides (234). An outline of the principles of aCGH is illustrated in Figure 2.3.

The resolution is dependent on the number of DNA fragments and their spacing along the genome. In addition to the higher resolution, the power of aCGH lies within the information available from each target sequence allowing access to multiple biological annotations along with chromosomal location.

1.3.6.2 Array comparative genomic hybridisation profiling in PDAC

To date, nine studies using aCGH technology for analysis of CNAs in PDAC have been published (235-243). The majority of these studies have focused on the analysis of pancreatic cancer cell lines, although primary tumours have been evaluated to a lesser extent, with similar concordance between cell lines and primary tumours (Table 1.6) (235, 240). As expected, the spectrum of gains and losses detected by aCGH is very similar to that observed by chromosomal CGH but with improved resolution of CNA boundaries.

Several amplifications events localised by aCGH correspond to known oncogene loci including KRAS (12p12.1), MYC (8q24) and AKT2 (19q13) (235-238, 242, 243). It is uncertain, however, if they are the real or sole target genes of these amplicons. The KRAS oncogene is known to be activated by point mutations rather than by gene amplifications.

The identification of recurrent chromosomal amplifications and deletions indicate that the current compendium of known genetic lesions represents a very limited collection of molecular mechanisms driving this disease. Studies have demonstrated that there are other possible target genes for the 12p12 amplification identifying as many as 20 potential targets for this region. Furthermore high-resolution mapping analyses have indicated that there are several independent amplicons at 12p, proximal and distal to the KRAS gene, suggesting that there might be several important genes that are activated in this region.

aCGH is also able to detect reliably homozygous and heterozygous deletions. In PDAC, regions showing copy number losses by aCGH correlate very well with chromosomal regions harbouring TSGs that are known to be altered in PDAC (235, 237, 238). Common homozygous deletions have been detected at the CDKN2A (9p21), SMAD4 (8q21) and the TP53 locus (17p31.1) (235, 237, 238) although these genes as well as others can be inactivated through various mechanisms e.g. epigenetic alterations that do not affect copy number, it is possible that regions of common loss identified by aCGH highlight additional TSGs important for PDAC pathogenesis.

Genome wide CNA analysis of PDAC has identified that SKAP2/SCAP2 is amplified, with amplification associated with increased expression of gene product and may have an important role in pancreatic tumourigenesis (244). A further approach has identified SEC11L3 as being deleted in the majority of PDACs and therefore potentially represents a TSG (239).

1.3.6.3 Clinical utility of arrayCGH in PDAC

Knowledge of CNAs can have immediate clinical use in diagnostics and potentially prognosis. Association of CNAs with prognosis has been found for a variety of tumour types, including prostate (245) and breast (246), however there is limited evidence for this in PDAC.

Table 1.6 PDAC aCGH studies reporting gene copy number changes

Study (Ref)	Array format	No. of samples	Gains	Losses
Aguirre et al, 2004 (235)	**cDNA**	**13 primaries**	5p15.13-15.33; 7p22.1-22.3; 7q21.11-32.2; 8p11.21-p12; 8q12.1-12.3; 8q21.3-24.3; 11q14.1-14.2; 17q12-23.2; 20p13-q13.33	4q34.1-35.2; 6q21-22.31; 8p12-23.3; 9p21.2-9p24.3; 17p11.1-13.3; 18q11.2-21.1; 18q22-23; 21p11.2-q11.2; 22q11.1-13.2
	14,160 clones	24 cell lines		
Bashyam et al, 2005 (237)	cDNA 39,632 clones	22 cell lines	6p21; 7q21; 11q13; 11q22; 12p11; 12p12; 14q24; 17q12; 19q13	6q35; 8p22; 8p23; 9p21; 18q21; 18q23; Xp
Gysin et al, 2005 (238)	BAC 2464 clones	25 cell lines	5p14.3-15.1; 8q24-24.2; 10p14; 11q13; 11q22; 12p11.2-12; 17q21.3; 20q11-qtel	3p14-p21; 6p24; 6q26; 8p22-23.2; 9p21 13q21-32; 16q23; 18q21.1; Xp22.3; Xq27
Heidenblad et al, 2004 (236)	BAC 3200 clones	16 cell lines	6p21-22; 7q21-31; 8p11-12; 8q23-24	9p21; 9p24; 9q32; 10p12; 10q22; 12q24
	cDNA 25,648 clones	15 cells lines	12p11-12; 18q11-12; 19q13.2	18q23
Holzmann et al, 2004 (240)	**cDNA 812 clones**	**6 primaries**	**1p22; 7p12; 7q21; 8q24; 11q12-q13**	
		13 cell lines	12p13; 12q13-15; 17q21	
Mahlamaki et al, 2002 (247)	cDNA 12,232 clones	13 cell lines	7q22; 11q13; 15q25; 17q21; 19p13.3; 19q13.1; 20q13.3; Xq28	
Nowak et al, 2005 (243)	BAC 5400 clones	9 cell lines	7p11.2-21.11; 7q31.32; 7q33	3p14; 4q31.3; 5q14.3; 6q24.3; 6q26; 8p23.1
		7 cell lines 17 xenografts	8q11.1-24; 11p13; 14q22.2; 20p12.2; 20q11.23-13.33; 20q13	9p21.3; 17p12; 18q21; 22q13.1

Studies in **bold** highlight where primary human tumours were analysed

1.3.7 Integrative genomics

As discussed, chromosomal instability is important in PDAC. Regions exhibiting CNA can affect expression of *cis*-localised TSGs and oncogenes. Several studies have integrated global patterns of gene expression and genomic data in cancer in an effort to identify alterations that are biologically relevant to tumourigenesis (248). While CNAs are structural changes, measuring the level of mRNA transcripts provides additional information on whether those changes have functional consequences. There have been initial reports of integrated genomic methods in PDAC, with limited relationship with patient prognosis. Furthermore, it may be that gene expression patterns are altered according to miRNA expression in human PDAC. There has been no such assessment performed in human PDAC at this time.

1.3.8 Hypotheses

Scope exists to improve the accuracy of the clinicopathological staging parameters and for the discovery of biomarkers that may add to existing prognostic criteria for PDAC, potentially resulting in the improved stratification of patient outcome. In the future this may provide the opportunity to modify treatment according to an improved characterisation of

PDAC allowing therapy to be targeted depending on the predicted outcome. From the appraisal of the literature a number of postulations are proposed that may improve the understanding of the clinical behavior of this challenging disease.

From review of the traditional pathological factors that influence prognosis, it is apparent that controversy exists on the issue of the frequency of resection margin involvement. The definition of an R0 margin varies and the perceived influence on prognosis is not universally accepted. It is hypothesised that resection margins are frequently involved and that not all involved margins have equal prognostic influence. The determination of resection margin involvement is an important issue as currently adjuvant chemotherapy allocation as part of randomised controlled trials is allocated according to R1 status. Individuals most likely to benefit from adjuvant therapy are those who have undergone a resection with no evidence of disease at the margins. Clearly in the context of investigating the influence of established and novel adjuvant therapies the issue of resection margin involvement following PD is an important one that merits further investigation.

Further to the issue of resection margin involvement, invasion into the peripancreatic fat, beyond the pancreas itself could potentially represent a more advanced process of disease. It is hypothesised that this pathological feature may influence survival and pattern of failure and warrants more detailed analysis. Potentially stratification of outcome according this factor may influence the targeting of adjuvant therapies.

Identification of biomarkers that can be assessed prior to treatment would be of particular value, not simply as prognostic markers but potentially as predictive tools in relation to treatment response. Despite investigations of numerous molecular pathways in PDAC for potential prognostic utility (249), inadequate study size and inadequate clinicopathological correlation has limited their worth. It is therefore proposed that assessment of established pathways integral to pancreatic cancer tumourigenesis at a protein level by means of IHC in a large resectional cohort might relate pathological features of disease to these aberrant pathways. It is hypothesised that by determining the prognostic capability of the best candidate protein markers from the literature in a large TMA cohort it will be possible to stratify outcome following resection of PDAC. Furthermore it may be possible to generate combinations of protein markers that describe subgroups of PDACs with variable prognosis.

Certainly detailed gene expression analysis of PDAC by microarray analysis has been undertaken, however only limited exploration of the relationship between gene expression patterns and clinicopathological factors exist. It is hypothesised that there is a potential for the development of novel gene sets or signatures in PDAC that describe pathological features, which could provide insight into the aggressive behaviour of this disease. Furthermore, it is proposed that a prognostic gene signature providing additional prognostic

information beyond traditional prognostic factors could be developed for PDAC, as has been generated for other cancer types. This could better characterise PDAC and allow stratification of outcome in addition to current pathological features.

Only limited miRNA profiling has so far been performed in human PDAC specimens. However, sufficient evidence exists for this class of molecule to possess an integral role in PDAC tumour biology, with a number of the established molecular aberrations previously discussed being impacted upon by alterations in the miRNAome. Furthermore, it is noted that minimal exploration of the relationship between miRNA expression patterns and clinicopathological factors exist. It is proposed that the investigation of a PDAC miRNA expression signature could provide additional prognostic information beyond traditional prognostic factors and stratify patient outcome following resection. Additionally, investigation of miRNA expression may provide insight into the established molecular signalling patterns.

To date nominal correlation between CNAs and human PDAC specimens have been performed, of which few have attempted to associate CNA with pathological features of the tumour or survival following resection. It is proposed that the CNAs identified by aCGH may associate with pathological features of pancreatic cancer and potentially with survival. Consequently, this may provide insight into the established molecular signalling patterns.

Finally, it is hypothesised that alterations in copy number that affect gene expression levels are potentially more likely to modify protein expression. The integration of gene expression data with copy number changes may allow those changes most likely to be causally implicated in PDAC tumour evolution to be identified. This has proven effective in various other types (250) but has not been undertaken in human PDAC studies previously. Similarly integration of mRNA expression patterns according to miRNA expression may provide insight into human PDAC biology.

1.4 Project aims and objectives

As described above, the identification and establishment of methods to better characterise PDAC so as improve stratification of outcome following resection is vital if there is to be progress in the management of this deadly disease. The aim of the present work was therefore to evaluate potential prognostic factors at various levels to better understand the clinical behaviour of PDAC. This included the investigation of candidate pathological and protein factors, in addition to a genome wide exploration of gene expression, miRNA expression and copy number aberrations within a large cohort of patients with pancreatic cancer. While it is hypothesised that this hierarchical approach will provide unique insight into the underlying tumour biology, the concept of stratification of therapy according to certain prognostic criteria brings clinical relevance to this work. This methodology may

result in improved stratification of patient survival beyond what is currently possible with conventional pathological criteria. Furthermore it may also identify novel biomarkers that have potential for application in the clinical management of PDAC.

Specifically, the objectives were to:

1) Determine whether rigorous pathological assessment of PDAC resection specimens, in particular of the frequency and site of resection margin involvement, could enhance patient stratification following resection for PDAC.
2) Determine whether the presence of peripancreatic fat invasion may enhance outcome prediction following resection for PDAC. Furthermore to investigate whether pathological factors including fat invasion are related with the site of tumour recurrence.
3) Validate the prognostic value of a number of previously studied protein biomarkers using IHC in a TMA cohort of PDAC patients so as improve patient outcome stratification following resection. Furthermore an attempt will be made to combine expression of these markers into a prognostic protein expression signature.
4) Identify microarray derived gene expression patterns using associated with PDAC and in particular gene expression profiles associated with clinicopathological factors focusing upon survival following resection in a fresh frozen tissue cohort. An attempt will be made to validate discovered prognostic gene expression signature within independent microarray data sets. Components of any prognostic gene expression signature will be validated by IHC in the larger TMA cohort.
5) Define a microarray derived PDAC miRNA expression profile and investigate the association of miRNA expression with clinicopathological factors and survival following resection to improve patient outcome stratification. Furthermore an attempt will be made to validate prognostic miRNA targets using PCR in an independent cohort of patients with PDAC.
6) Identify using aCGH genomic CNAs associated with PDAC and clinicopathological factors in fresh frozen tissue cohort. Furthermore the intention is to investigate whether individual CNAs in addition to the frequency of CNAs in the tumour are capable of stratifying patient outcome following resection.
7) Undertake a combined genomic integration approach to the study of PDAC by integrating gene expression, aCGH, as well as IHC analysis of protein expression in PDAC TMAs to identify genes for which mRNA expression is correlated with copy number status. In particular there will be a focus upon the identification of potential key regulators underlying PDAC tumourigenesis. A further aim is to investigate the downstream gene targets of a selection of miRNAs in PDAC.

2 Methods and Materials

2.1 Methods

2.1.1 Investigation of pathological prognostic factors

2.1.1.1 Pancreaticoduodenectomy cohort

All patients included in this thesis underwent surgery in the West of Scotland Pancreatic Unit, GRI, over a seventeen-year period (1st January 1992 to 31st December 2009). All patients underwent either classical or pylorus-preserving PD, performed by a team of four surgeons. Surgical death was defined as in-hospital mortality. This analysis was limited to patients undergoing PD for PDAC with curative intent. Patients undergoing a palliative bypass, who were unsuitable for a curative procedure, were excluded. The distribution of PDAC, ampullary, duodenal and cholangiocarcinoma resected over the study period is illustrated in Figure 2.1A and the inclusion of PDAC patients in each chapter is shown in Figure 2.1B with clinicopathological details presented in Table 2.1.

The decision to perform resection was made by a multi-disciplinary team including surgeons, oncologists, radiologists and pathologists. The criteria for resectability were: a) CT evidence of localised tumour in the head of the pancreas; b) no greater than 180° circumferential involvement of SMV; c) no overt arterial involvement (251).

2.1.1.2 Operative procedure

The mobilisation phase of a classical PD involves the anterior, duodenal and posterior aspects of the HOP being fully mobilised back to the midline, leaving the medial lymphovascular structures intact (Figure 3.1A, B). The transection phase requires division of the jejunum, proximal jejunal mesentery, bile duct, pancreas, mesopancreas (medial transection margin) and distal stomach/ duodenum (+/- vein resection) to allow resection completion. Transection margin frozen section analysis is performed to establish the presence of residual disease, with further pancreatic body resection undertaken if required. The majority (95%) of patients had classical PD with reconstruction by a four layer, duct to mucosa pancreaticojejunostomy.

The extent of resection remained constant during study, although the order in which individual steps were undertaken would vary, to facilitate early identification of locoregional inoperability. Uncinate process lesions or those sited medially would undergo an “artery first” exploration to ensure absence of arterial involvement, whereas lesions at the neck undergo an early dissection of the hepatico-duodenal ligament to ensure proximal clearance. Short segment (< 180°) venous involvement was managed by en-block resection and primary anastomosis. Arterial involvement was considered a contraindication to resection.

2.1.1.3 Adjuvant therapy protocol

Post-operatively, all patients were considered for adjuvant therapy. In the earlier years of the study, patients were considered for ESPAC-1 randomisation; in the later years, they were considered for ESPAC-3 randomisation. There is a range of five treatment options across both

these studies, including 5-FU with folinic acid, gemcitabine, radiotherapy, 5-FU with radiotherapy and no therapy. Follow-up comprised a standardised protocol of out-patient reviews. CT scans were not performed routinely during follow-up but only when local recurrence or metastatic disease was suspected. In patients with CT confirmed recurrent disease, the patient was considered for chemotherapy if oncologically naïve, or for adjuvant chemotherapy re-challenge. Neo-adjuvant therapy was not used during the study period.

2.1.1.4 Pathology assessment

The pathology reports from all patients undergoing PD for PDAC between 1992 and 2009 were reviewed. During the study period, the resection specimens were assessed by three senior pathologists (AKF, KO and JJG). AKF has led the local standardisation of "taking in" procedures and was a co-author of the RCPath National Pancreatic specimen guidelines (95). The gross and microscopic examination of PD specimens incorporated these guidelines and has done so since 1996. Prior to this time resection margins were not routinely inked.

Pathological assessment began with the four pancreatic margins (pancreatic transection, medial, posterior and anterior surface) being identified and inked (Figure 3.1C, D). The medial margin describes a column running down from, and as wide as, the pancreatic transection margin and containing the beds of the mesenteric vessels. The anterior margin comprises the pancreatic surface lying in front of the medial margin. The posterior margin comprises the smooth pancreatic surface lying behind the medial margin. Thereafter three cuts were made from the luminal aspect of the second part of the duodenum into the HOP, in a transverse plane and the specimen fixed for 24–48 hours. After fixation, the specimen was again examined, sectioned and characterised, recording tumour location, size and proximity to margins. Blocks were taken for microscopic examination as follows: multiple tumour blocks; adjacent circumferential margin(s); other circumferential margin(s); bile duct, gastric or duodenal and jejunal resection margins; ampulla if near tumour; and macroscopically normal pancreas, gallbladder and lymph nodes. Microscopic assessment and reporting included: maximum tumour diameter and extent and location of local spread; tumour grade; perineural and venous invasion; total lymph nodes examined and number positive. TNM staging was performed in accordance with the UICC/AJCC staging system (252) which corresponds to the RCPath Guidelines (95). Tumour grade was categorised into high for poorly differentiated tumours and low for moderately and well-differentiated tumours (83). The original H&E slides for the entire cohort were reassessed (NBJ) under the supervision of a consultant pathologist, with the specific aim of identification of resection margin involvement and peripancreatic fat invasion. Where there was ambiguity new sections were cut and stained.

As the standardised protocol driven studies (93, 96) assessed R1 status according to the RCPath criteria this methodology has been adopted in this work. The guidelines define

margin positivity as the presence of tumour at or ≤ 1 mm of a margin when assessed by microscopy of H&E stained slides (95). Marginal status was further categorised as: direct extension when directly infiltrating tumour was present at or ≤ 1 mm from a resection margin; or loco-regional extension when there was perineural, venous or lymphatic infiltration or tumour within a lymph node ≤ 1 mm from a margin. If major vessel resection was required to achieve a macroscopically negative resection the vessel margin is similarly assessed. To facilitate comparison with previous data, a parallel analysis of resection margin status was been performed according to the UICC/AJCC criteria, in which margins are regarded as positive only when tumour was present at the margin surface.

2.1.1.5 Site of recurrence

The first site/ sites of disease recurrence were classified as liver metastases or recurrence other than liver metastases. The latter included local recurrence (pancreatic bed and mesentery root), regional recurrence (soft tissues or lymph nodes beyond pancreatic bed or peritoneal cavity) or other distant recurrence (lungs or other distant organs). Radiographic findings consistent with recurrent disease were considered adequate proof, while only occasionally was tissue evidence obtained. Only the first site at presentation with recurrence was considered. Data regarding recurrence site were collated prospectively from the late 1990's.

2.1.1.6 Statistical analysis of clinicopathological data

The relationships between categorical variables were analysed using the Mantel–Haenszel (χ^2) test. The Mann-Whitney U test was used to compare continuous variables. The principal outcome measure was length of overall survival as measured from time of the original surgery. Length of survival following surgery and cause of death were obtained from prospectively maintained database and validated using the NHS Scotland Information Services Department (http://www.isdscotland.org). Kaplan-Meier survival analysis was used to analyse the overall survival from time of surgery with a Log-rank test to compare curves. Patients alive at time of follow-up point were censored. The last follow-up period for patients still alive was October 2010. A Cox proportional-hazards model was used for multivariate analysis to adjust for competing risk factors, and the hazard ratio (HR) with 95% confidence intervals (CIs) reported as an estimate of the risk of disease-specific death. Only variables found to be significant on univariate analysis at $p < 0.10$ were included in multivariate analysis in a backwards-stepwise fashion. Statistical significance was set at $p \leq 0.05$.

2.1.2 Investigation of immunohistochemical prognostic factors

2.1.2.1 TMA construction

Conventional IHC used whole tissue sections and therefore was reagent and sample intensive. More recently, TMA technology was developed as a high-throughput platform for gene validation enabling integration of DNA, RNA and protein expression, easing correlation of

targets with tumour and clinicopathological data. Appropriate H&E stained sections were reviewed. Multiple representative areas of tumour as well as normal pancreatic ducts, islets, duodenum and bile duct were marked on the slides. Due to the heterogeneous nature of PDAC, six cores were felt to be necessary to provide representation of the overall tumour. Areas were selected on the basis of: first, high tumour content (minimal inclusion of contaminants e.g. stromal tissue); second, definite invasive PDAC (avoiding PanIN) and third, tumour size (sufficient for 18 x 0.6 mm cores, leaving sufficient residual tissue).

2.1.2.2 Array design and construction

Prior to construction, the layout of the array was designed to incorporate: number of tumour cores (six) and normal cores (two) per patient; control tissue; ability to differentiate and orientate each TMA, and minimum distance between block to maximise space (Appendix Figure 11.1). Array outlines are traditionally asymmetrical to allow sample identification and ideally cores should be randomised and interspersed throughout the block

Arrays were constructed in a recipient block of Paraplast wax using a manual tissue arrayer. A hollow needle was used to remove a wax core at least 5.7 mm from the recipient block edges. A core of tumour was then removed from the first donor block, using its corresponding marked H&E slide as a guide. The tumour core was deposited in the recipient block, whose position was then changed using digital micrometres. A minimum distance of 0.8 mm was left between cores. This process was repeated, positioning, a total of 215, 0.6 mm cores (6 x 215 = 1290 cores), across 7 easily differentiated arrays, each in triplicate. A series of 10 control tissues (breast, testis, pancreatic ducts, pancreatic acinar tissue, islets, bile duct, duodenum, liver and prostate) were arrayed in duplicate in each array. Arrays were placed in a 40°C incubator for 15 minutes and followed by cooling prior to sectioning. A practice TMA (25 cores) was also created for antibody optimisation.

2.1.2.2.1 Sectioning

Arrays were sectioned using a tape-transfer system and a Leitz 1512 microtome. Prior to sectioning, tissue blocks were cooled to -10°C (Tissue Tec© cooler). An adhesive tape window was rolled onto the array surface. The microtome blade was positioned under one window edge and 5 μm sections were cut. The cut section was then fixed onto an adhesive slide by UV curing for 35 seconds. TPC solvent then released the tape window from the adhered section. Finally slides were baked at 80°C for 5 minutes and stored at 4°C.

2.1.2.2.2 Haematoxylin & eosin staining

Sections, de-waxed in Histoclear and taken through graded alcohol, were immersed in haematoxylin (4 minutes) then rinsed in water. Following brief immersion in acid alcohol, slides were placed in Scott's tap water for 1 minute, rinsed in water and then placed in eosin Y for 30 seconds. Sections were dehydrated through graded alcohol and Histoclear.

2.1.2.3 Immunohistochemistry

For the IHC protocol FFPE sections were dewaxed in xylene for 20 minutes and rehydrated through intermediate alcohols. Antigen retrieval was necessary in 15 cases, outlined below. Protocols were optimised using FFPE sections then applied to practice PDAC TMAs and then the final TMA sections. (Additional IHC was kindly performed by a pathology technician, ID). Sections were stained in a DAKO Autostainer as follows: firstly incubated in goat serum blocker for 20 minutes, then primary antibody for 30 minutes. Following washing in TBS/Tween, endogenous peroxidases were blocked in 0.3% hydrogen peroxidase for 5 minutes, then again washed in TBS/Tween. Detection was by Envision ChemMate for 30 minutes, followed by visualisation with 3,3-diaminobenzidine for 10 minutes and enhanced with copper sulphate. Antibody diluent was used for the negative controls. When enzyme digestion pre-treatment was required slides were digested in Tris buffer containing 0.1% Trypsin and 0.1% calcium chloride for 25 minutes at 37°C. When microwave pressure cooker pre-treatment was necessary, slides were immersed in boiling dH_20 containing 0.55g EDTA and 0.87% Tris base. Slides were heated at full pressure for 5 minutes then cooled.

2.1.2.3.1 Tissue microarray and image capture and archiving

Following staining of TMA sections, the slides were digitally captured, stored and archived by CO. The Slidepath Digital Image Hub (http://ld.dih.slidepath.com/login.php) was used as a cloud based digital microscope to visualise and score the TMAs. Scores were linked via a unique identifier to the tumour specimen allowing integration within SPSS.

2.1.2.3.2 TMA assay quantification - modified histoscore

The default method for analyses of TMAs has been by trained visual inspectors, (pathologist), using a semi-quantitative ordinal scoring system. This considers three factors: percentage of positive staining cells, staining intensity and percentage of core occupied by tumour. The troublesome feature of visual assessment, however, is the semi-quantitative nature, which reduces continuous biomarker expression to ordinal scaling. Scoring of the IHC was performed in this thesis using a weighted histoscore. When scoring each core, the investigator multiplies the proportion of cells staining by intensity of staining to give an overall histoscore out of 300 for each cell compartment (membrane, cytoplasm and nucleus). The proportion of cells staining is given as a percentage and the intensity is based upon a 0 - 3 scale, where 0 is nil, 1 is weak, 2 is moderate and 3 is strong staining. The total score out of 300 is achieved by adding the following: (0 x % not staining) + (1 x % weakly staining) + (2 x % moderately staining) + (3 x % strongly staining). For example, a section with 50% of tumour staining with an intensity of 1; 25% staining with intensity of 2; and 25% staining with an intensity of 3 would have a total histoscore of: (50 x 1) + (25 x 2) + (25 x 3) = 175.

All of the antibodies were scored by NBJ and double scored for the most part by the pathologist (KO) along with other adequately trained members of the research team (MM). Scoring consistency confirmed using the intra-class correlation coefficient (ICCC). If the histoscore varied by a difference of 50 or greater for any score then the two observers looked at the core again and came to an agreement about the appropriate score.

2.1.2.3.3 IHC evaluation

Semiquantitative analysis of protein expression was performed for the panel of putative prognostic markers using the Histoscore method. The correlations between all pairwise combinations of the studied putative prognostic markers in all specimens including: Lkb1, p21, cyclin D1, β-catenin, E-cadherin, COX-2, Bcl-2, pAkt, Ki67, SMAD4, GSK3β, TGFβ1 and p53 were evaluated by Spearman's Correlation Coefficient analysis. Measures of association were obtained between the prognostic markers and the clinicopathological factors.

2.1.2.3.4 Cutoff point determination for survival analysis

The cohort was dichotomised, divided into tertiles or quartiles according to the histoscores for each putative prognostic marker following which Kaplan-Meier analysis and Cox proportional-hazards modeling was executed. For Lkb1, p21, GSK3β and pAkt the cohort was divided into quartiles, with histoscore for the lower quartile corresponding to 100, 40, 20 and 100 respectively. For β-catenin, E-cadherin, Bcl-2, cyclin D1, TGFβ1 and COX-2 tertiles were determined and either the three groups were compared or the low and middle group/ middle and high group were compared with the remaining group. For p53 and SMAD4 absence or < 5% of tumour cells showing expression was set as the lower limit of expression as had previously been used in the literature, this corresponded to a histoscore of less than 15 that was used to distinguish high from low expression. Table 5.2 contains cut-offs used for each marker and justifying evidence for each.

2.1.2.3.5 Hierarchical clustering

IHC results were combined to create a multi-marker descriptor. The patients were clustered based on IHC expression of markers as a continuous variable. Hierarchical clustering of target protein expression using the average-linkage clustering algorithm was performed using the Cluster/Treeview software package (253). This was undertaken for all patients with IHC results available (119 patients) following log transformation to normalise the semi-quantitative histoscore results for each target.

2.1.3 Methods for genomic profiling in PDAC

2.1.3.1 RNA extraction protocol (TRIzol®)

Following bench and equipment cleansing with RNase Zap, macrodissected samples were homogenised in two stages. First appropriately sized (50 mg) frozen samples (-80°C) were

broken down in liquid N_2 using a pestle and mortar. These small fragments were added to 900 µL of TRIzol® in a MagNAlyser tube and left at room temperature for 5 minutes. Tubes were homogenated in a MagNAlyser for 30 seconds (6000 rpm) and left for 10 minutes.

200 µL of chloroform was added per mL of TRIzol®, tubes were shaken for 30 seconds then incubated for 10 minutes at room temperature. Samples were centrifuged in a Beckman centrifuge for 15 minutes at 13200 rpm (4°C). The clear top layer (aqueous) was removed and transferred to 1.5 mL eppendorf tube (contains RNA), to which 500 µL of isopropanol was added and vortexed for 10 seconds. Tubes were incubated (20°C) for 5 minutes then centrifuged for 10 minutes at 13200 rpm (4°C), causing RNA pellet precipitation. The tubes were emptied and excess liquid blotted. A further 400 µL of 75% ethanol was added to the pellet and gently shaken. The tubes were again spun for 10 minutes and the supernatant removed. The wash step and blotting were repeated and the samples left to dry for 5 minutes. The RNA was dissolved and re-suspended in 50 µL RNase free H_20 and stored at -80°C.

RNA samples contaminated with genomic DNA were treated with DNA-free (Ambion, Huntingdon, UK). RNA samples were incubated with 0.1 volume 10xDNAse buffer and 1 µL (2U) DNase at 37°C for 30 minutes. DNase was inactivated with 5 µL inactivation agent, which was then removed by centrifugation at 12000 rpm.

2.1.3.2 DNA extraction protocol

DNA extraction was performed in two stages. Initially the digestion step required 360 µL of Qiagen buffer ATL to be added to the 50 mg tumour sample. This was vortexed, 40 µL of proteinase K added and incubated overnight in a thermomixer at 55°C (450 rpm). The digested sample was then transferred into a fresh tube and placed in a 70°C heat block to inactivate the proteinase K. Samples were cooled to room temperature and briefly centrifuged (6,000 rpm). 8 µL of RNase A (100 mg/mL), was added then incubated for 2 minutes. The samples were centrifuged and 400 µL of Buffer AL added, mixed thoroughly and incubated in a circulating water bath. 440 µL of 100% ethanol was then added and vortexed. Samples were then centrifuged for 30 seconds. The sample mixture was split between two DNeasy Mini spin columns (660 µL each) then centrifuged for 1 minute. 500 µL AW1 Buffer was added and centrifuged for 1 minute. The DNeasy Mini spin columns were placed in fresh collection tubes. 500 µL of 80% ethanol was added to each column and centrifuged for 3 minutes (20,000 rpm) until dry. For DNA elution, 50 µL water added directly to each column, left to stand for 1 minute and centrifuged.

2.1.3.3 Nucleic acid quality assessment and quantification

RNA quantification and quality assessment was performed using the RNA 6000 Nano assay with the Agilent 2100 Bioanalyser standard protocol. 400 µL gel matrix was mixed with 4 µL sample buffer. 9 µL gel-dye mix was applied to the appropriate well in the RNA Nano

LabChip and pressure applied for 30 seconds, ensuring all capillaries were filled with gel. An additional 9 µL gel dye mix, 5 µL sample buffer and 1 µL RNA 6000 ladder were applied to appropriate wells. 1 µL sample buffer and sample were loaded to sample wells, the chip vortexed for 1 minute then run on the Agilent Bioanalyser. Samples with a RNA integrity number (RIN) > 7.0 were deemed suitable for downstream analysis. Quantification was performed using a NanoDrop ND-1000 UV-VIS Spectrophotometer measuring optical density (OD) at wavelengths of 230, 260 and 280 nm. The recorded values were:

- Cyanine 3 (Cy3)/ Cyanine 5 (Cy5) dye concentration (pmol/µL)
- RNA/DNA absorbance ratio (260 nm/280 nm)
- RNA/DNA concentration (ng/µL)

Sample purity was indicated by an OD_{260} nm/OD_{280} nm ratio reading of approximately 1.8 for DNA and 2.0 for RNA. For DNA a secondary measurement of nucleic acid purity is provided by the OD_{260} nm/OD_{230} nm ratio; a value < 1.8–2.2 suggests contamination.

2.1.4 Microarray experimentation

2.1.4.1 Gene expression microarray methodology

A workflow outlining the protocol for gene expression microarray analysis is shown in Figure 2.2A. Agilent 44K whole genome microarrays were used to assess gene expression. Figure 2.3 outlines the principles underlying microarray methods.

2.1.4.2 Preparation of labelling reaction

One colour microarray analysis required 1000 ng of total RNA to be added to a 1.5 mL microcentrifuge tube in an appropriate volume of nuclease free water to bring the combined volume to 11.5 µL. 1.2 µL of T7 promoter primer was added followed by 5 µL of diluted Spike-In mix. The primer and the template were denatured at 65°C for 10 minutes, followed by cooling on ice for 5 minutes. 8.5 µL of cDNA Master Mix was added to each sample tube. Samples were incubated in a 40°C water bath for 2 hours, transferred to a 65°C water bath for 15 minutes, then ice. Tumour RNA samples were then labelled with Cy3-CTP. Finally 60 µL of Transcription Master Mix were added to each sample and incubated at 40°C for 2 hours.

2.1.4.3 Purification of the labelled/amplified RNA

Purification of the labelled/amplified RNA required the addition of 20 µL of nuclease-free water to the cRNA sample, followed by 350 µL of Buffer RLT. 250 µL of ethanol (96%-100% purity) was added and mixed thoroughly. 700 µL of the cRNA sample was transferred to an RNeasy mini column in a 2 mL collection tube and centrifuged at 4°C for 30 seconds (13,000 rpm). The RNeasy column was transferred to a new tube, 500 µL of buffer RPE added and centrifuged again. A further 500 µL of buffer RPE was added to the column followed by centrifugation at 4°C for 60 seconds (13,000 rpm). The cleaned cRNA sample

was eluted by transferring the RNeasy column to a new 1.5 mL tube with the addition of 30 µL RNase-free water onto the filter membrane for 60 seconds, then centrifuging at 4°C for 30 seconds (13,000 rpm). The cRNA flow-through was incubated on ice.

2.1.4.4 Quantification of RNA

See section 2.1.3.3. Yield and specific activity of each reaction were determined as follows:

A) cRNA (ng/ µL) to determine the µg cRNA yield as follows: (*Concentration of cRNA*) x 30 µL (*elution volume*)/ 1000 = µg of cRNA.

B) cRNA (ng/ µL) and Cy3 (pmol/µL) to determine the specific activity as follows: (*Concentration of Cy3*)/ (*Concentration of cRNA*) x 1000 = pmol Cy3 per µg cRNA.

If yield was < 1.65 µg and the specific activity is < 9.0 pmol Cy3 per µg cRNA then the hybridisation step was not performed and instead cRNA preparation was repeated.

2.1.4.5 Preparation of samples for hybridisation

Prior to hybridisation 1.65 µg Cy3-labeled, amplified cRNA, 6 µL 10x Blocking agent, 1.2 µL 25x fragmentation buffer were combined and brought up to 30 µL with DEPC water and equilibrated to 60°C. To fragment RNA the mixture was incubated at 60°C for 30 minutes. 30 µL 2x GEx Hybridisation Buffer HI-RPM was added to the fragmentation mix at the appropriate volume to stop the reaction and mixed with care to avoid bubble formation. The mixture was then spun (13,000 rpm) for 1 minute and loaded onto the hybridisation chamber.

2.1.4.6 Hybridisation assembly for gene expression

100 µL of hybridisation sample mixture was dispensed onto the gasket well held in the SureHyb chamber base in a “drag and dispense” manner. A microarray slide was placed “active side” down onto the gasket slide, so the numeric barcode side is facing up and “Agilent” labeled barcode is facing down. The chamber cover was clamped onto both pieces and the chamber placed in the hybridisation oven (65°C) rotating at 15 rpm for 17 hours.

2.1.4.7 Microarray washing

During the post-hybridisation period, prior to washing the array slides were kept in the dark. The microarray slides were disassembled from the hybridisation chambers in a staining dish #1 (Gene Expression Wash Buffer 1 - 20°C), transferred to dish #2 (Gene Expression Wash Buffer 1 - 20°C) for 5 minutes then transferred to dish #3 (Gene Expression Wash Buffer 2 - 37°C on a warming plate) for 1 minute for a final wash step. Care was taken when removing the slides from the wash solution to ensure that no streaking and adequate drying. Slides were scanned immediately to minimise impact of oxidants on signal intensities.

2.1.4.8 MiRNA microarray methodology

Total RNA extraction methods differ in numerous ways and impact substantially on yield, inclusion of small RNAs, total RNA extraction and quantification of total RNA. It is therefore vital that uniform extraction method is used to obtain consistent miRNA profiles. miRNA

expression profiling was performed using Agilent's Human miRNA Microarrays (Version 2.0, based on Sanger miRBase version 10.1), carrying 723 human miRNAs (http://microrna.sanger.ac.uk). The workflow followed is shown in Figure 2.2C

2.1.4.9 MiRNA labelling reaction, ligation and purification

The initial step involved dephosphorylation of total RNA. The sample was diluted to 25 ng/ µL with 1xTE pH 7.5. To 4 µL of this sample, 3 µL of Calf Intestine Alkaline Phosphatase was added. Dephosphorylation was initiated by incubation at 37°C. 5 µL of DMSO was added followed by incubation in 100°C heat block for 5 minutes, then ice to halt the reaction. The ligation reaction was initiated by adding 8.0 µL of T4 RNA ligase master mix which comprised 10x T4 RNA ligase buffer (2.0 µL), dH_20 (1.0 µL), pCp-Cy3 (3.0 µL) and Ambion T4 RNA ligase (5U/ µL), bringing the reaction to 20 µL and incubated at 16°C for 2 hours. The sample was made up to 50 µL with 1xTE pH 7.5 buffer. To desalt the samples this volume was added to a Micro Bio-spin 6 column and eluted by centrifuging for 4 minutes.

2.1.4.10 Hybridisation, hybridisation assembly and washing steps

The 50 µL Cy3-labelled samples were dried with a speed-vac at 45°C, resuspended in 18 µL of RNase free water and 4.5 µL of 10xGE blocking agent. 22.5 µL of hiRM hybridisation buffer was added to each sample, with incubation at 100°C for 5 minutes followed by ice. The slide gasket arrangement was performed as in 2.1.4.6 however with 45 µL of hybridisation sample mixture and with the oven set at 20 rpm (55°C) for 20 hours incubation. miRNA microarrays washing was performed as for Gene Expression microarrays (2.4.6.7).

2.1.4.11 ArrayCGH methodology

The aCGH (244K Agilent array) protocol was performed according to Figure 2.2B workflow.

2.1.4.12 Restriction digestion of amplified gDNA

3.0 µg of genomic DNA was brought up to a final volume of 20.2 µL with DEPC water for both samples and controls. The aCGH procedure was initiated with the preparation of the Digestion Master Mix requiring per reaction 2 µL of DEPC water, 2.6 µL of 10x Buffer C, 0.2 µL BSA, 0.5 µL Alu I and 0.5 µL Rsa I. 5.8 µL of Digestion Master Mix was added to each tube and incubated at 37°C for 2 hours, then a heat block at 65°C for 20 minutes then to ice.

2.1.4.13 Fluorescent labeling of genomic DNA

Specimen samples required comparison with gender-matched reference DNA (pooled individuals). Specimens were labeled with Cy3 and reference DNA with Cy5. The 5 µL of Random Primers (Agilent Genomic DNA Labeling Kit PLUS) were added to each reaction tube containing 24 µL of digested gDNA. The sample tubes were transferred to a heat block at 95°C for 3 minutes and to ice for 5 minutes. The Labeling Master Mix including 10 µL 5x Buffer, 5 µL 10x dNTP, 4 µL of Cy3-dUTP/ Cy5-dUTP as appropriate (Reference Cy3, Tumour Cy5), 1 µL Exo-Klenow fragment with 21 µL of master mix added to each reaction

tube containing the gDNA and incubated at 37°C for 2 hours. Samples were placed on a heat block at 65°C for 10 minutes to inactivate the enzyme before chilling on ice.

2.1.4.14 Clean-up of labelled genomic DNA and preparation for hybridisation

To clean up the genomic DNA 430 µL of 1X TE (pH 8.0) was added to each reaction tube and the contents transferred to a Microcon YM-30 filter in a 1.5 mL microfuge tube. This was centrifuged for 10 minutes at 8,000 rpm at 20°C. A further 480 µL of 1X TE (pH 8.0) was added to each filter and centrifuged again. The purified sample was collected into fresh 1.5 mL microfuge tube following a 1 minute spin. Each sample volume was measured: if the volume > 80.5 µL, the sample was returned to its filter, spun again until volume was ≤ 80.5 µL. All sample volumes were then standardised with 1X TE (pH 8.0) to 80.5 µL. The yield and specific activity was then determined (2.1.3.3). The Cy5-labeled sample (tumour) and Cy3-labeled sample (reference DNA) were combined for a total mixture volume of 158 µL.

To the complementary labeled gDNA 50 µL Cot-1 DNA, 52 µL 10x blocking agent and 260 µL 2x hybridisation buffer, were added, centrifuged, incubated at 95°C for 3 minutes and transferred to a 37°C water bath for 30 minutes. Human Cot-1 DNA is essential to block repetitive sequences in the human genome. Tubes were spun for 1 minute at 17,900 rpm.

2.1.4.15 Hybridisation assembly and aCGH microarray washing

Hybridisation assembly was performed as in 2.1.4.6 however; hybridisation sample volume was 490 µL with the oven set at 15 rpm (65°C) for 17 hours incubation. The microarray slides were disassembled in dish #1 (Oligo aCGH Wash Buffer 1 at 20°C), then transferred to dish #2 (Oligo aCGH Wash Buffer 1 at 20°C) for 5 minutes before finally being transferred to dish #3 (Oligo aCGH Wash Buffer 2 at 37°C) for 1 minute for a final wash step and then scanned.

2.1.5 Microarray image processing

2.1.5.1 Microarray scanning and image acquisition and feature extraction

The fluorescent intensity data were collected from hybridised array slides by scanning them on the Agilent G2505B Microarray Scanner. Recommended scan settings were used for the Feature extraction software (v9.5, Agilent). Target probe location and identification details were then imported into the software, which provided a replicate spot average value for each probe. Absent or poor quality spots were identified on the screen array image and flagged. Abnormal spots occur either when flecks of dust interfere, in relation to problematic array construction, or with a hybridisation (bubble not rotating), or wash artefact. These were excluded from subsequent data analysis. Quality control metrics allowed poor quality hybridisations to be identified and excluded from downstream analysis.

2.1.6 Microarray data analysis

Since the advent of global expression profiling technologies a wealth of studies have been published reporting their application to biology, with particular focus on cancer. Although

there is currently no 'gold standard' solution for analysis and interpretation of expression data, there are a number of commonly used techniques and important principles.

2.1.6.1 Gene expression microarray data

Gene expression analysis was performed using the publically available BRB-ArrayTools software package. Array data generated from feature extraction were uploaded as .txt file using the appropriate filter (one colour Agilent 44K microarray). An excel file was created containing expression data and flagged (outlier probes). Gene expression probes annotation enrichment of the probe list was performed to include Gene Symbol and Refseq identifiers. Chromosomal probe position annotation data was also included at this point.

2.1.6.2 Normalisation and filtering

After excluding negative values with hybridisation intensity below background, normalisation was performed by using normalisation to the median array as reference. Genes showing minimal variation across the arrays were excluded from the analysis. Genes whose expression differed by at least 1.5 fold from the median in at least 20% of the arrays were retained.

2.1.6.3 Identification of differentially expressed genes

To identify differentially expressed genes between two groups, the class comparison analysis was performed computing a t-test separately for each gene using the normalised log-intensities for one-colour arrays. Class prediction algorithms were also used to identify genes best describing subgroups. Visualisation of differentially expressed genes was performed using multidimensional scaling methods.

2.1.6.4 Gene set comparison

The gene set comparison tool analyses pre-defined gene sets for differential expression among pre-defined classes. The pre-defined gene sets were based on Gene Ontology (GO) categories, BioCarta and Kyoto Encyclopedia of Genes and Genomes (KEGG) pathways, protein domains, transcription factor targets, miRNA targets and the Broad Institute's Molecular Signature Database gene set collections. The evaluation of which GO categories are differentially expressed among phenotype classes was performed using a functional class scoring analysis (254). This is potentially a more powerful method of identifying differentially expressed gene classes than over-representation analysis or annotation of gene lists based on individually analysed genes.

2.1.6.5 Gene expression microarray data survival analysis

The identification of genes whose expression associated with survival time following PD required the fitting of Cox proportional-hazards models relating survival to each gene, with p value computation for each gene to test the hypothesis that survival is independent of the expression level. Cross validation is an alternative to the test/ validation group method of estimating prediction accuracy while preserving the key separation principle. With leave-one-

out cross-validation (LOOCV), one case was omitted and a predictive classifier developed based on the remaining cases (*n-1)*. That classifier was used to classify the omitted case with a record made of the prediction result. A different case was omitted, with the one omitted initially now included and a new classifier developed from scratch on the new training set of *n-1* cases. That classifier was subsequently used to classify the omitted case with the prediction result recorded. In particular, the gene selection was repeated for each loop of the cross-validation, as failure to include the full dataset in the cross-validation fitting of the model would result in a highly biased estimate of prediction accuracy (255).

2.1.6.6 Gene set analysis survival

Similar to the gene set comparison, this method was used to identify sets of genes that are associated with survival following PD. A proportional-hazards model was fitted to survival time, one gene at a time and the corresponding p value for the gene set then computed.

2.1.7 MiRNA microarray data analysis

2.1.7.1.1 Normalisation and filtering

Following a similar method to the gene expression data analysis, an average value of the replicate spots for each miRNA were normalised and uploaded into BRB-ArrayTools. After excluding negative values with hybridisation intensity below background, normalisation was performed by using the median normalisation method and normalisation to the median array. 476 miRNAs with consistent log values present in > 50% of samples were selected. This filtering method was agreed upon *a priori* to eliminate probes with unreliable expression.

2.1.7.1.2 Identification of differentially expressed miRNAs

miRNAs that were differently expressed among groups using the class comparison analysis and the significance analysis of microarray (SAM) analysis ($p < 0.001$) were identified. Class prediction algorithms in BRB-ArrayTools were used to determine whether miRNA microarray expression patterns could accurately differentiate tumour from non-tumour tissue. For these analyses, Bayesian compound covariate and nearest centroid algorithms were arbitrarily chosen with the percentage of correctly identified tissues reported.

2.1.7.1.3 miRNA microarray survival analysis

Based on the dichotomised expression of the individual miRNAs using the median value as a cut-off, miRNAs were identified whose expression was significantly related to patient survival. A statistical significance level for each miRNA based on a univariate Cox proportional-hazards regression model was computed. These p values were then used in a multivariate permutation test in which the survival times and censoring indicators were randomly permutated among the arrays. miRNAs were considered statistically significant if the $p < 0.05$ according to a Log-rank analysis. By this means low and high-risk groups based on miRNA expression were determined.

2.1.7.2 Bioinformatic tools for miRNA enrichment analysis

Stem–loop quantitative RT–PCR has become the method of choice for quantitative and qualitative miRNA analysis (256). miRNAs are catalogued in the miRNA international Sanger database; in which each mature miRNA is assigned a unique identifier e.g. microRNA 21 is assigned miR-21. The most recent update Sanger v17.0 (April 2011), lists over 950 human miRNAs (http://www.mirbase.org). Although putative miRNA targets may be defined by bioinformatic algorithmic approach, the actual miRNA downstream influence cannot be reliably predicted by algorithm because it targets by imperfect base pairing. Prediction algorithms including PicTar, Targetscan and Miranda provide ranked lists of targets (257). Each miRNA can regulate several mRNA transcripts and conversely one mRNA can be regulated by several miRNAs. The predicted targets of miRNAs of interest were determined by using DIANA LAB (http://diana.cslab.ece.ntua.gr), which combines prediction algorithms from DIANA-microT v3.0, PicTar and Targetscan. Predicted targets were analysed with respect to over-representation within different biological pathways.

2.1.8 ArrayCGH data

2.1.8.1 Data quality evaluation and preparation for analysis

The aCGH text files were uploaded into the Agilent Genomic Workstation version 5.0 (Figure 2.2D). Initially quality control metrics (background noise, signal intensity and signal to noise) were used to evaluate the adequacy of hybridisations for downstream analysis. The reference versus specimen DNA spot intensity was calculated (i.e. Cy5/Cy3) and the median all of spot ratios within each block calculated. Normalisation of each spot intensity ratio was achieved by dividing the intensity ratio by the median of all spot ratios within each block. For each probe, the mean and standard deviation (SD) across the identical triplicate spots were calculated. Any spot with a SD > 0.2 was discarded from further analysis.

2.1.8.1.1 Dye-swap hybridisation

For 10 PDAC samples dye swap reactions were performed. Hybridisations were repeated with the specimen and reference dye labelling reversed (Cy5 or Cy3). This was designed to improve the accuracy of hybridisation results, as a genuine gain indicated by a high intensity ratio in the first hybridisation will be represented as a low intensity. Also, the dyes are incorporated differently within GC-rich DNA regions, generating artefactual false positives. Full aCGH experimentation dye swap was not performed due to prohibitive cost and little difference being noted in aberrations between dye swaps experiments.

2.1.8.2 Aberrations and copy number variation detection

Analysis of the volume of data generated by aCGH creates numerous challenges. Although the major aberrations in a genome are frequently evident by inspection, many tumours, owing to their non-diploid genomes or heterogeneity, have closely spaced ratio levels that partially overlap because of noise measurement. Use of smoothing by averaging the ratios on

neighbouring array elements improves the behaviour of thresholding but blurs the locations of boundaries and reduces the amplitude of aberrations, involving fewer elements than the smoothing window. A number of aberration detection algorithms were used and simultaneously remove noise from the data (Figure 2.2E): The Z-score algorithm is a quick method of detecting aberrant regions assessing genomic intervals with an over- or under-abundance of probes with log ratios that deviate significantly from baseline. It scores intervals using sliding window of specified fixed size. The Aberration Detection Method identifies all aberrant intervals with consistently high or low log ratios based on the statistical score. The algorithm automatically determines optimal size of a statistically significant aberration with incorporation of quality information about each log ratio measurement. The Hidden Markov Model algorithm identifies aberrant intervals based upon the individual likelihood of such signals in a genomic context (258). The Circular Binary Segmentation (CBS) is used to identify regions in chromosomes such that the copy numbers in each region are equal (259). For each chromosome, the data is recursively split until no further change points are found. Based on the segmentation mean log ratio data, copy number at a particular genomic location was assigned as one of five states: amplification, gain, no change, loss and homozygous deletion. Two methods were used to determine copy number status, the first method selects thresholds based on the segmented log ratios, while the second determines the thresholds based on a factor multiplied by the median absolute deviation of log ratio data of each array. One important goal for many aCGH studies is to identify the regions with frequent CNA among multiple samples using the Genomic Identification of Significant Targets in Cancer (GISTIC) tool (260) in BRB-CGHTools (further detailed in Chapter 8).

2.1.8.3 Pathway enrichment based on arrayCGH analysis

Gene enrichment associated with specific BioCarta or KEGG pathways was conducted based on chromosomal aberrations and presence of particular clinicopathological states. The test statistic was generated by consideration of the total number of specific pathway genes that fell into gain/ loss regions. The null-hypothesis being that the number of genes in the specific pathway in the gain/ loss regions is a random event. Analysis was conducted at 1) whole genome scale; 2) individual chromosomes; 3) on each individual chromosome arm.

2.1.8.4 Survival analysis based on arrayCGH data

The presence of particular genomic aberrations was correlated with outcome following PD similar to the mRNA survival correlation. BRB-CGHTools allowed survival correlation of genomic aberrations in a univariate manner using a Cox proportional-hazards model.

2.1.9 Reverse transcription

First strand cDNA synthesis was performed using Invitrogen's Superscript First Strand Synthesis System. 3 µL total RNA (1 µg/µL) was added to 21 µL DEPC water, 3 µL oligo $(dT)_{12\text{-}18}$ (500 µg/mL) and 3 µL 10 mM dNTPs. The mixture was heated to 65°C for 5 minutes

and chilled on ice. 12 µL 25 mM $MgCl_2$, 6 µL 0.1 M DTT, 6 µL 10X RT buffer and 3 µL RNase inhibitor was added, incubated at 42°C for 2 minutes and placed on ice. 3 µL (200 U) Superscript II Reverse Transcriptase was then added and incubated at 45°C for 50 minutes. The reaction was stopped by heating at 70°C for 15 minutes. 3 µL (6 U) *E. coli* RNase H was added and incubated at 37°C for 20 minutes to RNA complementary to the cDNA.

2.1.10 Polymerase chain reaction

PCR amplifications were performed using the DyNAMo™ Hot star SYBR® Green kit and the Opticon 2 DNA Engine. Each 50 µL DyNAMo reaction contained 25 µL 2x Master Mix (containing *T. brockianus* DNA Polymerase, SYBR Green I dye, optimised PCR buffer, 5 mM MgCl2, dNTP mix including dUTP), 0.5 µL each of two 25 µM oligonucleotide primers, 1 µL of input cDNA made up to the final volume with dH_20. Cycling conditions included an initial denaturation at 95°C for 10 minutes, with 40 cycles of denaturation at 94°C for 10 seconds, annealing for 20 seconds and extension at 72°C for 20 seconds. The relative transcript abundance of target genes were calculated based on the $2^{-\Delta\Delta CT}$ method (261).

2.1.11 MiRNA polymerase chain reaction

Reverse transcription (RT) was conducted with the mirVana™ quantitative (q)RT-PCR miRNA detection kit according to the manufacturer's instructions. The reaction master mix, containing mirVana™ 5 x RT Buffer, 1 x mirVana™ RT primer, Array-Script™ Enzyme Mix and nuclease-free water was mixed with 20 ng of each total RNA sample. The RT reaction was performed at 37°C for 30 minutes then 95°C for 10 minutes. Using the DyNAmo Hot star SYBR Green kit and the Opticon 2 DNA Engine. The PCR master mix containing mirVana™ 5 x PCR Buffer (with SYBR® Green), 50x ROX, SuperTaq Polymerase, mirVana™ PCR primers and RT products was processed as follows: 95°C for 3 minutes and then 95°C for 15 seconds, 60°C for 35 seconds for up to 40 cycles. All quantitative PCRs were normalised to the small nuclear RNA, U6, as the normalisation control. All assays were performed in triplicate.

2.1.12 Integration of gene expression and arrayCGH data

Integration of copy number variation with gene expression data was successfully achieved by a BRB-CGHTools CNA and gene expression integration function. Additionally, a further R based program, the Correlate analysis tool was used to integrate these technologies using Spearman's rho correlation and is discussed in more detail in Chapter 9.

2.2 Materials

Materials used in the experiments described in this thesis are listed below.

2.2.1 Statistical analysis of prognostic factors

IBM, SPSS Inc. (Chicago, Il, USA)
SPSS version 18

Microsoft® (Reading, UK)
Microsoft® Access database and Excel spreadsheet programs

2.2.2 Meta-analysis of prognostic immunohistochemical markers

Microsoft® (Reading, UK)
Microsoft® Access database and Excel spreadsheet programs

Cochrane collaboration (Oxford, UK)
REVMAN systematic review and meta-analysis software v5.0 (www.cochrane.org).

National Center for Biotechnology Information (NCBI)
http://www.ncbi.nlm.nih.gov/pubmed/

2.2.3 Equipment

Equipment standard to most laboratories not included in the list below, but used in this work, included: wet and dry ice, 37°C incubators, vortex mixers, refrigerators, freezers (-20°C and -70°C), liquid nitrogen, flasks for liquid nitrogen, microwave oven, pressure cooker, sterile and non-sterile glass pipettes, flasks, plastic bottles, beakers, measuring cylinders, aluminium foil, Clingfilm, autoclave tape, platform shaker, forceps, scalpels, spatulas, pestle, mortar, slide holders and magnetic stir bars.

Agilent Technologies UK Ltd (Stockport, UK)
2100 Bioanalyser
Agilent Microarray Scanner
Hybridisation Chamber, stainless
Hybridisation oven
Hybridisation oven rotator for Agilent Microarray Hybridisation Chambers
Human Genome CGH Microarray 244K
Human 4x44K mRNA gene expression arrays
Human MiRNA Version 2 microarrays

Anachem Ltd (Luton, UK)
Gilson PIPETMAN® pipettes (2 µL, 20 µL, 20 µL, 200 µL, 1000 µL) with separate sets for RNAase-free work and general use.

Beckman (RIIC) Ltd (High Wycombe, UK)
Centrifuge tubes
Microfuge® R centrifuge
GS-6R centrifuge
Vacuum spin centrifuge
Magnetic stir plate
Heat blocks
Thermomixer

Dako Cytomation (Ely, UK)
Auto stainer

Hamamatsu (Japan)

NanoZoomer Digital Pathology Scanner

Millipore (Watford, UK)

Milli-Q plus PF water purification system

MJ Research (Rayne, UK)

Opticon 2 DNA Engine

Qiagen

RNeasy Mini Kits

Stratagene Ltd (Cambridge, UK)

UV Stratalinker2400

Thermo Hybaid (Ashford, UK)

Ribolyser

Thermo Fisher Scientific (Waltham, Mass, USA)

NanoDrop ND-1000 UV-VIS Spectrophotometer

2.2.4 General plasticware

Becton Dickinson UK Ltd (Oxford, UK)

Falcon conical tubes (15 ml)

Elkay laboratory Products (UK) Ltd (Basingstoke, UK)

Microcentrifuge tubes (0.5, 1.5, 2.0 ml)

Standard pipette tips

Greiner Labortechnik Ltd (Stonehouse, UK)

Aerosol-resistant pipette tips (10 µL, 20 µL, 200 µL and 1000 µL)

2.2.5 Chemicals

Stock solutions were made up with distilled water. For RNA work, distilled water was pre-treated with diethylpyrocarbonate (DEPC).

Ambion (Huntingdon, UK)

RNase ZAP™

DNA ZAP™

Braun Medical Ltd (Sheffield, UK)

Water for injection

Fisher Scientific UK Ltd (Loughborough, UK)

Chloroform

Glycerol

Histoclear

Hydrochloric acid

Isopropanol

Methanol

Sodium chloride (5 M stock solution)

Sodium hydroxide (0.5 M stock solution)

Propan-2-ol

Tris base

Xylene

Hayman Ltd (James Borrough) (Witham, UK)

Absolute alcohol (ethanol, analytical reagent grade 100% and 70% stock solutions)

Sigma (Dorset, UK)

Acetonitrile

DEPC

Ethidium bromide (10 mg/mL stock solution)
Ethyleneidiaminetetracetic acid (EDTA)
Hydrogen peroxide
Phenol: chloroform: isoamyl alcohol (25:24:1)
Sodium acetate buffer solution

Surgipath Europe Ltd (Peterborough, UK)

Haematoxylin
Eosin Y

2.2.6 Buffer and other solutions

Stock solutions made with distilled water. For RNA work, distilled water was DEPC treated.

Phosphate Buffered Saline (PBS)
Sodium Citrate Buffer (0.1M Sodium citrate)
Tris Buffered Saline (TBS)/Tween (2.5 mL Tween)
TE (10mM Tris-HCL (pH 7.5), 1 mM EDTA (pH 7.5)

2.2.7 Tissue arrays

2.2.7.1 Primary tumours

Following curation of the pancreatic cancer database containing all pancreatic tumours managed within GRI from 1992 to January 2007, patients with appropriate tumours (n = 224) were selected for the creation of the pancreaticobiliary TMAs (Table 2.1, Figure 2.1B). Samples suitable for TMA inclusion were identified from pathology reports including 119 PDACs, 56 ampullary adenocarcinomas, 23 cholangiocarcinomas and ancillary tumours (Table 2.2). Only PDACs were studied in this thesis with ampullary, duodenal, distal bile duct adenocarcinomas, MCNs and IPMNs excluded from further analysis. Archival formalin fixed, paraffin embedded (FFPE) tumour specimens were obtained from the pathology archive of the Department of Pathology, GRI.

2.2.7.2 Ethical approval for immunohistochemical experiments

Ethical approval was granted by the North Glasgow Hospitals University NHS trust ethics committee for the formation of TMAs to allow the investigation of prognostic markers in pancreaticobiliary disease. Computerised records were pseudoanonymised to prevent association of pathological diagnosis and experimental results with individual patients.

2.2.7.3 TMA construction and sectioning

Beecher Instruments (Silver Spring, MD, USA)

Manual Tissue Multi-arrayer. Rotating platform allows construction of 4 arrays.
0.6 mm punches

Thermo Shandon UK (Runcorn, UK)

Paraplast® Paraffin

Instrumedics Inc (Hackensack, NJ, USA)

Paraffin Tape-Transfer Slides
Tape Windows

Leica Microsystems (UK) Ltd (Milton Keynes, UK)

1512 Rotary microtome

2.2.8 Immunohistochemistry

2.2.8.1 Primary antibodies

Dako Ltd (Ely, UK)

Ki67 (Monoclonal Mouse Anti-Human; MIB-1)
Bcl-2 (Monoclonal Mouse Anti-Human; clone 124)
β-catenin (Monoclonal Mouse Anti-Human; clone β-catenin)
E-cadherin (Monoclonal Mouse Anti-Human; clone NCH-38)
p53 (Monoclonal Mouse Anti-Human; clone DO-7)
p21 (Monoclonal Mouse Anti-Human; clone SX118)

Santa Cruz (Ca, USA)

SMAD-4 (Monoclonal Mouse Anti-Human; clone B-8)
TGFβ1 (Polyclonal Rabbit Anti-Human; clone sc146)
COX-2 (Polyclonal Rabbit Anti-Human)

Abcam (UK)

Lkb1 (Polyclonal Rabbit Anti-Human; clone ab58786)

Cell Signalling (Danvers, Ma, USA)

Phospho-AKT ser-473 (Monoclonal Rabbit Anti-Human; # 4060)
Phospho-mTOR ser-2448 (Polyclonal Rabbit Anti-Human; #2971)
GSK3β ser-9/21 (Polyclonal Rabbit Anti-Human; #9331)
PTEN (Polyclonal Rabbit Anti-Human; #9552)

Lab-Vision Neomarkers (Fremont, Ca, USA)

Cyclin D1 (Monoclonal Rabbit Anti-Human; clone SP4)

BD Biosciences, PharMingen (San Diego, Ca, USA)

Maspin (Monoclonal Mouse Anti-Human; clone G167-70)

2.2.8.2 Secondary staining

Vector Laboratories Ltd (Peterborough, UK)

ChemMate Envision Kit
Peroxidase Substrate Kit

2.2.9 Tissue microarray image acquisition, archiving and analysis software

Slidepath (Dublin, Ireland)

Digital Image Hub and Distiller
opTMA and Tissue Image Analyser

2.2.10 Samples for microarray and RT-PCR

2.2.10.1 Primary tumours

Immediately following resection, the specimens were transported on ice to the pathology department where a senior pathologist (KO, AKF, JJG) performed immediate tumour specimen sampling. The time from resection to freezing was kept to a minimum. 1-2 mm blocks of tumour were immediately frozen in liquid N_2 and stored at -70°C. Quality assessment was performed by H&E sectioning of these blocks to confirm the satisfactory presence of tumour (minimum 50% carcinoma content). 76 PDAC tissue samples were collected prospectively.

2.2.10.2 Ethical approval for microarray experiment

Ethical approval was granted by the North Glasgow Hospitals University NHS trust ethics committee for microarray experimentation. Informed consent was gained from all patients detailing the storage and use of their resected tissue specimen. This aspect of the study was granted specific approval with reference to the use of genomic DNA for research purposes. Samples were stored at -70°C within the GRI BioBank, managed by JH. The clinicopathological characteristics of the PDAC cohort are illustrated in Table 2.1.

2.2.11 Purchased DNA

Promega UK Ltd (Southampton, UK)

Male and female genomic DNA

2.2.12 RNA extraction

Ambion (Huntingdon, UK)

DNAzap®

RNasezap®

Invitrogen Life Technologies Ltd (Paisley, UK)

TRIzol® Reagent

2.2.13 DNase digestion of RNA

Ambion (Huntingdon, UK)

DNA-free™

2.2.14 DNA extraction

Qiagen Ltd (Crawley, UK)

Qiagen DNeasy Blood & Tissue Kit

Qiagen Proteinase K (>600 mAU/mL, solution)

Qiagen RNase A (100 mg/mL)

RLT buffer

RPE buffer

2.2.15 RNA and DNA quality assessment and quantification

Agilent technologies UK Ltd (Stockport, UK)

2100 Bioanalyser

RNA 6000 Nano Assay (RNA Series II Kit)

Thermo Fisher Scientific (Waltham, Mass, USA)

NanoDrop ND-1000 UV-VIS Spectrophotometer

2.2.16 Microarray experimentation

2.2.16.1 Gene expression microarray

Agilent technologies UK Ltd (Stockport, UK)

Gene Expression Hybridisation Kit

Low RNA Input Linear Amplification Kit, PLUS, One-Color

RNA Spike-In Kit, One-Color

Gene Expression Wash Buffer 1

Gene Expression Wash Buffer 2

Invitrogen (UK)

DNase/RNase-free distilled water

Human Cot-1 DNA

Sigma (Dorset, UK)
Triton® X-100

2.2.16.2 MicroRNA microarray experimentation

Agilent Technologies UK Ltd (Stockport, UK)
MiRNA labelling reagent and Hybridisation kit
Ambion (Huntingdon, UK)
T4 RNA ligase
Calf Intestine Alkaline Phosphatase (CIP)
X10 CIP buffer
Fisher Scientific UK Ltd (Loughborough, UK)
Dimethyl Sulphoxide (DMSO)
Sigma (Dorset, UK)
Triton® X-102
Bio-Rad Laboratories (Hercules, Ca, USA)
Bio-spin 6 column

2.2.16.3 ArrayCGH microarray experimentation

Agilent Technologies UK Ltd (Stockport, UK)
Agilent Genomic DNA Labeling Kit PLUS (50)
Agilent Oligo aCGH Hybridisation Kit (25)
Agilent Oligo aCGH Wash Buffer 1 and 2 set
Agilent Oligo aCGH Spike-in Kit (50)
Stabilisation and Drying Solution, 500 mL
Promega UK Ltd (Southampton, UK)
Acetylated bovine serum albumin (BSA) 10 µg/µL
1 x TE (pH 8.0), Molecular grade
Alu I (10 U/µL)
Rsa I (10 U/µL)
Human Genomic DNA (female)
Human Genomic DNA (male)
Millipore
Microcon YM-30 filter units

2.2.17 Microarray, genomic and pathway data analysis software

Agilent Technologies UK Ltd (Stockport, UK)
Agilent Feature Extraction (version 9.5)
Genespring version 10
Agilent CGH analytic suite
Partek
Partek
Biometric Research Branch (BRB)(National Cancer Institute, USA)
BRB Array Tools 3.9.0 http://linus.nci.nih.gov/BRB-ArrayTools.html
BRB CGH tools 1.1
IBM SPSS Inc. (Chicago, Ill, USA)
SPSS version 15
R www.r-project.org
Pollack Laboratory
Correlate

GeneGO™ Inc (St Joseph's, MI, USA) MetaCore™

MetaCore™ is an integrated software suite for functional analysis of experimental data. The scope of data types includes microarray, SNPs, aCGH, proteomics, metabolomics and pathway analysis. MetaCore™ is based on a proprietary manually curated database (MetaBase™) of human protein-protein, metabolic and signalling pathways. The analytical package includes data visualisation tools, multiple networking algorithms and filters.

2.2.18 Reverse transcription

Invitrogen Life technologies Ltd (Paisley, UK)

Superscript First Strand Synthesis System for RT-PCR

2.2.19 Polymerase chain reaction

2.2.19.1 Reagents

Finnzymes (Espoo, Finland)

DyNAmoHot star SYBR green Kit

2.2.19.2 Oligonucleotides

Oligonucleotide primer sequences used for RT-PCR validation of genes predicted by analysis of gene expression microarray data were as follows:

TGM2	*5'-CTGGTCACTAACCAACAT-3',*	*5'-GAGCAGGAGATAAAGTC-3'*
CLIC3	*5'*-GGACGGCGACAGGCTCAC-*3'*,	*5'*-AGGATCTCGGCGCTGTGC-*3'*
DUSP5	*5'-GTCCTCACCTCGCTACTC-3',*	*5'-CATCCACGCAACACTCAG-3'*

2.2.20 MicroRNA polymerase chain reaction

2.2.20.1 Reagents

Ambion (Huntingdon, UK)

MiRVANA™ qRT-PCR miRNA detection kit

MiRVANA™ qRT-PCR miRNA set for normalisation (U6)

SuperTaq™ polymerase

Finnzymes (Espoo, Finland)

DyNAmo Hot star SYBR green kit

2.2.20.2 Primer sets

Ambion (Huntingdon, UK)

hsa-miR-21	UAGCUUAUCAGACUGAUGUUGA
hsa-miR-29c	UAGCACCAUUUGAAAUCGGU
hsa-miR-30d	UGUAAACAUCCCCGACUGGAAG
hsa-miR-34a	UGGCAGUGUCUUAGCUGGUUGUU
hsa-miR-221	CCACACCGUAUCUGACACUUU
hsa-miR-224	CAAGUCACUAGUGGUUCCGUUUA

Table 2.1 Characteristics of the patient cohorts used in the thesis

*Demographic, operative, pathological and treatment characteristics of **A)** 148 PDAC patients analysed in Chapter 3. **B)** 189 PDAC patients analysed in Chapter 4. **C)** 119 PDAC patients included in the Tissue microarray analysed in Chapter 5. **D)** 48 PDAC patients for which tumours underwent gene expression microarray and miRNA expression microarray profiling in Chapter 6 and 7. **E)** The characteristics of a further 24 patients used as a validation cohort for miRNA expression in Chapter 7. **F)** The characteristics of the 45 patients undergoing aCGH profiling Chapter 8. Note that in Chapter 9 which overlapping data was only available for 37 patients.*

Characteristic	A) 148 Patient cohort	B) 189 Patient cohort	C) 119 Patient cohort	D) 48 Patient cohort	E) 24 Patient cohort	F) 45 Patient cohort
Demographic						
Gender (F: M)	73/75	86/103	59/60	19/29	10/14	19/26
Age (≤65/ > 65 yrs)	83/65	104/85	64/55	25/23	10/14	23/22
Pathological						
Tumour stage (T2/ T3)	14/134	18/171	13/106	4/44	1/23	5/40
Lymph node metastasis (no/ yes)	28/120	37/152	24/95	8/40	5/19	9/36
Tumour size (≤30/ > 30mm)	85/63	98/91	63/56	28/20	13/11	25/20
Tumour grade (low/ high)	99/49	127/62	85/34	32/16	17/7	31/14
Perineural invasion (no/ yes)	11/137	16/173	11/108	3/45	0/24	3/42
Venous invasion (no/ yes)	75/73	94/95	58/61	15/33	10/14	15/30
Lymphatic invasion (no/ yes)	109/39	131/58	84/35	31/17	15/9	30/15
Operative, treatment and outcome						
Vascular resection (no / yes)	130/18	158/31	106/13	36/12	16/8	34/11
Resection margin status (R0/ R1)	39/109	51/138	29/90	10/38	6/18	11/34
Adjuvant chemotherapy (no/ yes)	86/62	114/75	79/40	20/28	14/10	17/28
Survival (months) (median/ mean)	17.6/23.8	18.9/28.2	16.7/23.2	18.0/24.9	20.7/21.5	18.0/24.6

Table 2.2 Histological classification of tumours used in tissue microarrays

Expression pattern of a number of markers were assessed by immunohistochemistry in a series of 224 primary pancreaticobiliary tumours. The histological classification of the tumours is listed. All specimens were assessed and marked with supervision of a hepatobiliary pathologist prior to use (KO).

Tumour primary site and histology	No. of specimens
Total	224
Pancreatic	
Ductal adenocarcinoma	119
Cystadenocarcinoma mucinous	3
Adenosquamous carcinoma	2
Carcinosarcoma	1
Ampullary	
Adenocarcinoma	56
Common bile duct	
Cholangiocarcinoma	26
Duodenal	
Adenocarcinoma	17

Figure 2.1 Characteristics of patient cohorts used in the thesis

A) *Illustration of the pancreaticoduodenectomy specimens performed for PDAC, ampullary, duodenal and cholangiocarcinoma. Note for the year 2009, cases were recorded until June.*

B) *The PDAC cohort studied in this thesis illustrating the groups used in individual chapters, which are described in detail in Table 2.1.*

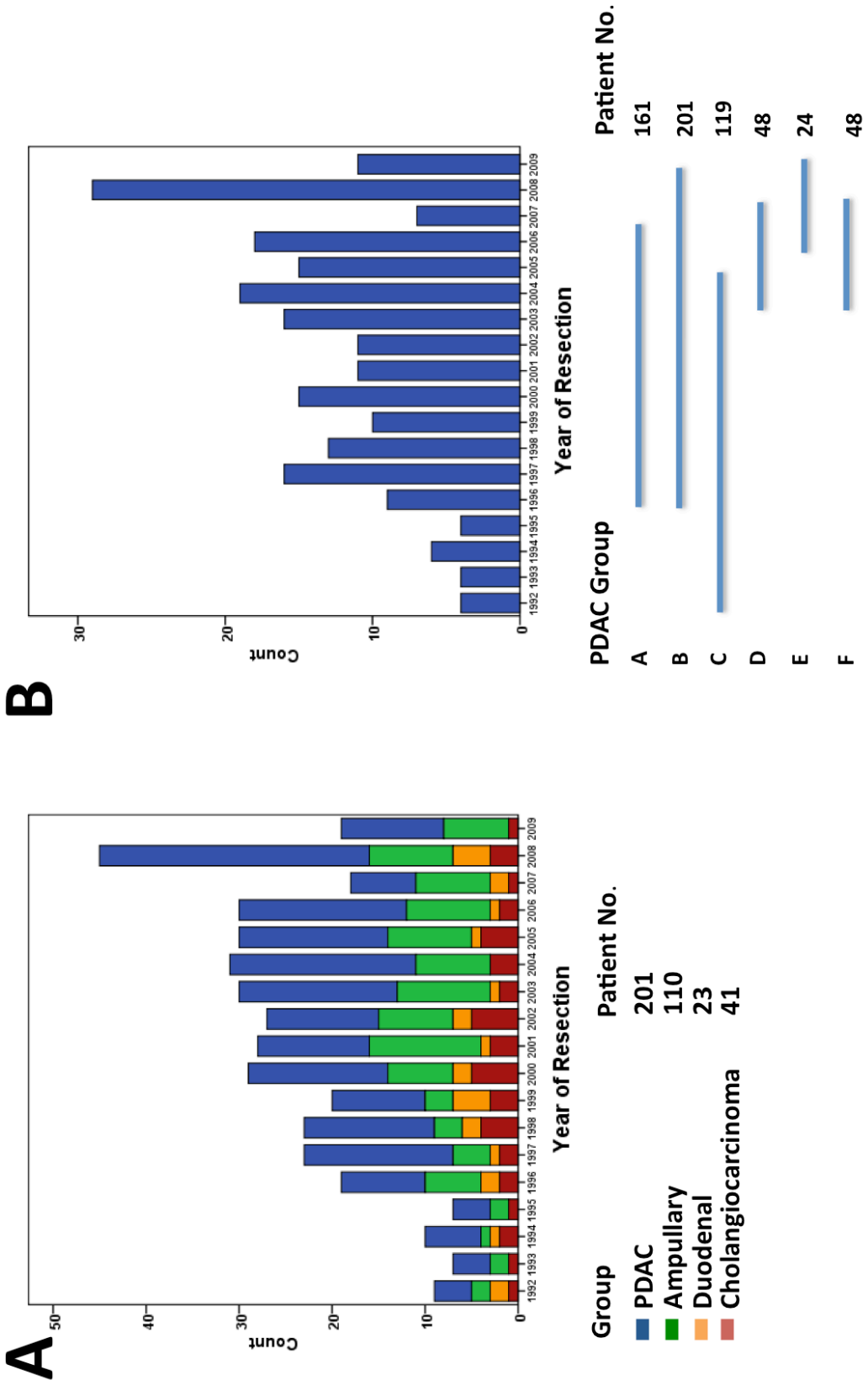

Figure 2.2 Microarray workflows and analysis schematics

Workflow for sample preparation and microarray processing for:

A) *Gene expression microarray,* ***B)*** *aCGH,* ***C)*** *microRNA expression microarray.*

D) *Schematic diagram of the aCGH data analysis process from image file acquisition to copy number aberration.*

E) *Detection algorithms for aCGH analysis. ADM – Aberration Detection Model, HMM – Hidden Markov Model , CBS – Circular Binary Segmentation.*

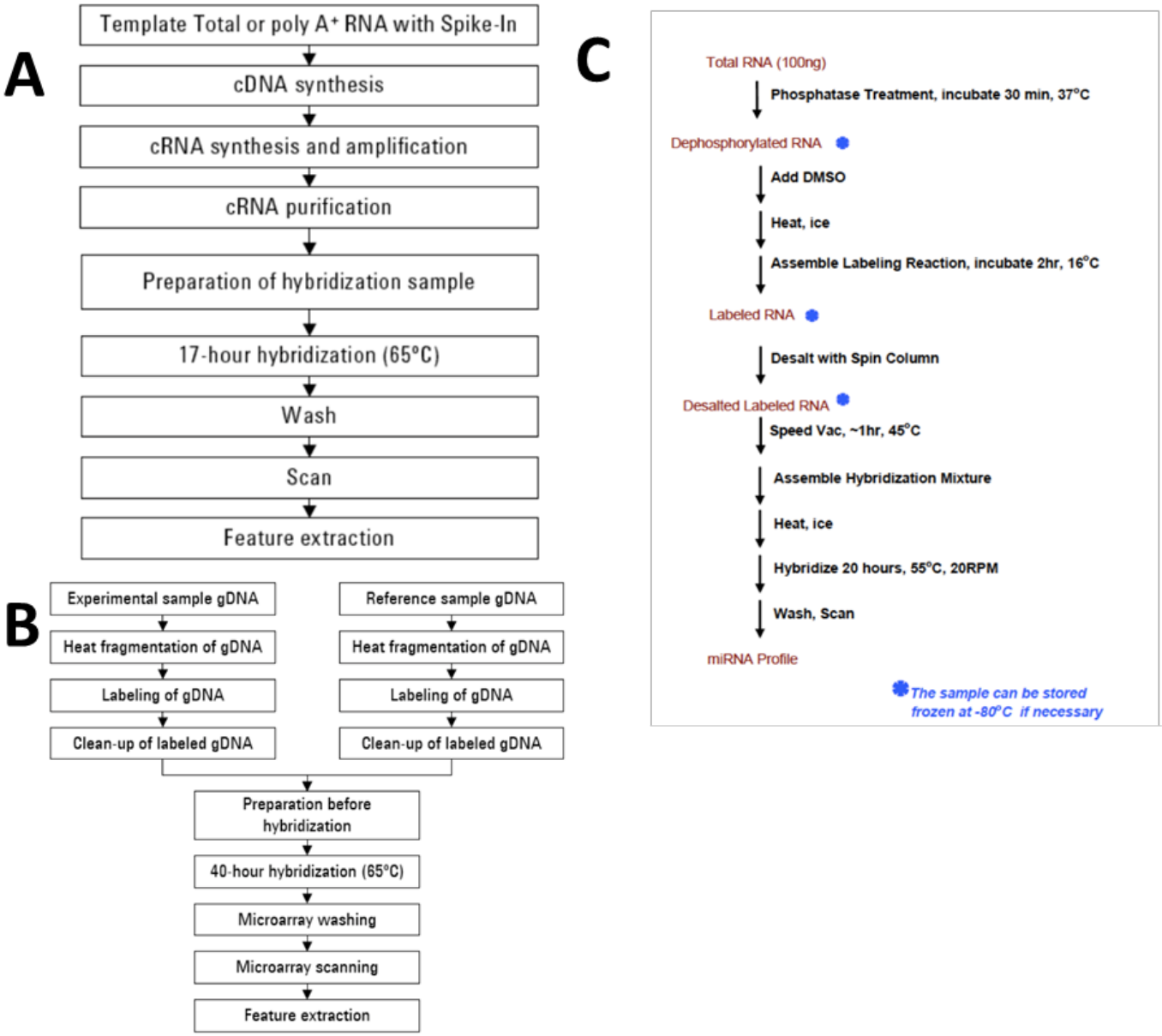

Figure 2.2

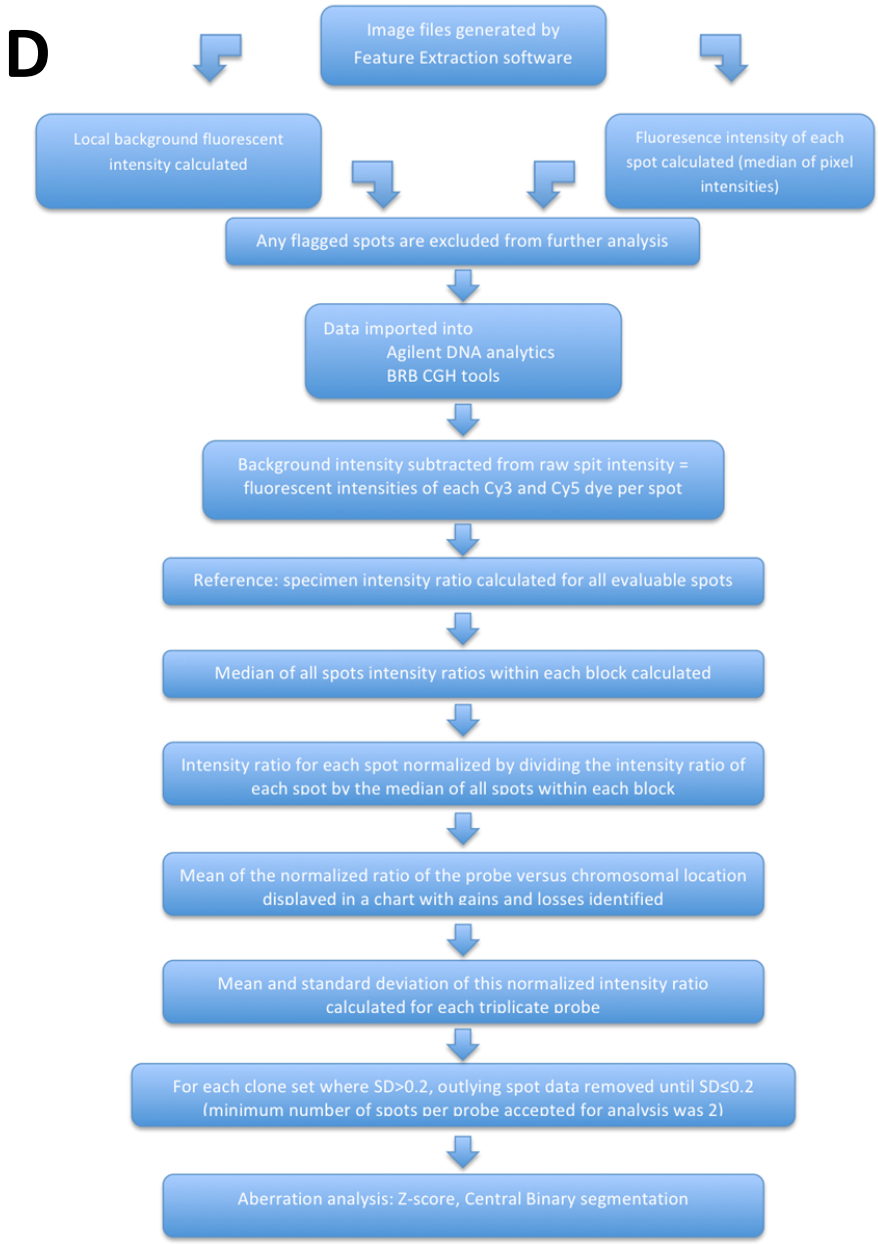
D
Image files generated by Feature Extraction software
Local background fluorescent intensity calculated
Fluoresence intensity of each spot calculated (median of pixel intensities)
Any flagged spots are excluded from further analysis
Data imported into Agilent DNA analytics BRB CGH tools
Background intensity subtracted from raw spit intensity = fluorescent intensities of each Cy3 and Cy5 dye per spot
Reference: specimen intensity ratio calculated for all evaluable spots
Median of all spots intensity ratios within each block calculated
Intensity ratio for each spot normalized by dividing the intensity ratio of each spot by the median of all spots within each block
Mean of the normalized ratio of the probe versus chromosomal location displayed in a chart with gains and losses identified
Mean and standard deviation of this normalized intensity ratio calculated for each triplicate probe
For each clone set where SD>0.2, outlying spot data removed until SD≤0.2 (minimum number of spots per probe accepted for analysis was 2)
Aberration analysis: Z-score, Central Binary segmentation
E
Detection Algorithms
Z-score
Detection of regions of fixed size with an over or under abundance of aberrant probes
ADM
Identification of significant aberrant regions of arbitrary size
HMM
Detection of probes likely to be aberrant can be grouped to form aberrant regions of any size
CBS
Identification of regions that have constant copy number. The regions are arbitrary in size

Figure 2.3 Images of microarray experimentation

A) Gene expression analysis. *Schematic depiction of a two-colour microarray-based expression profiling method. mRNA isolated from test and reference samples (or test and spike in RNA control for single colour experiment) are differently labelled using two different fluorescent dyes and then co-hybridised to a microarray comprising an ordered array of gene specific DNA probes (left). Labelled mRNAs bind their cognate probes on the microarray by Watson-Crick base pairing. Following hybridisation and imaging (centre), the ratio of red to green fluorescence for each gene spot reflects that gene's relative expression level in the test compared to reference sample approximately proportional to the number of molecules of cDNA bound to the probe. The AKT gene, shown in red spot on the scanned image, is more highly expressed in the test sample. Analysis of multiple samples produces a heatmap of gene expression ratios (right), each column represents a different sample and each row represent a different gene on the array. The column and rows have been ordered by unsupervised hierarchical cluster analysis to reveal patterns in the data, where the dendrogram (tree) branches indicate relationships among samples and genes.*

B) Array CGH analysis. *Schematic depiction of array-based comparative genomic hybridisation (aCGH) method. Genomic DNA (gDNA) isolated from tumour and normal samples is differentially labelled (shown as red and green dyes, respectively) and then co-hybridised to a microarray comprising DNA probes of known chromosome location. Following hybridisation and imaging, the ratio of red to green fluorescence for each DNA spot on the array reflects that gene's relative copy number in the tumour genome. The KRAS gene, shown as a red spot in the scanned image, is amplified in the tumour genome. Plotting fluorescence ratios by genome map position is useful in defining DNA amplifications and deletions. Illustrative data is shown for chromosome 12 (right) for a series of pancreatic tumours. Peaks to the right represent high copy number while peaks to the left represent low copy number.*

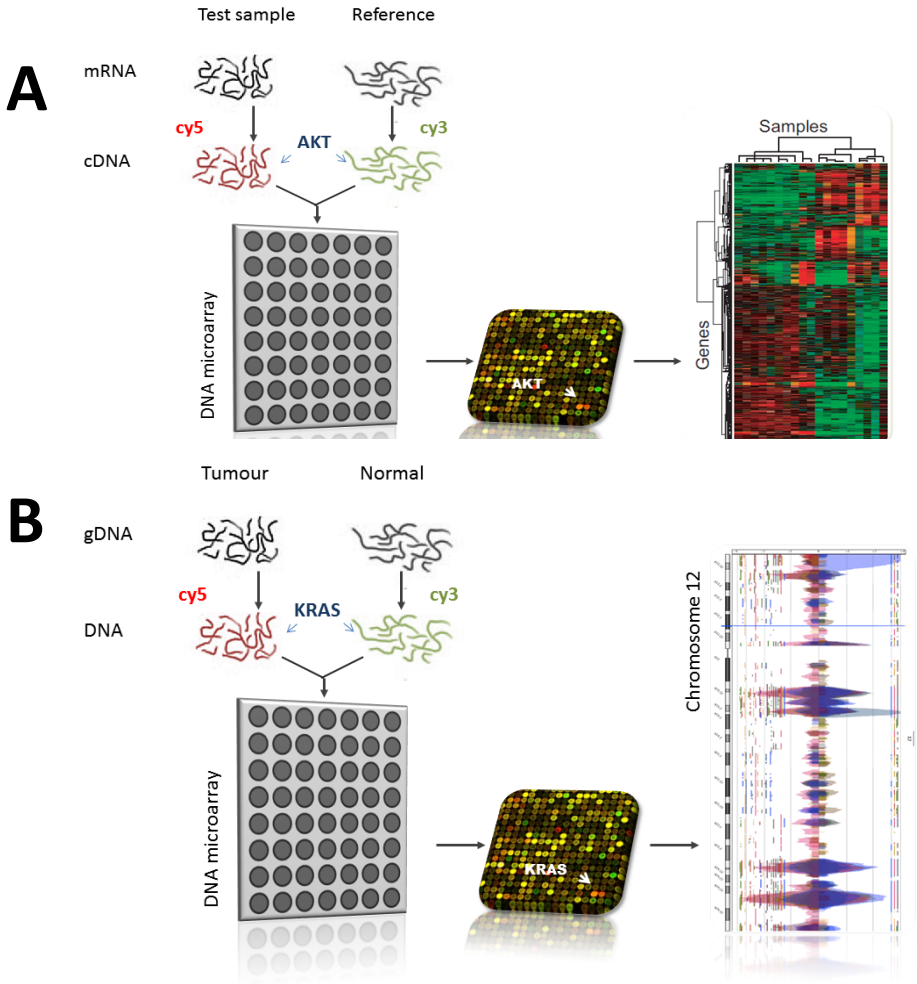

Introduction to Candidate Prognostic Marker Chapters

The first three results chapters of this thesis investigate candidate markers influencing prognosis in patients who have undergone resection for pancreatic cancer. In particular, the prognostic influence of resection margin status (Chapter 3), peripancreatic fat invasion (Chapter 4) and immunohistochemically assessed protein biomarkers (Chapter 5) will be investigated.

3 Positive Mobilisation Margins Alone Do Not Influence Survival Following Pancreatico-Duodenectomy for PDAC

3.1 Introduction

The impact of a microscopically positive resection margin on outcome following PD for PDAC has been variable. While some have shown it to have important independent prognostic significance, others have not (94, 262, 263). However, even after an R0 resection there remains a high rate of tumour recurrence with the majority of patients succumbing to the disease within 5 years (2, 61) of which 60–86% develop local recurrence (98, 99), suggesting considerable underestimation of true R1 status.

Currently all resection margins are considered important, with tumour at or close to any margin considered of equal prognostic significance. However, this may not be the case. Lymphovascular pancreatic drainage is a combination of mid- and foregut origins, resulting in a complex network which drains the HOP initially toward the midline or the hepaticoduodenal ligament, but not posteriorly to the retroperitoneum, anteriorly to the colon or laterally beyond the duodenum (264). During resection, mobilisation of the colon from the duodenum anteriorly or posteriorly from the inferior vena cava (IVC) and kidney restores the midline (embryological) position of the pancreas and does not transect any tissue, vascular or lymphatic planes. By contrast, division of the pancreatic parenchyma, the medial mesopancreas adjacent to the portal vein, SMA and SMV or hepaticoduodenal ligaments involves division of contiguous adventitia and lymphovascular outflow, which is the likely primary route of dissemination. The circumferential margin of a PD specimen consists of (a) transection margins where tissue has been surgically divided e.g. pancreatic body transection margin or mesopancreatic margin adjacent to mesenteric vessels and (b) mobilisation margins where two adjacent organ surfaces have been simply separated by developing embryological planes e.g. posterior margin, anterior surface or lateral duodenal margin. Therefore, tumour at or close to different margins of a PD specimen, although all currently defined as R1, may confer differing prognostic significance (82, 93, 265). Accurate assessment of R1 status following resection has important implications beyond prognosis. Currently, stratification within the setting of randomised control trials of adjuvant therapy is based partly upon margin positivity. Appropriate determination of those patients who would most benefit is vital if the true potential of novel and existing therapies is to be established.

3.1.1 Aim

Consequently, the aim of this chapter was to assess the frequency and prognostic impact of R1 status within the cohort, and furthermore, to determine the prognostic influence of tumour involvement of a mobilisation margin compared to a transection margin following PD for PDAC.

3.2 Methods

3.2.1 Operative procedure

Full details are outlined in section 2.1.1.2 and as illustrated in Figure 3.1A and B, during a PD the anterior, duodenal and posterior aspects of the HOP are fully mobilised back to the midline, leaving the medial lymphovascular structures intact.

3.2.2 Pathology assessment

The full pathology assessment is outlined in 2.1.1.4. The four pancreatic resection margins are identified and inked (Figure 3.1C, D). For this study, as the medial circumferential pancreatic resection margin requires tissue transection, as opposed to separation of planes, it was combined with the traditional transection margins (pancreatic body, duodenal, bile duct) to form the transection margin group ($R1_{Transection}$). The anterior pancreatic surface, posterior pancreatic margin and duodenal serosal margin were grouped together as mobilisation margins ($R1_{Mobilisation}$) (Figure 3.1E).

3.3 Results

3.3.1 Clinicopathological characteristics of the patient cohort

As inking of the pancreatic resection specimens had been standard pathology practice in the department since 1996, only the specimens since that time point until 2007 (time point of analysis), formed the cohort analysed in this chapter as described in Table 2.1.

3.3.2 Resection margin status relationship with pathological characteristics

When the RCPath criteria (R1 if tumour is ≤ 1 mm from margin) are applied, 109 (74%) of the 148 patients had histologically positive margins and were thus R1 resections. During the study period the R1 rate did not vary significantly being 76.3% prior to 2001 and 72.5% following this time. The relationship between the clinicopathological characteristics according to R0/R1 resection margin status is shown in Table 3.1. The only characteristics significantly associated with R1 status were the presence of lymph node metastasis and venous invasion. If the UICC/AJCC criteria (R1 only if tumour at margin surface) are applied, then 82 (55%) cases had histologically positive margins and were thus R1 resections. From this point on all results are according to the RCPath criteria. However, parallel analysis according to the UICC/AJCC criteria did not impact upon findings.

Of the 109 R1 resections, 63 (58%) had only a single margin involved and 46 (42%) had two or more margins involved (median size 30.0 versus 31.0 mm respectively, $p = 0.33$, Mann-Whitney U test). The overall frequency of involvement of each resection margin is shown in Table 3.2. For the 63 patients with a single margin involved, tumour was present at: posterior margin only ($R1_{Posterior}$) in 21; anterior surface only ($R1_{Anterior}$) in 14; medial margin only ($R1_{Medial}$) in 21 and pancreatic transection margin only in 7 patients (Table 3.3).

3.3.3 Survival and relationship with clinicopathological characteristics

The overall median survival for the 148 patients was 17.6 months (95%CI: 13.8-21.3). Univariate analysis of the clinicopathological characteristics in relation to survival is shown

in Table 3.2. The factors significantly associated with poorer overall survival were higher T stage, positive lymph node status, high tumour grade, venous invasion, tumour size > 30 mm, major vascular resection and R1 margin status.

3.3.4 Relationship between survival and resection margin status

The 109 (73.6%) patients with R1 resections had a significantly shorter overall survival compared to the 39 (26.4%) R0 resections, the median survival being 15.4 months (95% CI: 13.0–17.8) and 26.5 months (95%CI: 21.2–31.8) respectively (p = 0.011, Figure 3.1F). R1 resections were divided into single margin (n = 63), two margins (n = 39) or ≥ three margins involvement (n = 7). Multiple margin involvement was associated with poorer outcome: 8.4 months (95%CI: 7.9–9.0) for ≥ three margins versus 12.3 months (95%CI: 10.0–14.6) for two versus single margin 16.8 months (95%CI: 14.6–18.9) (Table 3.3). $R1_{Mobilisation}$ involvement ($R1_{Anterior}$, $R1_{Posterior}$ and duodenal serosa positive patients [n = 48]) had a significantly longer median survival of 18.9 months (95%CI: 13.7–24.8) compared to 11.1 months (95%CI: 7.1–15.0) (p < 0.001) for the $R1_{Transection}$ group ($R1_{Medial}$ and other traditional transection margins [n = 61]) (Table 3.3, Figure 3.1F, G). Patients with synchronous mobilisation and transection margin involvement were allocated to the $R1_{Transection}$ group. There was a non-significant difference in outcome between $R1_{Mobilsation}$ involvement compared to R0 cases: 18.9 months (95%CI: 13.1–24.8) versus 26.5 months (95%CI: 21.2–31.8) (p = 0.52). The outcome of resections identified to have tumour present at the margin did not differ significantly from those with tumour ≤ 1 mm from the margin, 13.9 months (95%CI: 10.8–17.1) versus 15.4 months (95%CI: 9.9–20.8) (p = 0.81) (Table 3.3). All survival comparisons were calculated using the Log-rank test.

3.3.5 Survival and resection margin status: multivariate analysis

Factors that independently adversely affected overall survival (Table 3.4) were high tumour grade (HR: 2.22; 95%CI: 1.51–3.28), higher tumour stage (HR: 2.11; 95%CI: 1.15–3.87), tumour size > 30 mm (HR: 1.55; 95%CI: 1.07–2.25) and R1 status (HR: 1.73; 95%CI: 1.13–2.63). A further multivariate analysis using $R1_{Transection}$ status did not alter the covariates present in the model but resulted in $R1_{Transection}$ contributing greater prognostic impact (HR: 2.76; 95%CI: 2.12–3.91).

3.4 Discussion

It is accepted that various pathological factors including tumour grade, lymph node status and perineural invasion influence outcome following PDAC resection (2, 61, 83, 86, 266). Additionally, while many investigators have reported resection margin involvement to be an independent prognostic factor (61, 87, 266, 267), a number have concluded otherwise (94, 251, 268, 269). Wide variation exists in the published R1 resection rates from 10–84% (Table 3.5) with many of the previous studies reporting particularly low rates of margin involvement failing to demonstrate that R1 status influences outcome. There is a concern

that these studies are under-reporting involved resection margin frequency. Furthermore, specific details of the involved individual margins are lacking in many of these reports.

Recently, these issues have been addressed by a seminal prospective study in which the standardised pathological examination of PD specimens was demonstrated to influence the R1 rate, with a positive correlation between R1 status and sampling frequency of circumferential margins (93). This protocol resulted in an R1 rate of 84%, which associated with outcome in univariate analysis with a trend towards multivariate significance. Further support was provided by an increase in R1 frequency from 14% to 76% following the introduction of a similar pathological protocol in an institute where all other factors remained constant (96). In another prospective standardised protocol of a periampullary cohort, R1 status predicted outcome although with a non-significant difference in the PDAC subgroup (270). Despite the high R1 rate of these studies, their overall survival figures matched studies reporting lower R1 rates. A recent retrospective analysis of a similar 163 patient cohort to that studied in this work revealed a comparable R1 rate (79%) (271).

Certainly based upon embryological origins, PD resection margins can be clearly differentiated. Moreover, while it is accepted that a positive resection margin adjacent to lymphovascular drainage of the HOP or a positive pancreatic body transection margin, which may occur due to errors in frozen section, would likely influence prognosis, it is felt that involvement of the mobilisation margins, devoid of lymphatic or venous drainage, may impact upon outcome to a lesser extent. It was the aim to determine firstly the prognostic impact of margin involvement and secondly the influence on survival conferred by the involvement of particular groups of margins, notably $R1_{Mobilisation}$ and $R1_{Transection}$ groups.

The strength of this cohort stems from no R2 resections being included owing to detailed radiological assessment preoperatively; a standardised surgical technique used throughout, and detailed consistent pathological reporting of resection margin status over the last decade in the West of Scotland Pancreatic Unit. The definition of pancreatic resection margins match closely those used in previous prospective studies (93, 96, 270), with the circumferential margins subdivided into the anterior pancreatic surface, and posterior and medial resection margin. The nomenclature surrounding the latter term is somewhat confusing (272, 273). Occasionally described as the retroperitoneal or uncinate margin, in this work it referred to the 3–4 cm^2 of HOP inferior to the pancreatic body transection margin, between the anterior and posterior resection margin.

Despite the retrospective nature of this study, resection margin involvement rate was high at 74%, matching rates achieved in studies that have applied prospective protocol driven specimen assessment (93, 96), but contrasting with the majority of the literature in this regard. In terms of demographics and clinicopathological characteristics, the studied cohort

compares favourably with these prospective studies and conforms to the accepted literature (61, 267). The overall high R1 rate in the present study may be a consequence of different specimen handling techniques, careful histological assessment of all soft tissue margins and use of ≤ 1 mm definition for margin involvement. Additional inclusion of tumour locoregional spread including lymph node invasion within the definition contributes a further 5% to the R1 total. These factors are common amongst the current study and those prospectively evaluating resection margin status (93, 96). The shared high rate of R1 resections in these studies is likely a reflection of high-quality reporting rather than inadequate operative technique. Furthermore, the studied cohort is in line with previous studies that have analysed the relative frequency of involvement of individual margins in R1 resections, with medial and posterior margins being most commonly involved (up to 77%) (93, 96, 270). Likewise, involvement of the anterior surface occurred less frequently, however, at a higher rate (36.7%) compared to previous studies (10–25%) (93, 274). One particular prospective evaluation found 10% involvement but only in 1% was it the only positive margin (96). Those with venous invasion and lymph node involvement were more likely to be R1, supporting claims that R1 tumours are more biologically aggressive (251). The use of a minimum clearance > 1 mm as a gauge of complete resection appears to be appropriate, as it was not possible to distinguish an improved outcome for those cases with tumour present ≤ 1 mm from the margin compared to those with tumour extending to the margin. Currently the RCPath (95) supports this definition, however, it is not explicit within other guidelines. However, in recent study optimal survival was achieved only when minimal clearance was more than 1.5 mm (275). The lack of detailed analysis regarding minimal distance of margin clearance represents a limitation of this analysis.

Despite the relatively high R1 rate, the overall median survival time is comparable to groups reporting a much lower rate of R1 resections. Univariate analysis revealed that traditional clinicopathological factors predict outcome, furthermore R1 status associated with worse outcome. Notably, R1 status was an independent predictor of poor outcome along with high T stage, large tumour size and high-grade. Involvement of two or more margins has been observed previously in over 40% of R1 cases (93, 96, 269) as the current data supports. Multiple margin involvement associated with a significantly worse outcome, a finding supported by a previous retrospective analysis of 79 patients (269). The influence of tumour infiltration at multiple margins does not appear to be merely a function of tumour size, as there were no significant differences in the mean maximum tumour diameter between those with single and multiple margin involvement ($p = 0.33$).

R1 sub-grouping by comparison of the embryologically separate $R1_{Mobilisation}$ group with the $R1_{Transection}$ group, revealed a significant prognostic benefit of an $R1_{Transection}$ negative

resection. This was despite the $R1_{Mobilisation}$ group containing nine patients with multiple positive mobilisation margins and no differences in adjuvant therapy. The favourable outcome is highlighted by a lack of difference in survival between the $R1_{Mobilisation}$ group and R0 cases. While the medial circumferential margin is a true transection margin, creation of the posterior margin or anterior surface, requires simple mobilisation of structures towards the midline. Anterior surface involvement has been previously shown to negatively impact upon outcome (274, 276), however, in the studied cohort, survival of this group was significantly better than $R1_{Transection}$ cases. Indeed, it has been suggested that anterior surface involvement should be assessed by a separate criterion with only tumour cells at this inked margin (not < 1 mm) counting (273).

It is clear from these data that $R1_{Transection}$ tumour presence has a deleterious impact on outcome compared to both $R1_{Mobilisation}$ and R0 cases. Consequently it is proposed that differentiation of $R1_{Posterior}$ from $R1_{Medial}$ involvement is paramount if these potential survival benefits are to be identified. Indeed, it has been shown that completion pancreatectomy for those with pancreatic body transection margin involvement can improve outcome (277). Additionally, routine use of an artery first approach (278) with intra-operative frozen sections could reduce the frequency of both pancreatic body transection and medial margin involvement. While inherent value is gained from accurate prognostic information for the individual, greater utility would be achieved if such information could be used to generate comparable cross-centre datasets and guide adjuvant therapy decisions. A recent meta-analysis of adjuvant therapy that considered marginal status concluded that while beneficial effects of chemotherapy were apparent in the R0 group this was not so for R1 cases (268). The rather low combined rate of R1 resections for this meta-analysis at 32% (18–83%) however, is in contrast with more recent standardised assessments including data generated by this work. Furthermore, a meta-analysis of radio-chemotherapy suggested that R1 cases experience survival benefit (279). If the efficacy of adjuvant therapy is indeed influenced by resection margin status then a standardised sampling and assessment technique is urgently required to ensure appropriate allocation of therapy in randomised control trials.

3.4.1 Summary

In conclusion, it has been demonstrated that the R1 rate in this cohort was 74% and it is an independent predictor of outcome. Furthermore, patients with $R1_{Mobilisation}$ tumour extension (posterior margin and anterior surface either singly or in combination) have a similar outcome to R0 resections, while true $R1_{Transection}$ involvement results in significant survival reduction. This is a single centre retrospective evaluation but should future validation of these findings occur in the form of a prospective protocol driven study, consideration of the $R1_{Mobilisation}$ group separately from those with $R1_{Transection}$ involvement may improve prognostication and serve to guide adjuvant therapy allocation with improved efficacy.

Figure 3.1 Prognostic influence of resection margin status

Intraoperative image of head of pancreas mobilisation

Creation of mobilisation margins: ***A)*** *Anterior surface and* ***B)*** *Posterior surface (without division of vascular or lymphatic structures).*

Pancreaticoduodenectomy specimen handling

C) *Pancreaticoduodenectomy resection specimen prior to formalin fixation illustrating the anterior pancreatic surface, medial margin including the SMV groove and pancreatic body transection margin. The smooth nature of the anterior pancreatic surface is in contrast to rough surface of the medial margin.*

D) *Inking of the specimen clearly identifies the medial resection margin including the SMV groove (yellow), which lies below the pancreatic body transection margin (blue) and separates the posterior resection margin (black) from the anterior pancreatic surface (green).*

E) *Illustration of* $R1_{Transection}$ *which includes medial and pancreatic body transection margins (broken line) and* $R1_{Mobilisation}$ *which includes anterior pancreatic surface and posterior margin (solid line).*

Kaplan-Meier survival curves following pancreaticoduodenectomy for PDAC

F) *Illustration of the survival benefit of an R0 resection in contrast to all other R1 resections. The median survival for the 39 R0 cases was 26.5 months compared to 15.4 months for the 109 R1 cases (Log-rank test, p = 0.011).*

G) *The median survival of the 48 R1 cases with mobilisation margin involvement* ($R1_{Mobilisation}$) *was 18.9 months compared to 11.1 months for the 61 R1 cases with transection margin involvement* ($R1_{Transection}$) ($p < 0.0001$). *There was no difference in survival when comparing* $R1_{Mobilisation}$ *with R0 resections (Log-rank test, p = 0.52).*

Figure 3.1

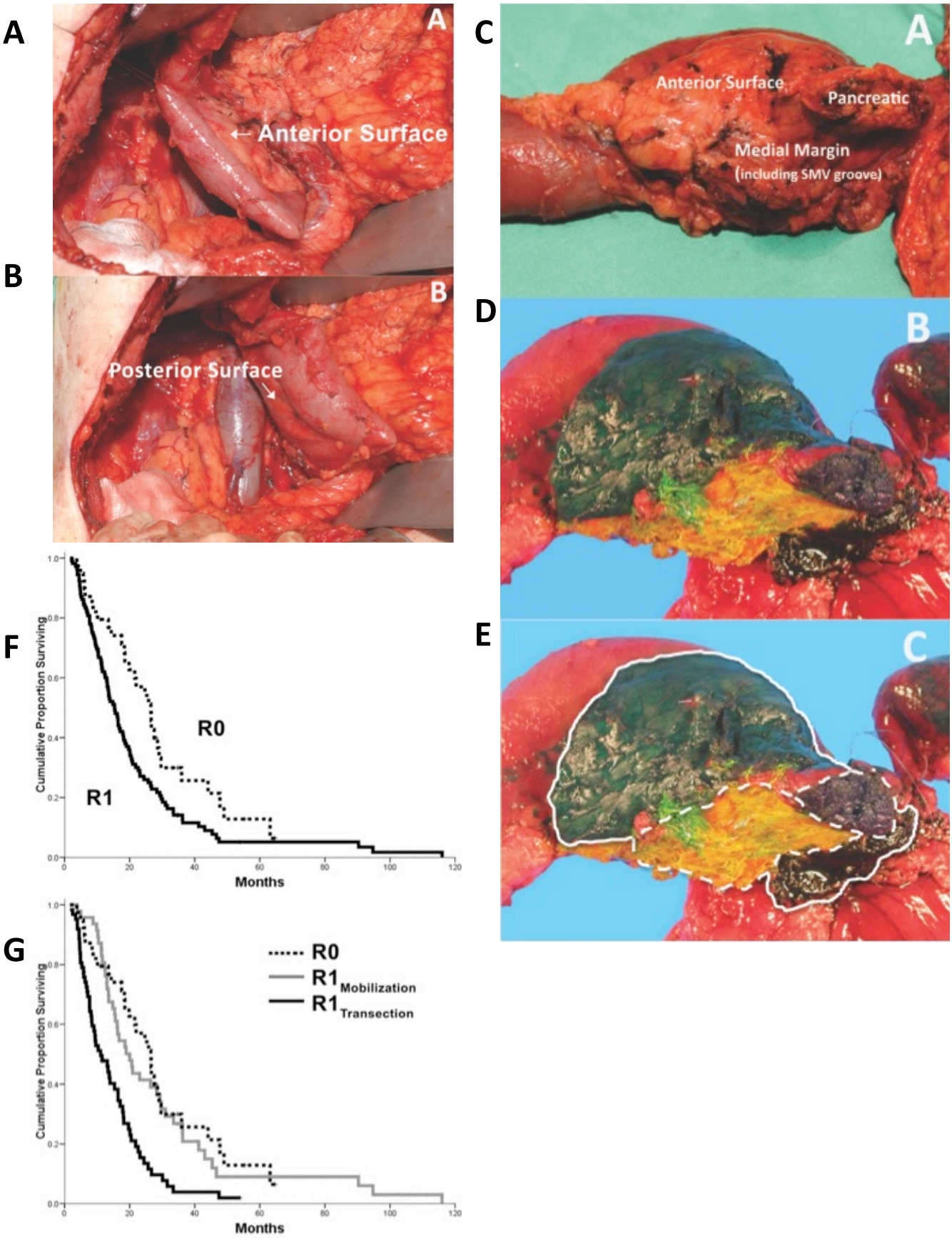
A
A
← Anterior Surface
B
B
Posterior Surface
C
A
Anterior Surface
Pancreatic
Medial Margin
(including SMV groove)
D
B
E
C
F
Cumulative Proportion Surviving
R0
R1
Months
G
Cumulative Proportion Surviving
R0
R1 Mobilization
R1 Transection
Months

Table 3.1 Demographic, operative, pathologic and treatment characteristics by resection margin status in 148 patients undergoing resection for PDAC

	No. (%) patients		
	R0 Resection	**R1 Resection**	**p value [a]**
Total No. of patients	39 (26.4)	109 (73.6)	
Gender			
Female	22 (56.4)	51 (46.8)	0.35
Male	17 (43.6)	58 (53.2)	
Age (yrs) [b]			
Median	65.1	64.1	0.31
Mean	63.8	61.8	
Range	41 - 77.1	40.2 - 77.6	
Tumour stage			
T2	5 (12.8)	9 (8.3)	0.53
T3	34 (87.2)	100 (91.7)	
Lymph node status			
N0	12 (30.8)	16 (14.7)	0.04
N1	27 (69.2)	93 (85.3)	
Tumour size (mm) [b]			
Median	28	30	0.16
Mean	29.1	33.3	
Range	5 - 55	15 - 65	
Tumour grade			
Low	24 (61.5)	75 (68.8)	0.43
High	15 (38.5)	34 (31.2)	
Perineural invasion			
No	4 (10.3)	7 (6.4)	0.48
Yes	35 (89.7)	102 (93.6)	
Venous invasion			
No	26 (66.7)	49 (45.0)	0.025
Yes	13 (33.3)	60 (55.0)	
Vascular resection			
No	36 (91.7)	94 (86.3)	0.40
Yes	3 (8.3)	15 (13.7)	
Adjuvant chemotherapy			
No	22 (56.5)	64 (58.7)	0.85
Yes	17 (43.5)	45 (41.3)	

[a] χ^2 tests were used to compare categorical variables.
[b] Mann-Whitney U test was used to compare continuous variables.

Table 3.2 Survival and relationship with clinicopathological characteristics in 148 patients undergoing PD for PDAC

Univariate analysis identifying significant prognostic factors.

Prognostic Variable	No. of Patients	Median Survival (months)	95% CI	p value [a]
Overall	148	17.6	14.7 - 19.4	-
Gender				
Female	73	18.2	14.8 - 21.5	0.11
Male	75	16.4	11.9 - 20.8	
Age (yrs)				
≤ 65	81	18.4	14.7 - 22.1	0.09
> 65	67	20.9	15.3 - 26.5	
Tumour stage				
T2	14	36.2	26.9 - 45.5	0.01
T3	134	16.2	13.4 - 19.3	
Lymph node status				
N0	28	21.8	2.8 - 40.8	0.01
N1	120	16.7	14.3 - 19.3	
Tumour size (mm)				
≤ 30	85	19.6	15.8 - 23.5	0.011
> 30	63	13.5	8.4 - 19.1	
Tumour grade				
Low	99	19.6	16.5 - 22.8	0.005
High	49	12.9	8.7 - 17.4	
Perineural invasion				
No	11	18.2	13.5 - 22.9	0.82
Yes	137	16.7	14.0 - 19.5	
Venous invasion				
No	75	20.9	15.8 - 26.1	0.005
Yes	73	15.4	12.1 - 18.6	
Resection margin status [b]				
R0	39	26.5	21.1 - 31.9	0.01
R1	109	15.4	13.0 - 17.8	
Vascular resection				
No	130	17.8	15.6 - 20.1	0.039
Yes	18	13.4	3.8 - 23.1	
Adjuvant chemotherapy				
No	86	14.8	9.9 - 19.7	0.37
Yes	62	18.0	14.4 - 21.7	

[a] p value according to Log-rank test

[b]

Mobilisation margins	No. (%)	Transection Margins	No. (%)
Posterior	48 (44.0)	Medial	50 (45.9)
Anterior surface	40 (36.7)	Pancreatic body	15 (13.7)
Duodenal surface	1 (0.9)	Bile duct	3 (2.7)
		Gastric	1 (0.9)
		Jejunal	0 (0)

Table 3.3 Survival relationship and resection margin status in 109 R1 resections

Margin Involvement	No. of cases (% of R1)	Median Survival (months)	95% CI	p value
Multiple margins				
1	63 (57.8)	16.8	14.6 - 18.9	[a]
2	39 (35.8)	12.3	10.0 - 14.6	
3 or more	7 (6.4)	8.4	7.9 - 9.0	
Mobilisation margin				
Posterior	21 (19.3)	28.3	12.3 - 44.8	0.25
Anterior surface	14 (12.8)	19.8	13.8 - 26.2	
Duodenal serosa	1 (0.9)	23.2	-	
Total mobilisation margins	48 (44.0)	18.9	13.1 - 24.8	< 0.001 [b]
Transection margin				
Medial	21 (19.3)	11.5	3.5 - 25.5	0.8
Pancreatic body transection	7 (6.4)	6.7	4.6 - 8.7	
Total transection margins [c]	61 (66.0)	11.1	7.1 - 15.1	
Tumour margin clearance				
At margin	84 (77.1)	13.9	10.8 - 17.1	0.81
Present within 1 mm	25 (22.9)	15.4	9.9 - 20.8	

[a] 1 margin versus 2 margins p = 0.049, 1 margin versus ≥ 3 margins p = 0.029, 2 margins versus ≥ 3 margins p = 0.121

[b] Log-rank test comparing total mobilisation margins ($R1_{Mobilisation}$) versus total transection margins ($R1_{Transection}$)

[c] All cases with transection margin involvement including synchronous mobilisation margin involvement

Table 3.4 Multivariate analysis including resection margin status in 148 patients

Prognostic Variable	Hazard Ratio	95% CI	p value
Age (yrs)			
≤ 65	1.00	-	0.12
> 65	1.34	0.93 - 1.94	
Tumour stage			
T2	1.00	-	0.01
T3	2.20	1.20 - 4.02	
Tumour size (mm)			
≤ 30	1.00	-	0.01
> 30	1.63	1.12 - 2.36	
Lymph node status			
N0	1.00	-	0.12
N1	1.51	0.91 - 2.51	
Resection margin status			
R0	1.00	-	0.009
R1	1.76	1.15 - 2.68	
Tumour grade			
Low	1.00	-	< 0.001
High	2.14	1.44 - 3.15	
Venous invasion			
No	1.00	-	0.38
Yes	1.18	0.81 - 1.72	
Vascular resection			
No	1.00	-	0.48
Yes	1.22	0.69 - 2.23	

Table 3.5 Summary of the studies evaluating the impact of margin status on survival

Study (ref)	Year	Study period	No. of Patients	R1 rate	R1 Survival (months) [a]	R0 Survival (months) [a]
Gall et al (280)	1991	1969-1987	260	17%	7	11
Willet et al (281)	1993	1978-1991	72	51%	12	20
Nitecki et al (282)	1995	1981-1991	172	16%	9	NA
Sperti et al (283)	1996	1970-1992	113	17%	7	14
Yeo et al (1)	1997	1990-1996	282	29%	10	18
Nishimura et al (284)	1997	1980-1995	157	45%	6	12
Millikan et al (285)	1999	1980-1997	75	29%	8	17
Sohn et al (266)	2000	1984-1999	616	30%	12	19
Benassai et al (286)	2000	1974-1995	75	20%	9	17
Neoptolemos et al (71)	2001	1994-2000	541	19%	11	17
Richter et al (287)	2003	1972-1998	194	37%	12	24
Wagner et al (2)	2004	1993-2001	165	24%	15	20
Kuhlmann et al (82)	2006	1992-2001	160	50%	10	16
Verbeke et al (93)	2006	1995-2003	26	85%	11	37
Winter et al (61)	2006	1970-2006	1175	42%	14	21
Raut et al (94)	2007	1990-2004	360	17%	22	28
Esposito et al (96)	2008	2005-2006	111	76%	15	22
Campbell et al (271)	2009	1997-2007	163	79%	14	25
Present Study	**2010**	**1996-2007**	**148**	**74%**	**15**	**27**

[a] Median survival (months)
NA, Not available

4 Peripancreatic Fat Invasion is an Independent Predictor of Poor Outcome Following Pancreaticoduodenectomy for PDAC

4.1 Introduction

Resection margin status and in particular the site of margin involvement appears to influence overall survival in PDAC. T stage correlates well with prognosis, however the prognostic impact of the different components determining T stage are less clear. In particular there is a lack of investigation of the influence of peripancreatic fat invasion. Therefore it is unclear whether local tumour invasion to each compartment constituting T3 stage progression (duodenum, bile duct and peripancreatic fat), carries with it equal prognostic impact.

Furthermore, in view of the variation in the reported frequency of resection margin involvement, investigation is required into the influence of R1 status and other pathological factors on recurrence pattern. In particular it may be proposed that spread into the surrounding adipose tissue could result in residual tumour in the pancreatic bed and hence negatively influence survival and associate with local recurrence.

4.1.1 Aim

In this chapter the influence of peripancreatic fat invasion on survival was investigated, furthermore the impact of clinicopathological factors including peripancreatic fat invasion on the pattern of primary recurrence was assessed.

4.2 Results

4.2.1 Clinicopathological characteristics of the patient cohort

As peripancreatic fat invasion could be assessed from standard H&E sections, the extended cohort available for analysis in this chapter (n = 189) covered the entire study period from 1992 until 2009 and is described in Table 2.1.

4.2.2 Peripancreatic fat invasion and relationship with clinicopathological characteristics

Detailed review of pathology specimens revealed that 51 (27%) patients had histological involvement of the peripancreatic fat (Figure 4.1A, B). During the study period the rate of peripancreatic fat invasion did not vary significantly being 29% prior to 2002 and 25% following this time. The relationship between clinicopathological and treatment characteristics of the cohort according to presence or absence of peripancreatic fat invasion is shown in Table 4.1. Excluding T stage, the only characteristics significantly associated with peripancreatic fat invasion were larger tumour size and lymph node metastasis. There was no significant difference in rate of peripancreatic fat invasion based on resection margin involvement. Of the 51 resections without evidence of resection margin involvement, 11 (22%) patients had histological evidence of peripancreatic fat invasion. For those patients identified as having peripancreatic fat invasion, 15 specimens (29%) showed evidence of

widespread adipose tissue invasion present at two or more locations. In 15 specimens (29%) it was present at the anterior or inferior aspect of the pancreas (six which had peripancreatic fat invasion adjacent to the common bile duct or ampulla), while 11 specimens (22%) had fat invasion near the medial/ SMV margin or the pancreatic transection region. In the remaining 10 specimens (20%) it was present at posterior or superior aspects.

4.2.3 Survival and relationship with clinicopathological characteristics

The factors significantly associated with poorer overall survival ($p < 0.05$, Log-rank test) were high T stage, tumour size > 30 mm, lymph node metastasis, high tumour grade, venous invasion, perineural invasion, R1 margin status, no adjuvant chemotherapy and peripancreatic fat invasion (Table 4.2).

4.2.4 Relationship between survival and determinants of T3 status including peripancreatic fat invasion

The presence of duodenal invasion (including spread to the ampulla) was not associated with a significant reduction in survival as shown in Table 4.2. The 86 (46%) patients with evidence of bile duct invasion had a shorter median survival compared to the 103 (55%) patients with no invasion; the median survival being 16.8 months (95%CI: 13.1–20.4) and 23.1 months (95%CI: 16.3–29.3) respectively ($p = 0.049$). The 51 (27%) patients with peripancreatic fat invasion had a significantly shorter overall survival compared to the 138 (73%) patients with no fat invasion, the median survival being 12.4 months (95%CI: 9.9–15.0) and 22.6 months (95%CI: 18.5–26.7) respectively ($p < 0.0001$) (Figure 4.1C). All survival comparisons were calculated using the Log-rank test.

4.2.5 Relationship between peripancreatic fat invasion, lymph node status, tumour size and survival

As peripancreatic fat invasion was related to lymph node involvement and more frequently present in larger tumours, survival was assessed according to both of these established prognostic markers stratified by the presence of peripancreatic fat invasion (Figure 4.1D, E). The presence of peripancreatic fat invasion had a significant negative impact on overall survival both for patients with lymph node involvement (median survival of 20.7 months [95%CI: 17.4–23.9] without fat invasion versus 13.3 months when fat invasion was present [95%CI: 10.4–16.2, $p = 0.035$]) and for those without lymph node metastases (median survival 36.6 months with no fat invasion [95%CI: 13.8–59.5] versus 10.1 months with fat invasion [95%CI: 1.9–17.1, $p = 0.012$]). Likewise peripancreatic fat invasion significantly negatively influenced the overall survival for patients with tumour size > 30 mm with a median survival of 20.0 months (95%CI: 14.1–25.9) versus 11.3 months (95%CI: 6.1–16.5, $p = 0.036$) when fat invasion was absent and present respectively. For those with tumours < 30 mm in size fat invasion significantly reduced overall survival with a median survival of 25.8 months (95% CI: 19.9–31.8) versus 13.3 months (95%CI: 11.0–15.6, $p = 0.014$) when

fat invasion was absent. While there was a trend towards peripancreatic fat invasion at the medial/SMV margin and transection margin being associated with a worse prognosis than other sites, sample size prevented more detailed analysis. All survival comparisons were calculated using the Log-rank test.

4.2.6 Relationship between fat invasion and adjuvant chemotherapy

For those patients receiving adjuvant therapy (n = 78), there was a range of five treatment options from both these studies, with 40 patients (51%) receiving 5-FU with folinic acid, 32 (41%) receiving gemcitabine, three (4%) receiving radiotherapy alone and three (4%) receiving 5-FU with radiotherapy. Of those who did not receive adjuvant therapy (n = 111), 11 (10%) were randomised to the observation arm of the ESPAC study. 4 patients (4%) were commenced on adjuvant chemotherapy however received only one cycle before suffering from complications. 2 patients (2%) had a previous malignant diagnosis (breast and colorectal) and so were not eligible for trial entry. 55 (50%) were considered unsuitable for randomisation on the basis of poor performance status, prolonged hospitalisation following resection or persistent pancreatic fistula. The remaining 39 (35%) patients declined randomisation.

There was a non-significant trend towards adjuvant chemotherapy being used less frequently in those patients with no peripancreatic fat invasion ($p = 0.15$, χ^2 test). Adjuvant radiotherapy was only rarely used in these patients, as its routine use was not supported by the outcome of the original ESPAC-1 study (251). Certainly adjuvant chemotherapy in any form provides a significant survival benefit within this cohort of PDAC (Table 4.2) ($p = 0.014$). For the 138 patients without peripancreatic fat invasion, when all chemotherapy regimens were combined, there was no significant improvement in outcome ($p = 0.41$). Subsequent analysis revealed that those patients receiving adjuvant gemcitabine (n = 27) did survive significantly longer (median overall survival 27.6 months, 95%CI: 21.3–33.4]) than those receiving 5-FU combinations (22.6 months, 95%CI: 15.9–29.2, $p = 0.048$) or no adjuvant therapies (19.8 months, 95%CI: 17.9–21.6, $p = 0.01$). Adjuvant chemotherapy (both 5-FU/ gemcitabine regimens) did significantly improve overall survival when employed in patients with peripancreatic fat invasion (median survival for patients receiving chemotherapy 16.2 months [95%CI: 11.7–20.7] versus 11.6 months [95%CI: 9.3–13.8] without adjuvant therapy, $p = 0.015$). All survival comparisons were calculated using the Log-rank test.

4.2.7 Peripancreatic fat invasion: multivariate analysis

Covariates that affected survival at the $p < 0.05$ level of significance were included in a multivariate Cox proportional-hazards model (Table 4.3). Factors that independently adversely affected overall survival were high tumour grade, higher tumour stage, lymph

node involvement, venous invasion, resection margin involvement and the histological presence of peripancreatic fat invasion (HR: 1.93, 95%CI: 1.18–3.45, p = 0.007). Adjuvant chemotherapy was associated with prolonged survival following resection.

Multivariate survival analysis was repeated including only T3 tumours (n = 171) (Table 4.4). Within this model peripancreatic fat invasion again independently negatively influenced survival (HR: 1.93, 95%CI: 1.18–3.45, p = 0.009) as did high grade, venous invasion and R1 status. Although adjuvant therapy continued to provide independent survival benefits following resection for the T3 only cohort, lymph node involvement was no longer an independent predictor of poor outcome (HR: 0.61, 95%CI: 0.40–0.95).

4.2.8 Impact of clinicopathological factors on disease recurrence

The median follow-up for censored patients was 25.8 months (95%CI: 19.0–32.5) and for all patients including those who had died, was 21.4 months (95%CI: 17.2–23.7). During the study period recurrent disease occurred in 144/189 patients (76%). Distant metastases (including liver and lung) occurred in 78 patients (54%) with 66 (46%) developing locoregional recurrence. Among the entire cohort, univariate analysis revealed that lymph node status and peripancreatic fat invasion were associated with local recurrence (Table 4.5). By multivariate analysis, only peripancreatic fat invasion (HR: 2.95, p < 0.001) remained independently associated with local recurrence. Further χ^2 test analysis revealed that recurrent disease was identified in 105/138 (76%) patients who had no evidence of peripancreatic fat invasion and in 39 (76%) patients who had evidence of peripancreatic fat invasion following resection (Table 4.6). Peripancreatic fat invasion affected the site of first recurrence, with 50.9% (26/51) of patients with locoregional recurrence in those tumours exhibiting peripancreatic fat invasion representing a significantly greater proportion than in the 29% (40/138) of patients whose tumours had no evidence (p = 0.002). High tumour grade was associated with distant metastases being the primary site of recurrence, with distant metastases developing in 53% (33/62) of those with high-grade tumours compared to 38% (48/126) of those with low-grade tumours. Resection margin status, perineural invasion, venous invasion, tumour size or use of adjuvant chemotherapy failed to impact on the pattern of recurrence following PD.

4.3 Discussion

While spread of tumour to the peripancreatic tissue including adipose tissue, upgrades the lesion from T2 to T3 disease, the individual prognostic influence of peripancreatic fat invasion has not previously been investigated following PD for PDAC. As discussed in the previous chapter progress has been made towards the redefinition of the pathology terminology associated with pancreatic resection margins and retroperitoneal spread (93,

270, 272). It was proposed therefore to determine the relationship of peripancreatic fat invasion with prognosis and its influence on the pattern of failure.

In the present chapter, peripancreatic fat invasion was evident in 27% of tumours. Peripancreatic fat invasion was associated significantly with larger tumours; however, it was a rare finding in the absence of lymph node metastases. It was demonstrated that peripancreatic fat invasion was significantly and independently associated with poorer survival (12.4 versus 22.6 months). The two other determinants of T3 disease are duodenal and common bile duct spread and while there was a trend towards poor survival in the latter group, this was not an independent prognostic factor. While the majority of tumours resected for PDAC are T3 (61), a figure supported by the current study, it was demonstrated that T3 categorisation has a spectrum of outcomes based upon the site of peripancreatic spread. Despite the association of peripancreatic fat invasion and lymph node involvement, it was demonstrated that even in those cases where adipose invasion was identified in the LN0 group, this associated with a significant survival reduction. If these results are confirmed then reclassification of the current pathological staging system (T3a and T3b) to account for this powerful prognostic factor may be appropriate.

Data on both patterns of failure and factors associated with disease recurrence following PD remain poorly defined. Distant recurrence is presumed to occur in the majority following potentially curative resection (94, 103) and this fact combined with the overall poor survival, results in the issue of local recurrence being largely ignored. Locoregional recurrence can have important clinical implications notably severe pain along with biliary and GI tract obstruction. Indeed when the pattern of recurrence was investigated in advanced PDAC according to a protocol of immediate autopsy to obtain primary and metastatic tissue, 12% showed no evidence of metastatic disease (265).

The incidence of local recurrence varies greatly in the literature. In terms of the pattern of failure in the present study, there was a slight excess of the first site of failure being distant metastases including liver (54%) compared to locoregional failure (46%). Some report locoregional recurrence rates from 50%–80%. In contrast, other studies in which the majority of patients received adjuvant chemo-radiotherapy have noted a lower risk of local recurrence (71, 94, 100, 103, 288, 289). In particular those studies utilising radiotherapy have noted local recurrence rates of 10–40%. In the present study although 74 patients received adjuvant therapy, only two patients received adjuvant radiotherapy.

Identification of patients who are at higher risk of local recurrence may be important. Factors previously correlated with pattern of recurrence include, a high degree of lymph node disease burden relating to local recurrence in N1 resection (103), although margin status failed to reach significance when adjustment was made for lymph node status. Margin

status did not significantly impact upon pattern of recurrence in a study of 360 patients treated by PD, which reported locoregional recurrence in 16.7% of R0 versus 13.4% of R1 resections (94). Peripancreatic fat invasion was found to associate with the pattern of recurrence, with invasion into the surrounding adipose tissue resulted in a significantly increased proportion of locoregional recurrence compared to those with no involvement of the peripancreatic fat (51.0% versus 28.9% respectively, $p = 0.002$). While many of the clinicopathological factors including resection margin status and lymph node status were not found to be associated with the site of primary recurrence, high-grade tumours were associated with recurrence at a distant site. This finding is in contrast to the findings of Asiyanbola and co-workers who identified high-grade tumours being associated with local recurrence (103). Regarding resection margin status, the discrepancy of R1 rates between recent studies and previous investigations (Table 3.5) may influence the association between patterns of failure and requires reassessment in future studies.

The identification of peripancreatic fat invasion at the time of assessment of resectability could potentially identify a group at high risk of locoregional recurrence and poor survival. In terms of preoperative imaging, dynamic enhanced MRI has a sensitivity and specificity equal to or better than that of helical CT for the detection of local tumour extension and vascular involvement (290). MRI was recently shown to demonstrate extrapancreatic neural plexus invasion successfully in patients with resected PDAC (291). 80% of patients with pathological proof of extrapancreatic neural plexus invasion had abnormal signal intensity in background fat on MRI. Unfortunately MRI was not available for all patients to enable correlation between preoperative macroscopic and microscopic appearance in the current study.

In a recent study, the term “isolated solitary ductal unit” described clusters of cancer cells forming solitary ducts completely surrounded by adipose tissue without accompanying acini, islets or fibrosis and appear to be a reliable indicator of adenocarcinoma (292). The identification of such cell clusters distant from the tumour bulk in the adipose tissue has implications for tumour size and margin characterisation. Identified in approximately 50% of resections a number of tumours were subsequently upstaged (T1 to T3). Certainly while this finding was of interest it requires validation, furthermore, no attempt was made to correlate the presence of “isolated solitary ducts” with outcome. The current cohort was not assessed for “isolated solitary ducts”, but as the reported rate was greater than direct extension of tumour into the adipose identified in the present study, recognition of these structures may further stratify outcome.

Evidence that the presence of increased intra-pancreatic fat is associated with poor outcome and disseminated disease was recently demonstrated in a case controlled analysis of 40

PDACs (293). The authors report that increased pancreatic fat may itself be a contributing factor to PDAC's aggressive phenotype. Great focus has been placed upon the role of the tumour microenvironment in PDAC tumourigenesis including inflammatory mediators, stellate cells and myofibroblasts (294). Potentially adipocytokines including leptin and adiponectin, produced as a result of tumour infiltration may influence the inflammatory milieu and contribute to the tumour microenvironment, enhancing PDAC tumourigenesis, as demonstrated in colorectal cancer (295).

A recent study identified that high total body adiposity (body mass index [BMI] > 35) correlated with an increased incidence of lymph node positivity (296). However, this finding was not corroborated in a recent larger study (297), and so the influence of adipose tissue on tumour progression remains unclear. BMI is a crude measure of adiposity therefore more accurate assessments of total body fat (cross sectional imaging), are required to answer whether total body, peri- or intratumoural adiposity influences tumour aggressiveness.

It is acknowledged that the present study has a number of limitations. Notably the cohort had a relatively low rate of adjuvant chemotherapy and this may explain why the presence of pancreatic fat invasion was associated with locoregional recurrence. Clearly this is the first study to identify the independent prognostic significance of pancreatic fat invasion and therefore the findings require validation in a further cohort, in particular the study should be repeated in a cohort receiving standardised adjuvant therapy. While the data regarding tumour recurrence was collected prospectively from 1999, evidence of local recurrence was based upon follow-up CT scan imaging and therefore there is potential for incorrect designation.

4.3.1 Summary

The results of this chapter demonstrate that the presence of peripancreatic fat invasion assessed by histological examination following PD for PDAC in 189 patients provides independent prognostic information in addition to the categorisation of T3 disease and other clinicopathological factors including resection margin status. Additionally, the presence of peripancreatic fat invasion, but not resection margin involvement, was associated with locoregional disease as the primary site of recurrence. Modification of future staging systems to improve outcome stratification may be justified if these findings are replicated. Furthermore, there is potential for this poor prognostic factor to be identified preoperatively by advanced cross sectional imaging techniques.

Table 4.1 Patient and tumour characteristics stratified by peripancreatic fat invasion

	No. (%) patients		
	Peripancreatic Fat Invasion		
	Absent	**Present**	**p value [a]**
Total No. of patients	138 (26.4)	51 (73.6)	
Gender			
Female	64 (46.4)	21 (41.2)	0.513
Male	74 (53.6)	30 (58.8)	
Age (yrs) [b]			
Median	63.6	64.8	0.289
Mean	62.2	64.2	
Range	37.4 - 77.6	38.9 - 86.0	
Tumour stage			
T2	18 (13.0)	0 (0)	0.001
T3	120 (87.0)	51 (100)	
Tumour size (mm) [b]			
Median	30.0	35	0.045
Mean	31.7	36.1	
Range	5 - 65	15 - 60	
Tumour grade			
Low	93 (67.4)	34 (66.7)	0.925
High	45 (32.6)	17 (33.3)	
Lymph node status			
N0	34 (24.6)	3 (5.8)	0.004
N1	104 (75.4)	48 (94.2)	
Margin involvement			
R0	40 (28.9)	11 (21.5)	0.359
R1	98 (71.1)	40 (78.5)	
Perineural invasion			
No	13 (9.4)	3 (5.9)	0.564
Yes	125 (91.6)	48 (94.1)	
Venous invasion			
No	74 (53.6)	21 (41.2)	0.129
Yes	64 (46.4)	30 (58.8)	
Vascular resection			
No	117 (84.7)	41 (80.4)	0.469
Yes	21 (15.3)	10 (19.6)	
Adjuvant therapy			
No	79 (57.2)	35 (68.6)	0.145
Yes	59 (42.8)	16 (31.4)	

[a] χ^2 tests were used to compare categorical variables.
[b] Mann-Whitney U test was used to compare continuous variables.

Table 4.2 Survival and relationship with clinicopathological characteristics in 189 patients undergoing PD for PDAC

Univariate analysis identifying significant prognostic factors.

Prognostic Variable	No. of Patients	Median Survival (months)	95% CI	p value [a]
Overall	189	18.9	15.7 – 22.2	-
Gender				
Female	86	20.4	16.1 – 24.7	0.072
Male	103	17.8	13.5 – 22.2	
Age (yrs)				
≤ 65	104	18.2	14.8 – 21.6	0.081
> 65	85	21.9	14.9 – 29.1	
Tumour stage				
T2	18	36.2	17.5 – 54.9	0.002
T3	171	17.8	15.0 – 20.7	
Peripancreatic fat invasion				
Absent	138	22.6	18.5 – 26.7	0.0001
Present	51	12.4	9.9 – 15.0	
Duodenal invasion				
Absent	60	22.3	15.4 – 29.8	0.155
Present	129	17.8	14.2 – 21.4	
Bile duct invasion				
Absent	103	23.1	16.3 – 29.3	0.049
Present	86	16.8	13.1 – 20.4	
Lymph node status				
N0	37	35.9	13.7 – 58.1	0.002
N1	152	18.4	15.6 – 21.1	
Tumour size (mm)				
< 30	98	21.8	15.8 – 27.8	0.022
≥ 30	91	16.2	11.7 – 20.6	
Tumour grade				
Low	127	21.8	16.8 – 26.8	0.028
High	62	13.1	9.0 – 17.2	
Perineural invasion				
Absent	16	18.2	13.5 – 22.9	0.023
Present	173	16.7	14.0 – 19.5	
Venous invasion				
Absent	94	24.7	18.3 – 31.1	0.001
Present	95	15.6	12.9 – 18.2	
Resection margin status				
R0	51	27.5	23.8 – 31.2	0.0001
R1	138	16.2	13.0 – 19.3	
Vascular resection				
No	158	19.8	16.1 – 23.5	0.056
Yes	31	13.4	7.02 – 19.9	
Adjuvant therapy				
No	114	14.8	9.7 – 19.8	0.021
Yes	75	21.9	16.9 – 26.9	

[a] p value according to Log-rank test

Table 4.3 Predictors of survival in 189 patients following PD - multivariate analysis

		Overall survival	
Prognostic variable	**Category**	**HR (95% CI)**	**p value**
Tumour stage	T2/ T3	2.45 (1.30 - 4.62)	0.006
Peripancreatic fat invasion	Absent/ Present	1.93 (1.18 - 3.45)	0.007
Bile duct invasion	Absent/ Present	1.11 (0.78 - 1.59)	0.542
Tumour size (mm)	<30/ ≥ 30	1.29 (0.89 - 2.15)	0.172
Lymph node status	Absent/ Present	1.89 (1.11 - 3.31)	0.025
Tumour grade	Low/ High	1.80 (1.25 - 2.61)	0.002
Perineural invasion	Absent/ Present	1.27 (0.53 - 3.04)	0.586
Venous invasion	Absent/ Present	1.42 (1.01 - 2.08)	0.045
Margin involvement	R0/ R1	1.91 (1.24 - 2.92)	0.003
Vein resection	No/ Yes	0.96 (0.57 - 1.63)	0.906
Adjuvant therapy	No/ Yes	0.61 (0.41 - 0.90)	0.014

Table 4.4 Predictors of survival in 171 T3 patients following PD - multivariate analysis

		Overall survival	
Prognostic variable	**Category**	**HR (95% CI)**	**p value**
Peripancreatic fat invasion	Absent/ Present	1.61 (1.11 - 2.58)	0.009
Bile duct invasion	Absent/ Present	1.09 (0.76 - 1.58)	0.625
Tumour size (mm)	<30/ ≥ 30	1.43 (0.99 - 2.08)	0.056
Lymph node status	Absent/ Present	1.45 (0.89 - 2.81)	0.102
Tumour grade	Low/ High	1.89 (1.29 - 2.79)	0.001
Venous invasion	Absent/ Present	1.49 (1.03 - 2.17)	0.033
Margin involvement	R0/ R1	1.86 (1.19 - 2.87)	0.006
Vein resection	No/ Yes	0.94 (0.55 - 1.61)	0.824
Adjuvant therapy	No/ Yes	0.63 (0.40 - 0.95)	0.038

Table 4.5 Factors associated with local recurrence following PD in 189 patients

Factors associated with local recurrence following resection: univariate and multivariate analysis.

	Univariate			Multivariate		
Prognostic variable	**Hazard Ratio**	**95% CI**	**p value**	**Hazard Ratio**	**95% CI**	**p value**
Tumour stage						
T2		-				
T3	1.95	0.77 – 4.89	0.155	-	-	-
Peripancreatic fat invasion						
Absent		-				
Present	3.31	1.92 – 5.70	< 0.001	2.95	1.71 – 5.10	< 0.001
Duodenal invasion						
Absent		-				
Present	1.04	0.61 – 1.75	0.884	-	-	-
Bile duct invasion						
Absent		-				
Present	1.20	0.72 – 1.99	0.472	-	-	-
Lymph node status						
N0		-				
N1	2.29	1.04 – 5.02	0.038	1.63	0.71 – 3.74	0.235
Tumour size (mm)						
≤ 30		-				
> 30	1.46	0.88 – 2.43	0.137	-	-	-
Tumour grade						
Low		-				
High	0.86	0.48 – 1.54	0.616	-	-	-
Perineural invasion						
Absent		-				
Present	0.43	0.13 – 1.40	0.163	-	-	-
Venous invasion						
Absent		-				
Present	1.47	0.87 – 2.47	0.144	-	-	-
Resection margin status						
R0		-				
R1	1.49	0.82 – 2.73	0.192	-	-	-
Adjuvant therapy						
No		-				
Yes	0.84	0.49 – 1.42	0.510	-	-	-

Table 4.6 Pattern of recurrence stratified by A) fat invasion and B) tumour grade

	Peripancreatic Fat Invasion		
A	**Absent n = 138 (%)**	**Present n = 51 (%)**	**p value [a]**
Site of first recurrence			
Liver/ distant metastases	65 (47.1)	13 (25.5)	0.002
Locoregional	40 (28.9)	26 (51.0)	
No Recurrence	33 (24.0)	12 (23.5)	0.889

	Tumour Grade		
B	**Low n = 126 (%)**	**High n = 62 (%)**	**p value [a]**
Site of first recurrence			
Liver/ distant metastases	48 (38.1)	33 (53.2)	0.041
Locoregional	47 (37.3)	16 (25.8)	
No Recurrence	32 (24.6)	13 (20.9)	0.813

[a] χ^2 tests were used to compare categorical variables

Figure 4.1 Prognostic influence of peripancreatic fat invasion

Illustrations of PDAC invading into the peripancreatic fat

A) *Low power image of fibro-fatty tissue containing infiltrating adenocarcinoma (black arrows).* ***B)*** *Higher power image of individual infiltrating ductal structures (black arrows). (Both haematoxylin-and-eosin).*

Kaplan-Meier survival curves for PDAC following PD – influence of peripancreatic fat invasion

C) *Illustration of the survival benefit associated with an absence of peripancreatic fat invasion in contrast to a resection with evidence of pancreatic fat invasion. The median survival for the 138 patients with no peripancreatic fat invasion was 22.6 months compared to 12.4 months for the 51 patients with fat invasion (Log-rank test, p = 0.0001).*

Kaplan-Meier survival curves interaction of lymph node status and tumour size with peripancreatic fat invasion

D) *Lymph node status stratified by peripancreatic fat invasion with peripancreatic fat invasion significantly reducing the survival for patients with lymph node negative resections. The overall median survival for LN0 patients with no fat invasion was 36.6 months, significantly longer than for LN0 patients with fat invasion (p = 0.012, Log-rank test). LN1 patients with fat invasion patients survived significantly longer (median survival of 20.7 months, 95%CI: 17.4–23.9) compared with LN1 patients with no fat invasion patients (median survival of 13.3 months, 95%CI: 10.4–16.2, p = 0.035, Log-rank test).*

E) *Tumour size stratified by peripancreatic fat invasion with peripancreatic fat invasion significantly reducing survival even when tumour is less than 30 mm in size. For patients with tumour size > 30 mm with no fat invasion the overall median survival was 20.0 months (95%CI: 14.1–25.9) versus 11.3 months (95%CI: 6.1–16.5, p = 0.036) when fat invasion was present (p = 0.036, Log-rank test). For small tumours fat invasion significantly reduced overall survival with a median survival of 25.8 months (95% CI: 19.9–31.8) versus 13.3 months (95%CI: 11.0–15.6, p = 0.014, Log-rank test) when fat invasion was absent.*

Figure 4.1

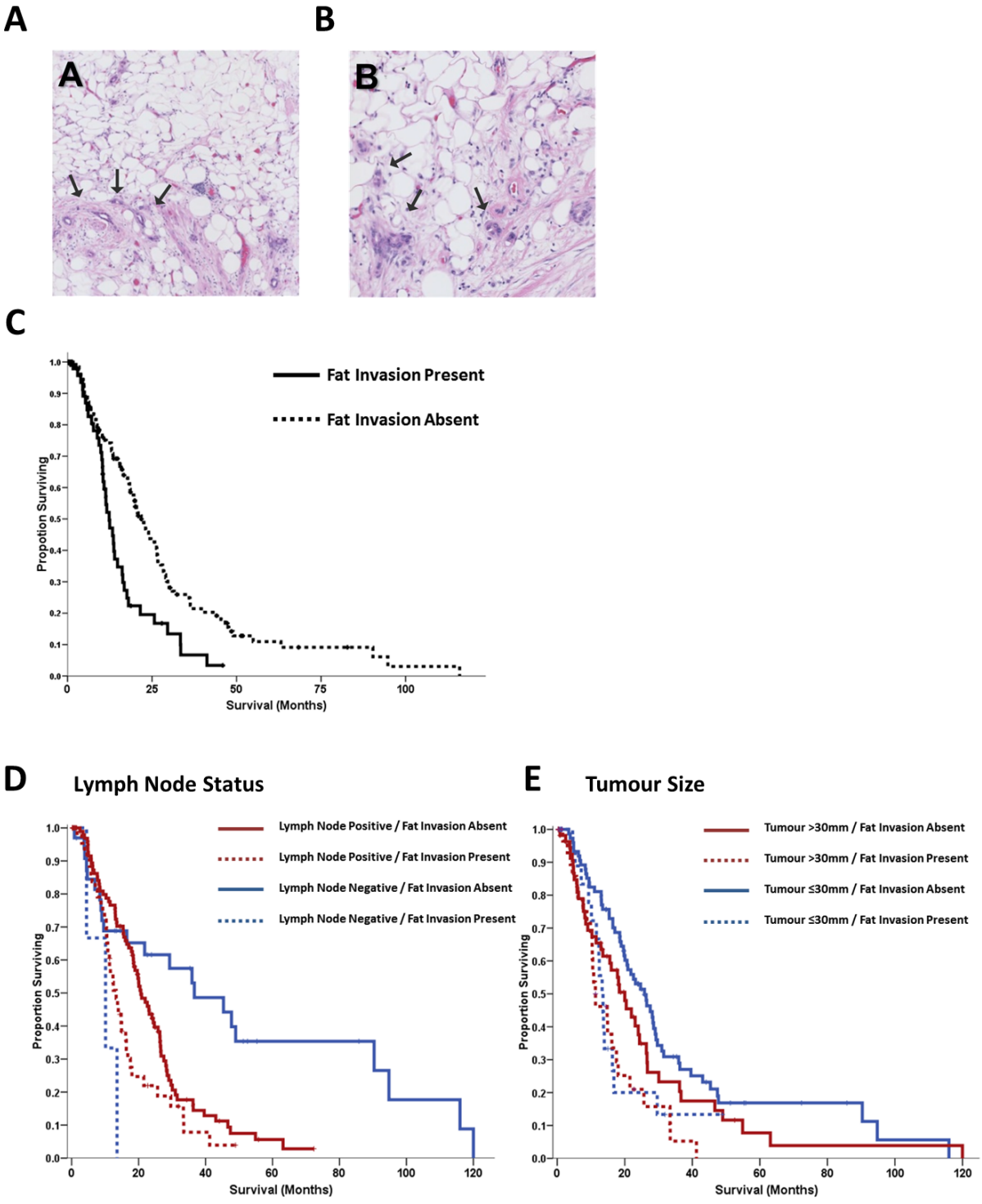
A
B
A
B
C
Fat Invasion Present
Fat Invasion Absent
Propotion Surviving
Survival (Months)
D
Lymph Node Status
Lymph Node Positive / Fat Invasion Absent
Lymph Node Positive / Fat Invasion Present
Lymph Node Negative / Fat Invasion Absent
Lymph Node Negative / Fat Invasion Present
Proportion Surviving
Survival (Months)
E
Tumour Size
Tumour >30mm / Fat Invasion Absent
Tumour >30mm / Fat Invasion Present
Tumour ≤30mm / Fat Invasion Absent
Tumour ≤30mm / Fat Invasion Present
Proportion Surviving
Survival (Months)

5 Tissue Biomarkers Associated With Prognosis in PDAC

5.1 Introduction

As discussed in the previous chapters, clinicopathological factors determined at PD establish risk stratification for patients with PDAC (61, 83, 84). Unfortunately, these factors alone do not account for all the observed variability in outcome. A need therefore exists for superior markers of prognosis to potentially enhance management of operable PDAC. Molecular analysis is one source of such clinically useful biomarkers. Indeed, tumours with similar clinicopathological characteristics can be shown to contain molecular aberrations, which may underpin some variances in clinical behaviour, as demonstrated in pancreatic as well as other cancers (3, 4, 169, 298).

A comprehensive review and meta-analysis of IHC based prognostic biomarkers following PDAC resection was performed (presented in part in this chapter) (299). While reviews have been published on the prognostic utility of IHC markers in PDAC (249, 300), the meta-analysis assessed the available data according to the REporting recommendations for tumour MARKer prognostic studies (REMARK) guidelines (301). The meta-analysis sought to determine candidate biomarkers for which there were sufficient evidence to support prospective validation in a controlled environment or the need for additional investigation due to insufficient rigor in the previous studies. Furthermore, it aimed to identify functional pathways potentially involved with PDAC prognosis prediction.

The search of the PDAC IHC prognostic literature yielded 1992 manuscripts (Figure 5.1A) of which 378 manuscripts were assessed. 83 high-quality cohort studies from 34 research groups met the eligibility criteria by presenting multivariable survival estimates for differential levels of candidate protein expression in operative cohorts. 21 clinicopathological factors were incorporated in one or more of the included studies' multivariate analyses. The most commonly included prognostic factor was lymph node involvement (Figure 5.1B). The frequency of clinical covariate integration is shown in Figure 5.1C. The 83 studies present data on 103 unique proteins, for 89 of which a multivariate HR and associated 95%CI were available from a single study only. For the remaining 14 markers, outcome data were available from two or more studies and could be combined to give a single summary statistic (299). The proteins evaluated for overall survival were sorted according to Hanahan-Weinberg functional capabilities of cancer (302), modified to include pancreatic differentiation markers, immunocompetence and markers associated with DNA damage repair and chemotherapeutic metabolism (Table 11.4). 84% of the candidate markers demonstrated a significant association with outcome ($p < 0.05$).

In summary, based on functional capabilities, markers facilitating invasion and metastases were most likely to be associated with prognosis. In total 21 markers were significantly associated with overall survival, however all were identified in single studies except for E-

cadherin for which data from two studies were included. Despite numerous studies investigating catenins none were eligible for analysis. Regulators of angiogenesis were also highlighted. The few markers related to pancreatic development yielded prognostic relevance, however the Wnt signalling pathway, vital in embryogenesis and GI cancer development, was underrepresented.

Rather than targeting a single marker, which potentially only evaluates marginal effects of proteins on prognosis, multi-marker phenotypes, defined here as combinations of clinicopathological and/ or tumour markers, may better identify prognostic sub-groups. 11/83 studies assessed the prognostic utility of multiple-markers. Notably, apoptotic marker combinations were more powerful than single protein evaluation (119) while Bcl-2 and lymph node status combined were more powerful than pathological status alone (303).

Certainly if clinically useful prognostic biomarkers for PDAC are to be achieved, the collective research community should address the persistence of incomplete adoption of the 2005 REMARK guidelines (301). The studies evaluating IHC markers in PDAC are generally limited in terms of power and with a failure to control consistently for clinicopathological factors. Therefore a need exists for the evaluation of these markers in a large dataset of PDAC patients with complete and mature follow-up.

5.1.1 Aim

To further elucidate the prognostic utility of signalling pathways in PDAC following PD, the relationship of candidate biomarkers with overall survival was assessed in a large PDAC TMA cohort using IHC. Selection of the best-evidenced markers biomarkers was based primarily upon findings from the systematic review (299) selected with the aim of testing their prognostic utility in a large cohort. To assist in the data presentation, the candidate markers' correlation with clinicopathological features and prognosis were made according to biological functional groupings: senescence, apoptosis, angiogenesis, invasion and metastasis, insensitivity to growth inhibition and self-sufficiency for growth signals. The primary goal was to determine whether these most evidenced markers associated independently with overall survival adjusting for clinicopathological features. Secondly, the study aimed to assess the cross-sectional relationship amongst individual markers. The final aim was to combine marker expression in a multi-marker phenotype, in an attempt to describe discrete subpopulations of patients based on protein expression, as a means to assess the relationship between the expression of functional groups of proteins and prognosis.

Figure 5.1 Manuscript selection algorithm and meta-analysis study characteristics

A) *Flow diagram of the literature search and selection of included studies.*
B) *Frequencies with which adjustments were made for various clinicopathological parameters.*
C) *Distributions of the total number of clinicopathological covariates that were adjusted for across the 83 eligible cohort studies.*

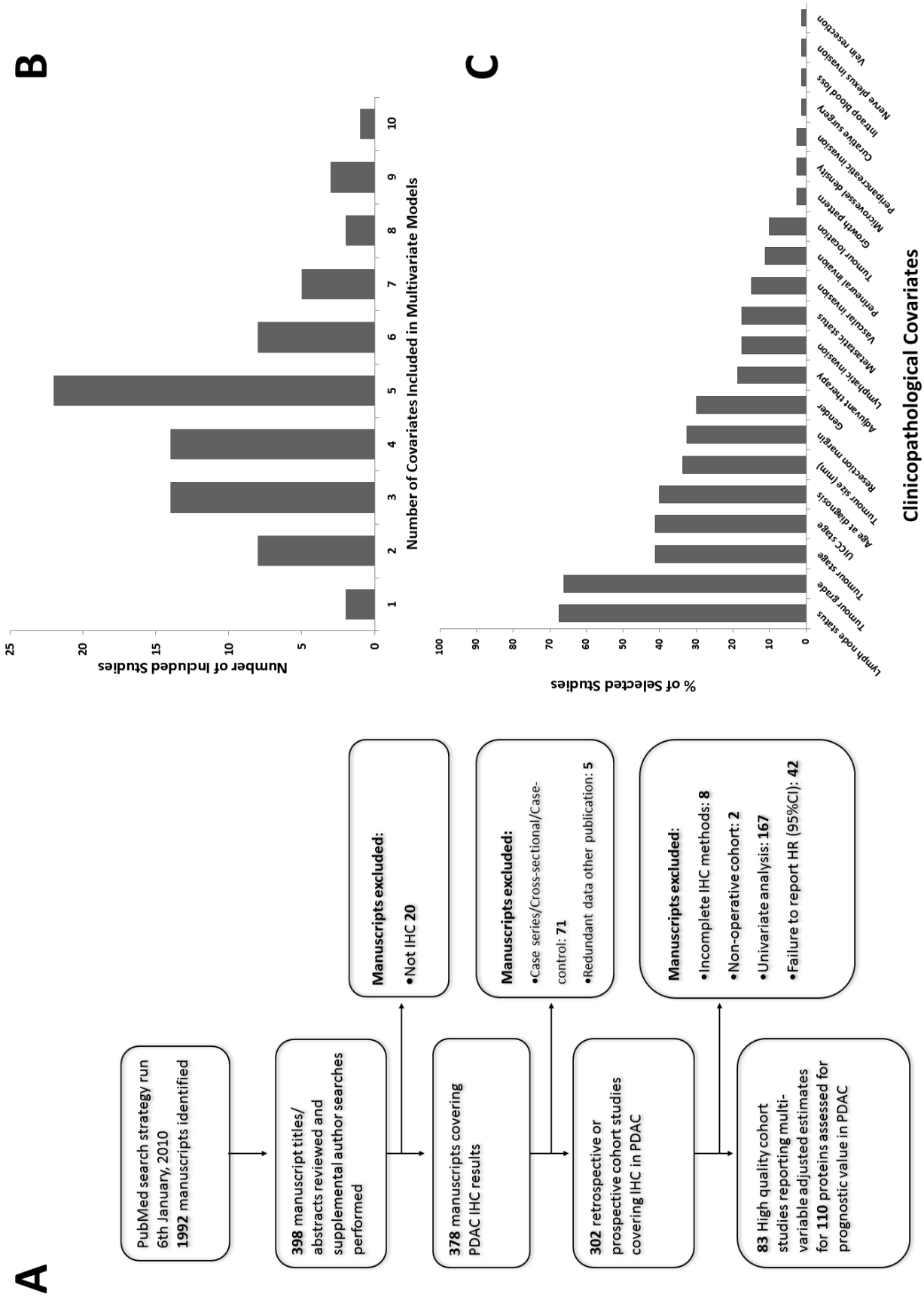

Figure 5.2 Algorithm for integrating protein expression and clinicopathological data

The prognostic relevance of a selection of protein biomarkers assessed within the tissue microarray cohort. The markers were grouped by functional characteristics. Association with other proteins, pathological features and survival was determined. An attempt was made to cluster the patients according to protein expression to potentially determine a multimarker phenotype.

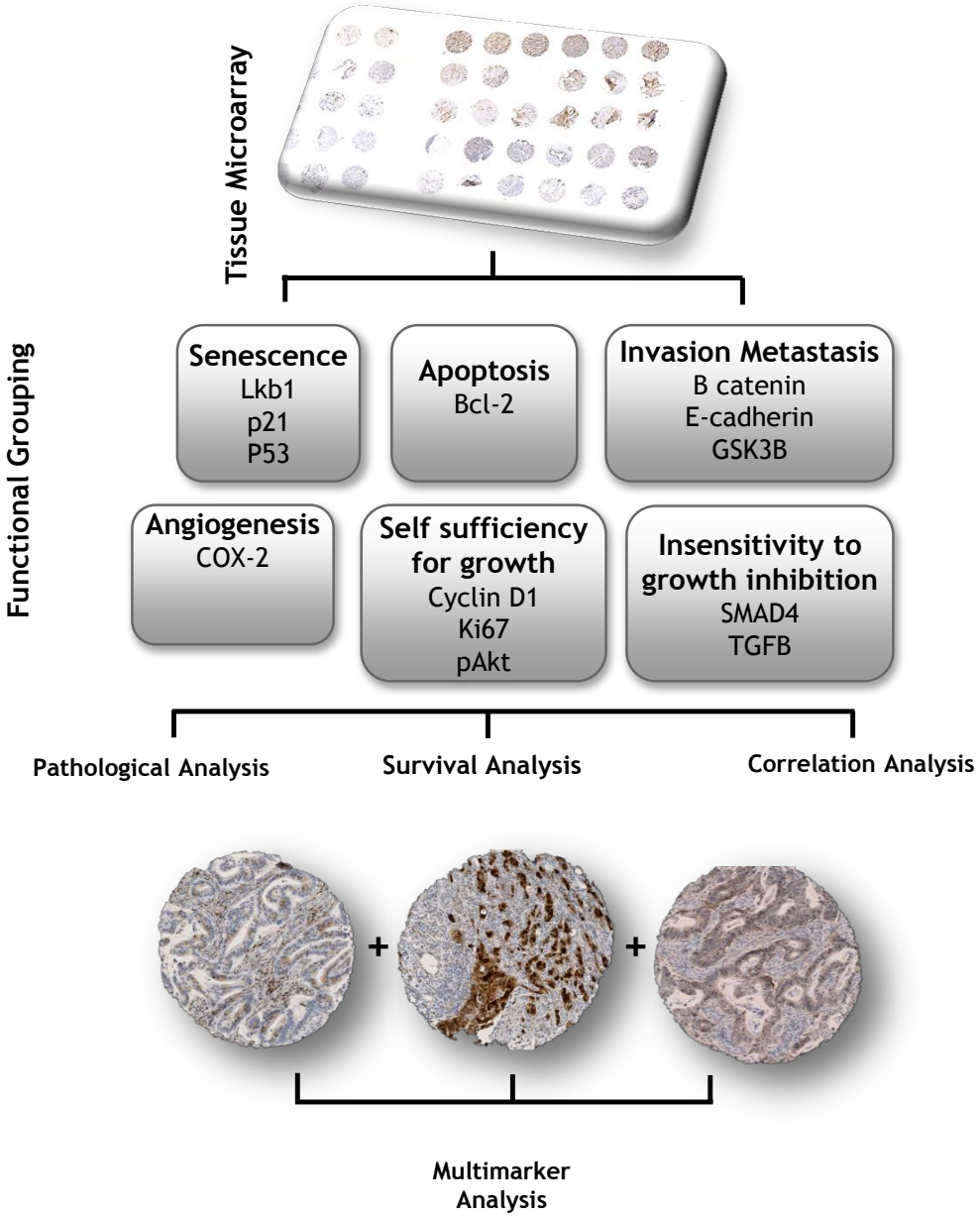

Table 5.1 Univariate survival analysis of factors affecting outcome in TMA cohort

Clinicopathological determinants of outcome in 119 patients with PDAC studied within the TMA cohort.

			Overall Survival		
Prognostic variable		**Patients (%)**	**Median (months)**	**95% CI**	**p value [a]**
Gender	Female	59 (49.0)	20.4	15.5 - 25.4	0.121
	Male	60 (51.0)	18.0	13.8 - 22.3	
Age (yrs)	≤ 65	64 (53.7)	18.1	13.6 - 20.5	0.104
	> 65	55 (46.2)	21.9	14.9 - 29.0	
Tumour stage	T2	13 (10.9)	36.2	17.5 - 54.9	0.002
	T3	106 (89.1)	17.6	14.5 - 20.6	
Tumour size (mm)	≤ 30	63 (52.9)	21.3	15.8 - 27.8	0.018
	> 30	56 (47.1)	16.1	11.7 - 20.6	
Tumour grade	Low	85 (71.4)	23.1	17.8 - 28.3	0.001
	High	34 (28.6)	13.1	9.10 - 17.2	
Lymph node status	Absent	24 (20.2)	35.9	10.4 - 61.5	0.001
	Present	95 (79.8)	18.4	15.6 - 21.2	
Margin involvement	R0	29 (24.4)	27.5	22.5 - 32.5	< 0.001
	R1	90 (75.6)	16.2	12.6 - 18.6	
Perineural invasion	Absent	11 (9.2)	54.4	21.6 - 83.6	0.014
	Present	108 (90.8)	18.5	15.7 - 21.8	
Venous invasion	Absent	58 (48.7)	24.7	18.3 - 31.1	0.001
	Present	61 (51.3)	15.6	12.8 - 18.2	
Vascular resection	No	116 (89.1)	18.4	14.7 - 22.1	0.088
	Yes	13 (10.9)	11.3	2.12 - 20.4	
Adjuvant therapy	No	79 (66.4)	14.8	9.71 - 19.8	0.051
	Yes	40 (33.6)	21.9	16.9 - 27.3	

[a] p value according to Log-rank test, CI = confidence interval

5.3 Results

5.3.1 Clinicopathological factors influencing outcome in the TMA cohort

The TMA cohort was limited to 119 patients for which adequate tissue blocks were available. The majority of patients in the TMA cohort had tumours that were T3, < 30 mm, low-grade, lymph node positive, R1, with perineural invasion (Table 2.1). Only 34% received postoperative chemotherapy. Details of the clinicopathological factors that influenced univariate survival analysis are displayed in Table 5.1 and Figure 11.1.

5.3.2 Prognostic influence of senescence markers

p21 and p53 have well established roles in the pathogenesis of PDAC and there is evidence to suggest that their aberrant expression can provide prognostic information. Recently it has been suggested that another genetic lesion, mutation of the Lkb1 gene, may influence p21 and p53 expression in PDAC. Investigation of Lkb1 expression in this PDAC cohort, along with assessment of the influence of p21 and p53 on outcome, would provide an opportunity to assess the interactions between these putative senescence-associated lesions.

5.3.3 Lkb1, p21 and p53: correlation with clinicopathological features

5.3.3.1 Lkb1 staining characteristics

The relevance of the Lkb1 pathway to PDAC progression was investigated. As expected Lkb1 staining was observed primarily in the cytoplasm of epithelial cells (Figure 11.3A) with presence in 98% of stained normal ductal tissue. In PDAC, 23% of cases expressed Lkb1 at a low level (histoscore < 100).

5.3.3.2 Lkb1 clinicopathological correlation

Expression levels of Lkb1 did not differ in terms of lymph node status or tumour size, however, high tumour stage and grade were significantly associated with lower median Lkb1 expression (Figure 5.3A, B). In univariate analysis, low Lkb1 expression (n = 27) was associated with significantly decreased overall median survival compared with high expression (n = 91) following resection, (12.9 months [95%CI: 10.5–15.4] versus 20.4 months [95%CI: 15.5–25.3], p = 0.008, Log-rank test) (Figure 5.3C, Table 5.2). Most importantly, in multivariate analysis, low Lkb1 expression remained an independent predictor of poor survival (HR: 1.90, 95%CI: 1.15–3.15, p = 0.012) (Table 5.3A).

5.3.3.3 p21 staining characteristics

p21 staining was evident in only the nuclear compartment of malignant epithelial cells (Figure 11.3A) and in 14% of normal pancreatic ductal tissue nuclei.

5.3.3.4 p21 clinicopathological correlation

p21 expression was not significantly altered in relation to clinicopathological parameters, however low p21 expression (n = 92) was associated with decreased overall survival following resection (16.2 months, 95%CI: 12.3–20.0), compared with high expression (n =

27) (30.1 months, 95%CI: 20.2–39.9, p = 0.005, Log-rank test) (Figure 5.3D, Table 5.2).

5.3.3.5 p53 staining characteristics

Investigation of whether p53 accumulation correlated with clinicopathological findings in PDAC was performed. p53 staining was evident in the nuclear compartment only (Figure 11.3A) and was present in only 3% of normal pancreatic ductal tissue.

5.3.3.6 p53 clinicopathological correlation

Although no significant associations were found with tumour progression parameters or overall survival (Table 5.3C), a significant correlation between p53 accumulation and lymph node metastasis was demonstrated. In particular, lymph node negative resections were associated with a lower tumour accumulation of p53, compared with lymph node positive resections (median histoscore 12.3 versus 64.7 [p = 0.019, Mann-Whitney U test]). Furthermore, specimens with a LNR < 50% were associated with lower tumour p53 accumulation, compared with resections with a LNR ≥ 50% (median histoscore 56.5 versus 103.8, [p = 0.011, Mann-Whitney U test]) (Figure 5.3G).

5.3.3.7 Interrelationship between the Lkb1, p21 and p53

Strikingly, in these PDAC specimens, Lkb1 expression was demonstrated to correlate directly with p21 expression (Figure 5.3F) (Spearman's rho (ρ) correlation coefficient = 0.34; p < 0.001). Significantly, high expression of both Lkb1 and p21 identified a group of patients with a more favourable outcome, with a median survival of 25.7 months (95%CI: 12.9–40.3) (Figure 5.3E). Multivariate analysis revealed that reduced p21 expression was an independent predictor of poor outcome (Table 5.3B). However, when both Lkb1 and p21 expression are entered into the multivariate model, p21 status was displaced (Table 5.3C).

Given the TP53 gene is frequently mutated in PDAC (40–70%) (304) and Lkb1 is down-regulated in around 20%, it was hypothesised that loss of Lkb1-mediated p53/p21 induction might be able to circumvent the need for p53 mutation in PDAC and thus should not be down-regulated in tumours with p53 mutated. Intriguingly, in tumours with low Lkb1 levels and hence low levels of p21, accumulation of mutant p53 was not observed (median histoscore = 4.00, n = 20). In contrast, in the subset of tumours that had low p21 with high Lkb1 expression, significantly higher levels of p53 were found, indicative of accumulation of mutant p53 (median histoscore = 71.3, n = 58, p = 0.05, Mann-Whitney U test, Figure 5.3H).

5.3.4 Discussion

5.3.4.1 Lkb1

In PDAC these data have shown that Lkb1 deficiency correlates with loss of p21 expression and with poorer prognosis, and that Lkb1 deficiency may act as an alternative to p53 mutation in pancreatic tumourigenesis. These results support the hypothesis that Lkb1 may

act as a TSG in the pancreas and that may function, at least in part, by inducing p21 expression (Figure 5.3I).

In the present study of PDAC, low levels of p21 and Lkb1 are correlated, data that are consistent with the previous findings that Lkb1 loss prevents culture induced cellular senescence (160) and allows BRAF mutant melanoma cells to proliferate (305). One important question that has been raised through the study of Lkb1 in mice (160) is whether biallelic mutations in Lkb1 are required for tumourigenesis. PJS patients develop benign hamartomas of the GI tract and develop IPMNs and cystadenomas. The previous work of Hezel and co-workers (306), showed complete loss of pancreatic Lkb1 leads to formation of benign cystadenomas, with cooperating oncogenic event required to drive carcinoma formation, and that the timing of the cooperating oncogenic event may be critical – if this occurs too late the tumour may not progress from a benign state.

Data from this chapter is consistent with this hypothesis; 27/118 tumours showed a down-regulation of Lkb1 compared to normal ductal epithelium and, remarkably, low levels of Lkb1 can act as an independent prognostic indicator of poor outcome in resected PDAC. The lack of Lkb1 mutations so far observed in human RAS-driven pancreatic tumours may instead be explained by down-regulation at the protein level, or inactivation of the gene by epigenetic means, since hypermethylation of Lkb1 in hamartomatous polyps and in tumours commonly associated with PJS has been demonstrated in the absence gene mutation (154).

5.3.4.2 p21

The CDK inhibitor p21 inhibits progression through the cell cycle mainly at S phase and the meta-analysis identified it as influencing prognosis in PDAC, while p27 did not (299). Although p21 expression did not correlate with any clinicopathological factors in the current chapter, loss of expression negatively impacted on survival independent of traditional prognostic factors. However, when Lkb1 expression was included in the multivariate analysis the influence of p21 was displaced providing more evidence that Lkb1 limits the p21 pathway. Remarkably, no PDAC tumours with low Lkb1 expression had high p21 expression. There was a subset of tumours that had low p21 with high Lkb1 expression presumably due to the fact that multiple different events can cause p21 down-regulation, e.g., TP53 mutation or TBX2 over-expression (307). Indeed this group of tumours exhibited high p53 levels; indicative of mutant p53 accumulation, suggesting Lkb1 deficiency can substitute for p53 mutation in pancreatic tumourigenesis.

5.3.4.3 p53

TP53 triggers cell cycle arrest or apoptosis via Bax in response to DNA damage, and is frequently mutated in PDAC predominantly through missense mutations (304). The fact that TP53 is mutated, rather than deleted, in the majority of cancers, suggests that mutant p53

provides some tumour cell growth advantage. Despite over 40 studies assessing the prognostic impact of p53, few identified a significant association. Pooling of the eligible data sets assessing overall survival impact failed to support a prognostic role for p53 in operable PDAC ($p = 0.14$) (299).

In pancreatic cancer TP53 mutation following an initiating activating KRAS mutation, frequently result in expression of a stable protein, $p53^{R175H}$, rather than complete loss of protein expression. Mice carrying endogenous p53 missense mutations in a model of Li Fraumeni syndrome, develop a distinct spectrum of tumours compared with those arising in p53 heterozygous null mice (osteosarcomas and carcinomas) (308). This indicates that the $p53^{R172H}$ mutant is not simply a loss-of function allele, but rather its tumourigenicity is enhanced through a gain-of-function or dominant negative function. These data also suggest that depending on tumour type and collaborating oncogenic or tumour suppressive events, mutant p53 may confer extra properties on tumour cells affecting cell proliferation, differentiation and metastasis. The IHC assessment of p53 performed in this chapter suggests that while p53 mutation status does not correlate with survival, the expression of mutant p53 was associated with metastasis promotion as measured by an increased LNR. These data suggest that strategies aimed at knocking down mutant or reactivating mutant p53 may have therapeutic efficacy in PDAC.

Table 5.2 Survival analysis of putative IHC prognostic markers in TMA cohort

Summary of univariate outcome according to the expression of IHC markers (Log-rank analysis). Includes immunostaining cut-offs that determine group allocation for survival analysis, as well as evidence for the selection of cut-off criteria.

					Overall Survival			
Protein marker	**Method to divide cohort**	**Comparison for univariate survival analysis**	**Histoscore threshold**	**Evidence for use**	**Category**	**Patients N = 119 (%)**	**Median (months)**	**95% (CI)**	**p value (Log-rank)**
p21	Quartiles	Highest quartile versus other groups	40	Intensity threshold used in literature	Low	92 (77.3)	16.2	12.3-20.0	0.005
					High	27 (22.7)	30.1	20.2-39.9	
Lkb1	Quartiles	Lowest quartile versus other groups	100	No prior evidence	Low	29 (24.3)	13.4	10.8-16.0	0.006
					High	89 (75.7)[b]	20.1	14.8-25.3	
p53	<5% cells	Histoscore ≤15 versus histoscore >15	15	Threshold used previously in literature	Low	41 (34.5)	17.1	14.3-19.9	0.15
					High	78 (65.5)	17.8	11.9-23.7	
Bcl-2	Tertiles	Lowest tertile versus other groups	40	Intensity threshold used in literature	Low	38 (31.9)	17.1	12.5-21.7	0.005
					High	81 (78.1)	24.4	13.1-35.6	
β-catenin	Tertiles	Three groups compared	100/ 200	Intensity threshold used in literature	Low	37 (30.5)	13.0	10.6-15.5	0.008
					Medium	38 (32.3)	18.4	14.3-22.5	
					High	44 (37.2)	25.7	17.1-34.2	
E-cadherin	Tertiles	Lowest tertile versus other groups	50	Intensity threshold used in literature	Low	26 (23.2)	10.3	7.9-12.6	0.006
					High	92 (76.8)	19.6	15.8-23.5	
GSK3β	Quartiles	Highest quartile versus other groups	20	No prior evidence	Low	100 (15.9)	18.0	13.9-22.1	0.015
					High	19 (84.1)	13.9	9.8-17.1	
COX-2	Tertiles	Three groups compared	100	Intensity threshold used in literature	Nil	19 (16.0)	39.6	19.6–59.6	0.001
					Low	79 (66.4)	17.1	13.6–20.5	
					High	21 (17.6)	9.0	7.9-10.2	
pAkt	Quartiles	Lowest quartile versus other groups	50	Intensity threshold used in literature	Low	27 (22.7)	24.7	16.9–42.5	0.031
					High	92 (77.3)	16.1	12.1–20.1	
Cyclin D1	Tertiles	Highest tertile versus other groups	100	Intensity threshold used in literature	Low	81 (78.1)	15.7	12.5–18.6	0.043
					High	38 (31.9)	21.8	15.5–28.3	
Ki67	Dichotomised	Low group versus high group	[a]	Method used previously in literature	Low	40 (33.6)	13.5	10.5–16.5	0.048
					High	79 (66.4)	20.1	16.8–23.4	
SMAD4	<5% cells	Histoscore ≤15 versus histoscore >15	15	Threshold used previously in literature	Low	38 (31.9)	17.6	14.5-20.8	0.027
					High	81 (68.1)	24.6	5.6-43.0	
TGFβ	Dichotomised	Low group versus high group	120	Method used previously in literature	Low	61 (51.3)	19.6	15.7 –22.4	0.52
					High	58 (48.7)	14.8	11.3 –18.3	

[a] *For Ki67 Histoscore not used as staining intensity uniform in nature, therefore only percentage of cells stained. Mean Ki67 % staining therefore used to dichotomise groups*

[b] *For Lkb1 only 118 patients available*

Table 5.3 Multivariate Cox regression analysis of markers of senescence

*Association of **A)** Lkb1, **B)** p21 and clinicopathological parameters with overall survival in 119 patients following PD for PDAC. In **C)** when Lkb1 and p21 expression are combined within the same multivariate analysis p21 is displaced from the model.*

A		**Overall survival**	
Prognostic variable	**Category**	**Hazard ratio (95% CI)**	**p value**
Tumour stage	T2/ T3	2.67 (1.37 - 5.23)	0.04
Lymph node involvement	Absent/ Present	1.11 (0.59 - 2.01)	0.76
Tumour size (mm)	<30/ ≥30	1.68 (1.10 - 2.54)	0.015
Tumour grade	Low/ High	2.81 (1.76 - 4.45)	0.0001
Venous invasion	Absent/ Present	0.98 (0.62 - 1.55)	0.94
Perineural invasion	Absent/ Present	0.89 (0.37 - 2.32)	0.82
Resection margin status	R0/ R1	2.62 (1.54 - 4.47)	0.0001
Lkb1 expression	**High/ Low**	**1.90 (1.15 - 3.12)**	**0.012**

B		**Overall survival**	
Prognostic variable	**Category**	**Hazard ratio (95% CI)**	**p value**
Tumour stage	T2/ T3	1.95 (0.99 - 3.81)	0.051
Lymph node involvement	Absent/ Present	1.42 (0.78 - 2.58)	0.26
Tumour size (mm)	<30/ ≥30	1.68 (1.10 - 2.54)	0.015
Tumour grade	Low/ High	2.11 (1.35 - 3.32)	0.001
Venous invasion	Absent/ Present	1.19 (0.77 - 1.82)	0.43
Perineural invasion	Absent/ Present	0.91 (0.34 - 2.12)	0.67
Resection margin status	R0/ R1	2.35 (1.39 - 3.95)	0.001
p21 expression	**Low/ High**	**0.57 (0.34 - 0.95)**	**0.031**

C		**Overall survival**	
Prognostic variable	**Category**	**Hazard ratio (95% CI)**	**p value**
Tumour stage	T2/ T3	2.67 (1.37 - 5.23)	0.04
Lymph node involvement	Absent/ Present	1.11 (0.59 - 2.01)	0.76
Tumour size (mm)	<30/ ≥30	1.68 (1.10 - 2.54)	0.15
Tumour grade	Low/ High	2.81 (1.76 - 4.45)	0.0001
Venous invasion	Absent/ Present	0.98 (0.62 - 1.55)	0.82
Perineural invasion	Absent/ Present	0.89 (0.37 - 2.32)	0.82
Resection margin status	R0/ R1	2.62 (1.54 - 4.47)	0.0001
p21 expression	**Low/ High**	**0.92 (0.54 - 1.56)**	**0.75**
Lkb1 expression	**High/ Low**	**1.90 (1.15 - 3.12)**	**0.012**

5.4 Prognostic influence of apoptosis markers

The apoptotic pathway is one of the most extensively investigated intracellular pathways; however, it comprises a multitude of signalling redundancies. As evident in the systematic review (299) various markers associated with apoptosis, including survivin, Bcl-2 and Bax were consistently and significantly associated with overall outcome in multiple studies, of which validation of the prognostic utility of Bcl-2 was performed.

5.4.1 Bcl-2: correlation with clinicopathological features and survival

Bcl-2 was expressed both within the nucleus and cytoplasm of PDAC epithelial cells, but not within the stromal component (Figure 11.3B). Bcl-2 was present in 11% of normal ductal tissue.

5.4.1.1 Bcl-2 clinicopathological correlation

Cytoplasmic expression levels of Bcl-2 did not differ in terms of clinicopathological features, however in univariate analysis, high Bcl-2 expression (n = 38) was associated with significantly prolonged overall survival compared with low or medium cytoplasmic expression (n = 81) following resection of PDAC, (24.4 months [95%CI: 13.1–35.6] versus 17.1 months [95%CI: 12.5–21.7, p = 0.005, Log-rank analysis]) (Figure 11.4) (Table 5.2). Notably, in multivariate analysis, high Bcl-2 expression remained an independent predictor of prolonged overall survival (HR: 0.37, 95%CI: 0.21–0.67, p = 0.001) (Table 5.4).

5.4.1.2 Correlation of Bcl-2 with other markers

Bcl-2 was weakly inversely correlated with p53 expression (Spearman's $\rho = -0.21$, $p = 0.048$), however, did not correlate significantly with any other marker.

5.4.2 Discussion

There is strong clinical data supporting a positive correlation between Bcl-2 expression and survival following pancreatic cancer resection (119, 303, 309, 310), although some studies found no correlation (311). In particular, evidence is provided by a high fraction of apoptotic cells correlating with longer overall survival following resection independent of lymph node involvement (119). Certainly the data from this chapter is the largest single study of the prognostic role of Bcl-2 in PDAC, validating the findings of previous studies. The observation that Bcl-2 positivity, an anti-apoptotic factor, results in longer survival is somewhat paradoxical and may only be explained when more information regarding the role of other members of the Bcl-2 family is obtained. However, this finding is mirrored in other malignancies including breast cancer where it provided prognostic value independent of the Nottingham Prognostic Index (312). This effect may be explained by a complex interaction of competitive dimerisations between pro- and anti-apoptotic proteins that govern a cell's fate in response to apoptotic stimuli (313). The tumourigenic potential of Bcl-2 has been suggested in animal models (314) and supported by over-expression in lymphoma as a result

of chromosomal translocation (315). However, it would appear that the mechanism of over-expression in other tumours including PDAC is less certain. These data describing a negative correlation between p53 and Bcl-2 reflects negative regulation by a p53-dependent mechanism in breast (316). A possible explanation for the prognostic role of Bcl-2 may be consequent on a nonapoptotic role, with *in vitro* experiments demonstrating that high Bcl-2 can result in dramatic growth inhibition in different cell types (315).

From the meta-analysis data it would appear that Bax expression is associated with a favourable outcome in PDAC, concordant with its physiological role (299). While, the intention was to assess Bax expression in this cohort and investigate not only its prognostic role but also the relationship with Bcl-2 expression, unfortunately reliable IHC staining could not be achieved in the PDAC TMA.

Table 5.4 Multivariate Cox regression analysis for Bcl-2

Clinicopathological parameters and Bcl-2 expression in patients undergoing resection for PDAC.

		Overall survival	
Prognostic variable	**Category**	**Hazard ratio (95% CI)**	**p value**
Tumour stage	T2/ T3	2.28 (1.42 - 3.64)	0.019
Lymph node positivity	Absent/ Present	1.38 (0.72 - 2.65)	0.332
Tumour size (mm)	< 30/ ≥ 30	1.83 (1.22 - 2.81)	0.005
Tumour grade	Low/ High	2.26 (1.43 - 3.65)	0.001
Venous invasion	Absent/ Present	1.45 (0.92 - 2.26)	0.118
Perineural invasion	Absent/ Present	0.98 (0.78 - 3.44)	0.882
Resection margin status	R0/ R1	2.53 (1.48 - 4.31)	0.001
Bcl-2 expression (cytoplasmic)	**Low/ High**	**0.37 (0.21 - 0.67)**	**0.001**
Adjuvant chemotherapy	No/ Yes	0.76 (0.47 - 1.23)	0.001

5.5 Prognostic influence of invasion and metastasis signalling markers

As identified within the meta-analysis, markers of invasion and metastasis were very strongly linked to outcome. Therefore, to further investigate the prognostic influence of markers of invasion and metastasis, β-catenin, E-cadherin and GSK3β IHC were performed on the PDAC TMAs.

5.5.1.1 β-catenin, E-cadherin and GSK3β: correlation with clinicopathological features and survival

Investigation of the relevance of the invasion and metastasis markers to pathological factors or prognosis in PDAC was performed. As expected β-catenin and E-cadherin staining was observed primarily in epithelial cell membranes but also within the cytoplasm and nucleus (Figure 11.3C). GSK3β staining was evident principally in the cytoplasm of epithelial cells with no evidence of staining in tumour stroma (Figure 11.3C). β-catenin, E-cadherin and GSK3β were present in 95%, 97% and 80% of normal ductal tissue respectively.

5.5.1.2 β-catenin clinicopathological correlation

In PDAC, 31% of cases expressed β-catenin at a low level (histoscore < 100). Membranous expression levels of β-catenin did not differ in terms of lymph node status, tumour size, tumour stage, perineural or venous invasion; however, high tumour grade was significantly associated with lower median β-catenin expression level (Figure 11.5A) ($p = 0.001$, Mann-Whitney U test). In univariate analysis high membranous expression (n = 36) resulted in a prolonged median overall survival of 25.7 months (95%CI: 17.1–34.3) versus medium expression (n = 38) of 18.4 months (95%CI: 14.3–22.5) and low expression (n = 44) of 13.1 months (95%CI: 10.5–15.50, $p = 0.006$, Log-rank test) (Table 5.2) (Figure 11.5B). Most importantly, in multivariate analysis, high membranous β-catenin expression remained an independent predictor of good outcome (HR: 0.54, 95%CI: 0.35–0.84, $p = 0.005$) (Table 5.5A).

5.5.1.3 E-cadherin clinicopathological correlation

In 23% of tumours, E-cadherin was expressed at a low level (histoscore < 50). High tumour grade was significantly associated with lower median membranous E-cadherin expression (Figure 11.5C) ($p = 0.002$, Mann-Whitney U test). In univariate analysis, high expression (n = 92) resulted in a prolonged median overall survival of 19.6 months (95% CI: 15.6–23.6) versus low expression (n = 26) of 10.3 months (95%CI: 7.3–13.2, $p = 0.002$, Log-rank test) (Table 5.2). Complete loss of membranous E-cadherin expression was noted in seven patients associating with a very poor overall median survival of 8.7 months (95%CI: 6.2–11.2). Most importantly, in multivariate analysis, high E-cadherin expression remained an independent predictor of good outcome (HR: 0.31, 95%CI: 0.18–0.53, $p < 0.0001$) (Table 5.5B).

5.5.1.4 GSK3β clinicopathological correlation

In PDAC the majority of cases showed negligible or no expression with 15.9% of cases (n = 19) expressing GSK3β at a high level (histoscore > 100). Expression levels of GSK3β did not differ in terms of lymph node status, tumour size, tumour stage, or the presence of venous invasion; however, the presence of perineural invasion was significantly associated with a higher mean GSK3β histoscore of 23.9 (95%CI: 16.9–30.9) compared to those tumours without perineural invasion with a histoscore of 5.5 (95%CI: 1.1–9.9) (Figure 11.5F) (Mann-Whitney U test, p = 0.025). In univariate analysis, low expression (n = 100) resulted in a prolonged overall survival of 27.8 months (95%CI: 22.0–33.8) versus high expression (n = 19) of 15.3 months (95%CI: 11.5–19.1, p = 0.015, Log-rank test) (Table 5.2) (Figure 11.5E). Most importantly, in multivariate analysis, high GSK3β expression remained an independent predictor of poor survival (HR: 1.4, 95%CI: 1.13–1.62, p = 0.011) (Table 5.5C)

5.5.1.5 Multivariate analysis including β-catenin, E-cadherin and GSK3β

All three markers provided prognostic information independent of the clinicopathological factors. When all were entered into a multivariate model both E-cadherin and GSK3β remained within the multivariate model along with other clinicopathological factors, however, β-catenin was removed (Table 5.5D).

5.5.1.6 Relationship between markers of invasion and metastasis

There was a strong positive correlation between membranous β-catenin and E-cadherin expression in this cohort (Spearman's $\rho = 0.843$, $p < 0.001$) (Figure 11.5G). Furthermore both β-catenin and E-cadherin were significantly inversely related to GSK3β ($\rho = -0.289$, $p = 0.031$; $\rho = -0.312$, $p = 0.025$) (Figure 11.5H, I). Cyclin D1 expression related inversely to GSK3β expression ($\rho = -0.277$, $p = 0.013$).

5.5.2 Discussion

β-catenin/ E-cadherin interactions are important for the maintenance of cell to cell adhesion and in contributing to β-catenin activation (317). A spectrum of expression for both proteins was observed. This study is the largest to date evaluating the prognostic role of the cadherin-catenin complex in PDAC, demonstrating loss of either membrane E-cadherin or β-catenin was indicative independently of poor prognosis. As demonstrated in this chapter, reduced E-cadherin expression has been shown to correlate with high tumour grade and poor patient survival (317-319). To ensure that tumour grade did not confound the prognostic utility of E-cadherin, sub-group analysis of the poorly differentiated tumours confirmed E-cadherin expression status provided additional prognostic value. Furthermore, although complete loss of expression of E-cadherin membranous expression was rare, this group had an especially poor outcome highlighting the potential prognostic role of this biomarker. This finding has been confirmed in recent large cohort assessing E-cadherin expression (320). A strong

correlation between the expression of these proteins was demonstrated (Figure 11.5G). For β-catenin a complete or near complete loss of expression was associated with an especially poor outcome. A previous study assessing β-catenin and E-cadherin expression in a small PDAC cohort suggested a consistent increase in cytoplasmic expression for both, suggesting translocation to this compartment (321). The present evaluation showed that cytoplasmic expression was less apparent in normal ducts; however, no correlation between cytoplasmic expression and survival was apparent. It is plausible that local environmental factors including hypoxia mediated by tumour-stromal interactions could suppress E-cadherin expression by transcriptional repression (322).

Recently diffuse expression of E-cadherin was associated with a deleterious outcome (320). Analysis of the variation in E-cadherin expression between TMA cores in the present data failed to identify a significant difference. Further analysis of whole sections may be necessary to confirm the prognostic impact of focal versus diffuse loss of E-cadherin and β-catenin expression.

The loss of E-cadherin in cancers is often attributed to the induction of an EMT program (149, 150). Clearly the prognostic relevance of loss of E-cadherin expression highlights the necessity for further investigation of the prognostic utility of EMT markers in human PDAC tissue. This has the potential to explain the loss of architecture structure and poor differentiation associated with loss of E-cadherin expression, while also providing targets for antimetastatic therapies.

The expression of nuclear β-catenin was not thought to be reproducible and therefore not formally assessed in this cohort. While it is characteristic of solid-pseudopapillary neoplasms, it is not a common feature of PDACs (323), and undifferentiated PDAC lacking E-cadherin expression typically lack nuclear β-catenin. Certainly, nuclear localisation is thought to be the mechanism by which β-catenin modifies gene expression and therefore future work is required to resolve the prognostic relevance of nuclear localisation.

The chapter provides the first evidence of GSK3β expression relating to perineural invasion and outcome in PDAC. These data suggest that increased expression of GSK3β was independently associated with reduced survival following resection underscoring the significance of GSK3β phosphorylation in PDAC. Furthermore, for the first time it has been demonstrated that GSK3β is inversely related to membranous expression of E-cadherin and β-catenin in resected specimens. This supports the theory that β-catenin expression is altered or inactivated in part by GSK3β. Certainly further interrogation of the interaction between GSK3β and β-catenin is required, however, it is has been suggested that GSK3β is potentially involved in the apparent resistance of pancreatic cell lines to radiotherapy (324).

Table 5.5 Multivariate Cox regression analysis for markers of invasion and metastases.

A) β-catenin, B) E-cadherin, C) GSK3β with overall survival following PD. In D) all three markers are included within the model.

A		Overall survival	
Prognostic variable	**Category**	**Hazard ratio (95% CI)**	**p value**
Tumour stage	T2/ T3	3.05 (1.54 - 6.02)	0.001
Lymph node positivity	Absent/ Present	1.22 (0.83 - 2.08)	0.11
Tumour size (mm)	< 30/ ≥ 30	1.74 (1.15 - 2.63)	0.009
Tumour grade	Low/ High	2.62 (1.64 - 4.19)	0.0001
Venous invasion	Absent/ Present	1.20 (0.77 - 1.88)	0.42
Perineural invasion	Absent/ Present	0.65 (0.34 - 1.72)	0.39
Resection margin status	R0/ R1	2.63 (1.59 - 4.61)	0.0001
β-catenin expression (membranous)	**Low/ High**	**0.54 (0.35 - 0.83)**	**0.005**

B		Overall survival	
Prognostic variable	**Category**	**Hazard ratio (95% CI)**	**p value**
Tumour stage	T2/ T3	2.20 (1.15 - 4.38)	0.018
Lymph node positivity	Absent/ Present	1.71 (0.99 - 3.11)	0.06
Tumour size (mm)	< 30/ ≥ 30	1.69 (1.10 - 2.61)	0.017
Tumour grade	Low/ High	2.27 (1.43 - 3.60)	0.0001
Venous invasion	Absent/ Present	1.37 (0.88 - 2.15)	0.16
Perineural invasion	Absent/ Present	0.54 (0.21 - 1.44)	0.22
Resection margin status	R0/ R1	2.51 (1.43 - 4.29)	0.002
E-cadherin expression (membranous)	**Low/ High**	**0.31 (0.18-0.53)**	**<0.0001**

C		Overall survival	
Prognostic variable	**Category**	**Hazard ratio (95% CI)**	**p value**
Tumour stage	T2/ T3	2.51 (1.27 - 4.95)	0.008
Lymph node positivity	Absent/ Present	1.59 (0.89 - 2.85)	0.11
Tumour size (mm)	< 30/ ≥ 30	1.23 (0.89 - 1.95)	0.17
Tumour grade	Low/ High	2.19 (1.39 - 3.46)	0.001
Venous invasion	Absent/ Present	1.18 (0.77 - 1.82)	0.44
Perineural invasion	Absent/ Present	1.12 (0.87 - 1.62)	0.39
Resection margin status	R0/ R1	1.92 (1.12 - 3.27)	0.01
GSK3β expression	**Low/ High**	**1.38 (1.19 - 1.77)**	**0.008**

D		Overall survival	
Prognostic variable	**Category**	**Hazard ratio (95% CI)**	**p value**
Tumour stage	T2/ T3	3.06 (1.54 - 6.11)	0.001
Lymph node positivity	Absent/ Present	1.19 (0.74 - 2.21)	0.57
Tumour size (mm)	< 30/ ≥ 30	1.72 (1.14 - 2.61)	0.01
Tumour grade	Low/ High	3.01 (1.89 - 4.80)	0.0001
Venous invasion	Absent/ Present	1.20 (0.78 - 1.89)	0.43
Perineural invasion	Absent/ Present	0.51 (0.19 - 1.37)	0.18
Resection margin status	R0/ R1	2.91 (1.69 - 5.03)	0.0001
β-catenin expression (membranous)	**Low/ High**	**0.71 (0.42 - 1.17)**	**0.18**
E-cadherin expression (membranous)	**Low/ High**	**0.34 (0.19 - 0.59)**	**0.0001**
GSK3β expression	**Low/ High**	**1.21 (1.01 - 1.46)**	**0.037**

5.6 Prognostic influence of angiogenesis markers

According to the meta-analysis, regulators of angiogenesis that influenced overall mortality following resection included eleven candidates, highlighting the importance of this functional grouping in PDAC. COX-2 was investigated in two studies with an elevated level associated with a significantly worse outcome (p = 0.002). Despite vascular endothelial growth factor (VEGF) being a heavily studied marker, only three studies were eligible (299), a combination of which did not suggest that over-expression influenced overall survival (HR: 1.34, 95%CI: 0.87–2.06, p = 0.18). There is strong epidemiological and experimental evidence to suggest that COX-2 plays an important role in both the development and progression of gastrointestinal malignancies. Having been identified as a robust prognostic marker (299), the prognostic role of COX-2 expression was chosen to be validated and integrated within the TMA cohort dataset.

5.6.1 COX-2: correlation with clinicopathological features and survival

COX-2 staining primarily was observed in the cytoplasm and membrane of epithelial cells and also within the nucleus (Figure 11.3B). COX-2 expression was not evident in the surrounding fibroblasts or inflammatory cells. COX-2 staining was present in 27% of stained normal ductal tissue.

5.6.1.1 COX-2 clinicopathological correlations

19 tumours (16%) had no COX-2 expression, while 100 (84%) had a degree of COX-2 cytoplasm expression of which 21 tumours (18%) had high expression of COX-2 (> 100 histoscore). COX-2 expression was lower in T2 compared to T3 tumours (p = 0.04, Mann-Whitney U test), while all tumours with an absence of perineural invasion had no or low expression of COX-2 (p = 0.03, Mann-Whitney U test). Furthermore large tumours demonstrated higher COX-2 expression (p = 0.02, Mann-Whitney U test). While COX-2 expression did not differ significantly based on lymph node positivity, those tumours with a LNR > 0.5 had significantly greater COX-2 than those tumours with a lower LNR (Figure 11.6B) (p = 0.035, Mann-Whitney U test). Expression levels of COX-2 did not significantly differ in terms of tumour grade, resection margin status, or venous invasion. Patients with high COX-2 expressing tumours were more likely to receive adjuvant therapy.

In univariate analysis, high COX-2 expression (histoscore > 100 [n = 21]) was associated with significantly reduced median overall survival (9.0 months, 95%CI: 7.9–10.2) compared to patients with low expression (n = 79) (17.1 months, 95%CI: 13.6–20.5) or no expression (n = 19) (39.6 months, 95%CI: 19.6–59.6, p = 0.001, Log-rank test) (Table 5.2) (Figure 11.6A). Most importantly, in a multivariate analysis, high COX-2 expression remained an independent predictor of poor survival (HR: 1.31, 95%CI: 1.05–1.71, p = 0.005) (Table 5.6).

5.6.1.2 Prognostic influence of COX-2 expression stratified by tumour size

Stratification by tumour size and COX-2 expression was performed to assess the joint effects of these factors (Figure 11.6C). Large tumours with high COX-2 cytoplasmic expression (n = 12) had significantly shortened survival (median 6.1 months, 95%CI: 2.5–9.7) compared to small tumours (n = 50) with low cytoplasmic COX-2 expression (20.7 months, 95%CI: 12.2–29.2, p = 0.002, Log-rank test). Among tumours > 30 mm, the mean size of the COX-2 negative tumours was similar to those of the COX-2 positive tumours (40.0 mm). Indicating the observed effect of COX-2 on survival is not the result of COX-2 expressing tumours being larger than low COX-2 expressing tumours. Furthermore, in a multivariate model stratified by tumour size (

Table 5.7), the HR associated with COX-2 expression in tumour < 30 mm in size was 1.19 (95%CI: 0.83–1.74) compared to a HR of 1.55 (95%CI: 1.06–2.28) in tumours ≥ 30 mm (p = 0.02).

5.6.1.3 Correlation of COX-2 expression with other markers

The correlation of COX-2 expression with important signalling pathways in PDAC was studied. High Lkb1 expression was associated with over expression of COX-2 (Figure 11.6D), ($\rho = 0.54$, $p < 0.001$). Stratification was then performed by both COX-2 and Lkb1 expression, identifying patients with low Lkb1 and elevated COX-2 expression (n = 9) with a very poor prognosis (7.1 months, 95%CI: 2.1–12.0, p = 0.001). β-catenin and E-cadherin cytoplasmic expression correlated strongly with COX-2 expression ($\rho = 0.61$, $p < 0.001$) ($\rho = 0.41$, $p < 0.001$), respectively (Figure 11.6E).

5.6.2 Discussion

Consistent with previous studies this work has confirmed that high COX-2 expression in PDAC tumour epithelium was independently associated with poor prognosis. Merati and co-workers studied patients receiving radiotherapy identifying worse survival for those high COX-2 expressors compared to low expressors (14.0 versus 19.5 months) (325). Juuti and co-workers showed that COX-2 expression was associated with worse overall survival independent of stage and tumour histological grade (326). Matsubayashi and co-workers confirmed that COX-2 expression was a poor prognosticator especially in tumours > 30 mm (327). In the current cohort tumour size > 30 mm was significantly associated with COX-2 expression confirming the previous study results (327). It should be noted, the 30 mm cut-off is not based on biological rationale but rather is a reflection of a common cutoff size used to determine the influence of size on outcome following resection. It was determined that a high LNR was associated with high COX-2 expression although lymph node positivity itself was not, a novel finding. In addition to being associated with poor prognosis in colorectal cancer it has been demonstrated that greater COX-2 expression correlated with larger tumour size, lymph node involvement and more advanced stage (328). The reason for the interaction between tumour size, COX-2 expression and outcome are unknown but could arise from the association of COX-2 expression with tumour hypoxia, which is more likely in larger tumours. The pro-survival characteristics of COX-2 may be more important for the survival of larger compared to smaller tumours. While COX-2 expression has an established

relationship with angiogenesis (329), no correlation with intratumoural venous invasion was identified.

It is uncertain whether COX-2 inhibition remains a worthwhile therapy for PDAC. Compared to strong evidence for COX-2 inhibition preventing colorectal cancer, epidemiological studies do not show the same chemo-preventative effect in PDAC. Despite initial promise, a phase II study of Celecoxib in addition to gemcitabine and cisplatin for advanced PDAC showed no benefit over chemotherapy alone (330). To ascertain whether inhibition has a therapeutic role requires patient selection based upon COX-2 expression status to avoid missing potential therapeutic benefit.

There is certainly molecular evidence that COX-2 plays an important role in PDAC progression, with inhibition limiting progression of PanINs in the $KRAS^{G12D}$ model (331). The precise molecular pathways impacted in this model are incompletely described, however, stronger cytoplasmic expressions of β-catenin and E-cadherin, suggests alterations in cell adhesion. There is evidence that COX-2 influences Lkb1 expression, with a PJS study comparing Lkb1 and COX-2 demonstrating that polyps expressing Lkb1 overexpressed COX-2, with the reverse also holding true (332). A murine study suggested that the RAS/RAF/MEK/ERK signalling pathway is most likely to mediate COX-2 induction in murine Lkb1 polyposis (333). In the present study a correlation was demonstrated between Lkb1 and COX-2 expression in PDAC in a novel investigation of this relationship. Furthermore it was identified for the first time that low Lkb1/ high COX-2 expression was associated with an especially poor outcome in human PDAC. Certainly it has been suggested that COX-2 may inactivate TSGs including Lkb1 (334), however, it appears that in PDAC a positive correlation exists suggesting a direct suppressive effect is not present in vivo. Further evidence of the interaction between COX-2 and Lkb1 has been provided by COX-2 inhibition resulting in suppression of PJS in Lkb1+/- mice (335).

Table 5.6 Multivariate Cox regression analysis including COX-2 expression

Clinicopathological parameters and COX-2 expression in patients undergoing resection for PDAC.

		Overall survival	
Prognostic variable	**Category**	**Hazard ratio (95% CI)**	**p value**
Tumour stage	T2/ T3	2.51 (1.27 - 4.95)	0.008
Lymph node positivity	Absent/ Present	1.59 (0.89 - 2.85)	0.11
Tumour size (mm)	< 30/ ≥ 30	1.23 (0.89 - 1.95)	0.17
Tumour grade	Low/ High	2.19 (1.39 - 3.46)	0.001
Venous invasion	Absent/ Present	1.18 (0.77 - 1.82)	0.44
Perineural invasion	Absent/ Present	1.12 (0.87 - 1.62)	0.39
Resection margin status	R0/ R1	1.92 (1.12 - 3.27)	0.01
COX-2 expression	**(Low/ High)**	**1.31 (1.05 - 1.71)**	**0.005**

Table 5.7 Multivariate Cox regression analysis of COX-2 expression according to size

Patient cohort (n = 119) stratified by tumours < 30 mm as compared to ≥ 30 mm.

		Overall survival	
	Category	**Hazard ratio (95% CI)**	**p value**
Small tumours			
Tumour stage	T2/ T3	2.11 (0.82 - 2.13)	0.122
Lymph node positivity	Absent/ Present	2.52 (1.20 - 5.28)	0.015
Tumour grade	Low/ High	2.19 (0.62 - 2.13)	0.67
Venous invasion	Absent/ Present	1.58 (0.85 - 2.91)	0.15
Perineural invasion	Absent/ Present	0.78 (0.17 - 3.67)	0.77
Resection margin status	R0/ R1	1.92 (1.12 - 3.27)	0.01
COX-2 expression	**(Low/ High)**	**1.19 (0.83 - 1.74)**	**0.34**
Large tumours			
Tumour stage	T2/ T3	2.25 (0.83 - 6.14)	0.11
Lymph node positivity	Absent/ Present	1.11 (0.54 - 2.91)	0.015
Tumour grade	Low/ High	5.47 (2.54 - 11.8)	0.0001
Venous invasion	Absent/ Present	1.09 (0.58 - 2.06)	0.78
Perineural invasion	Absent/ Present	0.84 (0.37 - 3.97)	0.67
Resection margin status	R0/ R1	2.51 (1.05 - 5.92)	0.037
COX-2 expression	**(Low/ High)**	**1.55 (1.06 - 2.28)**	**0.02**

5.7 Prognostic influence of self-sufficiency for growth signalling markers

Among the 22 proteins associated with limitless replicative potential that were assessed as part of the systematic review, pAkt and Ki67 appear to be most consistently associated with overall survival. Therefore the prognostic influence of cyclin D1, pAkt and Ki67 as markers representing the functional group of self-sufficiency for growth signalling was assessed.

5.7.1 Cyclin D1, pAkt and Ki67: correlation with clinicopathological features and survival

Cyclin D1 staining was evident only within the nucleus of malignant epithelial cells (Figure 11.3D), not within the surrounding fibroblasts or inflammatory cells. Cyclin D1 was rarely expressed in normal ductal tissue (11%). pAkt staining was evident within the cytoplasm and nucleus of tumour epithelium (Figure 11.3D), not in the surrounding fibroblasts or inflammatory cells. pAkt was expressed in 6% of normal ductal structures. Ki67 staining was evident only within the nuclear compartment of tumour epithelium with no staining evident in surrounding fibroblasts or inflammatory cells (Figure 11.3D). Ki67 was rarely present in the normal ducts (4%).

5.7.1.1 Cyclin D1 clinicopathological correlations

With the cohort separated into tertiles, the 32% expressing cyclin D1 at an elevated level (histoscore >100) were deemed high expressors. LN0 tumours had a significantly higher median cyclin D1 level (median histoscore 88.1 versus 62.3; p = 0.002) (Figure 11.7A), however, no other pathological factors were related.

In univariate analysis high cyclin D1 expression (n = 38) was associated with a better outcome (21.8 months, 95%CI: 15.5–28.3) than low cyclin D1 expression (n = 81) (15.7 months, 95%CI: 12.5–18.6, p = 0.043, Log-rank test) (Figure 11.7B) (Table 5.2). Cyclin D1 negative tumours where then stratified by lymph node status identifying a group of lymph node negative patients (n = 12) that had a very good prognosis median 35.9 months (95%CI: 23.7–49.3) versus 13.9 months (95%CI: 10.5–17.3). In a multivariate analysis high cyclin D1 remained an independent predictor of good outcome (HR: 0.61, 95%CI: 0.61–0.39, p = 0.026) (Table 5.8A).

5.7.1.2 pAkt clinicopathological correlations

With the cohort separated into quartiles, the lowest 25% of cases expressing pAkt with a histoscore > 50, were deemed low expressors. pAkt expression did not differ in terms of clinicopathological factors. Univariate analysis demonstrated that patients with low pAkt expressing tumours (n = 26) were associated with a prolonged median overall survival of 24.7 months (95%CI: 6.9–42.5) compared to those with high pAkt expression (n = 92) that had a median survival of 16.1 months (95%CI: 12.1–20.1) (p = 0.031, Log-rank Test) (Table 5.2) (Figure 11.7C). Most importantly, in a multivariate analysis, high pAkt expression

remained an independent predictor of poor survival (HR: 2.02, 95%CI: 1.19–3.43, p = 0.008) (Table 5.8B).

5.7.1.3 Ki67 clinicopathological correlations

The cohort was separated into two groups based on the median proliferative index value. Expression levels of Ki67 were not significantly related to any clinicopathological factor. Counter-intuitively elevated Ki67 was associated with a more favourable outcome following resection. Within univariate analysis low Ki67 (n = 59) expression was associated with a median survival of 13.5 months (95%CI: 10.5–16.5), significantly less than for those patients with tumours with high expression of Ki67 (n = 60) who had a median survival of 20.1 months (95%CI: 16.8–23.4) (p = 0.048, Log-rank test) (Figure 11.7D) (Table 5.2). Multivariate analysis however did not support Ki67 as a predictor of outcome (HR: 0.67, 95%CI: 0.43–1.20, p = 0.168) (Table 5.8C).

5.7.1.4 Correlation of Cyclin D1, pAkt and Ki67 expression with other markers

Cyclin D1 correlated extensively with other markers as demonstrated in Figure 11.7E. There was a strong positive correlation with SMAD4 ($\rho = 0.43$, $p < 0.001$), p21 ($\rho = 0.37$, $p < 0.001$), p53 ($\rho = 0.34$, $p = 0.002$) and COX-2 ($\rho = 0.39$, $p < 0.001$). pAkt expression correlated with Lkb1 ($\rho = 0.36$, $p = 0.005$), COX-2 ($\rho = 0.35$, $p < 0.001$) and Ki67 ($\rho = 0.29$, $p = 0.01$).

5.7.2 Discussion

Up-regulation of cyclin D1 is known to be important in the regulation of the cell cycle pathway, with an increase in expression permitting loss of G1 restriction point integrity. Of the 12 studies that assessed the prognostic significance of cyclin D1 in PDAC, four had found an association with outcome. These data provide evidence that supports cyclin D1 expression being associated with favourable outcome. The reason for this somewhat paradoxical relationship is not clear, although this relationship has previously been identified in a number of breast cancer studies (336). Further investigation of this relationship is required before any firm conclusion can be drawn particularly in view of the previous finding of cyclin E1 associating with poor outcome a single study. However, further validation of cyclin E1 by the original authors in a well-powered study failed to support the finding (337).

There is increasing evidence that Akt is activated in various cancers, and that this signalling pathway confers a potent survival signal (338). pAkt had been assessed for prognostic utility in only two previous studies; however both of these suggested it was an independent predictor of survival although in opposing directions. Certainly the data from this chapter is the largest single study of the prognostic role of pAkt in PDAC, providing support for a negative role in survival. The previous study suggesting pAkt expression was independently associated with a favourable outcome, was limited in size (339) and this limitation may in

part account for the conflicting results. Certainly, there are numerous genetic events that could lead to activation of Akt, including mutations of KRAS or PTEN. Certainly, the correlation of PTEN and pAkt expression is an important investigation that would provide further insight into this signalling pathway in PDAC. Further implications of pAkt associating with poor outcome include evidence that Akt activation inhibits gemcitabine-induced apoptosis, and the addition of Akt inhibitors enhances apoptosis (340).

Regarding Ki67 expression being associated with a favourable outcome, in view of the literature both for PDAC and for other cancers it is difficult at this time to rationalise this finding. The association was not borne out in multivariate analysis. Potentially a methodological error either at the staining or scoring level may account for these findings. Certainly this work does not support Ki67 as a useful prognostic marker in resected PDAC specimens. Theoretically this may be the result of chemosensitivity in those tumours with a higher proliferative rate responding to adjuvant chemotherapy, and therefore resulting in prolonged survival.

Table 5.8 Multivariate Cox regression analysis for self-sufficiency for growth signalling
*Correlation of **A)** Cyclin D1, **B)** pAkt, **C)** Ki67 with overall survival following PD.*

A		**Overall survival**	
Prognostic variable	**Category**	**Hazard ratio (95%CI)**	**p value**
Tumour stage	T2/ T3	2.23 (1.15 - 4.62)	0.018
Lymph node positivity	Absent/ Present	1.77 (0.93 - 3.31)	0.089
Tumour size (mm)	< 30/ ≥ 30	1.74 (1.14 - 2.65)	0.009
Tumour grade	Low/ High	2.29 (1.45 - 3.66)	< 0.001
Venous invasion	Absent/ Present	1.22 (0.70 - 1.99)	0.393
Perineural invasion	Absent/ Present	0.89 (0.57 - 2.01)	0.448
Resection margin status	R0/ R1	2.60 (1.51 - 4.35)	0.001
Cyclin D1 expression	**Low/ High**	**0.61 (0.39 - 0.94)**	**0.026**
B		**Overall survival**	
Prognostic variable	**Category**	**Hazard ratio (95%CI)**	**p value**
Tumour stage	T2/ T3	2.20 (1.12 - 4.32)	0.023
Lymph node positivity	Absent/ Present	1.87 (1.02 - 3.45)	0.049
Tumour size (mm)	< 30/ ≥ 30	1.62 (1.05 - 2.54)	0.034
Tumour grade	Low/ High	2.09 (1.33 - 3.31)	0.001
Venous invasion	Absent/ Present	1.23 (0.79 - 1.92)	0.355
Perineural invasion	Absent/ Present	1.09 (0.77 - 1.54)	0.448
Resection margin status	R0/ R1	2.27 (1.34 - 3.88)	0.002
pAkt expression	**Low/ High**	**2.03 (1.20 - 3.43)**	**0.008**
C		**Overall survival**	
Prognostic variable	**Category**	**Hazard ratio (95%CI)**	**p value**
Tumour stage	T2/ T3	2.05 (1.06 - 3.97)	0.034
Lymph node positivity	Absent/ Present	1.87 (1.02 - 3.45)	0.061
Tumour size (mm)	< 30/ ≥ 30	1.67 (1.05 - 2.51)	0.028
Tumour grade	Low/ High	2.01 (1.29 - 3.75)	0.002
Venous invasion	Absent/ Present	1.46 (0.93 - 2.31)	0.102
Perineural invasion	Absent/ Present	1.10 (0.77 - 1.54)	0.448
Resection margin status	R0/ R1	2.20 (1.29 - 3.73)	0.003
Ki67 expression	**Low/ High**	**0.67 (0.43 - 1.20)**	**0.168**

5.8 Prognostic influence of insensitivity to growth inhibition markers

The TGFβ pathway, which includes the TSG SMAD4, is inactivated in approximately 50% of PDAC, either by mutation of one allele plus loss of the other allele or by homozygous deletion of both alleles. Loss of the SMAD4 is an early event in PDAC, however combining two studies within the meta-analysis (341, 342), each reporting prognostic impact but in opposing directions, did not reveal any prognostic impact on overall survival (p = 0.21). A further component of the TGFβ pathway, TGFβ1 itself was also an independent predictor of outcome following resection. The prognostic influence of this functional grouping was assessed in PDAC TMA cohort.

5.8.1 SMAD4 and TGFβ1: correlation with clinicopathological features and survival

SMAD4 staining was evident within the nucleus and cytoplasm of tumour epithelium (Figure 11.3E), but not evident in surrounding fibroblasts or inflammatory cells. SMAD4 was present in the cytoplasm of normal ducts in 86% of specimens. TGFβ1 staining was evident within the nucleus and cytoplasm of tumour epithelium (Figure 11.3E), but was rarely present in the surrounding stromal tissue.

5.8.1.1 SMAD4 clinicopathological correlations

32% of patients (n = 38) had low or absent expression of SMAD4 in the cytoplasm of tumour cells compared to 68% with maintained expression (n = 81). Only 15% of patients (n = 18) had evidence of loss of expression of SMAD4 in the nucleus. Loss of SMAD4 expression did not correlate with any clinicopathological feature. Loss of SMAD4 expression in the cytoplasm (< 5% of tumour cells showing evidence of staining) was related to a significant reduction in survival with a median survival of 13.4 months (95%CI: 9.8–17.0) compared to 20.7 months (95%CI: 16.2–25.8) for tumours with SMAD4 expression maintained (p = 0.027, Log-rank test) (Table 5.2). Most importantly, in a multivariate analysis, low SMAD4 expression remained an independent predictor of poor survival (HR: 1.73, 95%CI: 1.11–2.69, p = 0.011) (Table 5.9). When nuclear expression was assessed however, there was no significant correlation with outcome with high SMAD4 high expression having a median survival of 17.6 months (95%CI: 14.6–20.8) compared to 24.6 months for those with low SMAD4 expression (95%CI: 5.6–43.0) (p = 0.33, Log-rank test).

5.8.1.2 TGFβ1 clinicopathological correlations

51% (n = 61) had low or absent expression of TGFβ1 in tumour cytoplasm compared to 49% with high expression (n = 58) (Histoscore = 120). TGFβ1 expression failed to correlate with any clinicopathological feature. Cytoplasmic expression in PDAC cells did not correlate significantly with outcome, as patients with high cytoplasmic expression (n = 58) survived for 14.8 months (95%CI: 11.3–18.3) compared to those patients with low

expression (n = 61) who survived 19.6 months (95%CI: 15.7–22.4, p = 0.52, Log-rank test) (Table 5.2).

5.8.1.3 Association of protein biomarker expression and site of recurrence

Limited investigation of the influence of molecular marker expression in PDAC on the site of primary recurrence has been performed. IHC based molecular markers were investigated for potential correlation with site of tumour recurrence within the TMA cohort. The median cytoplasmic expression of SMAD4 was significantly reduced in tumours with distant metastases as the primary site of failure (median histoscore = 10.2) compared with local recurrence (median histoscore = 26.8, p = 0.043) (Figure 11.8). All other IHC assessed markers failed to correlate significantly with site of recurrence.

5.8.2 Discussion

Using IHC, these data confirm that reduced SMAD4 expression is associated with poor survival (265) and furthermore on a subset of the total cohort it was confirmed that SMAD4 expression is significantly reduced in those patients who developed distant metastases as the primary site of failure. No other protein marker measured by IHC was associated with the site of tumour recurrence. IHC is not an ideal methodology for analysis of a gene inactivated by mutation, however a more recent study considering mutation analysis confirmed that, of the genes investigated, only inactivation of SMAD4 was associated with poor survival following resection (122). The utility of molecular markers to predict the pattern of recurrence has been evaluated in a study by Iacobuzio-Donahue and colleagues (122), in which tumours with extensive metastatic disease burden showed SMAD4 loss rates of 75%, compared to locally advanced PDAC from patients with no evidence of metastases which had a loss rate of only 22%. It has been suggested that the association between loss of SMAD4 and poor survival may result from an increased propensity of PDAC with inactivated SMAD4 to metastasise widely. Despite no other clinicopathological factor correlating with SMAD4 expression, the current study supports the concept that a poorer survival is associated with SMAD4 inactivation (342). None of this work however, confirms that SMAD4 plays a direct role in metastasis. Further correlation of molecular marker expression with site of recurrence may conceivably identify a group of patients that benefit from more aggressive neoadjuvant or adjuvant therapies. The association of SMAD4 gene inactivation with poor prognosis and an increased propensity to metastasise has direct clinical implications. Namely, patients with borderline resectable tumours, with especially high risk of resection margin involvement, might be spared the morbidity of surgical resection, as their tumours may be more likely to metastasise widely. Those patients with borderline resectable PDAC and *intact* SMAD4 may benefit from local control provided by neoadjuvant chemotherapy followed by PD.

While TGFβ1 is an integral component of PDAC tumour biology, these data do not confirm the previous prognostic literature and therefore do not support the use of TGFβ1 as an IHC marker of prognosis in the studied cohort.

Table 5.9 Multivariate Cox regression analysis for SMAD4 expression

Clinicopathological parameters and SMAD4 expression in patients undergoing resection for PDAC.

		Overall survival	
Prognostic variable	**Category**	**Hazard ratio (95%CI)**	**p value**
Tumour stage	T2/ T3	2.20 (1.13 - 4.28)	0.019
Lymph node positivity	Absent/ Present	1.10 (0.90 - 2.89)	0.061
Tumour size (mm)	< 30/ ≥ 30	1.73 (1.11 - 2.68)	0.015
Tumour grade	Low/ High	2.42 (1.53 - 3.95)	<0.001
Venous invasion	Absent/ Present	1.31 (0.83 - 2.07)	0.234
Perineural invasion	Absent/ Present	1.12 (0.89 - 1.34)	0.628
Resection margin status	R0/ R1	2.03 (1.19 - 3.46)	0.009
SMAD4 expression	**High/ Low**	**1.73 (1.11 - 2.69)**	**0.011**

5.9 Hierarchical clustering of protein expression defines subclasses of PDAC

While the previous sections have illustrated that individual or paired markers can have prognostic value, there is interest in the identification of protein expression patterns that relate to outcome. It is also hoped that investigation of the inter-relationships underlying a prognostic protein expression signature would provide information underlying PDAC tumour biology.

5.9.1 Hierarchical clustering based on all studied markers

Hierarchical clustering of the 119 patients based on all IHC markers studied for prognostic utility was performed. This identified 4 distinctive clusters as illustrated in Figure 5.4A. Cluster 1 (n = 30), cluster 2 (n = 13), cluster (n = 37) and cluster (n = 39). Correlation with clinicopathological features including survival was performed but failed to identify significant relationships.

5.9.2 Hierarchical clustering based on functional groups of markers

Subsequently hierarchical clustering was performed based on the functional groups. Firstly, the markers related to senescence appear to have an important role in pancreatic tumourigenesis. Although not a functional grouping described by Hanahan and Weinberg, members of this pathway are perturbed in PDAC development. The initial senescence grouping was expanded to include other important targets including pAkt and Bcl-2.

Hierarchical clustering of patients using markers related to senescence identified 5 distinctive clusters in Figure 5.4B. Cluster 1 (n = 37) is characterised by high pAkt expression and low p21 expression, cluster 2 (n = 27) by low expression of p53, p21 and Bcl-2. Cluster 3 (n = 30) demonstrated high expression of Lkb1 and pAkt, cluster 4 (n = 15) high expression of p53, Lkb1 and pAkt, while cluster 5 (n = 12) had high expression of p21, Lkb1 and low Bcl-2.

Subgroup analysis of the clusters based on pathological features revealed that 15/15 patients in cluster 4 had lymph node involvement (χ^2 test, p = 0.032). Venous invasion also differed significantly (χ^2 test, p = 0.039), with a trend towards a difference in R1 status (χ^2 test, p = 0.07) (Table 5.10). Furthermore, a higher proportion of liver metastases occurred as the primary site of failure in Cluster 5 patients (χ^2 test, p = 0.041) (Table 5.10). Survival analysis revealed a significant association with overall survival (p = 0.002, Log-rank test) with cluster 5 having the most favourable (47.7 months, 95%CI: 27.3–68.1) and cluster 4 the least favourable outcome (13.5 months, 95%CI: 9.3–17.6) (Figure 5.4C). A multivariate analysis was performed using cluster 5 as the reference group. This clustering based prognostic signature remained an independent predictor of good outcome following resection (HR: 0.49, 95%CI: 0.35–0.63, p = 0.004) (Table 5.11).

When patients were clustered by the expression pattern of invasion and metastases proteins, four clusters were identified (Figure 5.4D) although no clinicopathological correlations were demonstrated. Cluster 1 had a shortened survival compared to other clusters but this was not statistically significant ($p = 0.54$, Log-rank test) (Figure 5.4E).

5.9.3 Discussion

Using semi-quantitative scoring of protein expression in a large TMA cohort of PDAC samples, hierarchical clustering analysis was applied in an attempt to develop a multi-marker phenotype. The initial attempt to cluster the cohort based on a large panel of markers generated well-defined clusters, however, these did not correlate with survival. The expression of p53 and p21 appeared to drive this clustering pattern and so focus was given to clustering on the functional grouping of senescence with successful results. The cluster analysis introduces five subclasses of PDAC that can be distinguished by their overall survival following resection. Importantly, cluster 5, which showed down-regulation of Bcl-2 and p53 with up-regulation of p21, Lkb1 and pAkt was independently associated with a significantly prolonged survival. The relatively weak HR may suggest that further refinement of the protein expression signature is possible. However, it may be that molecular profiling cannot greatly supplement the prognostic value of the established clinicopathological factors such as resection margin status.

This is the first example of protein expression being utilised to cluster PDAC patients to firstly identify subgroups with aberrant pathway activation and secondly identify clusters that vary in survival outcome. It has provided an unbiased means of identifying marker profiles associated with prognosis. Failure to identify prognostic clusters related to markers of invasion and metastasis was disappointing in view of the influence of the individual markers, however, repetition with a modified selection of markers will be of interest.

Proteins are subject to modulation by intricate molecular interactions, employed in pathways to induce cellular effects. Rather than targeting investigations on individual protein targets, multi-marker phenotypes that include combinations of clinicopathological features and tumour markers can be helpful in the identification of poor prognostic subgroups, as demonstrated by a panel of 13 IHC markers identifying a high-risk group of node-negative colorectal tumours (343). Only a selection of markers have been utilised and further IHC to investigate additional pathways including angiogenesis and apoptosis will be important future steps.

5.10 Overall discussion

Even in the era of novel high-throughput molecular assays, IHC remains a versatile tool for cancer biology investigation. Providing a direct link between the characterisation of protein expression and histological appearance of a specimen (344), it additionally provides cellular localisation information. IHC is routinely employed as a relatively inexpensive diagnostic

test, however, it has failed to find routine application for prognostic markers in PDAC despite morphological features inadequately stratifying survival following surgery. While considered a homogenous disease, in which all patients develop metastases and progress rapidly to death, molecularly defined sub-groups of PDAC can identify patients with distinct clinicopathological features (299).

TMA technology has extended the utility of IHC-based biomarker assessment by facilitating high-throughput analysis across large cohorts (345), standardising staining conditions and reducing misclassification. This is a advancement as studies utilising TMA datasets more frequently report significant results in PDAC (299). Tremendous variation exists in the experimental procedures, including antigen retrieval, observer variability and cut-off point selection, which could potentially influence the prognostic value of the proposed association. It is likely that even adherence to the REMARK guidelines is not enough (301), as these do not currently adequately account for, or standardise variation in, the staining of individual proteins, which remains a considerable source of inter-study variation.

The data in the current chapter is the first time that semi-quantitative assessment of multiple markers has been performed in PDAC, with these results being consistent with the previous literature. While only an evaluation of a selection of markers; the majority of those chosen were prognostic based on a review of the literature. Such methodology requires large numbers and although the current work used a cohort of hundred and nineteen patients, further larger cohorts are required to test this profiling method. Despite use of a semi-quantitative scoring method, which resulted in a continuous score for protein expression, there is still the potential for bias associated with subjective categorical assessment. The use of automated quantitative image analysis has the potential to eliminate this bias (346), however the difficulty created by tissue heterogeneity and intense stromal reaction in PDAC has limited its use. The original intention was to assess immunostaining using an automated algorithm, however despite a great deal of time spent optimising the Slidepath image analysis software (data not shown), it was not possible to reliably identify all cellular compartments. It is hoped that with future with development this will become the routine method.

The chosen markers are not a complete set and systematic review of the literature suggests that markers such as S100A2 may serve as a powerful component of a profile. Ideally a further validation set would have been used to test any findings of the current work. In the future any further IHC prognostic profiling studies will be conducted with a definite test set and validation set structure. For PDAC research this degree of rigor is lacking as exemplified recently in assessment of S100A2 (337). The original intention had been to test

Bax as part of the apoptosis functional grouping. Unfortunately, antibody optimisation proved challenging in the PDAC TMA.

For the majority of markers the findings of the previous literature were confirmed. For E-cadherin and COX-2 these data provide a degree of confidence that these markers are prognostically independent of established clinicopathological factors in PDAC. A potential subsequent step is investigating the prognostic utility of these markers in preoperatively collected EUS-FNA specimens.

A completely novel aspect of this thesis has been the clustering of PDACs based on protein marker expression in an attempt to develop a multi-marker IHC prognostic signature. In this preliminary investigation, successful identification of clinically relevant subgroups of resected PDAC patients, based on markers relating to senescence and apoptosis, was performed. Further, more complete profiling is required in a further validation group before confident conclusions can be drawn. However, this work has provided evidence that such a method is useful in advancing understanding of the influence of pathways and protein expression on outcome in resected PDAC. Various methods have been employed in other cancers including the Classification and Regression Tree method (347), and therefore comparison of techniques would be necessary.

5.10.1 Summary

Scoring immunostaining for a number of markers by semi-quantitative evaluation methods may enhance the clinical value of IHC in PDAC. These data have provided evidence that hierarchical clustering of IHC expression data identifies patient sub-groups with significant variation in outcome. The assessment of multiple-markers and phenotype combinations may hold promise for the discrimination of prognosis in resectable PDAC.

Figure 5.3 Senescence signalling clinicopathological correlation

A) *Boxplot of Lkb1 median histoscore versus tumour grade: Low grade tumours (n = 81) exhibited a higher level of Lkb1 expression (median histoscore = 128) versus high-grade tumours (n = 33) (median histoscore = 100) (p = 0.01, Mann-Whitney U test).*

B) *Boxplot of Lkb1 median histoscore versus tumour stage: Stage T2 tumours (n = 13) had a higher level of Lkb1 expression (median histoscore = 150) versus stage T3 tumours (n = 111) (median histoscore = 105) (p = 0.02, Mann-Whitney U test).*

C) *Kaplan-Meier analysis showing cases with low Lkb1 expression (n = 29) have poorer outcome compared to those with high expression (n = 80) following PD (Log-rank test, p = 0.008).*

D) *Kaplan-Meier analysis illustrates that cases with p21 low expression (n = 92) have poorer outcome compared to those with high expression (n = 27) following PD (Log-rank test, p = 0.006).*

E) *Kaplan-Meier analysis illustrates that Lkb1high/p21high have a more favourable outcome compared to Lkb1high/p21low and Lkb1low /p21low cases (Log-rank test, p = 0.002).*

F) *Correlation of Lkb1 with p21 protein expression in 118 cases of PDAC (Spearman's $\rho = 0.34$; $p < 0.001$).*

G) *p53 drives metastasis of PDAC. p53 histoscore in relation to lymph node status in cases of PDAC (Lymph node (LN) negative, metastatic disease present in < 50% of lymph nodes sampled, metastatic disease present in > 50% of lymph nodes sampled) (Mann-Whitney U test). Mean number of nodes reviewed per resection = 21.*

H) *Boxplot of p53 histoscore in $Lkb1_{low}/p21_{low}$ tumours (Red bar, n = 20) compared with $Lkb1_{high}/p21_{low}$ tumours (Blue bar, n = 58) ($p < 0.05$, Mann-Whitney U test).*

I) *Lkb1 a serine/threonine kinase that activates the AMP kinase cascade. Furthermore it is a negative regulator of mTOR signalling and Lkb1 associates with p53 and regulates p53-dependent apoptosis and transactivation of p21.*

Figure 5.3

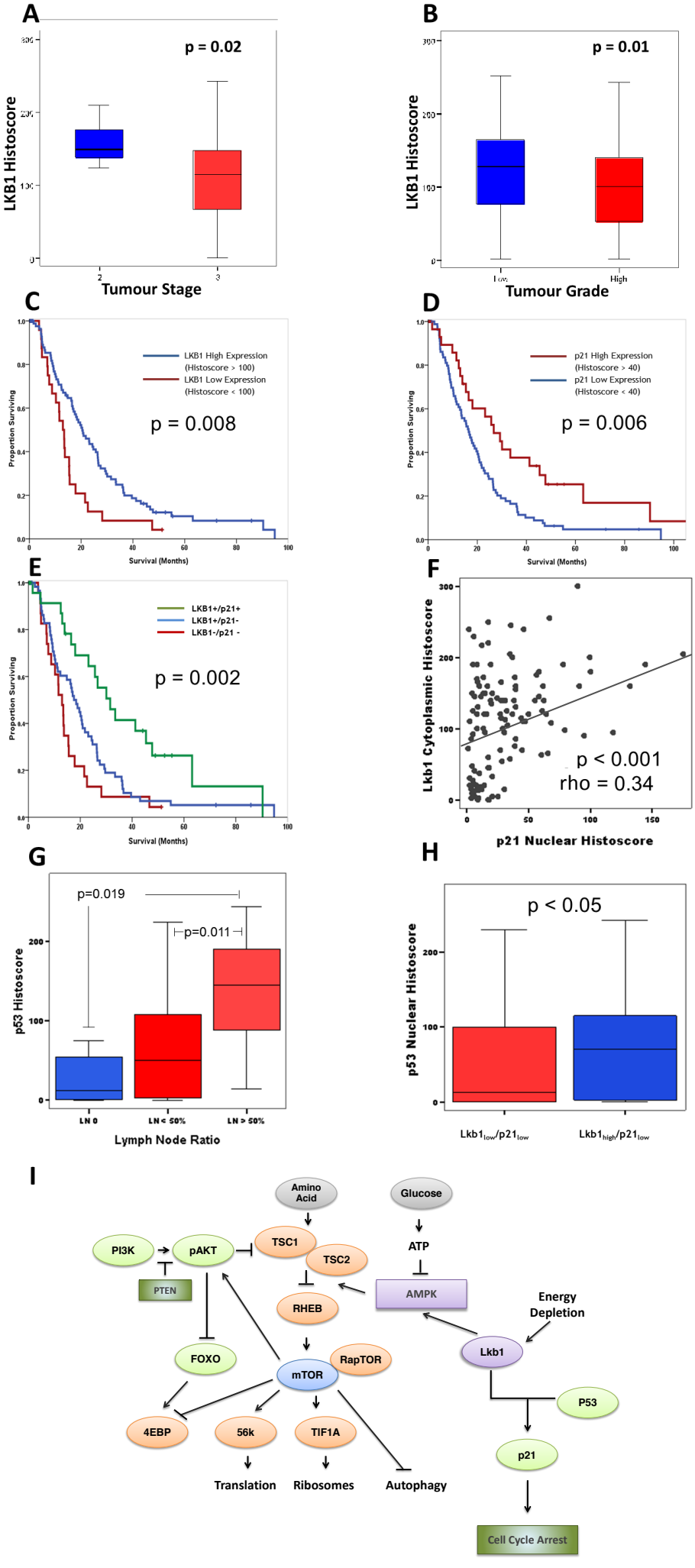
A
p = 0.02
LKB1 Histoscore
Tumour Stage
B
p = 0.01
LKB1 Histoscore
Tumour Grade
C
LKB1 High Expression (Histoscore > 100)
LKB1 Low Expression (Histoscore < 100)
p = 0.008
Proportion Surviving
Survival (Months)
D
p21 High Expression (Histoscore > 40)
p21 Low Expression (Histoscore < 40)
p = 0.006
Proportion Surviving
Survival (Months)
E
LKB1+/p21+
LKB1+/p21-
LKB1-/p21 -
p = 0.002
Proportion Surviving
Survival (Months)
F
p < 0.001
rho = 0.34
Lkb1 Cytoplasmic Histoscore
p21 Nuclear Histoscore
G
p=0.019
p=0.011
p53 Histoscore
LN 0
LN < 50%
LN > 50%
Lymph Node Ratio
H
p < 0.05
p53 Nuclear Histoscore
Lkb1low/p21low
Lkb1high/p21low
I
Amino Acid
Glucose
PI3K
pAKT
TSC1
TSC2
ATP
PTEN
AMPK
RHEB
Energy Depletion
FOXO
mTOR
RapTOR
Lkb1
P53
4EBP
56k
TIF1A
p21
Translation
Ribosomes
Autophagy
Cell Cycle Arrest

Figure 5.4 Hierarchical clustering related to IHC expression of senescence markers

A) *Hierarchical clustering of PDACs using Cluster and Treeview application based on all markers studied. Red represented high expression, green low expression. 4 clusters are defined. Cluster 1 had low expression of p53 and p21 as did Cluster 4. Cluster 3 had high expression of p53. Cluster 1 had specimens with low β-catenin and E-cadherin. The clustering failed to correlate with survival following resection. According to the logarithmic colour bar, red represents high protein expression while green represents low protein expression.*

B) *Hierarchical clustering of PDACs using Cluster and Treeview application based on senescence markers for 119 patients. 5 clusters are defined. Cluster 1 had high expression of pAkt and low expression of p21. Cluster 2 had low expression of p53, p21 and Bcl-2. Cluster 3 had high expression of Lkb1 and pAkt. Cluster 4 had high expression of p53, Lkb1 and pAkt while cluster 5 had high expression of p21, Lkb1 and low Bcl-2 expression.*

C) *Kaplan-Meier survival analysis for 119 PDACs with respect to overall survival according to senescence based cluster assignment. Cluster 5 survival time was significantly prolonged compared to the combination of the other clusters (Log-rank test, p = 0.002).*

D) *Hierarchical clustering of PDACs using Cluster and Treeview application based on invasion and metastases markers for 119 patients. Four clusters are defined. Cluster 1 had high expression of pAkt and low expression of p21. Cluster 2 had low expression of p53, p21 and Bcl-2. Cluster 3 had high expression of Lkb1 and pAkt. Cluster 4 had high expression of p53, Lkb1 and pAkt.*

E) *Kaplan-Meier survival analysis for 119 PDACs with respect to overall survival according to invasion and metastases based cluster assignment (Log-rank test, p = 0.54).*

Figure 5.4

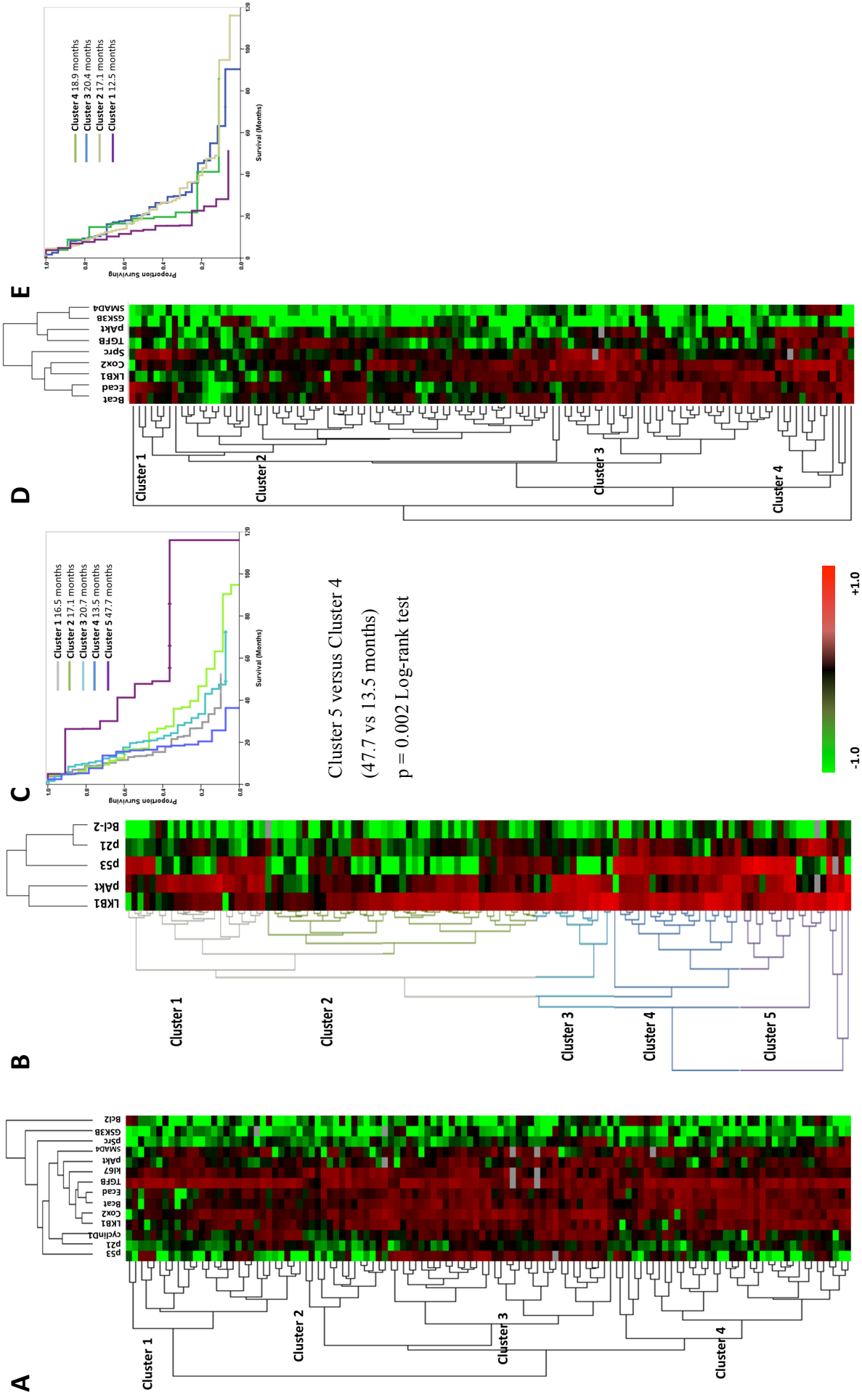
A
Cluster 1
Cluster 2
Cluster 3
Cluster 4
p53
p21
cyclinD1
LKB1
CoxII
Bcat
Ecad
TGFB
Ki67
pAkt
SMAD4
pSrc
GSK3B
Bcl2
B
Cluster 1
Cluster 2
Cluster 3
Cluster 4
Cluster 5
LKB1
pAkt
p53
p21
Bcl-2
C
Cluster 1 16.5 months
Cluster 2 17.1 months
Cluster 3 20.7 months
Cluster 4 13.5 months
Cluster 5 47.7 months
Survival (Months)
Proportion Surviving
Cluster 5 versus Cluster 4
(47.7 vs 13.5 months)
p = 0.002 Log-rank test
+1.0
-1.0
D
Cluster 1
Cluster 2
Cluster 3
Cluster 4
Bcat
Ecad
LKB1
CoxII
Spsrc
TGFB
pAkt
GSK3B
SMAD4
E
Cluster 4 18.9 months
Cluster 3 20.4 months
Cluster 2 17.1 months
Cluster 1 12.5 months
Survival (Months)
Proportion Surviving

Table 5.10 Comparison between senescence expression clusters and pathological characteristics

Pathological variable		Cluster 1+3 n = 37 (%)	Cluster 2+3 n = 57 (%)	Cluster 5 n = 12 (%)	Cluster 4 n = 15 (%)	p value [a]
Tumour stage	T2	3 (8)	5 (9)	4 (33)	1 (7)	0.299
	T3	34 (92)	52 (91)	8 (67)	14 (93)	
Tumour size (mm)	<30	16 (43)	35 (61)	7 (58)	6 (40)	0.226
	≥30	21(57)	22 (39)	5 (42)	9 (60)	
Tumour grade	Low	25 (68)	42 (73)	9 (75)	11 (73)	0.917
	High	12 (32)	15 (27)	3 (25)	4 (27)	
Lymph node status	Absent	7 (19)	12 (23)	6 (50)	0 (0)	0.032
	Present	30 (81)	45(77)	6 (50)	15 (100)	
Margin involvement	R0	12 (32)	12 (21)	5 (42)	1 (7)	0.07
	R1	25 (68)	45 (79)	7 (58)	14 (93)	
Perineural invasion	Absent	2 (5)	7 (13)	2 (20)	1 (7)	0.720
	Present	35 (95)	51(87)	10 (80)	14 (93)	
Venous invasion	Absent	13 (35)	34 (59)	8 (67)	5 (33)	0.039
	Present	24 (65)	23 (41)	4 (33)	10 (67)	
Site of first recurrence	Liver	9 (38)	11 (29)	8 (89)	5 (46)	0.041
	Other sites of recurrence	15 (62)	28 (71)	1 (11)	6 (54)	

[a] χ^2 tests were used to compare categorical variables
Cluster 1 and 3 were combined for purpose of this analysis

Table 5.11 Multivariate Cox regression analysis for multi-marker senescence signature

Prognostic significance of Cluster 5 compared to the other clusters.

		Overall Survival	
Prognostic variable	**Category**	**Hazard ratio (95% CI)**	**p value**
Tumour stage	T2/ T3	2.37 (1.21 - 4.66)	0.012
Lymph node involvement	Absent/ Present	1.53 (0.83 - 2.87)	0.175
Tumour size (mm)	< 30/ ≥ 30	1.56 (1.04 - 2.35)	0.031
Tumour grade	Low/ High	3.65 (2.19 - 5.79)	< 0.0001
Venous invasion	Absent/ Present	1.08 (0.68 - 1.70)	0.752
Perineural invasion	Absent/ Present	0.76 (0.46 - 1.89)	0.662
Resection margin status	R0/ R1	2.29 (1.37 - 3.85)	0.0001
Multi-marker senescence clustering	**Good/ Poor prognosis**	**0.49 (0.35 - 0.63)**	**0.004**

Introduction to genome wide analysis chapters

In the preceding chapters investigation of the influence of a number of candidate markers on outcome following pancreatic cancer resection was performed. The remaining four results chapters of the thesis will cover the investigation of potential prognostic markers in pancreatic cancer using a genome wide approach. In particular they will evaluate firstly in what way gene expression signatures vary according to clinicopathological features, including survival (Chapter 6). Secondly, the manner in which miRNA expression relates to clinicopathological states including survival (Chapter 7) and thirdly, how clinicopathological features impact upon copy number change (Chapter 8). Finally, data from these chapters will be integrated in an attempt to identify critical gene targets that may be involved in PDAC tumourigenesis (Chapter 9).

6 Gene Expression Molecular Profiles Associated with Diagnosis, Clinicopathological Criteria and Survival in Resectable PDAC

6.1 Introduction

Large-scale transcriptional profiling can identify differentially expressed genes and molecular signatures in numerous biological systems including malignancy (4). Recent efforts in cancer to derive clinical predictors of survival from gene expression data have focused on discrete patient groups clustered at either end of the survival spectrum. For pancreatic cancer several studies have identified differentially expressed genes compared with normal pancreas (Table 1.4), but there has been a scarcity of signatures developed for PDAC that relate to pathological features or prognosis.

6.1.1 Aim

The aim in this chapter was to investigate, using whole-genome oligonucleotide arrays, the gene expression signatures associated with clinicopathological states in patients with PDAC. Furthermore, the identification and validation of a prognostic gene expression signature was attempted. Additionally, validation of a recently generated PDAC prognostic gene signature was performed using the gene expression profiled cohort from this thesis.

6.2 Results

6.2.1 PDAC and normal pancreatic tissue: differentially expressed genes.

The analysis workflow for this chapter is shown in Figure 11.9. Gene expression profiling was performed for 48 primary PDACs and 10 matched normal pancreatic samples on Agilent 44K-Human oligonucleotide microarrays to generate signatures of malignant transformation. The clinicopathological features of the cohort are summarised in Table 2.1. Only patients for which fresh frozen tissue from which high quality RNA could be extracted were included in this analysis.

Following global normalisation and filtering of the array data, 31,296 of 44,200 features were available for analyses. Based on a group comparison t-test, 1359 genes were differentially expressed at $p < 0.001$, with 573 genes differentially expressed at $p < 0.0005$ (Figure 6.1). To increase the confidence that identified genes were relevant to pancreatic carcinogenesis, further selection of only those genes with $p < 1x10^{-5}$ and at least 2-fold deregulation between matched normal pancreatic tissue and PDACs was performed. 48 genes were up-regulated and 28 showed reduced expression (76 genes in total) (Table 11.5A, B).

6.2.2 Comparison of PDAC and normal pancreatic tissue: class prediction.

Gene expression levels in PDACs and normal pancreatic samples were explored to determine whether they were sufficiently different to discern the two groups. One classifier, support vector machines analysis, resulted in a correct prediction rate of 96%. A multidimensional scaling analysis plot (Figure 6.2A) illustrates PDAC separation from normal specimens based on the 573-gene classifier.

6.2.3 Functional annotation of differential gene expression: PDAC and normal.

A problem encountered in the analysis of expression data is biological interpretation of the generated gene lists. The functional annotation of differentially expressed lists and their affiliation with signalling pathways were interrogated using DAVID and GeneGo software. The search was targeted to the 76 genes with > 4-fold expression difference between PDAC and matched normal pancreatic tissue. Genes of interest included those known to be aberrant in PDAC: PSCA, S100P, S100A2 and several novel targets including: Aquaporin (AQP) 5, PITX1, CLIC3, IRX5 and TRIM29. 20 networks were generated with the most significant related to S100A2 and PITX1. Further detail is provided in Appendix 11.4.1 and Figure 11.11.

6.2.4 Gene expression analysis according to lymph node status

Gene expression patterns were then assessed according to lymph node status, potentially informing as to whether the propensity for lymph node spread is an inherent feature of the primary tumour. 138 genes that were differentially expressed ($p < 0.01$) between the lymph node–negative (LN0) and positive (LN1) PDACs (Table 11.6). 71 genes were down-regulated in LN1 tumours, and 67 were up-regulated compared with LN0 tumours. The most significantly up-regulated genes included VEGFB, MMP13 and SPEG. EYA4 and SERPINB11 were strongly down-regulated in the LN1 group. Group separation based on this 138-gene profile is displayed in Figure 6.2B. A class prediction analysis employing this set achieved sensitivity for the detection of LN1 tumours of 83% and a specificity of 66%. Functional gene annotation between LN0 and LN1 tumours is presented in Appendix 11.4.3.

6.2.5 Gene expression analysis according to resection margin status

Investigation as to whether R1 status associated with an altered gene expression signature identified 154 genes ($p < 0.005$) differentially expressed including MIP, SYVN1, PLOD2 and ADCY1 (Figure 11.11). There was significant enrichment for T cell mediated immune response, SODD/TNFR1 signalling pathway and PITX2 transcription.

6.2.6 Gene expression analysis according to peripancreatic fat invasion status

The presence of fat invasion was associated with differential expression of 739 genes ($p < 0.001$) with significant up-regulated targets including SCGB1A1, EPN1, NTRK3 and BOK while down-regulated genes included PCDH7, AQP4 and NOX-1. Pathway enrichment identified highlighted neural invasion and Wnt signalling.

6.2.7 Gene expression analysis according to other pathological factors

Additional gene expression analysis according to tumour grade, stage, venous invasion and site of recurrence are included in Appendix 11.4.4. These gene signatures, and their overlap, are illustrated in Figure 6.3. Three genes were differentially expressed in association with all four of tumour grade, stage, resection margin status and lymph node status: EPN3, TRIB3 and BTBD14B.

6.2.8 Prognostic gene expression signature following resection

Gene expression patterns were then investigated in the context of prognosis. Hierarchical average-linking clustering analysis was used initially, which grouped patients according to similar overall gene expression patterns for all genes. Two groups were identified containing 23 and 25 patients respectively (Figure 6.4A). Kaplan-Meier analysis of the resulting unsupervised clustering groups demonstrated a trend towards a significant difference (Figure 6.4B), with the median overall survival for the poor prognostic group (cluster 1) being 13.0 months (95%CI: 2.6–23.8) versus 26.4 months (95%CI: 23.8–29.0) for the favourable outcome group (cluster 2) ($p = 0.061$, Log-rank test).

As a survival difference was evident according to unsupervised gene expression cluster analysis, those genes most significantly associated with survival were defined using a Cox proportional-hazards model. This serially assessed the individual prognostic influence of all genes within the cohort (Figure 11.12). 332 genes most significantly associated with overall survival were identified ($p = 0.001$, Table 11.7) and used to re-cluster the 48 patients (Figure 6.5A). The two clusters differed significantly in terms of survival outcome, with the favourable prognosis group having a median overall survival of 39.6 months (95%CI: 16.6–62.5) versus 13.0 months (95%CI: 5.9–20.1) for the poor prognosis group (Log-rank test, $p < 0.001$, Figure 6.5B).

To determine the extent that survival could be predicted based on a multivariate prognostic index, a LOOCV model was used to classify patients into longer or shorter survival groups. Nine of the most powerful predictors of this 107-gene prediction model (Table 11.8) are illustrated in Figure 6.6A. The survival difference was statistically significant as determined by the permutation distribution of the cross validation Log-rank χ^2 statistic ($p < 0.05$). The longer surviving group (23 patients) had a median survival of 30.1 months (95% CI: 12.3–47.8) versus 13.0 months (95%CI: 5.1–20.9). A selection of powerful prognostic genes ($p < 1x10^{-6}$) included chloride ion transporter 3 (CLIC3), transglutaminase 2 (TGM2), dual specificity phosphatase 5 (DUSP5), NT5E and selenium binding protein 1 (SELENBP1) (Figure 6.6A). There was a trend towards high-grade tumours being associated with a high-risk gene profile ($p = 0.065$, χ^2 Test) and adjuvant therapy usage was more common in the low-risk group ($p = 0.045$, χ^2 Test) (Table 6.1). In addition to the overall survival profile, tumour stage, lymph node status, R1 status, venous, perineural invasion and adjuvant chemotherapy showed prognostic value ($p < 0.05$) within univariate analysis (Table 6.2, Figure 11.13). In multivariate analysis T stage, R1 status, adjuvant therapy allocation and the 107-gene survival profile yielded independent prognostic value (HR: 5.36, 95%CI: 2.22–12.9, $p < 0.001$, Table 6.3).

To assess which gene sets associated with survival, Gene Set Enrichment Analysis (GSEA) was performed. 140 GO groups were significant including cullin-RING ubiquitin ligase

complex, MAPKKK cascade and SMAD phosphorylation (Table 11.9). In terms of BioCarta and KEGG pathway analysis, 53/303 (Table 11.10) and 29/171 (Table 11.11) were associated with overall survival respectively including bone remodeling, Cyclin E destruction, CD40L and PPARα pathways, with predicted significant transcription factors shown in Table 11.12.

6.2.9 Methodological validation of component of the overall survival profile

To validate the gene expression microarray data, qRT-PCR was performed for the 48 samples included in the microarray analysis. 3 genes, CLIC3, DUSP5 and TGM2, were selected from the top scoring 107-gene survival profile according to biological plausibility. Relative expression levels for each gene were correlated with the corresponding microarray signal intensities confirming strong relationships for all three genes (Figure 6.6B).

6.2.10 CLIC3 validation analysis

As one of the most highly ranked genes in the prognostic signature, validation of the prognostic utility of CLIC3 was performed by analysing protein expression in the TMA cohort. CLIC3 was undetectable in either normal pancreatic ductal or acinar tissues (Figure 6.7A). Examination of early PanINs revealed that CLIC3 expression was low within well-organised epithelia (Figure 6.7A; green arrows), whereas dysplastic regions of the PanIN were more abundant in CLIC3 (Figure 6.7A; red arrows). CLIC3 was highly expressed in PDAC (Figure 6.7A) being localised to cytoplasmic granules, but also observable in the nucleus of cancers with high CLIC3 levels (Figure 6.7B). Moreover, CLIC3 expression was highly enriched in regions where tumours invaded normal tissue (Figure 6.7B), suggesting a role for CLIC3 in the invasive behaviour of PDAC. Levels of CLIC3 did not differ in terms of traditional clinicopathological factors, however in univariate survival analysis, high CLIC3 expression (n = 37) was associated with significantly decreased overall survival (11.5 months, 95%CI: 7.9–15.1) compared with low expression (n = 85) (20.5 months, 95%CI: 15.6–24.6, $p < 0.01$, Figure 6.7E). Moreover, tumours from patients with a LNR > 50% had elevated levels of CLIC3 compared to LN0 tumours ($p < 0.005$) and those with lower levels of lymph node involvement ($p = 0.01$, Figure 6.7F). In multivariate analysis, high CLIC3 protein expression remained a predictor of poor survival (HR: 1.34, 95%CI: 1.06–1.78, $p = 0.026$, Table 6.4), independent of grade and lymph node status.

Using CLIC3 PCR mRNA data, it was confirmed that consistent with the histoscore analysis, high levels of CLIC3 were associated with poor survival for the 48 patients with a median overall survival for high expressors being 15.4 months (95%CI: 9.6–21.7) versus 49.0 months (95%CI: 31.1–57.3) for low CLIC3 expressors (Figure 6.7H, $p = 0.012$). Multivariate analysis confirmed that CLIC3 gene expression remained independently prognostic (HR: 4.81, 95%CI: 1.86–12.3, $p = 0.001$, Table 6.5).

6.2.11 Validation of prognostic gene signature in independent cohorts

Validation of the prognostic value of the gene survival profile within two independent microarray cohorts was performed. The signature genes were mapped to the validation data sets by Genebank accession or UniGene Symbol. Using validation cohort 1 (348), the initial analysis confirmed no significant differences in the frequency of pathological variables between low (n = 13) and high-risk groups (n = 14) (Table 6.1).

Visualisation of the gene signature, along with successful stratification of the cohort into low and high-risk groups was performed (Figure 6.8A). The prognostic utility of the 107-gene profile was then explored along with T stage, grade, lymph node status and R1 status within the validation cohort. Patients in the high-risk group, as determined by the 107-gene survival profile, had a significantly poorer outcome (HR: 4.34, 95%CI: 1.55–12.2, p = 0.005, Table 6.6A, Figure 6.8B). The gene expression signature was an independent predictor of poor overall survival along with lymph node status.

Validation cohort 2 was then analysed (349), with no significant difference in the distribution of T stage or lymph node status according to the low (n = 50) and high-risk groups (n = 51) (Table 6.1). Seven patients who died within three months of resection were censored from analysis. Visualisation of the gene signature along with successful stratification into low (n = 51) and high-risk groups (n = 51) was performed (Figure 6.8C). Allocation to the high-risk group resulted in a trend towards poor survival (HR: 1.59, 95%CI: 0.96–2.64; p = 0.067, Table 6.6B, Figure 6.8D), along with lymph node status. A further stratification into low, medium and high-risk groups identified a subgroup with particularly poor prognosis (HR: 2.11, 95%CI: 1.15–3.87, p = 0.016, Table 6.6C, Figure 6.8E) independent of lymph node status.

6.2.12 Validation of subtype gene signature in an independent cohort

Validation cohort 1 had previously been used to develop a gene expression signature identifying three PDAC subtypes with differing prognosis. This prompted analysis of this 72-gene signature within the 48 patient cohort from this thesis, clustering the patients as illustrated in Figure 11.14A. 15 patients were identified as belonging to the classical PDAC cohort, 25 to the exocrine-like cohort and 8 to the quasi-mesenchymal (QM) type. The relationship between clinicopathological factors and the PDAssigner subtypes are shown in Table 11.13. As in the original study, stratification by PDAssigner subtype provided significant prognostic information (Figure 11.14B, Table 11.14). Classical subtype patients had a significantly longer overall survival (43.0 months) than those categorised as QM-subtype (13.0 months, p = 0.002, Log-rank test). A multivariate analysis revealed independent predictors of poor outcome included T stage, LN1 status, R1 status, adjuvant therapy and the QM-subtype (HR: 5.86, 95%CI: 2.07–16.5, p = 0.001, Table 11.15).

6.3 Discussion

This chapter focused on the development of a microarray derived gene expression profile for PDAC. These data support the hypothesis that a gene expression profile can distinguish between PDAC and comparative normal pancreas, and between tumours with differing pathological features. Furthermore, these data provide evidence that a PDAC gene expression signature can provide prognostic information following resection. Therefore, these results add to the understanding of the molecular basis underlying the clinical behavior of PDAC.

When a number of gene expression microarray studies were compared by meta-analyses, 568 genes were consistently deregulated in PDAC. There was little concordance between the respective gene sets generated by the individual studies, with only 22% described in the published individual analysis (3). Several potential reasons exist for the low concordance: first, tumour histology, and type of normal tissue used (commercial RNA, normal from resected tumours or donor organs) varied. Second, microdissection was not universally applied. Third, differing array technologies were used and fourth, no gold standard exists for microarray analysis. More recently, Badea and colleagues identified genes specifically overexpressed in tumour epithelium (350) by combining their data with other studies including stromal, normal, PDAC, CP and tumour cell lines (175), providing a robust list of differentially expressed genes.

In this chapter cataloguing the difference in gene expression pattern between normal pancreas tissue and PDAC, genes were identified with established PDAC associations as previously noted (Table 1.4). Of note were genes not previously identified as being dysregulated, including AQP5, a water channel, putative oncogene and prognostic factor in colorectal cancer, potentially acting through the ERK/p38 MAPK pathway which is known to be aberrant in PDAC (351). Pituitary homeobox 1 (PITX1) is a potential TSG in lung cancer, down-regulating the RAS pathway through RASAL1 (352). Remarkably, PITX1 expression was significantly up-regulated in PDAC suggesting an altered role in this cancer. Pathway enrichment highlighted Notch, SRC and Wnt signalling as well as novel pathways including PML and Reelin signalling. Transcription factors associated with differentially expressed genes included SP1, a potential contributor to the transcriptional response of PDAC cells to TGFβ (353).

In LN1 tumours, many genes are up-regulated that associate with cancer progression including VEGFB, IRF7, MMP13 and SPEG. A number of potential TSGs with low expression in the LN1 group included EYA4 and SERPINB11, the latter a putative squamous cell carcinoma TSG (354). Based on a class prediction analysis, LN1 tumours could be distinguished to an extent from LN0 tumours. It may therefore be possible to

determine by examining resected primary tumours whether it is associated with synchronous lymph node metastases. Two studies have assessed microarray PDAC gene expression stratified by lymph node status (355, 356), however, there was little overlap with the current data, possibly reflecting small cohort size, array platform and analytical strategy. It has been suggested that R1 status reflects an inherent biological tumour property rather than merely a pathological criteria (251). Supporting this theory, numerous genes were differently expressed, many which are recognised as having a role in carcinogenesis. Aquaporin 0 with a cell adhesion role (357), and CASP8, an apoptosis regulator (358), were down-regulated three-fold in the R1 group suggesting apoptosis control may be lost. While insufficient to definitively support the biological argument, it highlights the need for further evaluation. Overlap between the pathological based signatures revealed numerous shared components, which warrant further analysis.

A lack of long-term survivors following PDAC resection and hence a narrow outcome spectrum, creates a challenge for gene expression signature identification. This problem may be surmountable by large cohort size; however, tissue availability and reagent cost are limiting factors. Using a semi-supervised Cox proportional-hazards model (359), a 107-gene survival profile was identified ($p < 0.001$), which clustered the cohort into long- or short-survival groups. These results infer an underlying organisation within the gene expression profile of the PDAC tumours relating to patient survival may exist. By grouping the cohort into ‘high-risk’ and ‘low-risk’ groups, the overall survival profile maintained independent prognostic significance in multivariate analysis. Limited overlap between individual genes, was found between the present survival profile and those reported in previous non-prognostic PDAC microarray studies (3).

Investigation then focused on an individual component of the prognostic signature, CLIC3, with validation of this novel prognostic factor in a large patient group an encouraging finding. Further investigation of the molecular role of CLIC3 in PDAC tumourigenesis is necessary. The gene survival profile contains several interesting genes (Figure 6.6, Table 11.7) many that have potential biologically plausible roles in cancer that offer potential insight into PDAC biology. The validity of this approach is confirmed by the observation that for many of these genes, earlier non-array methodologies have indicated relevance to PDAC, e.g. PLAU associated with poor prognosis in the present study, as previously reported (360). Additional markers of interest that will require validation as performed for CLIC3 include DUSP5: expression of which has been shown to influence ERK signalling in a breast cancer cell model (361). This is first report of DUSP expression relating to pathological features in PDAC. SELENBP1: loss is associated with reduced survival in ovarian cancer (362). TGM2: may play a role in cell growth through anti-apoptosis

signalling and may predict poor prognosis in colon cancer (363). Caveolin-3: while there has been no previous report of CAV3 associating with outcome, caveolin-1, a scaffolding protein, has been reported to be a poor prognostic factor in PDAC (364). NT5E: a T lymphocyte signalling molecule that may prevent tumour death by inhibiting antitumour immunity (365).

Gene set analysis identified potential novel prognostic pathways in PDAC including stathmin, which associates with PIK3CA activation and is a marker of poor prognosis in endometrial cancer (366). CXCR4 expression was previously correlated with poor outcome in PDAC (367), possibly enhancing cell proliferation through AKT and ERK pathways. Interestingly E2F1 amplification has been associated with poor outcome in PDAC (241).

The gene survival profile was validated in two independent data sets (Table 6.7), demonstrating prognostic utility in both. The first dataset had been used previously to develop a gene signature describing three novel PDAC subtypes with disparate outcomes (PDAssigner) (348). Data was combined from two cohorts to generate the signature, however the study was limited by the small sample size (n = 27) of the original validation cohort. Successful validation of the PDAssigner signature within the 48 patient cohort from this thesis, confirmed the prognostic utility of this novel signature. The second validation cohort, profiled PDAC tumours compared to matched metastatic lesions (349). This identified a prognostic six-gene signature initially applied to training and validation cohort confirming the prognostic utility, independent of pathological factors. The signature included KLF6, FOSB, NFκBIZ, ATPA4, GSG1 and SIGLEC11. KLF6 is a transcription factor with a putative TSG role in ovarian cancer, with over-expression previously noted to be prognostic in PDAC (368). It should be noted that disparate outcomes between the test and validation set within this study might have influenced the development of this prognostic signature. This signature failed to stratify outcome in the 48 patient cohort from this thesis (data not shown).

It was encouraging that the gene survival profile developed in this chapter predicted outcome in two further datasets. The limited overlap of the prognostic gene signatures may suggest that multiple sets of gene expression biomarkers exist in PDAC that could be useful for prognostication. This may explain in part the heterogeneity associated with PDAC gene expression profiles studies, exemplified by the meta-analysis that identified only seven shared genes (3). Comparison of the prognostic profile developed in this study and the two previous prognostic classifiers indicate there are large differences in sample numbers, microarray platform and classifier design methodology. Out of the total 185 potentially prognostic genes identified, only five were shared between studies (Figure 6.8F). Validation of the PDAssigner signature in the present cohort supports the concept that gene expression

signatures can discriminate PDAC subtypes and stratify outcome. Of the genes shared between the PDAssigner set and the gene survival profile (S100A2, NT5E, PAPPA, LOX and TWIST) biological plausibility exists for each to have a role in PDAC. S100A2 has been discussed in the previous chapter, while TWIST has previously been noted to be over-expressed and associated with EMT in PDAC (149). Interestingly, TWIST overexpression has been shown to decrease E-cadherin expression (369) that was shown in the previous chapter to be associated with poor overall survival. These findings support the concept of a 'prognostic space' of genes that may have critical prognostic relevance. Although the true test of clinical efficacy for a prognostic signature lies in prospective validation, initial development requires demonstration of prognostic utility when testing retrospectively. While this signature is clearly not ready for clinical use, it provides a building block for development. The importance of reducing variability of study heterogeneity as outlined in other cancers (370) should now be applied to PDAC.

The failure to perform laser capture microdissection prior to RNA extraction represents a significant limitation of this work. Microdissection of tumour epithelium from surrounding stromal tissue and contaminating normal epithelium would have enhanced the ability to identify overexpressed transcripts in PDAC. A further factor limiting this analysis has been that normal comparison pancreatic tissue was derived from resected specimens, not true normal pancreas. This could have been achieved ideally by the use of normal pancreas tissue resected during donor harvesting. Attempted validation in the independent cohorts was limited by heterogeneity between the studies in terms of patients, treatment, methodology and uniformity of the clinicopathological factors included within multivariate analysis.

6.3.1 Summary

The original hypothesis proposed that a gene expression a signature could be generated that relates to outcome following resection of PDAC. In this chapter, a gene signature associated with PDAC has been described, which in addition to confirming previous pancreatic profiling studies, has identified potential tumourigenesis targets. Furthermore, a gene expression signature was described associated with poor prognosis independent of clinicopathological parameters and with validated utility in further independent cohorts of PDAC patients. It is hoped that the development of such classifiers will enhance the understanding of PDAC biology, and may lead to the development of more refined prognostic gene signatures.

Table 6.1 Association between overall gene survival profile and pathological characteristics

Training and validation cohorts were divided into two groups (low and high risk) according to their overall gene survival profile.

		Training Cohort			Validation Cohort 1			Validation Cohort 2		
Prognostic variable		**Low Risk n = 24 (%)**	**High Risk n = 24 (%)**	**p value [a]**	**Low Risk n = 13 (%)**	**High Risk n = 14 (%)**	**p value [a]**	**Low Risk n = 51 (%)**	**High Risk n = 51 (%)**	**p value [a]**
Gender	Female	11 (46)	8 (33)	0.556	-	-	-	-	-	-
	Male	13 (54)	16 (67)							
Age (yrs) [b]	< 65	13 (54)	14 (58)	0.973	5 (39)	9 (64)	0.257	-	-	-
	≥ 65	11 (46)	10 (42)		8 (61)	5 (36)				
Tumour stage [c]	T2	3 (13)	3 (13)	0.990	2 (18)	4 (36)	0.635	9 (18)	9 (19)	0.990
	T3	21 (87)	21 (87)		9 (82)	7 (64)		42 (82)	38 (81)	
Tumour size (mm)	< 30	14 (53)	14 (56)	0.721	-	-	-	-	-	-
	≥ 30	9 (47)	11 (44)							
Tumour grade	Low	19 (79)	13 (54)	0.125	10 (77)	6 (43)	0.120	-	-	-
	High	5 (21)	11 (46)		3 (23)	8 (57)				
Lymph node status [d]	Absent	6 (25)	4 (17)	0.724	4 (36)	3 (27)	0.997	17 (34)	11 (22)	0.187
	Present	18 (75)	20 (83)		7 (64)	11 (73)		33 (66)	40 (78)	
Margin involvement	R0	7 (29)	4 (21)	0.740	10 (77)	6 (43)	0.120			
	R1	17 (71)	21 (79)		3 (23)	8 (57)				
Perineural invasion	Absent	4 (17)	2 (8)	0.601	-	-	-	-	-	-
	Present	20 (83)	22 (92)							
Venous invasion	Absent	11 (46)	6 (25)	0.227	-	-	-	-	-	-
	Present	13 (54)	18 (75)							
Peripancreatic fat invasion	Absent	22 (92)	18 (75)	0.122						
	Present	2 (8)	6 (25)							
Adjuvant chemotherapy	No	7 (29)	14 (58)	0.085	-	-	-	-	-	-
	Yes	17 (71)	10 (42)							

[a] χ^2 tests were used to compare categorical variables. [b] For validation cohort 1 median age was 68 yrs
[c] For validation cohort 2 tumour stage data available only for 98 patients. [d] For validation cohort 2 lymph node status available for 101 patients.

Table 6.2 Clinicopathological factors associated with survival-48 patient PDAC cohort

Factors univariately associated with survival following PD.

Prognostic Variable	**No. of Patients**	**Median Survival**	**95% CI**	**p value [a]**
Overall	48	26.3	15.7 - 36.9	-
Gender				
Female	19	28.3	15.3 - 41.3	0.072
Male	29	18.0	7.07 - 28.9	
Age (yrs)				
≤ 65	27	26.3	14.1 - 38.5	0.711
> 65	21	27.5	15.9 - 39.1	
Tumour stage				
T2	6	36.2	17.5 - 54.9	0.017
T3	42	17.8	15.7 - 36.9	
Lymph node status				
N0	10	38.9	29.7 - 49.1	0.007
N1	38	18.0	7.55 - 28.5	
Tumour size (mm)				
< 30	28	28.3	25.6 - 31.1	0.089
≥ 30	20	17.6	3.8 - 31.3	
Tumour grade				
Low	32	26.4	15.1 - 37.7	0.091
High	16	13.4	9.01 - 17.8	
Perineural invasion				
Absent	6	27.5	23.8 - 31.2	0.003
Present	42	16.2	13.0 - 19.3	
Venous invasion				
Absent	17	49.0	23.3 - 74.7	0.006
Present	31	16.5	13.3 - 19.6	
Resection margin status				
R0	12	49.0	38.9 - 59.1	0.009
R1	36	17.8	12.6 - 23.1	
Peripancreatic fat invasion				
Absent	40	27.4	15.4 - 39.4	0.066
Present	8	16.2	14.1 - 18.2	
Adjuvant chemotherapy				
No	20	11.5	2.89 - 20.0	0.042
Yes	28	27.5	24.7 - 30.3	

[a] p value calculated from Log-rank analysis

Table 6.3 Prognostic value of the overall gene survival profile adjusted for other clinicopathological parameters within a multivariate analysis

		Overall survival			
Prognostic variable	**Category**	**HR (95% CI)**	**p value** [a]	**HR (95% CI)**	**p value** [b]
Tumour stage	T2/ T3	4.22 (0.93 - 19.1)	0.062	3.14 (1.12 - 9.6)	0.046
Tumour size (mm)	< 30/ ≥ 30	1.96 (0.95 - 3.99)	0.065	1.91 (0.94 - 3.87)	0.075
Lymph node status	Absent/ Present	1.84 (0.36 - 9.39)	0.464	2.56 (0.91 - 7.68)	0.066
Tumour grade	Low/ High	2.52 (1.08 - 5.86)	0.032	1.84 (0.77 - 4.46)	0.172
Perineural invasion	Absent/ Present	3.56 (0.77 - 8.04)	0.222	1.56 (0.77 - 3.04)	0.612
Venous invasion	Absent/ Present	2.68 (1.09 - 6.61)	0.031	1.56 (0.54 - 4.47)	0.411
Margin involvement	R0/ R1	3.92 (1.25 - 12.3)	0.019	4.32 (2.08 - 7.19)	0.002
Peripancreatic fat invasion	Yes/No	2.04 (0.91 - 3.74)	0.253	1.93 (0.85 - 3.12)	0.353
Adjuvant chemotherapy	Yes/ No	0.34 (0.14 - 0.81)	0.014	0.27 (0.11 - 0.65)	0.003
Gene survival profile	Low/ High Risk	-	-	5.36 (2.22 - 12.9)	< 0.001

[a] Multivariate Cox proportional-hazards regression analysis (n = 48) – clinicopathological parameters only.
[b] Multivariate Cox proportional-hazards regression analysis (n = 48) – including gene survival profile.

Table 6.4 Multivariate prognostic influence of CLIC3: IHC validation analysis

CLIC3 protein expression assessed by IHC in 118 patents. Only clinical variables prognostic within univariate analysis included in multivariate model.

		Overall survival	
Prognostic variable	**Category**	**HR (95% CI)**	**p value**
Tumour stage	T2/ T3	2.08 (1.07 - 4.05)	0.031
Tumour size (mm)	< 30/ ≥ 30	1.65 (1.06 - 2.65)	0.026
Lymph node status	Absent/ Present	1.54 (0.76 - 2.93)	0.121
Margin involvement	R0/ R1	2.23 (1.32 - 3.76)	0.003
Tumour grade	Low/ High	2.07 (1.29 - 3.29)	0.002
Perineural invasion	Absent/ Present	0.71 (0.27 - 1.85)	0.482
Venous invasion	Absent/ Present	1.32 (0.85 - 2.09)	0.213
Peripancreatic fat invasion	Absent/ Present	1.78 (1.12 - 2.87)	0.019
CLIC3 (cytoplasm) [a]	Low/ High	1.34 (1.06 - 1.78)	0.026
Adjuvant chemotherapy	Yes/ No	0.76 (0.46 - 1.16)	0.112

[a] CLIC3 median expression used to determine low and high grouping

Table 6.5 Multivariate prognostic influence of CLIC3: RT-PCR validation analysis

CLIC3 mRNA expression assessed by RT-PCR in 48 patients. Only clinical variables prognostic within univariate analysis included in multivariate model.

		Overall survival	
Prognostic variable	**Category**	**HR (95% CI)**	**p value**
Tumour stage	T2/ T3	2.29 (1.35 - 3.82)	0.023
Tumour size (mm)	< 30/ ≥ 30	2.67 (1.08 - 6.57)	0.033
Lymph node status	Absent/ Present	2.43 (0.81 - 9.11)	0.199
Margin involvement	R0/ R1	2.83 (1.77 - 4.14)	0.002
Tumour grade	Low/ High	1.83 (0.71 - 4.68)	0.210
Venous invasion	Absent/ Present	2.10 (0.78 - 5.68)	0.142
Peripancreatic fat invasion	Absent/ Present	1.54 (0.87 - 3.77)	0.232
CLIC3 expression [a]	Low/ High	4.81 (1.86 - 12.3)	0.001
Adjuvant chemotherapy	Yes/ No	0.34 (0.12 - 0.93)	0.036

[a] CLIC3 median expression used to determine low and high grouping

Table 6.6 Prognostic utility of prognostic gene signature within validation cohorts

A) *Multivariate analysis in independent validation cohort 1 (27 patients).*

		Univariate		Multivariate		Multivariate	
Prognostic Factor	**Category**	**HR (95% CI)**	**p value**	**HR (95% CI)**	**p value**	**HR (95% CI)**	**p value**
Age (yrs)	<65/ ≥ 65	1.27 (0.50 - 3.18)	0.616	-	-	-	-
Tumour stage	T2/ T3	2.20 (0.64 - 7.61)	0.211	-	-	-	-
Lymph node status	Absent/ Present	3.79 (1.08 - 13.3)	0.038	5.77 (1.49 - 22.5)	0.011	5.42 (1.43 - 20.5)	0.013
Tumour grade	Low/ High	2.44 (0.96 - 6.19)	0.061	3.79 (1.35 - 10.7)	0.012	2.53 (0.84 - 7.65)	0.100
Margin involvement	R0/ R1	1.59 (0.63 - 3.88)	0.341	-	-	-	-
Gene survival profile	Low/ High risk	3.14 (1.20 - 8.19)	0.020	-	-	4.34 (1.55 - 12.2)	0.005

B) *Multivariate analysis in independent validation cohort 2 (101 patients) 2 risk groups comparison.*

		Univariate		Multivariate	
Prognostic Factor	**Category**	**HR (95% CI)**	**p value**	**HR (95% CI)**	**p value**
Tumour stage	T2/ T3	0.89 (0.48 - 1.65)	0.720	-	-
Lymph node status	Absent/ Present	1.93 (1.08 - 3.45)	0.027	1.85 (1.05 - 3.26)	0.035
Gene survival profile	Low/ High risk	1.87 (1.18 - 3.15)	0.017	1.59 (0.96 - 2.64)	0.067

C) *Multivariate analysis in independent validation cohort 2 (101 patients) 3 risk groups comparison.*

		Univariate		Multivariate	
Prognostic Factor	**Category**	**HR (95% CI)**	**p value**	**HR (95% CI)**	**p value**
Tumour stage	T2/ T3	0.89 (0.48 - 1.65)	0.720	-	-
Lymph node status	Absent/ Present	1.93 (1.08 - 3.45)	0.027	1.81 (1.02 - 3.19)	0.042
Gene survival profile	Low risk	-	-	-	-
	Medium risk	1.51 (0.78 - 2.89)	0.213	1.27 (0.68 - 2.38)	0.454
	High risk	2.68 (1.42 - 5.04)	0.002	2.11 (1.15 - 3.87)	0.016

Table 6.7 Comparison of PDAC prognostic and pathological gene expression studies

Comparison of the 2 prior studies that have generated a PDAC prognostic gene signature and the study generating a signature associated with lymph node status.

Study (ref)	**Signature**	**Platform**	**Signature model**	**Classification**	**Survival Analysis**	**Hazard ratio (95% CI)**	**p value**
Stratford et al (349)	6 genes (101 pts)	Agilent	SAM/ X-tile classification	Genes associated with metastatic cohort	Multivariate Independent cohort	4.1 (1.7 - 10.0)	0.002
Collisson et al (348)	72 genes (27 pts)	Affymetrix	Unsupervised Clustering	Exocrine-like Quasi-mesenchymal Classical PDAC	Multivariate	0.21 (0.068 - 0.65)	0.024
Kim et al (355)	155 genes (10 pts)	Applied Biosystems	Supervised hierarchical clustering	Lymph node negative/ positive	NA	NA	NA
This study	107 genes (48 pts)	Agilent	Semi-supervised	Cox proportional-hazards risk index	Multivariate Independent cohort	5.36 (2.22 - 12.9)	< 0.001

SAM – Significance analysis of microarray
NA – Not applicable
pts – patients

Figure 6.1 Hierarchical clustering of gene expression profiles for 48 PDAC versus 10 normal pancreas specimens

Clustering of 573 genes differentially expressed (vertical axis) (Class comparison test, $p < 0.0005$) between normal pancreas tissues (Green) compared to PDAC (Orange - horizontal bar). Red represents high gene expression while blue represents low gene expression.

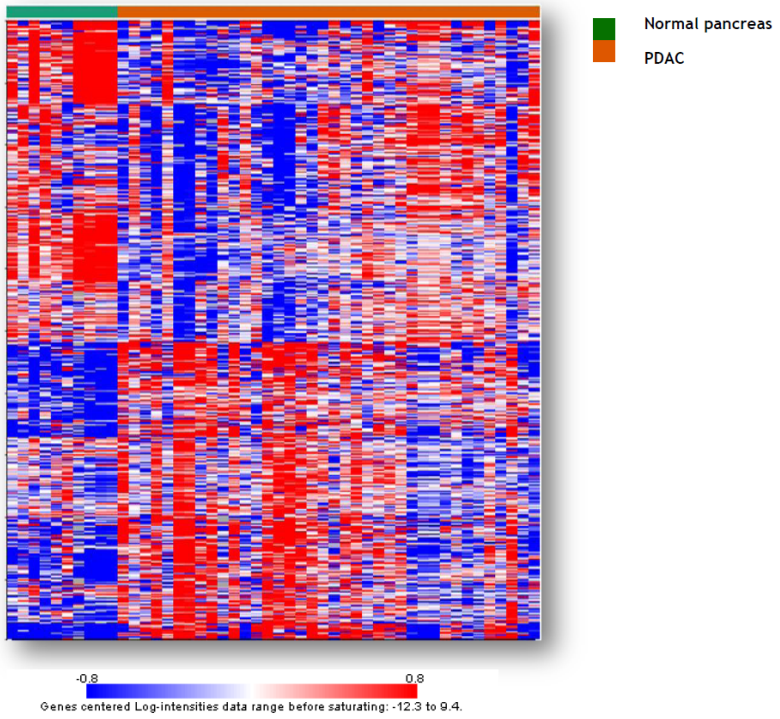

Figure 6.2 Multidimensional association plots: gene expression

A) *Multidimensional association plot of 48 PDACs (**red**) and 10 matched control pancreatic tissue samples (**green**) based on the set of 573 differentially expressed genes.*

B) *Multidimensional association plot of 9 lymph node negative (**blue**) and 39 lymph node positive (**red**) PDACs based on the set of 138 differentially expressed genes.*

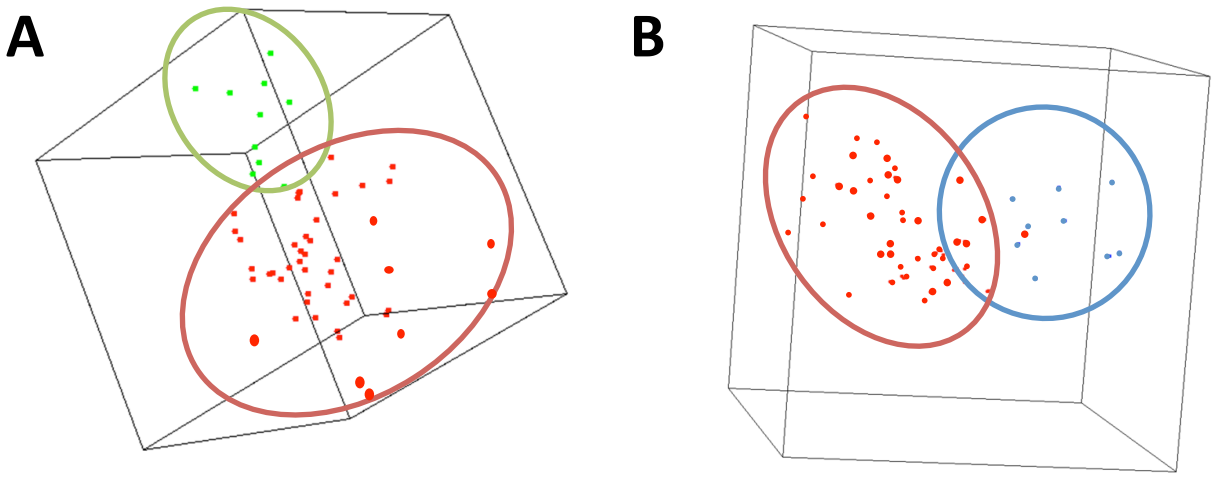

Figure 6.3 Gene expression associated with clinicopathological features in PDAC

Venn diagram of genes that are associated in PDAC with tumour grade, tumour stage, lymph node status and resection margin status. The numbers are attached to lists of the genes associated with each component of the diagram. The genes in the boxes are over expressed. Genes associated with the presence of peripancreatic fat invasion are listed separately at bottom left: those genes which are common in two groups in the Venn diagram are shown in black, those common to three or more are highlighted in red.

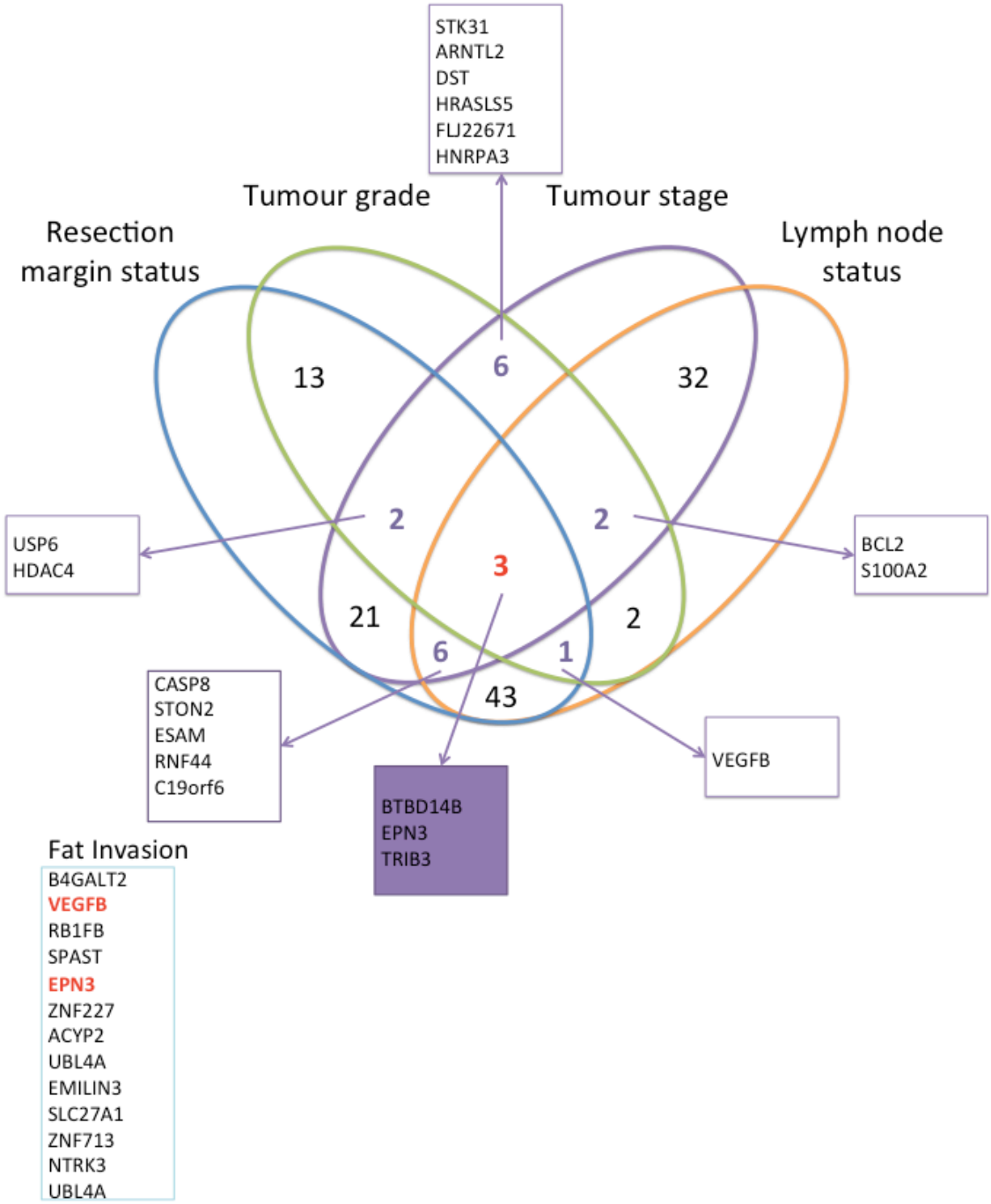

Figure 6.4 Unsupervised hierarchical clustering and resulting survival curves

A) *Dendrogram created by unsupervised clustering demonstrating two major groups of patients.*

B) *Kaplan-Meier survival curve based on the two groups of patients from A (Log-rank test, p = 0.061).*

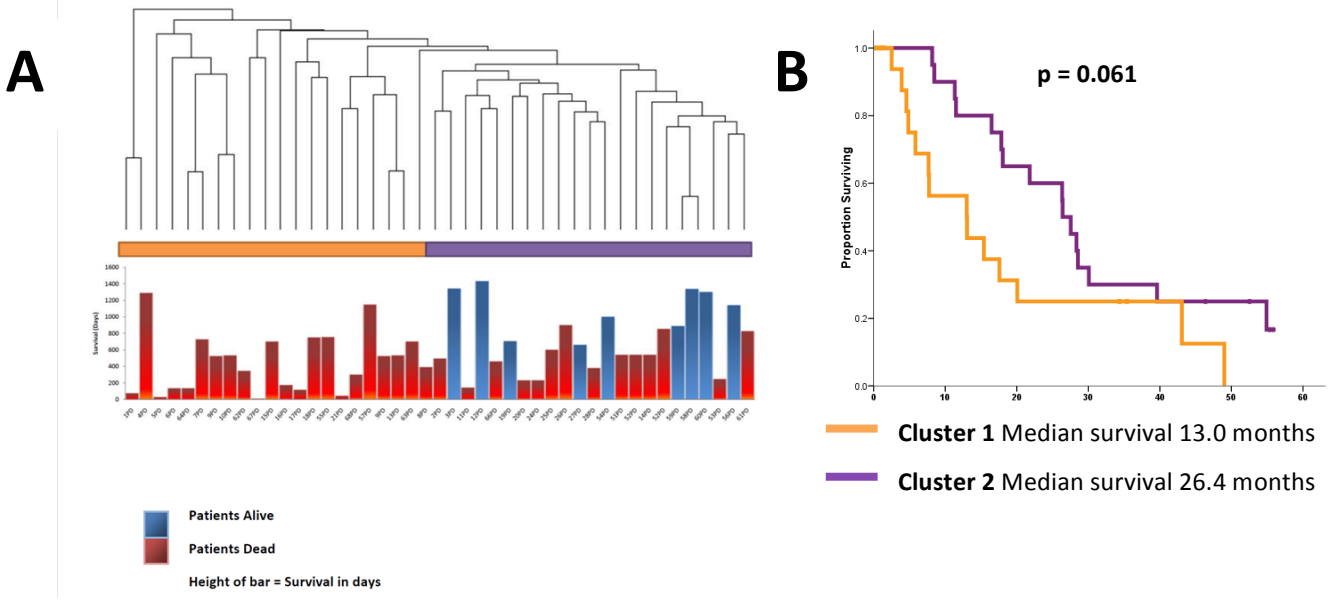

Figure 6.5 Semi-supervised gene survival analysis

A) *Cluster matrix of 332 genes most significantly associated with survival. The matrix colours represent up- (red) or down-regulation (blue) relative to the median for each gene. Column height in the bar graph below the matrix represents length of survival (days) following resection; green bars represent patients alive at follow-up. The dendrogram depicts the two major patient groups.*

B) *The Kaplan-Meier survival curves illustrate the divergence in survival between the good prognosis group (39.6 months) (**Blue**) and the poor prognosis group (13.0 months) (**Red**) (Log-rank test, p < 0.001).*

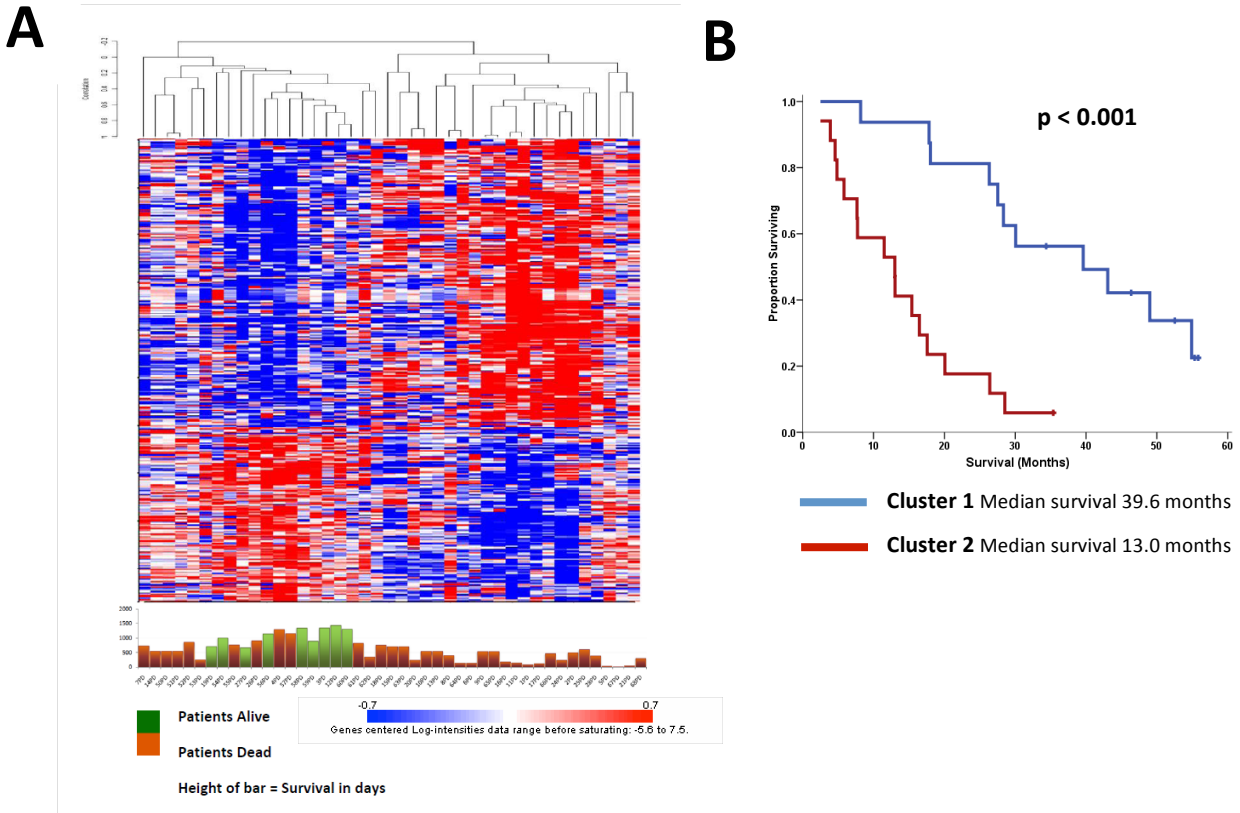

Figure 6.6 Analysis of the prognostic gene signature

A) *From the top 25 genes most significantly related to survival in univariate analysis, survival curves are presented for 9 candidate genes (Log-rank analysis).*

B) *Scatter plots showing the microarray gene expression signal versus the ΔCt obtained by qRT-PCR for three individual genes. Validated genes were CLIC3, DUSP5 and TGM2. A ΔCt of the gene is obtained by subtracting the mean Ct value of GAPDH from the mean Ct value of the gene. Both axes are on the log_2 scale.*

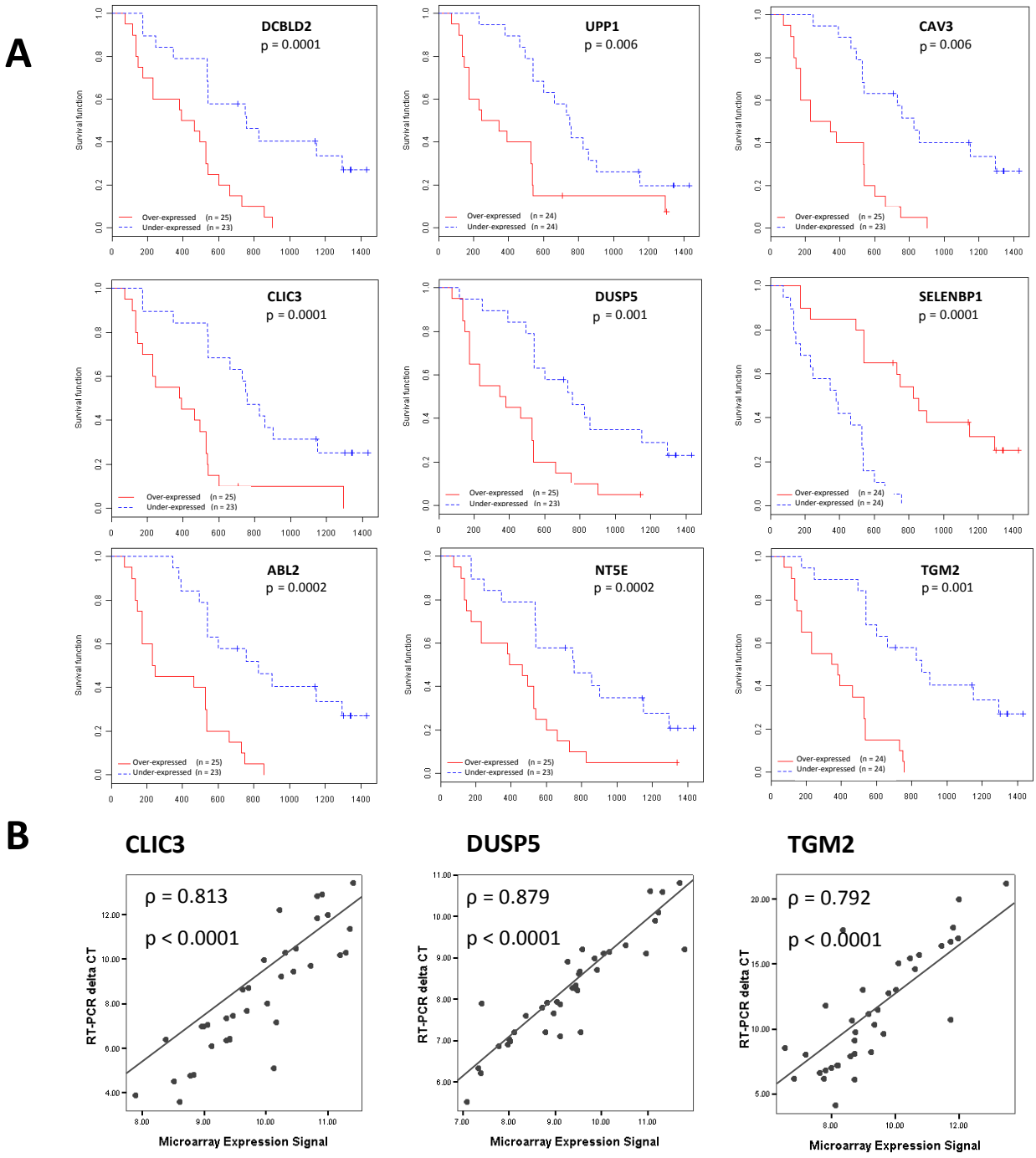

Figure 6.7 CLIC3 validation and survival analysis

A) *CLIC3 levels in normal pancreatic tissue, PanIN and PDAC. Green arrows indicate preserved normal structure of ductal epithelium; red arrows point to dysplastic areas.*

B) *H&E and CLIC3 IHC of an invasive margin of PDAC. High magnification of CLIC3 immunostaining in PDAC showing granular cytoplasmic and nuclear distributions.*

C) *CLIC3 IHC scoring of PDAC TMA; negative (0), weak (1), moderate (2), strong (3) and insets with corresponding H&E staining.*

D) *Box plot illustrating stratification of PDAC patients into low and high CLIC3 expressors based on histoscore.*

E) *Kaplan-Meier analysis indicates that patients with high CLIC3 expression (n = 37) have a poorer outcome than those with low expression (n = 81) following tumour resection (Log-rank test, $p < 0.01$).*

F) *Box plot indicating that tumours from patients with more than 50% lymph node involvement have increased levels of CLIC3 in comparison to those with no lymph node involvement (Mann-Whitney U test, $p = 0.005$) and those with less than 50% lymph node positivity following resection (Mann-Whitney U test, $p = 0.01$).*

G) *Box plot illustrating stratification of PDAC patients into low and high CLIC3 expressors based on normalised mean gene expression.*

H) *Kaplan-Meier analysis showing that patients with high CLIC3 mRNA expression (n = 31) have a poorer survival than those with low expression (n = 17) following tumour resection (Log-rank test, $p = 0.001$).*

Figure 6.7

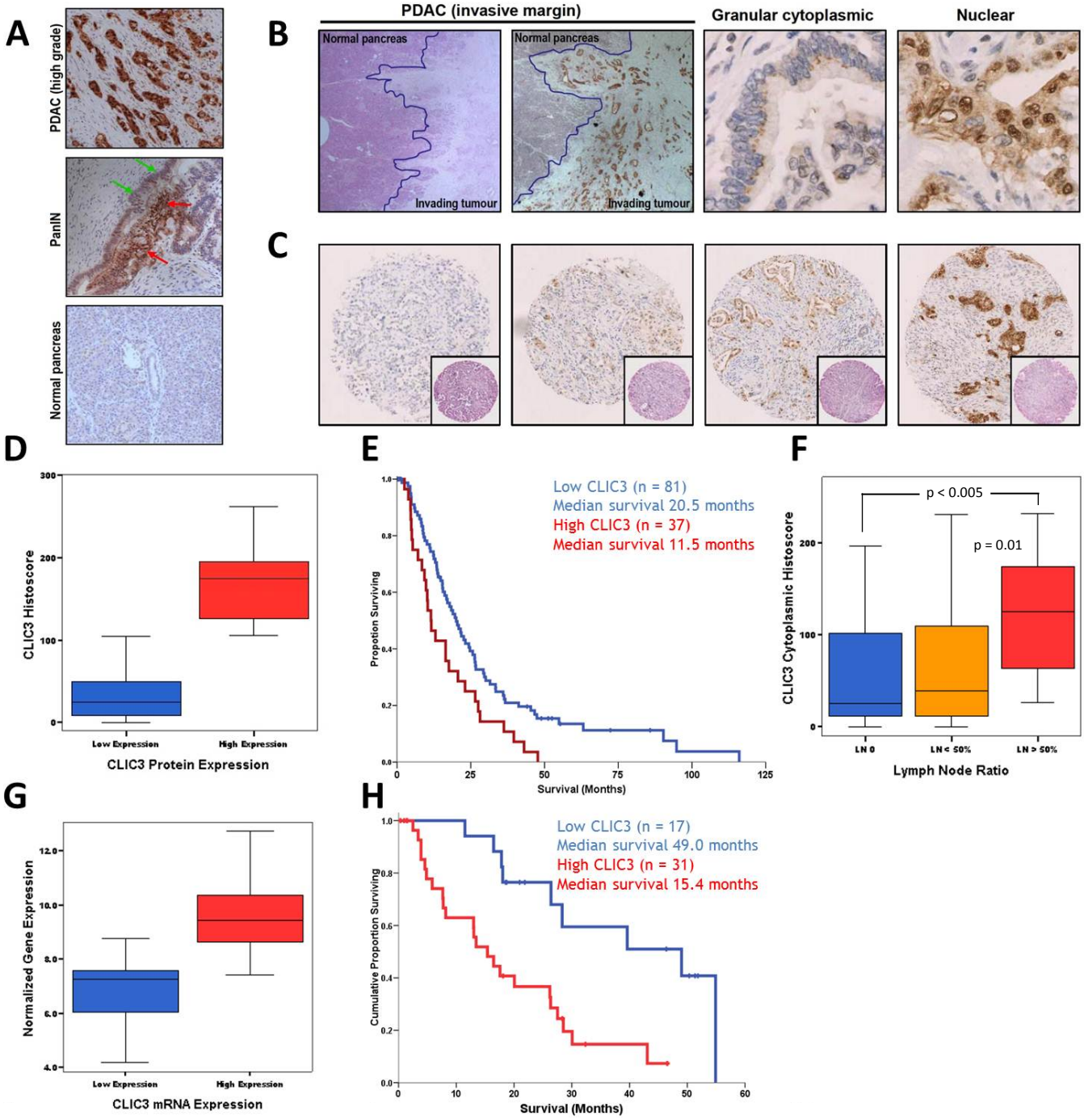
A
PDAC (high grade)
PanIN
Normal pancreas
B
PDAC (invasive margin)
Granular cytoplasmic
Nuclear
Normal pancreas
Invading tumour
Normal pancreas
Invading tumour
C
D
CLIC3 Histoscore
Low Expression
High Expression
CLIC3 Protein Expression
E
Low CLIC3 (n = 81)
Median survival 20.5 months
High CLIC3 (n = 37)
Median survival 11.5 months
Propotion Surviving
Survival (Months)
F
p < 0.005
p = 0.01
CLIC3 Cytoplasmic Histoscore
LN 0
LN< 50%
LN > 50%
Lymph Node Ratio
G
Normalized Gene Expression
Low Expression
High Expression
CLIC3 mRNA Expression
H
Low CLIC3 (n = 17)
Median survival 49.0 months
High CLIC3 (n = 31)
Median survival 15.4 months
Cumulative Proportion Surviving
Survival (Months)

Figure 6.8 Validation of the 107-gene prognostic profile in independent cohorts

A) *Visualisation of the 107-gene profile for validation cohort 1 (27 independent samples). Samples are ranked according to their prognostic risk score. Red represents high gene expression while green represents low gene expression.*

B) *Kaplan-Meier survival plot of overall survival estimates for the 27 samples in validation cohort 1, low (21.6 months) versus high risk (6.6 months, p = 0.005, Log-rank analysis).*

C) *Visualisation of the profile for validation cohort 2 (102 independent samples). Samples are ranked according to their prognostic risk score.*

D) *Kaplan-Meier survival plot of overall survival estimates of the 102 samples in validation cohort 2, low (22.0 months) versus high risk (16.0 months, p = 0.013, Log-rank analysis).*

E) *Kaplan-Meier survival plot of overall survival estimates of the 102 samples in validation cohort 2, low (21.6 months) versus medium (18.0 months) versus high risk (13.0 months, overall p = 0.003, Log-rank analysis).*

F) *Gene overlap between PDAC prognostic signatures. The overlap of genes between the studies was limited to 5 from a total of 185 genes (PAPPA, TWIST, NT5E, S100A2, LOX). Potentially, all the identified signatures form subsets of a larger PDAC prognostic super-group. Green – prognostic-based signature, Blue – pathological based signature, Yellow – over-lapping signatures.*

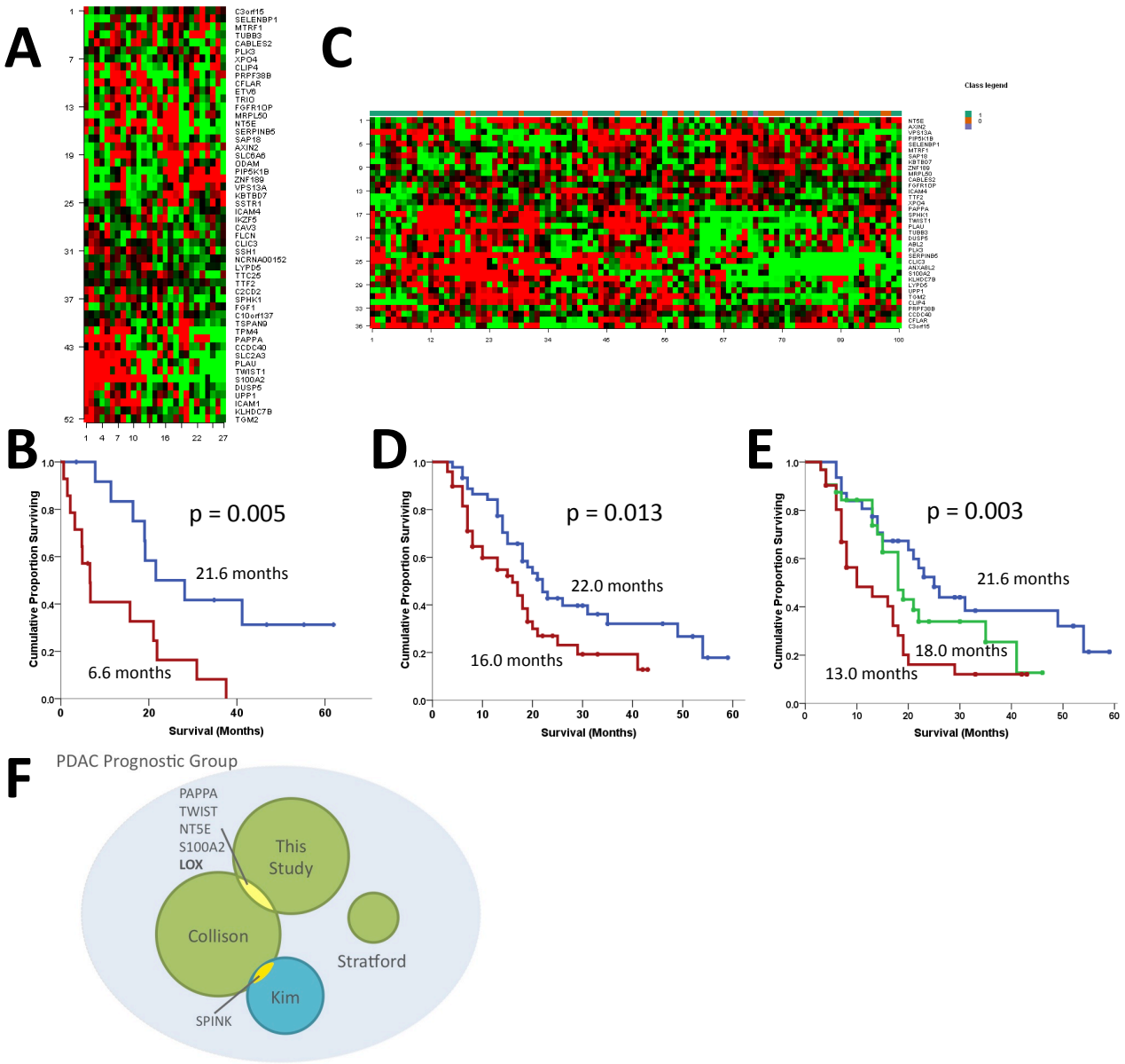

7 microRNA Molecular Profiles Associated with Diagnosis, Clinicopathological Criteria and Survival in Resectable PDAC

7.1 Introduction

The analysis of protein expression and mRNA expression levels has contributed to defining the molecular network of PDAC carcinogenesis. Although the investigation of gene and protein expression has yielded new information, it has become apparent that studying non-coding RNA gene products may provide additional insights into PDAC biology (371). To date only three large-scale profiles of miRNAs in PDAC have been published (219, 220, 225).

7.1.1 Aim

Given the diagnostic, prognostic and therapeutic potential for miRNAs in cancer, the aim of the current chapter was to investigate the genome wide miRNA expression profile in a 48 patient PDAC cohort and corresponding normal tissues and to correlate this molecular signature, not only with diagnosis, but also with clinicopathological variables including patient survival. A subset of candidate miRNAs was validated by RT-PCR in the 48 patients and in a further 24 patients.

7.2 Results

7.2.1 miRNA expression profiles between PDAC and normal pancreas

The initial miRNA profiling was performed on 48 patients with resectable PDAC who underwent PD as described in the previous chapter (Table 2.1). A further 24 patients were used as a validation set (Table 2.1). The prognostic influence of clinicopathological factors were evaluated univariately and multivariately in Chapter 6 (Table 6.2, Table 6.3).

The miRNA expression profiles in 48 PDACs and 10 paired samples of non-cancerous pancreas tissue were analysed and compared according to the workflow in Figure 11.15. 97 miRNAs showed statistically different expression between the two groups ($p < 0.001$, t-test class comparison). 39 miRNAs were up-regulated and 58 were down-regulated in cancer (the top 25 up and down-regulated miRNAs are shown in Table 7.1 [complete list in Table 11.16]). miRNAs up-regulated in PDAC compared to normal pancreas included miR-10a, miR-21, miR-143 and miR-145; miRNAs down-regulated in PDAC compared to normal included miR-148, miR-216 and miR-217. Using a multivariate permutation test to control for multiple comparisons, the probability of identifying 97 miRNAs by chance at $p < 0.001$, was estimated at 0. A comparison of the miRNA profiles for PDAC and normal pancreatic tissue is illustrated in Figure 7.1A, with hierarchical clustering demonstrated in Figure 7.1B. Further analysis of global miRNA profiles enabled PDAC and normal pancreas to be distinguished with 95% accuracy using the Bayesian compound covariate and with 90% accuracy using the nearest centroid class prediction algorithms (10-fold cross-validation). This supports the hypothesis of systematic change in miRNA expression during PDAC formation.

7.2.2 miRNA profiles related to clinicopathological features

28 miRNAs were identified that differed based on tumour grade; 23 for tumour stage; 15 for lymph node status; 19 for venous invasion; 11 for resection margin status; 6 for peripancreatic fat invasion and 14 associated with site of recurrence ($p < 0.001$, t-test class comparison). No significant differences were associated with perineural invasion. These miRNA signatures, and their overlap, are illustrated in Figure 7.2. Three miRNAs were differentially expressed in association with tumour grade, stage and lymph node status; miR-21, miR-146a and miR-628. No miRNA was identified as differently expressed according to patient gender or age.

7.2.3 miRNA expression profiles associated with survival

In a similar manner to the gene expression survival analysis in the previous chapter, miRNA expression profiles and patient survival following resection were investigated. Univariate analysis revealed, that, out of 476 probes that passed the filtering criteria, 20 miRNAs (Table 7.2) were associated significantly with survival ($p < 0.05$, Log-rank test). This analysis was visualised by hierarchical clustering, which demonstrated the ability of the highest ranked miRNAs to cluster the 48 specimens according to survival (Figure 7.3A). Poor outcome was associated with low expression of 11 miRNAs and high expression of 9 miRNAs. Kaplan-Meier analysis according to expression of the 20 miRNAs shows a significant difference in survival between low- and high-risk groups (Figure 7.3B). The poorest PDAC prognosis was associated with low expression of miR-29c, miR-30d, miR-34a, and/ or high expression of miR-21, miR-221 and miR-224.

7.2.4 RT-PCR analysis of the most prognostic miRNAs

Using RT-PCR, for the six individual miRNAs, high expression of miR-29c, miR-30d and miR-34a was confirmed as associating with better prognosis (Figure 7.3C). miR-30d high expression associated with a median overall survival of 30.7 months (95%CI: 15.4–44.7) versus low expression 18.0 months (95%CI: 12.2–23.9, $p = 0.017$); miR-34a high expression 43.1 months (95%CI: 20.1–66.1) versus low expression 13.4 months (95%CI: 7.7–19.1, $p < 0.001$); and miR-29c high expression 39.6 months (95%CI: 15.6–66.1) versus low expression 16.7 months (95%CI: 9.3–23.6, $p < 0.001$).

Furthermore, high expression of miR-21, miR-221 and miR-224 associated with poorer prognosis. Thus, miR-21 high expression was associated with a median overall survival of 16.5 months (95%CI: 11.4-21.6) versus 30.1 months (95%CI: 14.2–49.9, $p = 0.012$) for low expression; miR-224 high expression of 17.6 months (95%CI: 10.5–24.7) versus 29.8 months (95%CI: 15.1–45.0, $p = 0.023$) for low expression; and miR-221 high expression of 16.5 months (95%CI: 9.4–23.5) versus 28.3 months (95%CI: 23.9–32.7, $p = 0.025$) for low expression (Table 7.3). All survival comparisons were calculated using the Log-rank test.

7.2.5 miRNA expression associated with site of recurrence

Of the six PCR validated miRNAs, only miR-30d showed significantly different expression based on recurrence site. 14/21 (67%) patients with distant recurrence showed low miR-30d expression, compared with 5/16 (31%) of those with local recurrence ($p = 0.047$, χ^2 test). Likewise, 12/16 (75%) with liver metastases as the primary site of failure showed low expression of miR-30d, by comparison with 8/21 (38%) for patients with recurrence elsewhere ($p = 0.03$, χ^2 test).

7.2.6 Multivariate analysis identifies three prognostic miRNAs

The six prognostic miRNAs identified on univariate analysis were included in separate multivariate models (48 patients) along with established prognostic clinicopathological factors. High miR-21 expression (HR: 3.22, 95%CI: 1.21–8.58, $p = 0.019$) remained an independent predictor of poor outcome, while high expression of miR-30d (HR: 0.31, 95%CI: 0.12–0.79, $p = 0.014$) and miR-34a (HR: 0.15, 95%CI: 0.06–0.37, $p < 0.001$) independently predicted better survival (Table 7.4).

7.2.7 Validation of prognostic miRNAs in an independent cohort

A further validation series of 24 independent PDAC samples was used to evaluate the prognostic significance of a miRNA associated with poor outcome (miR-21) and a miRNA associated with favourable outcome (miR-34a) following resection. The validation group did not differ significantly in terms of pathological features compared to the original 48 patient cohort (Table 2.1). Both miRNAs were prognostic using a univariate comparison (Log-rank test). Patients with high miR-21 expression again had a poorer outcome (13.7 months, 95%CI: 4.7–12.1) compared to low miR-21 expression (25.7 months, 95%CI: 20.2–31.1, $p = 0.031$, Figure 7.4A). High miR-34a expression was associated again with good outcome (26.6 months, 95%CI: 14.9–38.3) compared to low miR-34a expression (6.1 months, 95%CI: 1.75–10.5, $p < 0.001$, Figure 7.4B).

7.2.8 The predictive utility of miR-21

miR-21 expression was analysed along with adjuvant chemotherapy allocation and survival. As the group characteristics were similar, a pooled comparison across the combined 72-patient cohort (48 original + 24 validation PDACs) was performed. 38 patients received chemotherapy, and 34 did not. Univariate survival comparisons were calculated using the Log-rank test. Adjuvant chemotherapy was associated with improved survival: 21.8 months (95%CI: 12.6–31.0) versus 13.0 months (95%CI: 8.5–18.0, $p = 0.05$). 34 patients had high miR-21 and 38 had low expression, with low miR-21 associated with better outcome compared to high miR-21: 11.5 months (95%CI: 8.2–14.8) versus 26.7 months (95%CI: 24.8–28.6, $p = 0.001$). Thus both receipt of chemotherapy and miR-21 levels are prognostic factors; but is miR-21 predictive of therapeutic response?

Of the patents with low miR-21 expression, 21 received chemotherapy and 17 did not, and administration of chemotherapy was not associated with improvement in survival: 27.5 months (95%CI: 23.6–31.4) versus 26.6 months (95%CI: 23.1–30.0) without chemotherapy ($p = 0.74$). In contrast, in patients with high miR-21 expression, 16 received chemotherapy and 18 did not. Adjuvant chemotherapy was associated with a significant increase in overall survival, from 7.1 months (95%CI: 1.0–14.3) without chemotherapy to 16.4 months (95%CI: 12.3–18.4) with chemotherapy (Figure 7.4C). However, the study is limited by small sample size and utility as a predictive marker should be tested in an adequately powered, prospective study. Thus in patients with tumours expressing high miR-21 adjuvant chemotherapy resulted in prolonged overall survival ($p = 0.008$); in contrast, for those with low miR-21 expressing tumours, no survival advantage could be demonstrated. Multivariate analysis of this combined cohort demonstrated high miR-21 expression predicted poor prognosis while adjuvant therapy was associated with improved survival (Table 7.5A). Subgroup multivariate analysis demonstrated that adjuvant therapy was only an independent predictor of outcome for the low miR-21 group (Table 7.5B, C).

7.2.9 Bioinformatic enrichment of miRNA survival profiles

Given that biological significance of miRNA deregulation is assumed to relate to the effect of miRNAs on their cognate protein-coding gene targets, the predicted targets of the six most prognostic miRNAs were analysed to gain further insight into the biological pathways potentially deregulated in PDAC. The analysis was performed using three algorithms, Targetscan 5.0 (372), PicTar (373) and DIANA-microT v3.0 (374), which are commonly used to predict human miRNA targets. Prediction results of the genes statistically most likely to be targets of these miRNAs show putative target cancer-related genes as follows: for miR-34a, BCL2, E2F2, CCNE2, PDGFRA and CDK6; for miR-30d, CCNE2, MAPK8, SOS1, KRAS and BCL2; for miR-29c, IGF1, COL4A1, PTEN, LAMC1, VEGFA and PDGFC; for miR-21, YOD1, PLAG1 and STAG2; for miR-221, TGFβ, CDKN1B, RALA and PTEN; and for miR-224, SMAD4 and CDK6.

To investigate the biological consequence of altered expression of these miRNAs, a bioinformatic analysis was conducted, using DIANA-mirPath, to group the predicted targets of these miRNAs by KEGG pathway. miRNAs associated with poor prognosis demonstrated enrichment for MAPK signalling, TGFβ signalling, Wnt signalling and p53 signalling (Figure 11.16, Table 11.17). For these poor prognosis pathways, the only common target gene was UBE2D3, an ubiquitin-conjugating enzyme that is a target of the retinoid signalling pathway (375). miRNAs associated with favourable prognosis demonstrated enrichment for focal adhesion pathways, ECM-receptor interaction pathways and phosphatidylinositol signalling (Figure 11.17, Table 11.18). For these good prognosis pathways, shared target genes were

Sirt-1, CALCR and RARB. Further investigation of miR-21 targets, miR-34a regulation and expression profiles associated with these miRNAs are presented in Chapter 9.

7.3 Discussion

In this chapter, global miRNA profiling in 48 resected PDAC specimens was performed using miRNA microarrays. These data show that miRNA expression profiling can identify novel clinicopathological correlations for PDAC including a signature of prognostic miRNAs. Detailed miRNA profiles have previously been generated from PDAC cell and animal models (376). Additionally three large-scale profiles of miRNAs in human PDAC have been published (219, 220, 225).

This cohort is the second largest in the miRNA microarray profiling literature behind that of Bloomston and co-workers in which 65 PDACs were profiled (225). 21 miRNAs were significantly up-regulated in that study with four down-regulated in the PDAC specimens compared with normal pancreatic tissue. CP miRNA expression profile was similar to that of PDAC tumour specimens, however the normal pancreatic tissue profile was quite distinct from both. This was the first attempt to correlate miRNA expression with clinicopathological factors including survival. Comparing the miRNA expression profile of lymph node positive cases only, they identified six miRNAs associated with outcome (miR-30a-3p, miR-105, miR-127, miR-187, miR-452 and miR-518a-2). Two additional miRNAs were also identified, miR-196a-2 and miR-219, overexpression of which were associated with poor survival. The importance of miR-196 confirms the findings of Szafranska and co-workers. The expression profiles of miRNAs generated in this thesis broadly agree with the prior literature, which provides credence to the novel candidates that were reported.

First, in this thesis an evaluation of PDAC miRNA profiles identified 39 miRNAs that were up-regulated and 58 miRNAs that were down-regulated in PDAC in comparison to normal pancreatic tissue ($p < 0.001$). In particular, miR-21, miR-155 and miR-10a were significantly over-expressed in PDAC compared to normal (miR-21 showing a 5.6 fold increase), with miR-130b, miR-148 and miR-216 being under-expressed. There is considerable overlap between miRNA expression profiles generated in recent PDAC microarray analyses (220) and the current study, far more than was evident in mRNA profiling studies (3). Principally a result of the smaller number of potential targets this overlap supports the robustness of miRNA methodology as, despite different extraction and analysis techniques, remarkably similar profiles result. A true advantage for miRNA profiling is their small size lessens susceptibility to degradation in FFPE tissue, allowing for wider application of profiling on large cohorts of banked tissue samples.

Over-expressed miRNAs including miR-21, miR-145 and miR-155 all commonly associate with malignancy (377, 378), however miR-23a and miR-103 were novel over-expressed

targets that warrant further investigation. It was identified that miRNA expression correlated with clinicopathological features. Notably, high tumour grade was associated with the greatest number of aberrant miRNAs followed by T stage and venous invasion. R1 status was associated with significantly aberrant miRNA expression suggesting tumour biology variation may underlie this detrimental pathological state (251). Three miRNAs were commonly differentially expressed in association with tumour grade, stage and lymph node status; miR-21 emerged once again along with miR-146a and miR-628. This finding suggests a number of miRNAs are shared amongst tumours with advanced features. Although this type of analysis is novel in PDAC, the results concur with previous cancer related miRNA studies. In gastric carcinoma, miR-146a expression was associated with lymph node positivity (379). In a neuroblastoma sequencing study, miR-628 was identified as a putative TSG, being expressed in tumours with favourable outcome (380). miR-21 expression has been correlated with stage and lymph node metastasis in various malignancies (377, 378).

Global miRNA profiling with multivariate Cox regression analysis identified numerous miRNAs that were significantly associated with overall survival following resection in the studied cohort. The overlap with differentially expressed miRNAs based on pathological factors included only miR-21, miR-30d and miR-125. While many were novel associations, high miR-21 expression was confirmed as independently associated with poor overall survival, supporting previous reports (221), including in-situ hybridisation assessment, in which miR-21 was prognostic in node-negative patients (381). The proposed oncogenic properties of this almost ubiquitously expressed molecule are supported by functional investigations demonstrating that inhibition reduced proliferation of cancer cell lines including breast, hepatocellular and PDAC (382-384). Conversely, miR-21 precursor transfection enhanced invasion in a breast cancer model (385) in addition to pancreatic cancer (384).

This work identified numerous novel miRNA prognostic associations in particular miR-30d and miR-34a. The miR-34 family is strongly implicated as serving a tumour suppressor role in malignancy (386) and in a p53-deficient pancreatic cancer cell model, miR-34a transfection resulted in restoration of the p53 TSG function (387). In NSCLC, it was shown to be down-regulated, with low levels correlated with a high probability of relapse (388). The current data support a tumour suppressive role for miR-34a as higher than median expression was independently associated with a favourable outcome following resection in the test cohort and univariately in the validation set.

High miR-30d expression was identified as an independent marker of good prognosis in the test set. While not previously implicated in PDAC, over-expression of miR-30d is associated with poor outcome in hepatocellular carcinoma (389). miR-29c has not previously been

correlated with survival in PDAC but in mesothelioma, miR-29 expression associated with favourable outcome, and overexpression in a cell model resulted in decreased invasion (390). Similarly in mantle cell lymphoma, miR-29 was down-regulated compared to normal lymphocytes with under-expression associating with reduced survival (391).

The miR-221/222 cluster is up-regulated in PDAC cell lines and likely promotes proliferation as in other tumours (392). miR-222 over-expression was previously associated with poorer outcome following PDAC resection (223). While miR-221 has been associated with increasing PanIN grade (393), the current data is the first to associate miR-221 or miR-224 expression with overall survival. The novel survival associations for miR-29c, miR-30d, miR-34a, miR-221 and miR-224 warrant validation studies to investigate potential roles in PDAC tumourigenesis.

miR-196a is a notable target previously demonstrated by Bloomston and co-workers (225) that was not identified as prognostic in the present analysis. Subsequently no further investigation of this target was performed and therefore potential prognostic utility cannot be excluded. miR-196a expression did correlate with lymph node positivity, T3 tumours, venous invasion and resection margin involvement, supporting a disease progression role. Expression profile differences may be explained by RNA extraction and analysis platform variation. It should be noted that discrepancy in miRNA profiling between these data and the Bloomston study might be explained by their extraction of RNA from paraffin cores.

These results suggest that miR-21 had prognostic utility for all patients regardless of adjuvant therapy status supporting its role as a prognostic marker. However, if miR-21 expression is causal to poor therapeutic outcome, antagomirs (394) targeting this molecule may yield therapeutic benefits in high expressors. This assessment of miR-21 predictive utility was confounded by limited sample size and a non-standardised chemotherapy regimen. Giovannetti and co-workers studied the relationship between miR-21 over-expression in PDAC and gemcitabine resistance (221), with high expressors having poorer prognosis. Transfection of pre-miR-21 was seen to decrease the anti-proliferative and apoptotic influence of gemcitabine in cell culture model. Hwang and co-workers showed that in both test and validation cohorts, low miR-21 expressors benefited from adjuvant chemotherapy (222) with longer survival. However, miR-21 expression did not predict overall survival in the adjuvant therapy group.

The pathway enrichment analysis conducted for putative mRNA targets of miRNAs associated with poor outcome highlighted established pathways underlying PDAC including Wnt, TGFβ and MAPK signalling. Putative target genes commonly targeted by the good prognosis miRNAs were identified by a combination of on-line computational approaches

and indicate the cancer-associated genes are potentially regulated by these miRNAs. Additional studies are required to validate these targets.

This study was not without limitations, principally the failure to perform laser capture microdissection, instead using bulk-dissected pancreatic tumour tissue for RNA extraction again compromises these results. The technique used enables the stromal and potentially inflammatory components, which play an increasingly recognised role in carcinogenesis and tumour progression, to be evaluated alongside epithelial components. Despite this potential benefit, microdissection would have enhanced localisation of miRNA expression to individual tissue compartments.

Despite prognostic significance of miRNA profiling demonstrated in the current study, clinical utility may be more influenced by measurement prior to resection. miRNA analysis in PDAC tissue obtained by EUS-FNA has already been performed (395), with a combination of qRT-PCR miR-196 and miR-217 measurement enhancing traditional cytological assessment in distinguishing CP from malignancy, with potential to enhance the clinical management algorithm of borderline resectable cases and target neoadjuvant therapy. The stability and robustness of miRNAs was demonstrated by recent quantification in serum. Measurement of a miRNA panel including miR-21, miR-210, miR-155 and mir-196a suggested that a plasma miRNA profile could provide a sensitive and specific PDAC biomarker assay (396). If serum levels are confirmed as matching the promising early tumour based studies, this family of biomarkers may serve as a long-sought screening tool for PDAC, potentially allowing high-risk groups to be risk stratified. While diagnosis of malignancy is invariably determined by preoperative biopsy, this approach is not sensitive for evaluating the existence or extent of metastatic disease. Circulating miRNAs could provide a promising approach to the timely detection and diagnosis of both primary and occult metastatic disease.

7.3.1 Summary

In conclusion, this chapter has confirmed PDAC is associated with extensive alterations of miRNA expression that may deregulate cancer-related genes. The miRNA profiles of PDAC correlated with clinicopathological features including lymph node status and tumour grade and furthermore various miRNAs possessed independent prognostic utility following resection including miR-21 and miR-34a.

Table 7.1 Top 50 miRNAs dysregulated in PDAC compared with normal tissue

25 up- and down-regulated miRNAs, ranked by p-value.

miRNA ID	Chromosomal location	Parametric p-value [b]	FDR	Mean of intensities normal	Mean of intensities PDAC	Fold-change[a]
MicroRNAs with higher expression in PDAC						
hsa-let-7i	12q14.1	< 1e-07	< 1e-07	413.44	1683.51	4.00
hsa-miR-23a	19p13.13	< 1e-07	< 1e-07	1737.84	4847.53	2.78
hsa-miR-107	10q23.31	1.00E-07	6.67E-06	345.58	1037.51	3.03
hsa-miR-223	Xp11.3	1.00E-07	6.67E-06	166.79	1163.35	7.14
hsa-miR-143	5q32	2.00E-07	1.22E-05	123.34	871.28	7.14
hsa-miR-27a	19p13.13	3.00E-07	1.69E-05	498.56	2184.78	4.35
hsa-miR-214	1q24.3	5.00E-07	2.29E-05	178.47	548.68	3.03
hsa-miR-199a-5p	1q24.3	8.00E-07	3.26E-05	622.14	1739.08	2.78
hsa-miR-103	5q34	1.40E-06	4.89E-05	164.5	388.54	2.38
hsa-miR-145	5q32	1.70E-06	5.67E-05	430.4	1666.69	3.85
hsa-miR-21	17q23.2	3.60E-06	9.79E-05	4517.4	17083.78	3.85
hsa-miR-142-5p	17q22	9.60E-06	0.000214	85.14	323.35	3.85
hsa-miR-10a	17q21.32	1.15E-05	0.000241	75.01	256.77	3.45
hsa-miR-130a	22q11.21	1.40E-05	0.00027	373.22	750.09	2.00
hsa-miR-100	11q24.1	1.60E-05	0.000301	114.39	322.7	2.86
hsa-miR-142-3p	17q22	1.79E-05	0.000313	287.25	1105.55	3.85
hsa-miR-505	Xq27.1	2.64E-05	0.000431	16.74	29.38	1.75
hsa-miR-150	19p13.33	2.75E-05	0.000439	60.5	203.4	3.33
hsa-miR-155	21q21.3	5.16E-05	0.000689	31.1	68.26	2.17
hsa-miR-146b-5p	10q24.32	6.55E-05	0.000829	150.45	461.85	3.03
hsa-miR-331-3p	12 q22	8.54E-05	0.000995	188.16	340.2	1.82
hsa-miR-24	9q22.32	9.92E-05	0.00112	1778.84	3226.44	1.82
hsa-miR-34a	1p36.22	0.0001034	0.00114	234.08	474.37	2.04
hsa-miR-222	Xp11.3	0.0001202	0.0013	93.06	222.24	2.38
hsa-miR-221	Xp11.3	0.0001454	0.00148	64.03	134.47	2.08
MicroRNAs with reduced expression in PDAC						
hsa-miR-130b	22 q11.21	< 1e-07	< 1e-07	654.34	82.01	0.13
hsa-miR-345	14 q32.2	< 1e-07	< 1e-07	82.87	7.76	0.09
hsa-miR-617	12 q21.31	< 1e-07	< 1e-07	68.05	10.46	0.15
hsa-miR-887	5 p15.1	< 1e-07	< 1e-07	38.28	11.92	0.31
hsa-miR-708	11 q14.1	< 1e-07	< 1e-07	76	8.21	0.11
hsa-miR-139-3p	11 q13.4	< 1e-07	< 1e-07	110.5	35.76	0.32
hsa-miR-564	3 p21.31	1.00E-07	6.67E-06	165.43	25.53	0.15
hsa-miR-874	5 q31.2	5.00E-07	2.29E-05	250.53	113.9	0.45
hsa-miR-148a	7 p15.2	9.00E-07	3.48E-05	2315.13	331.76	0.14
hsa-miR-575	4 q21.22	1.10E-06	4.04E-05	564.79	128.95	0.23
hsa-miR-33b*	17 p11.2	2.20E-06	7.02E-05	28.61	9.92	0.35
hsa-miR-28-3p	3 q28	2.30E-06	7.03E-05	57.43	12.78	0.22
hsa-miR-324-3p	17 p13.1	3.40E-06	9.60E-05	655.4	303.3	0.46
hsa-miR-216a	2 p16.1	4.00E-06	0.000105	1546.12	49.51	0.03
hsa-miR-665	14 q32.2	5.60E-06	0.000142	30.54	5.26	0.17
hsa-miR-381	14 q32.31	5.80E-06	0.000142	79.4	41.38	0.52
hsa-miR-648	22 q11.21	6.60E-06	0.000156	61.58	6.79	0.11
hsa-miR-30a	6 q13	1.00E-05	0.000216	1618.77	631.19	0.39
hsa-miR-494	14 q32.31	1.25E-05	0.000255	4154.24	658.18	0.16
hsa-miR-148b	7 p15.2	1.74E-05	0.000313	16.44	.2.90	0.11
hsa-miR-29c	1 q32.2	1.75E-05	0.000313	5482.41	2708.27	0.50
hsa-miR-141	12 p13.31	2.14E-05	0.000365	5732.12	1434.94	0.25
hsa-miR-30c-1*	1 p34.2	2.28E-05	0.00038	8.67	2.89	0.33
hsa-miR-30d	8 q24.22	3.42E-05	0.000534	869.87	483.39	0.56
hsa-miR-217	2 p16.1	3.68E-05	0.000563	350.89	44.22	0.12

FDR = false discovery rate

[a] PDAC / Normal expression

[b] p value reported are the result of class comparison analysis of microRNA expression patterns from 48 PDAC tumours compared to 10 normal pancreatic tissue samples using Biometric Research Branch (BRB) Array Tools 3.9.

Table 7.2 Microarray analysis identified miRNAs univariately associated with survival

Analysis performed for 48 patients with PDAC ($p < 0.05$).

miRNA id	Parametric p-value	Hazard ratio [a]	SD of log intensities
hsa-miR-30d	0.0008	0.16	0.494
hsa-miR-29c	0.0055	0.407	0.684
hsa-miR-154*	0.0085	4.958	0.708
hsa-miR-21	0.0086	2.527	0.883
hsa-miR-224	0.0093	2.031	0.947
hsa-miR-34a	0.0128	0.395	0.607
hsa-miR-455	0.0147	3.151	0.543
hsa-miR-378	0.0152	0.464	0.759
hsa-miR-423	0.0178	0.412	0.582
hsa-miR-30a	0.0213	0.506	0.817
hsa-miR-31	0.0220	1.26	2.099
hsa-miR-125b*	0.0222	0.421	0.788
hsa-miR-221	0.0232	2.007	0.713
hsa-miR-33a	0.0243	0.288	0.482
hsa-miR-141	0.0344	0.716	1.336
hsa-miR-181b	0.0352	2.166	0.644
hsa-miR-193	0.0393	7.083	0.757
hsa-miR-223	0.0415	0.257	0.475
hsa-miR-186	0.0426	3.344	0.344
hsa-miR-30c	0.0495	0.637	0.777

[a] Hazard ratio < 1 miRNA expression associated with good outcome

Hazard ratio > 1 miRNA expression associated with poor outcome

* Denotes complementary miRNA sequence

SD – standard deviation

Table 7.3 Association of miRNA expression levels measured by RT-PCR with overall survival: univariate analysis

microRNA	No. of Patients	Median Survival (months)	95% CI	p value [a]
miR-21				
Low	25	30.1	14.2 - 49.9	
High	23	16.5	11.4 - 21.6	0.012
miR-29c				
Low	25	16.7	9.32 - 23.6	
High	23	39.6	15.6 - 63.6	0.002
miR-30d				
Low	25	18.0	12.2 - 23.9	
High	23	30.7	15.4 - 44.7	0.017
miR-34a				
Low	24	13.4	7.73 - 19.1	
High	24	43.1	20.1 - 66.1	< 0.001
miR-221				
Low	23	28.3	23.9 - 32.7	
High	25	16.5	9.4 - 23.5	0.025
miR-224				
Low	24	30.9	15.1 - 45.0	
High	24	17.6	10.5 - 24.7	0.023

[a] p value calculated from Log-rank analysis

Table 7.4 Multivariate Cox regression analysis including miRNA expression levels in 48 patients with PDAC

		Overall survival	
		Multivariate Analysis	
Model [a]	**Category**	**HR (95% CI)**	**p value**
A			
miR-21	Low/ High	3.22 (1.21 - 8.58)	0.019
B			
miR-30d	Low/ High	0.30 (0.12 - 0.79)	0.014
C			
miR-221	Low/ High	0.92 (0.34 - 2.54)	0.881
D			
miR-224	Low/ High	0.67 (0.25 - 1.76)	0.673
E			
miR-29c	Low/ High	0.53 (0.19 - 1.47)	0.227
F			
miR-34a	Low/ High	0.15 (0.06 - 0.37)	0.001

[a] Tumour stage, tumour grade, venous invasion, margin involvement, peripancreatic fat invasion, adjuvant therapy included in each multivariate model with includes a single miRNA.

Table 7.5 Prognostic miRNAs: multivariate analysis of combined 72 patient cohort

A) *All 72 patients.* ***B)*** *38 patients with low miR-21 expression (less than median expression value). C) 34 patients with high miR-21 expression (greater than median expression).*

		Overall survival	
		Multivariate	
Prognostic factor	**Category**	**HR (95% CI)**	**p value**
A) All 72 patients			
Tumour stage	T2/ T3	2.36 (0.96 - 6.33)	0.079
Lymph node status	Absent/ Present	2.17 (0.85 - 5.78)	0.104
Tumour grade	Low/ High	2.26 (1.25 - 4.08)	0.007
Tumour size (mm)	< 30/ ≥ 30	1.83 (1.03 - 3.26)	0.041
Venous invasion	Absent/ Present	1.23 (0.73 - 2.33)	0.382
Margin involvement	R0/ R1	3.45 (1.71 - 6.95)	0.001
Peripancreatic fat invasion	No/ Yes	2.22 (1.08 - 4.58)	0.033
Adjuvant therapy	No/ Yes	0.47 (0.28 - 0.78)	0.009
miR-21 expression	Low/High	4.45 (2.45 - 8.13)	0.001
B) Low miR-21 expression 38 patients			
Tumour stage	T2/ T3	2.61 (0.72 - 8.56)	0.147
Lymph node status	Absent/ Present	2.37 (0.56 - 9.61)	0.261
Tumour grade	Low/ High	2.75 (1.06 - 7.27)	0.041
Tumour size (mm)	< 30/ ≥ 30	1.51 (0.57 - 4.01)	0.404
Venous invasion	Absent/ Present	1.52 (0.52 - 4.38)	0.438
Margin involvement	R0/ R1	4.40 (1.49 - 12.9)	0.007
Peripancreatic fat invasion	No/ Yes	1.89 (1.12 – 5.70)	0.089
Adjuvant therapy	No/ Yes	0.51 (0.21 - 1.20)	0.120
C) High miR-21 expression 34 patients			
Tumour stage	T2/ T3	2.01 (0.36 - 11.3)	0.428
Lymph node status	Absent/ Present	2.95 (0.93 - 8.91)	0.124
Tumour grade	Low/ High	2.15 (0.83 - 5.61)	0.117
Tumour size (mm)	< 30/ ≥ 30	1.24 (0.53 - 2.92)	0.623
Venous invasion	Absent/ Present	1.17 (0.44 - 3.19)	0.895
Margin involvement	R0/ R1	7.51 (1.93 - 13.2)	0.001
Peripancreatic fat invasion	No/ Yes	2.35 (1.34 - 4.91)	0.055
Adjuvant therapy	No/ Yes	0.24 (0.09 - 0.61)	0.003

Figure 7.1 Differentially expressed microRNAs in PDAC versus normal pancreas

A) *Scatterplot characterisation of dysregulated miRNAs by microarray profiling: 48 PDAC and 10 normal pancreatic samples. Following global normalisation of the raw log array data, mean normal pancreatic tissue expression was plotted on the x-axis, and mean cancer expression plotted on the y-axis. Important microRNAs are highlighted by label. Spot size indicates the fold-change relative to median value. The centre line represents no expression difference between PDAC and normal pancreatic tissue. Colour is only to facilitate visualization.*

A

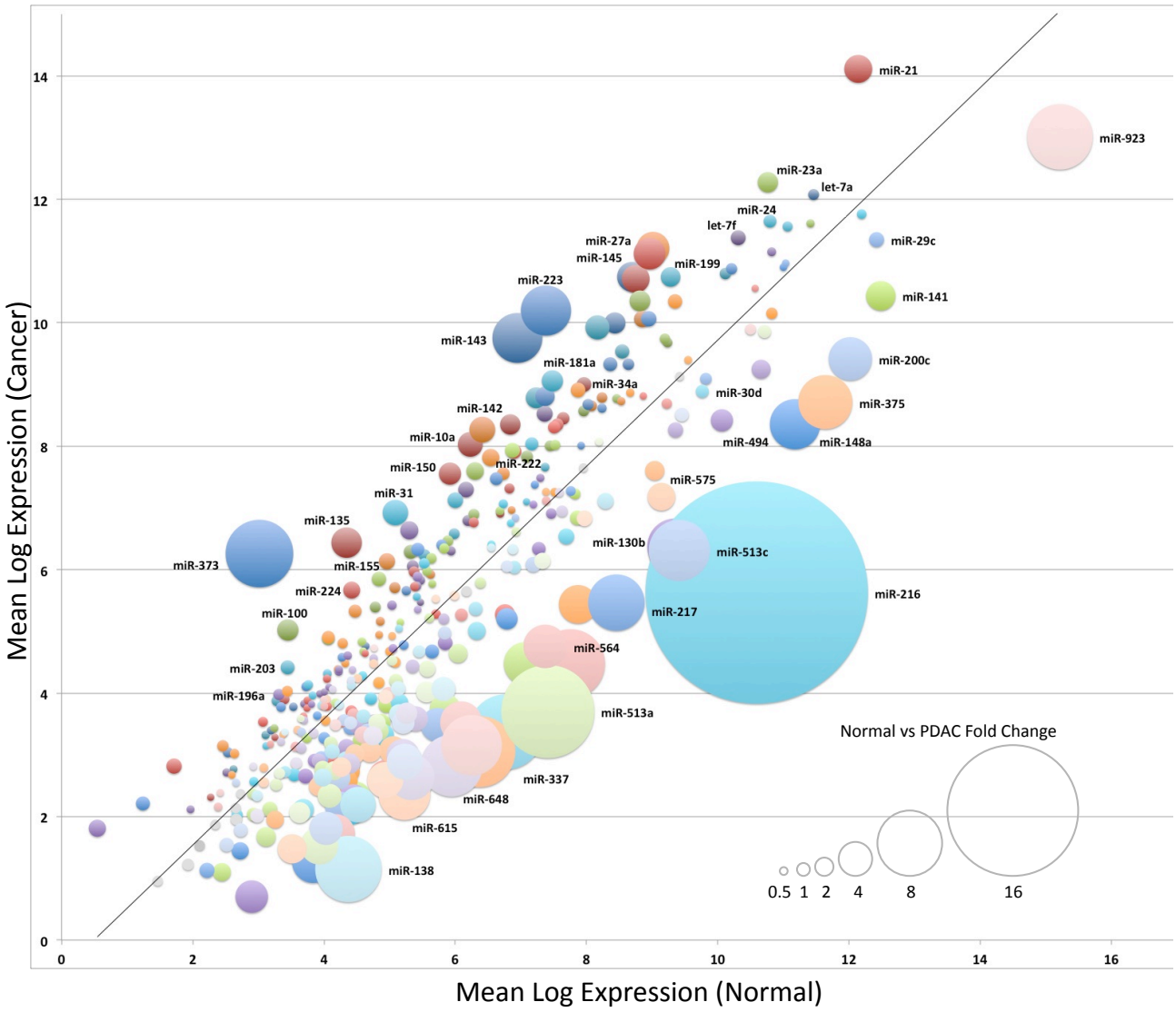

Figure 7.1 Differentially expressed microRNAs in PDAC versus normal pancreas

B) *Supervised average linkage clustering with centred Pearson correlation using 48 PDACs and 10 normal pancreatic samples. miRNAs are in rows with the samples in columns. The non-tumour normal pancreatic samples are on the right highlighted in green, with tumour samples highlighted in blue. The expression colour bar is shown below the dendrogram. Red indicates a miRNA expression higher than the average expression across all samples, blue indicates a lower expression.*

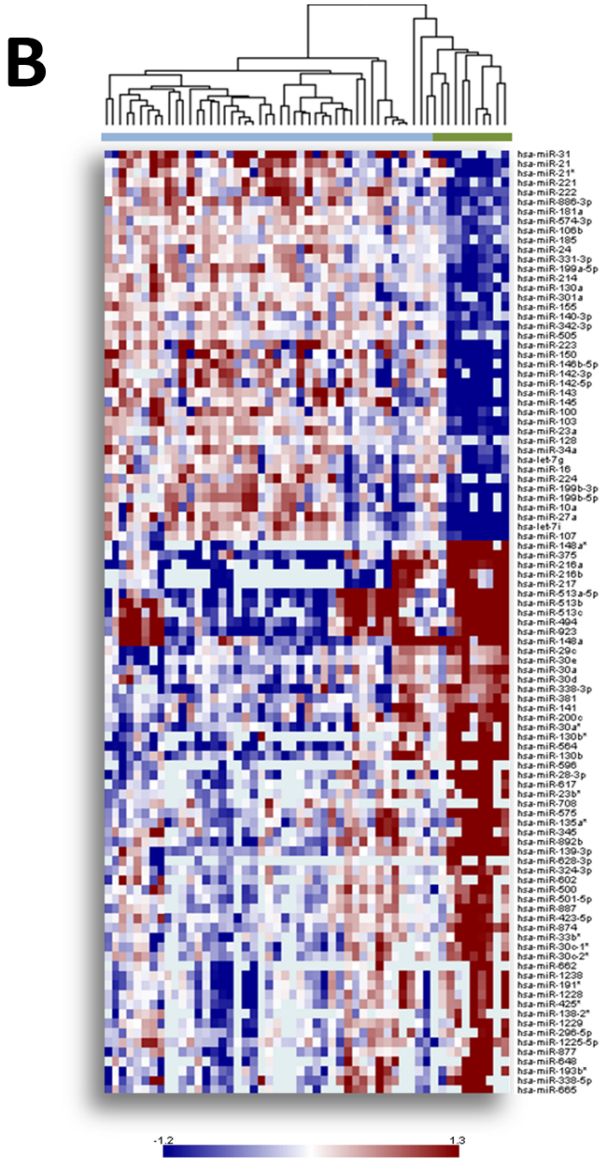

Figure 7.2 MiRNAs associated with traditional clinicopathological features in PDAC

Venn diagram of miRNAs that are associated in PDAC with tumour grade, tumour stage and lymph node status. The numbers are attached to lists of the miRNAs associated with each component of the diagram. miRNAs associated with the presence of venous invasion, resection margin involvement and liver metastases as the site of initial recurrence are listed separately at bottom left: those miRNAs which are common to those in the Venn diagram are highlighted in red.

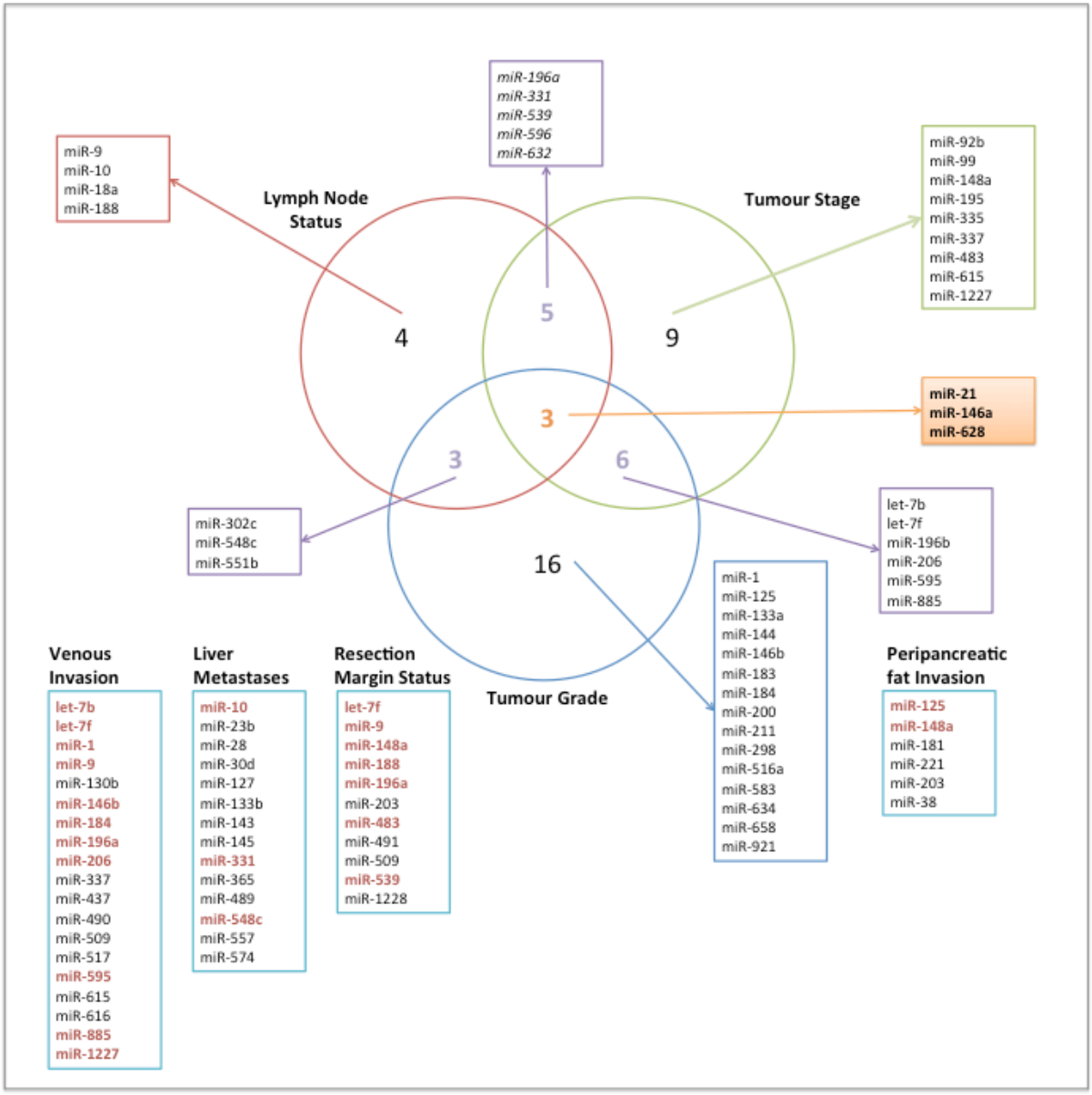

Figure 7.3 Identification and validation of prognostic miRNAs in PDAC

A) *Hierarchical clustering of 48 resected PDACs based on the top 20 survival associated miRNAs (miRNA expression by microarray: red indicates up-regulation; blue indicates down-regulation). In the survival identifier row, samples coloured green indicate survival over 2 years, while red indicates survival below 6 months.*

B) *Kaplan-Meier analysis of the 20 miRNA predictor demonstrates a significance difference in survival time based on microarray expression (Log-rank test, p = 0.02) between low-risk and high-risk groups.*

C) *Kaplan-Meier analysis of the RT-PCR validation. High expression of miR-29c, miR-30d and miR-34a is associated with favourable survival while high expression of miR-21, miR-224 and miR-221 expression is associated with poor survival. Here, miRNA expression levels were measured by qRT-PCR, with high expression levels of miRNA corresponding to a value greater than the median expression. p values are based on Log-rank test.*

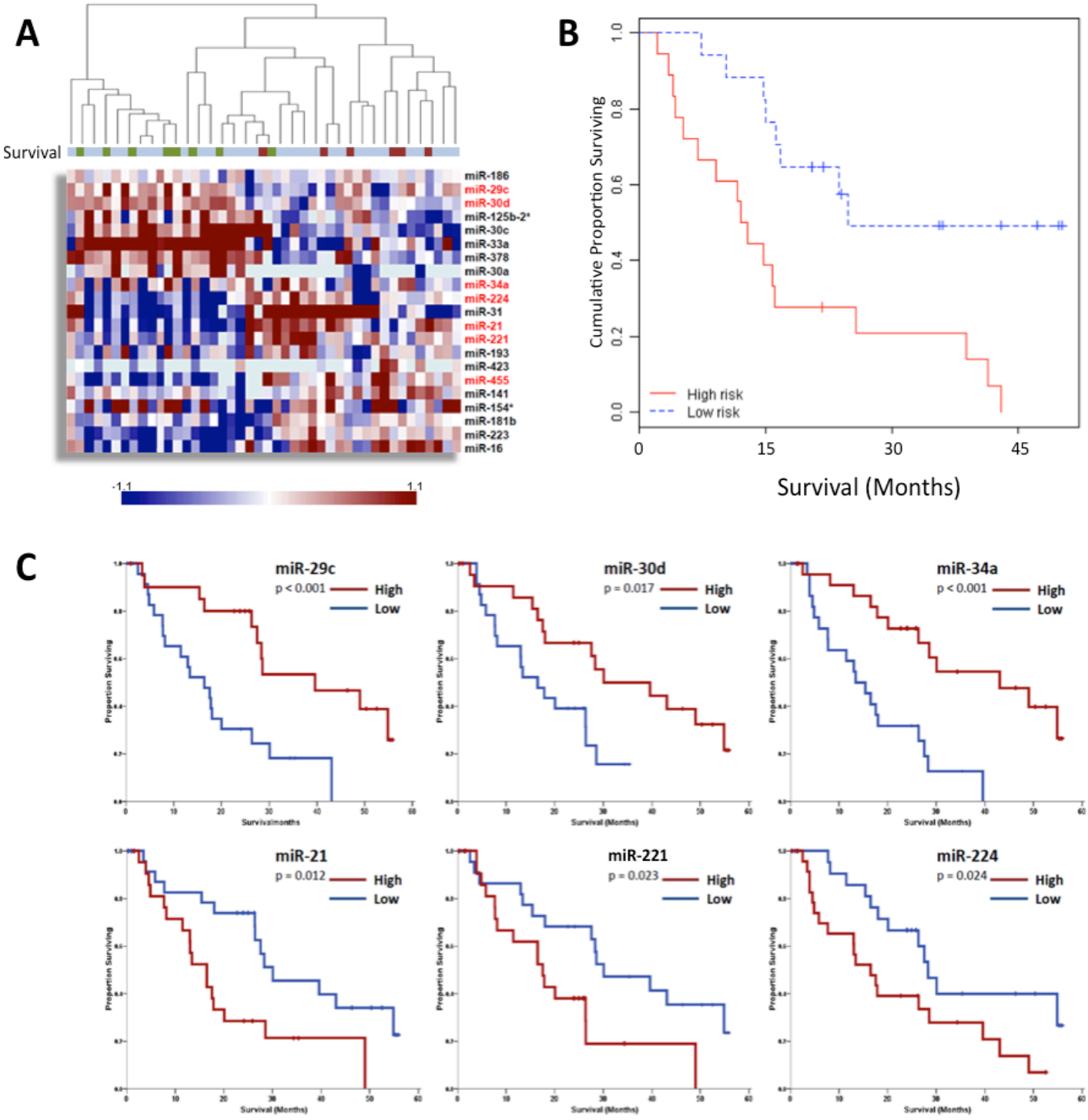

Figure 7.4 Further validation of prognostic miRNAs and predictive utility of miR-21

*Survival analyses confirming high expression of **A)** miR-21 (p = 0.031) and low expression of **B)** miR-34a (p < 0.001) was associated with poor survival following resection in a validation cohort of 24 PDAC patients. **C)** Combined analysis of 72-patient cohort examining associations between mir-21 expression and receipt of adjuvant chemotherapy with overall survival. In patients with low tumoural miR-21 expression, adjuvant chemotherapy failed to significantly influence overall survival (p = 0.74), while in patients with high miR-21 expression, chemotherapy was associated with significantly prolonged survival (p = 0.008). miRNA expression levels measured by qRT-PCR were converted into discrete variable by division of samples into two classes (low and high expression) based on median values as the threshold. p values based on Log-rank test.*

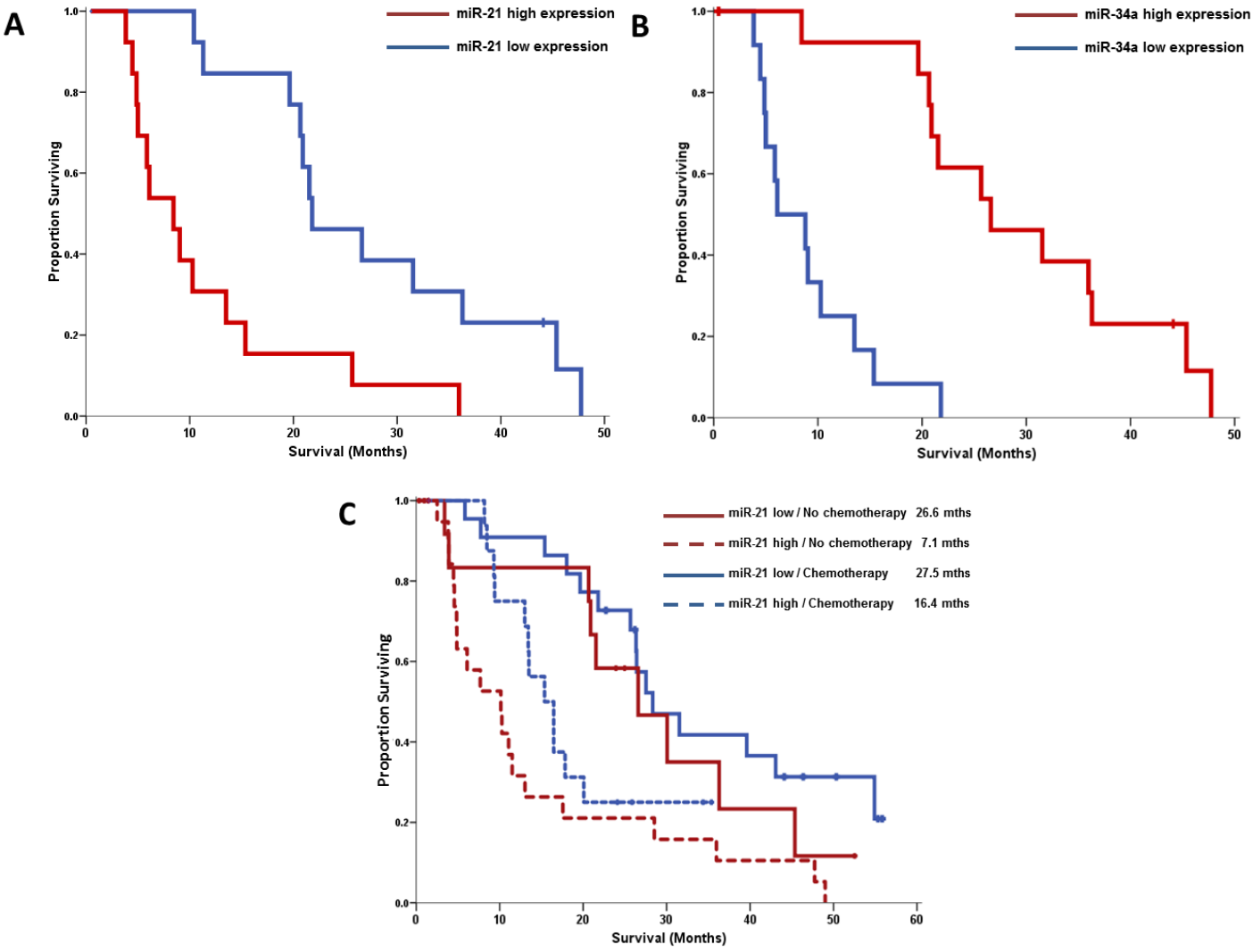

8 Array Comparative Genomic Hybridisation Profiles Associated with Clinicopathological Criteria and Survival in Resectable PDAC

8.1 Introduction

As discussed, PDAC is associated with a series of chromosomal aberrations. aCGH allows a unique view of the genomic instability that a tumour has undergone before diagnosis. The number of genomic CNAs and the specific loci involved, such as whole chromosome gain, loss, high-level amplification and homozygous deletions, are quantifiable. The type, degree and locations of these changes may have prognostic and therapeutic implications for PDAC.

8.1.1 Aim

The aim of the present chapter was to undertake a detailed analysis using aCGH of chromosomal imbalances in a cohort of 45 resected PDACs. A further objective was to identify CNAs associated with clinicopathological features including survival.

8.2 Results

8.2.1 Combination of previous aCGH data

The data from previous studies assessing CNA with aCGH in PDAC (Table 1.6) were used to create a CNA frequency plot (Figure 8.1). The first striking feature is that the frequency of deletion is greater than for amplification. Furthermore the location of several established TSGs is clear. The amplifications tend to be focal and assist in the identification of target oncogenes. The lack of frequent amplifications suggests that oncogene over-expression by gene amplification may not be a common mechanism in PDAC. From the frequent deletions in the PDAC genome it appears that suppression of TSGs by deletion may be a common feature of PDAC.

8.2.2 Assessment of copy number aberration in pancreatic cancer samples

In total, 45 PDACs had a copy number profile constructed and analysed for this chapter according to the workflow in Figure 11.18, with the cohort characteristics described in Table 2.1. As in the previous two chapters, only patients with fresh frozen tissue of suitable quality were included. Unfortunately this cohort did not overlap completely with the cohort that underwent gene expression and miRNA profiling from the previous chapters as a result of insufficient residual tissue (overlap = 37). Following aCGH hybridisations and removal of arrays with sub-standard hybridisation, analysis was performed as outlined in Figure 2.2D. The results for all samples and for each chromosome were plotted as for chromosome 17 (Figure 8.2). The analysis of CNAs was assessed using various algorithms (Figure 2.2E) previously utilised in similar analyses on a variety of tumour types, of which the CBS algorithm was found to be the most useful (259). A table of gains and losses in chromosomal regions for the entire cohort were compiled (Table 11.19). Diagrammatic representations of the CBS algorithm results are presented in Figure 8.3. Numerous aberrations were confirmed, previously identified in PDAC both in large-scale genomic profiling studies and by other molecular techniques.

8.2.3 Pathway enrichment analysis for arrayCGH

Pathway analysis allowed for the enrichment of a large number of aberrantly expressed regions according to specific gene sets. The results for KEGG and BioCarta pathway enrichment are shown in Table 11.34 and Table 11.35 respectively. There was clear enrichment of pathways previously identified as important in PDAC, with regions of gain associated with Jak-Stat, Notch, Wnt, NFκB signalling, ERBB2 and IL-5 pathways, as well as ECM receptor interaction, ubiquitin proteolysis, leukocyte transendothelial migration and haematopoietic cell lineage. Similarly there was pathway enrichment of genes with loss including TGFβ signalling, PTEN dependent cell cycle arrest, GnRH signalling pathway, Parkinson disease pathway, autophagy and apoptosis. Other novel pathways included PITX2 regulation, SUMOylation and PPARδ pathways.

8.2.4 Genomic identification of significant targets in cancer (GISTIC) analysis

The level of discordance between chromosomal abnormalities evident from recent studies highlights the need to determine 'controlling' genetic modifications. Strikingly different studies of the same tumour type often report 'regions of interest' that are highly discordant. In lung cancer for example, two similar studies reported 48 and 93 regions of interest, respectively (397, 398) with < 5% overlap. Although perfect agreement should not be expected, such a high level of disagreement is disconcerting. One possible explanation is the true number of cancer-related regions is extremely large, with each containing only a small and variable subset of regions. Alternatively, many reported regions are random events of no biologic significance. Most methods do not account for background levels of random chromosomal aberration. The GISTIC method was developed to help identify CNAs more likely to drive cancer pathogenesis, with greater weight given to high amplitude events, that are less likely to represent random aberrations.

8.2.4.1 GISTIC methodology

GISTIC identifies the frequent and significant CNAs through two key steps (Figure 8.4). Firstly, identifying a statistic (G score) involving both frequency of occurrence and aberration amplitude. Second, assessing the significance of each CNA compared to results expected by chance. The method accounts for multiple-hypothesis testing and assigns a *q value* to each result, reflecting the probability that the event is due to chance fluctuation. For each significant region, a 'peak region' with the greatest frequency and amplitude of aberration is identified. Each peak is tested to determine whether the signal is due primarily to broad events, focal events, or overlapping events of both types.

8.2.4.2 GISTIC results

Table 11.21 demonstrates the significant regions of gain and loss identified by the GISTIC method in the 45 patient cohort. As expected the number of significant areas of copy number loss outnumber regions of gain. The overall genome-wide view of the CNAs is shown in

Figure 8.5A. The overall pattern is complex, with almost every region of the genome altered in at least one tumour. Nonetheless, 6 broad and 23 focal events are significant in regions of copy number loss (1p36.23-p36.21, 16p13.3-q24.3, 17p13.3-q25.3, 18q12.1-q23, 19p13.3-q13.43, 21q22.3, 22p13.33-q13.33), while 9 focal events were significant in regions of copy number gain. The peak regions were compared to the location of common PDAC aberrations (KRAS, TP53, CDKN2A, SMAD4, LKB1, BRCA, PDX-1, HER2, c-MYC, EGFR, TGFβ1 and AKT). Five from 12 genes were found to correspond with one of 23 peak regions. KRAS was not overexpressed, however, it is well known to have altered expression resulting from mutation rather than CNA. Various peaks were identified containing genes aberrant in other cancers (CHAF1A, DPP6, EXOC4, SMURF1 and BOP1). This analysis suggests that CNAs involving these genes are relevant to PDAC pathogenesis and should be further characterised. In particular GSTT1 was identified as being significantly amplified in this cohort, having previously been associated with a predictive role in PDAC patients receiving 5-FU adjuvant therapy (399). The remaining regions are not associated with known cancer genes (ADAM18, MGRN1, SIRBP1 and RNPC3) highlighting the importance of systematic analysis.

8.2.4.3 Consistency across independent dataset

The GISTIC algorithm results were validated within an independent PDAC study (400), which used similar Agilent aCGH arrays (44K versus 244K) to profile 30 tumours. At first glance there appears to be striking differences, attributable in part to differing methodologies. Applying the GISTIC algorithm to the previous study identifies similar regions as identified in the studied cohort (Table 8.1), although the total number was reduced due to diminished array density. The most obvious CNAs were as expected, losses of SMAD4 and CDKN2A, gain of c-MYC, with broad aberrations of chromosome 4, 13, 17 and 18. Novel markers identified included MLLT3, a putative regulator of erythroid cell fate, implicated in acute myeloid leukaemia (401) but novel in PDAC. SMURF2 knockdown in breast cancer cells has been shown to enhance cell migration (402). Interestingly analysis of both datasets revealed increased DPP6 copy number and decreased DUSP22 copy number. The overlap between the data sets was not as high as expected.

8.2.5 Association of clinicopathological factors with copy number aberrations

Overall, cases with a phenotype indicating increased malignant potential had a higher degree of aberrations. Lymph node status, tumour stage, grade, venous invasion, size, pancreatic fat invasion and resection margin status were assessed (Appendix 11.6.5). Then the frequency of CNAs was compared and associated with different pathological states at a probe level, to identify whether CNA frequency was a potential driver accounting for these pathological states (comparison standardised at $p < 0.001$) (Figure 8.6A). Tumour grade and venous

invasion appeared to be associated with greater CNA frequency, suggesting these disease features are particularly associated with copy number change.

8.2.6 Prognostic impact of copy number aberration in PDAC

In order to determine whether CNAs in PDAC correlated with overall survival, a Cox proportional-hazards model was created to identify statistically significant individual clones. 1120 clones were identified on chromosomes 1, 7, 8, 9, 11, 18 and 21, which harboured loci significantly associated with outcome ($p < 0.001$, Log-rank test) (Figure 8.6B). The list of 250 genes and loci are shown in Table 11.32. As illustrated in Table 8.2, genes for which high copy number associated with poor outcome were located on chromosome 9, with PRSS3 (9p11.2) identified as the most prognostic aberration. Genes for which copy number loss associated with poor prognosis were found on chromosome 7 and 18 including EPHA1, CLCN1 and SHH.

Based on the common regions of aberrations identified, patients whose tumours had greater than the median number of aberrations had a significantly poorer prognosis (11.5 months) than those patients whose tumours had less than the median number of aberrations (28.3 months, $p = 0.002$, Log-rank test, Figure 8.6C).

8.2.6.1.1 CNA and outcome: univariate and multivariate analysis

To determine the extent that survival was determined by the presence or absence of chromosomal aberrations, outcome following resection was compared for a selection of aberrations associating with poor and favourable outcome (Table 8.2). Kaplan-Meier analysis of a selection of the genes in which CNA related to outcome is shown in Figure 8.7. In a multivariate model, copy number gain associated with STMN1 (1p36.1) yielded independent prognostic significance (HR: 3.6, 95%CI: 1.38–9.94; $p = 0.009$, Log-rank test) in addition to tumour stage, size, grade and R1 status (Table 8.4A). Conversely, copy number loss of EPH1A (7q34) yielded prognostic information (HR: 0.26, 95%CI: 0.11–0.59; $p = 0.001$, Log-rank test) when analysed separately along with tumour stage, size, grade, R1 status and adjuvant therapy (Table 8.4B). GSEA was performed to identify genes with CNAs relating to outcome correlated with known gene sets including GO, BioCarta and KEGG pathways (Table 11.33).

8.3 Discussion

The main objective of this chapter was to explore and catalogue the genomic aberrations in a 45 patient PDAC cohort using a high-density oligonucleotide aCGH platform. This allowed confirmation of numerous regions of recurrent chromosomal loss and gain, the spectrum of which was consistent with previously published conventional CGH and aCGH studies. The present study represents the highest resolution assessment of the PDAC genome using aCGH, and was envisioned as a means to identify new aberrations involved in PDAC tumourigenesis and prognosis.

The volume of data generated by this method of genomic profiling is problematical. While obvious CNAs can be selected from the background change, subtle high-definition changes are more challenging. Pathway enrichment analysis was applied successfully, confirming Jak-Stat, Ras, Notch and Wnt as demonstrating copy number gain. Novel pathways derived from genes with copy number loss identified by enrichment included PITX2 and SUMOlyation. Small ubiquitin-like modifiers (SUMOs) mediate post-translational modification and while not previously assessed in PDAC, SENP1 is up-regulated in thyroid tumours (403).

The GISTIC algorithm has proven useful in CNA identification in numerous malignancies (260) but this is the first application in PDAC. It is likely that some copy number alterations are secondary to random genomic instability associated with cancer in general. The GISTIC analysis method provides a potential means to identify recurrent changes that are concordant across data sets and less likely to represent random passenger events. Fifty percent of events in the current study involved known cancer related genes, with some not previously associated with PDAC and these genes deserve further investigation. GISTIC appears to have identified a manageable number of recurrent events, although studies with a larger sample size may identify further low prevalence events. Notable targets that were identified included CHAF1A, EXOC4, BOP1 and SMURF1. Chromatin assembly factor 1A (CHAF1A) is vital in chromatin assembly, prognostic in breast cancers (404) but yet to be assessed in PDAC. Exocyst complex component 4 (EXOC4) is frequently deleted in colon cancer (405), which contrasts the current finding in PDAC. Ribosome biogenesis protein (BOP1) (8q24) is frequently associated with increased gene dosage in colorectal cancer (406). A number of genes have not been subjected to analysis in malignant disease including ADAM18, MGRN1, SIRBP1 and RNPC3. The concordance amongst the independent dataset further supports the validity of this methodology. Ideally further datasets would be validated. In particular, studies using another technology platform would be beneficial, but unfortunately to date none are publically available.

Correlations between CNAs at various loci and clinicopathological parameters were identified. While CNAs related with pathological states, have potential to inform pathobiology, CNAs associated with outcome are more likely to have clinical utility. A notable finding was the wide range both in terms of numbers and pattern of CNAs observed between samples. No cases showed a total absence of CNAs. Importantly, the loss rate and range reported within this study is close to that previously published (407). There were few losses or gains of whole chromosomes indicating the majority of genomic instability in PDAC occurs at a sub-chromosomal level. Overall, specimens with highly malignant phenotypes had more frequent CNAs. It is of interest that loci associated with lymph node

metastasis, venous invasion, tumour grade and stage were for the majority different, suggesting that in PDAC, invasive and metastatic potential stem from diverse molecular mechanisms.

Of CNAs associated with lymph node status, though genes with evidence of copy number gain were rare, many with reduced copy number were implicated in cancer progression. These included EP300, ADSL, Cyclin E and CSNK1E. The latter is a member of the circadian genes implicated in Wnt/β-catenin signalling in breast cancer cells (408). While the small number of LN0 specimens (n = 9) limits the analysis, there appears to be genuine difference in CNAs between the LN1 and LN0 specimens. High-grade tumours had significantly more CNAs than low-grade tumours. In particular, Ift88 (intraflagellar transport protein 88), one of the most aberrant, is required for ciliogenesis and mediates SHH pathway dependent tumourigenesis in basal cell carcinoma (409). A further potential novel TSG, Klotho (13q12), is a regulator of senescence and an apoptosis promoter in lung cancer cell lines (410). Furthermore LATS2 (13q11) of the HIPPO-LATS signalling pathway, has roles in genomic stability maintenance (411). More advanced stage was associated with chromosome 1 CNAs (1p13), including the putative oncogene VAV3, not previously investigated in PDAC but implicated in breast cancer (412). High LMO4 expression in PDAC has been associated with favourable outcome (413), a result supported by the evidence of reduced copy number in T3 disease in the current data.

To date in a single study, pathological data was integrated with CNAs demonstrating concordance with the presence of venous invasion and lymph node metastasis (241). For venous invasion, while aberrant genes previously reported do not feature highly in the present comparison, the chromosomes that harbour these CNAs are similar: chromosomes 20, 19, 18, 11, 9, 8 and 1 (previous study), compared with 22, 19, 17, 11, 9, 8 and 1 in this study. Interestingly the loci significantly altered in the previous study match with the current data, with 19q31.3 the most significant in both. For lymph node metastasis the similarity was less obvious, with 3 loci that showed more evidence of loss in lymph node metastasis being SCYA21 (9p13), ATM (11q22) and RAD51L3 (17q12). HGF, MLL5 and CDK6 (all 7q21-22) were gained more frequently in the lymph node positive group (241). However, an unusual finding of that study was that the frequency of gains exceeded losses. It is established in PDAC and supported by the present study that the contrary is more often the case. Loukopoulos and co-workers (241) identified gain of LUNX, E2F1 and DNMT3b (20q11), loss of p73 (1p36) and gain of PPM1D (17q23) as having prognostic value independent of pathological variables, however only loci 1p36 was prognostic in the studied cohort. This could result from variability in methodology, patient cohort and data analysis

techniques. Of these, lack of specimen processing consistency and lack of standardisation of data analysis are the most likely contributors to variability.

Despite the considerable variation in genomic profile of the current cohort, genes were identified, the copy number status of which associated with outcome and therefore may yield potential prognostic value. PRSS3 (9p31) was most significantly related to outcome, with gain of this region associated with poor prognosis. PRSS3 has been assessed in CP but CNA of this gene was not shown to be related to this disease state (414). Furthermore it has been proposed as a potential TSG in bladder cancer (415). Additionally, within the 9p31.1 region is CBE1 (ciliated bronchial epithelium 1), important for lung and ciliated cell development (416) but which has yet to be implicated in carcinogenesis.

Of particular interest, p21 Activated Kinase 4 (PAK4) (19q13.1) was amplified in 37 (65%) cases and was associated with a poor overall survival, although not with other clinicopathological features. It was clearly identified amongst a region of amplification in proximity to c-MYC (see supplementary data). The GISTIC algorithm identified PAK4 as a region with recurrent amplification, and it is a component of the T-cell receptor-signalling pathway identified by pathway enrichment analysis. PAK4 was identified in an original PDAC cell line aCGH study (247), and more recently was noted to be amplified in 73 PDACs (417). PAK4 has also been identified as promoting pancreatic cell invasion along with RIOK, with both genes members of Rho signalling pathways (418). Certainly this appears to be an important aberration that warrants further investigation. In Chapter 6, AQPs were identified as being over expressed in PDAC. Gain of AQP3 and AQP7 were of particular interest, supported by previous studies demonstrating that $AQP3^{null}$ mice are resistant to the development of skin tumours (419). PAX5 at 9q13, previously noted as amplified in PDAC, was identified as a gene in which increased copy number associated with poor prognosis. Identified as up-regulated in IPMNs (420), this finding of CNA correlating with clinicopathological factors is novel. STMN1 (1p36.1), a microtubule-regulator was identified by GSEA (Chapter 6) as being up-regulated, with inhibition in pancreatic cancer cell lines reducing growth (421).

Potential novel PDAC TSGs identified by this study included RIN1 (11q13.2). In breast cancer cell lines, RIN1 expression inhibited tumour progression implicating a growth suppressor role. However, expression can potentiate cell signalling processes in NSCLC suggesting a context-specific role (422). Cst6 (11q13) has been identified as a TSG in renal cell carcinoma (423) although, conversely, in a previous study, it promoted pancreatic cell line growth (424). While copy number losses were more common than gains, it would appear that genes with evidence of a gain in copy number are proportionally more likely to be associated with outcome. Prognostic copy number loci identified by aCGH were

demonstrated to provide independent prognostic information. In particular, preserved copy number of EPH1A was associated with favourable outcome (HR = 0.26). Aberrant expression of ephrin proteins is recognised as influencing tumour progression, with low EPH1A expression correlated previously with poor survival in colorectal cancer (425).

The main limitation of this aCGH analysis was the use of non-laser microdissected tumour material for DNA extraction. While cancer cell contamination with normal cells is a well-known issue in aCGH, spiking experiments (mixing various amounts of non-tumoural DNA with a known glioblastoma xenograft samples) showed that aCGH of a sample with tumour cell percentage less than 50% agreed to an extent with genomic profiles obtained from 100% tumoural DNA, though chromosomal and gains and losses were more difficult to identify (426). As is recommended, detailed histological review of each tumour specimen was performed to ensure sufficient tumour cell percentage and the absence of necrotic material. Tumour heterogeneity is a further factor that may complicate the interpretation of aCGH data. Despite these limitations credible results were generated identifying a similar loss and gain pattern to studies using microdissection techniques (239). Therefore these data support previous studies using macrodissected tumour specimens that have also shown similar copy number pattern (427).

DNA quality still remains a crucial factor in performing successful aCGH. Generally, high molecular weight DNA can be easily obtained from fresh frozen tumour material but quality can be related to extraction technique. Given the high cost of aCGH analysis it is essential to reduce the number of failures through adequate DNA assessment prior to hybridisation. All the samples included within this study had DNA gel electrophoresis performed and passed the quality control steps. Unfortunately DNA gel electrophoresis might not adequately predict sample compliancy for further analysis, indicating that factors other than size may influence success. Clearly, copy number profiling of additional tumours should be carried out to resolve further the concordant CNAs.

8.3.1 Summary

In the previous chapters, dysregulation of gene expression was demonstrated to play an important role in PDAC prognosis. aCGH has the ability to identify CNAs at a high-resolution in cancer. In this chapter, using a high-density aCGH platform, a series of CNAs was identified that conforms to the results of previous studies. In this chapter, in addition to cataloguing novel PDAC CNAs, aberration signatures correlating with various tumour pathological features, including lymph node status, tumour grade, venous invasion and stage, have been elucidated. Furthermore, a high a rate of CNA was associated with poor outcome and a number of novel chromosomal loci that correlate with outcome following resection, including 1p36.1 and 7q34, were identified.

Figure 8.1 Frequency of genomic regions found altered within compiled data set

Data from the previous pancreatic cancer aCGH studies were compiled to generate the below diagram. To simplify the selection of regions found altered in the data, bins of 100kb size were made and the data sorted into respective bins. The frequency that a bin with either amplification or deletion was found. The y-axis is the frequency while x-axis is the chromosomal position for all chromosomes on one axis. Dashed vertical lines signify the chromosome ends. Amplifications are plotted in red above the origin while deletions are plotted in green and are plotted below. Several genes well known to be involved in pancreatic cancer are marked.

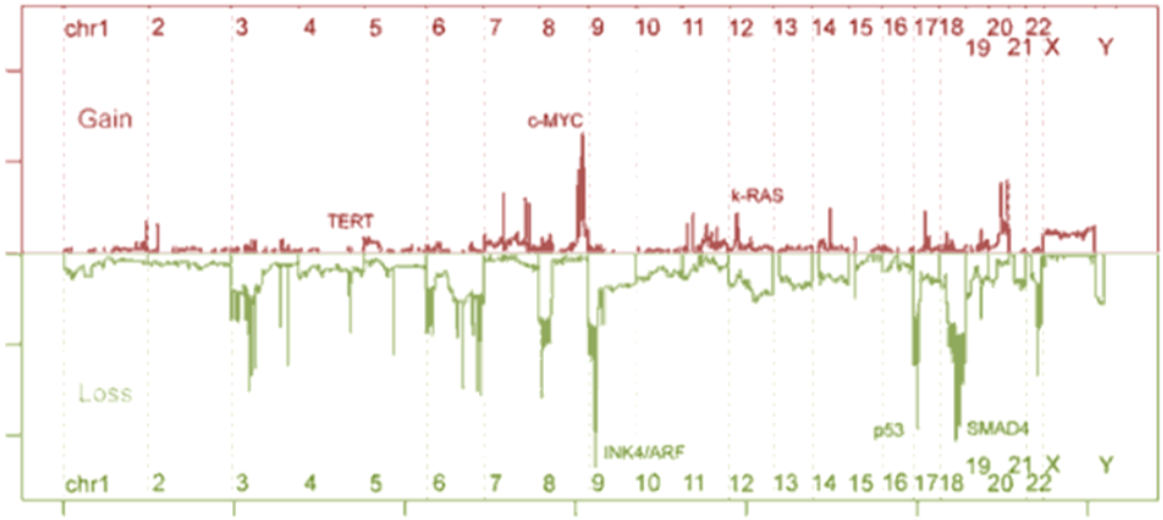

Figure 8.2 Plot of probes of all samples for Chromosome 17

Each dot represents a single probe. Red dots represent probes with increased copy number while green represent probes that have decreased copy number. Probes without significant variation from the normal copy number (between log -0.5 to 0.5) are not shown. The x-axis represents chromosomal location while the y-axis represents the degree of copy number gain or loss.

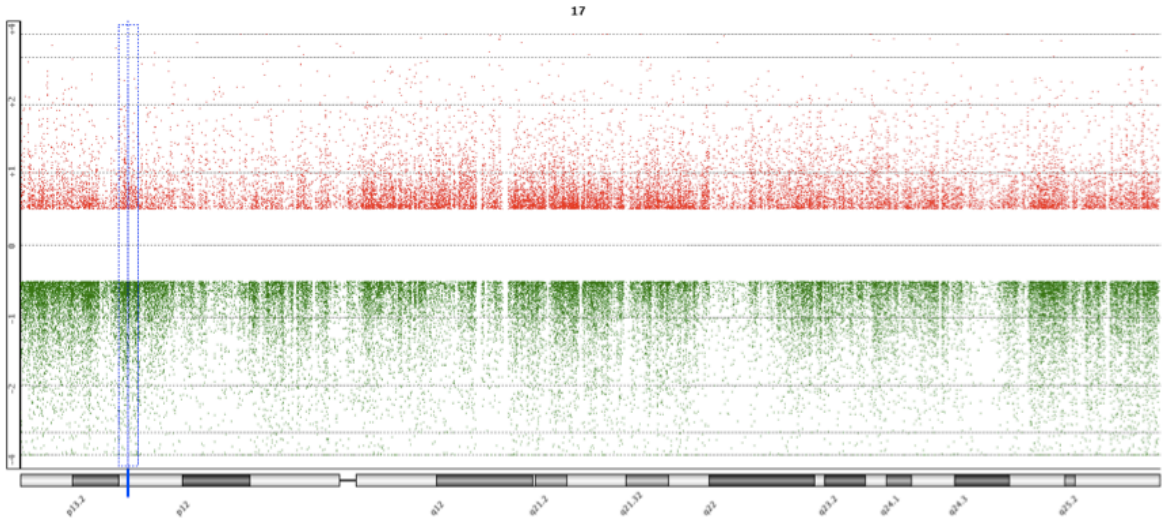

Figure 8.3 Summary penetrance plot of genome wide alterations - 45 PDAC patients

Demonstrates the frequency distribution of copy number aberrations amongst the studied cohort from this thesis (45 patients). Individual chromosomal perspective with genetic losses shown in red and genetic gains shown in blue (Partek analysis). As expected the losses were more frequent than gains.

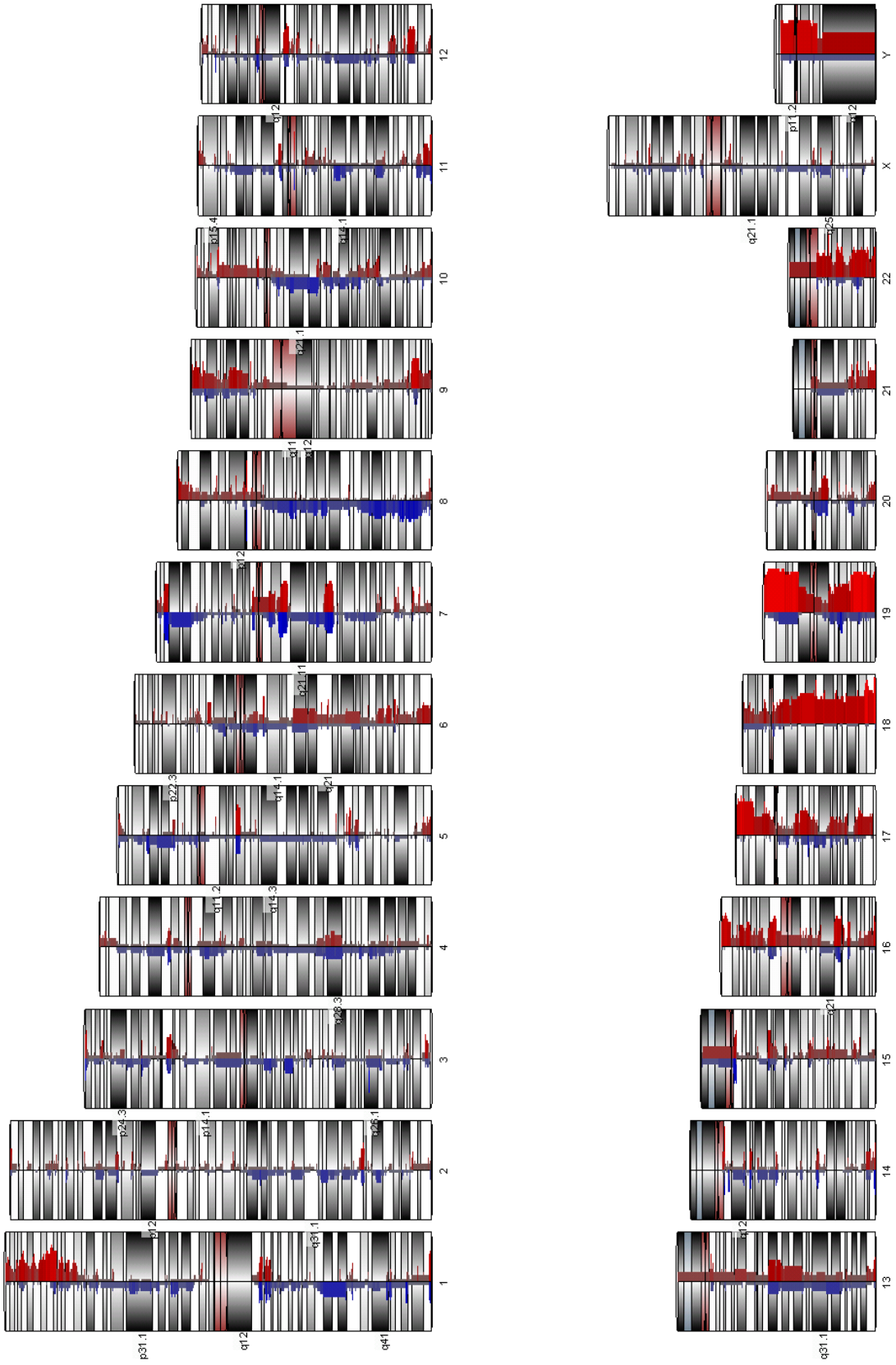

Figure 8.4 Overview of the GISTIC method

Following identification of location and magnitude of copy number aberrations in a number of tumours, Genomic identification of significant targets in cancer (GISTIC) scores each genomic marker with a G score that is proportional to the total magnitude of aberrations at each location. Additionally, permutating the locations in each tumour, GISTIC determines the frequency with which a given score would be attained if the events were due to chance and randomly distributed. A significance threshold (green line) is determined such that significant scores are unlikely to occur by chance alone. Alterations are deemed significant if they occur in regions that surpass this threshold.

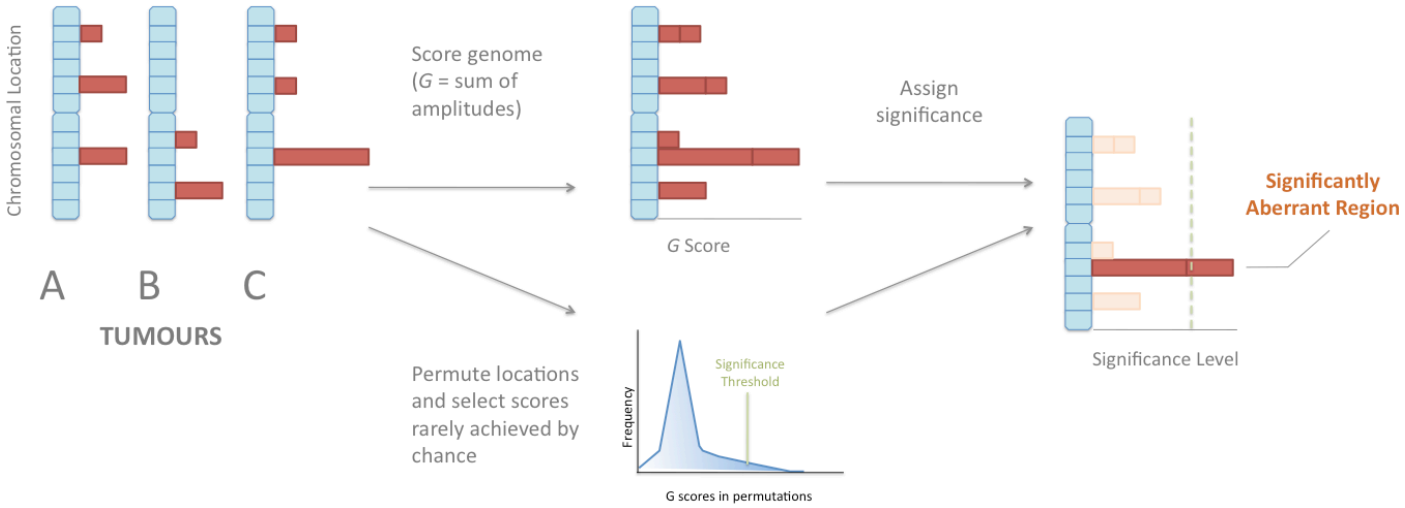

Figure 8.5 Significant broad and focal copy number alterations in the PDAC genome

A) *Amplifications (red) and deletion (blue), determined by segmentation analysis of the normalised signal intensities from 244K CGH arrays are displayed across the genome (chromosomal positions, indicated along the y axis, are proportional to marker density) for 45 PDACs (x axis). Broad events close in size to the chromosome arm are the most prominent, including amplification of Chr 13 and deletion of Chr 18.*

B) *GISTIC analysis of CNAs in PDAC. The statistical significance of the aberrations identified is displayed as FDR q values to account for multiple hypothesis testing. Chromosome positions are indicated along the y axis. Broad Events (indicated by* ***purple*** *bar for amplification and* ***orange*** *bar for deletion) and focal events surpass the significance threshold (green line). The locations of the peak regions and the known cancer related genes and non-cancer related genes within those peaks are indicated on the right of each panel.*

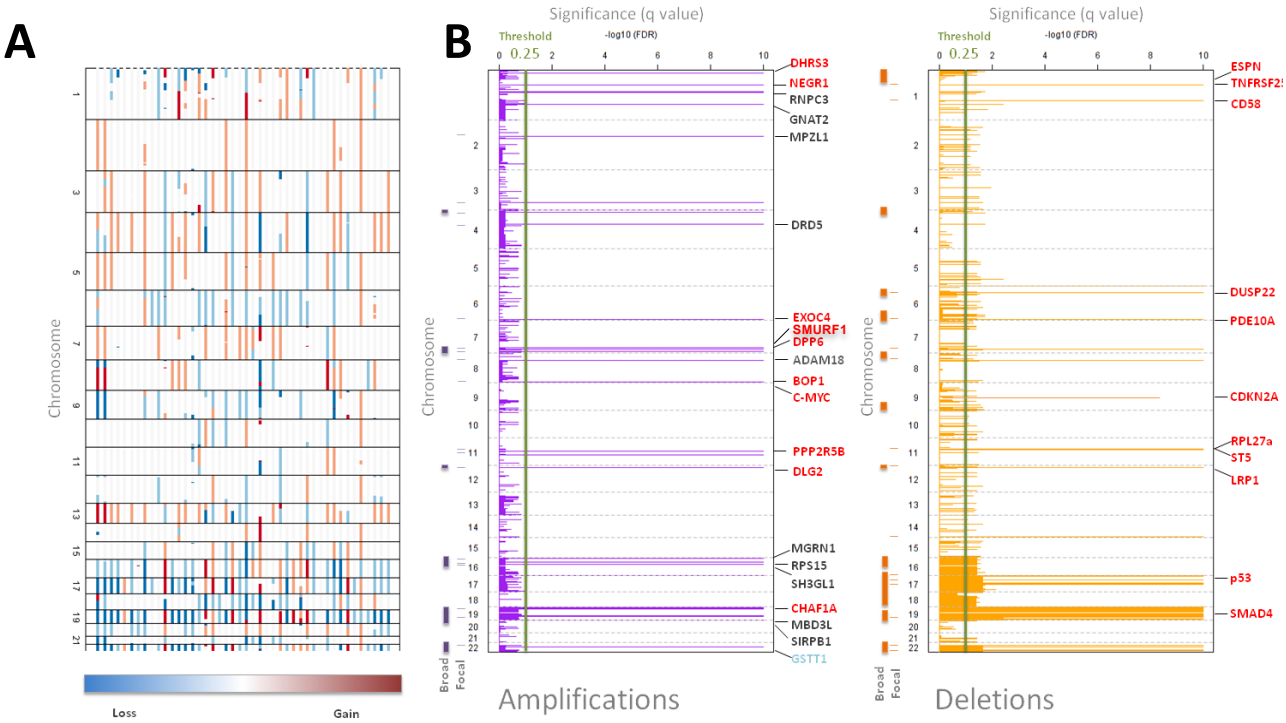

Figure 8.6 Relationship between copy number aberration and clinicopathological status

A) *The frequency of copy number aberrations plotted against each pathological variable (significance threshold $p < 0.001$). Venous invasion was associated with the greatest number of aberrations.*

B) *Chromosomal aberrations associated with prognosis. Red columns percentage of all chromosomal regions passing the filtering criteria that map to each chromosome. Blue columns, percentage of the prognostic copy number aberration regions that map to each chromosome.*

C) *Correlation between recurrent copy number aberrations and survival. Kaplan-Meier plot of 43 patients with PDAC groups according to the number of common regions of aberrations involved per sample. Samples grouped according to median number of aberrations. The group with low number of aberrations had a median survival of 11.5 months versus 28.3 months for high number of aberrations (Log-rank test, $p = 0.002$).*

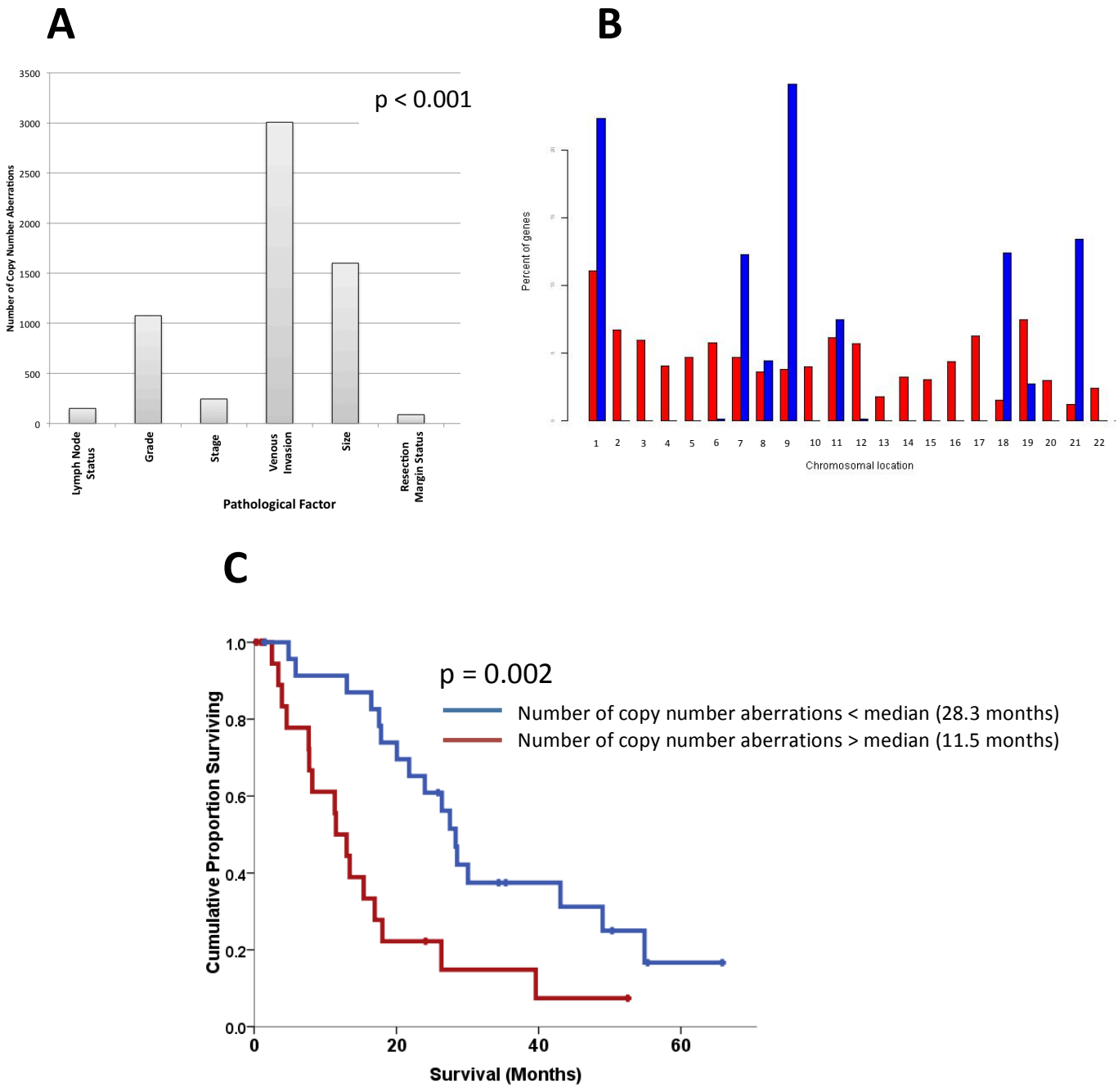

Figure 8.7 Overall survival rate of patients with PDAC according to the presence or absence of chromosomal abnormalities

Overall survival for patients with potential oncogenes with chromosomal loss of loci on chromosome 9, 21 and 1 and patients without such loss. Overall survival for patients with potential tumour suppressor genes with chromosomal loss of loci on chromosome 7, 11 and 18 and patients without such loss. Red lines indicate greater than median copy number state. Log-rank test was used to compare the Kaplan-Meier curves.

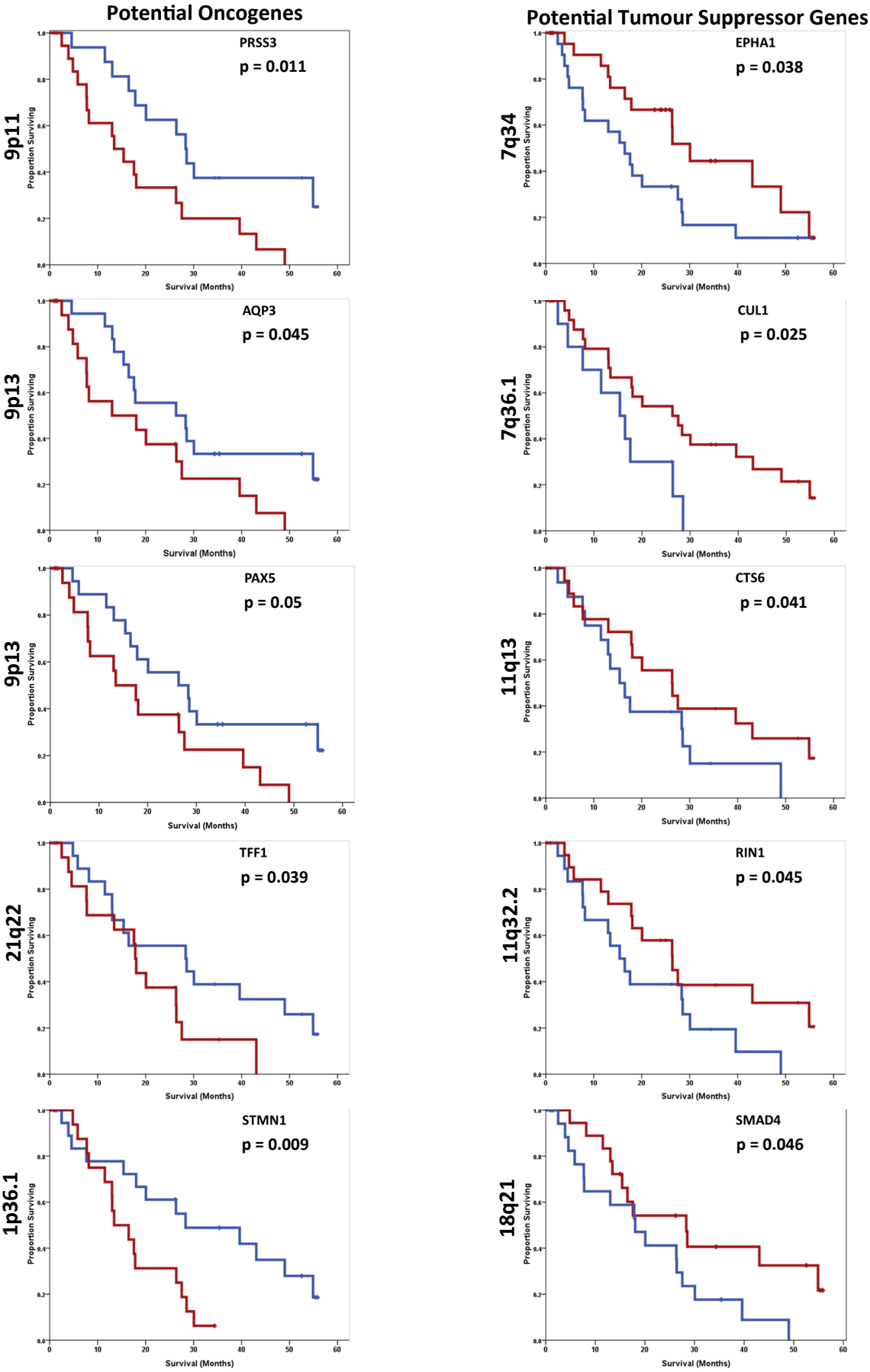

Table 8.1 CNAs calculated according to GISTIC methodology: validation cohort

A) Copy number gains ***B)*** *Copy number losses.*

A) Copy number gains

	Chromosome	Start	End	Cytoband	Number	Gene symbol
1	7	30239404	30272380	7q36.2	1	DPP6
2	9	20810273	23680273	9p21.3	24	KIAA1797, PTPLAD2, IFNB1, IFNW1, IFNA21, IFNA4, IFNA7, IFNA10, IFNA16, IFNA17, IFNA14, IFNA5, KLHL9, IFNA6, IFNA13, IFNA2, IFNA8, IFNA1, IFNE1, MTAP,
3	18	49394375	49985354	18q21.2	1	MBD2

B) Copy number losses

	Chromosome	Start	End	Cytoband	Number	Gene symbol
1	1	103875725	104009263	1p21.1	6	RNPC3, AMY2B, AMY2A, AMY1A, AMY1C, AMY1B
2	3	60267262	60497674	3p14.2	1	FHIT
3	6	23859385	23895884	6p25.3	1	DUSP22
4	9	19775974	20510469	9p22.1-p21.3	2	SLC24A2, MLLT3
5	9	24022718	25899346	9p21.3-p21.2	1	TUSC1 CDKN2A, CDKN2B, DMRTA1, ELAVL2
6	17	11168774	11892479	17p13.1-p12	3	DNAH9, ZNF18, MAP2K4
7	17	36847553	37242665	17q21.2	18	KRT38, KRT32, KRT35, KRT36, KRT13, KRT15, KRT19, KRT9, KRT14, KRT16, KRT17, EIF1, GAST, HAP1, JUP, SC65, FKBP10, NT5C3L
8	17	57398761	59063757	17q23.2-q23.3	13	MED13, EFCAB3, METTL2A, TLK2, MRC2, MARCH10, TANC2, CYB561, ACE, KCNH6, WDR68, CCDC44, MAP3K3
9	17	59223504	60360566	17q23.3-q24.1	22	DDX42, FTSJ3, PSMC5, SMARCD2, CSH2, GH2, CSH1, CSHL1, GH1, CD79B, SCN4A, ICAM2, ERN1, TEX2, LOC645993, PECAM1, C17orf60, POLG2, DDX5, CCDC45, SMURF2, LRRC37A3
10	18	46764796	75904995	18q21.2-q23	85	ELAC1, SMAD4, MEX3C, DCC, MBD2, POLI, STARD6, C18orf54, C18orf26, RAB27B, CCDC68, TCF4, TXNL1, WDR7, ST8SIA3, ONECUT2, FECH, NARS, ATP8B1, NEDD4L, ALPK2, MALT1, ZNF532, SEC11C, GRP, RAX, CPLX4, LMAN1, CCBE1, PMAIP1, MC4R, CDH20, RNF152, PIGN, KIAA1468, TNFRSF11A, ZCCHC2, PHLPP, BCL2, KDSR, VPS4B, SERPINB5, SERPINB12, SERPINB13, SERPINB4, SERPINB3, SERPINB11, SERPINB7, SERPINB2, SERPINB10, HMSD, SERPINB8, CDH7, CDH19, DSEL, TXNDC10, CCDC102B, DOK6, CD226, RTTN, SOCS6, CBLN2, NETO1, FBXO15, C18orf55, CYB5A, C18orf51, CNDP2, CNDP1, ZNF407, ZADH2, TSHZ1, C18orf62, ZNF516, ZNF236, MBP, GALR1, SALL3, ATP9B, NFATC1, CTDP1, KCNG2, PQLC1, TXNL4A, C18orf22
11	19	34789822	35127151	19q12	5	POP4, PLEKHF1, C19orf12, CCNE1, C19orf2

Table 8.2 Chromosomal location of prognostic copy number aberrations

	Copy number aberrations associated with prognosis		
Prognostic Influence	**Chromosome**	**Locus**	**Gene name**
Poor prognosis associated with high copy number	Chromosome 9	9p11.2	PRSS3
		9p13.3	UBE2R2, UBAP1, UBAP2, KIF24, NUDT2, CBE1
		9q12	ACO1, SMU1, BAG1
		9p13	APTX, B4GALT1, SPINK4, AQP7, AQP3, PAX5, PGM5, PIP5K1B, KLF9
	Chromosome 21	21q22.3	CBS, RIPK4, PRDM15, C2CD2, ABCG1, TFF1, TMPRSS3
	Chromosome 7	7q21.3	SMURF1
	Chromosome 1	1p	RPS6KA1
		1p36.1	STMN1, HGMN2
		1p34	HADC1
		1p35.1	S100PBP
		1p34.3	CLDN19, EIF2C3
	Chromosome 18	18q12-21	MAPK4
		18q12.1	GALNT1
		18q21.1	MYO5B
		18q21.3	DCC, SERPINB4, SERPINB5
		18q21.33	BCL2
		18q22.2	SOCS6
	Chromosome 19	19q13	SIRT2, DLL3
		19q13.1	NFKβIB
		19q13.2	PAK4, SYCN, FBXO27
Poor prognosis associated with low copy number	Chromosome 7	7q32	PRSS1, CLCN1
		7q34	PRSS2, PIP, EPHA1
		7q33-q35	EPHB6
		7q33-q34	TRPV6
		7q35	TRPV5, NOBOX
		7q36	PTPRN2, MNX1, LMBR1, SHH, EN2
		7q36.1	CUL1, NOS3, CDK5, CENTG3, PRKAG2
		7q22	PDGFA PRKAR1B
	Chromosome 18	18q21	PIAS2, SMAD2, SMAD4, SMAD7
	Chromosome 9	9p21	MTAP, PLAA, CDKN2A, CDKN2B

Table 8.3 Survival in 45 patients undergoing PD stratified according to the presence or absence of chromosomal copy number aberrations

High gene dosage associated with poor outcome (red). Low gene dosage associated with poor outcome (blue).

			Overall survival (months)	
Gene	**Copy number aberration**	**Chromosomal Loci**	**Median (95% CI)**	**p value**
PRSS3	Low	9p11	26.3 (9.2 - 43.5)	0.011
	High		15.6 (7.7 - 23.3)	
AQP3	Low	9p13	25.4 (4.5 - 48.2)	0.45
	High		13.0 (8.9 - 17.2)	
PAX5	Low	9p13	28.9 (9.1 - 43.5)	0.05
	High		13.4 (4.4 - 22.8)	
TFF1	Low	21q22	28.3 (3.2 - 53.4)	0.039
	High		17.8 (16.9 - 18.7)	
STMN1	Low	1p36.1	32.3 (5.5 - 53.2)	0.009
	High		12.1 (5.7 - 19.1)	
PAK4	Low	19q13.2	25.1 (14.4 - 36.2)	0.031
	High		13.8 (8.9 - 18.8)	
SIRT2	Low	19q13	26.3 (13.9 - 38.7)	0.022
	High		16.5 (11.9 - 20.9)	
EPHA1	High	7q34	16.5 (9.7 - 23.2)	0.038
	Low		30.1 (23.9 - 36.3)	
CUL1	High	7q36.1	15.4 (7.7 - 23.1)	0.025
	Low		26.7 (13.9 - 38.3)	
CST6	High	11q13	14.8 (9.5 - 19.9)	0.041
	Low		*26.1 (13.2 - 39.5)*	
RIN1	High	11q32.2	15.4 (9.1 - 21.7)	0.045
	Low		26.4 (17.4 - 35.4)	
SMAD4	High	18q21	28.3 (13.5 - 43.2)	0.046
	Low		18.0 (8.5 - 27.5)	

Table 8.4 Prognostic value of the copy number aberration adjusted for other clinicopathological parameters within a Cox regression multivariate analysis

*Assessment of **A)** STMN1 and **B)** EPH1A in 45 patients undergoing aCGH assessment of their tumours.*

A		**Overall survival**	
Prognostic variable	**Category**	**HR (95% CI)**	**p value**
Tumour stage	T2/ T3	4.83 (1.19 - 26.4)	0.044
Tumour size (mm)	< 30/ ≥ 30	2.61 (1.01 - 6.80)	0.049
Lymph node status	Absent/ Present	2.78 (0.55 - 14.3)	0.270
Tumour grade	Low/ High	6.34 (2.31 - 16.2)	0.001
Venous invasion	Absent/ Present	3.65 (1.22 - 10.9)	0.022
Margin involvement	R0/ R1	3.87 (1.35 - 11.9)	0.024
Peripancreatic fat invasion	Absent/ Present	3.89 (0.95 - 16.3)	0.062
Adjuvant therapy	Yes/ No	0.52 (0.17 - 1.04)	0.069
STMN1 (1p36.1)	Low/ High	3.50 (1.48 - 8.44)	0.003

B		**Overall survival**	
Prognostic variable	**Category**	**HR (95% CI)**	**p value**
Tumour stage	T2/ T3	3.84 (0.85 - 17.4)	0.081
Tumour size (mm)	< 30/ ≥ 30	2.27 (1.03 - 5.04)	0.041
Lymph node status	Absent/ Present	2.21 (0.37 - 13.1)	0.383
Tumour grade	Low/ High	2.11 (0.89 - 4.98)	0.089
Venous invasion	Absent/ Present	1.29 (0.46 - 3.68)	0.627
Margin involvement	R0/ R1	8.67 (2.35 - 31.9)	0.001
Peripancreatic fat invasion	Absent/ Present	2.33 (0.77 - 5.27)	0.344
Adjuvant therapy	Yes/ No	0.33 (0.13 - 0.82)	0.017
EPH1A (7q34)	Low/ High	0.26 (0.11 - 0.59)	0.001

9 Integration of Genome Wide Methodologies

9.1 Introduction

Parallel gene copy number change and gene expression analysis can be used to distinguish potential target genes that may drive tumour progression from those that are merely co-amplified bystander genes. Because gene amplification is expected to lead to overexpression at the mRNA level and subsequently at the protein level, these features can be used as hallmarks to distinguish the potential target genes. Indeed, genes with copy number driving changes in expression are likely to be functionally significant even if occurring in only few cases.

Integration of the wealth of information collected from the genome wide studies of gene expression, miRNA expression, aCGH and protein expression may achieve superior utilisation of the data. Following the hypothesis that alterations in copy number that affect gene expression levels will be likely to be modify protein expression, the integration of expression data with copy number changes has the potential to highlight those changes most likely to be causally implicated in tumour evolution. Investigation of the influence of the miRNAs identified in Chapter 7 on target protein expression, as well as potential regulators of miRNA expression, has the potential to provide a unique insight into PDAC tumour biology in resected human specimens.

9.1.1 Aim

The aim of this chapter was to investigate:

1) The relationship between gene expression and aCGH CNA data, to identify amplifications that potentially drive gene expression, with validation to be performed at protein level of potentially interesting targets (Figure 9.1A).

2) The relationship between aCGH data with miRNA expression data, to identify if regions of aberrant copy number change correlate with differentially expressed miRNAs.

3) The relationship between miRNA expression data, protein expression data and gene expression data, to investigate the downstream effects of miRNAs, as well as potential regulators, focusing in particular on miR-21 and miR-34a from Chapter 7.

Figure 9.1 Integration of genomic data to identify key regulators of PDAC

A) *Gene expression and copy number data integration workflow to identify underlying key regulator genes (only 37 samples were integrated as not all of the samples in Chapter 6 and Chapter 8 were dual profiled).*
B) *miRNA expression, protein expression data and copy number integration workflow to investigate regulators and validate targets of clinically relevant miRNAs (43 samples had both protein expression and miRNA expression data available).*

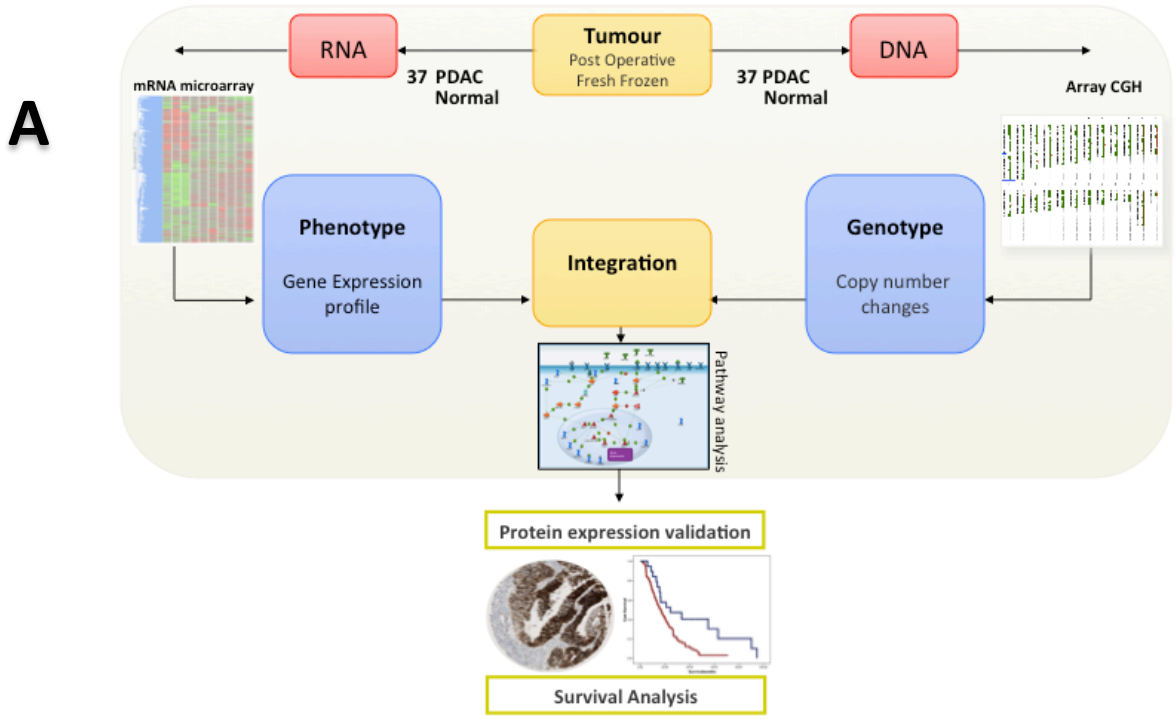

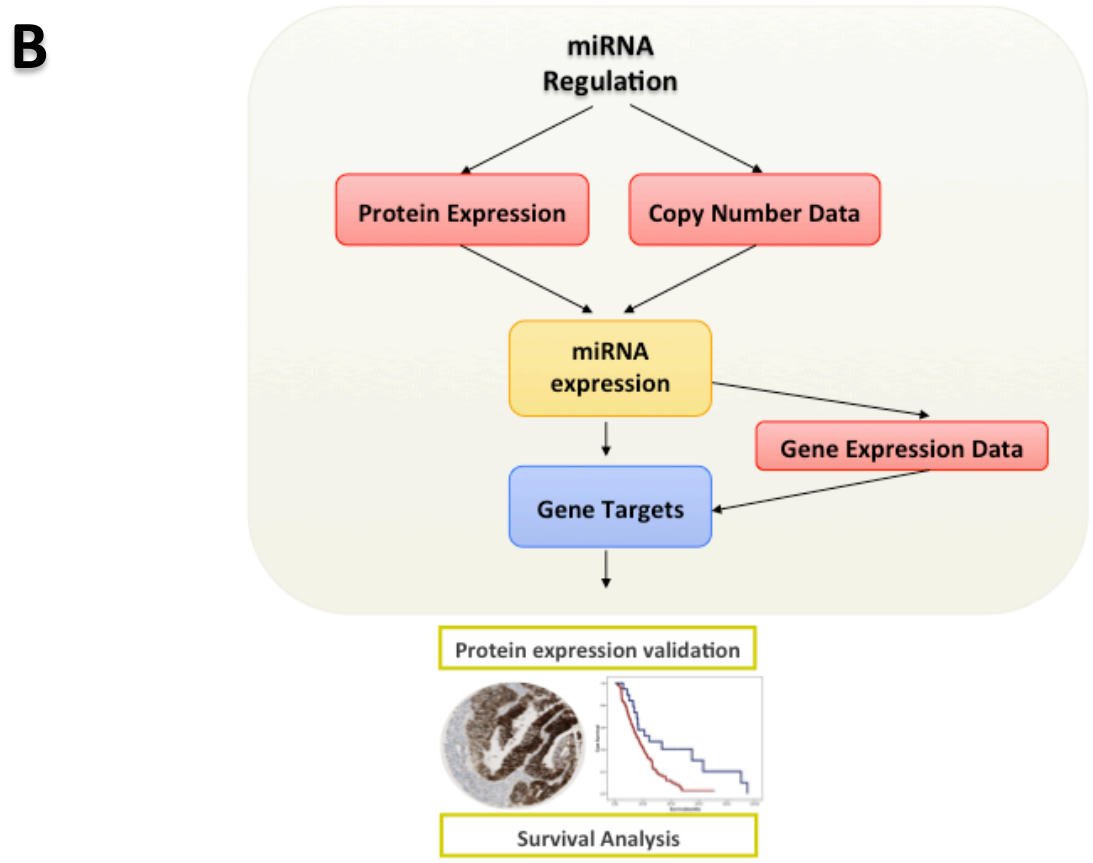

9.2 Results

9.2.1 Genomic clustering of differentially expressed genes

Assessment of whether genes differentially expressed in PDAC revealed a predilection for certain chromosomes was performed. The genomic clustering of 1262 genes differentially expressed in PDAC compared to normal tissue ($p = 0.01$, class comparison t-test) revealed genes on chromosomes 3, 8, 11 and 17 were more frequently differentially expressed compared to other chromosomes (Figure 9.2A). It was apparent that chromosomes 2, 6, 9 and 13 contained significantly more genes that had high expression levels.

9.2.2 Integrative genomic workflow of copy number and gene expression in PDAC

Genomic integration of CNA and gene expression levels has been successfully used in previous microarray studies investigating parallel expression in PDAC cell lines to highlight potentially interesting targets (237, 238, 242, 428). However, to date only limited integrative genomic analysis has been performed in human PDAC specimens.

Using the Correlate analysis tool, gene expression and aCGH CNA data for 37 PDAC patients studied in Chapter 6 and 8 were integrated to identify regions of CNA associated with concordant gene over-expression (Figure 9.1A). Figure 9.2B charts the frequency of correlated CNAs by chromosomal arm, with Figure 9.2C illustrating the chromosomal frequency aberration plot overlaid with regions containing over-expressed genes. For each chromosome a list of genes that had a correlated copy number (CN) and gene expression relationship was calculated with the most significantly correlated targets illustrated in Table 11.36. Almost all chromosomal regions contain some genes with concordant aberrant expression with regions 1q, 8q, 10q and 19q having the most. The fifty most correlated genes are illustrated in Table 11.37.

To further select this list the following criteria was applied: 1) normal versus PDAC specific copy number gain or loss; 2) differential gene expression between normal and PDAC; and 3) copy number significantly correlated with gene expression. A cut-off of > 1.5 fold-change in the median gene expression level was applied generating a shortlist of 17 genes with a significant gene dosage relationship. All are cancer related genes, however many are novel in PDAC (GATA6, ROR2, HNF4A, SMURF1, GPC5, N-Cor, FBI-1, DYRK1A, NFκB, ROCK1, HINT2, mTOR, WISP3, SIRT2, SIRT6, CTLA4 and WNT7B) suggesting that these genes may hold increased biological relevance (Table 9.1). By applying further cut-offs of log2 ratio > 0.3 (threshold for gain) and expression fold-change of > 5.0 (a more stringent cut-off for over-expression) five genes were highlighted as shown in Figure 9.3.

The most significant networks associated with the correlated genes are shown in Table 11.37 (Figure 11.24). GO analysis highlighted the apoptosis and cell death as being significantly enriched along with chromatin remodeling. The networks illustrated in Figure 9.4A and B

highlight the relationship between HNF4A, N-Cor, FBI-1 and ROCK1. The relation of DYRK1A to a number of other correlated genes is highlighted in Figure 9.4C.

9.2.3 Validation of targets identified by copy number and gene expression integration: mTOR

A target meeting the most stringent criteria between gene expression and CN gene dosage was mTOR (Figure 9.5B, Spearman's ρ correlation coefficient = 0.391, p = 0.001), which was selected to be validated at the protein level by IHC in the TMA cohort (Figure 9.5A), to determine whether this approach to biological target identification is useful.

9.2.3.1 Clinicopathological correlation of mTOR protein expression

Examination of tissue sections corresponding to early PanINs confirmed that mTOR expression was low within well-organised epithelia. mTOR did not vary according to tumour size, grade, stage, venous invasion, perineural invasion or R1 status. However, tumours from patients with a LNR > 50% had significantly elevated levels of mTOR compared to those with LNR < 50% and LN0 patients (Figure 9.5C).

In univariate survival analysis, high mTOR expression (n = 21; top quartile threshold histoscore 150) was associated with significantly decreased survival (11.6 months, 95%CI: 7.3–15.9) compared with low expression (n = 98, rest of cohort) (19.6 months, 95%CI: 14.8–24.4) following resection (p = 0.003, Log-rank test, Figure 9.5D, Table 9.2). In multivariate analysis, high mTOR expression is an independent predictor of poor survival (HR: 1.72, 95%CI: 1.08–2.92, p = 0.044, Table 9.3) along with tumour stage, size, grade, peripancreatic fat invasion and R1 status.

There is good evidence that mTOR acts as a downstream effector of PI3K/Akt signalling, linking growth factor signals with protein translation, cell growth and proliferation. Given the role played by mTOR in pAkt signalling an attempt was made to determine whether mTOR expression correlated with Lkb1 signalling. mTORC1 has emerged as a critical effector downstream of Lkb1, which as previously identified in Chapter 5 was associated with poor prognosis in PDAC. mTOR is thought to suppress tumour growth by negatively regulating mTORC1 signalling via AMPK. Lkb1 phosphorylates and activates AMPK, which in turn negatively regulates mTORC1 signalling through activation of TSC2 and direct inhibition of the mTOR binding partner Raptor (158). Furthermore, in tumours with Lkb1 loss, mTOR may play a key role downstream of Lkb1/AMPK metabolic signalling (429). The role and importance of mTOR as Lkb1/AMPK's mediator in PDAC remains to be elucidated. The relationship between Lkb1 and mTOR protein expression was investigated initially, however this failed to reveal a significant correlation (ρ = 0.32, p = 0.45, not illustrated). Stratification by mTOR and Lkb1 expression revealed that patients with low mTOR/ high Lkb1 expression had a particularly good outcome (23.1 months, 95%CI: 17.2–29.2) compared to those with

high mTOR/ low Lkb1 expression (6.3 months, 95%CI: 2.6–9.8, p = 0.001, Log-rank test, Figure 9.5H, Table 9.2).

Consistent with a role for mTOR in the COX-2 pathway, a clear correlation was detected between mTOR and COX-2 expression ($\rho = 0.31$, $p < 0.003$) (Figure 9.5E). Furthermore, GSK3β expression correlated closely with mTOR levels ($\rho = 0.571$, $p < 0.001$) (Figure 9.5F) supporting previous evidence that Wnt signalling may stimulate the mTOR pathway via GSK3β (430).

Cellular senescence, characterised by irreversible loss of proliferative potential and a distinct morphology, can be induced by CDK inhibitors including p21. Furthermore mTOR inhibition by rapamycin has been shown to prevent permanent loss of proliferative potential in arrested cells (431). Interestingly, when p21 and mTOR expression was plotted, a correlation was detected ($\rho = 0.339$, $p < 0.001$) (Figure 9.5G). Further stratification of mTOR by p21 expression revealed low mTOR/ low p21 expression was associated with a good outcome in 24 patients (29.3 months, 95%CI: 17.4–41.1) compared to a poor outcome in 14 patients with high mTOR/ high p21 expression (8.3 months, 95%CI: 3.3–13.3, p = 0.001, Log-rank test, Table 9.2).

9.2.4 miRNA integrative analysis

9.2.4.1 Integration of genomic aberration and miRNA expression

More than half of known miRNAs have been aligned to genomic fragile sites or regions associated with cancers (432). A neuroblastoma study investigating the relationship between CNAs and miRNA expression has indicated amplification of the n-MYC transcription factor significantly affected tumour miRNA expression (433).

To determine if large-scale genomic gains and losses might impact upon miRNA expression in PDAC, gains and losses of genomic regions, as determined by aCGH, were correlated with miRNA expression for 37 patients. Overlaying miRNA positions onto CNA plots for all PDAC samples was performed to identify overlap. From general inspection of each chromosome, areas of CNA (amplification or deletion) were often associated with the position of miRNA loci (Appendix 11.7.2). The miRNAs with matched CNA are illustrated in Table 9.4. Notably, regions associated with miRNA clusters were often associated with dense CNA regions. Regarding the miRNAs identified as prognostic in Chapter 8, CNAs correlated with miR-21 and miR-30d position in addition to miR-34a (Figure 9.6A). miR-148 and miR-181 identified as differentially expressed also corresponded with regions of CNA. Other notable miRNAs, miR-10a and miR-196a, previously identified as differentially expressed and prognostic in prior studies, correlated with CNA in the current cohort.

9.2.4.2 Integration of miRNA targets with mRNA expression

Given that miRNAs can have multiple targets and that each protein-coding gene can be targeted by multiple miRNAs, it has been suggested that more than one third of human genes could be regulated by miRNAs. From this perspective, the networks of post-transcriptional regulatory relationships tend to be highly complex. While target prediction software can predict potential interactions, all are compromised by a significant fraction of false positives caused by the limited comprehension of the molecular basis of miRNA-target pairing, and also by the context dependency of post-transcriptional regulation.

Integration of miRNA target predictions and gene expression profiles using matched samples may enable a better understanding of the influence of miRNA-gene expression integration. To our knowledge, there has been no previous attempt to combine miRNA and mRNA expression in a single analysis with the goal of elucidating post-transcriptional interactions in PDAC. Using Targetscan prediction software the predicted mRNA targets of differentially expressed miRNAs (PDAC versus normal pancreas) were compared with the differential gene expression microarray (PDAC versus normal pancreas) data. As is illustrated in Figure 9.6B only approximately 10% of mRNAs predicted by Targetscan were represented in the gene expression data for both up and down-regulated gene sets. However, despite this low rate, there was considerable overlap in terms of pathway enrichment between the predicted gene target list and the true gene expression data namely TGFβ signalling, Notch signalling, Wnt signalling, ubiquitin proteolysis and MAPK signalling pathways ($p < 0.0001$, GeneGo enrichment analysis).

9.2.4.3 Investigation of potential targets of miR-21 and miR-34a in PDAC

In Chapter 6 miR-21 and miR-34a appeared to be important components in PDAC molecular biology. Data was integrated at a miRNA, protein, gene expression and copy number level, potentially exploring the role these miRNAs play in PDAC (Figure 9.1B). The biological significance of miRNA deregulation is presumed to relate to the effect of miRNAs on their cognate protein-coding gene targets. To dissect the molecular basis underlying the poor prognosis associated with over-expression of miR-21 and under-expression of miR-34a, the gene targets of these miRNAs likely involved in PDAC tumourigenesis were tested. Of the 48 patients whose tumours underwent miRNA profiling, 43 had corresponding tissue present on the TMA. The miRNA PCR expression levels were correlated with protein expression using IHC (Figure 9.7A,B [Maspin and PTEN], Figure 11.3 [p53, Bcl-2, cyclin D1]).

Firstly miR-21 targeted proteins Bcl-2, maspin and PTEN were studied. As previous studies have suggested that miR-21 regulates apoptosis in tumour cells (214), Bcl-2 expression at the protein level was correlated. These data revealed high miR-21 levels were associated with elevated Bcl-2 expression ($p = 0.003$, Figure 9.7C). A positive correlation between miR-21

expression and maspin protein expression was identified ($p < 0.001$, Figure 9.7D), whereas miR-21 expression was negatively correlated with PTEN protein expression ($p = 0.004$, Figure 9.7E). A potential mechanism for the prognostic influence of miR-21 is provided by the evidence that low PTEN protein expression is independently associated with a poor outcome when assessed in the larger cohort (n = 117) (HR: 0.58, 95%CI: 0.38-0.88, $p = 0.011$, Figure 9.7F).

Consistent with *in vitro* study evidence (434), there was an inverse association between miR-34a expression in the 43 patients and cyclin D1 protein expression potentially impacting on cell-cycle arrest (Figure 9.7G). Furthermore, it was shown that miR-34a down-regulation is associated with increased expression of Bcl-2 (Figure 9.7H).

9.2.4.4 Regulation of miR-34a expression in PDAC

As discussed earlier p53 coordinates response to cellular stresses altering target gene expression culminating in apoptosis, cell-cycle arrest and increased DNA repair. Supporting previous *in vitro* data (435), miR-34a expression was identified as significantly associating with p53 expression in human PDAC specimens (Figure 9.7I). Although loss of p53 would be expected to reduce miR-34a expression, this is unlikely to account entirely for reduced miR-34a expression, as there was not a direct correlation between complete loss of p53 and the magnitude of miR-34a down-regulation (Figure 9.7I). Therefore, other mechanisms, in addition to p53 inactivation likely contribute to the reduction of miR-34a abundance (435). Integrating the aCGH data identified loss of copy number for the miR-34a region in 15/37 specimens. Deletion of the genomic interval encompassing miR-34a (1p36) is a common feature in various malignancies (436). Previously high-resolution copy number assessment analysis of pancreatic cancer cell lines (437) demonstrated hemizygous loss of the miR-34a locus. These data therefore support the concepts that gene deletion, lack of activation by p53 and possibly other mechanisms contribute to the under-expression of miR-34a in some human PDACs (Figure 9.7J).

9.2.4.5 Gene expression profiles associated with miR-21 and miR-34a expression

To determine the effects of miR-21 and miR-34a expression on mRNA expression, gene expression profiles of PDACs with low-expression against high-expression for both miRNAs (according to median expression level) were compared. For miR-21, there was a significant difference between these groups, with up-regulation of 561 mRNA transcripts and down-regulation of 517 ($p < 0.01$, Table 11.39A). PDCD4, a miR-21 target, was notably down-regulated, while MMP7 and MMP9 were up-regulated in the high miR-21 group. For miR-34a, there was a significant difference between these groups with up-regulation of 389 mRNA transcripts and down-regulation of 318 ($p < 0.05$, Table 11.39B).

To better understand the potential global effects of miR-21 and miR-34a expression on the PDAC transcriptome, GO classifications of the up- and down-regulated genes were examined. For miR-21, over-enriched GO terms among up-regulated genes included cytoskeleton organisation ($p = 1.2x10^{-5}$), blood vessel development and angiogenesis ($p = 4.1x10^{-4}$) and regulation of apoptosis ($p = 3.1x10^{-3}$). Genes assigned to the terms MAPK signalling pathway ($p = 9.2x10^{-3}$), regulation of caspase activity ($p = 4.3x10^{-4}$) and cell-cycle ($p = 8.1x10^{-3}$) were enriched amongst down-regulated genes. For miR-34a, over-enriched GO terms among up-regulated genes included cell division ($p = 8.1x10^{-6}$), response to DNA damage ($p = 2.9x10^{-3}$) and serine/threonine kinase activity ($p = 5.1x10^{-3}$). Moreover, genes assigned to the terms wound healing ($p = 1.8x10^{-4}$), chemotaxis ($p = 1.2x10^{-4}$) and apoptosis ($p = 7.1x10^{-3}$) were enriched amongst down-regulated genes. Nonetheless, the majority of genes differently expressed between the groups are certainly not related to miR-21 or miR-34a status.

9.3 Discussion

In this chapter there has been an attempt to combine and integrate data generated within earlier chapters of the thesis. The aim was to firstly identify underlying targets that could potentially drive pancreatic cancer progression and secondly to investigate findings from earlier chapters related to PDAC tumour biology, in particular those associated with miRNAs.

Since the development of high throughput profiling technology such as aCGH, the number of studies combining CNA with gene expression data has steadily increased, however studies which include paired data from the same patient are limited. Integrated analysis of both copy number and gene expression microarray data could provide additional insight regarding the role of CNA in the pathogenesis of pancreatic cancer as shown in other cancers (438).

Tumours often harbour CNAs altering dosage of thousands of genes. However, due to tissue-specific expression or feedback regulation, expression levels of these genes may remain unaltered. Because the effects of CNAs are mediated by changes in gene expression, the subset of genes exhibiting concordant changes in both DNA copy number and gene expression (e.g. amplified and over expressed genes) are likely to be enriched for candidate oncogenes. To date, combined analysis of DNA copy number and gene expression microarrays has revealed a major and direct effect of allelic imbalance on gene expression in many cancers, including breast (439) and NSCLC (397). At a global level, 40-60% of the genes in higher-level amplifications showed elevated expression (439), while 10% of highly over expressed genes were amplified. In low level CNAs, only 10% of the genes have been reported to show concordant changes in gene expression (439).

While several software tools have been developed for copy number or gene expression analysis individually, few methods have been developed for their integration (440, 441). Integration remains challenging even when transcriptional and genomic arrays originate from

the same manufacturer. Studies have classified samples according to the presence of chromosomal abnormalities, and subsequently tested for difference in gene expression between altered and unaltered samples using a gene-wise test similar to the student's t-statistic (235, 439). Adler and co-workers used a classification approach as the first step in a stepwise linkage analysis of signatures, testing for copy number difference between groups of breast cancer samples with and without a wound expression signature (250). All solutions have limitations, and while these strategies highlight potential targets, validation is essential to confirm biological relevance.

Previously, in a PDAC cell line study investigating concordance of CNA with gene expression, 60% of genes within highly amplified genomic regions displayed associated overexpression (235). A more recent study revealed that 18% of amplified loci and 15% of individual amplifications observed contained genes demonstrating concurrent overexpression (241). This discrepancy may be explained by different tissue sources (cell lines versus tumours) with the cell line study focusing upon individual genes rather than chromosomal loci. The most frequently concordant copy number and expression changes identified in the later study were SMURF1, TRRAP (7q22.1), BCAS1 (20q13.2) and VCL (10q22.1). SMURF1 may inhibit TGFβ signalling (442) and was associated with nodal metastasis. TRRAP, a c-Myc cofactor, along with SMURF1, was shown to be amplified in PDAC cell lines (237).

Using an integrative approach a number of numerous concordantly expressed genes related to cancer were identified, many of which were novel associations for PDAC. More than one target gene was over-expressed in some amplicons in the current study, as in prior work (235, 241). Importantly, SMURF1 was identified as showing evidence of copy number gain *and* high expression levels in the studied cohort, strongly supporting a biological role in PDAC and verifying the findings of the previous study (241). Focusing on mTOR, there is increasing evidence is amassing that it plays a critical role in PDAC biology. It was demonstrated that within the studied cohort a spectrum of expression exists, with over-expression at the protein level associated independently with poor prognosis. mTOR expression has important implications beyond prognosis, potentially as a predictive marker for rapamycin related therapies (443). These data furthermore provide novel insights into the role of mTOR in pathways important in human PDAC, including Lkb1 and p21.

Although the exploratory nature of this approach is recognised, it is felt that the findings of a prognostic influence for mTOR expression in a larger TMA group at a protein level supports the hypothesis that an integrative genomic analysis can identify important gene targets in PDAC. The analysis identified other interesting candidates that may have similarly biologically significant roles in PDAC including FBI-1, DYRK1A, SIRT-2 and HNF4A, in

addition to SMURF1. FBI-1, a transcriptional repressor, is a putative oncogenic factor over-expressed in various cancer types, and was recently shown to repress transcription of the TSG ARF, leading indirectly to p53 inactivation (444). Furthermore, FBI-1 has been demonstrated to repress other p53 pathway components including p21, and has been proposed as a master regulator of this pathway (445). Ultimately, validation at the protein level along with functional validation within animal and cell based models will be necessary to confirm the influence of such targets in PDAC tumourigenesis.

The strength of the analysis in the present chapter was the availability of copy number and expression data from matched patients with the ability to correlate findings with clinical outcome. To our knowledge this is the largest cohort of individuals with PDAC to be investigated with aCGH and gene expression microarray data. The integration of these data identified novel genes which otherwise would not have been selected from analysis of either dataset alone. The use of a large TMA resource coupled with outcome data provided robust protein level validation, enabled the prognostic influence of mTOR to be evaluated and allowed the integration of expression with other components of PDAC biology.

The miRNA profiling study conducted in Chapter 6 provided a number of clinically relevant targets, in particular miR-21 and miR-34a. An attempt was made to gain further insight into the role played by these miRNAs, as well as to elucidate factors that govern their expression. These data support the suggestion that miR-21 targets genes integral to PDAC tumourigenesis including PTEN (446), loss of which in turn correlates independently with poor outcome. The prognostic influence of PTEN loss is an important finding, not previously reported, confirming that it has an integral role in human PDAC biology. Maspin has been implicated as a tumour suppressor in malignancies including prostate cancer (447), with miR-21 inhibition a potential mechanism by which invasion and metastasis is achieved (448). In contrast, maspin expression has been associated with poor outcome following PDAC resection (449). The finding of a positive correlation between maspin and miR-21 expression suggests further investigation of this relationship is also warranted. The positive association of miR-21 and Bcl-2 appears somewhat paradoxical. As demonstrated in Chapter 5, Bcl-2 expression appears to be associated with a favourable outcome. This finding is interesting and will require further consideration and investigation.

miR-34a has been demonstrated to be induced by p53 (435) and subsequently these data provide evidence supporting this finding in human PDAC. Furthermore, these results suggest that miR-34a down-regulation is associated with increased expression of cyclin D1, which adds to previous evidence that miR-34a regulates cell-cycle progression in part by targeting G1-phase regulators (434). Restoration of miR-34a in human pancreatic cells has previously been shown to inhibit Bcl-2 expression, inhibiting growth and invasion, inducing apoptosis

and G1/G2 arrest (387), a finding that these data support. However, the Bcl-2 outcome data from Chapter 5 suggest that the situation in human PDAC is more complex.

These findings of the investigation of potential mechanisms for miR-34a regulation in human PDAC are novel, interesting, and potentially provide evidence for the manipulation of this miRNA in pancreatic cancer. Integration of copy number changes with miRNA expression data confirmed findings of other cancers that areas of aberration frequently correspond to the location of miRNAs in PDAC. Further investigations are required to elucidate whether these overlaps are directly responsible for altered miRNA expression in each instance, although these data provide an important starting point.

Previous analysis of gene expression in pancreatic cell lines, according to induced miR-34a status, identified up-regulation of cell-cycle, DNA repair and mitotic checkpoint categories along with down-regulation of angiogenesis related genes (435). Although there was some overlap between the GO identified in the current study, this was certainly not complete, explained by the numerous miRNAs dysregulated in human PDAC. The role of miR-34a in apoptosis is supported by the enrichment of established anti-apoptotic factors amongst the down-regulated targets. The finding of a differential gene expression signature, according to miRNA expression, is interesting, proving utility for this method of analysis and providing insight into the broad influence of miRNAs in PDAC. Evaluation of the influence of miR-21 and miR-34a expression on gene expression signatures in cell culture and animal models will be necessary before firm conclusions are drawn.

It was hoped that integration of copy number and gene expression data might identify potential ‘driver’ genes that influence PDAC tumour biology and prognosis. As the Agilent platform was chosen to conduct genomic analysis, corresponding Agilent software (DNA analytics) had the potential ability to undertake integration analysis. However, the software enabled only integration of two-colour gene expression files with aCGH data. As the gene expression data had been collected on the Agilent one colour platform, this hampered further integration analysis, forcing us to identify other solutions. This was provided by the open source R programming language based program BRB-ArrayTools (255) and the Correlate analysis tool (359).

Small cohort size was a significant limitation to this strategy as has been highlighted elsewhere in this thesis. While the correlation coefficients between CNA and gene expression targets were not especially strong, it is believed that this strategy is sound and unbiased, but would benefit from a larger study group. In an attempt to identify the most potentially critical targets, further stringent cut-offs were applied.

The true worth of this approach in terms of discovery of novel critical genes in PDAC will only be known when further investigation and validation of the targets is performed at a

protein level for HNF4A, FBI-1, SIRT2, DYRK1A, SMURF1 and others, as has been performed for mTOR. While this approach can lead to discovery of critical genes, which may be novel, it should be noted that certain genomic events do not directly translate into gene expression changes. Therefore, when integrating such datasets it should be remembered that RNA and subsequent protein expressions are often also subjected to complex post-transcriptional regulation, including the effects of miRNAs.

For the investigation of miRNA targets, further functional validation including silencing of miRNA expression followed by re-expression within a cell model will be necessary in order to confirm these downstream effects.

9.3.1 Summary

In this chapter, integration of the component findings from earlier chapters of the thesis, including gene expression and aCGH data, to identify genes with novel key regulatory functions in PDAC tumourigenesis, has been performed. There was successful identification of mTOR gene expression correlating with copy number status, and mTOR protein expression associating with outcome in the validation TMA set. Furthermore, a number of cancer related genes have been identified, not previously investigated in PDAC for which CN and gene expression are associated. Subsequent studies should investigate the functional role of these gene targets in PDAC, including FBI-1 and SMURF1. Finally, the integration of miRNA data with other genomic data and protein expression data was investigated, highlighting regulatory influences and down-stream targets of miR-21 and miR-34a in human PDAC.

Table 9.1 Genes with a significant correlation between expression and copy number

The following gene targets showed evidence of gene expression correlating with copy number change. Chromosomal location is shown along with whether the gene has previously been implicated in cancer, has been shown to have prognostic utility, or has been associated with PDAC previously in the literature.

Gene target	Chromosomal location	Implicated in cancer	Prognostic utility in cancer	Previously implicated in PDAC
BVES	6q21	Yes	N/A	No
DYRK1A	21q22.13	Yes	N/A	No
FBI-1	19p13.3	Yes	Yes	No
GATA6	18q11.2	Yes	Yes	Yes
GPC5	13q32	Yes	Yes	No
HINT2	9p13.3	Yes	N/A	No
HNF4A	20q13.12	Yes	Yes	Yes
mTOR	1p36.2	Yes	Yes	Yes
N-Cor	17p11.2	Yes	Yes	No
NFκB	4q24	Yes	Yes	Yes
ROCK1	18q11.1	Yes	Yes	Yes
ROR2	9q22	Yes	Yes`	No
SIRT2	19q13	Yes	Yes	No
SIRT6	19p13.3	Yes	N/A	No
SMURF1	7q21.3	Yes	Yes	Yes
WISP3	6q21	Yes	Yes	No
WNT7B	22q13	Yes	N/A	No

N/A – not yet assessed

Table 9.2 Univariate survival analysis for mTOR expression

*Prognostic influence of **A)** mTOR expression, **B)** mTOR expression stratified by Lkb1 expression, **C)** mTOR expression stratified by p21 expression at the protein level as assessed by IHC.*

		Overall Survival			
		Patients N = 119 (%)	**Median (months)**	**95% (CI)**	**p value [a]**
A					
mTOR	Low	98 (27.7)	19.6	14.8 - 24.4	0.003
	High	21 (82.3)	11.6	7.3 - 15.9	
B					
mTOR/ Lkb1	Low/High	77 (64.7)	23.1	17.2 - 29.2	0.020
	Low/Low	21 (17.6)	13.5	12.5 - 14.5	
	High/High	15 (12.6)	13.9	7.8 - 20.0	0.047
	High/Low	8 (6.7)	6.3	2.6 - 9.8	
C					
mTOR/ p21	Low/High	24 (20.2)	29.3	17.4 - 41.1	0.019
	Low/Low	74 (62.2)	17.8	14.3 - 21.4	
	High/High	7 (5.8)	18.0	9.9 - 26.0	0.020
	High/Low	14 (11.7)	8.3	3.3 - 13.3	

[a] p value according to Log-rank test

[b] For for mTOR/ Lkb1 Low/High versus High/Low $p < 0.0001$

[c] For for mTOR/ p21 Low/High versus High/Low $p < 0.0001$

Table 9.3 Multivariate Cox regression survival analysis according to mTOR expression

mTOR protein expression assessed in the TMA with clinicopathological parameters including overall survival for 119 patients undergoing resection for PDAC.

		Overall survival	
Prognostic factor	**Category**	**HR (95% CI)**	**p value**
Tumour stage	T2/ T3	2.16 (1.07 - 4.28)	0.043
Tumour size (mm)	< 30/ ≥ 30	1.58 (1.05 - 2.44)	0.031
Lymph node status	Absent/ Present	1.70 (0.89 - 3.25)	0.101
Margin involvement	R0/ R1	2.19 (1.29 - 3.74)	0.004
Tumour grade	Low/ High	2.18 (1.35 - 3.48)	0.001
Peripancreatic fat invasion	Absent/ Present	1.68 (1.05 - 2.70)	0.031
Perineural invasion	Absent/ Present	0.82 (0.29 - 1.74)	0.679
Venous invasion	Absent/ Present	1.28 (0.86 - 1.99)	0.267
mTOR (Cytoplasm)	**Low/ High**	**1.77 (1.06 - 2.99)**	**0.032**

Table 9.4 Correlation of copy number aberration with microRNA expression

Chromosome Position	Copy Number Aberration	miRNA
1q36	Loss	**miR-34a**
2q35	Loss	miR-26b, miR-375, miR-153-1
2q37.1	Loss	miR-1244, miR-1471, miR-562
3p21.31	Gain	miR-1226, miR-495, miR-566
3q29	Loss	miR-570
3q27.1	Loss	miR-1224
5q31.2	Gain	miR-1289-2, miR-874, miR-866
5q35.2	Loss	miR-1271, miR-341, miR-1229
6p21.33	Gain	miR-877, miR-1236, miR-1275, miR-219
6q13	Loss	miR-30a-2
7p22.1	Loss	miR-589, miR-584, miR-906b, miR-206, miR-335
8p11.21	Loss	miR-486
8q24.22	Loss	miR-30b, **miR-30d**
9p21.3	Loss	miR-491, miR-31
9p21.1	Loss	miR-878
9q22.32	Loss	Let-7b, miR-23b
9q34.11	Loss	miR-199b, miR-219-2
10q24.32	Gain	miR-608, miR-146b, miR-1307
11q12.3-11q13.4	Gain	miR-1237, miR-19a-2, miR-612
12q13.12–12q14.1	Loss	miR-1291, miR-1293, **miR-196a-2**, **miR-148b**, miR-1228, miR-616, miR-
13q21.1	Loss	miR-1297
14q32.32	Loss	miR-203, miR-1247, miR-345, miR-496, miR-377, miR-541, miR-409, miR-412, miR-410
15q15.1	Loss	miR-626, miR-1282, miR-627
15q22.31	Loss	miR-1272
16q21	Loss	miR-138
16q13.13	Gain	miR-548b
16q13.12	Gain	miR-484, miR-193b, miR-365-1 and miR-1972
16q22.1	Loss	miR-1538, miR-1972, miR-140
17q23.2	Gain	miR-142, miR-301, miR-454, **miR-21**
17q21.32	Loss	**miR-10a, miR-196a-1**
17q11.2	Loss	miR-1288, miR-33b, miR-1180
18q12.2	Gain	miR-187
19q13.2	Loss	miR-1181, miR-1238, miR-638, miR-199a-1
19q13.12	Gain	miR-24-2, miR-27a, miR-23a, **miR-181c**, **miR-181d**
19q13.33	Loss	miR-220 and miR-150
19q13.42	Gain	Multiple miRNAs
20q13.13	Gain	miR-1259
20q11.22	Gain	miR-1825, miR-644, miR-1289-1, miR-499
21q21.1	Loss	miR-99a, let-7c
22q13.2	Loss	miR-1281, miR-33a
22q11.22	Loss	miR-650

microRNA in Bold – identified as differentially expressed in previous chapter

microRNA in Red – identified as differentially expressed in prior literature

Figure 9.2 Integration of gene expression with copy number aberrations

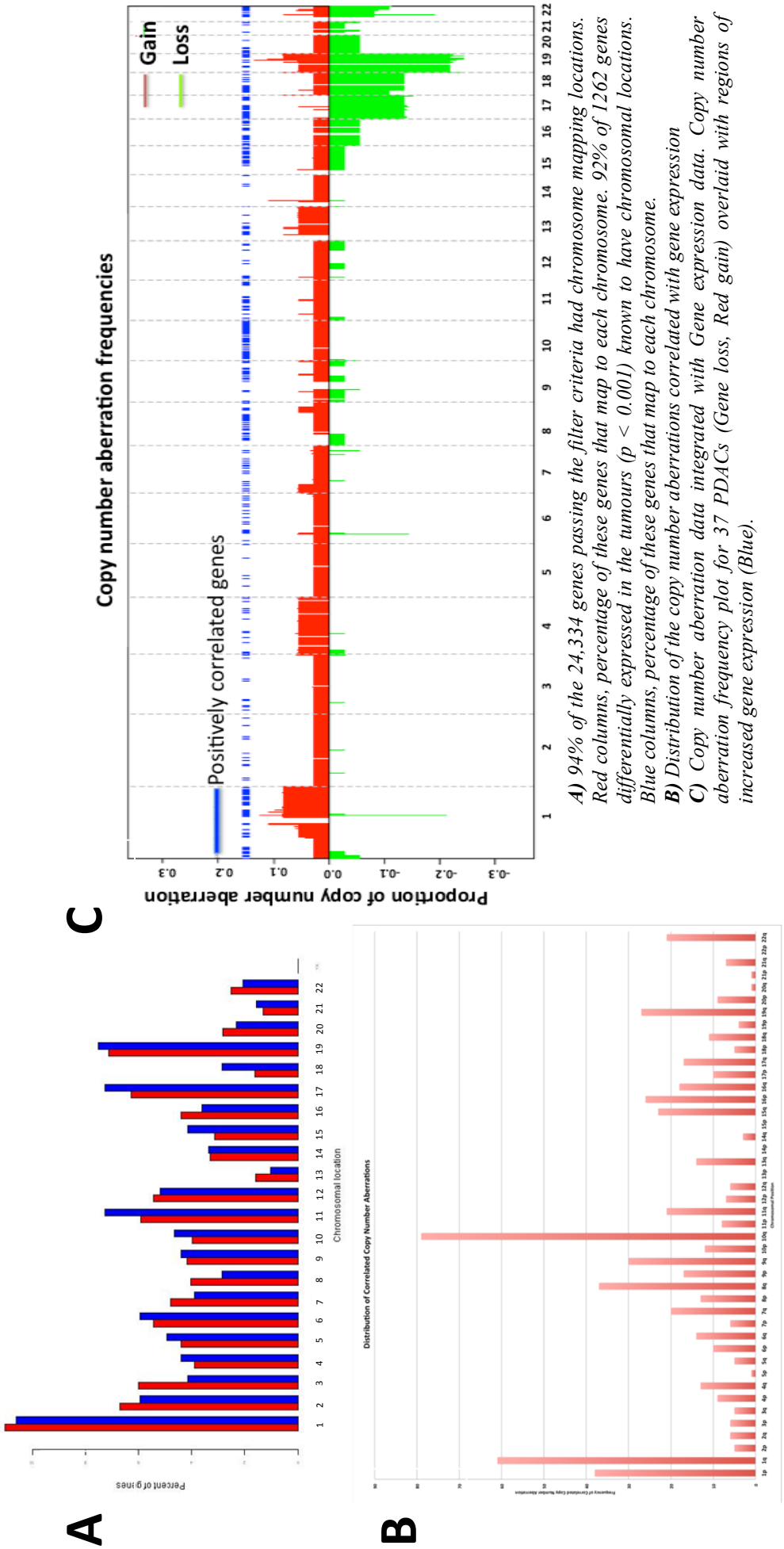

A) 94% of the 24,334 genes passing the filter criteria had chromosome mapping locations. Red columns, percentage of these genes that map to each chromosome. 92% of 1262 genes differentially expressed in the tumours ($p < 0.001$) known to have chromosomal locations. Blue columns, percentage of these genes that map to each chromosome.
***B)** Distribution of the copy number aberrations correlated with gene expression*
***C)** Copy number aberration data integrated with Gene expression data. Copy number aberration frequency plot for 37 PDACs (Gene loss, Red gain) overlaid with regions of increased gene expression (Blue).*

Figure 9.3 Correlation between copy number aberration and gene expression in PDAC

Scatter plot shows correlation between copy number changes (y-axis) and gene expression levels (x-axis represents gene expression fold change) of individual genes within regions with genomic gains. Five genes (mTOR, FBI-1, HNF4A, SIRT2 and DYRK1A) fulfilled the most stringent criteria (log_2 ratio > 0.3 [equals gain] and expression fold-change > 5.0). mTOR was subsequently taken forward for validation at the protein level.

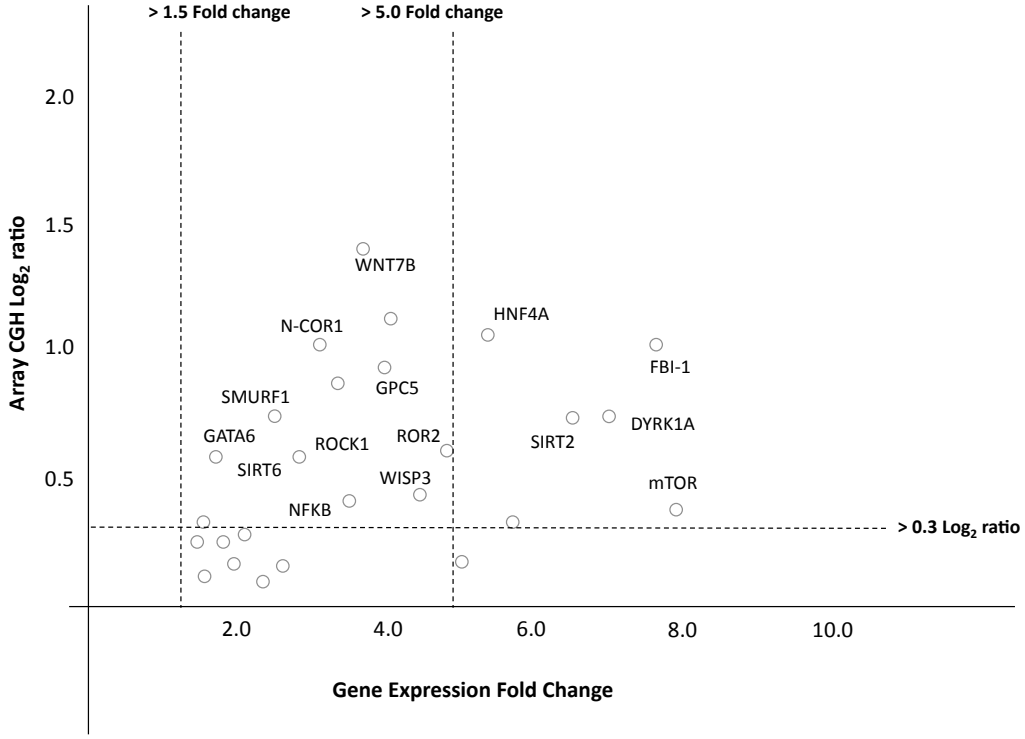

Figure 9.4 Networks generated from genomic integration derived gene list

A) *Top scoring interaction network of genes with highly correlated copy number and expression change indicating that HNF4A is strongly interconnected (correlated genes highlighted by).*

B) *Focus upon FBI-1, N-COR, HNF4A, which appear to interact with the transcription factor SP1.*

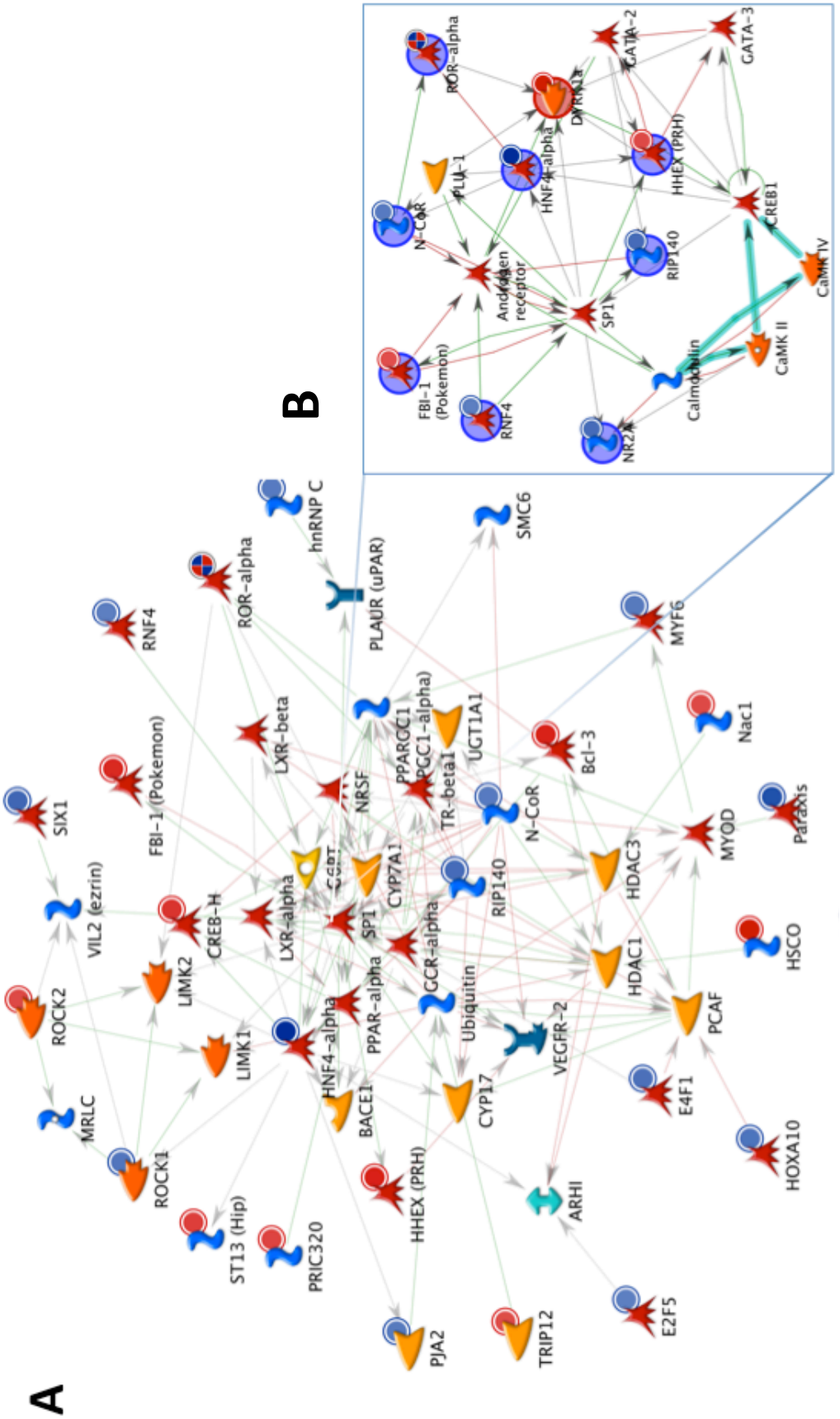

Figure 9.4

C) *HNF4A and DYRK1a (highlighted in orange) are clearly linked to many dysregulated genes as well as Notch and Ras.*

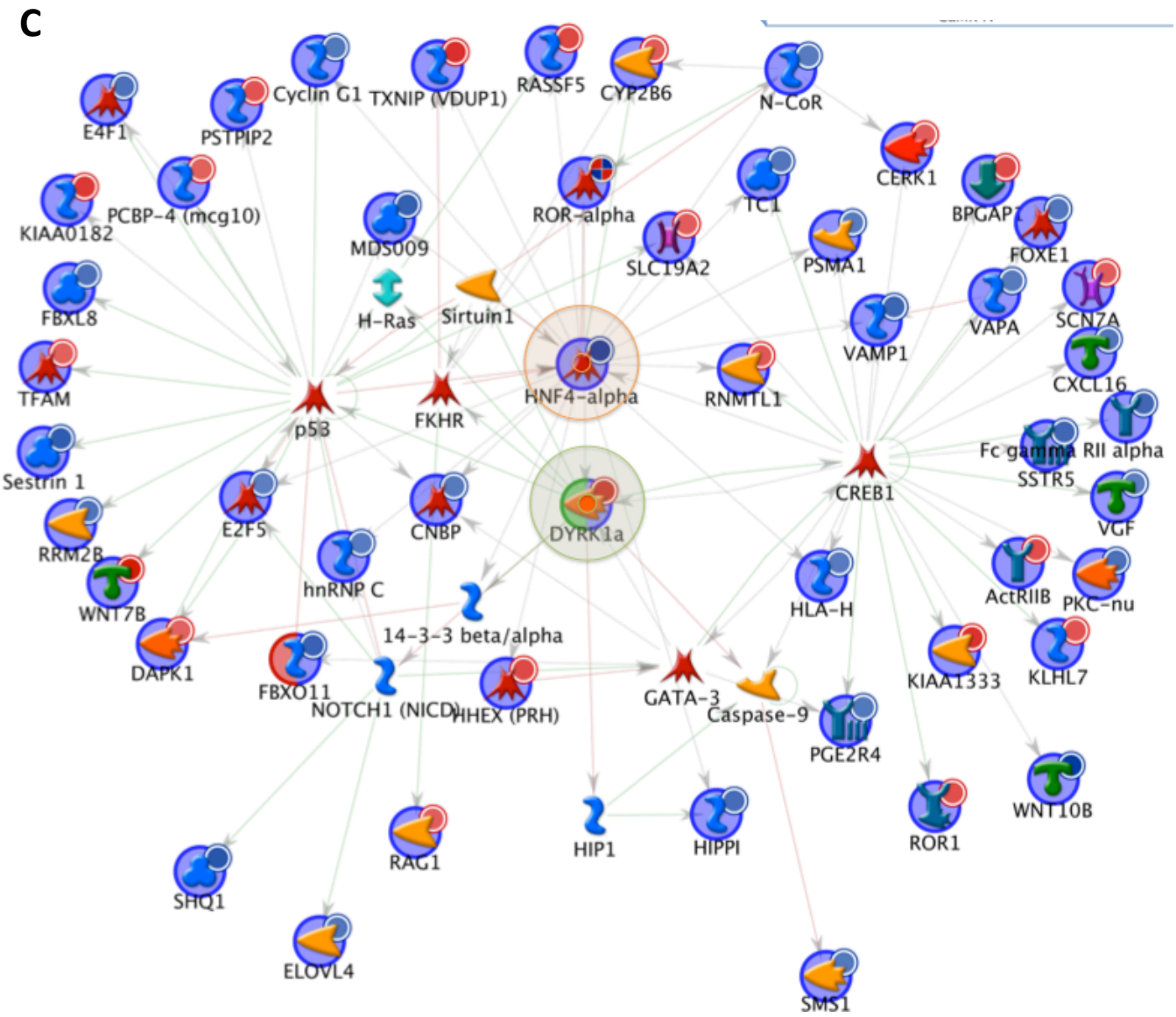

Figure 9.5 mTOR: clinicopathological association

A) *Representative immunostaining of mTOR in PDAC TMA: illustrating no staining, low, moderate and strong staining. Epithelial cytoplasmic staining was evaluated for this analysis.*

B) *Correlation between mTOR DNA copy number and its mRNA expression in 37 PDAC specimens (Spearman's rho (ρ) correlation coefficient = 0.391, p = 0.001).*

C) *Box plot indicating that tumours from patients with more than 50% lymph node involvement have increased levels of mTOR (median histoscore 235) in comparison to those with no lymph node involvement (median histoscore 181) (p = 0.005) and those with less than 50% lymph node positivity (median histoscore 207) following resection (p = 0.01, Mann-Whitney U test).*

D) *Kaplan-Meier analysis indicates that patients with high mTOR expression (n = 21) (median 19.6 months) have a poorer outcome than those with low expression (n = 98) (median 11.5 months) following tumour resection (Log-rank test, p = 0.003).*

Spearman's correlation indicating positive correlations between mTOR cytoplasmic levels and cytoplasmic levels of ***E)*** *GSK3β* ***F)*** *COX-2 and* ***G)*** *p21.*

H) *Kaplan-Meier analysis indicates that patients with low mTOR expression and high Lkb1 expression (n = 77) have a more favourable outcome than those with high mTOR expression and low Lkb1 expression (n = 8) following tumour resection (Log-rank test, p = 0.005).*

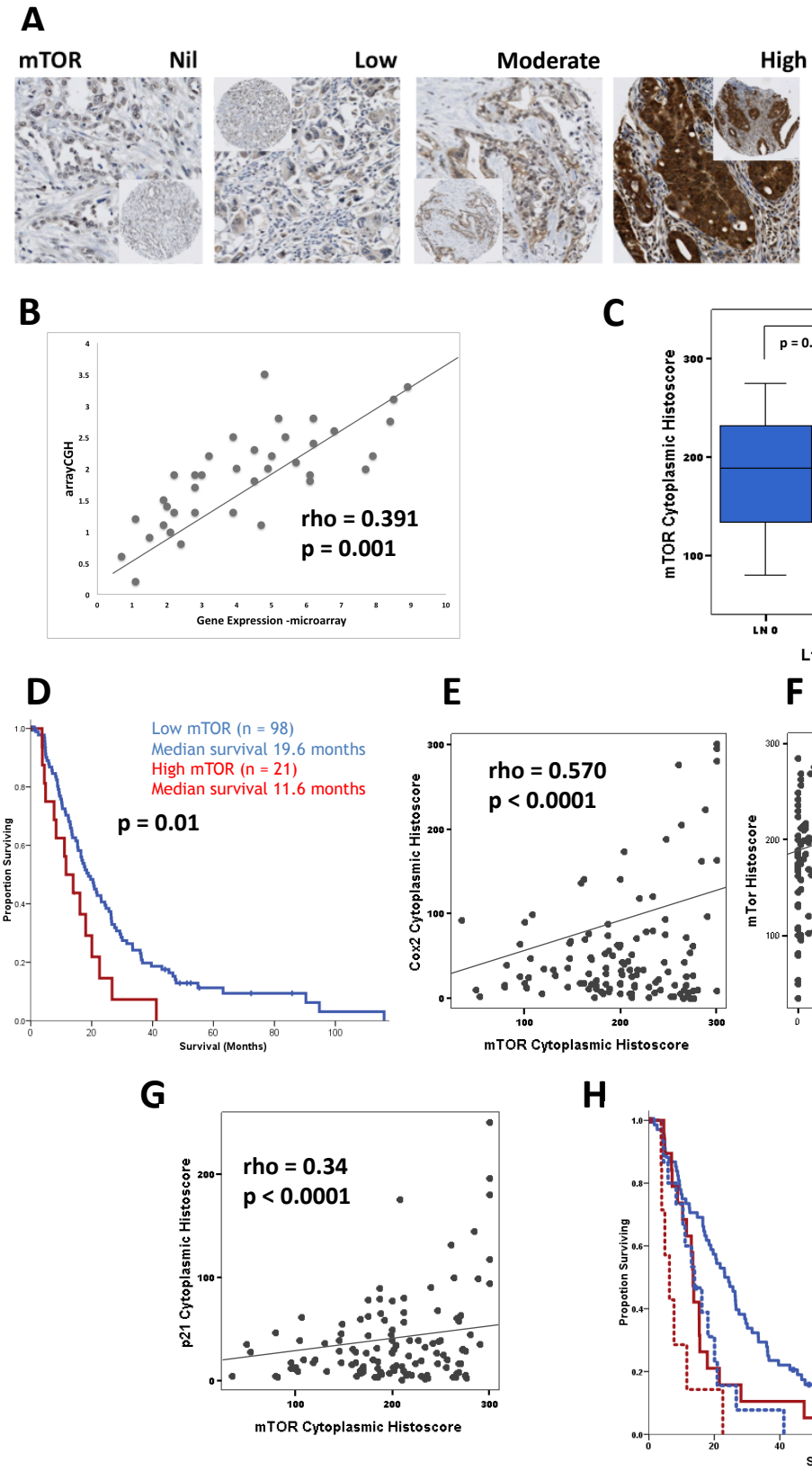
A
mTOR
Nil
Low
Moderate
High
B
arrayCGH
Gene Expression -microarray
rho = 0.391
p = 0.001
C
p = 0.005
p = 0.01
mTOR Cytoplasmic Histoscore
LN 0
LN < 50%
LN > 50%
Lymph Node Ratio
D
Low mTOR (n = 98)
Median survival 19.6 months
High mTOR (n = 21)
Median survival 11.6 months
p = 0.01
Proportion Surviving
Survival (Months)
E
rho = 0.570
p < 0.0001
Cox2 Cytoplasmic Histoscore
mTOR Cytoplasmic Histoscore
F
rho = 0.31
p = 0.003
mTor Histoscore
GSK3 Histoscore
G
rho = 0.34
p < 0.0001
p21 Cytoplasmic Histoscore
mTOR Cytoplasmic Histoscore
H
Low mTOR, High Lkb1
Low mTOR, Low Lkb1
High mTOR, High Lkb1
High mTOR, Low Lkb1
p = 0.005
Propotion Surviving
Survival (Months)

Figure 9.6 Integration of miRNA expression with copy number and gene expression data

A) *This figure illustrates copy number aberrations for all 45 patients for which aCGH copy number data (y-axis) was available overlaid on chromosomal location (x-axis) including the location of various miRNAs. Each colour represents an individual patient, with aberrations represented by a series of peaks as well as horizontal coloured bars. Areas of dense colouration represent overlap of copy number aberration shared between individual tumours. For miR-21 and miR-30d positions are highlighted in red. The overlap of other miRNAs of interest is illustrated in the supplementary data.*

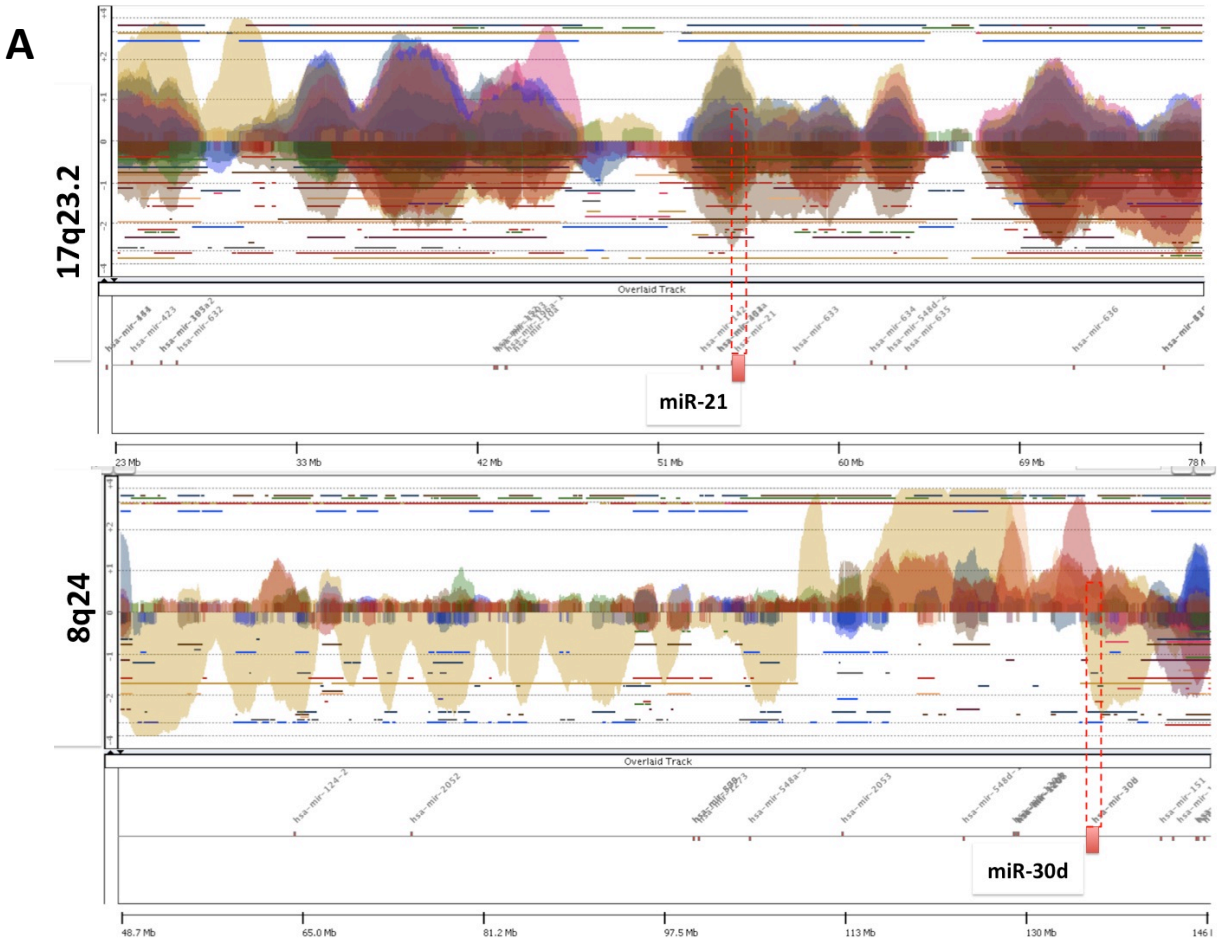

Figure 9.6

B) *mRNA and miRNA integration in a matched comparison of PDAC tumours. Comparison was performed of the* ***predicted*** *gene targets (generated by Targetscan software) of the differentially expressed miRNAs (green circle – down regulated miRNA targets and Red circle – up regulated miRNA targets) with genes* ***differentially*** *expressed according to gene expression microarray analysis (orange circle). Only approximately 10% overlap was achieved in terms of genes targets. However, pathway enrichment for the overlapping genes was significantly enriched for TGFβ signalling, Notch signalling, Wnt signalling, Ubiquitin proteolysis and MAPK signalling pathways known to be important in PDAC ($p < 0.0001$, GeneGo comparison analysis).*

B

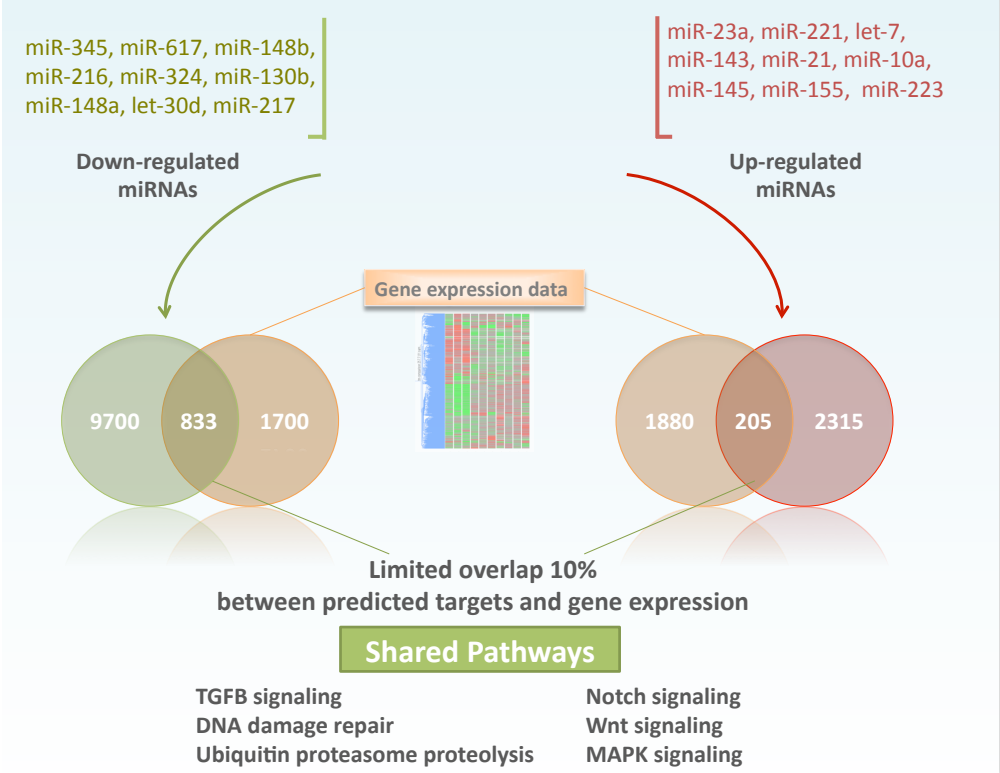

Figure 9.7 Investigation of gene targets of miR-21 and miR-34a in human PDAC

*Representative immunostaining of **A)** maspin in PDAC TMA: illustrating no staining, low, moderate and strong staining. Epithelial cytoplasmic staining was evaluated for this analysis. Representative immunostaining of **B)** PTEN in PDAC TMA: illustrating no staining, low, moderate and strong staining. Epithelial cytoplasmic staining was evaluated for this analysis.*

***C - E)** Correlation plots of RT-PCR miR-21 expression (relative expression) versus cytoplasmic Bcl-2 protein expression (Spearman's ρ correlation coefficient = 0.411, $p = 0.003$), cytoplasmic maspin expression (Spearman's $\rho = 0.653$, $p < 0.001$) and cytoplasmic PTEN expression (Spearman's $\rho = 0.43$, $p = 0.004$) ($n = 43$). IHC assessed using a semi-continuous histoscore.*

***F)** Kaplan-Meier analysis illustrating that patients with low PTEN have poorer outcome ($n = 38$, 13.0 months) compared to those with medium PTEN expression ($n = 41$, 16.7 months) and high PTEN expression ($n = 38$, 26.6 months) following pancreaticoduodenectomy (Log-rank test, $p = 0.01$). The cohort was divided into tertiles according to the cytoplasmic PTEN histoscore.*

***G - H)** Correlation plots of miR-34a expression with histoscore cytoplasmic Bcl-2 protein expression (Spearman's $\rho = -0.496$, $p = 0.001$) and histoscore nuclear cyclin D1 protein expression (Spearman's $\rho = -0.293$, $p = 0.043$) ($n = 43$).*

***I)** Correlation of histoscore nuclear p53 protein expression with miR-34a expression (Spearman's $\rho = 0.392$, $p = 0.01$) ($n = 43$).*

***J)** Proposed factors regulating miR-34a expression in human PDAC.*

Figure 9.7

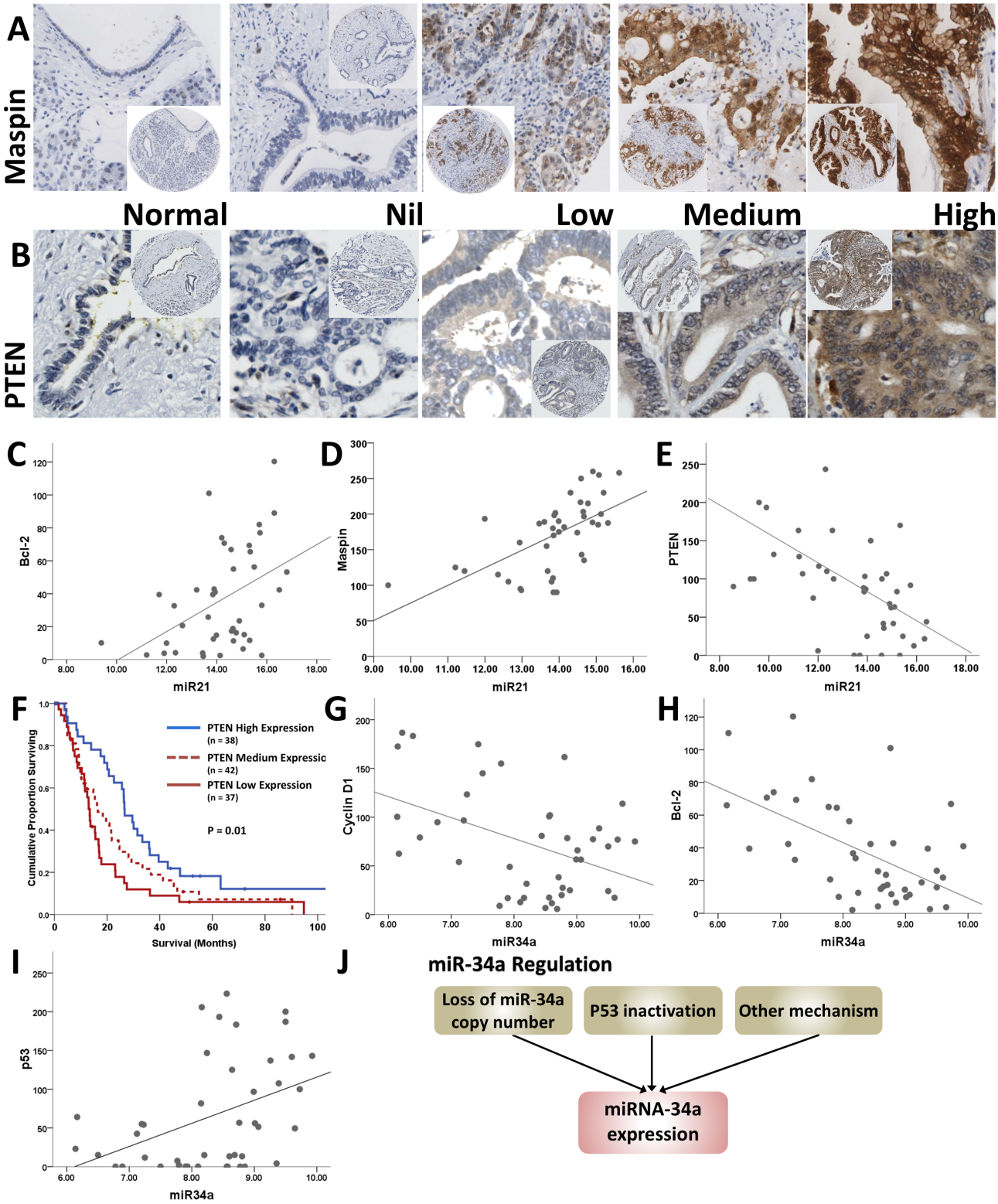
A
Maspin
Normal
Nil
Low
Medium
High
B
PTEN
C
Bcl-2
miR21
D
Maspin
miR21
E
PTEN
miR21
F
Cumulative Proportion Surviving
Survival (Months)
PTEN High Expression (n = 38)
PTEN Medium Expressio (n = 42)
PTEN Low Expression (n = 37)
P = 0.01
G
Cyclin D1
miR34a
H
Bcl-2
miR34a
I
p53
miR34a
J
miR-34a Regulation
Loss of miR-34a copy number
P53 inactivation
Other mechanism
miRNA-34a expression

10 Overall Discussion and Conclusion

10.1 Thesis summary

The present thesis investigates a number of approaches to the enhancement of the prediction of prognosis for patients undergoing resection for PDAC. Before any novel molecular aspects of prognostication can be assessed, the established clinical and pathological factors should be rigorously tested. This was performed in Chapter 3 that focused firstly on resection margin involvement, a factor for which the reported frequency varies considerably in the literature. The pathological staging criteria for PDAC were further refined by analysis of the prognostic influence of fat invasion on outcome in Chapter 4. IHC molecular prognostic candidates were reviewed in Chapter 5 with validation for a number of these candidate markers performed in the studied cohort and combined in an attempt to develop a multi-marker IHC prognostic signature. In the second half of the thesis, gene expression microarray analysis was applied to perform genome-wide profiling of 48 PDAC tumours, identifying genes related to pathological features and with survival as presented in Chapter 6. The prognostic gene signature obtained was subsequently independently validated in a further cohort. miRNA microarray profiling was performed in Chapter 7 and identified novel associations with tumour pathology in addition to prognostic associations. In Chapter 8 aCGH analysis was used to profile the genomic aberrations of the cohort, which were then associated with clinicopathological factors. Integration of the genomic technologies was outlined in Chapter 9 identifying genes for which expression correlated with genomic aberrations, highlighting potentially important genes involved in PDAC tumour biology. Figure 10.1 provides a summary diagram of the project with the key findings highlighted.

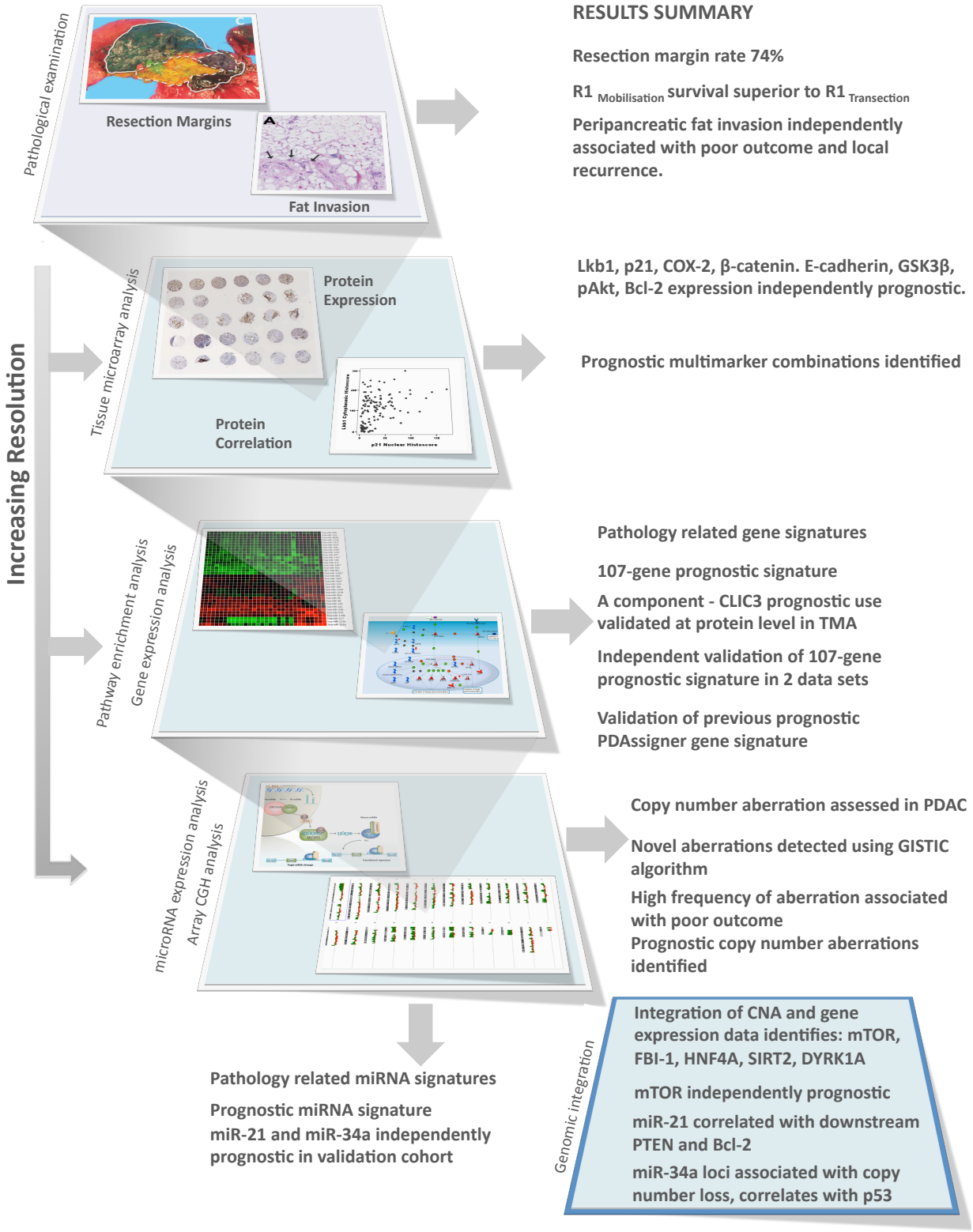

Figure 10.1 Summary of project: hierarchical approach to prognostication

An attempt has been made to enhance traditional pathological variables, initially by rigorous assessment. Focussing on individual protein biomarkers, prognosis was then assessed with IHC. Clinicopathological associations and outcome prediction based on gene expression level was carried out, with further focus towards the investigation of the prognostic influence of miRNA expression and copy number. Finally integration of copy number and gene expression patterns to identify potentially important regulatory targets in PDAC was performed.

10.2 Final discussion

Sir William Osler (1849-1919) anticipated the concept of personalised medicine when he recognised:

> "*Variability is the law of life, and as no two faces are the same, so no two bodies are alike, and no two individuals react alike and behave alike under abnormal conditions we know as disease"*

PDAC represents a dilemma, remaining a devastating disease with few long-term survivors despite great efforts from the surgical and oncological community over the last 50 years. PD remains the standard therapy for patients with resectable disease (1), however despite optimisation of operative technique and post-operative management, complications affect up to 60% (451), and resection still harbours a perioperative mortality rate of 2-6% (452). Overall median survival following resection, remains at best 23 months, despite adjuvant therapy and therefore caution must be exercised when selecting candidates for surgical resection. Conventional cancer staging has been based upon a combination of pathological factors, many which are subjective by their nature (degree of differentiation) or difficult to assess with confidence (venous invasion). This system has proven useful for decades and is the basis of current clinical practice. Current thinking dictates that PDAC is managed simply as non-resectable or resectable, however the evidence suggests that the situation is far more complex. The early recurrence to which many patients succumb following resection underlines that PDAC represents a spectrum of disease that is not adequately described by current clinicopathological staging (450).

The resection margin involvement rate of over 70% suggests that PDAC is in essence a systemic disease from the time of presentation in almost all patients with the diffuse infiltrative nature of the disease generating a tremendous challenge. Chapter 3 highlighted the importance of a rigorous systematic pathological examination with a proposed redefinition of the resection margin status, the first novel outcome of the thesis. Based on the innovative concept of embryologically derived ($R1_{Mobilisation}$) versus surgically created ($R1_{Transection}$) margins, it was demonstrated that the former group experienced a significantly prolonged survival following resection and it can therefore be concluded that in PDAC, not all positive margins are of equal prognostic significance. This important pathological information may impact the individualisation of adjuvant therapy. Despite detailed investigation of the prognostic influence of individual margin involvement, the prognostic relevance of minimal distance of resection margin clearance warrants analysis in an extended dataset to determine the optimum cut-off point for margin positivity potentially for each of the resection margins. This would be a further important step towards the standardisation of pancreatic specimen pathology reporting.

Related to this concept, Chapter 4 illustrated a further observation that peripancreatic fat invasion by PDAC, considered in current staging systems to promote disease from T2 to T3, provided independent prognostic information. Furthermore, although resection margin status failed to predict the site of recurrence, the presence of pancreatic fat invasion was associated with local recurrence. If true effects of adjuvant therapy are to be resolved, these findings highlight the importance of adequately controlling for such pathological factors prior to the allocation of adjuvant treatment in randomised controlled trials.

Review of the substantial prognostic IHC literature revealed that translational success is lacking in PDAC (299). The paucity of clinically useful prognostic molecular biomarkers may result from inadequate methodology, limited cohort size or flawed analyses. Numerous potential candidate markers were identified, for which the prognostic utility was validated in the TMA cohort in Chapter 5. In this section an attempt was made to combine the expression of markers within a multi-marker analysis, initially for all markers, then based on functional groupings. Application of this methodology is again novel in PDAC and successfully identified a cluster of patients with good outcome. This reinforced the concept that pathway analysis and molecular signatures may provide additional prognostic utility compared to single markers alone in the inherently complex system of cancer. Strong evidence that loss of E-cadherin expression, high COX-2 expression and high pAkt expression are associated with poor prognosis was provided and moreover demonstrated for the first time in PDAC that loss of Lkb1, alone and in combination with p21 expression was associated with a very poor outcome. Following potential enhancement to outcome stratification by integrating IHC marker expression in resected specimens, further investigation of the utility of the prognostic markers in preoperatively collected EUS-FNA cytology samples will be performed in future work including evaluation of Lkb1, E-cadherin, COX-2 and pAkt expression.

A genome wide approach was subsequently applied in an effort to identify novel molecular targets related to PDAC behaviour, with gene expression microarray profiling of the studied cohort presented in Chapter 6. The identification of variation in gene expression patterns according to clinicopathological factors was successful. While previously performed in other cancer types, this depth of analysis was novel for PDAC at the commencement of this project. Furthermore, as initially was proposed, a gene expression profile was developed that was able to describe groups of patients with good and poor survival, independent of the established pathological features previously described. The analysis was extended by successfully confirming the prognostic utility of an individual component of the signature, the chloride ion transporter CLIC3, at a protein level in the TMA cohort. This important role for CLIC3 in PDAC was a further novel discovery resulting from this thesis. It is planned to

undertake functional validation of this molecule within a pancreatic cancer cell line model in an attempt to determine the mechanisms by which expression translates to clinical behaviour. It is putatively involved with cell invasion through association with cytoskeletal actin (453). Crucially, validation of the 107-gene survival profile was successful within an independent PDAC cohort.

This work has provided evidence that in PDAC, despite a relatively narrow spectrum of survival outcomes following resection, prognostic signatures can be developed, at a protein and gene expression level. This is only the first step, as a considerable gap exists in terms of prognostic signature development for PDAC compared with other malignancies (370). Successful validation of the prognostic gene signature within an independent cohort is certainly encouraging. Subsequently, the previously developed PDAssigner signature (348) not only subtyped the patients but also demonstrated prognostic value in the studied cohort, delivering further evidence supporting prognostic signatures in PDAC. It was noted that limited gene overlap existed between the profiles. However, it may be that a core 'super-group' of shared genes govern the aggressive behaviour of PDAC and the overlapping genes provide an important avenue for investigation. It was interesting to note that one of the shared genes, Twist1, as discussed earlier, is a component of the EMT grouping and is capable of suppressing E-cadherin expression (149, 150). Potentially, Twist1 may be key in relating the poor prognosis gene-expression signature identified in Chapter 6 with the deleterious outcome associated with loss of E-cadherin demonstrated in Chapter 5. However, whether increased Twist1 expression is the cause or a consequence of reduced E-cadherin in PDAC, as demonstrated in a murine model of breast cancer metastasis, would require further investigation (454). Previous investigation of Twist1 expression in human PDAC revealed minimal protein expression (149), but demonstrated that expression was strongly linked to tumour cell hypoxia. Certainly, assessment of Twist1 expression in this human PDAC cohort, invasion and motility assays and investigation of its ability to suppress E-cadherin is warranted.

The generated prognostic gene expression profile was relatively large (107 genes), and future analysis will likely focus on refining it. CLIC3 was a component of the novel gene survival profile and therefore further steps will include validation of additional high-ranking components of the prognostic signature including SELENBP1, TGM2, NT5E and DUSP5, at a protein level within an extended TMA cohort to determine if they can stratify outcome. Furthermore functional validation of targets not previously investigated in pancreatic cancer is planned. It should be noted that while a signature of genes can yield prognostic value, there is no guarantee that the components will provide such useful information individually.

The miRNAome expression profile of the resected PDAC cohort in Chapter 7 identified a reassuringly similar signature to that described previously (220), despite differences in experimental and analysis techniques. This highlights the utility of miRNAs as a cancer-profiling tool and emphasises their potential importance as prognostic biomarkers. The findings of previous reports that proposed miR-21 to have prognostic utility were confirmed and furthermore novel roles for a number of miRNAs in PDAC were identified. In particular, the novel finding that loss of miR-34a expression was associated with poor outcome in this cohort was important. It is intended therefore to extend the investigation of this critical target. The expression of miR-34a in a PDAC cell model will be manipulated to assess the impact on cell behaviour and down-stream targets. Furthermore, evaluation of miR-34a will be extended to a larger TMA cohort using in-situ hybridisation. Unfortunately, attempts at validation of the miRNA signature in a further dataset were not possible, as no such dataset is currently available. As was emphasised, it is the robustness of measurement and lack of degradation of miRNAs, which lends to their usefulness. Of interest, further miRNA microarray profiling on FFPE samples matched to the fresh frozen cohort was undertaken. This provided similar profiles (data not shown), although with reduced intensity and supports the pursuit of paraffin and cytology based miRNA evaluation.

The prognostic utilities of CNAs were investigated in Chapter 8. At the time, this aCGH assessment was of an unmatched resolution in PDAC, and employed analysis techniques novel for pancreatic cancer, including the GISTIC algorithm. The expected pattern of chromosomal aberration in PDAC was confirmed and, subsequently, numerous novel CNAs were identified. Of note it was demonstrated that a high frequency of CNA was associated with a poor prognosis. The GISTIC algorithm was subsequently applied to a further cohort of PDAC patients, however a lack of outcome data limited the ability to validate prognostic regions. It should be noted that validation experiments for the targets identified by aCGH, in particular fluorescent in situ hybridization, are necessary to confirm these findings.

Integration of CNA and gene expression data was performed in Chapter 9 to identify over-expressed genes that were concordantly amplified, potentially representing fundamental regulator genes. While the categorical identification of regulatory genes that influence PDAC progression was not successful, the identification of a number of genes with a positive gene dosage relationship was achieved. A notable correlated target was mTOR, expression of which was found to be prognostic at a protein level in the TMA cohort. Further interrogation of other genes with correlative gene dosage including FBI-1, SIRT2 and HNF4a will form the basis of future projects to determine the clinical impact of targets identified by integration of copy number and gene expression, as was performed for mTOR. The relationship of miR-21 and miR-34a expression and potential protein targets and

regulators was subsequently investigated. This provided unique insight into human PDAC, suggesting miR-21 correlates inversely with PTEN expression at the protein level, while miR-34a related inversely to p53. Integration of miRNA with mRNA data is still at an early stage, however enrichment for biologically plausible downstream targets of both miR-21 and miR-34a was demonstrated. Further bioinformatic enhancements may well yield further information from this important dataset.

10.2.1 Implications for staging and management algorithms

Conventionally, prognostic gene expression signatures developed from the study of cancer patients undergoing standard treatment can be used to identify patients with a poor prognosis, who may require more aggressive treatment (5). It is anatomical, not molecular features that currently determine PDAC resectability and the decision to administer neoadjuvant and adjuvant therapy. Improvements in the selection algorithm for therapy are mandatory if there is to be improvement in outcome and quality of life for these patients.

When validated, the use of prognostic markers or signatures may allow redefinition of this paradigm, supplementing current pathological staging criteria and guiding personalised treatment decisions for individual patients. This may result, for example, in neoadjuvant therapy being offered according to biological considerations, in addition to anatomical criteria of resectability, maximising benefits associated with treatment, prolonging survival and benefitting quality of life by avoiding the morbidity of resection in those unlikely to derive benefit.

Gene expression signatures offer potential for the optimisation of management decisions of individual cancer patients. However, the intrinsic complexity of cancer biology, the difficulties associated with high-dimensional data analysis and the lack of focus in the development and validation of prognostic signatures have generated formidable challenges in the move towards more predictive and prognostic surgical oncology. Prognostic signatures must be constructed and validated with particular attention paid to the clinical or therapeutic goal from inception, and ideally, a novel signature should be validated within the context of randomised control trials (370).

The findings of the present thesis raise several important issues concerning factors affecting prognosis in PDAC. Firstly, can clinical management algorithms be adapted to include molecular biomarkers identified at the preoperative stage? A potential strategy may be preoperative biomarker identification that provides prognostic information that could modify the strategy for a borderline resectable patient from definite resection, to a chemotherapeutic option with palliative surgery and therefore potentially enhance quality of life with a reduction in morbidity.

Such a personalised medicine strategy is paramount for a disease such as PDAC, as only by this manner could targeted therapies options based on marker expression be instigated in a

timely manner so as to enhance efficacy. EUS-FNA tissue presents numerous challenges for downstream molecular analysis. Principally, only small volumes of cellular material are yielded. Secondly, owing to the heterogeneity of PDAC, much of the material will be stromal or inflammatory. Differentiating CP from PDAC creates a diagnostic dilemma and any marker must ideally be specific for PDAC if it is to yield prognostic utility. While difficulties have arisen with gene expression analysis of EUS retrieved samples, it may be that miRNA expression provides an avenue of investigation owing to their robustness, as well as potential for measurement in serum and FFPE specimens (381).

Future genome-wide analysis of PDAC may be superseded by direct sequencing projects, with the recent completion of the Pancreatic Cancer Genome Project marking a considerable milestone, determining all the exons of all coding genes in 24 PDACs (455). 12 core signalling pathways were highlighted: apoptosis, regulation of G_1/S phase transition, integrin signalling, JNK signalling, KRAS signalling, regulation of invasion, DNA damage control, small non-KRAS GTPase-dependent signalling, TGFβ, Hh and Wnt/Notch signalling. The authors argue that PDAC as a general entity should no longer be considered; rather individualisation of a patient's cancer is necessary. This proposed the potential for the identification of mutational state, gene expression, methylation state and miRNA expression pattern preoperatively, targeting appropriate neoadjuvant therapy, extent of resection, adjuvant regimen and post-operative prognosis. It was encouraging that data from this thesis supports many of signalling pathways defined by this landmark study.

Through quantitative analysis of the timing of such genetic events, hope for PDAC treatment was recently provided by the discovery that a broad time window exists for the events illustrated in Figure 1.1B (456). With the initiating mutation being followed by a decade prior to the birth of the founding malignancy, which requires five years to develop metastatic ability and two years preceding death. This exceptionally detailed genotyping study provides evidence that theoretically opportunities for modification of disease progression by targeting the discussed pathways, may indeed be plausible.

10.2.2 Limitations of the thesis

It should be noted that although this study investigated gene expression at the level of the transcriptome and miRNAome with additional CNA analysis, it failed to consider all potential levels of regulation. A great number of target genes in PDAC undergo methylation, which can also be studied using microarray technology (457). Further, important limitations of this thesis relate to the tissue utilised for the genome wide approach, as has been highlighted earlier. Comparison between PDAC and normal tissue was restricted by the normal tissue originating from resection specimens, not from true normal specimens (e.g. donor resections) and therefore caution must be exercised when considering results for both the mRNA and miRNA chapters. Additionally, failure to perform laser capture

microdissection of the PDAC specimens, instead using macrodissected pancreatic tumour tissue for RNA extraction, was a limiting factor. This enabled the stromal, and potentially also the inflammatory components that play an increasingly recognised role in carcinogenesis and tumour progression, to be evaluated alongside the epithelial components. However, despite this potential benefit, microdissection would have enhanced localisation of mRNA and miRNA expression to the individual tissue compartments. It is hoped, however that preoperative profiling based upon biopsy examination may become an important component of the PDAC clinical management algorithm. Material obtained by this means will undoubtedly be a mixture of tumour epithelium, stromal and normal tissue. Therefore, this strategy has worth in determining markers that may be used in the future to stratify patients based on preoperative assessment. Furthermore, a similar strategy was employed by another established group investigating prognostic gene signatures in PDAC (349). Comparison with CP tissue was originally planned, however poor quality of the extracted RNA prevented assessment by microarray methodology.

10.3 Conclusion

Currently the prediction of prognosis following resection for PDAC is based solely on pathological factors, for which consensus is only now being reached. For breast cancer, routine management is enhanced by molecular prognostic classification e.g. HER-2 status. Unfortunately, despite a wealth of molecular investigation in PDAC, the prognostic value of this approach is to date limited.

This thesis describes the investigation of prognostic indicators for patients with PDAC using firstly a candidate marker approach followed by a genome wide approach. The clinical parameter of survival has been used as a means to investigate the underlying tumour biology, and to determine whether poor prognosis after resection can be tied to any pathological or molecular aspect.

The proposed enhancements to the current pathological classifications should create a firm foundation on which to stratify patient outcome robustly according to molecular targets. In addition to enhancing aspects of conventional pathological staging, the detailed, unbiased genome-wide analysis has successfully identified potentially novel aspects of PDAC biology (Figure 10.1). Most importantly, a number of novel factors that appear to stratify prognosis for resectable pancreatic cancer patients at a pathological and molecular level have been identified as a result of this thesis including evidence of gene expression signatures and miRNA expression patterns.

These findings have the potential, following validation, to refine outcome stratification post-operatively, and may in the future form the initial steps towards an individualisation of management for patients with resectable pancreatic cancer.

References

1. Yeo CJ, Cameron JL, Sohn TA, Lillemoe KD, Pitt HA, Talamini MA, Hruban RH, Ord SE, Sauter PK, Coleman J, Zahurak ML, Grochow LB, Abrams RA. Six hundred fifty consecutive pancreaticoduodenectomies in the 1990s: pathology, complications, and outcomes. Ann Surg. 1997;226:248-57.
2. Wagner M, Redaelli C, Lietz M, Seiler CA, Friess H, Buchler MW. Curative resection is the single most important factor determining outcome in patients with pancreatic adenocarcinoma. Br J Surg. 2004;91:586-94.
3. Grutzmann R, Boriss H, Ammerpohl O, Luttges J, Kalthoff H, Schackert HK, Kloppel G, Saeger HD, Pilarsky C. Meta-analysis of microarray data on pancreatic cancer defines a set of commonly dysregulated genes. Oncogene. 2005;24:5079-88.
4. Golub TR, Slonim DK, Tamayo P, Huard C, Gaasenbeek M, Mesirov JP, Coller H, Loh ML, Downing JR, Caligiuri MA, Bloomfield CD, Lander ES. Molecular classification of cancer: class discovery and class prediction by gene expression monitoring. Science. 1999;286:531-7.
5. van de Vijver MJ, He YD, van't Veer LJ, Dai H, Hart AA, Voskuil DW, Schreiber GJ, Peterse JL, Roberts C, Marton MJ, Parrish M, Atsma D, Witteveen A, Glas A, Delahaye L, van der Velde T, Bartelink H, Rodenhuis S, Rutgers ET, Friend SH, Bernards R. A gene-expression signature as a predictor of survival in breast cancer. N Engl J Med. 2002;347:1999-2009.
6. CancerStats. http://info.cancerresearchuk.org/cancerstats/. Accessed 23 January 2011.
7. Klein AP, Brune KA, Petersen GM, Goggins M, Tersmette AC, Offerhaus GJ, Griffin C, Cameron JL, Yeo CJ, Kern S, Hruban RH. Prospective risk of pancreatic cancer in familial pancreatic cancer kindreds. Cancer Res. 2004;64:2634-8.
8. Amundadottir L, Kraft P, Stolzenberg-Solomon RZ, Fuchs CS, Arslan AA, Jacobs EJ, LaCroix A, Zheng W, Albanes D, Bamlet W, Berg CD, Berrino F, Chanock SJ, Hartge P, Hoover RN. Genome-wide association study identifies variants in the ABO locus associated with susceptibility to pancreatic cancer. Nat Genet. 2009;41:986-90.
9. Pernick NL, Sarkar FH, Philip PA, Arlauskas P, Shields AF, Vaitkevicius VK, Dugan MC, Adsay NV. Clinicopathologic analysis of pancreatic adenocarcinoma in African Americans and Caucasians. Pancreas. 2003;26:28-32.
10. Petersen GM, Hruban RH. Familial pancreatic cancer: where are we in 2003? J Natl Cancer Inst. 2003;95:180-1.
11. Shi C, Klein AP, Goggins M, Maitra A, Canto M, Ali S, Schulick R, Palmisano E, Hruban RH. Increased Prevalence of Precursor Lesions in Familial Pancreatic Cancer Patients. Clin Cancer Res. 2009;15:7737-43.
12. Wang L, Brune KA, Visvanathan K, Laheru D, Herman J, Wolfgang C, Schulick R, Cameron JL, Goggins M, Hruban RH, Klein AP. Elevated cancer mortality in the relatives of patients with pancreatic cancer. Cancer Epidemiol Biomarkers Prev. 2009;18:2829-34.
13. Howes N, Lerch MM, Greenhalf W, Stocken DD, Ellis I, Simon P, Truninger K, Ammann R, Cavallini G, Charnley RM, Jansen J, Mountford R, Whitcomb DC, Neoptolemos JP. Clinical and genetic characteristics of hereditary pancreatitis in Europe. Clin Gastroenterol Hepatol. 2004;2:252-61.
14. Threadgold J, Greenhalf W, Ellis I, Howes N, Lerch MM, Simon P, Jansen J, Charnley R, Laugier R, Frulloni L, Olah A, Delhaye M, Ihse I, Schaffalitzky de Muckadell OB, Andren-Sandberg A, Imrie CW, Martinek J, Gress TM, Mountford R, Whitcomb D, Neoptolemos JP. The N34S mutation of SPINK1 (PSTI) is associated with a familial pattern of idiopathic chronic pancreatitis but does not cause the disease. Gut. 2002;50:675-81.
15. Chari ST, Leibson CL, Rabe KG, Timmons LJ, Ransom J, de Andrade M, Petersen GM. Pancreatic cancer-associated diabetes mellitus: prevalence and temporal association with diagnosis of cancer. Gastroenterology. 2008;134:95-101.
16. Huxley R, Ansary-Moghaddam A, Berrington de Gonzalez A, Barzi F, Woodward M. Type-II diabetes and pancreatic cancer: a meta-analysis of 36 studies. Br J Cancer. 2005;92:2076-83.
17. Li D, Yeung SC, Hassan MM, Konopleva M, Abbruzzese JL. Antidiabetic therapies affect risk of pancreatic cancer. Gastroenterology. 2009;137:482-8.
18. Caygill CP, Hill MJ, Hall CN, Kirkham JS, Northfield TC. Increased risk of cancer at multiple sites after gastric surgery for peptic ulcer. Gut. 1987;28:924-8.
19. de Martel C, Llosa AE, Friedman GD, Vogelman JH, Orentreich N, Stolzenberg-Solomon RZ, Parsonnet J. Helicobacter pylori infection and development of pancreatic cancer. Cancer Epidemiol Biomarkers Prev. 2008;17:1188-94.

20. Swift M, Chase CL, Morrell D. Cancer predisposition of ataxia-telangiectasia heterozygotes. Cancer Genet Cytogenet. 1990;46:21-7.
21. Coughlin SS, Calle EE, Patel AV, Thun MJ. Predictors of pancreatic cancer mortality among a large cohort of United States adults. Cancer Causes Control. 2000;11:915-23.
22. Fuchs CS, Colditz GA, Stampfer MJ, Giovannucci EL, Hunter DJ, Rimm EB, Willett WC, Speizer FE. A prospective study of cigarette smoking and the risk of pancreatic cancer. Arch Intern Med. 1996;156:2255-60.
23. Blackford A, Parmigiani G, Kensler TW, Wolfgang C, Jones S, Goggins M, Jaffee EM, Iacobuzio-Donahue CA, Maitra A, Klein A, Cameron JL, Olino K, Schulick R, Winter J, Vogelstein B, Velculescu VE, Kinzler KW, Hruban RH. Genetic mutations associated with cigarette smoking in pancreatic cancer. Cancer Res. 2009;69:3681-8.
24. Ye W, Lagergren J, Weiderpass E, Nyren O, Adami HO, Ekbom A. Alcohol abuse and the risk of pancreatic cancer. Gut. 2002;51:236-9.
25. Talamini G, Falconi M, Bassi C, Sartori N, Salvia R, Caldiron E, Frulloni L, Di Francesco V, Vaona B, Bovo P, Vantini I, Pederzoli P, Cavallini G. Incidence of cancer in the course of chronic pancreatitis. Am J Gastroenterol. 1999;94:1253-60.
26. Bansal P, Sonnenberg A. Pancreatitis is a risk factor for pancreatic cancer. Gastroenterology. 1995;109:247-51.
27. Malka D, Hammel P, Maire F, Rufat P, Madeira I, Pessione F, Levy P, Ruszniewski P. Risk of pancreatic adenocarcinoma in chronic pancreatitis. Gut. 2002;51:849-52.
28. Berrington de Gonzalez A, Sweetland S, Spencer E. A meta-analysis of obesity and the risk of pancreatic cancer. Br J Cancer. 2003;89:519-23.
29. Nothlings U, Wilkens LR, Murphy SP, Hankin JH, Henderson BE, Kolonel LN. Meat and fat intake as risk factors for pancreatic cancer: the multiethnic cohort study. J Natl Cancer Inst. 2005;97:1458-65.
30. Larsson SC, Hakansson N, Giovannucci E, Wolk A. Folate intake and pancreatic cancer incidence: a prospective study of Swedish women and men. J Natl Cancer Inst. 2006;98:407-13.
31. Hezel AF, Kimmelman AC, Stanger BZ, Bardeesy N, Depinho RA. Genetics and biology of pancreatic ductal adenocarcinoma. Genes Dev. 2006;20:1218-49.
32. Nakata B, Wang YQ, Yashiro M, Nishioka N, Tanaka H, Ohira M, Ishikawa T, Nishino H, Hirakawa K. Prognostic value of microsatellite instability in resectable pancreatic cancer. Clin Cancer Res. 2002;8:2536-40.
33. Seidel G, Zahurak M, Iacobuzio-Donahue C, Sohn TA, Adsay NV, Yeo CJ, Lillemoe KD, Cameron JL, Hruban RH, Wilentz RE. Almost all infiltrating colloid carcinomas of the pancreas and periampullary region arise from in situ papillary neoplasms: a study of 39 cases. Am J Surg Pathol. 2002;26:56-63.
34. Abraham SC, Wu TT, Hruban RH, Lee JH, Yeo CJ, Conlon K, Brennan M, Cameron JL, Klimstra DS. Genetic and immunohistochemical analysis of pancreatic acinar cell carcinoma: frequent allelic loss on chromosome 11p and alterations in the APC/beta-catenin pathway. Am J Pathol. 2002;160:953-62.
35. Abraham SC, Klimstra DS, Wilentz RE, Yeo CJ, Conlon K, Brennan M, Cameron JL, Wu TT, Hruban RH. Solid-pseudopapillary tumors of the pancreas are genetically distinct from pancreatic ductal adenocarcinomas and almost always harbor beta-catenin mutations. Am J Pathol. 2002;160:1361-9.
36. Maitra A, Fukushima N, Takaori K, Hruban RH. Precursors to invasive pancreatic cancer. Adv Anat Pathol. 2005;12:81-91.
37. Luttges J, Galehdari H, Brocker V, Schwarte-Waldhoff I, Henne-Bruns D, Kloppel G, Schmiegel W, Hahn SA. Allelic loss is often the first hit in the biallelic inactivation of the p53 and DPC4 genes during pancreatic carcinogenesis. Am J Pathol. 2001;158:1677-83.
38. Buchholz M, Braun M, Heidenblut A, Kestler HA, Kloppel G, Schmiegel W, Hahn SA, Luttges J, Gress TM. Transcriptome analysis of microdissected pancreatic intraepithelial neoplastic lesions. Oncogene. 2005;24:6626-36.
39. Li C, Heidt DG, Dalerba P, Burant CF, Zhang L, Adsay V, Wicha M, Clarke MF, Simeone DM. Identification of pancreatic cancer stem cells. Cancer Res. 2007;67:1030-7.
40. Hermann PC, Huber SL, Herrler T, Aicher A, Ellwart JW, Guba M, Bruns CJ, Heeschen C. Distinct populations of cancer stem cells determine tumor growth and metastatic activity in human pancreatic cancer. Cell Stem Cell. 2007;1:313-23.

41. Habbe N, Shi G, Meguid RA, Fendrich V, Esni F, Chen H, Stoffers DA, Konieczny SF, Leach SD, Maitra A. Spontaneous induction of murine pancreatic intraepithelial neoplasia (mPanIN) by acinar cell targeting of oncogenic Kras in adult mice. PNAS. 2008;105:18913-8.
42. Stanger BZ, Stiles B, Lauwers GY, Bardeesy N, Mendoza M, Wang Y, Greenwood A, Cheng KH, McLaughlin M, Brown D, Depinho RA, Wu H, Melton DA, Dor Y. Pten constrains centroacinar cell expansion and malignant transformation in the pancreas. Cancer Cell. 2005;8:185-95.
43. Pelaez-Luna M, Takahashi N, Fletcher JG, Chari ST. Resectability of presymptomatic pancreatic cancer and its relationship to onset of diabetes: a retrospective review of CT scans and fasting glucose values prior to diagnosis. Am J Gastroenterol. 2007;102:2157-63.
44. Minniti S, Bruno C, Biasiutti C, Tonel D, Falzone A, Falconi M, Procacci C. Sonography versus helical CT in identification and staging of pancreatic ductal adenocarcinoma. J Clin Ultrasound. 2003;31:175-82.
45. Catalano C, Laghi A, Fraioli F, Pediconi F, Napoli A, Danti M, Reitano I, Passariello R. Pancreatic carcinoma: the role of high-resolution multislice spiral CT in the diagnosis and assessment of resectability. Eur Radiol. 2003;13:149-56.
46. Phoa SS, Tilleman EH, van Delden OM, Bossuyt PM, Gouma DJ, Lameris JS. Value of CT criteria in predicting survival in patients with potentially resectable pancreatic head carcinoma. J Surg Oncol. 2005;91:33-40.
47. Hanninen EL, Ricke J, Amthauer H, Rottgen R, Bohmig M, Langrehr J, Pech M, Denecke T, Rosewicz S, Felix R. Magnetic resonance cholangiopancreatography: image quality, ductal morphology, and value of additional T2- and T1-weighted sequences for the assessment of suspected pancreatic cancer. Acta Radiol. 2005;46:117-25.
48. Lytras D, Connor S, Bosonnet L, Jayan R, Evans J, Hughes M, Garvey CJ, Ghaneh P, Sutton R, Vinjamuri S, Neoptolemos JP. Positron emission tomography does not add to computed tomography for the diagnosis and staging of pancreatic cancer. Dig Surg. 2005;22:55-61.
49. Lemke AJ, Niehues SM, Hosten N, Amthauer H, Boehmig M, Stroszczynski C, Rohlfing T, Rosewicz S, Felix R. Retrospective digital image fusion of multidetector CT and 18F-FDG PET: clinical value in pancreatic lesions--a prospective study with 104 patients. J Nucl Med. 2004;45:1279-86.
50. Dewitt J, Devereaux BM, Lehman GA, Sherman S, Imperiale TF. Comparison of endoscopic ultrasound and computed tomography for the preoperative evaluation of pancreatic cancer: a systematic review. Clin Gastroenterol Hepatol. 2006;4:717-25.
51. Kosugi C, Furuse J, Ishii H, Maru Y, Yoshino M, Kinoshita T, Konishi M, Nakagohri T, Inoue K, Oda T. Needle tract implantation of hepatocellular carcinoma and pancreatic carcinoma after ultrasound-guided percutaneous puncture: clinical and pathologic characteristics and the treatment of needle tract implantation. World J Surg. 2004;28:29-32.
52. Raut CP, Grau AM, Staerkel GA, Kaw M, Tamm EP, Wolff RA, Vauthey JN, Lee JE, Pisters PW, Evans DB. Diagnostic accuracy of endoscopic ultrasound-guided fine-needle aspiration in patients with presumed pancreatic cancer. J Gastrointest Surg. 2003;7:118-26.
53. Maithel SK, Maloney S, Winston C, Gonen M, D'Angelica MI, Dematteo RP, Jarnagin WR, Brennan MF, Allen PJ. Preoperative CA 19-9 and the yield of staging laparoscopy in patients with radiographically resectable pancreatic adenocarcinoma. Ann Surg Oncol. 2008;15:3512-20.
54. Koopmann J, Fedarko NS, Jain A, Maitra A, Iacobuzio-Donahue C, Rahman A, Hruban RH, Yeo CJ, Goggins M. Evaluation of osteopontin as biomarker for pancreatic adenocarcinoma. Cancer Epidemiol Biomarkers Prev. 2004;13:487-91.
55. Neoptolemos JP, Dunn JA, Stocken DD, Almond J, Link K, Beger H, Bassi C, Falconi M, Pederzoli P, Dervenis C, Fernandez-Cruz L, Lacaine F, Pap A, Spooner D, Kerr DJ, Friess H, Buchler MW. Adjuvant chemoradiotherapy and chemotherapy in resectable pancreatic cancer: a randomised controlled trial. Lancet. 2001;358:1576-85.
56. Jones L, Russell C, Mosca F, Boggi U, Sutton R, Slavin J, Hartley M, Neoptolemos JP. Standard Kausch-Whipple pancreatoduodenectomy. Dig Surg. 1999;16:297-304.
57. McKay A, Mackenzie S, Sutherland FR, Bathe OF, Doig C, Dort J, Vollmer CM, Jr., Dixon E. Meta-analysis of pancreaticojejunostomy versus pancreaticogastrostomy reconstruction after pancreaticoduodenectomy. Br J Surg. 2006;93:929-36.
58. Tran KT, Smeenk HG, van Eijck CH, Kazemier G, Hop WC, Greve JW, Terpstra OT, Zijlstra JA, Klinkert P, Jeekel H. Pylorus preserving pancreaticoduodenectomy versus standard Whipple procedure: a prospective, randomized, multicenter analysis of 170 patients with pancreatic and periampullary tumors. Ann Surg. 2004;240:738-45.

59. Karpoff HM, Klimstra DS, Brennan MF, Conlon KC. Results of total pancreatectomy for adenocarcinoma of the pancreas. Arch Surg. 2001;136:44-7; discussion 8.
60. Riall TS, Cameron JL, Lillemoe KD, Campbell KA, Sauter PK, Coleman J, Abrams RA, Laheru D, Hruban RH, Yeo CJ. Pancreaticoduodenectomy with or without distal gastrectomy and extended retroperitoneal lymphadenectomy for periampullary adenocarcinoma--part 3: update on 5-year survival. J Gastrointest Surg. 2005;9:1191-204.
61. Winter JM, Cameron JL, Campbell KA, Arnold MA, Chang DC, Coleman J, Hodgin MB, Sauter PK, Hruban RH, Riall TS, Schulick RD, Choti MA, Lillemoe KD, Yeo CJ. 1423 pancreaticoduodenectomies for pancreatic cancer: A single-institution experience. J Gastrointest Surg. 2006;10:1199-210.
62. Muscari F, Suc B, Kirzin S, Hay JM, Fourtanier G, Fingerhut A, Sastre B, Chipponi J, Fagniez PL, Radovanovic A. Risk factors for mortality and intra-abdominal complications after pancreatoduodenectomy: multivariate analysis in 300 patients. Surgery. 2006;139:591-8.
63. Tseng JF, Raut CP, Lee JE, Pisters PW, Vauthey JN, Abdalla EK, Gomez HF, Sun CC, Crane CH, Wolff RA, Evans DB. Pancreaticoduodenectomy with vascular resection: margin status and survival duration. J Gastrointest Surg. 2004;8:935-49.
64. van der Gaag NA, Rauws EA, van Eijck CH, Bruno MJ, van der Harst E, Kubben FJ, Nio CY, de Castro SM, Busch OR, van Gulik TM, Bossuyt PM, Gouma DJ. Preoperative biliary drainage for cancer of the head of the pancreas. N Engl J Med. 2010;362:129-37.
65. Bilimoria KY, Bentrem DJ, Ko CY, Stewart AK, Winchester DP, Talamonti MS. National failure to operate on early stage pancreatic cancer. Ann Surg. 2007;246:173-80.
66. Kalser MH, Ellenberg SS. Pancreatic cancer. Adjuvant combined radiation and chemotherapy following curative resection. Arch Surg. 1985;120:899-903.
67. Oettle H, Post S, Neuhaus P, Gellert K, Langrehr J, Ridwelski K, Schramm H, Fahlke J, Zuelke C, Burkart C, Gutberlet K, Kettner E, Schmalenberg H, Weigang-Koehler K, Bechstein WO, Niedergethmann M, Schmidt-Wolf I, Roll L, Doerken B, Riess H. Adjuvant chemotherapy with gemcitabine vs observation in patients undergoing curative-intent resection of pancreatic cancer: a randomized controlled trial. JAMA. 2007;297:267-77.
68. Regine WF, Winter KA, Abrams RA, Safran H, Hoffman JP, Konski A, Benson AB, Macdonald JS, Kudrimoti MR, Fromm ML, Haddock MG, Schaefer P, Willett CG, Rich TA. Fluorouracil vs gemcitabine chemotherapy before and after fluorouracil-based chemoradiation following resection of pancreatic adenocarcinoma: a randomized controlled trial. JAMA. 2008;299:1019-26.
69. Corsini MM, Miller RC, Haddock MG, Donohue JH, Farnell MB, Nagorney DM, Jatoi A, McWilliams RR, Kim GP, Bhatia S, Iott MJ, Gunderson LL. Adjuvant radiotherapy and chemotherapy for pancreatic carcinoma: the Mayo Clinic experience (1975-2005). J Clin Oncol. 2008;26:3511-6.
70. Herman JM, Swartz MJ, Hsu CC, Winter J, Pawlik TM, Sugar E, Robinson R, Laheru DA, Jaffee E, Hruban RH, Campbell KA, Hidalgo M, Diaz LA, Jr., Yeo C, Cameron JL, Schulick RD, Abrams R. Analysis of fluorouracil-based adjuvant chemotherapy and radiation after pancreaticoduodenectomy for ductal adenocarcinoma of the pancreas: results of a large, prospectively collected database. J Clin Oncol. 2008;26:3503-10.
71. Neoptolemos JP, Stocken DD, Friess H, Bassi C, Dunn JA, Hickey H, Beger H, Fernandez-Cruz L, Dervenis C, Lacaine F, Falconi M, Pederzoli P, Pap A, Spooner D, Kerr DJ, Buchler MW. A randomized trial of chemoradiotherapy and chemotherapy after resection of pancreatic cancer. N Engl J Med. 2004;350:1200-10.
72. Neoptolemos JP, Stocken DD, Bassi C, Ghaneh P, Cunningham D, Goldstein D, Padbury R, Moore MJ, Gallinger S, Mariette C, Wente MN, Izbicki JR, Friess H, Lerch MM, Dervenis C, Olah A, Butturini G, Doi R, Lind PA, Smith D, Valle JW, Palmer DH, Buckels JA, Thompson J, McKay CJ, Rawcliffe CL, Buchler MW. Adjuvant chemotherapy with fluorouracil plus folinic acid vs gemcitabine following pancreatic cancer resection: a randomized controlled trial. JAMA. 2010;304:1073-81.
73. Evans DB, Varadhachary GR, Crane CH, Sun CC, Lee JE, Pisters PW, Vauthey JN, Wang H, Cleary KR, Staerkel GA, Charnsangavej C, Lano EA, Ho L, Lenzi R, Abbruzzese JL, Wolff RA. Preoperative gemcitabine-based chemoradiation for patients with resectable adenocarcinoma of the pancreatic head. J Clin Oncol. 2008;26:3496-502.
74. Gillen S, Schuster T, Meyer Zum Buschenfelde C, Friess H, Kleeff J. Preoperative/neoadjuvant therapy in pancreatic cancer: a systematic review and meta-analysis of response and resection percentages. PLoS medicine. 2010;7:e1000267.

75. Donahue TR, Isacoff WH, Hines OJ, Tomlinson JS, Farrell JJ, Bhat YM, Garon E, Clerkin B, Reber HA. Downstaging chemotherapy and alteration in the classic computed tomography/magnetic resonance imaging signs of vascular involvement in patients with pancreaticobiliary malignant tumors: influence on patient selection for surgery. Arch Surg. 2011;146:836-43.
76. Varadhachary GR, Tamm EP, Abbruzzese JL, Xiong HQ, Crane CH, Wang H, Lee JE, Pisters PW, Evans DB, Wolff RA. Borderline resectable pancreatic cancer: definitions, management, and role of preoperative therapy. Ann Surg Oncol. 2006;13:1035-46.
77. Koniaris LG, Staveley-O'Carroll KF, Zeh HJ, Perez E, Jin XL, Maley WR, Zabari G, Bartlett DL, Khanna A, Franceschi D, Schoeniger LO. Pancreaticoduodenectomy in the presence of superior mesenteric venous obstruction. J Gastrointest Surg. 2005;9:915-21.
78. Lesko LJ, Atkinson AJ, Jr. Use of biomarkers and surrogate endpoints in drug development and regulatory decision making: criteria, validation, strategies. Annu Rev Pharmacol Toxicol. 2001;41:347-66.
79. Tonini GP, Boni L, Pession A, Rogers D, Iolascon A, Basso G, Scaruffi P, Lo Cunsolo C, Marchese N, Milanaccio C, Conte M, Bruzzi P, De Bernardi B. MYCN oncogene amplification in neuroblastoma is associated with worse prognosis, except in stage 4s: the Italian experience with 295 children. J Clin Oncol. 1997;15:85-93.
80. Sobin LH, Wittekind C. International Union Against Cancer TNM Classification of Malignant Tumours. New York: Wiley–Liss; 2003.
81. Kloppel G, Lingenthal G, von Bulow M, Kern HF. Histological and fine structural features of pancreatic ductal adenocarcinomas in relation to growth and prognosis: studies in xenografted tumours and clinico-histopathological correlation in a series of 75 cases. Histopathology. 1985;9:841-56.
82. Kuhlmann KF, de Castro SM, Wesseling JG, ten Kate FJ, Offerhaus GJ, Busch OR, van Gulik TM, Obertop H, Gouma DJ. Surgical treatment of pancreatic adenocarcinoma; actual survival and prognostic factors in 343 patients. Eur J Cancer. 2004;40:549-58.
83. Luttges J, Schemm S, Vogel I, Hedderich J, Kremer B, Kloppel G. The grade of pancreatic ductal carcinoma is an independent prognostic factor and is superior to the immunohistochemical assessment of proliferation. J Pathol. 2000;191:154-61.
84. Riediger H, Keck T, Wellner U, zur Hausen A, Adam U, Hopt UT, Makowiec F. The lymph node ratio is the strongest prognostic factor after resection of pancreatic cancer. J Gastrointest Surg. 2009;13:1337-44.
85. Kayahara M, Nagakawa T, Konishi I, Ueno K, Ohta T, Miyazaki I. Clinicopathological study of pancreatic carcinoma with particular reference to the invasion of the extrapancreatic neural plexus. Int J Pancreatol. 1991;10:105-11.
86. van Roest MH, Gouw AS, Peeters PM, Porte RJ, Slooff MJ, Fidler V, de Jong KP. Results of pancreaticoduodenectomy in patients with periampullary adenocarcinoma: perineural growth more important prognostic factor than tumor localization. Ann Surg. 2008;248:97-103.
87. Allema JH, Reinders ME, van Gulik TM, Koelemay MJ, Van Leeuwen DJ, de Wit LT, Gouma DJ, Obertop H. Prognostic factors for survival after pancreaticoduodenectomy for patients with carcinoma of the pancreatic head region. Cancer. 1995;75:2069-76.
88. Luttges J, Vogel I, Menke M, Henne-Bruns D, Kremer B, Kloppel G. The retroperitoneal resection margin and vessel involvement are important factors determining survival after pancreaticoduodenectomy for ductal adenocarcinoma of the head of the pancreas. Virchows Arch. 1998;433:237-42.
89. Yekebas EF, Bogoevski D, Cataldegirmen G, Kunze C, Marx A, Vashist YK, Schurr PG, Liebl L, Thieltges S, Gawad KA, Schneider C, Izbicki JR. En bloc vascular resection for locally advanced pancreatic malignancies infiltrating major blood vessels: perioperative outcome and long-term survival in 136 patients. Ann Surg. 2008;247:300-9.
90. Tseng JF, Tamm EP, Lee JE, Pisters PW, Evans DB. Venous resection in pancreatic cancer surgery. Best Pract Res Clin Gastroenterol. 2006;20:349-64.
91. Han SS, Jang JY, Kim SW, Kim WH, Lee KU, Park YH. Analysis of long-term survivors after surgical resection for pancreatic cancer. Pancreas. 2006;32:271-5.
92. Furukawa H, Okada S, Saisho H, Ariyama J, Karasawa E, Nakaizumi A, Nakazawa S, Murakami K, Kakizoe T. Clinicopathologic features of small pancreatic adenocarcinoma. A collective study. Cancer. 1996;78:986-90.
93. Verbeke CS, Leitch D, Menon KV, McMahon MJ, Guillou PJ, Anthoney A. Redefining the R1 resection in pancreatic cancer. Br J Surg. 2006;93:1232-7.

94. Raut CP, Tseng JF, Sun CC, Wang H, Wolff RA, Crane CH, Hwang R, Vauthey JN, Abdalla EK, Lee JE, Pisters PW, Evans DB. Impact of resection status on pattern of failure and survival after pancreaticoduodenectomy for pancreatic adenocarcinoma. Ann Surg. 2007;246:52-60.
95. The Royal College of Pathologists. Standards and Minimum Datasets for Reporting Cancers. Minimum Dataset for the Histopathological Reporting of Pancreatic, Ampulla of Vater and Bile Duct Carcinoma. : The Royal College of Pathologists: London; 2002.
96. Esposito I, Kleeff J, Bergmann F, Reiser C, Herpel E, Friess H, Schirmacher P, Buchler MW. Most pancreatic cancer resections are R1 resections. Ann Surg Oncol. 2008;15:1651-60.
97. Isaji S, Kawarada Y, Uemoto S. Classification of pancreatic cancer: comparison of Japanese and UICC classifications. Pancreas. 2004;28:231-4.
98. Kayahara M, Nagakawa T, Ueno K, Ohta T, Takeda T, Miyazaki I. An evaluation of radical resection for pancreatic cancer based on the mode of recurrence as determined by autopsy and diagnostic imaging. Cancer. 1993;72:2118-23.
99. Van den Broeck A, Sergeant G, Ectors N, Van Steenbergen W, Aerts R, Topal B. Patterns of recurrence after curative resection of pancreatic ductal adenocarcinoma. Eur J Surg Oncol. 2009;35:600-4.
100. Massucco P, Capussotti L, Magnino A, Sperti E, Gatti M, Muratore A, Sgotto E, Gabriele P, Aglietta M. Pancreatic resections after chemoradiotherapy for locally advanced ductal adenocarcinoma: analysis of perioperative outcome and survival. Ann Surg Oncol. 2006;13:1201-8.
101. Breslin TM, Hess KR, Harbison DB, Jean ME, Cleary KR, Dackiw AP, Wolff RA, Abbruzzese JL, Janjan NA, Crane CH, Vauthey JN, Lee JE, Pisters PW, Evans DB. Neoadjuvant chemoradiotherapy for adenocarcinoma of the pancreas: treatment variables and survival duration. Ann Surg Oncol. 2001;8:123-32.
102. Westerdahl J, Andren-Sandberg A, Ihse I. Recurrence of exocrine pancreatic cancer--local or hepatic? Hepatogastroenterology. 1993;40:384-7.
103. Asiyanbola B, Gleisner A, Herman JM, Choti MA, Wolfgang CL, Swartz M, Edil BH, Schulick RD, Cameron JL, Pawlik TM. Determining pattern of recurrence following pancreaticoduodenectomy and adjuvant 5-flurouracil-based chemoradiation therapy: effect of number of metastatic lymph nodes and lymph node ratio. J Gastrointest Surg. 2009;13:752-9.
104. Hruban RH, van Mansfeld AD, Offerhaus GJ, van Weering DH, Allison DC, Goodman SN, Kensler TW, Bose KK, Cameron JL, Bos JL. K-ras oncogene activation in adenocarcinoma of the human pancreas. A study of 82 carcinomas using a combination of mutant-enriched polymerase chain reaction analysis and allele-specific oligonucleotide hybridization. Am J Pathol. 1993;143:545-54.
105. Grippo PJ, Nowlin PS, Demeure MJ, Longnecker DS, Sandgren EP. Preinvasive pancreatic neoplasia of ductal phenotype induced by acinar cell targeting of mutant Kras in transgenic mice. Cancer Res. 2003;63:2016-9.
106. Calhoun ES, Jones JB, Ashfaq R, Adsay V, Baker SJ, Valentine V, Hempen PM, Hilgers W, Yeo CJ, Hruban RH, Kern SE. BRAF and FBXW7 (CDC4, FBW7, AGO, SEL10) mutations in distinct subsets of pancreatic cancer: potential therapeutic targets. Am J Pathol. 2003;163:1255-60.
107. Okami K, Wu L, Riggins G, Cairns P, Goggins M, Evron E, Halachmi N, Ahrendt SA, Reed AL, Hilgers W, Kern SE, Koch WM, Sidransky D, Jen J. Analysis of PTEN/MMAC1 alterations in aerodigestive tract tumors. Cancer Res. 1998;58:509-11.
108. Ruggeri BA, Huang L, Wood M, Cheng JQ, Testa JR. Amplification and overexpression of the AKT2 oncogene in a subset of human pancreatic ductal adenocarcinomas. Mol Carcinog. 1998;21:81-6.
109. Schlieman MG, Fahy BN, Ramsamooj R, Beckett L, Bold RJ. Incidence, mechanism and prognostic value of activated AKT in pancreas cancer. Br J Cancer. 2003;89:2110-5.
110. Bruns CJ, Koehl GE, Guba M, Yezhelyev M, Steinbauer M, Seeliger H, Schwend A, Hoehn A, Jauch KW, Geissler EK. Rapamycin-induced endothelial cell death and tumor vessel thrombosis potentiate cytotoxic therapy against pancreatic cancer. Clin Cancer Res. 2004;10:2109-19.
111. Chien Y, White MA. RAL GTPases are linchpin modulators of human tumour-cell proliferation and survival. EMBO reports. 2003;4:800-6.
112. Holcomb B, Yip-Schneider M, Schmidt CM. The role of nuclear factor kappaB in pancreatic cancer and the clinical applications of targeted therapy. Pancreas. 2008;36:225-35.
113. Fujioka S, Sclabas GM, Schmidt C, Frederick WA, Dong QG, Abbruzzese JL, Evans DB, Baker C, Chiao PJ. Function of nuclear factor kappaB in pancreatic cancer metastasis. Clin Cancer Res. 2003;9:346-54.

114. Schutte M, Hruban RH, Geradts J, Maynard R, Hilgers W, Rabindran SK, Moskaluk CA, Hahn SA, Schmiegel W, Baylin SB, Kern SE, Herman JG. Abrogation of the Rb/p16 tumor-suppressive pathway in virtually all pancreatic carcinomas. Cancer Res. 1997;57:3126-30.
115. Serrano M, Hannon GJ, Beach D. A new regulatory motif in cell-cycle control causing specific inhibition of cyclin D/CDK4. Nature. 1993;366:704-7.
116. Bardeesy N, Aguirre AJ, Chu GC, Cheng KH, Lopez LV, Hezel AF, Feng B, Brennan C, Weissleder R, Mahmood U, Hanahan D, Redston MS, Chin L, Depinho RA. Both p16(Ink4a) and the p19(Arf)-p53 pathway constrain progression of pancreatic adenocarcinoma in the mouse. PNAS. 2006;103:5947-52.
117. Esposito I, Kleeff J, Abiatari I, Shi X, Giese N, Bergmann F, Roth W, Friess H, Schirmacher P. Overexpression of cellular inhibitor of apoptosis protein 2 is an early event in the progression of pancreatic cancer. J Clin Pathol. 2007;60:885-95.
118. Evans JD, Cornford PA, Dodson A, Greenhalf W, Foster CS, Neoptolemos JP. Detailed tissue expression of bcl-2, bax, bak and bcl-x in the normal human pancreas and in chronic pancreatitis, ampullary and pancreatic ductal adenocarcinomas. Pancreatology. 2001;1:254-62.
119. Magistrelli P, Coppola R, Tonini G, Vincenzi B, Santini D, Borzomati D, Vecchio F, Valeri S, Castri F, Antinori A, Nuzzo G, Caraglia M, Picciocchi A. Apoptotic index or a combination of Bax/Bcl-2 expression correlate with survival after resection of pancreatic adenocarcinoma. J Cell Biochem. 2006;97:98-108.
120. Massague J. TGFbeta in Cancer. Cell. 2008;134:215-30.
121. Peng B, Fleming JB, Breslin T, Grau AM, Fojioka S, Abbruzzese JL, Evans DB, Ayers D, Wathen K, Wu T, Robertson KD, Chiao PJ. Suppression of tumorigenesis and induction of p15(ink4b) by Smad4/DPC4 in human pancreatic cancer cells. Clin Cancer Res. 2002;8:3628-38.
122. Blackford A, Serrano OK, Wolfgang CL, Parmigiani G, Jones S, Zhang X, Parsons DW, Lin JC, Leary RJ, Eshleman JR, Goggins M, Jaffee EM, Iacobuzio-Donahue CA, Maitra A, Cameron JL, Olino K, Schulick R, Winter J, Herman JM, Laheru D, Klein AP, Vogelstein B, Kinzler KW, Velculescu VE, Hruban RH. SMAD4 gene mutations are associated with poor prognosis in pancreatic cancer. Clin Cancer Res. 2009;15:4674-9.
123. Duda DG, Sunamura M, Lefter LP, Furukawa T, Yokoyama T, Yatsuoka T, Abe T, Inoue H, Motoi F, Egawa S, Matsuno S, Horii A. Restoration of SMAD4 by gene therapy reverses the invasive phenotype in pancreatic adenocarcinoma cells. Oncogene. 2003;22:6857-64.
124. Kleeff J, Ishiwata T, Maruyama H, Friess H, Truong P, Buchler MW, Falb D, Korc M. The TGF-beta signaling inhibitor Smad7 enhances tumorigenicity in pancreatic cancer. Oncogene. 1999;18:5363-72.
125. Zavadil J, Bottinger EP. TGF-beta and epithelial-to-mesenchymal transitions. Oncogene. 2005;24:5764-74.
126. Levy L, Hill CS. Smad4 dependency defines two classes of transforming growth factor {beta} (TGF-{beta}) target genes and distinguishes TGF-{beta}-induced epithelial-mesenchymal transition from its antiproliferative and migratory responses. Mol Cell Biol. 2005;25:8108-25.
127. Jeanes A, Gottardi CJ, Yap AS. Cadherins and cancer: how does cadherin dysfunction promote tumor progression? Oncogene. 2008;27:6920-9.
128. Wong AS, Gumbiner BM. Adhesion-independent mechanism for suppression of tumor cell invasion by E-cadherin. J Cell Biol. 2003;161:1191-203.
129. Li YJ, Ji XR. Relationship between expression of E-cadherin-catenin complex and clinicopathologic characteristics of pancreatic cancer. World J Gastroenterol. 2003;9:368-72.
130. Juhaszova M, Zorov DB, Kim SH, Pepe S, Fu Q, Fishbein KW, Ziman BD, Wang S, Ytrehus K, Antos CL, Olson EN, Sollott SJ. Glycogen synthase kinase-3beta mediates convergence of protection signaling to inhibit the mitochondrial permeability transition pore. J Clin Invest. 2004;113:1535-49.
131. Chan TA, Wang Z, Dang LH, Vogelstein B, Kinzler KW. Targeted inactivation of CTNNB1 reveals unexpected effects of beta-catenin mutation. PNAS. 2002;99:8265-70.
132. Barton CM, Staddon SL, Hughes CM, Hall PA, O'Sullivan C, Kloppel G, Theis B, Russell RC, Neoptolemos J, Williamson RC. Abnormalities of the p53 tumour suppressor gene in human pancreatic cancer. Br J Cancer. 1991;64:1076-82.
133. Schutte M, da Costa LT, Hahn SA, Moskaluk C, Hoque AT, Rozenblum E, Weinstein CL, Bittner M, Meltzer PS, Trent JM. Identification by representational difference analysis of a homozygous deletion in pancreatic carcinoma that lies within the BRCA2 region. PNAS. 1995;92:5950-4.

134. Couch FJ, Johnson MR, Rabe KG, Brune K, de Andrade M, Goggins M, Rothenmund H, Gallinger S, Klein A, Petersen GM, Hruban RH. The prevalence of BRCA2 mutations in familial pancreatic cancer. Cancer Epidemiol Biomarkers Prev. 2007;16:342-6.
135. Berman DM, Karhadkar SS, Maitra A, Montes De Oca R, Gerstenblith MR, Briggs K, Parker AR, Shimada Y, Eshleman JR, Watkins DN, Beachy PA. Widespread requirement for Hedgehog ligand stimulation in growth of digestive tract tumours. Nature. 2003;425:846-51.
136. Hebrok M, Kim SK, St Jacques B, McMahon AP, Melton DA. Regulation of pancreas development by hedgehog signaling. Development. 2000;127:4905-13.
137. Feldmann G, Habbe N, Dhara S, Bisht S, Alvarez H, Fendrich V, Beaty R, Mullendore M, Karikari C, Bardeesy N, Ouellette MM, Yu W, Maitra A. Hedgehog inhibition prolongs survival in a genetically engineered mouse model of pancreatic cancer. Gut. 2008;57:1420-30.
138. Jimeno A, Feldmann G, Suarez-Gauthier A, Rasheed Z, Solomon A, Zou GM, Rubio-Viqueira B, Garcia-Garcia E, Lopez-Rios F, Matsui W, Maitra A, Hidalgo M. A direct pancreatic cancer xenograft model as a platform for cancer stem cell therapeutic development. Mol Cancer Ther. 2009;8:310-4.
139. Apelqvist A, Li H, Sommer L, Beatus P, Anderson DJ, Honjo T, Hrabe de Angelis M, Lendahl U, Edlund H. Notch signalling controls pancreatic cell differentiation. Nature. 1999;400:877-81.
140. Miyamoto Y, Maitra A, Ghosh B, Zechner U, Argani P, Iacobuzio-Donahue CA, Sriuranpong V, Iso T, Meszoely IM, Wolfe MS, Hruban RH, Ball DW, Schmid RM, Leach SD. Notch mediates TGF alpha-induced changes in epithelial differentiation during pancreatic tumorigenesis. Cancer Cell. 2003;3:565-76.
141. Murtaugh LC, Stanger BZ, Kwan KM, Melton DA. Notch signaling controls multiple steps of pancreatic differentiation. PNAS. 2003;100:14920-5.
142. Sundaram MV. The love-hate relationship between Ras and Notch. Genes Dev. 2005;19:1825-39.
143. Lowy AM, Fenoglio-Preiser C, Kim OJ, Kordich J, Gomez A, Knight J, James L, Groden J. Dysregulation of beta-catenin expression correlates with tumor differentiation in pancreatic duct adenocarcinoma. Ann Surg Oncol. 2003;10:284-90.
144. Katoh M. Integrative genomic analyses of WNT11: transcriptional mechanisms based on canonical WNT signals and GATA transcription factors signaling. Int J Mol Med. 2009;24:247-51.
145. Harper JW, Adami GR, Wei N, Keyomarsi K, Elledge SJ. The p21 Cdk-interacting protein Cip1 is a potent inhibitor of G1 cyclin-dependent kinases. Cell. 1993;75:805-16.
146. Collado M, Gil J, Efeyan A, Guerra C, Schuhmacher AJ, Barradas M, Benguria A, Zaballos A, Flores JM, Barbacid M, Beach D, Serrano M. Tumour biology: senescence in premalignant tumours. Nature. 2005;436:642.
147. Nakajima S, Doi R, Toyoda E, Tsuji S, Wada M, Koizumi M, Tulachan SS, Ito D, Kami K, Mori T, Kawaguchi Y, Fujimoto K, Hosotani R, Imamura M. N-cadherin expression and epithelial-mesenchymal transition in pancreatic carcinoma. Clin Cancer Res. 2004;10:4125-33.
148. Bolos V, Peinado H, Perez-Moreno MA, Fraga MF, Esteller M, Cano A. The transcription factor Slug represses E-cadherin expression and induces epithelial to mesenchymal transitions: a comparison with Snail and E47 repressors. J Cell Sci. 2003;116:499-511.
149. Hotz B, Arndt M, Dullat S, Bhargava S, Buhr HJ, Hotz HG. Epithelial to mesenchymal transition: expression of the regulators snail, slug, and twist in pancreatic cancer. Clin Cancer Res. 2007;13:4769-76.
150. von Burstin J, Eser S, Paul MC, Seidler B, Brandl M, Messer M, von Werder A, Schmidt A, Mages J, Pagel P, Schnieke A, Schmid RM, Schneider G, Saur D. E-cadherin regulates metastasis of pancreatic cancer in vivo and is suppressed by a SNAIL/HDAC1/HDAC2 repressor complex. Gastroenterology. 2009;137:361-71, 71 e1-5.
151. Shirts BH, Burt RW, Mulvihill SJ, Cannon-Albright LA. A population-based description of familial clustering of pancreatic cancer. Clin Gastroenterol Hepatol. 2010;8:812-6.
152. Begg CB, Orlow I, Hummer AJ, Armstrong BK, Kricker A, Marrett LD, Millikan RC, Gruber SB, Anton-Culver H, Zanetti R, Gallagher RP, Dwyer T, Rebbeck TR, Mitra N, Busam K, From L, Berwick M. Lifetime risk of melanoma in CDKN2A mutation carriers in a population-based sample. J Natl Cancer Inst. 2005;97:1507-15.
153. de vos tot Nederveen Cappel WH, Offerhaus GJ, van Puijenbroek M, Caspers E, Gruis NA, De Snoo FA, Lamers CB, Griffioen G, Bergman W, Vasen HF, Morreau H. Pancreatic carcinoma in carriers of a specific 19 base pair deletion of CDKN2A/p16 (p16-leiden). Clin Cancer Res. 2003;9:3598-605.

154. Esteller M, Avizienyte E, Corn PG, Lothe RA, Baylin SB, Aaltonen LA, Herman JG. Epigenetic inactivation of LKB1 in primary tumors associated with the Peutz-Jeghers syndrome. Oncogene. 2000;19:164-8.
155. Giardiello FM, Brensinger JD, Tersmette AC, Goodman SN, Petersen GM, Booker SV, Cruz-Correa M, Offerhaus JA. Very high risk of cancer in familial Peutz-Jeghers syndrome. Gastroenterology. 2000;119:1447-53.
156. Qanungo S, Haldar S, Basu A. Restoration of silenced Peutz-Jeghers syndrome gene, LKB1, induces apoptosis in pancreatic carcinoma cells. Neoplasia. 2003;5:367-74.
157. Sato N, Rosty C, Jansen M, Fukushima N, Ueki T, Yeo CJ, Cameron JL, Iacobuzio-Donahue CA, Hruban RH, Goggins M. STK11/LKB1 Peutz-Jeghers gene inactivation in intraductal papillary-mucinous neoplasms of the pancreas. Am J Pathol. 2001;159:2017-22.
158. Shaw RJ, Kosmatka M, Bardeesy N, Hurley RL, Witters LA, DePinho RA, Cantley LC. The tumor suppressor LKB1 kinase directly activates AMP-activated kinase and regulates apoptosis in response to energy stress. PNAS. 2004;101:3329-35.
159. Karuman P, Gozani O, Odze RD, Zhou XC, Zhu H, Shaw R, Brien TP, Bozzuto CD, Ooi D, Cantley LC, Yuan J. The Peutz-Jegher gene product LKB1 is a mediator of p53-dependent cell death. Mol Cell. 2001;7:1307-19.
160. Bardeesy N, Sinha M, Hezel AF, Signoretti S, Hathaway NA, Sharpless NE, Loda M, Carrasco DR, DePinho RA. Loss of the Lkb1 tumour suppressor provokes intestinal polyposis but resistance to transformation. Nature. 2002;419:162-7.
161. Slater EP, Langer P, Niemczyk E, Strauch K, Butler J, Habbe N, Neoptolemos JP, Greenhalf W, Bartsch DK. PALB2 mutations in European familial pancreatic cancer families. Clinical genetics. 2010;78:490-4.
162. Wilentz RE, Goggins M, Redston M, Marcus VA, Adsay NV, Sohn TA, Kadkol SS, Yeo CJ, Choti M, Zahurak M, Johnson K, Tascilar M, Offerhaus GJ, Hruban RH, Kern SE. Genetic, immunohistochemical, and clinical features of medullary carcinoma of the pancreas: A newly described and characterized entity. Am J Pathol. 2000;156:1641-51.
163. Klein AP, Borges M, Griffith M, Brune K, Hong SM, Omura N, Hruban RH, Goggins M. Absence of deleterious palladin mutations in patients with familial pancreatic cancer. Cancer Epidemiol Biomarkers Prev. 2009;18:1328-30.
164. Shi C, Hruban RH, Klein AP. Familial pancreatic cancer. Archives of pathology & laboratory medicine. 2009;133:365-74.
165. Kleihues P, Schauble B, zur Hausen A, Esteve J, Ohgaki H. Tumors associated with p53 germline mutations: a synopsis of 91 families. Am J Pathol. 1997;150:1-13.
166. McWilliams R, Highsmith WE, Rabe KG, de Andrade M, Tordsen LA, Holtegaard LM, Petersen GM. Cystic fibrosis transmembrane regulator gene carrier status is a risk factor for young onset pancreatic adenocarcinoma. Gut. 2005;54:1661-2.
167. Hingorani SR, Petricoin EF, Maitra A, Rajapakse V, King C, Jacobetz MA, Ross S, Conrads TP, Veenstra TD, Hitt BA, Kawaguchi Y, Johann D, Liotta LA, Crawford HC, Putt ME, Jacks T, Wright CV, Hruban RH, Lowy AM, Tuveson DA. Preinvasive and invasive ductal pancreatic cancer and its early detection in the mouse. Cancer Cell. 2003;4:437-50.
168. Hingorani SR, Wang L, Multani AS, Combs C, Deramaudt TB, Hruban RH, Rustgi AK, Chang S, Tuveson DA. Trp53R172H and KrasG12D cooperate to promote chromosomal instability and widely metastatic pancreatic ductal adenocarcinoma in mice. Cancer Cell. 2005;7:469-83.
169. Perou CM, Sorlie T, Eisen MB, van de Rijn M, Jeffrey SS, Rees CA, Pollack JR, Ross DT, Johnsen H, Akslen LA, Fluge O, Pergamenschikov A, Williams C, Zhu SX, Lonning PE, Borresen-Dale AL, Brown PO, Botstein D. Molecular portraits of human breast tumours. Nature. 2000;406:747-52.
170. Wang Y, Jatkoe T, Zhang Y, Mutch MG, Talantov D, Jiang J, McLeod HL, Atkins D. Gene expression profiles and molecular markers to predict recurrence of Dukes' B colon cancer. J Clin Oncol. 2004;22:1564-71.
171. Schena M. Genome analysis with gene expression microarrays. Bioessays. 1996;18:427-31.
172. Sorlie T, Perou CM, Tibshirani R, Aas T, Geisler S, Johnsen H, Hastie T, Eisen MB, van de Rijn M, Jeffrey SS, Thorsen T, Quist H, Matese JC, Brown PO, Botstein D, Eystein Lonning P, Borresen-Dale AL. Gene expression patterns of breast carcinomas distinguish tumor subclasses with clinical implications. PNAS. 2001;98:10869-74.
173. van 't Veer LJ, Dai H, van de Vijver MJ, He YD, Hart AA, Mao M, Peterse HL, van der Kooy K, Marton MJ, Witteveen AT, Schreiber GJ, Kerkhoven RM, Roberts C, Linsley PS, Bernards R,

Friend SH. Gene expression profiling predicts clinical outcome of breast cancer. Nature. 2002;415:530-6.
174. Wang Y, Klijn JG, Zhang Y, Sieuwerts AM, Look MP, Yang F, Talantov D, Timmermans M, Meijer-van Gelder ME, Yu J, Jatkoe T, Berns EM, Atkins D, Foekens JA. Gene-expression profiles to predict distant metastasis of lymph-node-negative primary breast cancer. Lancet. 2005;365:671-9.
175. Grutzmann R, Foerder M, Alldinger I, Staub E, Brummendorf T, Ropcke S, Li X, Kristiansen G, Jesnowski R, Sipos B, Lohr M, Luttges J, Ockert D, Kloppel G, Saeger HD, Pilarsky C. Gene expression profiles of microdissected pancreatic ductal adenocarcinoma. Virchows Arch. 2003;443:508-17.
176. Argani P, Rosty C, Reiter RE, Wilentz RE, Murugesan SR, Leach SD, Ryu B, Skinner HG, Goggins M, Jaffee EM, Yeo CJ, Cameron JL, Kern SE, Hruban RH. Discovery of new markers of cancer through serial analysis of gene expression: prostate stem cell antigen is overexpressed in pancreatic adenocarcinoma. Cancer Res. 2001;61:4320-4.
177. Gress TM, Wallrapp C, Frohme M, Muller-Pillasch F, Lacher U, Friess H, Buchler M, Adler G, Hoheisel JD. Identification of genes with specific expression in pancreatic cancer by cDNA representational difference analysis. Genes Chromosomes Cancer. 1997;19:97-103.
178. Han H, Bearss DJ, Browne LW, Calaluce R, Nagle RB, Von Hoff DD. Identification of differentially expressed genes in pancreatic cancer cells using cDNA microarray. Cancer Res. 2002;62:2890-6.
179. Iacobuzio-Donahue CA, Maitra A, Olsen M, Lowe AW, van Heek NT, Rosty C, Walter K, Sato N, Parker A, Ashfaq R, Jaffee E, Ryu B, Jones J, Eshleman JR, Yeo CJ, Cameron JL, Kern SE, Hruban RH, Brown PO, Goggins M. Exploration of global gene expression patterns in pancreatic adenocarcinoma using cDNA microarrays. Am J Pathol. 2003;162:1151-62.
180. Logsdon CD, Simeone DM, Binkley C, Arumugam T, Greenson JK, Giordano TJ, Misek DE, Kuick R, Hanash S. Molecular profiling of pancreatic adenocarcinoma and chronic pancreatitis identifies multiple genes differentially regulated in pancreatic cancer. Cancer Res. 2003;63:2649-57.
181. Tan ZJ, Hu XG, Cao GS, Tang Y. Analysis of gene expression profile of pancreatic carcinoma using cDNA microarray. World J Gastroenterol. 2003;9:818-23.
182. Iacobuzio-Donahue CA, Maitra A, Shen-Ong GL, van Heek T, Ashfaq R, Meyer R, Walter K, Berg K, Hollingsworth MA, Cameron JL, Yeo CJ, Kern SE, Goggins M, Hruban RH. Discovery of novel tumor markers of pancreatic cancer using global gene expression technology. Am J Pathol. 2002;160:1239-49.
183. Crnogorac-Jurcevic T, Efthimiou E, Nielsen T, Loader J, Terris B, Stamp G, Baron A, Scarpa A, Lemoine NR. Expression profiling of microdissected pancreatic adenocarcinomas. Oncogene. 2002;21:4587-94.
184. Friess H, Ding J, Kleeff J, Fenkell L, Rosinski JA, Guweidhi A, Reidhaar-Olson JF, Korc M, Hammer J, Buchler MW. Microarray-based identification of differentially expressed growth- and metastasis-associated genes in pancreatic cancer. Cell Mol Life Sci. 2003;60:1180-99.
185. Chelala C, Hahn SA, Whiteman HJ, Barry S, Hariharan D, Radon TP, Lemoine NR, Crnogorac-Jurcevic T. Pancreatic Expression database: a generic model for the organization, integration and mining of complex cancer datasets. BMC Genomics. 2007;8:439.
186. Segara D, Biankin AV, Kench JG, Langusch CC, Dawson AC, Skalicky DA, Gotley DC, Coleman MJ, Sutherland RL, Henshall SM. Expression of HOXB2, a retinoic acid signaling target in pancreatic cancer and pancreatic intraepithelial neoplasia. Clin Cancer Res. 2005;11:3587-96.
187. Ishikawa M, Yoshida K, Yamashita Y, Ota J, Takada S, Kisanuki H, Koinuma K, Choi YL, Kaneda R, Iwao T, Tamada K, Sugano K, Mano H. Experimental trial for diagnosis of pancreatic ductal carcinoma based on gene expression profiles of pancreatic ductal cells. Cancer Sci. 2005;96:387-93.
188. Grutzmann R, Pilarsky C, Ammerpohl O, Luttges J, Bohme A, Sipos B, Foerder M, Alldinger I, Jahnke B, Schackert HK, Kalthoff H, Kremer B, Kloppel G, Saeger HD. Gene expression profiling of microdissected pancreatic ductal carcinomas using high-density DNA microarrays. Neoplasia. 2004;6:611-22.
189. Lowe AW, Olsen M, Hao Y, Lee SP, Taek Lee K, Chen X, van de Rijn M, Brown PO. Gene expression patterns in pancreatic tumors, cells and tissues. PLoS One. 2007;2:e323.
190. Cao D, Hustinx SR, Sui G, Bala P, Sato N, Martin S, Maitra A, Murphy KM, Cameron JL, Yeo CJ, Kern SE, Goggins M, Pandey A, Hruban RH. Identification of novel highly expressed genes in pancreatic ductal adenocarcinomas through a bioinformatics analysis of expressed sequence tags. Cancer Biol Ther. 2004;3:1081-9.

191. Hustinx SR, Cao D, Maitra A, Sato N, Martin ST, Sudhir D, Iacobuzio-Donahue C, Cameron JL, Yeo CJ, Kern SE, Goggins M, Mollenhauer J, Pandey A, Hruban RH. Differentially expressed genes in pancreatic ductal adenocarcinomas identified through serial analysis of gene expression. Cancer Biol Ther. 2004;3:1254-61.
192. Crnogorac-Jurcevic T, Efthimiou E, Capelli P, Blaveri E, Baron A, Terris B, Jones M, Tyson K, Bassi C, Scarpa A, Lemoine NR. Gene expression profiles of pancreatic cancer and stromal desmoplasia. Oncogene. 2001;20:7437-46.
193. Nakamura T, Furukawa Y, Nakagawa H, Tsunoda T, Ohigashi H, Murata K, Ishikawa O, Ohgaki K, Kashimura N, Miyamoto M, Hirano S, Kondo S, Katoh H, Nakamura Y, Katagiri T. Genome-wide cDNA microarray analysis of gene expression profiles in pancreatic cancers using populations of tumor cells and normal ductal epithelial cells selected for purity by laser microdissection. Oncogene. 2004;23:2385-400.
194. Li A, Omura N, Hong SM, Goggins M. Pancreatic cancer DNMT1 expression and sensitivity to DNMT1 inhibitors. Cancer Biol Ther. 2010;9.
195. Jones PA, Baylin SB. The fundamental role of epigenetic events in cancer. Nat Rev Genet. 2002;3:415-28.
196. Ueki T, Toyota M, Sohn T, Yeo CJ, Issa JP, Hruban RH, Goggins M. Hypermethylation of multiple genes in pancreatic adenocarcinoma. Cancer Res. 2000;60:1835-9.
197. Wada M, Yazumi S, Takaishi S, Hasegawa K, Sawada M, Tanaka H, Ida H, Sakakura C, Ito K, Ito Y, Chiba T. Frequent loss of RUNX3 gene expression in human bile duct and pancreatic cancer cell lines. Oncogene. 2004;23:2401-7.
198. Fukushima N, Sato N, Sahin F, Su GH, Hruban RH, Goggins M. Aberrant methylation of suppressor of cytokine signalling-1 (SOCS-1) gene in pancreatic ductal neoplasms. Br J Cancer. 2003;89:338-43.
199. Rosty C, Ueki T, Argani P, Jansen M, Yeo CJ, Cameron JL, Hruban RH, Goggins M. Overexpression of S100A4 in pancreatic ductal adenocarcinomas is associated with poor differentiation and DNA hypomethylation. Am J Pathol. 2002;160:45-50.
200. Sato N, Maitra A, Fukushima N, van Heek NT, Matsubayashi H, Iacobuzio-Donahue CA, Rosty C, Goggins M. Frequent hypomethylation of multiple genes overexpressed in pancreatic ductal adenocarcinoma. Cancer Res. 2003;63:4158-66.
201. Calin GA, Croce CM. MicroRNA signatures in human cancers. Nat Rev Cancer. 2006;6:857-66.
202. Lee Y, Jeon K, Lee JT, Kim S, Kim VN. MicroRNA maturation: stepwise processing and subcellular localization. EMBO J. 2002;21:4663-70.
203. Lee Y, Ahn C, Han J, Choi H, Kim J, Yim J, Lee J, Provost P, Radmark O, Kim S, Kim VN. The nuclear RNase III Drosha initiates microRNA processing. Nature. 2003;425:415-9.
204. Filipowicz W, Bhattacharyya SN, Sonenberg N. Mechanisms of post-transcriptional regulation by microRNAs: are the answers in sight? Nat Rev Genet. 2008;9:102-14.
205. Tomari Y, Zamore PD. Perspective: machines for RNAi. Genes Dev. 2005;19:517-29.
206. Bartel DP, Chen CZ. Micromanagers of gene expression: the potentially widespread influence of metazoan microRNAs. Nat Rev Genet. 2004;5:396-400.
207. O'Connell RM, Taganov KD, Boldin MP, Cheng G, Baltimore D. MicroRNA-155 is induced during the macrophage inflammatory response. Proc Natl Acad Sci U S A. 2007;104:1604-9.
208. Calin GA, Dumitru CD, Shimizu M, Bichi R, Zupo S, Noch E, Aldler H, Rattan S, Keating M, Rai K, Rassenti L, Kipps T, Negrini M, Bullrich F, Croce CM. Frequent deletions and down-regulation of micro- RNA genes miR15 and miR16 at 13q14 in chronic lymphocytic leukemia. PNAS. 2002;99:15524-9.
209. Cummins JM, He Y, Leary RJ, Pagliarini R, Diaz LA, Jr., Sjoblom T, Barad O, Bentwich Z, Szafranska AE, Labourier E, Raymond CK, Roberts BS, Juhl H, Kinzler KW, Vogelstein B, Velculescu VE. The colorectal microRNAome. PNAS. 2006;103:3687-92.
210. Visone R, Russo L, Pallante P, De Martino I, Ferraro A, Leone V, Borbone E, Petrocca F, Alder H, Croce CM, Fusco A. MicroRNAs (miR)-221 and miR-222, both overexpressed in human thyroid papillary carcinomas, regulate p27Kip1 protein levels and cell cycle. Endocr Relat Cancer. 2007;14:791-8.
211. Iorio MV, Ferracin M, Liu CG, Veronese A, Spizzo R, Sabbioni S, Magri E, Pedriali M, Fabbri M, Campiglio M, Menard S, Palazzo JP, Rosenberg A, Musiani P, Volinia S, Nenci I, Calin GA, Querzoli P, Negrini M, Croce CM. MicroRNA gene expression deregulation in human breast cancer. Cancer Res. 2005;65:7065-70.

212. Esquela-Kerscher A, Slack FJ. Oncomirs - microRNAs with a role in cancer. Nat Rev Cancer. 2006;6:259-69.
213. Cimmino A, Calin GA, Fabbri M, Iorio MV, Ferracin M, Shimizu M, Wojcik SE, Aqeilan RI, Zupo S, Dono M, Rassenti L, Alder H, Volinia S, Liu CG, Kipps TJ, Negrini M, Croce CM. miR-15 and miR-16 induce apoptosis by targeting BCL2. PNAS. 2005;102:13944-9.
214. Chan JA, Krichevsky AM, Kosik KS. MicroRNA-21 is an antiapoptotic factor in human glioblastoma cells. Cancer Res. 2005;65:6029-33.
215. Lu J, Getz G, Miska EA, Alvarez-Saavedra E, Lamb J, Peck D, Sweet-Cordero A, Ebert BL, Mak RH, Ferrando AA, Downing JR, Jacks T, Horvitz HR, Golub TR. MicroRNA expression profiles classify human cancers. Nature. 2005;435:834-8.
216. Calin GA, Ferracin M, Cimmino A, Di Leva G, Shimizu M, Wojcik SE, Iorio MV, Visone R, Sever NI, Fabbri M, Iuliano R, Palumbo T, Pichiorri F, Roldo C, Garzon R, Sevignani C, Rassenti L, Alder H, Volinia S, Liu CG, Kipps TJ, Negrini M, Croce CM. A MicroRNA signature associated with prognosis and progression in chronic lymphocytic leukemia. N Engl J Med. 2005;353:1793-801.
217. Volinia S, Calin GA, Liu CG, Ambs S, Cimmino A, Petrocca F, Visone R, Iorio M, Roldo C, Ferracin M, Prueitt RL, Yanaihara N, Lanza G, Scarpa A, Vecchione A, Negrini M, Harris CC, Croce CM. A microRNA expression signature of human solid tumors defines cancer gene targets. PNAS. 2006;103:2257-61.
218. Yu SL, Chen HY, Chang GC, Chen CY, Chen HW, Singh S, Cheng CL, Yu CJ, Lee YC, Chen HS, Su TJ, Chiang CC, Li HN, Hong QS, Su HY, Chen CC, Chen WJ, Liu CC, Chan WK, Li KC, Chen JJ, Yang PC. MicroRNA signature predicts survival and relapse in lung cancer. Cancer Cell. 2008;13:48-57.
219. Lee EJ, Gusev Y, Jiang J, Nuovo GJ, Lerner MR, Frankel WL, Morgan DL, Postier RG, Brackett DJ, Schmittgen TD. Expression profiling identifies microRNA signature in pancreatic cancer. Int J Cancer. 2007;120:1046-54.
220. Szafranska AE, Davison TS, John J, Cannon T, Sipos B, Maghnouj A, Labourier E, Hahn SA. MicroRNA expression alterations are linked to tumorigenesis and non-neoplastic processes in pancreatic ductal adenocarcinoma. Oncogene. 2007;26:4442-52.
221. Giovannetti E, Funel N, Peters GJ, Del Chiaro M, Erozenci LA, Vasile E, Leon LG, Pollina LE, Groen A, Falcone A, Danesi R, Campani D, Verheul HM, Boggi U. MicroRNA-21 in pancreatic cancer: correlation with clinical outcome and pharmacologic aspects underlying its role in the modulation of gemcitabine activity. Cancer Res. 2010;70:4528-38.
222. Hwang JH, Voortman J, Giovannetti E, Steinberg SM, Leon LG, Kim YT, Funel N, Park JK, Kim MA, Kang GH, Kim SW, Del Chiaro M, Peters GJ, Giaccone G. Identification of microRNA-21 as a biomarker for chemoresistance and clinical outcome following adjuvant therapy in resectable pancreatic cancer. PLoS One. 2010;5:e10630.
223. Greither T, Grochola LF, Udelnow A, Lautenschlager C, Wurl P, Taubert H. Elevated expression of microRNAs 155, 203, 210 and 222 in pancreatic tumors is associated with poorer survival. Int J Cancer. 2010;126:73-80.
224. Ikenaga N, Ohuchida K, Mizumoto K, Yu J, Kayashima T, Sakai H, Fujita H, Nakata K, Tanaka M. MicroRNA-203 expression as a new prognostic marker of pancreatic adenocarcinoma. Ann Surg Oncol. 2010;17:3120-8.
225. Bloomston M, Frankel WL, Petrocca F, Volinia S, Alder H, Hagan JP, Liu CG, Bhatt D, Taccioli C, Croce CM. MicroRNA expression patterns to differentiate pancreatic adenocarcinoma from normal pancreas and chronic pancreatitis. JAMA. 2007;297:1901-8.
226. Yu S, Lu Z, Liu C, Meng Y, Ma Y, Zhao W, Liu J, Yu J, Chen J. miRNA-96 suppresses KRAS and functions as a tumor suppressor gene in pancreatic cancer. Cancer Res. 2010;70:6015-25.
227. Solomon E, Borrow J, Goddard AD. Chromosome aberrations and cancer. Science. 1991;254:1153-60.
228. Weir BA, Woo MS, Getz G, Perner S, Ding L, Beroukhim R, Lin WM, Province MA, Kraja A, Zakowski MF, Zhang Q, Beer DG, Wistuba, II, Watson MA, Garraway LA, Ladanyi M, Travis WD, Pao W, Rubin MA, Gabriel SB, Gibbs RA, Varmus HE, Wilson RK, Lander ES, Meyerson M. Characterizing the cancer genome in lung adenocarcinoma. Nature. 2007;450:893-8.
229. van Heek NT, Meeker AK, Kern SE, Yeo CJ, Lillemoe KD, Cameron JL, Offerhaus GJ, Hicks JL, Wilentz RE, Goggins MG, De Marzo AM, Hruban RH, Maitra A. Telomere shortening is nearly universal in pancreatic intraepithelial neoplasia. Am J Pathol. 2002;161:1541-7.
230. Hackett JA, Greider CW. Balancing instability: dual roles for telomerase and telomere dysfunction in tumorigenesis. Oncogene. 2002;21:619-26.

231. Nigg EA. Centrosome aberrations: cause or consequence of cancer progression? Nat Rev Cancer. 2002;2:815-25.
232. Kowalski J, Morsberger LA, Blackford A, Hawkins A, Yeo CJ, Hruban RH, Griffin CA. Chromosomal abnormalities of adenocarcinoma of the pancreas: identifying early and late changes. Cancer Genet Cytogenet. 2007;178:26-35.
233. Kallioniemi OP, Kallioniemi A, Piper J, Isola J, Waldman FM, Gray JW, Pinkel D. Optimizing comparative genomic hybridization for analysis of DNA sequence copy number changes in solid tumors. Genes Chromosomes Cancer. 1994;10:231-43.
234. Solinas-Toldo S, Lampel S, Stilgenbauer S, Nickolenko J, Benner A, Dohner H, Cremer T, Lichter P. Matrix-based comparative genomic hybridization: biochips to screen for genomic imbalances. Genes Chromosomes Cancer. 1997;20:399-407.
235. Aguirre AJ, Brennan C, Bailey G, Sinha R, Feng B, Leo C, Zhang Y, Zhang J, Gans JD, Bardeesy N, Cauwels C, Cordon-Cardo C, Redston MS, DePinho RA, Chin L. High-resolution characterization of the pancreatic adenocarcinoma genome. PNAS. 2004;101:9067-72.
236. Heidenblad M, Schoenmakers EF, Jonson T, Gorunova L, Veltman JA, van Kessel AG, Hoglund M. Genome-wide array-based comparative genomic hybridization reveals multiple amplification targets and novel homozygous deletions in pancreatic carcinoma cell lines. Cancer Res. 2004;64:3052-9.
237. Bashyam MD, Bair R, Kim YH, Wang P, Hernandez-Boussard T, Karikari CA, Tibshirani R, Maitra A, Pollack JR. Array-based comparative genomic hybridization identifies localized DNA amplifications and homozygous deletions in pancreatic cancer. Neoplasia. 2005;7:556-62.
238. Gysin S, Rickert P, Kastury K, McMahon M. Analysis of genomic DNA alterations and mRNA expression patterns in a panel of human pancreatic cancer cell lines. Genes Chromosomes Cancer. 2005;44:37-51.
239. Harada T, Baril P, Gangeswaran R, Kelly G, Chelala C, Bhakta V, Caulee K, Mahon PC, Lemoine NR. Identification of genetic alterations in pancreatic cancer by the combined use of tissue microdissection and array-based comparative genomic hybridisation. Br J Cancer. 2007;96:373-82.
240. Holzmann K, Kohlhammer H, Schwaenen C, Wessendorf S, Kestler HA, Schwoerer A, Rau B, Lichter P, Gress T, Bentz M. Genomic DNA-chip hybridization reveals a higher incidence of genomic amplifications in pancreatic cancer than conventional comparative genomic hybridization and leads to the identification of novel candidate genes. Cancer Res. 2004;64:4428-33.
241. Loukopoulos P, Shibata T, Katoh H, Kokubu A, Sakamoto M, Yamazaki K, Kosuge T, Kanai Y, Hosoda F, Imoto I, Ohki M, Inazawa J, Hirohashi S. Genome-wide array-based comparative genomic hybridization analysis of pancreatic adenocarcinoma: identification of genetic indicators that predict patient outcome. Cancer Sci. 2007;98:392-400.
242. Mahlamaki EH, Kauraniemi P, Monni O, Wolf M, Hautaniemi S, Kallioniemi A. High-resolution genomic and expression profiling reveals 105 putative amplification target genes in pancreatic cancer. Neoplasia. 2004;6:432-9.
243. Nowak NJ, Gaile D, Conroy JM, McQuaid D, Cowell J, Carter R, Goggins MG, Hruban RH, Maitra A. Genome-wide aberrations in pancreatic adenocarcinoma. Cancer Genet Cytogenet. 2005;161:36-50.
244. Harada T, Chelala C, Bhakta V, Chaplin T, Caulee K, Baril P, Young BD, Lemoine NR. Genome-wide DNA copy number analysis in pancreatic cancer using high-density single nucleotide polymorphism arrays. Oncogene. 2008;27:1951-60.
245. Paris PL, Andaya A, Fridlyand J, Jain AN, Weinberg V, Kowbel D, Brebner JH, Simko J, Watson JE, Volik S, Albertson DG, Pinkel D, Alers JC, van der Kwast TH, Vissers KJ, Schroder FH, Wildhagen MF, Febbo PG, Chinnaiyan AM, Pienta KJ, Carroll PR, Rubin MA, Collins C, van Dekken H. Whole genome scanning identifies genotypes associated with recurrence and metastasis in prostate tumors. Hum Mol Genet. 2004;13:1303-13.
246. Callagy G, Pharoah P, Chin SF, Sangan T, Daigo Y, Jackson L, Caldas C. Identification and validation of prognostic markers in breast cancer with the complementary use of array-CGH and tissue microarrays. J Pathol. 2005;205:388-96.
247. Mahlamaki EH, Barlund M, Tanner M, Gorunova L, Hoglund M, Karhu R, Kallioniemi A. Frequent amplification of 8q24, 11q, 17q, and 20q-specific genes in pancreatic cancer. Genes Chromosomes Cancer. 2002;35:353-8.
248. Camps J, Nguyen QT, Padilla-Nash HM, Knutsen T, McNeil NE, Wangsa D, Hummon AB, Grade M, Ried T, Difilippantonio MJ. Integrative genomics reveals mechanisms of copy number alterations responsible for transcriptional deregulation in colorectal cancer. Genes Chromosomes Cancer. 2009;48:1002-17.

249. Garcea G, Neal CP, Pattenden CJ, Steward WP, Berry DP. Molecular prognostic markers in pancreatic cancer: a systematic review. Eur J Cancer. 2005;41:2213-36.
250. Adler AS, Lin M, Horlings H, Nuyten DS, van de Vijver MJ, Chang HY. Genetic regulators of large-scale transcriptional signatures in cancer. Nat Genet. 2006;38:421-30.
251. Neoptolemos JP, Stocken DD, Dunn JA, Almond J, Beger HG, Pederzoli P, Bassi C, Dervenis C, Fernandez-Cruz L, Lacaine F, Buckels J, Deakin M, Adab FA, Sutton R, Imrie C, Ihse I, Tihanyi T, Olah A, Pedrazzoli S, Spooner D, Kerr DJ, Friess H, Buchler MW. Influence of resection margins on survival for patients with pancreatic cancer treated by adjuvant chemoradiation and/or chemotherapy in the ESPAC-1 randomized controlled trial. Ann Surg. 2001;234:758-68.
252. Exocrine pancreas. In: Greene FL PD, Fleming ID, et al, eds. AJCC Cancer Staging Manual. Chicago: Springer; 2002. p. 157–64.
253. Eisen MB, Spellman PT, Brown PO, Botstein D. Cluster analysis and display of genome-wide expression patterns. PNAS. 1998;95:14863-8.
254. Pavlidis P, Qin J, Arango V, Mann JJ, Sibille E. Using the gene ontology for microarray data mining: a comparison of methods and application to age effects in human prefrontal cortex. Neurochem Res. 2004:29:1213-22.
255. Simon R, Radmacher MD, Dobbin K, McShane LM. Pitfalls in the use of DNA microarray data for diagnostic and prognostic classification. J Natl Cancer Inst. 2003;95:14-8.
256. Chen C, Ridzon DA, Broomer AJ, Zhou Z, Lee DH, Nguyen JT, Barbisin M, Xu NL, Mahuvakar VR, Andersen MR, Lao KQ, Livak KJ, Guegler KJ. Real-time quantification of microRNAs by stem-loop RT-PCR. Nucleic Acids Res. 2005;33:e179.
257. Min H, Yoon S. Got target? Computational methods for microRNA target prediction and their extension. Exp Mol Med. 2010;42:233-44.
258. Shah SP, Cheung KJ, Jr., Johnson NA, Alain G, Gascoyne RD, Horsman DE, Ng RT, Murphy KP. Model-based clustering of array CGH data. Bioinformatics. 2009;25:i30-8.
259. Olshen AB, Venkatraman ES, Lucito R, Wigler M. Circular binary segmentation for the analysis of array-based DNA copy number data. Biostatistics. 2004;5:557-72.
260. Beroukhim R, Getz G, Nghiemphu L, Barretina J, Hsueh T, Linhart D, Vivanco I, Lee JC, Huang JH, Alexander S, Du J, Kau T, Thomas RK, Shah K, Soto H, Perner S, Prensner J, Debiasi RM, Demichelis F, Hatton C, Rubin MA, Garraway LA, Nelson SF, Liau L, Mischel PS, Cloughesy TF, Meyerson M, Golub TA, Lander ES, Mellinghoff IK, Sellers WR. Assessing the significance of chromosomal aberrations in cancer: methodology and application to glioma. PNAS. 2007;104:20007-12.
261. Livak KJ, Schmittgen TD. Analysis of relative gene expression data using real-time quantitative PCR and the 2(-Delta Delta C(T)) Method. Methods. 2001;25:402-8.
262. Bouvet M, Gamagami RA, Gilpin EA, Romeo O, Sasson A, Easter DW, Moossa AR. Factors influencing survival after resection for periampullary neoplasms. Am J Surg. 2000;180:13-7.
263. Schmidt CM, Powell ES, Yiannoutsos CT, Howard TJ, Wiebke EA, Wiesenauer CA, Baumgardner JA, Cummings OW, Jacobson LE, Broadie TA, Canal DF, Goulet RJ, Jr., Curie EA, Cardenes H, Watkins JM, Loehrer PJ, Lillemoe KD, Madura JA. Pancreaticoduodenectomy: 20-year experience 516 patients. Arch Surg. 2004;139:718-25.
264. Pissas A. Anatomoclinical and anatomosurgical essay on the lymphatic circulation of the pancreas. Anat Clin. 1984;6:255-80.
265. Iacobuzio-Donahue CA, Fu B, Yachida S, Luo M, Abe H, Henderson CM, Vilardell F, Wang Z, Keller JW, Banerjee P, Herman JM, Cameron JL, Yeo CJ, Halushka MK, Eshleman JR, Raben M, Klein AP, Hruban RH, Hidalgo M, Laheru D. DPC4 gene status of the primary carcinoma correlates with patterns of failure in patients with pancreatic cancer. J Clin Oncol. 2009;27:1806-13.
266. Sohn TA, Yeo CJ, Cameron JL, Koniaris L, Kaushal S, Abrams RA, Sauter PK, Coleman J, Hruban RH, Lillemoe KD. Resected adenocarcinoma of the pancreas-616 patients: results, outcomes, and prognostic indicators. J Gastrointest Surg. 2000;4:567-79.
267. Jarufe NP, Coldham C, Mayer AD, Mirza DF, Buckels JA, Bramhall SR. Favourable prognostic factors in a large UK experience of adenocarcinoma of the head of the pancreas and periampullary region. Dig Surg. 2004;21:202-9.
268. Butturini G, Stocken DD, Wente MN, Jeekel H, Klinkenbijl JH, Bakkevold KE, Takada T, Amano H, Dervenis C, Bassi C, Buchler MW, Neoptolemos JP. Influence of resection margins and treatment on survival in patients with pancreatic cancer: meta-analysis of randomized controlled trials. Arch Surg. 2008;143:75-83.
269. Sasson AR, Hoffman JP, Ross EA, Kagan SA, Pingpank JF, Eisenberg BL. En bloc resection for locally advanced cancer of the pancreas: is it worthwhile? J Gastrointest Surg. 2002;6:147-57.

270. Westgaard A, Tafjord S, Farstad IN, Cvancarova M, Eide TJ, Mathisen O, Clausen OP, Gladhaug IP. Resectable adenocarcinomas in the pancreatic head: the retroperitoneal resection margin is an independent prognostic factor. BMC Cancer. 2008;8:5.
271. Campbell F, Smith RA, Whelan P, Sutton R, Raraty M, Neoptolemos JP, Ghaneh P. Classification of R1 resections for pancreatic cancer: the prognostic relevance of tumour involvement within 1 mm of a resection margin. Histopathology. 2009;55:277-83.
272. Khalifa MA, Maksymov V, Rowsell C. Retroperitoneal margin of the pancreaticoduodenectomy specimen: anatomic mapping for the surgical pathologist. Virchows Arch. 2009;454:125-31.
273. Verbeke CS. Resection margins and R1 rates in pancreatic cancer-are we there yet? Histopathology. 2008;52:787-96.
274. Nagakawa T, Sanada H, Inagaki M, Sugama J, Ueno K, Konishi I, Ohta T, Kayahara M, Kitagawa H. Long-term survivors after resection of carcinoma of the head of the pancreas: significance of histologically curative resection. J Hepatobiliary Pancreat Surg. 2004;11:402-8.
275. Chang DK, Johns AL, Merrett ND, Gill AJ, Colvin EK, Scarlett CJ, Nguyen NQ, Leong RW, Cosman PH, Kelly MI, Sutherland RL, Henshall SM, Kench JG, Biankin AV. Margin clearance and outcome in resected pancreatic cancer. J Clin Oncol. 2009;27:2855-62.
276. Tsuchiya R, Noda T, Harada N, Miyamoto T, Tomioka T, Yamamoto K, Yamaguchi T, Izawa K, Tsunoda T, Yoshino R. Collective review of small carcinomas of the pancreas. Ann Surg. 1986;203:77-81.
277. Schmidt CM, Glant J, Winter JM, Kennard J, Dixon J, Zhao Q, Howard TJ, Madura JA, Nakeeb A, Pitt HA, Cameron JL, Yeo CJ, Lillemoe KD. Total pancreatectomy (R0 resection) improves survival over subtotal pancreatectomy in isolated neck margin positive pancreatic adenocarcinoma. Surgery. 2007;142:572-8.
278. Horiguchi A, Ishihara S, Ito M, Nagata H, Shimizu T, Furusawa K, Kato R, Katada K, Miyakawa S. Pancreatoduodenectomy in which dissection of the efferent arteries of the head of the pancreas is performed first. J Hepatobiliary Pancreat Surg. 2007;14:575-8.
279. Stocken DD, Buchler MW, Dervenis C, Bassi C, Jeekel H, Klinkenbijl JH, Bakkevold KE, Takada T, Amano H, Neoptolemos JP. Meta-analysis of randomised adjuvant therapy trials for pancreatic cancer. Br J Cancer. 2005;92:1372-81.
280. Gall FP, Kessler H, Hermanek P. Surgical treatment of ductal pancreatic carcinoma. Eur J Surg Oncol. 1991;17:173-81.
281. Willett CG, Lewandrowski K, Warshaw AL, Efird J, Compton CC. Resection margins in carcinoma of the head of the pancreas. Implications for radiation therapy. Ann Surg. 1993;217:144-8.
282. Nitecki SS, Sarr MG, Colby TV, van Heerden JA. Long-term survival after resection for ductal adenocarcinoma of the pancreas. Is it really improving? Ann Surg. 1995;221:59-66.
283. Sperti C, Pasquali C, Piccoli A, Pedrazzoli S. Survival after resection for ductal adenocarcinoma of the pancreas. Br J Surg. 1996;83:625-31.
284. Nishimura Y, Hosotani R, Shibamoto Y, Kokubo M, Kanamori S, Sasai K, Hiraoka M, Ohshio G, Imamura M, Takahashi M, Abe M. External and intraoperative radiotherapy for resectable and unresectable pancreatic cancer. Int J Radiat Oncol Biol Phys. 1997;39:39-49.
285. Millikan KW, Deziel DJ, Silverstein JC, Kanjo TM, Christein JD, Doolas A, Prinz RA. Prognostic factors associated with resectable adenocarcinoma of the head of the pancreas. Am Surg. 1999;65:618-23.
286. Benassai G, Mastrorilli M, Quarto G, Cappiello A, Giani U, Forestieri P, Mazzeo F. Factors influencing survival after resection for ductal adenocarcinoma of the head of the pancreas. J Surg Oncol. 2000;73:212-8.
287. Richter A, Niedergethmann M, Sturm JW, Lorenz D, Post S, Trede M. Long-term results of partial pancreaticoduodenectomy for ductal adenocarcinoma of the pancreatic head: 25-year experience. World J Surg. 2003;27:324-9.
288. Further evidence of effective adjuvant combined radiation and chemotherapy following curative resection of pancreatic cancer. Gastrointestinal Tumor Study Group. Cancer. 1987;59:2006-10.
289. Talamonti MS, Small W, Jr., Mulcahy MF, Wayne JD, Attaluri V, Colletti LM, Zalupski MM, Hoffman JP, Freedman GM, Kinsella TJ, Philip PA, McGinn CJ. A multi-institutional phase II trial of preoperative full-dose gemcitabine and concurrent radiation for patients with potentially resectable pancreatic carcinoma. Ann Surg Oncol. 2006;13:150-8.

290. Irie H, Honda H, Kaneko K, Kuroiwa T, Yoshimitsu K, Masuda K. Comparison of helical CT and MR imaging in detecting and staging small pancreatic adenocarcinoma. Abdom Imaging. 1997;22:429-33.
291. Zhang XM, Mitchell DG, Witkiewicz A, Verma S, Bergin D. Extrapancreatic neural plexus invasion by pancreatic carcinoma: characteristics on magnetic resonance imaging. Abdom Imaging. 2009;34:634-41.
292. Bandyopadhyay S, Basturk O, Coban I, Thirabanjasak D, Liang H, Altinel D, Adsay NV. Isolated solitary ducts (naked ducts) in adipose tissue: a specific but underappreciated finding of pancreatic adenocarcinoma and one of the potential reasons of understaging and high recurrence rate. Am J Surg Pathol. 2009;33:425-9.
293. Mathur A, Zyromski NJ, Pitt HA, Al-Azzawi H, Walker JJ, Saxena R, Lillemoe KD. Pancreatic steatosis promotes dissemination and lethality of pancreatic cancer. J Am Coll Surg. 2009;208:989-94.
294. Farrow B, Albo D, Berger DH. The role of the tumor microenvironment in the progression of pancreatic cancer. J Surg Res. 2008;149:319-28.
295. Ratke J, Entschladen F, Niggemann B, Zanker KS, Lang K. Leptin stimulates the migration of colon carcinoma cells by multiple signaling pathways. Endocr Relat Cancer. 2010;17:179-89.
296. Fleming JB, Gonzalez RJ, Petzel MQ, Lin E, Morris JS, Gomez H, Lee JE, Crane CH, Pisters PW, Evans DB. Influence of obesity on cancer-related outcomes after pancreatectomy to treat pancreatic adenocarcinoma. Arch Surg. 2009;144:216-21.
297. Tsai S, Choti MA, Assumpcao L, Cameron JL, Gleisner AL, Herman JM, Eckhauser F, Edil BH, Schulick RD, Wolfgang CL, Pawlik TM. Impact of Obesity on Perioperative Outcomes and Survival Following Pancreaticoduodenectomy for Pancreatic Cancer: A Large Single-Institution Study. J Gastrointest Surg. 2010;14:1143-50.
298. Iacobuzio-Donahue CA, Ashfaq R, Maitra A, Adsay NV, Shen-Ong GL, Berg K, Hollingsworth MA, Cameron JL, Yeo CJ, Kern SE, Goggins M, Hruban RH. Highly expressed genes in pancreatic ductal adenocarcinomas: a comprehensive characterization and comparison of the transcription profiles obtained from three major technologies. Cancer Res. 2003;63:8614-22.
299. Jamieson NB, Carter CR, McKay CJ, Oien KA. Tissue biomarkers for prognosis in pancreatic ductal adenocarcinoma: a systematic review and meta-analysis. Clin Cancer Res. 2011;17:3316-31.
300. Ghaneh P, Kawesha A, Evans JD, Neoptolemos JP. Molecular prognostic markers in pancreatic cancer. J Hepatobiliary Pancreat Surg. 2002;9:1-11.
301. McShane LM, Altman DG, Sauerbrei W, Taube SE, Gion M, Clark GM. REporting recommendations for tumor MARKer prognostic studies (REMARK). Nat Clin Pract Oncol. 2005;2:416-22.
302. Hanahan D, Weinberg RA. The hallmarks of cancer. Cell. 2000;100:57-70.
303. Sinicrope FA, Evans DB, Leach SD, Cleary KR, Fenoglio CJ, Lee JJ, Abbruzzese JL. bcl-2 and p53 expression in resectable pancreatic adenocarcinomas: association with clinical outcome. Clin Cancer Res. 1996;2:2015-22.
304. Scarpa A, Capelli P, Mukai K, Zamboni G, Oda T, Iacono C, Hirohashi S. Pancreatic adenocarcinomas frequently show p53 gene mutations. Am J Pathol. 1993;142:1534-43.
305. Zheng B, Jeong JH, Asara JM, Yuan YY, Granter SR, Chin L, Cantley LC. Oncogenic B-RAF negatively regulates the tumor suppressor LKB1 to promote melanoma cell proliferation. Mol Cell. 2009;33:237-47.
306. Hezel AF, Gurumurthy S, Granot Z, Swisa A, Chu GC, Bailey G, Dor Y, Bardeesy N, Depinho RA. Pancreatic LKB1 deletion leads to acinar polarity defects and cystic neoplasms. Mol Cell Biol. 2008;28:2414-25.
307. Prince S, Carreira S, Vance KW, Abrahams A, Goding CR. Tbx2 directly represses the expression of the p21(WAF1) cyclin-dependent kinase inhibitor. Cancer Res. 2004;64:1669-74.
308. Olive KP, Tuveson DA, Ruhe ZC, Yin B, Willis NA, Bronson RT, Crowley D, Jacks T. Mutant p53 gain of function in two mouse models of Li-Fraumeni syndrome. Cell. 2004;119:847-60.
309. Nio Y, Iguchi C, Yamasawa K, Sasaki S, Takamura M, Toga T, Dong M, Itakura M, Tamura K. Apoptosis and expression of Bcl-2 and Bax proteins in invasive ductal carcinoma of the pancreas. Pancreas. 2001;22:230-9.
310. Dong M, Zhou JP, Zhang H, Guo KJ, Tian YL, Dong YT. Clinicopathological significance of Bcl-2 and Bax protein expression in human pancreatic cancer. World J Gastroenterol. 2005;11:2744-7.

311. Sun CY, Wang BL, Hu CQ, Peng RY, Gao YB, Gu QY, Wang DW. Expression of the bcl-2 gene and its significance in human pancreatic carcinoma. Hepatobiliary Pancreat Dis Int. 2002;1:306-8.
312. Callagy GM, Pharoah PD, Pinder SE, Hsu FD, Nielsen TO, Ragaz J, Ellis IO, Huntsman D, Caldas C. Bcl-2 is a prognostic marker in breast cancer independently of the Nottingham Prognostic Index. Clin Cancer Res. 2006;12:2468-75.
313. Westphal S, Kalthoff H. Apoptosis: targets in pancreatic cancer. Mol Cancer. 2003;2:6.
314. McDonnell TJ, Korsmeyer SJ. Progression from lymphoid hyperplasia to high-grade malignant lymphoma in mice transgenic for the t(14; 18). Nature. 1991;349:254-6.
315. Pietenpol JA, Papadopoulos N, Markowitz S, Willson JK, Kinzler KW, Vogelstein B. Paradoxical inhibition of solid tumor cell growth by bcl2. Cancer Res. 1994;54:3714-7.
316. Miyashita T, Krajewski S, Krajewska M, Wang HG, Lin HK, Liebermann DA, Hoffman B, Reed JC. Tumor suppressor p53 is a regulator of bcl-2 and bax gene expression in vitro and in vivo. Oncogene. 1994;9:1799-805.
317. Lilien J, Balsamo J. The regulation of cadherin-mediated adhesion by tyrosine phosphorylation/dephosphorylation of beta-catenin. Curr Opin Cell Biol. 2005;17:459-65.
318. Schipper JH, Frixen UH, Behrens J, Unger A, Jahnke K, Birchmeier W. E-cadherin expression in squamous cell carcinomas of head and neck: inverse correlation with tumor dedifferentiation and lymph node metastasis. Cancer Res. 1991;51:6328-37.
319. Jawhari A, Jordan S, Poole S, Browne P, Pignatelli M, Farthing MJ. Abnormal immunoreactivity of the E-cadherin-catenin complex in gastric carcinoma: relationship with patient survival. Gastroenterology. 1997;112:46-54.
320. Hong SM, Li A, Olino K, Wolfgang CL, Herman JM, Schulick RD, Iacobuzio-Donahue C, Hruban RH, Goggins M. Loss of E-cadherin expression and outcome among patients with resectable pancreatic adenocarcinomas. Mod Pathol. 2011;24:1237-47.
321. Zeng G, Germinaro M, Micsenyi A, Monga NK, Bell A, Sood A, Malhotra V, Sood N, Midda V, Monga DK, Kokkinakis DM, Monga SP. Aberrant Wnt/beta-catenin signaling in pancreatic adenocarcinoma. Neoplasia. 2006;8:279-89.
322. Yang J, Weinberg RA. Epithelial-mesenchymal transition: at the crossroads of development and tumor metastasis. Dev Cell. 2008;14:818-29.
323. Cao D, Maitra A, Saavedra JA, Klimstra DS, Adsay NV, Hruban RH. Expression of novel markers of pancreatic ductal adenocarcinoma in pancreatic nonductal neoplasms: additional evidence of different genetic pathways. Mod Pathol. 2005;18:752-61.
324. Watson RL, Spalding AC, Zielske SP, Morgan M, Kim AC, Bommer GT, Eldar-Finkelman H, Giordano T, Fearon ER, Hammer GD, Lawrence TS, Ben-Josef E. GSK3beta and beta-catenin modulate radiation cytotoxicity in pancreatic cancer. Neoplasia. 2010;12:357-65.
325. Merati K, said Siadaty M, Andea A, Sarkar F, Ben-Josef E, Mohammad R, Philip P, Shields AF, Vaitkevicius V, Grignon DJ, Adsay NV. Expression of inflammatory modulator COX-2 in pancreatic ductal adenocarcinoma and its relationship to pathologic and clinical parameters. Am J Clin Oncol. 2001;24:447-52.
326. Juuti A, Louhimo J, Nordling S, Ristimaki A, Haglund C. Cyclooxygenase-2 expression correlates with poor prognosis in pancreatic cancer. J Clin Pathol. 2006;59:382-6.
327. Matsubayashi H, Infante JR, Winter J, Klein AP, Schulick R, Hruban R, Visvanathan K, Goggins M. Tumor COX-2 expression and prognosis of patients with resectable pancreatic cancer. Cancer Biol Ther. 2007;6:1569-75.
328. Sheehan KM, Sheahan K, O'Donoghue DP, MacSweeney F, Conroy RM, Fitzgerald DJ, Murray FE. The relationship between cyclooxygenase-2 expression and colorectal cancer. JAMA. 1999;282:1254-7.
329. Toomey DP, Murphy JF, Conlon KC. COX-2, VEGF and tumour angiogenesis. Surgeon. 2009;7:174-80.
330. El-Rayes BF, Zalupski MM, Shields AF, Ferris AM, Vaishampayan U, Heilbrun LK, Venkatramanamoorthy R, Adsay V, Philip PA. A phase II study of celecoxib, gemcitabine, and cisplatin in advanced pancreatic cancer. Invest New Drugs. 2005;23:583-90.
331. Funahashi H, Satake M, Dawson D, Huynh NA, Reber HA, Hines OJ, Eibl G. Delayed progression of pancreatic intraepithelial neoplasia in a conditional Kras(G12D) mouse model by a selective cyclooxygenase-2 inhibitor. Cancer Res. 2007;67:7068-71.
332. Wei C, Amos CI, Rashid A, Sabripour M, Nations L, McGarrity TJ, Frazier ML. Correlation of staining for LKB1 and COX-2 in hamartomatous polyps and carcinomas from patients with Peutz-Jeghers syndrome. J Histochem Cytochem. 2003;51:1665-72.

333. Rossi DJ, Ylikorkala A, Korsisaari N, Salovaara R, Luukko K, Launonen V, Henkemeyer M, Ristimaki A, Aaltonen LA, Makela TP. Induction of cyclooxygenase-2 in a mouse model of Peutz-Jeghers polyposis. PNAS. 2002;99:12327-32.
334. Wagner TM, Mullally JE, Fitzpatrick FA. Reactive lipid species from cyclooxygenase-2 inactivate tumor suppressor LKB1/STK11: cyclopentenone prostaglandins and 4-hydroxy-2-nonenal covalently modify and inhibit the AMP-kinase kinase that modulates cellular energy homeostasis and protein translation. J Biol Chem. 2006;281:2598-604.
335. Udd L, Katajisto P, Rossi DJ, Lepisto A, Lahesmaa AM, Ylikorkala A, Jarvinen HJ, Ristimaki AP, Makela TP. Suppression of Peutz-Jeghers polyposis by inhibition of cyclooxygenase-2. Gastroenterology. 2004;127:1030-7.
336. Gillett C, Smith P, Gregory W, Richards M, Millis R, Peters G, Barnes D. Cyclin D1 and prognosis in human breast cancer. Int J Cancer. 1996;69:92-9.
337. Biankin AV, Kench JG, Colvin EK, Segara D, Scarlett CJ, Nguyen NQ, Chang DK, Morey AL, Lee CS, Pinese M, Kuo SC, Susanto JM, Cosman PH, Lindeman GJ, Visvader JE, Nguyen TV, Merrett ND, Warusavitarne J, Musgrove EA, Henshall SM, Sutherland RL. Expression of S100A2 calcium-binding protein predicts response to pancreatectomy for pancreatic cancer. Gastroenterology. 2009;137:558-68, 68 e1-11.
338. Brognard J, Dennis PA. Variable apoptotic response of NSCLC cells to inhibition of the MEK/ERK pathway by small molecules or dominant negative mutants. Cell Death Differ. 2002;9:893-904.
339. Javle MM, Yu J, Khoury T, Chadha KS, Iyer RV, Foster J, Kuvshinoff BW, Gibbs JF, Geradts J, Black JD, Brattain MG. Akt expression may predict favorable prognosis in cholangiocarcinoma. J Gastroenterol Hepatol. 2006;21:1744-51.
340. Ng SSW, Tsao MS, Chow S, Hedley DW. Inhibition of phosphatidylinositide 3-kinase enhances gemcitabine-induced apoptosis in human pancreatic cancer cells. Cancer Res. 2000;60:5451-5.
341. Tascilar M, Skinner HG, Rosty C, Sohn T, Wilentz RE, Offerhaus GJ, Adsay V, Abrams RA, Cameron JL, Kern SE, Yeo CJ, Hruban RH, Goggins M. The SMAD4 protein and prognosis of pancreatic ductal adenocarcinoma. Clin Cancer Res. 2001;7:4115-21.
342. Biankin AV, Morey AL, Lee CS, Kench JG, Biankin SA, Hook HC, Head DR, Hugh TB, Sutherland RL, Henshall SM. DPC4/Smad4 expression and outcome in pancreatic ductal adenocarcinoma. J Clin Oncol. 2002;20:4531-42.
343. Zlobec I, Minoo P, Baumhoer D, Baker K, Terracciano L, Jass JR, Lugli A. Multimarker phenotype predicts adverse survival in patients with lymph node-negative colorectal cancer. Cancer. 2008;112:495-502.
344. Taylor CR. Standardization in immunohistochemistry: the role of antigen retrieval in molecular morphology. Biotech Histochem. 2006;81:3-12.
345. Packeisen J, Korsching E, Herbst H, Boecker W, Buerger H. Demystified...tissue microarray technology. Mol Pathol. 2003;56:198-204.
346. Kreizenbeck GM, Berger AJ, Subtil A, Rimm DL, Gould Rothberg BE. Prognostic significance of cadherin-based adhesion molecules in cutaneous malignant melanoma. Cancer Epidemiol Biomarkers Prev. 2008;17:949-58.
347. Karamitopoulou E, Lugli A, Panayiotides I, Karakitsos P, Peros G, Rallis G, Patsouris ES, Terracciano L, Zlobec I. Systematic assessment of protein phenotypes characterizing high-grade tumour budding in mismatch repair-proficient colorectal cancer. Histopathology. 2010;57:233-43.
348. Collisson EA, Sadanandam A, Olson P, Gibb WJ, Truitt M, Gu S, Cooc J, Weinkle J, Kim GE, Jakkula L, Feiler HS, Ko AH, Olshen AB, Spellman PT, Hanahan D, Gray JW. Subtypes of pancreatic ductal adenocarcinoma and their differing responses to therapy. Nat Med. 2011;17:500-3.
349. Stratford JK, Bentrem DJ, Anderson JM, Fan C, Volmar KA, Marron JS, Routh ED, Caskey LS, Samuel JC, Der CJ, Thorne LB, Calvo BF, Kim HJ, Talamonti MS, Iacobuzio-Donahue CA, Hollingsworth MA, Perou CM, Yeh JJ. A six-gene signature predicts survival of patients with localized pancreatic ductal adenocarcinoma. PLoS Med. 2010;7:e1000307.
350. Badea L, Herlea V, Dima SO, Dumitrascu T, Popescu I. Combined gene expression analysis of whole-tissue and microdissected pancreatic ductal adenocarcinoma identifies genes specifically overexpressed in tumor epithelia. Hepatogastroenterology. 2008;55:2016-27.
351. Zhang Z, Chen Z, Song Y, Zhang P, Hu J, Bai C. Expression of aquaporin 5 increases proliferation and metastasis potential of lung cancer. J Pathol. 2010;221:210-20.
352. Chen Y, Knosel T, Ye F, Pacyna-Gengelbach M, Deutschmann N, Petersen I. Decreased PITX1 homeobox gene expression in human lung cancer. Lung Cancer. 2007;55:287-94.

353. Jungert K, Buck A, Buchholz M, Wagner M, Adler G, Gress TM, Ellenrieder V. Smad-Sp1 complexes mediate TGFbeta-induced early transcription of oncogenic Smad7 in pancreatic cancer cells. Carcinogenesis. 2006;27:2392-401.
354. Shiiba M, Nomura H, Shinozuka K, Saito K, Kouzu Y, Kasamatsu A, Sakamoto Y, Murano A, Ono K, Ogawara K, Uzawa K, Tanzawa H. Down-regulated expression of SERPIN genes located on chromosome 18q21 in oral squamous cell carcinomas. Oncol Rep. 2010;24:241-9.
355. Kim HN, Choi DW, Lee KT, Lee JK, Heo JS, Choi SH, Paik SW, Rhee JC, Lowe AW. Gene expression profiling in lymph node-positive and lymph node-negative pancreatic cancer. Pancreas. 2007;34:325-34.
356. Hirono S, Yamaue H, Hoshikawa Y, Ina S, Tani M, Kawai M, Ushijima M, Matsuura M, Saiki Y, Saiura A, Yamamoto J, Miki Y, Noda T. Molecular markers associated with lymph node metastasis in pancreatic ductal adenocarcinoma by genome-wide expression profiling. Cancer Sci. 2010;101:259-66.
357. Kumari SS, Varadaraj K. Intact AQP0 performs cell-to-cell adhesion. Biochem Biophys Res Commun. 2009;390:1034-9.
358. Fulda S. Caspase-8 in cancer biology and therapy. Cancer Lett. 2009;281:128-33.
359. Bair E, Tibshirani R. Semi-supervised methods to predict patient survival from gene expression data. PLoS Biol. 2004;2:E108.
360. Smith R, Xue A, Gill A, Scarlett C, Saxby A, Clarkson A, Hugh T. High expression of plasminogen activator inhibitor-2 (PAI-2) is a predictor of improved survival in patients with pancreatic adenocarcinoma. World J Surg. 2007;31:493-502.
361. Nunes-Xavier CE, Tarrega C, Cejudo-Marin R, Frijhoff J, Sandin A, Ostman A, Pulido R. Differential up-regulation of MAP kinase phosphatases MKP3/DUSP6 and DUSP5 by Ets2 and c-Jun converge in the control of the growth arrest versus proliferation response of MCF-7 breast cancer cells to phorbol ester. J Biol Chem. 2010;285:26417-30.
362. Kim H, Kang HJ, You KT, Kim SH, Lee KY, Kim TI, Kim C, Song SY, Kim HJ, Lee C. Suppression of human selenium-binding protein 1 is a late event in colorectal carcinogenesis and is associated with poor survival. Proteomics. 2006;6:3466-76.
363. Miyoshi N, Ishii H, Mimori K, Tanaka F, Hitora T, Tei M, Sekimoto M, Doki Y, Mori M. TGM2 is a novel marker for prognosis and therapeutic target in colorectal cancer. Ann Surg Oncol. 2010;17:967-72.
364. Goetz JG, Lajoie P, Wiseman SM, Nabi IR. Caveolin-1 in tumor progression: the good, the bad and the ugly. Cancer Metastasis Rev. 2008;27:715-35.
365. Jin D, Fan J, Wang L, Thompson LF, Liu A, Daniel BJ, Shin T, Curiel TJ, Zhang B. CD73 on tumor cells impairs antitumor T-cell responses: a novel mechanism of tumor-induced immune suppression. Cancer Res. 2010;70:2245-55.
366. Salvesen HB, Carter SL, Mannelqvist M, Dutt A, Getz G, Stefansson IM, Raeder MB, Sos ML, Engelsen IB, Trovik J, Wik E, Greulich H, Bo TH, Jonassen I, Thomas RK, Zander T, Garraway LA, Oyan AM, Sellers WR, Kalland KH, Meyerson M, Akslen LA, Beroukhim R. Integrated genomic profiling of endometrial carcinoma associates aggressive tumors with indicators of PI3 kinase activation. PNAS. 2009;106:4834-9.
367. Marechal R, Demetter P, Nagy N, Berton A, Decaestecker C, Polus M, Closset J, Deviere J, Salmon I, Van Laethem JL. High expression of CXCR4 may predict poor survival in resected pancreatic adenocarcinoma. Br J Cancer. 2009;100:1444-51.
368. Hartel M, Narla G, Wente MN, Giese NA, Martignoni ME, Martignetti JA, Friess H, Friedman SL. Increased alternative splicing of the KLF6 tumour suppressor gene correlates with prognosis and tumour grade in patients with pancreatic cancer. Eur J Cancer. 2008;44:1895-903.
369. Alexander NR, Tran NL, Rekapally H, Summers CE, Glackin C, Heimark RL. N-cadherin gene expression in prostate carcinoma is modulated by integrin-dependent nuclear translocation of Twist1. Cancer Res. 2006;66:3365-9.
370. Subramanian J, Simon R. Gene expression-based prognostic signatures in lung cancer: ready for clinical use? J Natl Cancer Inst. 2010;102:464-74.
371. Ryu JK, Hong SM, Karikari CA, Hruban RH, Goggins MG, Maitra A. Aberrant MicroRNA-155 expression is an early event in the multistep progression of pancreatic adenocarcinoma. Pancreatology. 2010;10:66-73.
372. Lewis BP, Burge CB, Bartel DP. Conserved seed pairing, often flanked by adenosines, indicates that thousands of human genes are microRNA targets. Cell. 2005;120:15-20.

373. Krek A, Grun D, Poy MN, Wolf R, Rosenberg L, Epstein EJ, MacMenamin P, da Piedade I, Gunsalus KC, Stoffel M, Rajewsky N. Combinatorial microRNA target predictions. Nat Genet. 2005;37:495-500.
374. Papadopoulos GL, Alexiou P, Maragkakis M, Reczko M, Hatzigeorgiou AG. DIANA-mirPath: Integrating human and mouse microRNAs in pathways. Bioinformatics. 2009;25:1991-3.
375. Gudas LJ, Wagner JA. Retinoids regulate stem cell differentiation. J Cell Physiol. 2011;226:322-30.
376. Kent OA, Mullendore M, Wentzel EA, Lopez-Romero P, Tan AC, Alvarez H, West K, Ochs MF, Hidalgo M, Arking DE, Maitra A, Mendell JT. A resource for analysis of microRNA expression and function in pancreatic ductal adenocarcinoma cells. Cancer Biol Ther. 2009;8:2013-24.
377. Schetter AJ, Leung SY, Sohn JJ, Zanetti KA, Bowman ED, Yanaihara N, Yuen ST, Chan TL, Kwong DL, Au GK, Liu CG, Calin GA, Croce CM, Harris CC. MicroRNA expression profiles associated with prognosis and therapeutic outcome in colon adenocarcinoma. JAMA. 2008;299:425-36.
378. Avissar M, McClean MD, Kelsey KT, Marsit CJ. MicroRNA expression in head and neck cancer associates with alcohol consumption and survival. Carcinogenesis. 2009;30:2059-63.
379. Tchernitsa O, Kasajima A, Schafer R, Kuban RJ, Ungethum U, Gyorffy B, Neumann U, Simon E, Weichert W, Ebert MP, Rocken C. Systematic evaluation of the miRNA-ome and its downstream effects on mRNA expression identifies gastric cancer progression. J Pathol. 2010;222:310-9.
380. Schulte JH, Marschall T, Martin M, Rosenstiel P, Mestdagh P, Schlierf S, Thor T, Vandesompele J, Eggert A, Schreiber S, Rahmann S, Schramm A. Deep sequencing reveals differential expression of microRNAs in favorable versus unfavorable neuroblastoma. Nucleic Acids Res. 2010;38:5919-28.
381. Dillhoff M, Liu J, Frankel W, Croce C, Bloomston M. MicroRNA-21 is overexpressed in pancreatic cancer and a potential predictor of survival. J Gastrointest Surg. 2008;12:2171-6.
382. Krichevsky AM, Gabriely G. miR-21: a small multi-faceted RNA. J Cell Mol Med. 2009;13:39-53.
383. Meng F, Henson R, Wehbe-Janek H, Ghoshal K, Jacob ST, Patel T. MicroRNA-21 regulates expression of the PTEN tumor suppressor gene in human hepatocellular cancer. Gastroenterology. 2007;133:647-58.
384. Moriyama T, Ohuchida K, Mizumoto K, Yu J, Sato N, Nabae T, Takahata S, Toma H, Nagai E, Tanaka M. MicroRNA-21 modulates biological functions of pancreatic cancer cells including their proliferation, invasion, and chemoresistance. Mol Cancer Ther. 2009.
385. Lu Z, Liu M, Stribinskis V, Klinge CM, Ramos KS, Colburn NH, Li Y. MicroRNA-21 promotes cell transformation by targeting the programmed cell death 4 gene. Oncogene. 2008;27:4373-9.
386. Hermeking H. The miR-34 family in cancer and apoptosis. Cell Death Differ. 2010;17:193-9.
387. Ji Q, Hao X, Zhang M, Tang W, Yang M, Li L, Xiang D, Desano JT, Bommer GT, Fan D, Fearon ER, Lawrence TS, Xu L. MicroRNA miR-34 inhibits human pancreatic cancer tumor-initiating cells. PLoS One. 2009;4:e6816.
388. Gallardo E, Navarro A, Vinolas N, Marrades RM, Diaz T, Gel B, Quera A, Bandres E, Garcia-Foncillas J, Ramirez J, Monzo M. miR-34a as a prognostic marker of relapse in surgically resected non-small-cell lung cancer. Carcinogenesis. 2009;30:1903-9.
389. Yao J, Liang L, Huang S, Ding J, Tan N, Zhao Y, Yan M, Ge C, Zhang Z, Chen T, Wan D, Yao M, Li J, Gu J, He X. MicroRNA-30d promotes tumor invasion and metastasis by targeting Galphai2 in hepatocellular carcinoma. Hepatology. 2010;51:846-56.
390. Pass HI, Goparaju C, Ivanov S, Donington J, Carbone M, Hoshen M, Cohen D, Chajut A, Rosenwald S, Dan H, Benjamin S, Aharonov R. hsa-miR-29c* is linked to the prognosis of malignant pleural mesothelioma. Cancer Res. 2010;70:1916-24.
391. Zhao JJ, Lin J, Lwin T, Yang H, Guo J, Kong W, Dessureault S, Moscinski LC, Rezania D, Dalton WS, Sotomayor E, Tao J, Cheng JQ. microRNA expression profile and identification of miR-29 as a prognostic marker and pathogenetic factor by targeting CDK6 in mantle cell lymphoma. Blood. 2010;115:2630-9.
392. Galardi S, Mercatelli N, Giorda E, Massalini S, Frajese GV, Ciafre SA, Farace MG. miR-221 and miR-222 expression affects the proliferation potential of human prostate carcinoma cell lines by targeting p27Kip1. J Biol Chem. 2007;282:23716-24.
393. du Rieu MC, Torrisani J, Selves J, Al Saati T, Souque A, Dufresne M, Tsongalis GJ, Suriawinata AA, Carrere N, Buscail L, Cordelier P. MicroRNA-21 is induced early in pancreatic ductal adenocarcinoma precursor lesions. Clin Chem. 2010;56:603-12.

394. Mattes J, Yang M, Foster PS. Regulation of microRNA by antagomirs: a new class of pharmacological antagonists for the specific regulation of gene function? Am J Respir Cell Mol Biol. 2007;36:8-12.
395. Szafranska AE, Doleshal M, Edmunds HS, Gordon S, Luttges J, Munding JB, Barth RJ, Jr., Gutmann EJ, Suriawinata AA, Marc Pipas J, Tannapfel A, Korc M, Hahn SA, Labourier E, Tsongalis GJ. Analysis of microRNAs in pancreatic fine-needle aspirates can classify benign and malignant tissues. Clin Chem. 2008;54:1716-24.
396. Wang J, Chen J, Chang P, LeBlanc A, Li D, Abbruzzesse JL, Frazier ML, Killary AM, Sen S. MicroRNAs in plasma of pancreatic ductal adenocarcinoma patients as novel blood-based biomarkers of disease. Cancer Prev Res. 2009;2:807-13.
397. Tonon G, Wong KK, Maulik G, Brennan C, Feng B, Zhang Y, Khatry DB, Protopopov A, You MJ, Aguirre AJ, Martin ES, Yang Z, Ji H, Chin L, Depinho RA. High-resolution genomic profiles of human lung cancer. PNAS. 2005;102:9625-30.
398. Zhao X, Weir BA, LaFramboise T, Lin M, Beroukhim R, Garraway L, Beheshti J, Lee JC, Naoki K, Richards WG, Sugarbaker D, Chen F, Rubin MA, Janne PA, Girard L, Minna J, Christiani D, Li C, Sellers WR, Meyerson M. Homozygous deletions and chromosome amplifications in human lung carcinomas revealed by single nucleotide polymorphism array analysis. Cancer Res. 2005;65:5561-70.
399. Jiao L, Bondy ML, Hassan MM, Chang DZ, Abbruzzese JL, Evans DB, Smolensky MH, Li D. Glutathione S-transferase gene polymorphisms and risk and survival of pancreatic cancer. Cancer. 2007;109:840-8.
400. Maser RS, Choudhury B, Campbell PJ, Feng B, Wong KK, Protopopov A, O'Neil J, Gutierrez A, Ivanova E, Perna I, Lin E, Mani V, Duke V, Foroni L, Fielding AK, Goldstone AH, Rowe JM, Wang YA, Look AT, Stratton MR, Chin L, Futreal PA, DePinho RA. Chromosomally unstable mouse tumours have genomic alterations similar to diverse human cancers. Nature. 2007;447:966-71.
401. Meyer C, Kowarz E, Hofmann J, Renneville A, Zuna J, Trka J, Ben Abdelali R, Macintyre E, De Braekeleer E, De Braekeleer M, Delabesse E, de Oliveira MP, Ilencikova D, Molkentin M, Burmeister T, Dingermann T, Klingebiel T, Marschalek R. New insights to the MLL recombinome of acute leukemias. Leukemia. 2009;23:1490-9.
402. Fukunaga E, Inoue Y, Komiya S, Horiguchi K, Goto K, Saitoh M, Miyazawa K, Koinuma D, Hanyu A, Imamura T. Smurf2 induces ubiquitin-dependent degradation of Smurf1 to prevent migration of breast cancer cells. J Biol Chem. 2008;283:35660-7.
403. Huang Y, Guigon CJ, Fan J, Cheng SY, Zhu GZ. Pituitary homeobox 2 (PITX2) promotes thyroid carcinogenesis by activation of cyclin D2. Cell Cycle. 2010;9.
404. Polo SE, Theocharis SE, Klijanienko J, Savignoni A, Asselain B, Vielh P, Almouzni G. Chromatin assembly factor-1, a marker of clinical value to distinguish quiescent from proliferating cells. Cancer Res. 2004;64:2371-81.
405. Ashktorab H, Schaffer AA, Daremipouran M, Smoot DT, Lee E, Brim H. Distinct genetic alterations in colorectal cancer. PLoS One. 2010;5:e8879.
406. Killian A, Sarafan-Vasseur N, Sesboue R, Le Pessot F, Blanchard F, Lamy A, Laurent M, Flaman JM, Frebourg T. Contribution of the BOP1 gene, located on 8q24, to colorectal tumorigenesis. Genes Chromosomes Cancer. 2006;45:874-81.
407. Iacobuzio-Donahue CA, van der Heijden MS, Baumgartner MR, Troup WJ, Romm JM, Doheny K, Pugh E, Yeo CJ, Goggins MG, Hruban RH, Kern SE. Large-scale allelotype of pancreaticobiliary carcinoma provides quantitative estimates of genome-wide allelic loss. Cancer Res. 2004;64:871-5.
408. Kim SY, Dunn IF, Firestein R, Gupta P, Wardwell L, Repich K, Schinzel AC, Wittner B, Silver SJ, Root DE, Boehm JS, Ramaswamy S, Lander ES, Hahn WC. CK1epsilon is required for breast cancers dependent on beta-catenin activity. PLoS One. 2010;5:e8979.
409. Wong SY, Seol AD, So PL, Ermilov AN, Bichakjian CK, Epstein EH, Jr., Dlugosz AA, Reiter JF. Primary cilia can both mediate and suppress Hedgehog pathway-dependent tumorigenesis. Nat Med. 2009;15:1055-61.
410. Chen B, Wang X, Zhao W, Wu J. Klotho inhibits growth and promotes apoptosis in human lung cancer cell line A549. J Exp Clin Cancer Res. 2010;29:99.
411. Visser S, Yang X. LATS tumor suppressor: a new governor of cellular homeostasis. Cell Cycle. 2010;9:3892-903.
412. Lee K, Liu Y, Mo JQ, Zhang J, Dong Z, Lu S. Vav3 oncogene activates estrogen receptor and its overexpression may be involved in human breast cancer. BMC Cancer. 2008;8:158.

413. Murphy NC, Scarlett CJ, Kench JG, Sum EY, Segara D, Colvin EK, Susanto J, Cosman PH, Lee CS, Musgrove EA, Sutherland RL, Lindeman GJ, Henshall SM, Visvader JE, Biankin AV. Expression of LMO4 and outcome in pancreatic ductal adenocarcinoma. Br J Cancer. 2008;98:537-41.
414. Masson E, Le Marechal C, Chen JM, Ferec C. Absence of mesotrypsinogen gene (PRSS3) copy number variations in patients with chronic pancreatitis. Pancreas. 2008;37:227-8.
415. Marsit CJ, Karagas MR, Schned A, Kelsey KT. Carcinogen exposure and epigenetic silencing in bladder cancer. Ann N Y Acad Sci. 2006;1076:810-21.
416. Yoshisue H, Puddicombe SM, Wilson SJ, Haitchi HM, Powell RM, Wilson DI, Pandit A, Berger AE, Davies DE, Holgate ST, Holloway JW. Characterization of ciliated bronchial epithelium 1, a ciliated cell-associated gene induced during mucociliary differentiation. Am J Respir Cell Mol Biol. 2004;31:491-500.
417. Chen S, Auletta T, Dovirak O, Hutter C, Kuntz K, El-Ftesi S, Kendall J, Han H, Von Hoff DD, Ashfaq R, Maitra A, Iacobuzio-Donahue CA, Hruban RH, Lucito R. Copy number alterations in pancreatic cancer identify recurrent PAK4 amplification. Cancer Biol Ther. 2008;7:1793-1802.
418. Kimmelman AC, Hezel AF, Aguirre AJ, Zheng H, Paik JH, Ying H, Chu GC, Zhang JX, Sahin E, Yeo G, Ponugoti A, Nabioullin R, Deroo S, Yang S, Wang X, McGrath JP, Protopopova M, Ivanova E, Zhang J, Feng B, Tsao MS, Redston M, Protopopov A, Xiao Y, Futreal PA, Hahn WC, Klimstra DS, Chin L, DePinho RA. Genomic alterations link Rho family of GTPases to the highly invasive phenotype of pancreas cancer. PNAS. 2008;105:19372-7.
419. Hara-Chikuma M, Verkman AS. Aquaporin-3 facilitates epidermal cell migration and proliferation during wound healing. J Mol Med. 2008;86:221-31.
420. Prasad NB, Biankin AV, Fukushima N, Maitra A, Dhara S, Elkahloun AG, Hruban RH, Goggins M, Leach SD. Gene expression profiles in pancreatic intraepithelial neoplasia reflect the effects of Hedgehog signaling on pancreatic ductal epithelial cells. Cancer Res. 2005;65:1619-26.
421. Jiang L, Chen Y, Chan CY, Wang X, Lin L, He ML, Lin MC, Yew DT, Sung JJ, Li JC, Kung HF. Down-regulation of stathmin is required for TGF-beta inducible early gene 1 induced growth inhibition of pancreatic cancer cells. Cancer Lett. 2009;274:101-8.
422. Tomshine JC, Severson SR, Wigle DA, Sun Z, Beleford DA, Shridhar V, Horazdovsky BF. Cell proliferation and epidermal growth factor signaling in non-small cell lung adenocarcinoma cell lines are dependent on Rin1. J Biol Chem. 2009;284:26331-9.
423. Morris MR, Ricketts C, Gentle D, Abdulrahman M, Clarke N, Brown M, Kishida T, Yao M, Latif F, Maher ER. Identification of candidate tumour suppressor genes frequently methylated in renal cell carcinoma. Oncogene. 2010;29:2104-17.
424. Hosokawa M, Kashiwaya K, Eguchi H, Ohigashi H, Ishikawa O, Furihata M, Shinomura Y, Imai K, Nakamura Y, Nakagawa H. Over-expression of cysteine proteinase inhibitor cystatin 6 promotes pancreatic cancer growth. Cancer Sci. 2008;99:1626-32.
425. Herath NI, Doecke J, Spanevello MD, Leggett BA, Boyd AW. Epigenetic silencing of EphA1 expression in colorectal cancer is correlated with poor survival. Br J Cancer. 2009;100:1095-102.
426. Johnson NA, Hamoudi RA, Ichimura K, Liu L, Pearson DM, Collins VP, Du MQ. Application of array CGH on archival formalin-fixed paraffin-embedded tissues including small numbers of microdissected cells. Lab Invest. 2006;86:968-78.
427. Kitoh H, Ryozawa S, Harada T, Kondoh S, Furuya T, Kawauchi S, Oga A, Okita K, Sasaki K. Comparative genomic hybridization analysis for pancreatic cancer specimens obtained by endoscopic ultrasonography-guided fine-needle aspiration. J Gastroenterol. 2005;40:511-7.
428. Heidenblad M, Lindgren D, Veltman JA, Jonson T, Mahlamaki EH, Gorunova L, van Kessel AG, Schoenmakers EF, Hoglund M. Microarray analyses reveal strong influence of DNA copy number alterations on the transcriptional patterns in pancreatic cancer: implications for the interpretation of genomic amplifications. Oncogene. 2005;24:1794-801.
429. Mahoney CL, Choudhury B, Davies H, Edkins S, Greenman C, Haaften G, Mironenko T, Santarius T, Stevens C, Stratton MR, Futreal PA. LKB1/KRAS mutant lung cancers constitute a genetic subset of NSCLC with increased sensitivity to MAPK and mTOR signalling inhibition. Br J Cancer. 2009;100:370-5.
430. Inoki K, Ouyang H, Zhu T, Lindvall C, Wang Y, Zhang X, Yang Q, Bennett C, Harada Y, Stankunas K, Wang CY, He X, MacDougald OA, You M, Williams BO, Guan KL. TSC2 integrates Wnt and energy signals via a coordinated phosphorylation by AMPK and GSK3 to regulate cell growth. Cell. 2006;126:955-68.
431. Demidenko ZN, Zubova SG, Bukreeva EI, Pospelov VA, Pospelova TV, Blagosklonny MV. Rapamycin decelerates cellular senescence. Cell Cycle. 2009;8:1888-95.

432. Calin GA, Sevignani C, Dumitru CD, Hyslop T, Noch E, Yendamuri S, Shimizu M, Rattan S, Bullrich F, Negrini M, Croce CM. Human microRNA genes are frequently located at fragile sites and genomic regions involved in cancers. PNAS. 2004;101:2999-3004.
433. Bray I, Bryan K, Prenter S, Buckley PG, Foley NH, Murphy DM, London WB, McGrady PW, Higgins DG, O'Meara A, O'Sullivan M, Stallings RL. Widespread dysregulation of MiRNAs by MYCN amplification and chromosomal imbalances in neuroblastoma: association of miRNA expression with survival. PLoS One. 2009;4:e7850.
434. Sun F, Fu H, Liu Q, Tie Y, Zhu J, Xing R, Sun Z, Zheng X. Downregulation of CCND1 and CDK6 by miR-34a induces cell cycle arrest. FEBS letters. 2008;582:1564-8.
435. Chang TC, Wentzel EA, Kent OA, Ramachandran K, Mullendore M, Lee KH, Feldmann G, Yamakuchi M, Ferlito M, Lowenstein CJ, Arking DE, Beer MA, Maitra A, Mendell JT. Transactivation of miR-34a by p53 broadly influences gene expression and promotes apoptosis. Mol Cell. 2007;26:745-52.
436. Bagchi A, Papazoglu C, Wu Y, Capurso D, Brodt M, Francis D, Bredel M, Vogel H, Mills AA. CHD5 is a tumor suppressor at human 1p36. Cell. 2007;128:459-75.
437. Calhoun ES, Hucl T, Gallmeier E, West KM, Arking DE, Maitra A, Iacobuzio-Donahue CA, Chakravarti A, Hruban RH, Kern SE. Identifying allelic loss and homozygous deletions in pancreatic cancer without matched normals using high-density single-nucleotide polymorphism arrays. Cancer Res. 2006;66:7920-8.
438. Phillips JL, Hayward SW, Wang Y, Vasselli J, Pavlovich C, Padilla-Nash H, Pezullo JR, Ghadimi BM, Grossfeld GD, Rivera A, Linehan WM, Cunha GR, Ried T. The consequences of chromosomal aneuploidy on gene expression profiles in a cell line model for prostate carcinogenesis. Cancer Res. 2001;61:8143-9.
439. Hyman E, Kauraniemi P, Hautaniemi S, Wolf M, Mousses S, Rozenblum E, Ringner M, Sauter G, Monni O, Elkahloun A, Kallioniemi OP, Kallioniemi A. Impact of DNA amplification on gene expression patterns in breast cancer. Cancer Res. 2002;62:6240-5.
440. Carrasco DR, Tonon G, Huang Y, Zhang Y, Sinha R, Feng B, Stewart JP, Zhan F, Khatry D, Protopopova M, Protopopov A, Sukhdeo K, Hanamura I, Stephens O, Barlogie B, Anderson KC, Chin L, Shaughnessy JD, Jr., Brennan C, Depinho RA. High-resolution genomic profiles define distinct clinico-pathogenetic subgroups of multiple myeloma patients. Cancer Cell. 2006;9:313-25.
441. Albertson DG, Collins C, McCormick F, Gray JW. Chromosome aberrations in solid tumors. Nat Genet. 2003;34:369-76.
442. Zhu H, Kavsak P, Abdollah S, Wrana JL, Thomsen GH. A SMAD ubiquitin ligase targets the BMP pathway and affects embryonic pattern formation. Nature. 1999;400:687-93.
443. Garrido-Laguna I, Tan AC, Uson M, Angenendt M, Ma WW, Villaroel MC, Zhao M, Rajeshkumar NV, Jimeno A, Donehower R, Iacobuzio-Donahue C, Barrett M, Rudek MA, Rubio-Viqueira B, Laheru D, Hidalgo M. Integrated preclinical and clinical development of mTOR inhibitors in pancreatic cancer. Br J Cancer. 2010;103:649-55.
444. Maeda T, Hobbs RM, Merghoub T, Guernah I, Zelent A, Cordon-Cardo C, Teruya-Feldstein J, Pandolfi PP. Role of the proto-oncogene Pokemon in cellular transformation and ARF repression. Nature. 2005;433:278-85.
445. Choi WI, Jeon BN, Yun CO, Kim PH, Kim SE, Choi KY, Kim SH, Hur MW. Proto-oncogene FBI-1 represses transcription of p21CIP1 by inhibition of transcription activation by p53 and Sp1. J Biol Chem. 2009;284:12633-44.
446. Park JK, Lee EJ, Esau C, Schmittgen TD. Antisense inhibition of microRNA-21 or -221 arrests cell cycle, induces apoptosis, and sensitizes the effects of gemcitabine in pancreatic adenocarcinoma. Pancreas. 2009;38:190-9.
447. Hall DC, Johnson-Pais TL, Grubbs B, Bernal R, Leach RJ, Padalecki SS. Maspin reduces prostate cancer metastasis to bone. Urol Oncol. 2008;26:652-8.
448. Zhu S, Wu H, Wu F, Nie D, Sheng S, Mo YY. MicroRNA-21 targets tumor suppressor genes in invasion and metastasis. Cell Res. 2008;18:350-9.
449. Cao D, Zhang Q, Wu LS, Salaria SN, Winter JW, Hruban RH, Goggins MS, Abbruzzese JL, Maitra A, Ho L. Prognostic significance of maspin in pancreatic ductal adenocarcinoma: tissue microarray analysis of 223 surgically resected cases. Mod Pathol. 2007;20:570-8.
450. Katz MH, Wang H, Fleming JB, Sun CC, Hwang RF, Wolff RA, Varadhachary G, Abbruzzese JL, Crane CH, Krishnan S, Vauthey JN, Abdalla EK, Lee JE, Pisters PW, Evans DB. Long-term survival after multidisciplinary management of resected pancreatic adenocarcinoma. Ann Surg Oncol. 2009;16:836-47.

451. DeOliveira ML, Winter JM, Schafer M, Cunningham SC, Cameron JL, Yeo CJ, Clavien PA. Assessment of complications after pancreatic surgery: A novel grading system applied to 633 patients undergoing pancreaticoduodenectomy. Ann Surg. 2006;244:931-7.
452. Eppsteiner RW, Csikesz NG, McPhee JT, Tseng JF, Shah SA. Surgeon volume impacts hospital mortality for pancreatic resection. Ann Surg. 2009;249:635-40.
453. Singh H, Cousin MA, Ashley RH. Functional reconstitution of mammalian 'chloride intracellular channels' CLIC1, CLIC4 and CLIC5 reveals differential regulation by cytoskeletal actin. FEBS J. 2007;274:6306-16.
454. Onder TT, Gupta PB, Mani SA, Yang J, Lander ES, Weinberg RA. Loss of E-cadherin promotes metastasis via multiple downstream transcriptional pathways. Cancer Res. 2008;68:3645-54.
455. Jones S, Zhang X, Parsons DW, Lin JC, Leary RJ, Angenendt P, Mankoo P, Carter H, Kamiyama H, Jimeno A, Hong SM, Fu B, Lin MT, Calhoun ES, Kamiyama M, Walter K, Nikolskaya T, Nikolsky Y, Hartigan J, Smith DR, Hidalgo M, Leach SD, Klein AP, Jaffee EM, Goggins M, Maitra A, Iacobuzio-Donahue C, Eshleman JR, Kern SE, Hruban RH, Karchin R, Papadopoulos N, Parmigiani G, Vogelstein B, Velculescu VE, Kinzler KW. Core signaling pathways in human pancreatic cancers revealed by global genomic analyses. Science. 2008;321:1801-6.
456. Campbell PJ, Yachida S, Mudie LJ, Stephens PJ, Latimer C, McLaren S, Lin ML, McBride DJ, Varela I, Leroy C, Jia M, Menzies A, Butler AP, Teague JW, Griffin CA, Burton J, Swerdlow H, Quail MA, Stratton MR, Iacobuzio-Donahue C, Futreal PA. The patterns and dynamics of genomic instability in metastatic pancreatic cancer. Nature. 2010;467:1109-13.
457. Shi H, Maier S, Nimmrich I, Yan PS, Caldwell CW, Olek A, Huang TH. Oligonucleotide-based microarray for DNA methylation analysis: principles and applications. J Cell Biochem. 2003;88:138-43.

11 Appendices

11.1 Appendix 1 - Chapter 1 data

11.1.1 Summary of IHC prognostic biomarker studies in PDAC

Table 11.1 IHC molecular prognostic markers in PDAC

Excel file: contains detailed list with diagrammatic representation of PDAC IHC literature. This details the strength of prognostic studies both in terms of numbers and the level of significance (univariate/ multivariate) for over 400 IHC studies.

11.2 Appendix 2 - Chapter 2 data

11.2.1 Supplementary methods

The seven hepatopancreaticobiliary TMAs containing 248 specimens with 6 tumour cores and 2 normal cores for each specimen.

Excel file: Maps of the TMAs 1-7.

An example of a TMA map is shown in Figure 11.1.

11.3 Appendix 3 - Chapter 5 data

Table 11.2 All prognostic IHC studies reviewed in systematic review and meta-analysis

Excel file: detailing the 398 studies that were reviewed for the purpose of the systematic review and meta-analysis.

Table 11.3 Sample, study and methodological characteristics of the high quality cohort studies included in the systematic review

PDF file: details of the 83 main studies outlining the sample, study and methodological characteristics of the high quality cohort studies included in this systematic review are recorded within a supplementary table.

Figure 11.1 Tissue microarray map

Illustrating control tissue, PDAC cores (blue), ampullary adenocarcinoma cores (green), cholangiocarcinoma cores (orange), duodenal adenocarcinoma cores (purple) and normal cores (blue). The pattern of the control cores is altered on each TMA to allow orientation and differentiation of the TMAs.

Table 11.4 Proteins related to overall survival for resectable PDAC

Summary of the multivariate hazard ratios with 95% CIs for the eligible proteins, ranked according to Hanahan-Weinberg functional capabilities.

Protein	Total No. (PD)	Reference group	Compartment	HR (95% CI)	p value
Evading Apoptosis					
Bax*	126 (113)	<10% cells +	C, N	0.31 (0.17-0.56)	0.0001
Bcl-2*	227 (183)	<5% cells +	C, N	0.41 (0.27-0.63)	<0.0001
Survivin*	119 (106)	<10% cells +	C, N	0.46 (0.29-0.73)	0.001
Insensitivity to Antigrowth Signals					
14-3-3σ	300	Compared to ND	M, C	1.4 (0.9-2.20)	0.14
IEX-1*	78 (48)	<25% cells +	C	1.84 (1.22–2.82)	0.004
GADD45	72 (38)	<50% cells +	M, C	1.38 (0.78–2.45)	0.26
p21*	148 (37)	No stain	N	0.49 (0.33-0.73)	0.09
p27	352 (336)	<20% cells +	N	1.11 (0.84-1.47)	0.47
SMAD4	300	No stain	C	1.20 0.91-1.59)	0.21
SMAD7*	71	Compared to ND	C	0.39 (0.18-0.83)	0.014
TGFB-1*	61(31)	<30 cells +	C	0.44 (0.23-0.86)	0.015
Limitless Replicative Potential					
Akt*	65 (50)	Immunoscore < 100	C	0.40 (0.20-1.10)	0.043
pAkt	104 (89)	Relative to ND	C	0.59 (0.33-1.07)	0.08
Caveolin*	79	<50% cells +	M, C	1.88 (1.04-3.39)	0.036
Cyclin E*	75	<10% cells +	N	2.48 (1.39-4.41)	0.0021
EGFR	65 (50)	Immunoscore < 100	M	1.80 (0.80-4.20)	>0.05
Ezrin*	73	No stain	M, C	2.93 (1.58-2.30)	0.02
Erk	65 (50)	Immunoscore < 100	C	0.80 (0.30-2.10)	>0.05
pErk*	65 (50)	Immunoscore < 100	C	3.52 (1.41-9.01)	0.003
GPR54	53 (38)	No stain	C	1.22 (0.74-2.0)	0.43
HDGF*	50	Compared to ND 90% cells +	N, C	0.26 (0.08-0.65)	0.0026
Her2*	129 (88)	HerceptTest score 0-1	M	1.81 (1.07-3.04)	0.025
Ki67*	84	<10% cells +	N	2.42 (1.87-3.14)	0.005
MAP4K4*	66	<10% cells +	C	2.16 (1.10-4.23)	0.025
Metastin*	53 (38)	No stain	C	2.08 (1.1-4.7)	0.03
P53	287 (213)	<1% cells +	N	1.26 (0.93-1.70)	0.14
PPAR*	129	No stain	N	2.46 (1.04-5.78)	0.039
Rel65/P65‡	82	Semiquantitative score <6	N, C	RR 3.49	0.02
S100A2*	162 (75)	<30% cells +	C	3.23 (1.58-6.62)	0.0014
	439 (296)			1.87 (1.25-2.81)	0.0024
S100A4*	72	No stain	C	1.81 (1.01-3.27)	0.048
S100A6*	60	No stain	C	2.85 (1.43-5.71)	0.003
Skp2*	46 (35)	< 20% cells	N	6.05 (1.43-25.1)	0.014
VCP/p97*	83	Less than ND	C	2.42 (1.11-2.26)	<0.01
Transcription Factors					
LMO2*	164	<10% cells +	N	0.43 (0.28-0.66)	<0.001
LMO4*	120 (75)	<50% cells +	N	0.46 (0.21-0.99)	0.049
HMGA*	89 (83)	No stain	N	12.5 (2.70-57.5)	0.001
SP-1 *	42	<20% cells +	N	2.99 (1.06-8.46)	0.039
Tissue Invasion and Metastasis					
α5β1 Integrin*	31	<15% cells +	C	4.10 (1.15-14.7)	0.030
α6β1 Integrin*	42 (35)	<50% cells +	C, M	0.55 (0.29-0.78)	0.026
Actinin-4*	173	Relative to ND	M, C	2.23 (1.61-3.39)	0.000009
ADAM9*	59	No stain	M, C	2.85 (1.21-6.71)	<0.05
Claudin 18*	166	No stain	M	0.52 (0.32-0.84)	0.013
CXCR4*	71	Immunoscore ≤3	C	2.54 (1.27-5.1)	0.001
Cytokeratin 20*	76 (67)	No stain	M	2.15 (1.13-4.12)	0.02
Dysadherin*	125	<20% cells +	M	2.17 (1.14-4.14)	0.019
E-cadherin*	197	>90% cells +	M	1.80 (1.33-2.42)	0.0001
Galectin-3*	104	Staining < pancreatic nerve	C	2.06 (1.23-3.46)	0.006
Laminin γ2*	48	No stain	C, M	2.41 (1.18-4.93)	0.0161
Li-cadherin*	102	<25% cells +	M	2.04 (1.16-3.61)	0.01
Maspin*	229	<5% cells +	N, C	2.43 (1.36-4.34)	0.01
MMP7*	70	<30% +	C	3. 09 (1.22-10.8)	0.022
PAI-2*	46 (39)	No stain	C	2.72 (1.13-6.53)	0.001
PGP9.5*	65	<50% cells +	C	0.37 (0.21-0.65)	0.0006
SPARC (stromal) *	299	<10% cell +	S	1.89 (1.31-2.74)	0.001
Syndecan (stromal) *	144	<5% area +	S	1.70 (1.21-2.38)	0.002
Synuclein-γ*	62	<10% cells +	C, N	3.4 (1.51-7.51)	0.003
TROP2*	197 (105)	Immunoscore <4	M	1.8 (1.1-3.0)	0.009
UPAR*	42 (35)	<50% cells +	C	0.49 (0.28-0.82)	0.006
Angiogenesis					
APN/CD13*	50	<10% cells +	M, C	0.4 (0.19-0.84)	0.016
COX-2*	485 (384)	Immunoscore 0/+ <10% cells	C	1.39 (1.13-1.71)	0.002
DKK-3*	154	No stain	C	0.6 (0.40-0.94)	0.024
FGF	104 (80)	Immunoscore <1	C, S	1.56 (0.92-2.66)	0.098
FLT-1*	76 (30)	AQUA	C, M	9.87 (2.04-47.7)	0.004
HIF-1*	58	No stain	C	2.22 (0.99-4.99)	0.05
Midkine*	75	<10% cells +	C	2.14 (1.29-3.71)	0.003
PD-ECGF*	144	No stain	C	2.03 (1.22-3.38)	0.007
PEDF*	80 (61)	No cytoplasmic stain	C	0.39 (0.22-0.70)	0.0016
Tissue factor*	113 (78)	<25% cells +	C, M	2.01 (1.21-3.34)	0.008
VEGF	202 (178)	<10% cells +	C	1.34 (0.87-2.06)	0.18
Pancreatic Differentiation and Stem Cell Like Function					
CD133*	80	No stain	C	2.15 (1.21-3.87)	0.009
HOXB2*	59	<20% cells +	N	5.01 (2.36-10.6)	<0.0001
MUC-4*	135 (116)	<5% cells +	M, C	2.13 (1.24-3.65)	0.006
PDX-1*	35	>50% cells +	C	0.53 (0.28-0.95)	0.03
Chemotherapy					
ERCC	64	AQUA	C	1.54 (0.80-2.94)	0.194
GLUT-1*	60 (44)	No stain	M	2.81 (1.1-8.0)	0.034
hCNT3*	45	Median scoring <150	C	2.65 (1.19-5.87)	0.017
hENT1*	45	Median scoring <80	C	3.42 (1.44-8.81)	0.005
OPRT	99 (40)	No stain	C	0.90 (0.61-1.35)	0.62
RRM1*	64	AQUA	N	1.89 (1.01-3.48)	0.046
Thymidylate synthase	132 (116)	≤2 score	C	1.05 (0.73-1.51)	0.8
Altered Immunocompetence					
CD74*	68	<70% cells +	C	2.00 (1.3-3.2)	0.003
ILR1	31	<15% cells +	C	1.64 (0.38-7.02)	0.506
PD-L1*	51	<10% cells +	C	2.29 (1.12-4.68)	0.022
RCAS*	80 (61)	<5% cells +	C, M	3.09 (1.33-7.21)	0.009

HR = Hazard ratio, CI = Confidence interval, PD = Pancreaticoduodenectomy, C = Cytoplasm, M = Membrane, N = Nuclear, S = Stromal, ND = Normal distribution, RR = Relative risk

* For associations representing data from single study, p values calculated by multivariate Cox proportional-hazards modelling. For associations representing data from multiple studies, combined summary HRs are those calculated for the fixed effects general inverse variance method. Proteins with a statistical significance of $p < 0.05$ are marked.

‡ Prognostic significant only node negative cases (n = 26)

Figure 11.2 Kaplan-Meier survival curves of 119 patients undergoing PDAC resection

Clinicopathological factors significantly related to outcome for the TMA cohort (Log-rank test).

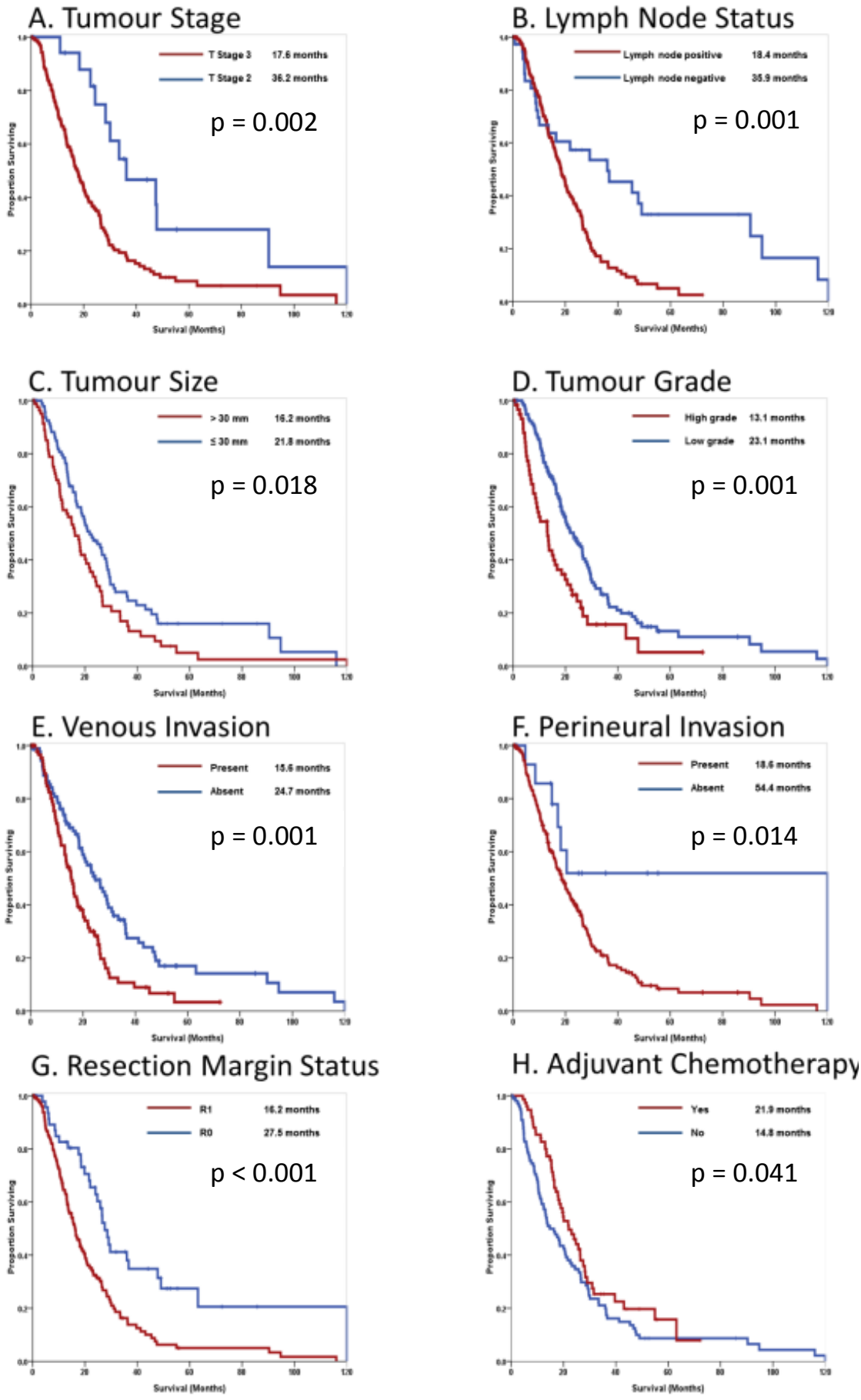

Median survival time illustrated

p value derived from Log-rank analysis

Figure 11.3 Immunohistochemical staining for multiple prognostic markers

A) *Lkb1, p21 and p53 immunostaining of normal pancreatic ductal tissue on tissue microarray (TMA)***.** *Representative immunostaining of Lkb1, p21 and p53 in PDAC TMA: illustrating no staining, low, moderate and strong staining.*

B) *COX-2 and Bcl-2 immunostaining of normal pancreatic ductal tissue on TMA. Representative immunostaining of COX-2 and Bcl-2 in PDAC TMA: illustrating no staining, low, moderate and strong staining.*

C) *β-catenin, E-cadherin and GSK3β immunostaining of normal pancreatic ductal tissue on TMA. Representative immunostaining of B-catenin, E-cadherin and GSK3β in PDAC TMA: illustrating no staining, low, moderate and strong staining.*

D) *Cyclin-D1, pAkt and Ki67 immunostaining of normal pancreatic ductal tissue on TMA. Representative immunostaining of cyclin-D1, pAkt and Ki67 in PDAC TMA: illustrating no staining, low, moderate and strong staining.*

E) *SMAD4 and TGFβ immunostaining of normal pancreatic ductal tissue on TMA. Representative immunostaining of SMAD4 and TGFβ in PDAC TMA: illustrating no staining, low, moderate and strong staining.*

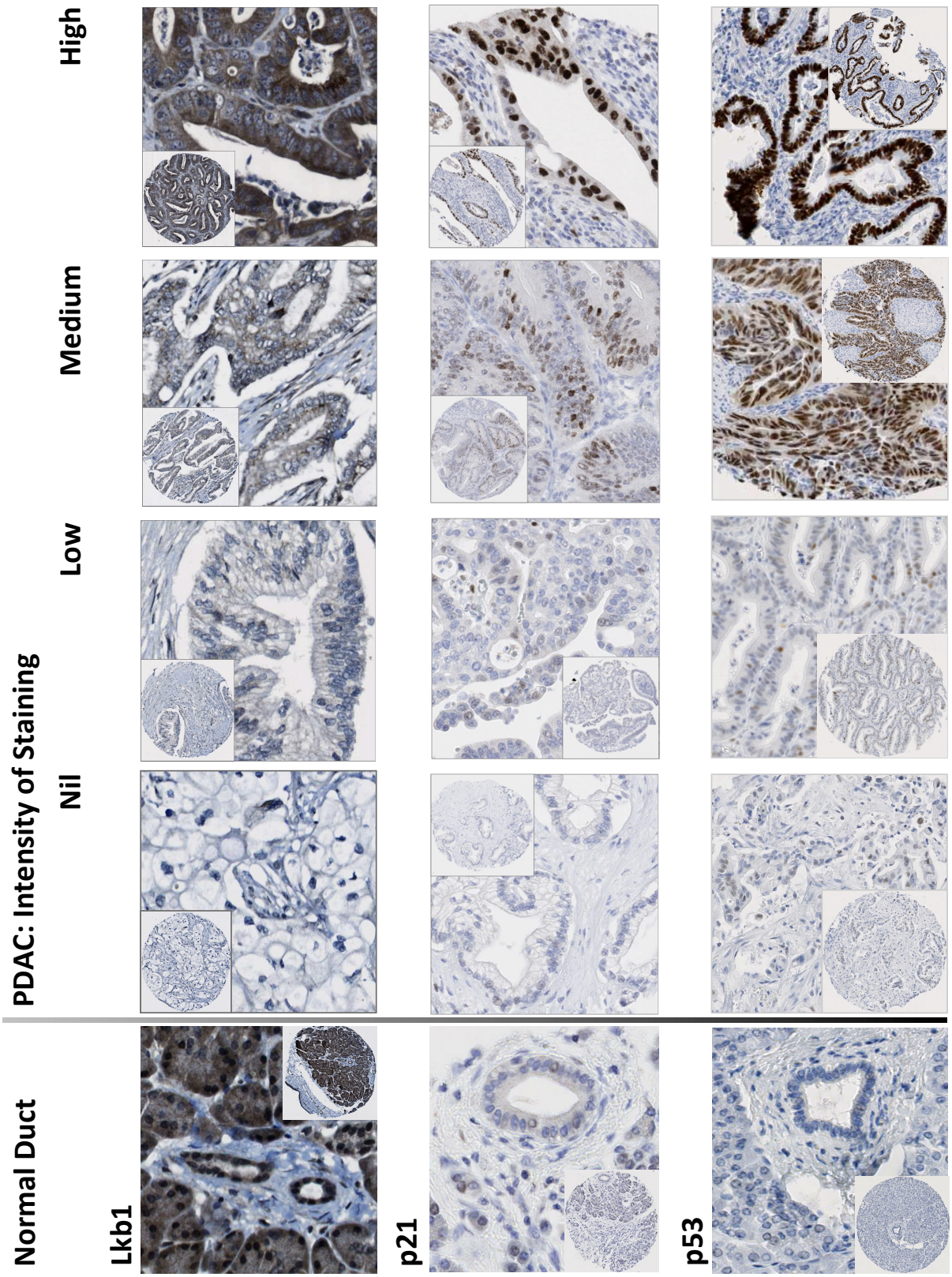
A
PDAC: Intensity of Staining
High
Medium
Low
Nil
Normal Duct
Lkb1
p21
p53

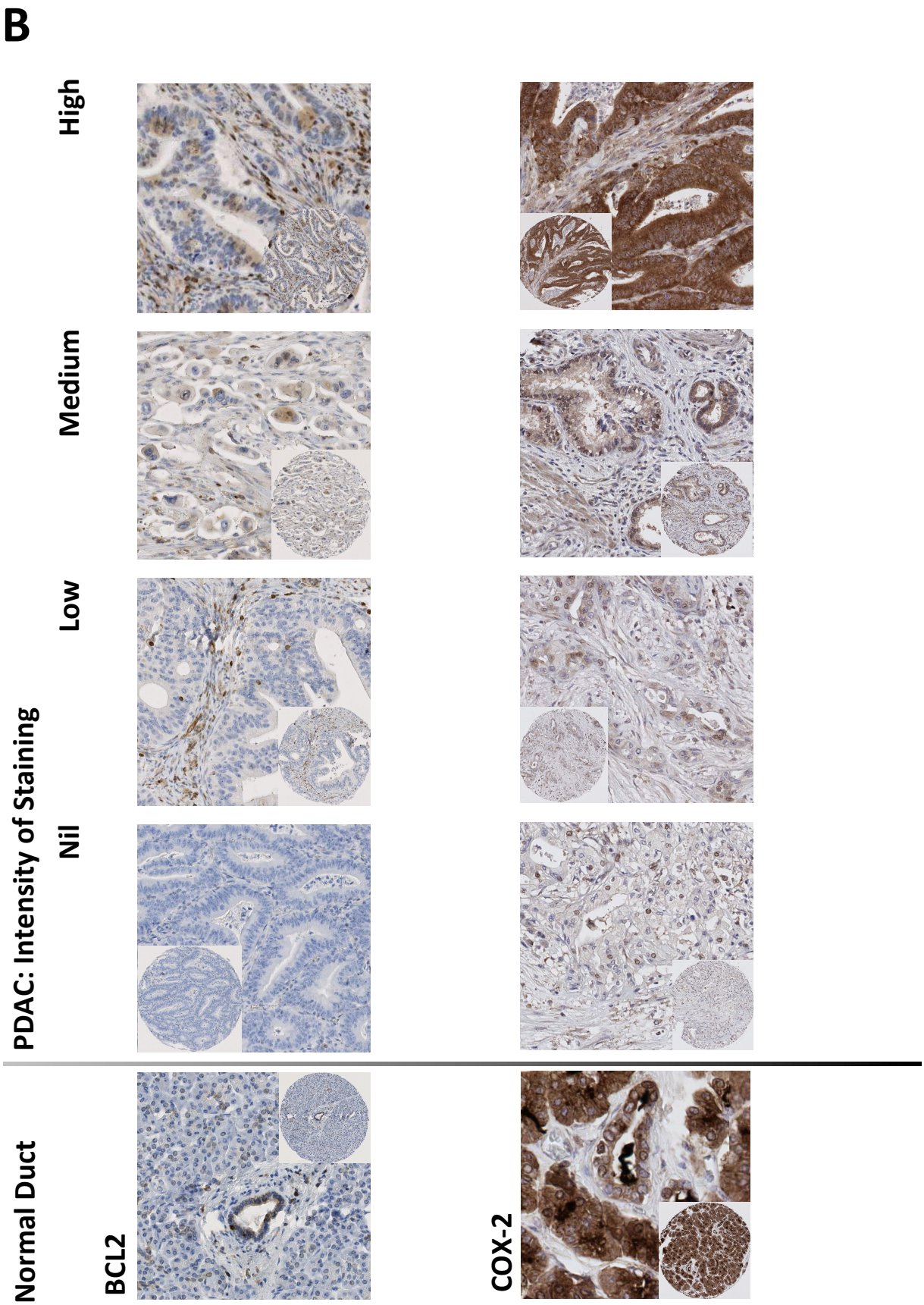
B
High
Medium
Low
Nil
PDAC: Intensity of Staining
Normal Duct
BCL2
COX-2

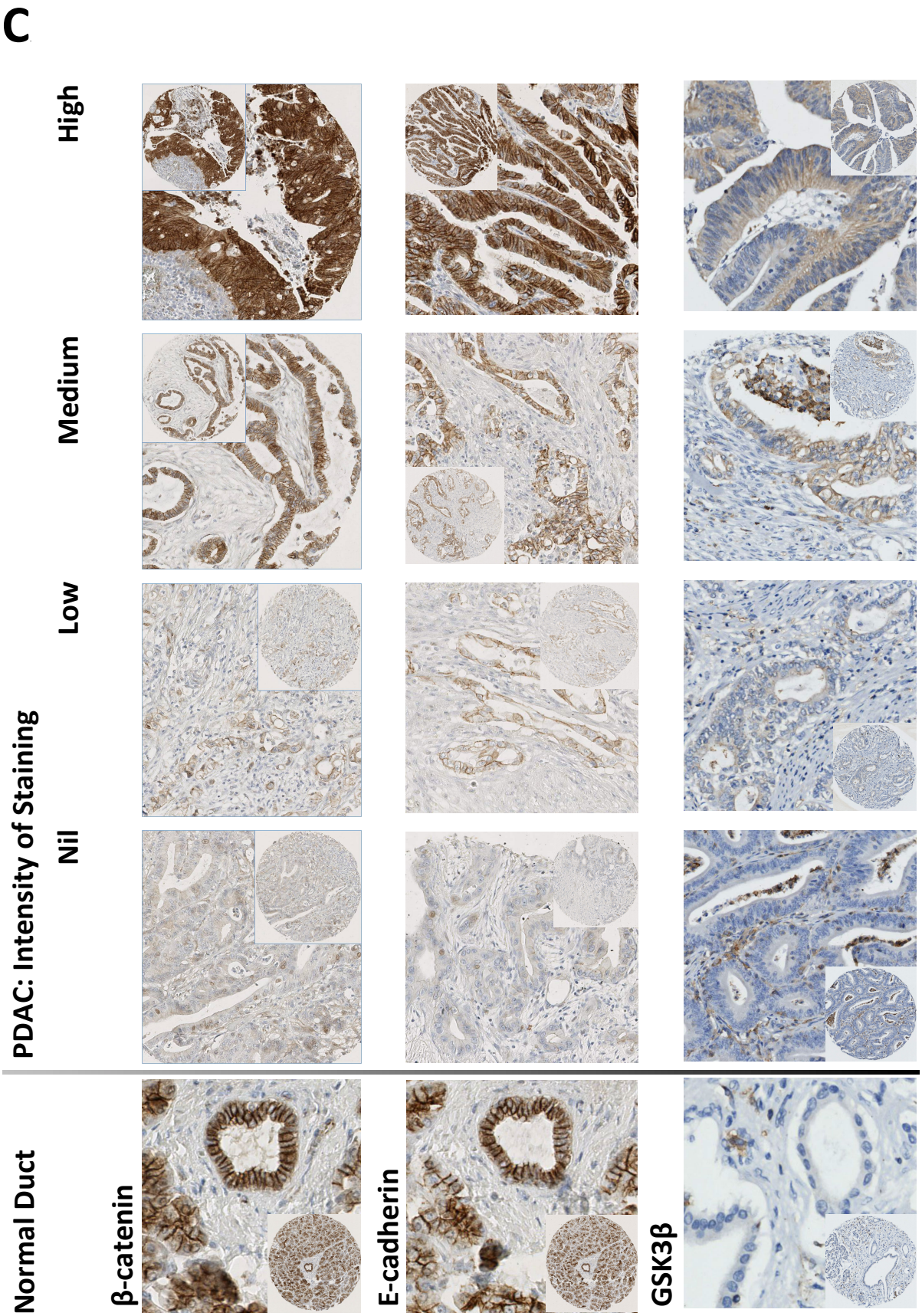
C
PDAC: Intensity of Staining
High
Medium
Low
Nil
Normal Duct
β-catenin
E-cadherin
GSK3β

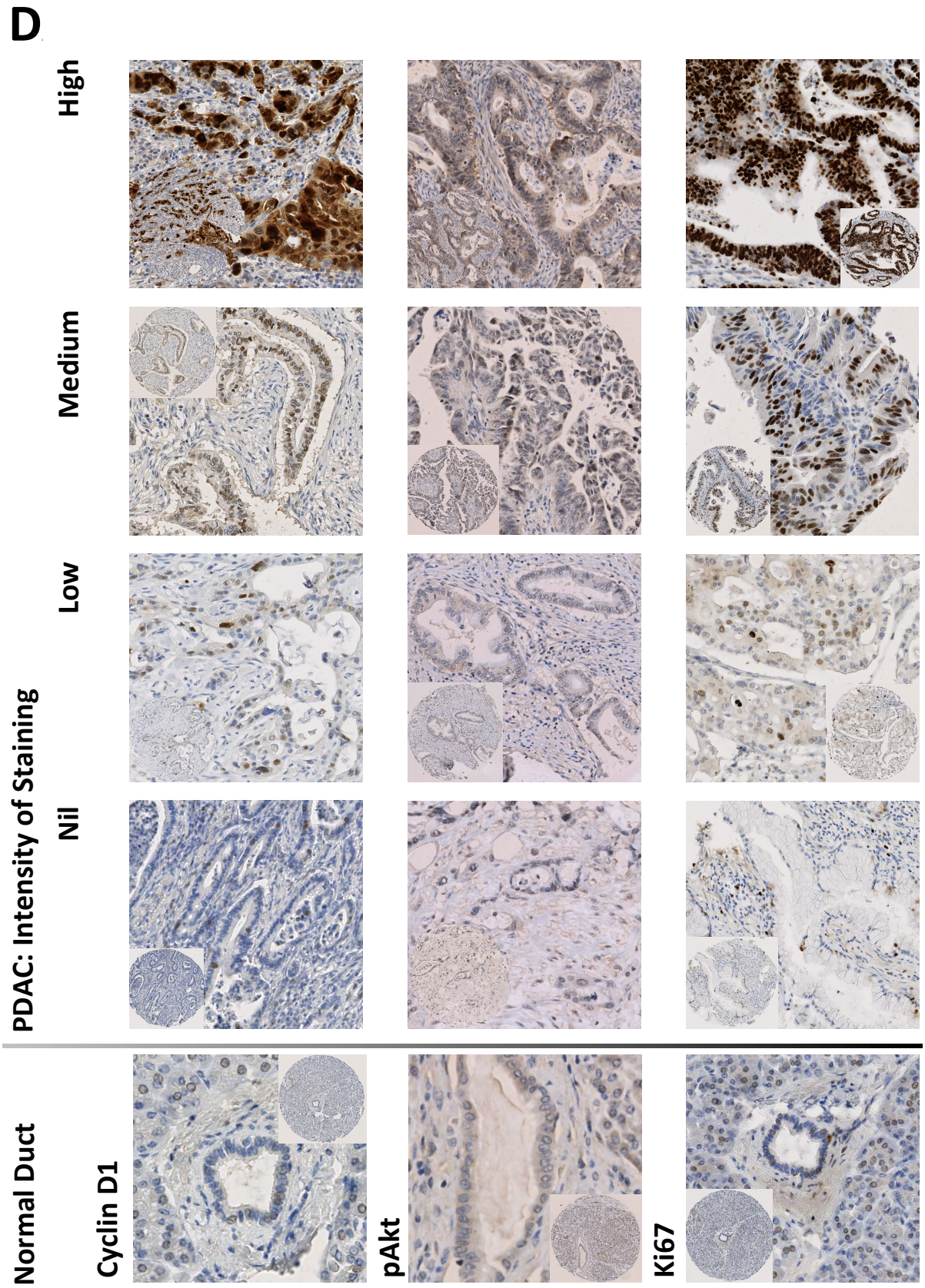
D
PDAC: Intensity of Staining
High
Medium
Low
Nil
Normal Duct
Cyclin D1
pAkt
Ki67

E

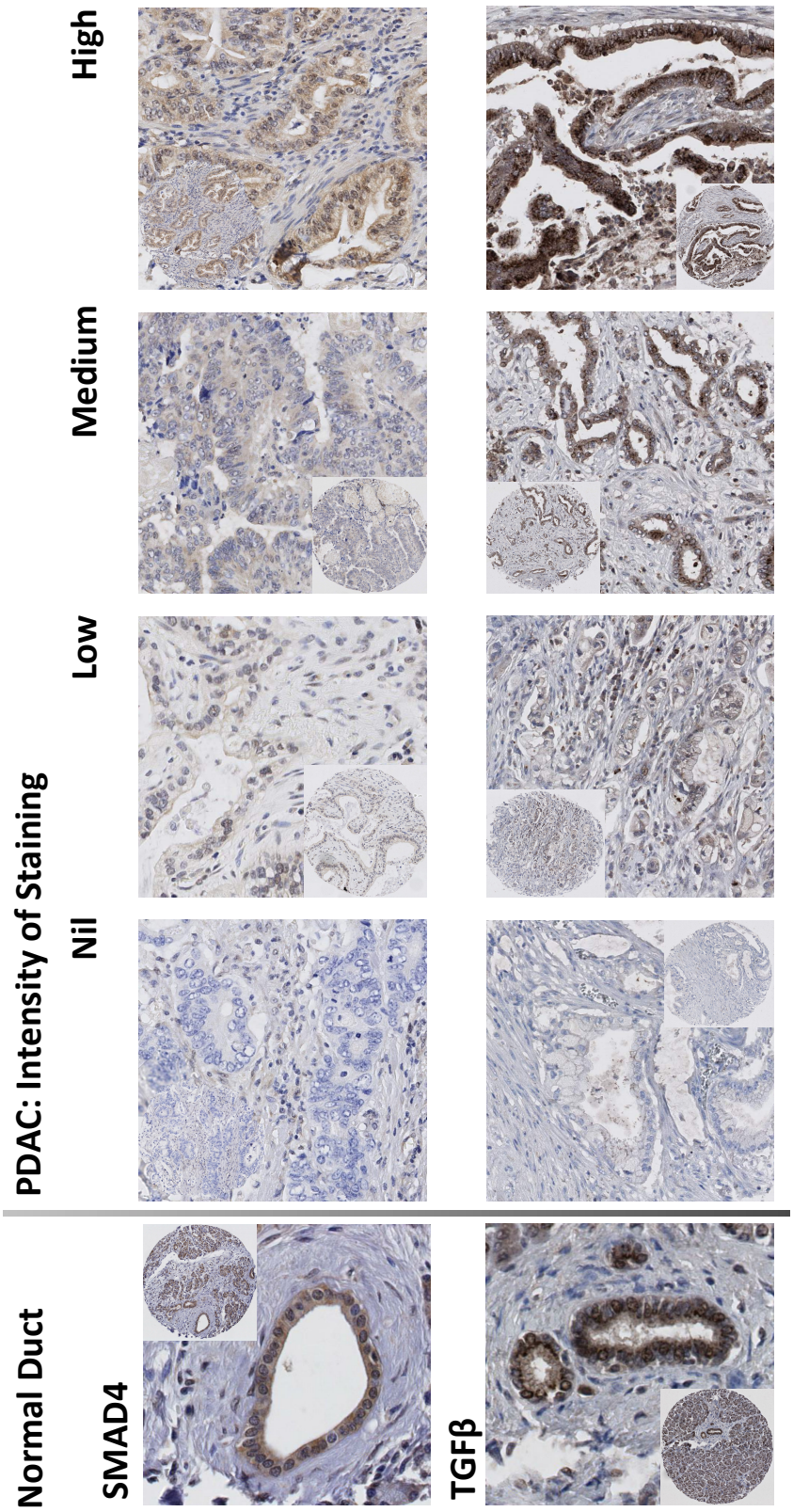
High
Medium
Low
Nil
PDAC: Intensity of Staining
Normal Duct
SMAD4
TGFβ

Figure 11.4 Kaplan-Meier survival curves for Bcl-2 expression

High Bcl-2 expression (n = 38) have prolonged outcome compared to those with low Bcl-2 expression (n = 81) following PD (p = 0.005, Log-rank test).

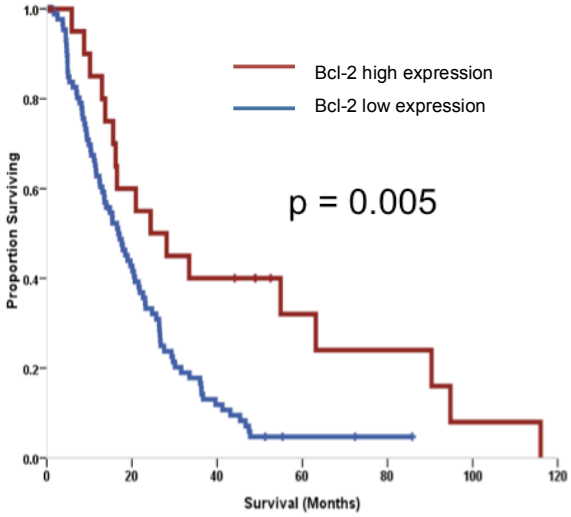

Figure 11.5 Invasion and metastasis signalling clinicopathological correlation

A) *Boxplot of membranous β-catenin expression according to tumour grade: Low grade tumours (n = 85) exhibited a higher level of β-catenin expression (median histoscore 128.2) versus high-grade tumours (n = 34) (median histoscore 76.5) (p < 0.0001, Mann-Whitney U test).*

B) *Kaplan-Meier analysis showing cases with high membranous β-catenin expression (n = 36) have better outcome compared to those with medium expression (n = 38) and far better than those with low expression (n = 44) following PD (p = 0.009, Log-rank test).*

C) *Boxplot of E-cadherin median histoscore versus tumour grade: Low grade tumours (n = 85) exhibited a higher level of β-catenin expression (median histoscore 143.0) versus high-grade tumours (n = 34) (median histoscore 93.1) (p < 0.0001, Mann-Whitney U test).*

D) *Kaplan-Meier analysis showing cases with high E-cadherin expression (n = 94) have better outcome compared to those with low expression (n = 25) following PD (p = 0.009, Log-rank test).*

E) *Kaplan-Meier analysis showing cases with high GSK3β expression (n = 19) have a worse outcome compared to those with low expression (n = 100) following PD (p = 0.015, Log-rank test).*

F) *Boxplot of GSK3β median histoscore compared to perineural invasion: tumours with an absence of perineural invasion (n = 12) exhibited a lower level of GSK3β expression (median histoscore 128.0) compared to tumours with perineural invasion (n = 117) (median histoscore 76.5) (p = 0.01, Mann-Whitney U test).*

G) *Correlation of β-catenin with E-cadherin protein expression in 119 cases of PDAC (Spearman's ρ correlation coefficient = 0.892; p < 0.001).*

H) *Correlation of β-catenin with GSK3β protein expression in 119 cases of PDAC (Spearman's ρ correlation coefficient =-0.289; p = 0.031).*

I) *Correlation of E-cadherin protein with GSK3β protein expression in 118 cases of PDAC (Spearman's ρ correlation coefficient = -0.312; p = 0.025).*

Figure 11.5

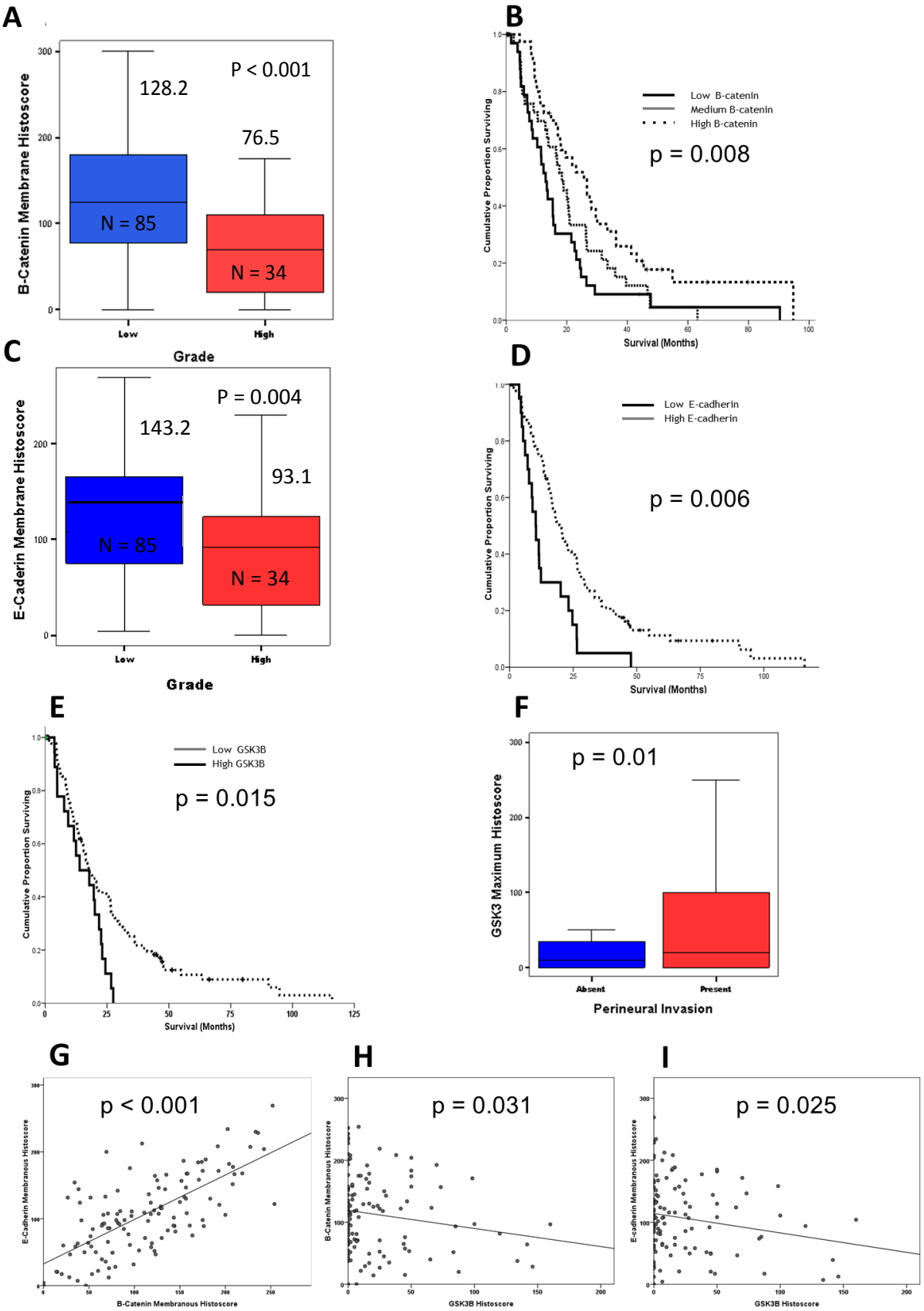
A
B-Catenin Membrane Histoscore
P < 0.001
128.2
76.5
N = 85
N = 34
Low
High
B
Cumulative Proportion Surviving
Low B-catenin
Medium B-catenin
High B-catenin
p = 0.008
Survival (Months)
C
Grade
E-Caderin Membrane Histoscore
P = 0.004
143.2
93.1
N = 85
N = 34
Low
High
Grade
D
Cumulative Proportion Surviving
Low E-cadherin
High E-cadherin
p = 0.006
Survival (Months)
E
Cumulative Proportion Surviving
Low GSK3B
High GSK3B
p = 0.015
Survival (Months)
F
GSK3 Maximum Histoscore
p = 0.01
Absent
Present
Perineural Invasion
G
p < 0.001
E-Cadherin Membranous Histoscore
B-Catenin Membranous Histoscore
H
p = 0.031
B-Catenin Membranous Histoscore
GSK3B Histoscore
I
p = 0.025
E-cadherin Membranous Histoscore
GSK3B Histoscore

Figure 11.6 COX-2 clinicopathological correlation

A) *Kaplan-Meier analysis showing PDACs with no COX-2 expression (n = 19) have better outcome compared to those with low expression (n = 79) and far better than those with high expression (n = 21) following pancreaticoduodenectomy (Log-rank test, p = 0.001).*

B) *Boxplot of COX-2 median cytoplasmic histoscore according to lymph node ratio (LNR). This demonstrates that PDAC with a LNR > 0.5 had significantly higher COX-2 expression than tumours with a LNR < 0.1 (p = 0.035) or a LNR 0.1–0.5 (p = 0.011, Mann-Whitney U test).*

C) *Kaplan-Meier analysis for patients with pancreatic ductal adenocarcinoma undergoing pancreaticoduodenectomy stratified by tumour size and cytoplasmic COX-2 expression. Large tumours with high cytoplasmic expression of COX-2 had a significantly shortened survival (median survival 6.1 months, 95%CI: 2.5–9.7) compared to small tumours with low cytoplasmic COX-2 expression (20.7 months, 95%CI: 12.2–29.2) (Log-rank test, p = 0.002).*

Investigation of the correlation between inflammatory pathways and β-catenin expression and Lkb1 expression in pancreatic cancer. Plot ***D)*** *illustrates a positive correlation between cytoplasmic Lkb1 expression and cytoplasmic COX-2 expression (Spearman's ρ correlation coefficient = 0.55, p < 0.001). Plot* ***E)*** *illustrates a positive correlation between membranous β-catenin expression and cytoplasmic COX-2 expression (Spearman's ρ correlation coefficient = 0.61, p < 0.001).*

Figure 11.6

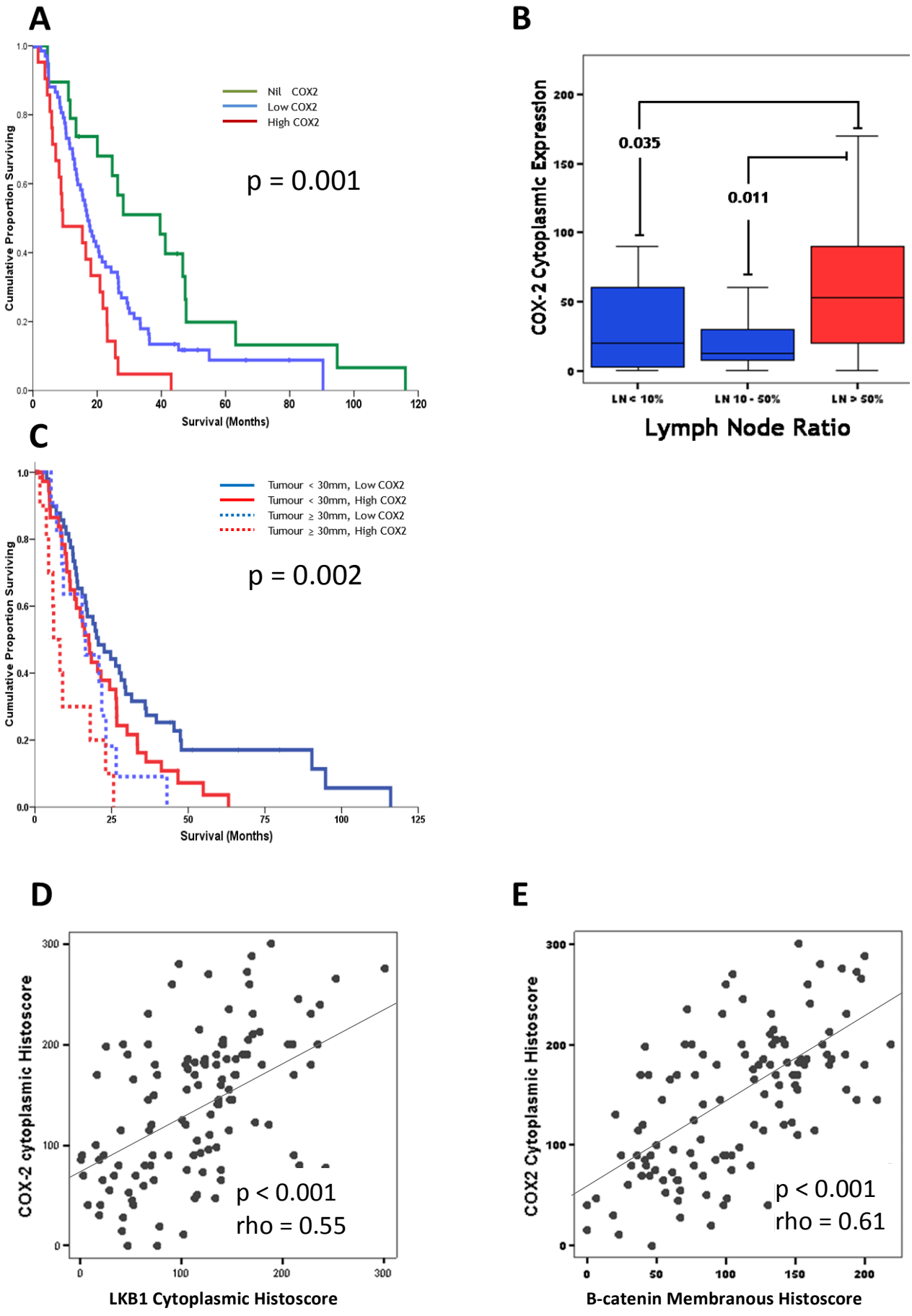
A
Nil COX2
Low COX2
High COX2
p = 0.001
Cumulative Proportion Surviving
Survival (Months)
B
0.035
0.011
COX-2 Cytoplasmic Expression
LN < 10%
LN 10 - 50%
LN > 50%
Lymph Node Ratio
C
Tumour < 30mm, Low COX2
Tumour < 30mm, High COX2
Tumour ≥ 30mm, Low COX2
Tumour ≥ 30mm, High COX2
p = 0.002
Cumulative Proportion Surviving
Survival (Months)
D
p < 0.001
rho = 0.55
COX-2 cytoplasmic Histoscore
LKB1 Cytoplasmic Histoscore
E
p < 0.001
rho = 0.61
COX2 Cytoplasmic Histoscore
B-catenin Membranous Histoscore

Figure 11.7 Self-sufficiency for growth signals clinicopathological correlation

A) *Boxplot of cyclin D1 expression (mean nuclear histoscore) according to lymph node status. This demonstrates that PDAC with lymph node involvement had significantly higher nuclear cyclin D1 expression (histoscore = 88.1) than lymph node negative tumours (histoscore = 62.3) (p = 0.002).*

B) *Kaplan-Meier analysis showing cases with low nuclear cyclin D1 expression (n = 38) have poorer outcome compared to those with high cyclin D1 expression (n = 81) following PD (p = 0.043).*

C) *Kaplan-Meier analysis showing cases with low pAkt expression (n = 26) have poorer outcome compared to those with high pAkt expression (n = 92) following PD (p = 0.031).*

D) *Kaplan-Meier analysis showing cases with low Ki67 expression (n = 40) have poorer outcome compared to those with high Ki67 expression (n = 79) following PD (p = 0.048).*

E) *Scatter plots demonstrating significant correlations between cyclin D1 versus SMAD4, p21, p53, COX-2 and pAkt versus Lkb1, COX-2 and Ki67.*

Figure 11.7

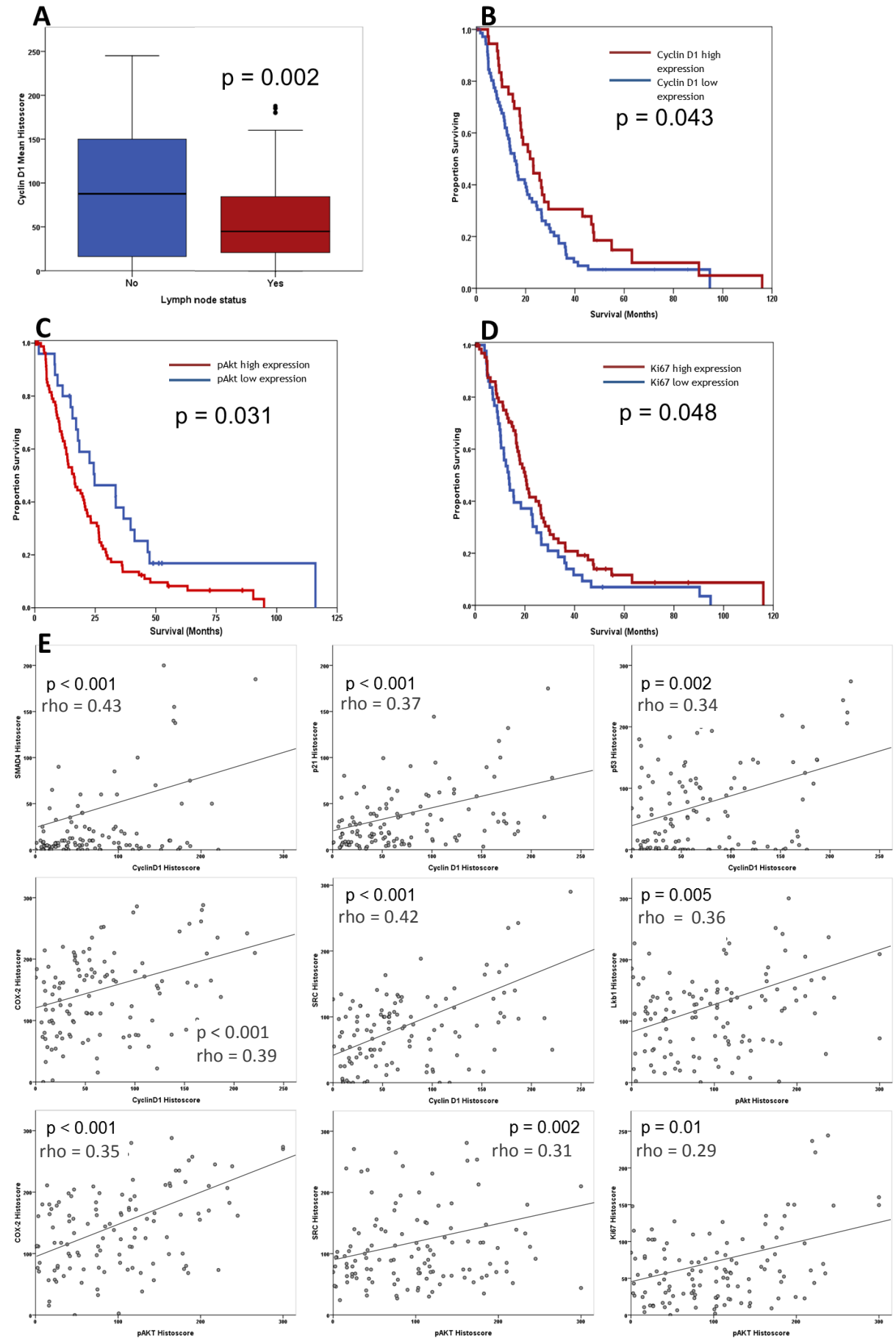
A
p = 0.002
Cyclin D1 Mean Histoscore
No
Yes
Lymph node status
B
Cyclin D1 high expression
Cyclin D1 low expression
p = 0.043
Proportion Surviving
Survival (Months)
C
pAkt high expression
pAkt low expression
p = 0.031
Proportion Surviving
Survival (Months)
D
Ki67 high expression
Ki67 low expression
p = 0.048
Proportion Surviving
Survival (Months)
E
p < 0.001
rho = 0.43
SNAD4 Histoscore
CyclinD1 Histoscore
p < 0.001
rho = 0.37
p21 Histoscore
Cyclin D1 Histoscore
p = 0.002
rho = 0.34
p53 Histoscore
CyclinD1 Histoscore
COX-2 Histoscore
p < 0.001
rho = 0.39
CyclinD1 Histoscore
p < 0.001
rho = 0.42
SRC Histoscore
Cyclin D1 Histoscore
p = 0.005
rho = 0.36
Lkb1 Histoscore
pAkt Histoscore
p < 0.001
rho = 0.35
COX-2 Histoscore
pAKT Histoscore
p = 0.002
rho = 0.31
SRC Histoscore
pAKT Histoscore
p = 0.01
rho = 0.29
Ki67 Histoscore
pAKT Histoscore

Figure 11.8 Insensitivity to growth inhibition clinicopathological correlation

A) *Kaplan-Meier analysis showing cases with low SMAD4 expression (n = 38) have poorer outcome compared to those with high SMAD4 expression (n = 81) following PD (p = 0.027, Log-rank test).*

B) *Kaplan-Meier analysis showing that there was no significant difference in survival when cases were stratified by high nuclear SMAD4 expression (n = 18) compared to those with low nuclear SMAD4 expression (n = 101) following PD (p = 0.33, Log-rank test).*

C) *Box plot illustrating that SMAD4 cytoplasmic expression is significantly reduced in the patients with distant metastases as the site of primary recurrence compared with patients with locoregional recurrence (n = 119) (p = 0.043, Mann-Whitney U test).*

D) *Kaplan-Meier analysis showing cases with low TGFβ expression (n = 58) have poorer outcome compared to those with high TGFβ expression (n = 61) following PD (p = 0.52, Log-rank test).*

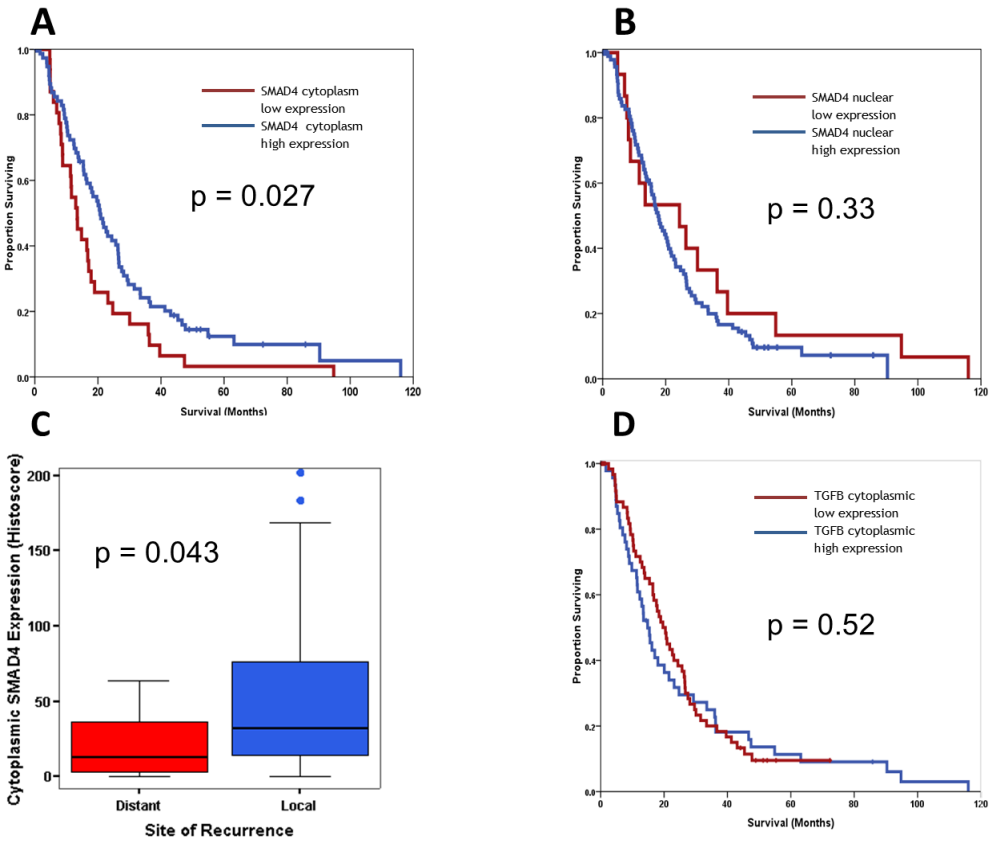

11.4 Appendix 4 - Chapter 6 data: gene expression analysis

Figure 11.9 Workflow for gene expression analysis

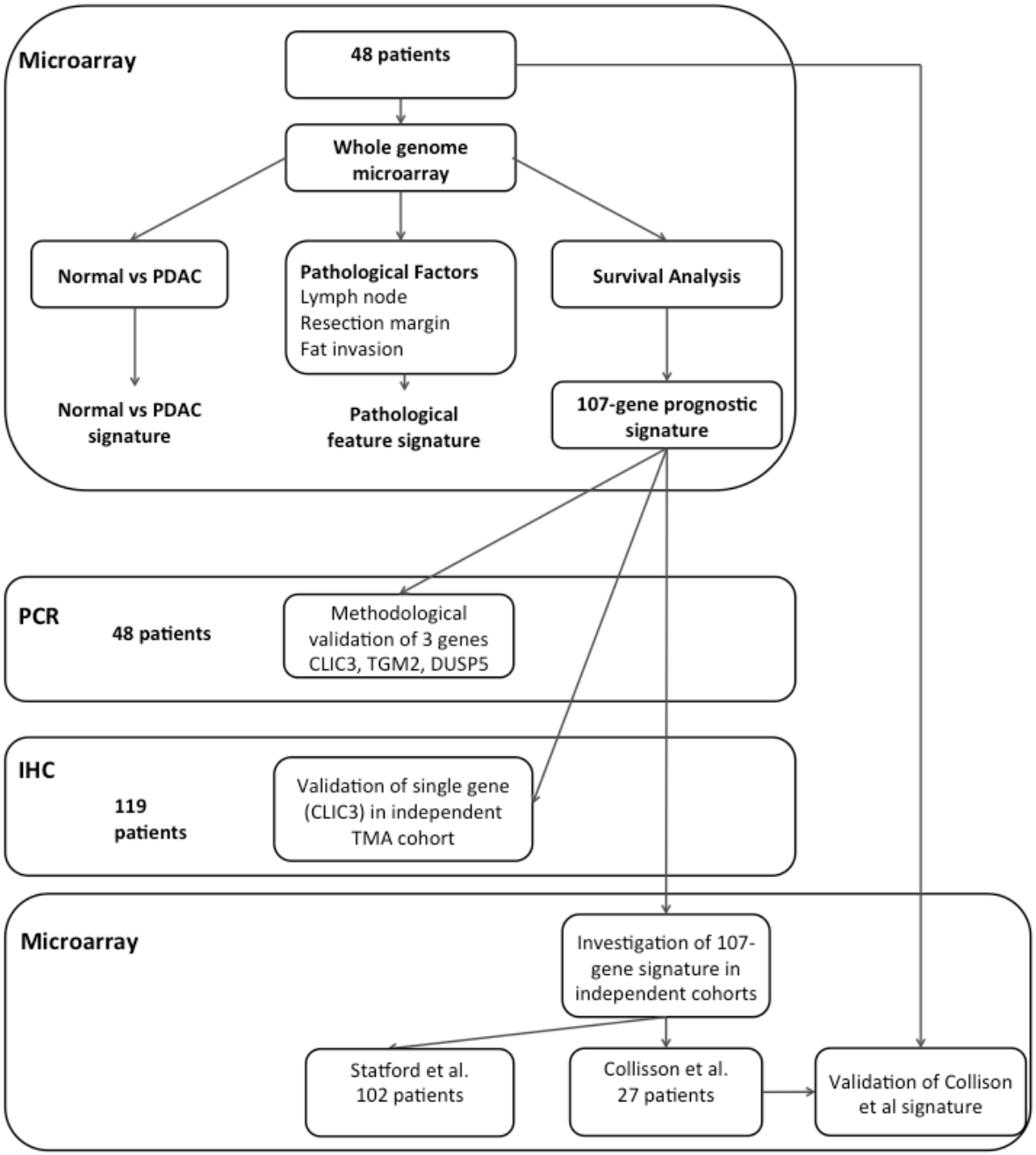

Table 11.5 Gene expression analysis PDAC expression compared to normal

A) *Normal compared to PDAC Expression – Top-ranking genes that are over-expressed in adenocarcinoma according to class comparison analysis.*

	p value	FDR	Mean of intensities Normal	Mean of intensities PDAC	Fold-change	Gene symbol
1	9.20E-06	0.0265	29.603603	596.14868	20.13	SLC6A14
2	2.25E-05	0.0346	174.24368	2851.7966	16.36	BU561469
3	4.44E-05	0.0362	7.3665823	85.257437	11.57	KIAA1751
4	8.70E-06	0.0265	11.461412	123.75292	10.79	RGMA
5	2.00E-07	0.0066	14.699395	156.18087	10.62	PITX1
6	2.90E-06	0.0240	604.32194	6181.0892	10.22	KCNN4
7	9.00E-06	0.0265	471.59831	4722.6931	10.01	S100A2
8	7.10E-06	0.0265	10.748666	97.607011	9.080	IRX5
9	2.90E-05	0.0349	10.412082	80.891683	7.769	KRT25
10	5.20E-06	0.0265	24.502371	174.31092	7.114	ANXA8
11	5.03E-05	0.0362	18.791259	129.06359	6.868	CLIC3
12	3.71E-05	0.0362	9.111906	60.163119	6.602	C22orf31
13	9.87E-05	0.0409	641.30998	3051.3393	4.757	SLPI
14	8.59E-05	0.0379	4.5105534	20.965454	4.648	AY358257
15	3.94E-05	0.0362	5066.9297	23322.939	4.602	SLPI
16	1.95E-05	0.0346	5.8254282	24.825513	4.261	SBEM
17	6.25E-05	0.0366	2492.5448	9345.3777	3.749	HK2
18	1.18E-05	0.0301	174.07675	604.85081	3.474	RASAL1
19	8.70E-05	0.0379	225.01426	747.53575	3.322	LRP8
20	3.06E-05	0.0349	4.6848161	14.856006	3.171	SYNJ2
21	4.04E-05	0.0362	197.19961	617.92819	3.133	ENST000344771
22	6.76E-05	0.0366	1723.9604	5366.4828	3.112	PPIAL4
23	2.15E-05	0.0346	182.12179	496.19765	2.724	BE175081
24	2.89E-05	0.0349	11.136005	29.439917	2.643	TEX101
25	7.40E-06	0.0265	2124.4875	5566.3461	2.620	CDC42SE1
26	2.54E-05	0.0349	1000.2137	2426.3753	2.425	CENTD3
27	6.66E-05	0.0366	119.94376	286.02612	2.384	ANTXR1
28	4.51E-05	0.0362	654.12123	1533.6597	2.344	CK300181
29	2.10E-06	0.0232	765.33427	1747.6469	2.283	LOC346887
30	3.22E-05	0.0349	376.95561	826.35329	2.192	ENST000304465
31	2.16E-05	0.0346	275.75525	592.95394	2.150	PCGF3
32	7.34E-05	0.0366	309.4988	640.83925	2.070	C10orf46
33	3.37E-05	0.0349	306.83499	625.34318	2.038	STK36
34	9.49E-05	0.0398	1367.3796	2766.702	2.023	STK10
35	6.12E-05	0.0366	142.14929	281.17789	1.978	RNF24
36	4.81E-05	0.0362	558.78264	1029.5207	1.842	SRP19
37	5.98E-05	0.0366	285.0244	474.9469	1.666	C1orf91

B) *Normal compared to PDAC expression - Top-ranking genes that are over-expressed in normal pancreas according to class comparison analysis*

	p value	FDR	Mean of intensities Normal	Mean of intensities PDAC	Fold-change	Gene symbol
	3.17E-05	0.035	10690.099	1108.6405	0.107	IGLV6-57
2	5.46E-05	0.037	1502.6972	414.66778	0.276	LIFR
3	1.55E-05	0.032	5733.3895	1624.8153	0.283	MGAT4A
4	7.24E-05	0.037	89.701475	25.734754	0.286	LOC283130
5	4.95E-05	0.036	131.85456	38.322091	0.290	FOXP2
6	6.05E-05	0.037	219.5271	74.467313	0.339	ANKRD20A2
7	6.12E-05	0.037	74.805225	25.633275	0.342	THC2427156
8	2.94E-05	0.035	470.5038	164.82408	0.350	MUC2
9	8.35E-05	0.038	184.46679	65.536563	0.355	MGC24039
10	3.32E-05	0.035	152.18094	54.232766	0.356	AK024684
11	1.38E-05	0.032	48238.104	17249.547	0.357	EEF2
12	6.45E-05	0.037	201.35086	73.5744	0.365	GGT6
13	7.36E-05	0.037	864.87331	340.49585	0.393	SEC63
14	7.05E-05	0.037	1111.881	448.11133	0.403	AFARP1
15	4.22E-05	0.036	50010.966	21829.872	0.436	SLC25A5
16	2.30E-05	0.035	22335.682	10197.005	0.456	CR609307
17	4.77E-05	0.036	4796.9933	2224.5141	0.463	SUCLG1
18	1.97E-05	0.035	1779.3884	827.9703	0.465	THC2399272
19	9.12E-05	0.039	12617.176	5893.2473	0.467	PCK2
20	7.52E-05	0.037	12953.394	6352.5998	0.490	SLC25A6
21	6.68E-05	0.037	40453.384	20084.033	0.496	LOC158345
22	7.45E-05	0.037	19475.239	9991.179	0.513	ENST00000361461
23	7.61E-05	0.037	2496.5669	1323.2366	0.530	C9orf103
24	7.34E-05	0.037	3113.1042	1682.3848	0.540	FAM13A1
25	8.49E-05	0.038	35126.78	19191.811	0.546	GNB2L1
26	5.84E-05	0.037	40488.368	22293.52	0.550	LOC388524
27	5.24E-05	0.037	62835.275	34644.777	0.551	MGC27348
28	5.33E-05	0.037	4304.1064	2484.2743	0.577	C9orf95

The Full list of normal versus PDAC gene expression analysis - 573 genes differentially expressed are displayed within a supplementary excel file. T-test statistical comparison with threshold for significance at $p < 0.0005$.

11.4.1 Functional annotation of gene expression data

The following supplementary data is contained in separate Excel files

1) Normal versus PDAC – Expression analysis, GSEA
2) Normal versus PDAC – Network analysis, GeneGO
3) Lymph node status – Expression analysis, GSEA
4) Lymph node status – Network analysis, GeneGO
5) Tumour stage – Expression analysis, GSEA
6) Tumour stage – Network analysis, GeneGO
7) Tumour grade – Expression analysis, GSEA
8) Tumour grade – Network analysis, GeneGO
9) Venous invasion – Expression analysis, GSEA
10) Resection margin status – Expression analysis, GSEA
11) Liver recurrence – Expression analysis, GSEA

11.4.2 Functional annotation of normal versus PDAC

Functional annotation identified enrichment for ubiquitin ligase activity, wound healing, kallikreins and maspin. By analysing GO groups, rather than individual genes the analysis was simplified, the number of comparisons reduced, enabling findings among biologically related genes to reinforce one another. 161 GO groups whose expression was differentially regulated between PDAC and normal pancreatic tissue were identified including: autophagy, apoptosis, extracellular matrix degradation, cell cycle, SMAD nuclear translocation and SUMO binding.

11.4.3 Functional annotation according to lymph node status

Functional annotation based on lymph node status identified 26 networks with VEGF-B, VEGFR-2, C/EBP and E2A being important nodes. GO enrichment highlighted 49 gene sets including, regulation of DNA repair and cell adhesion by integrins as being integral. In terms of BioCarta and KEGG pathway analysis 67/304 and 4/170 are associated with lymph node status respectively including CXCR4, Wnt and PDGF signalling pathways.

11.4.4 Gene expression analysis according to pathological features

Investigation into gene expression patterns according to tumour grade was performed. Potentially this could identify underlying genes that drive the progression of high-grade tumours that are associated with poorer outcome. 892 probes were differentially expressed at $p = 0.001$, with 219 features differentially expressed at $1x10^{-5}$. Of these 76 genes were up-regulated in the high-grade tumours and 65 genes were up-regulated in low-grade tumours. The clustering of 219 genes is illustrated in Figure 11.11. Amongst the most significantly dysregulated genes were DSCR3, MFI2, NGFR, EREG, EEF2K, SEM6AD and NTRK2.

Network analysis revealed the important genes that were integral in the 30 networks (Appendix 11.4.1). GSEA highlighted 225/3265 gene sets including apoptosis, chromatin remodeling, SMAD4 re-localisation and senescence as being strongly implicated in high-grade associated genes. Interestingly high-grade tumours were associated with neurogenesis and wound healing response. In terms of BioCarta and KEGG pathway analysis 10/304 and 15/170 are associated with grade respectively including mitotic spindle regulation, Wnt signalling and cytokine-cytokine interactions. GSEA identified STAT5A, HIF1A, SP1, STAT3 and NFκB among key transcription factors.

There was a significant difference in gene expression pattern between T2 and T3 tumours for 408 genes ($p < 0.005$), with clustering illustrated in Figure 11.11. The most significant genes associated with tumour stage included STK31, WNT10A, CDKN2A, HOXB7 and STAB2. Network analysis revealed the important genes that were integral in the top 30 networks (Appendix 11.4.1).

The presence of intratumoural venous invasion was associated with an altered gene expression signature identifying 439 genes at $p < 0.005$, with 77 genes at $p < 0.001$ which were then clustered (Figure 11.11). The most significant genes included GALNT8, ENOSF1, PAQR9, NXF3, FGFRL1 and CD80. To investigate the biological associations of venous invasion a bioinformatic analysis grouped the genes by GO terms. In addition to associations with more general GO terms (168/3265), there was a significant enrichment for genes associated with IL-6 production. In terms of BioCarta and KEGG pathway analysis 13/304 and 5/170 were associated with venous invasion respectively including B-lymphocyte surface molecules and JNK pathway activation. GSEA identified the transcription factors PAX5 and JUN target the differentially expressed genes.

In terms of site of tumour recurrence comparing liver metastases with metastases at another site identified an altered gene expression signature in the primary tumour. 136 genes were identified that associated with liver metastases as the primary site of recurrence ($p = 0.001$) with clustering illustrated in Figure 11.11. The most significant included SLC26A9, CFL2, CDH13, CNTN1, KLK11 and MUC1. GO analysis identified 176 gene sets differentially expressed including lymphocyte activation, cell proliferation, regulation of immune system processes, histone H4 acetylation and cell adhesion. Pathway enrichment revealed a preponderance of interesting gene sets including recruitment of Src kinases, Rho cell motility signalling and Trka receptor signalling pathway. STAT6 was identified by transcription factor enrichment analysis.

Table 11.6 Gene expression analysis: lymph node status

Gene expression according to lymph node status – Top ranking genes that are over-expressed in LN1 versus LN0 tumours according to class comparison analysis (Top-ranking over (red) and under (green) expressed genes).

	Parametric p value	Mean intensities Normal	Mean intensities PDAC	Fold-change	Clone	Gene symbol
1	0.00925	103.02	15.70	0.15	A_23_P145507	EYA4
2	0.00097	233.05	44.47	0.19	A_32_P215943	LOC126536
3	0.01017	152.01	38.67	0.25	A_23_P128235	KRT1
4	0.00033	30.30	8.40	0.28	A_23_P255027	MGC15705
5	0.00049	93.22	27.33	0.29	A_32_P25419	BE766438
6	0.00308	32.72	10.78	0.33	A_24_P272381	A_24_P272381
7	0.00951	25.50	8.83	0.35	A_23_P422240	UROC1
8	0.00447	25.56	8.92	0.35	A_23_P130411	SERPINB11
9	0.00709	1360.40	516.82	0.38	A_24_P252020	TRIM41
10	0.00217	801.30	306.36	0.38	A_23_P218144	LTBP2
11	0.00014	93.23	36.72	0.39	A_24_P407742	A_24_P407742
12	0.00035	276.71	111.89	0.40	A_32_P149011	CN479126
13	0.00011	75.38	30.85	0.41	A_32_P195137	AW858928
14	0.00333	412.32	172.44	0.42	A_32_P235274	AW276332
15	0.00843	114.05	47.91	0.42	A_32_P80231	BM973227
16	0.00644	114.37	48.37	0.42	A_32_P98793	THC2283716
17	0.00923	42.07	17.93	0.43	A_32_P44840	PDE4DIP
18	0.00818	49.62	22.25	0.45	A_24_P100382	GK
19	0.00103	282.20	127.67	0.45	A_24_P247749	RAB21
20	0.00586	9.76	39.59	4.06	A_23_P138931	MMP13
21	0.00145	1853.82	6388.79	3.45	A_23_P338919	SPEG
22	0.00104	5.43	16.41	3.02	A_23_P25615	SOHLH2
23	0.00559	17.64	51.20	2.90	A_24_P162293	RAB6IP2
24	0.00608	11.93	33.53	2.81	A_24_P920573	AB015616
25	0.00157	3129.27	7939.58	2.54	A_23_P33511	AX721087
26	0.00484	11.95	28.88	2.42	A_23_P302750	ATAD3B
27	0.00353	18.26	42.67	2.34	A_23_P85082	OTEX
28	0.00912	1462.74	3359.47	2.30	A_23_P41804	NKD2
29	0.00806	8.74	20.06	2.30	A_23_P131183	GBX2
30	0.00129	8.64	19.63	2.27	A_23_P114857	PLA2G2E
31	0.00090	3599.48	7950.29	2.21	A_23_P431360	ZNF219
32	0.00795	61.82	136.35	2.21	A_24_P37253	MGC52057
33	0.00661	106.61	235.09	2.21	A_23_P357504	THC2251776
34	0.00420	7.78	16.95	2.18	A_32_P206050	ENST00000229088
35	0.00088	16.77	36.18	2.16	A_32_P43711	SOCS7
36	0.00105	42.47	89.82	2.11	A_23_P55564	ZCCHC2
37	0.00857	208.45	440.37	2.11	A_23_P130735	SLC6A16
38	0.00565	904.77	1889.04	2.09	A_23_P150693	FJX1

11.4.5 Gene expression survival analysis

Detailed gene set enrichment analysis regarding genes associated with survival following resection of PDAC with curative intent is presented within an Excel file.

Table 11.7. 332 genes associated with survival in 48 patients with PDAC following resection. Univariate analysis (significance threshold p < 0.001)

Supplementary Excel file

Table 11.8. Risk Prediction model 107 genes

Supplementary Excel file

Table 11.9. Gene set enrichment survival analysis - Gene Ontology

Supplementary Excel file

Table 11.10. Gene set enrichment survival analysis – BioCarta

	BioCarta Pathway	Pathway description	Number of genes	LS permutation p value	KS permutation p value	Efron-Tibshirani's GSA test p value
1	h_ranklPathway	Bone Remodelling	11	0.00087	0.02003	0.015 (+)
2	h_pparaPathway	Mechanism of Gene Regulation by Peroxisome Proliferators via PPARa(alpha)	85	0.00263	0.01429	0.075 (-)
3	h_cptPathway	Mitochondrial Carnitine Palmitoyltransferase (CPT) System	5	0.00699	0.00054	0.015 (-)
4	h_fbw7Pathway	Cyclin E Destruction Pathway	12	0.033	0.02925	< 0.005 (-)
5	h_erythPathway	Erythrocyte Differentiation Pathway	19	0.04972	0.09612	< 0.005 (+)
6	h_eponfkbPathway	Erythropoietin mediated neuroprotection through NF-kB	16	0.05133	0.13807	< 0.005 (+)
7	h_ck1Pathway	Regulation of ck1/cdk5 by type 1 glutamate receptors	23	0.06184	0.02828	< 0.005 (-)
8	h_cd40Pathway	CD40L Signalling Pathway	12	0.32113	0.40259	< 0.005 (+)

Table 11.11. Gene set enrichment survival analysis – KEGG

	Kegg Pathway	Pathway description	Number of genes	LS permutation p value	KS permutation p value	Efron-Tibshirani's GSA test p value
1	hsa00760	Nicotinate and nicotinamide metabolism	45	0.0018	0.2016	0.035 (+
2	hsa03320	PPAR signalling pathway	95	0.00191	0.00439	0.045 (+
3	hsa00010	Glycolysis / Gluconeogenesis	80	0.0045	0.01285	0.08 (+
4	hsa00071	Fatty acid metabolism	61	0.00902	0.03374	< 0.005 (-
5	hsa00051	Fructose and mannose metabolism	67	0.0098	0.00033	0.035 (-
6	hsa00640	Propanoate metabolism	52	0.03934	0.00582	< 0.005 (-
7	hsa00624	1- and 2-Methylnaphthalene degradation	36	0.04783	0.19506	< 0.005 (-
8	hsa00930	Caprolactam degradation	15	0.06489	0.06063	< 0.005 (-
9	hsa00562	Inositol phosphate metabolism	56	0.09593	0.53891	< 0.005 (-
10	hsa00561	Glycerolipid metabolism	79	0.15125	0.46882	< 0.005 (-
11	hsa00625	Tetrachloroethene degradation	10	0.18629	0.00218	0.245 (-

Table 11.12. Gene set enrichment survival analysis – Transcription Factors

	Transcription Factor gene sets	Number of genes	LS permutation p value	KS permutation p value	Efron-Tibshirani's GSA test p value
1	**JUND_T01978**	14	0.0001	0.00863	< 0.005 (+)
2	**TP73_T04931**	16	0.00436	0.0055	< 0.005 (+)
3	**ATF1_T00968**	103	0.0045	0.29326	0.055 (-)
4	**TP73L_T06131**	7	0.01592	0.00123	0.04 (+)
5	**JUNB_T01977**	8	0.01924	0.09646	< 0.005 (+)

Figure 11.10 Network analysis normal versus PDAC

A) *Network including S100A2, PITX1, MASPIN (blue circle = differentially expressed in current data set) – links with p53, uPAR, a5/B1 integrins. Generated from GeneGO analysis.*

B) *Network including BCL-3, MMP13, FAK2 – links with c-MYC, NFκB and TGFβ.*

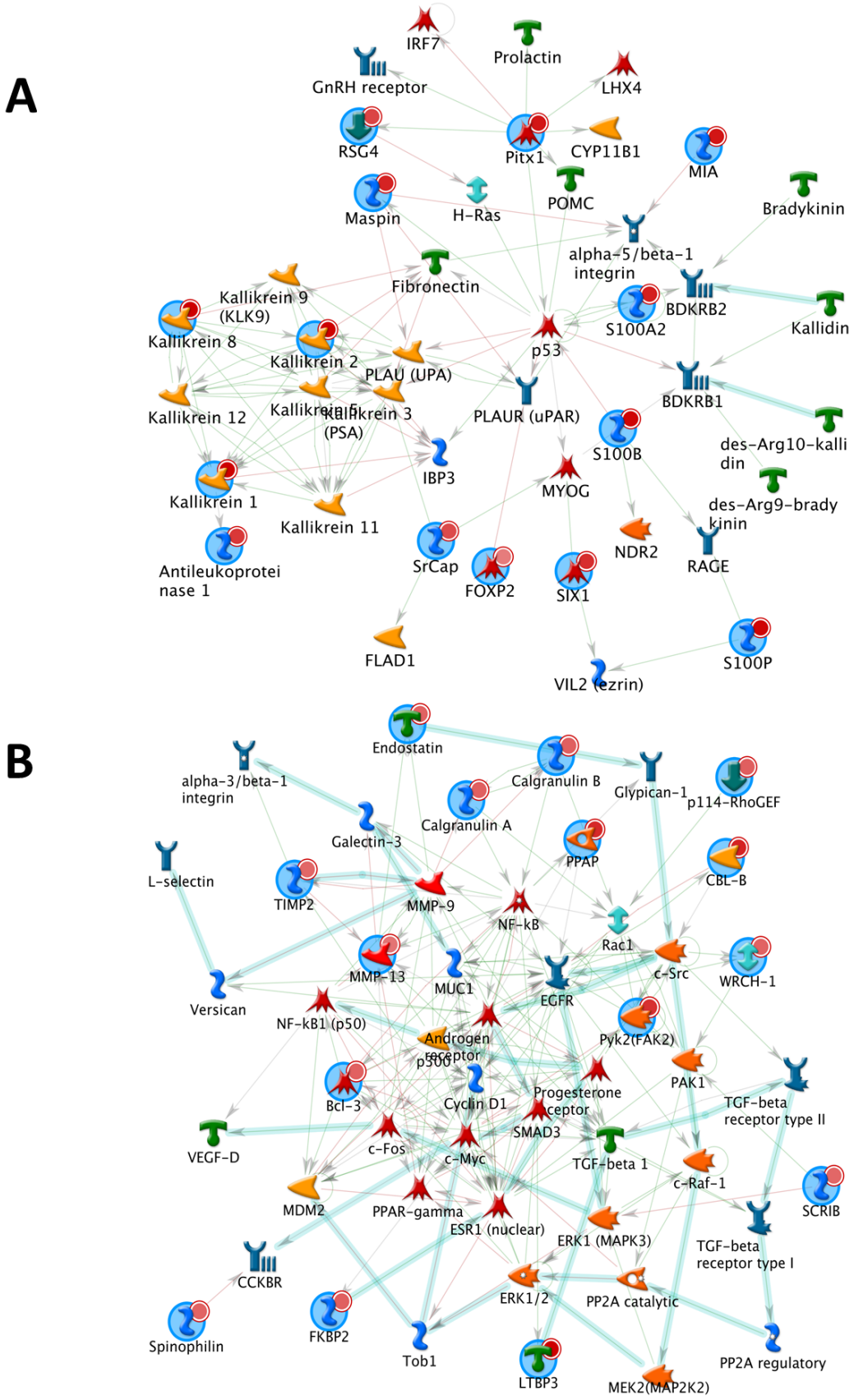

Figure 11.11 Hierarchical clustering according to clinicopathological factors

Lymph node status (284 genes), tumour grade (219 genes), tumour stage (264 genes), venous invasion (77 genes), resection margin status (154 genes) and site of recurrence (136 genes) ($p < 0.0001$, group comparison t-test).

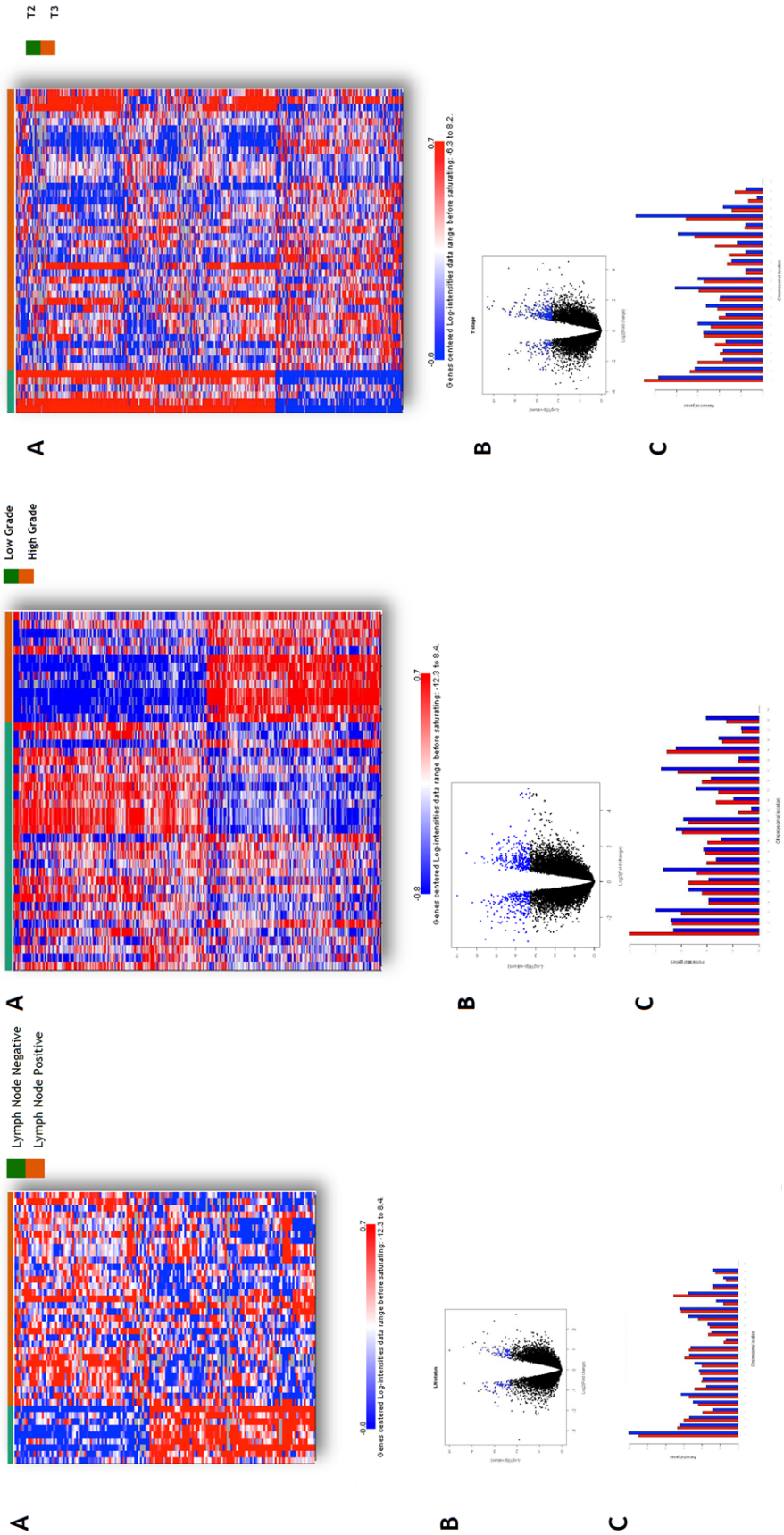

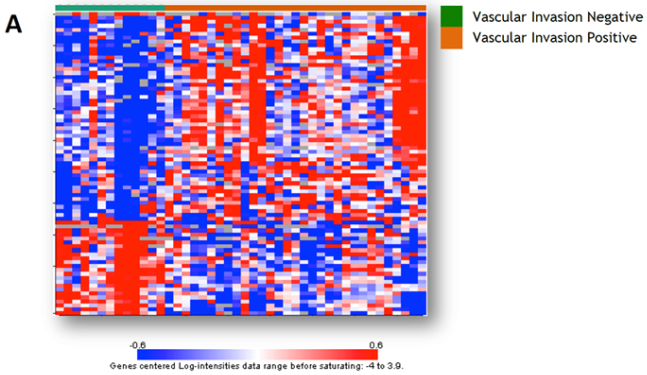
A
Vascular Invasion Negative
Vascular Invasion Positive
-0.6
0.6
Genes centered Log-intensities data range before saturating: -4 to 3.9.
B
C

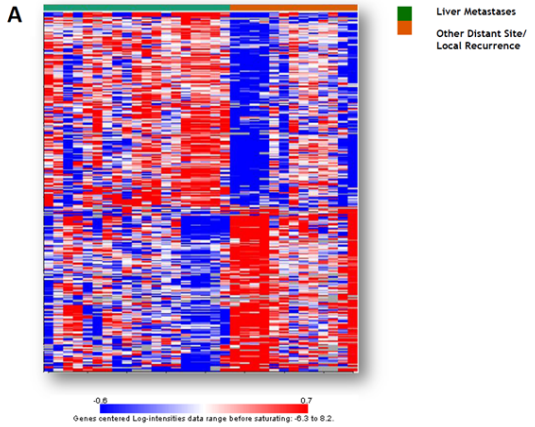
A
Liver Metastases
Other Distant Site/
Local Recurrence
-0.6
0.7
Genes centered Log-intensities data range before saturating: -6.3 to 8.2.
B
C

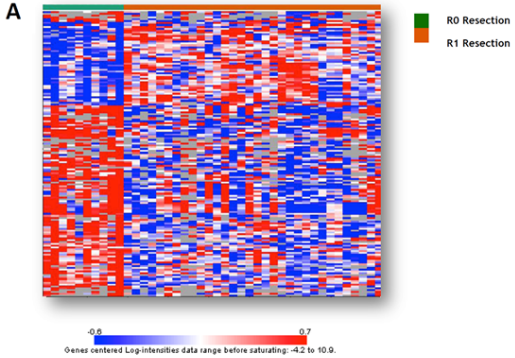
A
R0 Resection
R1 Resection
-0.8
0.7
Genes centered Log-intensities data range before saturating: -4.2 to 10.9.
B
C

Figure 11.12 Methodology of the identification and selection of prognostic signature

Serial Kaplan-Meier analyses were performed of the all genes identifying those with $p < 0.05$ (Log-rank test).

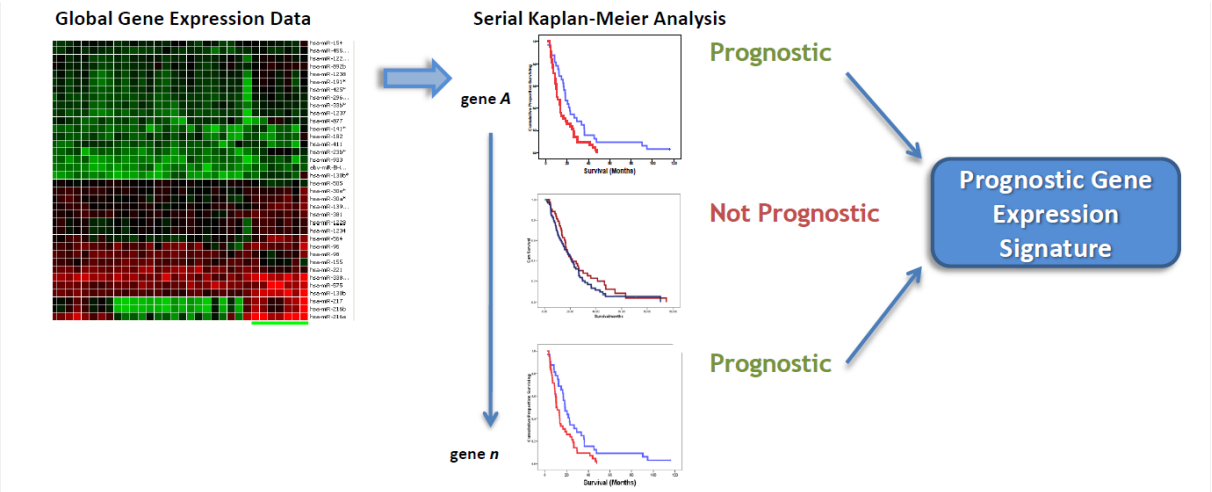

Figure 11.13 Kaplan-Meier survival curves of clinicopathological parameters for 48 patients cohort - gene expression profiled

High tumour stage, lymph node invasion, perineural invasion, resection margin involvement and venous invasion were significantly associated with survival (Log-rank test).

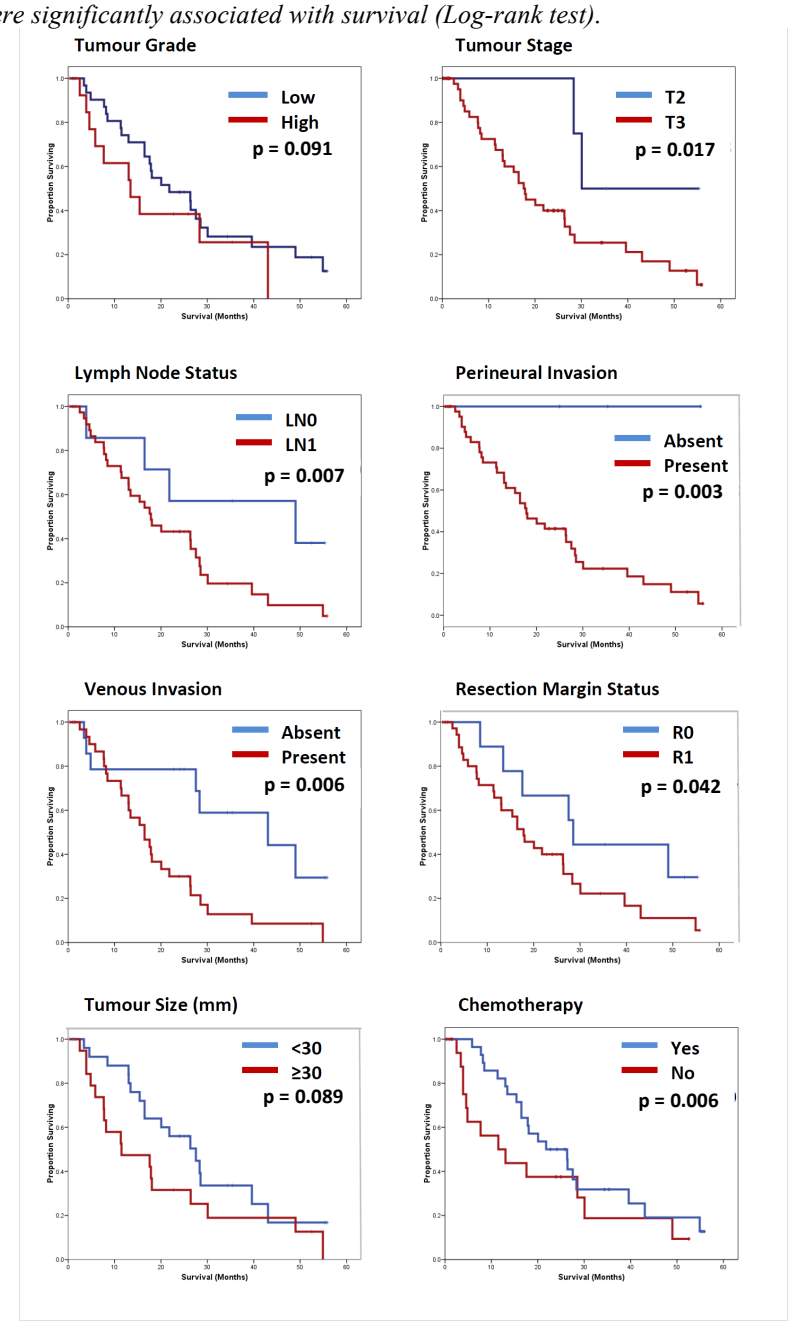

Figure 11.14 Subtypes of PDAC according to PDAssigner signature and their prognostic significance

A) *Heat map visualisation of the 72-gene PDAssigner classifier identifying three subtypes of PDAC in 48 patient cohort. Coloured sidebars indicate genes up-regulated in classical (purple), exocrine-like (blue) and Quasi-mesenchymal-subtype (orange). More that 72 genes are displayed in the figure, as there were multiple probes available for some genes on the Agilent 44K array. Red represents high gene expression while green represents low gene expression.*

B) *A Kaplan-Meier survival analysis according to PDAssigner subtypes comparing patient with classical (purple), exocrine-like (blue) and QM subtype (orange). p value according to Log-rank analysis.*

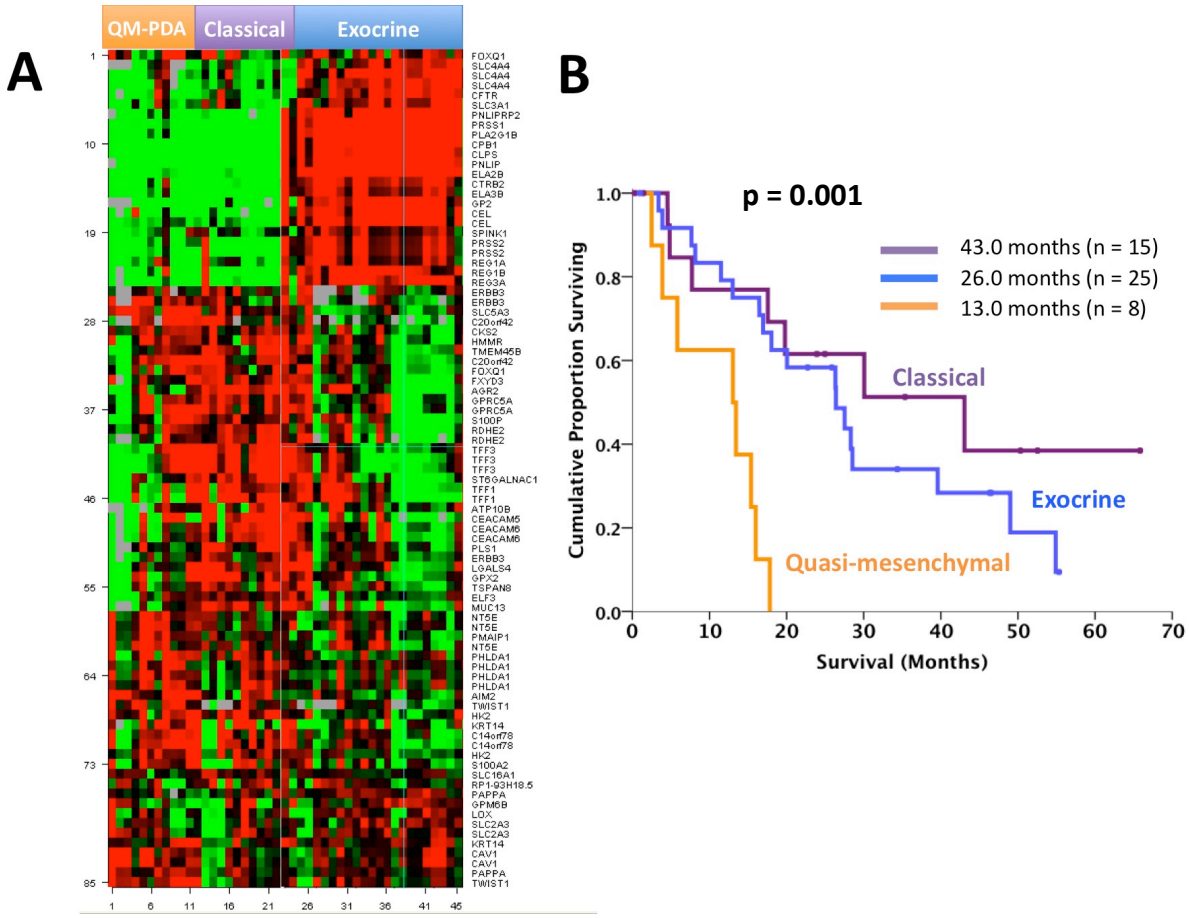

Table 11.13 Association between PDAssigner signature and pathological characteristics

48 patient cohort divided according to PDAssigner subtype.

		PDAssigner Signature			
Prognostic factor	**Category**	**Classical n = 15 (%)**	**Exocrine n = 25 (%)**	**QM n = 8 (%)**	**p value [a]**
Age (years)	< 65	7 (47)	16 (64)	9 (62)	0.541
	≥ 65	8 (53)	9 (36)	3 (38)	
Gender	F	7 (47)	11 (44)	2 (25)	0.570
	M	8 (53)	14 (56)	6 (75)	
Tumour stage	T2	3 (20)	3 (12)	0 (0)	0.383
	T3	12 (80)	22 (88)	8 (100)	
Lymph node status	Absent	4 (27)	5 (20)	1 (12)	0.720
	Present	11 (73)	20 (80)	7 (88)	
Tumour grade	Low	9 (60)	20 (80)	2 (22)	0.011
	High	6 (40)	5 (20)	7 (88)	
Tumour size (mm)	< 30	8 (53)	16 (64)	3 (38)	0.406
	≥ 30	7 (47)	9 (36)	5 (62)	
Margin involvement	R0	6 (40)	6 (24)	1 (12)	0.325
	R1	9 (60)	19 (76)	7 (88)	

[a] χ^2 tests were used to compare categorical variables.

QM – Quasi-mesenchymal

Table 11.14 Validation of PDAssigner signature in 48 patient cohort

Overall survival times of the PDAssigner subgroups were compared by means of Kaplan-Meier survival curves (Log-rank test).

		Survival (median)	
Prognostic factor	**PDAC Subtype (n)**	**Months (95% CI)**	**p value (Log-rank test)**
PDAssigner signature	QM (8)	13.0 (2.5 - 23.6)	0.002 (QM versus classical)
			0.001 (QM versus EXO)
	Exocrine-like (25)	26.4 (15.9 - 36.9)	0.312 (EXO versus classical)
	Classical (15)	43.1 (12.2 - 73.9)	-

QM – Quasi-mesenchymal, EXO – Exocrine-like

Table 11.15 Prognostic utility of PDAssigner signature within independent set of 48 patients

Univariate and multivariate Cox proportional hazards analysis was performed demonstrating that the PDAssigner signature was an independent prognostic factor.

		Univariate		**Multivariate**	
Prognostic factor	**Category**	**HR (95% CI)**	**p value**	**HR (95% CI)**	**p value**
Age (yrs)	<65/ > 65	0.95 (0.66 - 1.37)	0.811	-	-
Gender	M/F	1.23 (0.60 - 2.53)	0.568	-	-
Tumour stage	T2/ T3	2.79 (1.47 - 9.23)	0.074	3.54 (1.47 - 18.6)	0.015
Tumour size (mm)	<30/ ≥30	1.82 (0.89 - 3.71)	0.098	1.98 (0.89 - 4.38)	0.09
Lymph node status	Absent/ Present	3.92 (1.32 - 11.5)	0.010	4.10 (0.98 - 17.2)	0.054
Tumour grade	Low/ High	1.68 (0.95 - 3.32)	0.087	1.57 (0.62 - 3.99)	0.345
Margin involvement	R0/ R1	3.60 (1.35 - 9.51)	0.011	3.91 (1.15 - 13.3)	0.029
Adjuvant therapy	Yes/ No	0.50 (0.24 - 1.03)	0.072	0.35 (0.16 - 0.56)	0.001
Peripancreatic fat invasion	No/ Yes	1.77 (0.95 – 3.44)	0.069	1.59 (0.89 – 3.83)	0.219
PDAssigner signature	EXO + Classical / QM [a]	5.15 (1.97 - 13.4)	0.001	5.86 (2.07 - 16.5)	0.001

QM – Quasi-mesenchymal, EXO – Exocrine-like

[a] Exocrine-like subtypes and Classical were combined and compared with the poor prognosis Quasi-mesenchymal subtypes for the purpose of this analysis.

11.5 Appendix 5 - Chapter 7 Data: miRNA analysis

Figure 11.15 Workflow for miRNA expression analysis

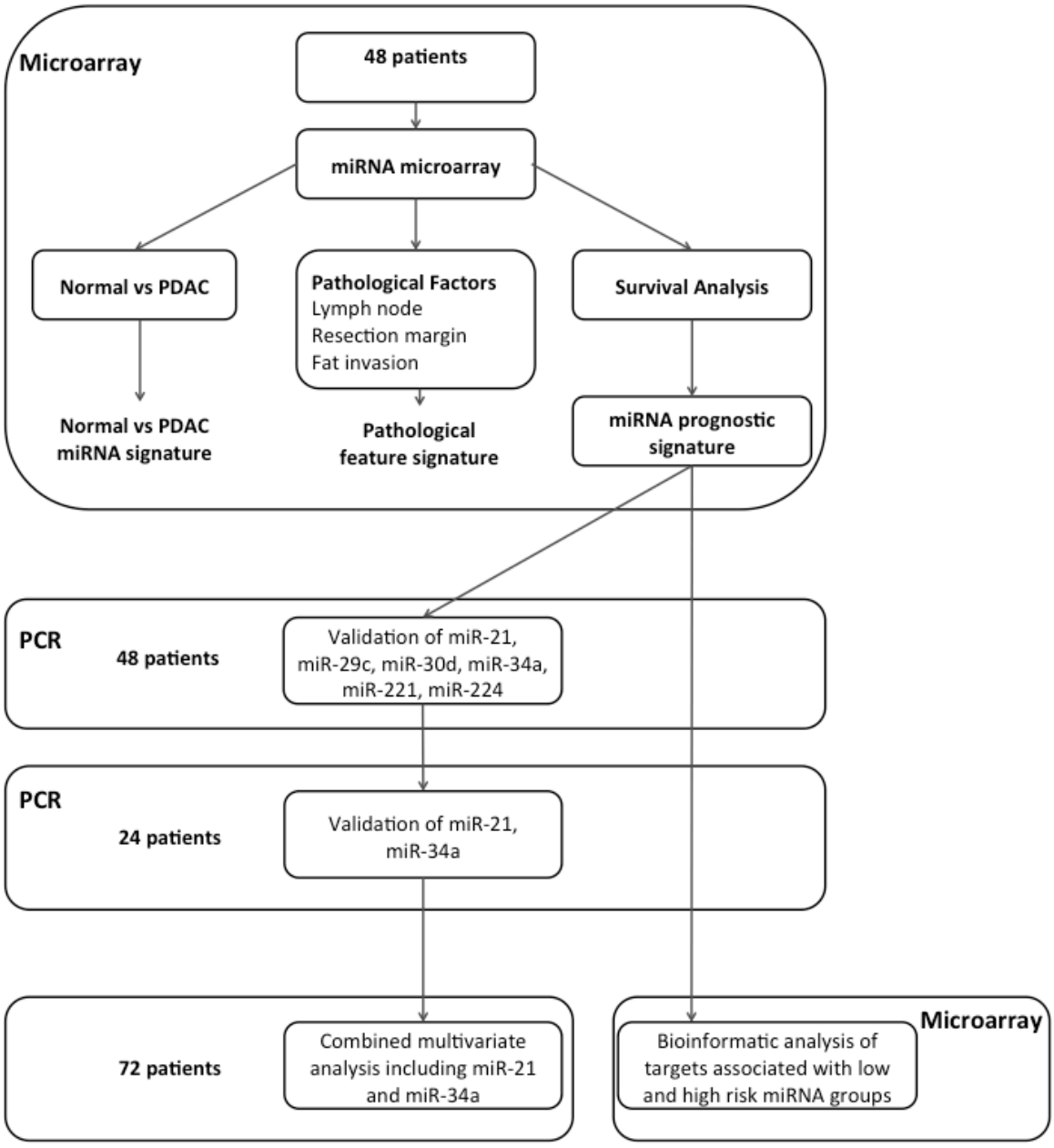

11.5.1 miRNA expression profiles between PDAC and normal pancreas

Table 11.16 miRNAs up-regulated and down-regulated in PDAC compared with normal pancreatic tissue

97 microRNAs showed a statistically different expression p < 0.001 ranked by p-value.

	p value	FDR	Mean of intensities in normal pancreas	Mean of intensities in PDAC	Fold-change	miRNA id
1	< 1e-07	< 1e-07	654.34	82.01	7.98	hsa-miR-130b
2	< 1e-07	< 1e-07	82.87	7.76	10.68	hsa-miR-345
3	< 1e-07	< 1e-07	68.05	10.46	6.5	hsa-miR-617
4	< 1e-07	< 1e-07	38.28	11.92	3.21	hsa-miR-887
5	< 1e-07	< 1e-07	413.44	1683.51	0.25	hsa-let-7i
6	< 1e-07	< 1e-07	76	8.21	9.26	hsa-miR-708
7	< 1e-07	< 1e-07	110.5	35.76	3.09	hsa-miR-139-3p
8	< 1e-07	< 1e-07	1737.84	4847.53	0.36	hsa-miR-23a
9	1.00E-07	6.67E-06	165.43	25.53	6.48	hsa-miR-564
10	1.00E-07	6.67E-06	345.58	1037.51	0.33	hsa-miR-107
11	1.00E-07	6.67E-06	166.79	1163.35	0.14	hsa-miR-223
12	2.00E-07	1.22E-05	123.34	871.28	0.14	hsa-miR-143
13	3.00E-07	1.69E-05	498.56	2184.78	0.23	hsa-miR-27a
14	4.00E-07	2.10E-05	56.49	16.69	3.38	hsa-miR-892b
15	5.00E-07	2.29E-05	250.53	113.9	2.2	hsa-miR-874
16	5.00E-07	2.29E-05	178.47	548.68	0.33	hsa-miR-214
17	6.00E-07	2.59E-05	516.88	2389.01	0.22	hsa-miR-199b-3p
18	8.00E-07	3.26E-05	622.14	1739.08	0.36	hsa-miR-199a-5p
19	9.00E-07	3.48E-05	2315.13	331.76	6.98	hsa-miR-148a
20	1.10E-06	4.04E-05	564.79	128.95	4.38	hsa-miR-575
21	1.40E-06	4.89E-05	164.5	388.54	0.42	hsa-miR-103
22	1.70E-06	5.67E-05	430.4	1666.69	0.26	hsa-miR-145
23	2.20E-06	7.02E-05	28.61	9.92	2.88	hsa-miR-33b*
24	2.30E-06	7.03E-05	57.43	12.78	4.49	hsa-miR-28-3p
25	3.20E-06	9.40E-05	30.81	6.04	5.11	hsa-miR-193b*
26	3.40E-06	9.60E-05	655.4	303.3	2.16	hsa-miR-324-3p
27	3.60E-06	9.79E-05	4517.4	17083.78	0.26	hsa-miR-21
28	4.00E-06	0.000105	1546.12	49.51	31.23	hsa-miR-216a
29	5.60E-06	0.000142	30.54	5.26	5.81	hsa-miR-665
30	5.80E-06	0.000142	79.4	41.38	1.92	hsa-miR-381
31	6.60E-06	0.000156	61.58	6.79	9.07	hsa-miR-648
32	8.90E-06	0.000204	36.91	10.61	3.48	hsa-miR-877
33	9.60E-06	0.000214	85.14	323.35	0.26	hsa-miR-142-5p
34	1.00E-05	0.000216	1618.77	631.19	2.56	hsa-miR-30a
35	1.15E-05	0.000241	75.01	256.77	0.29	hsa-miR-10a
36	1.25E-05	0.000255	4154.24	658.18	6.31	hsa-miR-494
37	1.32E-05	0.000262	11.43	2.79	4.1	hsa-miR-628-3p
38	1.40E-05	0.00027	373.22	750.09	0.5	hsa-miR-130a
39	1.60E-05	0.000301	114.39	322.7	0.35	hsa-miR-100
40	1.74E-05	0.000313	152145.09	16410.36	9.27	hsa-miR-923
41	1.75E-05	0.000313	5482.41	2708.27	2.02	hsa-miR-29c
42	1.79E-05	0.000313	287.25	1105.55	0.26	hsa-miR-142-3p
43	2.14E-05	0.000365	5732.12	1434.94	3.99	hsa-miR-141
44	2.28E-05	0.00038	8.67	2.89	3	hsa-miR-30c-1*
45	2.64E-05	0.000431	16.74	29.38	0.57	hsa-miR-505
46	2.75E-05	0.000439	60.5	203.4	0.3	hsa-miR-150
47	3.42E-05	0.000534	869.87	483.39	1.8	hsa-miR-30d
48	3.68E-05	0.000563	526.52	206.27	2.55	hsa-miR-338-3p
49	4.07E-05	0.000604	25.36	10.03	2.53	hsa-miR-425*
50	4.16E-05	0.000604	117.08	260.44	0.45	hsa-miR-886-3p
51	4.20E-05	0.000604	216.04	22.01	9.81	hsa-miR-513b
52	4.44E-05	0.000627	170.11	12.78	13.31	hsa-miR-513c
53	4.63E-05	0.00064	350.89	44.22	7.93	hsa-miR-217
54	4.71E-05	0.00064	143.69	265.85	0.54	hsa-miR-342-3p
55	5.16E-05	0.000689	31.1	68.26	0.46	hsa-miR-155
56	5.29E-05	0.000693	20.69	1.83	11.32	hsa-miR-596
57	5.53E-05	0.000712	22.44	10.32	2.17	hsa-miR-30c-2*
58	6.55E-05	0.000829	150.45	461.85	0.33	hsa-miR-146b-5p
59	6.95E-05	0.000865	78.9	190.63	0.41	hsa-miR-21*
60	7.63E-05	0.000933	19.05	4.45	4.28	hsa-miR-338-5p
61	7.91E-05	0.000938	681.95	80.51	8.47	hsa-miR-513a-5p
62	7.92E-05	0.000938	24.24	12.01	2.02	hsa-miR-501-5p
63	8.54E-05	0.000995	188.16	340.2	0.55	hsa-miR-331-3p
64	9.57E-05	0.0011	29.91	9.6	3.12	hsa-miR-191*
65	9.92E-05	0.00112	1778.84	3226.44	0.55	hsa-miR-24
66	0.0001034	0.00114	234.08	474.37	0.49	hsa-miR-34a
67	0.0001038	0.00114	16.54	5.94	2.79	hsa-miR-23b*
68	0.0001202	0.0013	93.06	222.24	0.42	hsa-miR-222
69	0.0001245	0.00132	20.75	6.25	3.32	hsa-miR-138-2*
70	0.0001275	0.00134	119.55	65.77	1.82	hsa-miR-423-5p
71	0.0001426	0.00147	1069.58	349.9	3.06	hsa-miR-200c
72	0.0001454	0.00148	64.03	134.47	0.48	hsa-miR-221
73	0.000159	0.0016	165.12	450.78	0.37	hsa-miR-199b-5p
74	0.0001628	0.00161	63.31	97.34	0.65	hsa-miR-185
75	0.0001734	0.0017	136.49	235.66	0.58	hsa-miR-140-3p

76	0.0002126	0.00205	55.49	87.53	0.63	hsa-miR-574-3p
77	0.0002294	0.00218	3190.52	447.45	7.13	hsa-miR-375
78	0.0002323	0.00218	449.96	1319.37	0.34	hsa-miR-16
79	0.0002342	0.00218	24.15	9.45	2.56	hsa-miR-602
80	0.0002429	0.00221	80.35	32.22	2.49	hsa-miR-30a*
81	0.0002435	0.00221	40.3	5.93	6.79	hsa-miR-662
82	0.0002612	0.00234	20.92	3.64	5.74	hsa-miR-130b*
83	0.0002683	0.00237	234.1	43.43	5.39	hsa-miR-216b
84	0.0003096	0.00271	27.49	42.15	0.65	hsa-miR-128
85	0.00035	0.00302	29.3	10.88	2.69	hsa-miR-1238
86	0.000417	0.00352	108.17	36.85	2.94	hsa-miR-135a*
87	0.0004184	0.00352	17.03	7.41	2.3	hsa-miR-1229
88	0.0004223	0.00352	57.55	26.18	2.2	hsa-miR-1228
89	0.0004344	0.00358	16.44	2.96	5.56	hsa-miR-148a*
90	0.0004917	0.00401	270.36	427.11	0.63	hsa-miR-106b
91	0.0005371	0.00433	28.57	57.71	0.5	hsa-miR-301a
92	0.0005453	0.00435	20.29	7.97	2.55	hsa-miR-296-5p
93	0.0006722	0.00531	34.19	17.99	1.9	hsa-miR-500
94	0.0007406	0.00578	461.4	1135.97	0.41	hsa-let-7g
95	0.0008157	0.0063	260.35	428.93	0.61	hsa-miR-181a
96	0.0008253	0.00631	1812.86	1014.97	1.79	hsa-miR-1225-5p
97	0.000986	0.00746	903.3	558.93	1.62	hsa-miR-30e

11.5.2 Bioinformatic enrichment of miRNA survival profiles

The predicted targets of the six most prognostic miRNAs were investigated to gain further insight into the biological pathways potentially deregulated in PDAC.

Table 11.17. miRNAs associated with poor prognosis demonstrated enrichment for MAPK signalling, TGFβ signalling, Wnt signalling and p53 signalling.

Supplementary Excel file

Table 11.18. miRNAs associated with favourable prognosis demonstrated enrichment for focal adhesion pathways, ECM-receptor interaction pathways and phosphatidy-linositol signalling.

Supplementary Excel file

Figure 11.16 Bioinformatics enrichment of miRNAs associated with favourable outcome.

A) *Pathway enrichment of the targets of miRNA-29c, miRNA-30d and miRNA-34a demonstrating union and intersections.*

B) *Enrichment of Focal Adhesion and* ***C)*** *ECM-receptor interaction KEGG pathways for miRNA-29c, miRNA-30d and miRNA-34a target expression.*

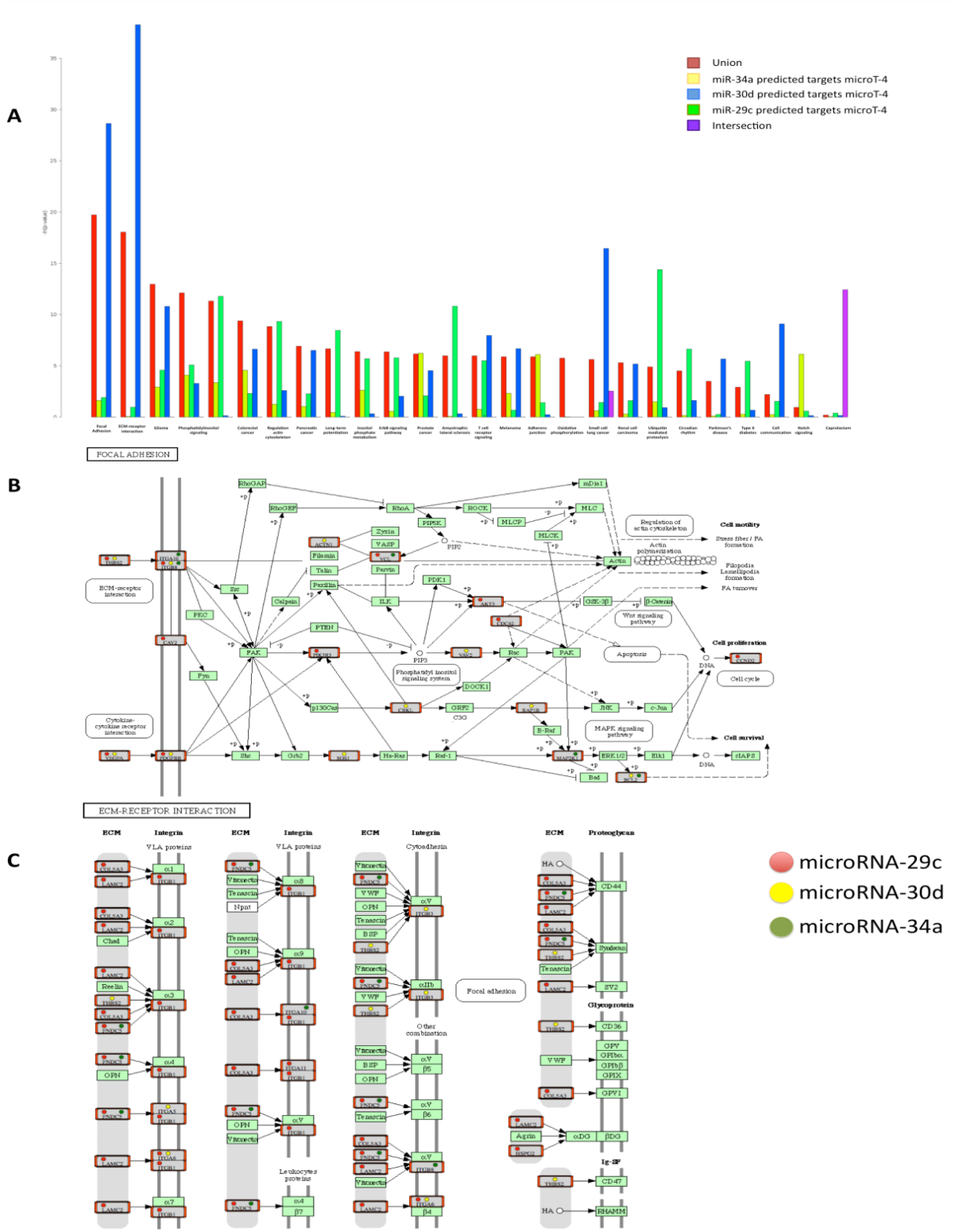

Figure 11.17 Bioinformatics enrichment of miRNAs associated with poor outcome.

A) *Pathway enrichment of the targets of miRNA-21, miRNA-221 and miRNA-224 demonstrating union and intersections.*

B) *Enrichment of TGFβ and* ***C)*** *MAPKinase KEGG pathways for miRNA-21, miRNA-221 and miRNA-224 target expression.*

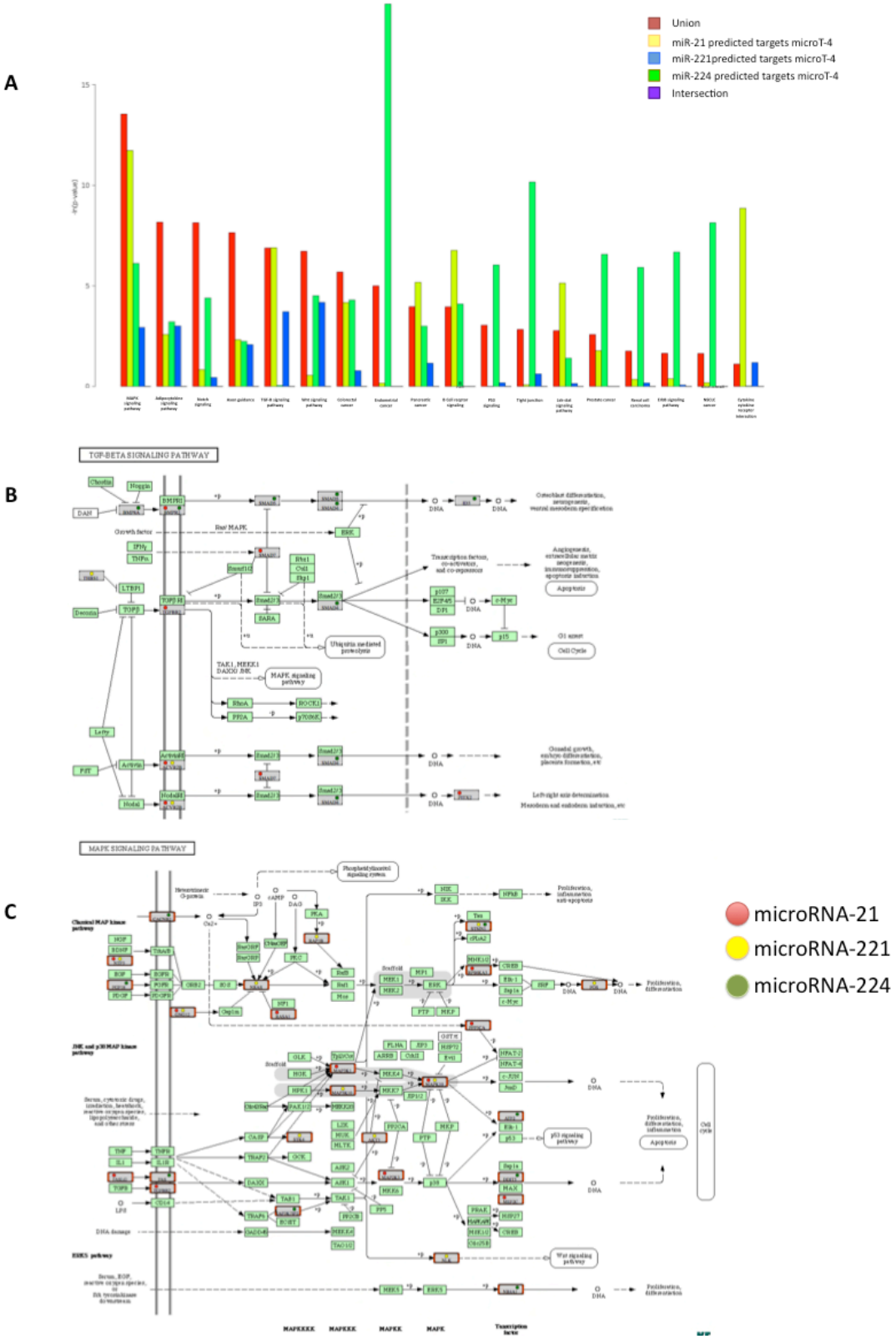

11.6 Appendix 6 - Chapter 8 data: arrayCGH analysis

Figure 11.18 Workflow for aCGH analysis

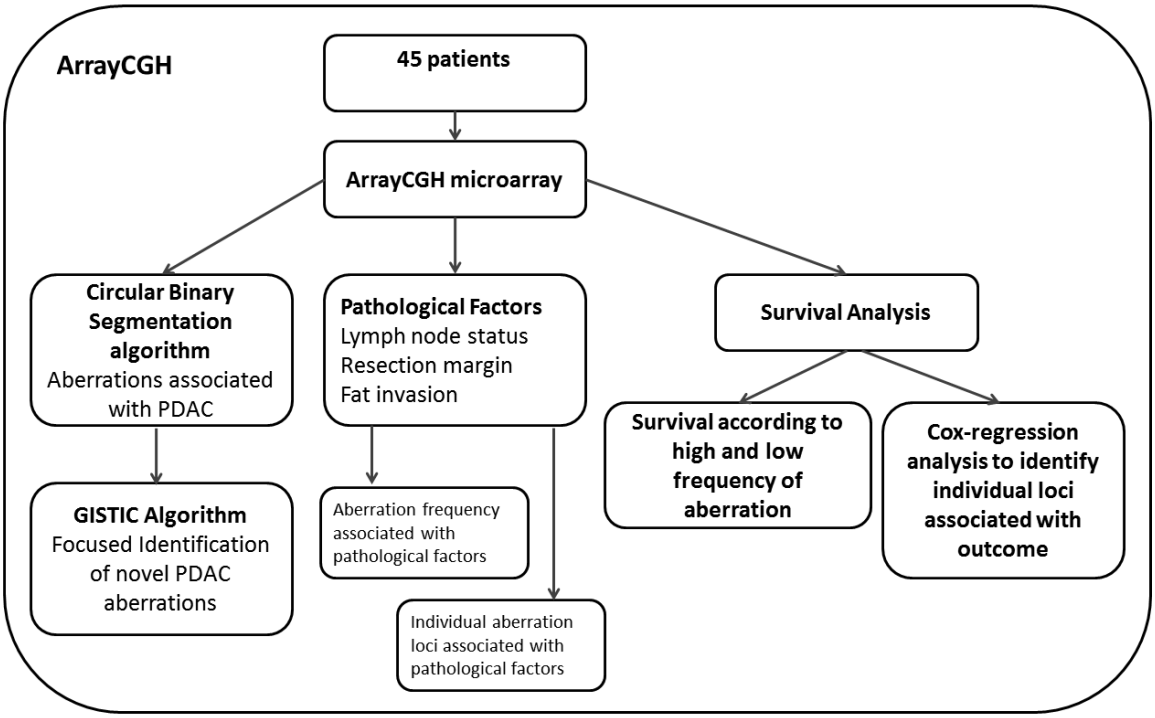

11.6.1 ArrayCGH analysis: linking copy number aberrations with known gene alterations

Figure 11.19 Plots demonstrating established copy number aberrations

Investigation as to whether amplification events localised by aCGH corresponded to important PDAC oncogenes. ***A) KRAS*** *(12p12.1) this oncogene is known to be activated by point mutation, not gene amplification. There was little copy number aberration activity at the KRAS locus or even around it within this cohort.* ***B) MYC*** *(8q24) is associated with a frequent copy number aberrations both copy number gains and losses. While many samples displayed aberrations in this position, there was a further aberrant locus in the region proximal to the MYC locus 18q24.12-18q24.21 in which multiple genes have evidence of amplification in a number of samples. These included ATAD2, FBXO32 and MTSS1.* ***C) AKT2*** *(19q13) showed evidence of copy number aberration with amplification evident in some of the patient samples. Notably however proximal to the AKT2 locus there was a large region with numerous high copy number changes which included PAX1, PAK4, NCCRP1, FBXO27 and PAPL.*

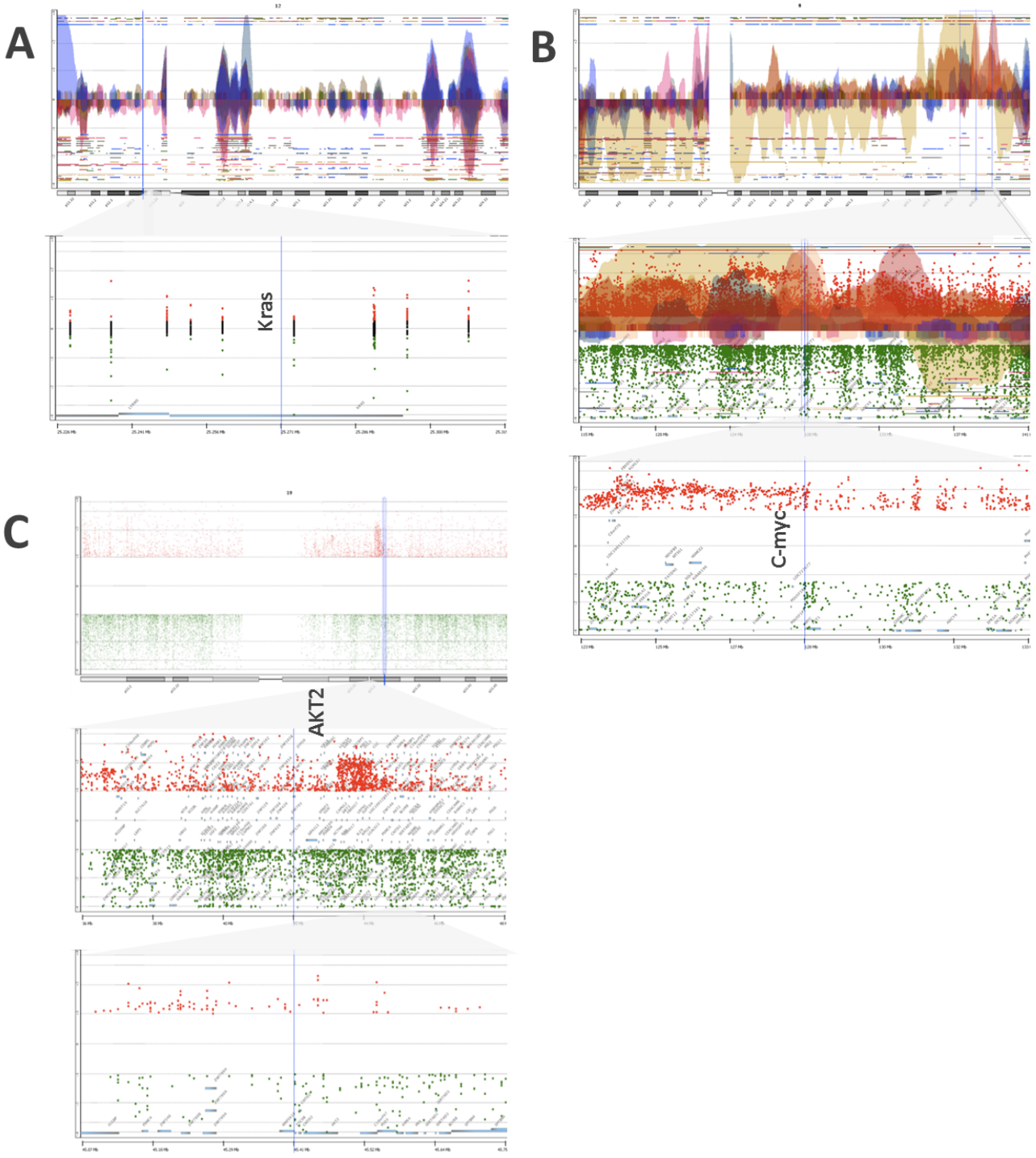

Figure 11.19 Plots demonstrating established copy number aberrations

Tumour suppressor genes. D) *$p16^{INK}$ (9p21) was reduced in copy number in many of the PDAC samples in this cohort confirming previous reports.* ***E) TP53 (****17p13.1) is a known TSG in PDAC. While this gene certainly is a site of copy number loss with some cases showing evidence of deletion, there is however, a great deal of copy number aberrations within the short arm of chromosome 17, in particular copy number losses, many of which are more profound that of TP53.* ***F) SMAD4*** *(18q21) lies amongst a multitude of loss of copy number regions throughout the chromosome in multiple regions. More than 50% of tumours within this cohort experienced loss of copy number within a number of these loci.*

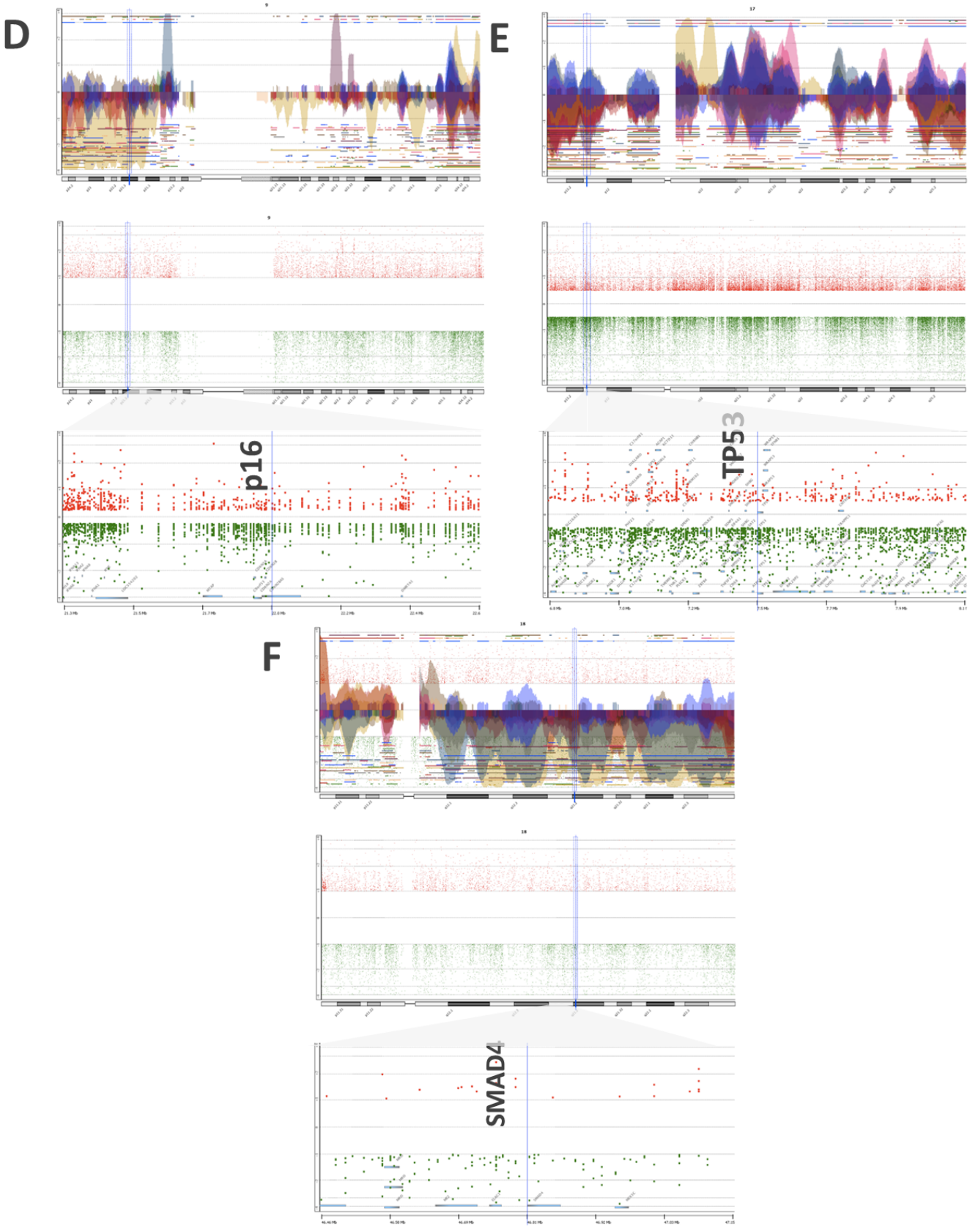

11.6.2 Circular binary segmentation analysis

Table 11.19 Segmentation analysis table for all samples
Supplementary Excel file

11.6.3 Pathway analysis according to copy number aberration

Table 11.20 KEGG pathway analysis: individual chromosomes
Supplementary Excel file

11.6.4 Genomic identification of significant targets in cancer (GISTIC) analysis

Table 11.21 Supplementary for the GISTIC analysis for PDAC cohort
Supplementary Excel file

11.6.5 Association of clinicopathological factors with CNAs in PDAC

Detailed tables cataloguing differences in CNAs according to clinicopathological variables are contained in within an Excel file:

Table 11.22 Differences in CNA based on lymph node status.

Table 11.23 Gene List enrichment analysis for CNA according to lymph node status A) BioCarta pathway analysis B) KEGG pathway analysis C) GSEA.

Table 11.24 Differences in CNA based on tumour grade (low versus high)

Table 11.25 Gene list enrichment analysis for CNA according to tumour grade A) BioCarta pathway analysis B) KEGG pathway analysis C) GSEA.

Table 11.26 Differences in CNA based on T2 versus T3 stage tumours.

Table 11.27 Gene list enrichment analysis for CNA according to tumour stage A) BioCarta Pathway analysis B) KEGG pathway analysis C) GSEA.

Table 11.28 Differences in CNA based on venous invasion.

Table 11.29 Gene list enrichment analysis for CNA according to venous invasion A) BioCarta Pathway analysis B) KEGG pathway analysis C) GSEA.

Table 11.30 Differences in CNA based on tumour size.

Table 11.31 Gene list enrichment analysis for CNA according to tumour size A) BioCarta pathway analysis B) KEGG pathway analysis C) GSEA D) Transcription factors E) Protein domains: PFAM F) Protein domains: SMART.

Table 11.32 Loci significantly associated with overall survival in 45 PDAC patients undergoing pancreaticoduodenectomy (250 most significant).

Table 11.33 Tables of gene sets associated with outcome: A) BioCarta pathway analysis B) KEGG pathway analysis C) GSEA D) miRNA targets E) Transcription factors F) Protein domains.

Table 11.34 BIOCARTA pathway analysis: all chromosomes

A) Pathway enrichment in genes with gain:

	Pathway	Description	No. of genes	Gene symbol	p value
1	h_stat3Pathway	Stat3 Signalling Pathway	5	FRAP1, MAPK3, STAT3, TYK2, JAK3	0.008
2	h_sumoPathway	Basic Mechanisms of SUMOylation	5	SUMO1, UBE2I, SUMO2, UBA2, SAE1	0.009
3	h_eif4Pathway	Regulation of eIF4e and p70 S6 Kinase	17	FRAP1, MKNK1, PIK3CA, EIF4G1, EIF4E,, PIK3R1, EIF4EBP1, PABPC1, PTEN, AKT1, MAPK3, EIF4A1, PDK2, RPS6KB1, PRKCA, MAPK1	0.01
4	h_stemPathway	Regulation of hematopoiesis by cytokines	16	CSF1, CD8A, IL8, IL2, IL3, CSF2, IL5, IL4, IL9, IL6, EPO, IL7, CD4, CSF3, SLC4A1, IL11	0.014
5	h_fosbPathway	FOSB gene expression and drug abuse	5	GRIA2, CDK5, PPP1R1B, JUND, FOSB	0.016
6	h_pitx2Pathway	Multi-step Regulation of Transcription by Pitx2	14	HDAC1, CTNNB1, GSK3B, LEF1, PITX2, APC, FZD1, TRRAP, LDB1, WNT1, AXIN1, CREBBP, MED1, EP300	0.017
7	h_nfatPathway	NFAT and Hypertrophy of the heart (Transcription in broken heart)	36	NPPA, ACTA1, AGT, CAMK1, RAF1, GSK3B, PIK3CB, PPP3CA, FGF2, HAND2, MEF2C, CAMK4, HBEGF, CSNK1A1, HAND1, NKX2-5, EDN1, PRKAR1B, GATA4, MAPK8, HRAS, F2, IGF1, AKT1, MAP2K1, CREBBP, MAPK3, CTF1, MYH2, RPS6KB1, NFATC1, CALR, ELSPBP1, FKBP1A, MAPK1, LIF	0.018
8	h_s1pPathway	SREBP control of lipid synthesis	6	SCAP, HMGCS1, MBTPS1, SREBF1, LDLR, SREBF2	0.021
9	h_bcrmolecule	B Cell Receptor Complex	2	CD79B, CD79A	0.033
10	h_lympathway	Adhesion and Diapedesis of Lymphocytes	14	VCAM1, SELE, CD34, IL1A, ITGA4, IL8, ITGB1, ITGAL, SLC4A1, ICAM2, PECAM1, MADCAM1, ICAM1, ITGB2	0.034

B) Pathway enrichment in genes with loss

	Pathway	Description	No. of genes	Gene symbol	p value
1	h_pelp1Pathway	Pelp1 Modulation of Estrogen Receptor Activity	7	ESR1, CREBBP, MAPK3, PELP1, SRC, MAPK1, EP300	0.001
2	h_TGFβPathway	TGF beta signalling pathway	17	ZFYVE9, TGFBR2, SKIL, APC, MAP3K7, TGFBR1, MAP2K1, SMAD3, CREBBP, MAPK3, CDH1, SMAD2, SMAD7, SMAD4, TGFB1, MAP3K7IP1, EP300	0.002
3	h_smPathway	Spliceosomal Assembly	13	SNRPG, SNRPC, SNRPF, SNRPA1, SFRS2, SNRPD1, SNRPA, SNRPD2, U2AF2, SNRPB, SNRPB2, U2AF1, SNRPD3	0.01
4	h_sumoPathway	Basic Mechanisms of SUMOylation	5	SUMO1, UBE2I, SUMO2, UBA2, SAE1	0.012
5	h_npcPathway	Mechanism of Protein Import into the Nucleus	10	RCC1, RANBP2, NUP210, NUP153, RAN, NUTF2, KPNB1, KPNA2, NUP62, RANGAP1	0.013
6	h_granulocytesPathway	Adhesion and Diapedesis of Granulocytes	16	SELP, SELE, IL1A, IL8, TNF, C5, IFNG, SELPLG, ITGAL, ITGAM, CSF3, SLC4A1, ICAM2, PECAM1, ICAM1, ITGB2	0.015
7	h_s1pPathway	SREBP control of lipid synthesis	6	SCAP, HMGCS1, MBTPS1, SREBF1, LDLR, SREBF2	0.018
8	h_carm-erPathway	CARM1 and Regulation of the Estrogen Receptor	24	SPEN, ERCC3, GTF2E1, PPARGC1A, MEF2C, SRA1, HDAC2, ESR1, TBP, CCND1, PHB2, GRIP1, NCOR2, GTF2A1, CREBBP, PELP1, POLR2A, MED1, BRCA1, GTF2F1, CARM1, RLN3, NRIP1, EP300	0.025
9	h_carm1Pathway	Transcription Regulation CARM1	8	CREB1, PRKAR1B, RXRA, CREBBP, RARA, CARM1, NCOA3, EP300	0.029
10	h_hdacPathway	Control of skeletal myogenesis by HDAC & calcium/calmodulin-dependent kinase (CaMK)	16	CAMK1, PIK3CB, PPP3CA, MYOD1, IGF1, AKT1, IGF1R, MEF2A, MAPK7, HDAC5, MAP2K6, NFATC1, INSR, AVP, CABIN1, YWHAH	0.033
11	h_il22bppathway	IL22 Soluble Receptor Signalling Pathway	10	IL22RA1, STAT1, IL22RA2, IL10RA, IL22, STAT5A, STAT3, SOCS3, TYK2, JAK3	0.033
12	h_vdrPathway	Control of Gene Expression by Vitamin D Receptor	25	ARID1A, HDAC1, NCOA1, TOP2B, SMARCC1, ACTL6A, BAZ1B, NCOA2, RXRA, VDR, SMARCD1, SUPT16H, SNW1, COPS2, TSC2, CREBBP, NCOR1, MED1, SMARCE1, CHAF1A, CARM1, SMARCA4, PRMT1, NCOA3, EP300	0.036
13	h_ctcfPathway	CTCF: First Multivalent Nuclear Factor	16	FRAP1, TGFBR3, PIK3CB, SMAD1, CDKL3, SMAD5, CDKN2A, PTEN, CDKN1B, CTCF, TP53, RPS6KB1, CD79B, SMAD4, TGFB1, CD79A	0.04
14	h_neutrophilPathway	Neutrophil and Its Surface Molecules	7	SELE, CD44, ITGAL, ITGAM, PECAM1, ICAM1, ITGB2	0.041
15	h_cb1rPathway	Metabolism of Anandamide,	5	PLD1, CNR1, BAAT, PLD2, PLD3	0.042
16	h_pyk2Pathway	Links between Pyk2 and Map Kinases	23	JUN, SHC1, SOS1, CAMK1, RAF1, RAC1, PTK2B, GNAQ, MAPK8, HRAS, PAK1, MAP2K1, MAPK3, BCAR1, MAP2K4, MAP2K3, PRKCA, GRB2, MAP2K2, SRC, PLCG1, CRKL, MAPK1	0.044
17	h_fosbPathway	FOSB gene expression and drug abuse	5	GRIA2, CDK5, PPP1R1B, JUND, FOSB	0.047
18	h_pparPathway	Basic mechanism of action of PPARa, PPARb(d)	4	PPARG, PPARD, RXRA, PPARA	0.048
19	h_mapkPathway	MAPKinase Signalling Pathway	73	RPS6KA1, MAP3K6, MKNK1, JUN, SHC1, MAPKAPK2, MAP4K3, MAP4K4, MAP3K2, ATF2, STAT1, CREB1, RAF1, MAPKAPK3, MAP3K13, PAK2, MAPK10, NFKB1, RAPGEF2, MAPK9, RIPK1, DAXX, MAPK13, MAP3K7, MAP3K5, MAP3K4, RPS6KA2, RAC1, BRAF, IKBKB, TGFBR1, HRAS,	0.049

Table 11.35 KEGG pathway analysis: all chromosomes

A) Pathway enrichment in genes with gain

	Pathway	Description	No. of genes	Gene Symbol	p value
1	hsa00040	Pentose and glucuronate interconversions	15	UGP2, RPE, UGT1A3, UGDH, UGT2B17, UGT2B15, UGT2B10, UGT2B7, UGT2B11, UGT2B28, UGT2B4, UGT2A2, GUSB, AKR1B1, DCXR	0.002
2	hsa00150	Androgen and estrogen metabolism	42	PRMT6, HSD3B2, HSD3B1, HSD17B7, HSD11B1, SRD5A2, UGT1A3, METTL6, HEMK1, UGT2B17, UGT2B15, UGT2B10, UGT2B7, UGT2B11, UGT2B28, UGT2B4, UGT2A2, SULT1E1, SRD5A1, HSD17B8, WBSCR22, METTL2B, AKR1D1, CYP11B1, CYP11B2, HSD17B3, AKR1C4, PRMT3, BCO2, PRMT8, PRMT5, LCMT2, LCMT1, HSD11B2, PRMT7, HSD17B2, HSD17B1, CARM1, SULT2A1, SULT2B1, PRMT1, PRMT2	0.004
3	hsa04060	Cytokine-cytokine receptor interaction	234	TNFRSF18, TNFRSF4, TNFRSF14, TNFRSF25, TNFRSF9, TNFRSF8, TNFRSF1B, IL22RA1, IL28RA, CSF3R, MPL, LEPR, IL23R, IL12RB2, CSF1, IL6R, XCL2, XCL1, FASLG, TNFSF18, TNFSF4, IL10, IL19, IL20, TGFB2, TPO, IL1R2, IL1R1, IL10RA, TNFRSF1A, LTBR, CD27, ACVR1B, AMHR2, INHBC, INHBE, IFNG, IL26, IL22, KITLG, TNFRSF19, FLT3, FLT1, TNFSF11, TNFSF13B, IL25, TGFB3, PLEKHO2, TNFRSF12A, TNFRSF17, IL4R, IL21R, CTF1, SLC4A1, NGFR, GH2, GH1, TNFRSF11A, AMH, TNFSF9, CD70, TNFSF14, , EPOR, IL12RB1, IL28B, IL28A, IL29, TGFB1, FLT3LG, IL11, BMP2, GDF5, CD40, BMP7, RTEL1, IFNAR2, IL10RB, IFNAR1, IFNGR2, LIF, OSM, CSF2RB, IL2RB, PDGFB, TNFRSF13C	0.008
4	hsa04930	Type II diabetes mellitus	40	PRKCZ, PIK3CD, FRAP1, PIK3R3, PKLR, CACNA1E, PRKCE, PRKCD, CACNA1D, PIK3CB, SLC2A2, PIK3CA, ADIPOQ, MAPK10, PIK3R1, MAPK9, TNF, GCK, PIK3CG, IKBKB, MAFA, MAPK8, KCNJ11, ABCC8, CACNA1C, SOCS2, PDX1, IRS2, PKM2, SOCS1, MAPK3, SLC2A4, PIK3R5, CACNA1G, SOCS3, SOCS6, INSR, CACNA1A, PIK3R2, MAPK1	0.01
5	hsa04640	Hematopoietic cell lineage	77	CSF3R, CSF1, FCGR1A, IL6R, CD1D, CD1A, CD1C, CD1B, CD1E, CD55, CR2, CR1, CD34, TPO, CD8A, CD8B, IL1R2, IL1R1, IL1A, IL1B, ITGA6, ITGA4, IL5RA, GP9, MME, THPO, GP5, TFRC, CD38, KIT, GYPA, IL7R, ITGA2, IL3, CSF2, IL5, IL4, CD14, TNF, HLA-DRA, HLA-DRB1, IL6, CD36, EPO, IL7, IL11RA, IL2RA, DNTT, CD59, CD44, MS4A1, CD5, CD3E, CD3D, CD3G, CD9, CD4, ITGA5, KITLG, FLT3, ANPEP, IL4R, CD19, ITGAM, GP1BA, CSF3, ITGA2B, ITGB3, ITGA3, CD7, FCER2, EPOR, CD22, CD37, FLT3LG, CD33, IL11	0.016
6	hsa00920	Sulphur metabolism	13	BPNT1, CHST13, SULT1E1, PAPSS1, CHST12, PAPSS2, SUOX, CHST11, SULT1A2, SULT1A1, SULT1A4, SULT2A1, SULT2B1	0.019
7	hsa04664	Fc epsilon RI signalling pathway	72	PIK3CD, PLA2G2E, PLA2G2A, PLA2G5, PLA2G2D, PLA2G2F, PIK3R3, VAV3, NRAS, FCER1A, FCER1G, PLA2G4A, AKT3, SOS1, PRKCE, PDK1, INPP5D, RAF1, PRKCD, PIK3CB, PIK3CA, MAPK10, PLA2G12A, PIK3R1, IL3, CSF2, IL5, IL13, IL4, LCP2, MAPK9, TNF, MAPK13, FYN, RAC1, PIK3CG, LYN, SYK, VAV2, MAPK8, PLA2G12B, HRAS, MS4A2, GAB2, KRAS, PLA2G1B, SOS2, AKT1, , PLA2G10, LAT, MAPK3, PLCG2, PIK3R5, MAP2K4, MAP2K3, PRKCA, MAP2K6, GRB2, RAC3, MAP2K2, VAV1, MAP2K7, PIK3R2, AKT2, PLCG1, MAPK1, PLA2G3, RAC2, PLA2G6,	0.02
8	hsa00860	Porphyrin and chlorophyll metabolism	25	UROD, PPOX, EPRS, UGT1A3, CPOX, CP, UGT2B17, UGT2B15, UGT2B10, UGT2B7, UGT2B11, UGT2B28, UGT2B4, UGT2A2, FTMT, BLVRA, GUSB, ALAD, UROS, HMBS, MMAB, HMOX2, FECH, BLVRB, HMOX1	0.026
9	hsa04670	Leukocyte transendothelial migration	102	PIK3CD, CDC42, CLDN19, PIK3R3, VCAM1, VAV3, GNAI3, RAP1A, NCF2, RASSF5, ACTN2, ROCK2, CTNNA2, CXCR4, RAPGEF4, ITGA4, CTNNB1, RHOA, GNAI2, CLDN18, PIK3CB, CLDN11, PIK3CA, CLDN1, CLDN16, RHOH, TXK, IL8, PF4, PPBP, CXCL13, PIK3R1, OCLN, CXCL14, CTNNA1, LRRTM2, ITK, MAPK13, CLDN20, ……, PLCG2, CYBA, CLDN7, PIK3R5, SLC4A1, PECAM1, PRKCA, ACTG1, ROCK1, VAV1, ICAM1, PIK3R2, ACTN4, VASP, GRLF1, PRKCG, PLCG1, MMP9, JAM2, CLDN17, CLDN8, ITGB2, CLDN5, NCF4, RAC2, MAPK12, MAPK11	0.031
10	hsa04120	Ubiquitin mediated proteolysis	43	CDC20, ANAPC1, UBE2E3, CUL3, VHL, UBE2E2, UBE2E1, ANAPC4, UBE2D3, ANAPC10, FBXW7, SKP2, SKP1, CDC23, UBE2D2, FBXW11, UBE2D4, SMURF1, CUL1, TCEB1, WWP1, UBR5, UBE2R2, CUL2, UBE2D1, BTRC, ARPC3, ANAPC5, CDC16, HERC2, NEDD4, HERC1, TCEB2, WWP2, CDC27, SMURF2, ANAPC11, NEDD4L, CDC34, FZR1, ITCH, UBE2C, RBX1	0.035
11	hsa00071	Fatty acid metabolism	48	CYP4A11, CYP4A22, CPT2, ACADM, ALDH9A1, HADHA, HADHB, ACADL, ACSL3, ACAA1, ACOX2, ACAD11, EHHADH, ACOX3, ADH5, ADH4, ADH6, ADH1A, ADH1B, ADH1C, ADH7, HADH, ACSL1, HSD17B4, ALDH7A1, ACSL6, PECI, ACAT2, ADHFE1, ALDH1B1, ACSL5, ECHS1, CPT1A, ACAT1, ACAD10, ALDH2, ACADS, ALDH1A3, DCI, ALDH3A2, ALDH3A1, ACOX1, GCDH, CYP4F8, CYP4F12, CYP4F11, CPT1C, CPT1B	0.04
12	hsa03010	Ribosome	79	RPL22, TCEB3, RPS8, RPL5, FAM69A, RPS27, RPS7, RPS27A, RPL31, RPL37A, RPL32, RPL15, RPSA, RPL14, RPL29, RPL24, RPL35A, RPL9, RPL34, RPS3A, RPL37, RPS23, RPS14, RPL26L1, RPS12, RPS20, RPL7, RPL30, MRPL13, RPL8, RPS11, RPS9, RPL28,	0.046

B) Pathway enrichment in genes with loss

	Pathway	Description	No. of genes	Gene symbol	p value
1	hsa00791	Atrazine degradation	8	ADAR, APOBEC2, APOBEC1, APOBEC3A, APOBEC3B, APOBEC3C, APOBEC3F, APOBEC3G	0.003
2	hsa04612	Antigen processing and presentation	71	NFYC, CTSS, RFX5, CD8A, CD8B, CREB1, HSPA9, CD74, CANX, HLA-F, HLA-G, FLJ45422, HLA-E, HLA-B, LTA, HSPA1L, HSPA1A, HSPA1B, HLA-DRA, HLA-DRB1, HLA-DQA1, HLA-DQB1, HLA-DQA2, HLA-DOB, TAP2, TAP1, HLA-DMB, HLA-DMA, HLA-DOA, HLA-DPA1, HLA-DPB1, TAPBP, NFYA, HSP90AB1, CTSB, IFNA21, IFNA4, IFNA7, IFNA10, IFNA16, IFNA17, IFNA14, IFNA5, IFNA6, IFNA13, IFNA2, IFNA8, IFNA1, HSPA5, HSPA8, CD4, KLRD1, KLRC3, KLRC2, KLRC1, NFYB, RFXAP, PSME1, PSME2, RNF31, LGMN, HSP90AA1, PDIA3, B2M, CIITA, CALR,	0.003
3	hsa04650	Natural killer cell mediated cytotoxicity	117	PIK3CD, LCK, PIK3R3, VAV3, NRAS, SHC1, CD48, CD244, FCER1G, FCGR3A, FCGR3B, SH2D1B, CD247, FASLG, SOS1, PPP3R1, ZAP70, RAF1, PIK3CB, TNFSF10, PIK3CA, SH3BP2, PPP3CA, CASP3, PIK3R1, CSF2, LCP2, HLA-G, FLJ45422, HLA-E, HLA-B, MICB, TNF, NCR3, NCR2, FYN, IFNGR1, ULBP2, ULBP1, ULBP3, RAC1, PIK3CG, PPP3CC, TNFRSF10B, TNFRSF10D, TNFRSF10A, PTK2B, IFNB1, IFNA21, IFNA4, IFNA7, IFNA10, IFNA16, IFNA17, IFNA14, IFNA5, IFNA6, IFNA13, IFNA2, IFNA8, IFNA1, SHC3, SYK, PPP3R2, VAV2, PRF1, PPP3CB, FAS, HRAS, PAK1, PTPN6, KLRD1, KLRK1, KLRC3, KLRC2, KLRC1, KRAS, IFNG, NFATC4, GZMB, SOS2, PRKCG, KIR2DL1, KIR2DL4, KIR3DL2, NCR1, PLCG1, NFATC2, IFNAR2, IFNAR1, IFNGR2, ITGB2, BID, MAPK1,	0.003
4	hsa00460	Cyanoamino acid metabolism	7	GBA, GBA3, SHMT1, GGT7, GGTLC2, GGT5, GGT1	0.012
5	hsa04370	VEGF signalling pathway	68	PIK3CD, CASP9, PLA2G2E, PLA2G2A, PLA2G5, PLA2G2D, PLA2G2F, CDC42, PIK3R3, NRAS, SH2D2A, PLA2G4A, MAPKAPK2, AKT3, PPP3R1, RAF1, MAPKAPK3, PIK3CB, PIK3CA, KDR, PPP3CA, PLA2G12A, PIK3R1, MAPK13, VEGFA, RAC1, HSPB1, PIK3CG, , PPP3R2, PLA2G12B, PPP3CB, HRAS, BAD, HSPB2, KRAS, PXN, PLA2G1B, NFATC4, AKT1, CHP, MAP2K1, PLA2G10, MAPK3, NFATC3, NFAT5, PLCG2, PIK3R5, PRKCA, SPHK1, RAC3, NFATC1, SHC2, MAP2K2, PIK3R2, AKT2, PRKCG, SRC, PLCG1, NFATC2, MAPK1, PLA2G3, RAC2, PLA2G6, , MAPK11	0.013
6	hsa00603	Glycosphingolipid biosynthesis - globoseries	13	B3GALNT1, HEXB, FUT9, ST3GAL1, GBGT1, ST8SIA1, HEXA, ST3GAL2, FUT2, FUT1, B3GALT5, NAGA, A4GALT	0.022
7	hsa00770	Pantothenate and CoA biosynthesis	24	PANK4, PPCS, DPYD, NAAA, PANK3, SIRT5, ENPP3, ENPP1, VNN3, VNN2, DPYS, ENPP2, SIRT1, PANK1, BCAT1, PPCDC, NTAN1, COASY, SIRT7, ILVBL, SIRT2, BCAT2, PANK2, UPB1	0.024
8	hsa01510	Neurodegenerative Disorders	34	PARK7, PINK1, PSEN2, CASP8, ALS2, HTT, UCHL1, CASP6, FBXW7, CASP3, PARK2, APBA1, HSPA5, CASP7, BAD, CASP1, GAPDH, ATN1, PSEN1, CREBBP, GFAP, MAPT, NGFR, GRB2, BCL2, APLP1, APOE, BAX, PRNP, BCL2L1, APP, SOD1, NEFH, EP300	0.028
9	hsa00590	Arachidonic acid metabolism	53	PLA2G2E, PLA2G2A, PLA2G5, PLA2G2D, PLA2G2F, CYP4A11, CYP4A22, GPX7, CYP2J2, PTGS2, PLA2G4A, GPX1, PGDS, CYP2U1, PLA2G12A, GPX3, LTC4S, GPX6, GPX5, TBXAS1, EPHX2, PTGS1, PTGES2, PTGES, AKR1C3, ALOX5, PLA2G12B, , CYP2E1, LTA4H, PLA2G1B, GPX2, PLA2G10, ALOX15, ALOX12, ALOX15B, ALOX12B, GPX4, CYP4F3, CYP4F2, CYP2B6, GGT7, PTGIS, CBR1, CBR3, GGTLC2, GGT5, GGT1, PLA2G3, PLA2G6	0.031
10	hsa04630	Jak-STAT signalling pathway	140	PIK3CD, IL22RA1, IL28RA, CSF3R, MPL, PIK3R3, JAK1, LEPR, IL23R, IL12RB2, PIAS3, IL6R, IL10, IL19, IL20, AKT3, TPO, SOS1, SOCS5, SPRED2, STAM2, STAT1, STAT4, IL5RA, CISH, CBLB, PIK3CB, IL12A, PIK3CA, IL2, IL21, SPRY1, …., CNTF, CLCF1, CCND1, IL10RA, CBL, CCND2, PTPN6, STAT2, STAT6, IFNG, IL26, IL22, SOCS2, SPRY2, IRF9, SOS2, SOCS4, AKT1, SPRED1, PIAS1, CREBBP, SOCS1, IL4R, IL21R, CTF1, PIK3R5, CSF3, STAT5B, STAT5A, STAT3, GH2, GH1, GRB2, SOCS3, PIAS2, SOCS6, PIAS4, TYK2, EPOR, JAK3, IL12RB1, PIK3R2, IL28B, IL28A, IL29, AKT2, CBLC, IL11, BCL2L1, IFNAR2, IL10RB, IFNAR1, IFNGR2, LIF, OSM, CSF2RB, IL2RB, EP300	0.031
11	hsa04912	GnRH signalling pathway	90	CALML6, PLA2G2E, PLA2G2A, PLA2G5, PLA2G2D, PLA2G2F, CDC42, JUN, PRKACB, NRAS, PLA2G4A, CACNA1S, ADCY3, SOS1, CALM2, MAP3K2, ITPR1, RAF1, PRKCD, CACNA1D, ADCY5, PLD1, GNRHR, MAPK10, PLA2G12A, CAMK2D, ADCY2, HBEGF, CAMK2A, MAPK9, ITPR3, MAPK13, CGA, MAP3K4, CAMK2B, ADCY1, EGFR, GNRH1, PTK2B, OS2, CALM1, PLCB2, MAP2K1, ADCY9, PLA2G10, , GRB2, GNA11, MAP2K2, MAP2K7, PRKACA, CALM3, LHB, GNRH2, PLCB1, PLCB4, SRC, GNAS, MAPK1, PLA2G3, PLA2G6, ATF4, MAPK12,	0.033
12	hsa03010	Ribosome	79	RPL22, TCEB3, RPS8, RPL5, FAM69A, RPS27, RPS7, RPS27A, RPL31, RPL37A, RPL32, RPL15, RPSA, RPL14, RPL29, RPL24, RPL35A, RPL9, RPL34, RPS3A, RPL37, RPS23, RPS14, RPL26L1, RPS18, RPS10, RPL10A, RPS12, RPS20, RPL7, RPL30, MRPL13, RPL8, RPS6, RPL35, RPL12, RPL7A, RPS24, RPLP2, RPL27A, RPS13, FAU, RPS3, RPS25, RPL41, RPL6, RPLP0, RPL21, RPL10L, RPS29, RPL36AL, RPS27L, RPL4, RPLP1, RPS17, RPL3L, RPS2, RPS15A, RPL13, RPL23A, RPL23, RPL19, RPL27, RPL38, RPL17, RPS15, RPL36, RPL18A, UBA52, RPS16, RPS19, RPL18,	0.038
13	hsa04140	Regulation of autophagy	27	PRKAA2, ATG7, ATG3, PIK3R4, PRKAA1, ATG12, ATG5, IFNA21, IFNA4, IFNA7, IFNA10, IFNA16, IFNA17, IFNA14, IFNA5, IFNA6, IFNA13, IFNA2, IFNA8, IFNA1, GABARAPL1, IFNG, ULK1, GABARAP, ULK2, BECN1, PIK3C3	0.04
14	hsa04664	Fc epsilon RI signalling pathway	72	PIK3CD, PLA2G2E, PLA2G2A, PLA2G5, PLA2G2D, PLA2G2F, PIK3R3, VAV3, NRAS, FCER1A, FCER1G, PLA2G4A, AKT3, SOS1, PRKCE, PDK1, INPP5D, RAF1, PRKCD, PIK3CB, PIK3CA, MAPK10, PLA2G12A, PIK3R1, IL3, CSF2, IL5, IL13, IL4, LCP2, MAPK9, TNF, MAPK13, FYN, RAC1, PIK3CG, LYN, SYK, VAV2, MAPK8, PLA2G12B, HRAS, MS4A2, GAB2, KRAS, PLA2G1B, SOS2, AKT1, MAP2K1, PLA2G10, LAT, MAPK3, PLCG2, PIK3R5, MAP2K4, MAP2K3, PRKCA, MAP2K6, GRB2, RAC3, MAP2K2, VAV1,	0.04

11.6.5.1 Lymph node status: copy number aberration

Comparison was made between LN1 PDAC tumours and LN0 resections which revealed significant differences in CNA associated with chromosomes 8, 9, 17 and 22. The respective frequency plots are illustrated in Figure 11.20. 150 clones were significantly different between the groups ($p < 0.05$). The site of the significantly altered aberrations and associated genes are illustrated in Table 11.22. In particular there was increased copy number of the gene KEL (7q33) in the LN1 group as well as RBM28 and IMPDH1 (7q32.1) and BTNL3 (5q35.3). The majority of differences between the groups were the result of decreased copy number of genes in the LN1 group compared to the LN0 group. The genes with the most significant decrease in copy number were MAFF, TMEM184B, CSNK1E, DMC1, MGAT3, CACNA1L, MAP3K7IP1, SYNGR1 (22q13.1), PDGFB (22q12.3-q13.1) and RBX1, EP300 (22q13.2). Similarly SPIN1, NXNL2, SHC3CKS2 (9q22.1) and SEMA4D (9q22.2) were reduced in copy number, as were CCL1, CCL8 (17q11.2), CCT6B, RFFL, AMAC1, PEX12 (17q12) and MYC (8q24.1).

BioCarta enrichment revealed that 3/288 gene sets were significant, while for KEGG enrichment 12/164 gene sets were significant including Jak-Stat signalling, cytokine-cytokine interactions, circadian rhythm, antigen processing and toll-like receptor signalling. GSEA analysis using the Broad institute curated gene sets revealed enrichment for previously identified PDAC sets, homeobox gene targets, HOXA5, which encodes a transcription factor previously shown to play important roles in embryogenesis and tumourigenesis and a MYC transcription factor gene set.

11.6.5.2 Tumour grade: copy number aberration

Comparison between low and high-grade tumours revealed numerous significant differences in copy number associated with regions on chromosomes 4, 13 and 17. 1076 clones had significantly altered CNA between the groups ($p < 0.05$) as illustrated in Figure 11.21 with the most significant CNAs and associated genes shown in Table 11.24. The genes that differed most were located on 13q including IFT88, PDX1 (13q12.1), LATS2, FGF9 (13q11-q12), CDK8, FLT-1, FLT-3, klotho (13q12), CDX2, BRCA2 (13q12.3), SMAD9 (13q12-q14), CCNA1 (13q12.3-q13) and RB1 (13q14.2). For all of these reduced copy number was associated with higher-grade disease. On chromosome 17q increased copy number was associated with: ERBB2 (17q11.2-q12), RARA, BRCA1, WNT3, WNT9B (17q21), IGFBP4, TNS4, CCR7 (17q12-q21.1), STAT3 (17q21.31), ADAM11, HOXB1-9 (17q21.3) and NGFR (17q21-q22). On chromosome 4 a number of regions harboured genes in which copy number loss was associated with higher grade including: IL8 (4q13-q21), EREG, EPGN (4q13.3), BMP3 (4q21) and NFκB at 4q24.

BioCarta enrichment revealed that 5/288 gene sets were significant including proepithelian conversion to epithelin, wound repair control and the IFN-β enhancer. For KEGG enrichment 6/164 gene sets were significant including the cell communication and antigen processing. GSEA analysis identified established pancreatic cancer sets, including RNA polymerase II and III.

11.6.5.3 Tumour stage: copy number aberration

Comparison between T2 and T3 tumours revealed a number of significant differences in CNA associated with chromosome 1, as illustrated in Figure 11.22 with the most significant CNAs and

associated genes shown in Table 11.26. 244 clones had significantly altered copy number expression between the two groups ($p < 0.05$). While high copy number of the gene RBM28 (7q32.1) was associated with T3 tumours all other significant copy number differences between the groups were located on chromsome 1p. The most significant were WNT2B (1p13), RHOC (1p13.1), PRMT6, VAV3 and CHI3L2 (1p13.3) and NGF (1p13.1). Other significant regions of chromsome 1 according to T stage included 1p22 which harboured LMO4 (1p22.3), MSH4 and ASB17 (1p31).

BioCarta enrichment revealed that 5/288 gene sets were significant including parkin of the ubiquitin-proteasomal pathway, interferon signalling pathway and the PPARα pathway. For KEGG enrichment 12/164 gene sets were significant including autophagy regulation, toll-like receptor signalling and natural killer cell mediated cytotoxicity. GSEA identified that 57/1399 gene sets were significantly different notably p53-signalling pathway.

11.6.5.4 Venous invasion: copy number aberration

CNAs associated with venous invasion were located on chromosomes 1, 2, 5, 13 and 19. The frequency plots for each group are illustrated in Figure 11.23. Although 3006 clones had significantly altered copy CNA between the two groups ($p < 0.01$), the majority of significant copy number differences were located on chromsome 1q including ARHGAP26, SLC9A11, KLKL20, serpinC1, PAPPA2 (1q25.1), ABL2 (1q24-q25), LHX4 (1q25.2) and TPR (1q25) for which a gain in copy number was associated with venous invasion. Chromosome 17 also had differences in of chemokines CCL7, CCL8 (17q11.2-q12) and members of the Notch signalling pathway NLE1 (17q12) and MMP28 (17q11-q21.1).

BioCarta enrichment revealed that 19/288 gene sets were significant including AKT signalling pathway. KEGG enrichment 6/164 gene sets were significant including cytokine interactions. GSEA revealed enrichment for a myeloma gene-set illustrating that the regulation of IL-6 target genes required the activation of Stat3.

11.6.5.5 Perineural invasion: copy number aberration

Unfortunately it was not possible to assess differences in CNA based on the presence of perineural invasion as all except two tumours from the 45 examined had evidence of perineural invasion.

11.6.5.6 Tumour size: copy number aberration

Comparison based on tumour size revealed a number of significant differences in CNA associated with chromosomes 9 and 15, with the most significant shown in Table 11.30. 627 clones had significantly altered copy number expression between the two groups ($p < 0.01$). The majority of significant copy number differences between the groups were associated with copy number loss associated with larger tumour size. The most significant loss of copy number were located on chromsome 15q in particular retinoid-related orphan receptor alpha (RORA) (15q22.2), NDN, BMF, DLL4 involved in Notch signalling pathway (15q14), THBS1 (15q15) and TP53BP1 (15q15-q21). Other signifcantly different aberrations were located on the long arm of chromsome 9 with IKBAP (9q31), TNC, TNFSF8 (9q33), TNFSF15, DEC1 (9q32) and TLR4 (9q32-q33).

BioCarta enrichment revealed 3/288 gene sets were significant including: TGFB signalling, spliceosomal assembly, SMAD binding, Notch signalling and caspase activity. For KEGG

enrichment 3/164 were significant including cell adhesion molecules and proteasome. GSEA revealed 57/1399 gene sets were significant including targets of HOXA5. Common transcription factors identified included EGFR, USF1, MAZR and ELK-1. Enrichment for protein domains that were common amongst the genes with CNAs included the S100, serpin, chromatin organisation modifier, CRAL/TRIO, TNF and histone domains.

11.6.5.7 Resection margin status: copy number aberration

Comparison based on resection margin status revealed significant differences in CN associated with chromosomes 7 and 11. 88 clones had significantly altered copy number expression between the two groups ($p < 0.01$). The majority of significant copy number differences between the groups were located on chromsome 11q including CCND1, MYEOV, CTSF (11q13), BRMS1 (11q-13q13.2), FGF19, TSGA10P (11q13.1), TBX10 (11q13.2), FGF4 (11q13.3), LRP5 (11q13.4) and RHOD (11q14.3) for all of which a decrease in copy number associated with R1 status. BioCarta enrichment revealed that 4/288 gene sets were significant including the activity of tubby proteins.

11.6.5.8 GSEA related to survival according to copy number aberration

Enrichment analysis was performed to identify if genes with CNAs relating to outcome correlated with known gene sets (Table 11.33). Using a Cox proportional-hazards model 1) the LS/KS permutation test finds gene sets which have more genes differentially expressed with survival times than expected by chance and 2) Goeman's Global test finds gene sets which are associated with survival times. According to GO enrichment analysis 92/3434 gene sets were significant. LS/KS permutation test found 56 significant gene sets Goeman's Global test found 36 significant gene sets.

Prognostic gene set enrichment analysis. Using the list of gene sets available at the Broad institute 105/1399 gene sets were significant ($p < 0.005$). The LS/KS permutation test found 44 significant gene sets while Goeman's Global test found 61 significant gene sets.

Prognostic pathway enrichment analysis. Using the BioCarta pathway gene sets 10/ 288 investigated gene sets were significant ($p < 0.005$). The LS/KS permutation test found 6 significant gene sets. Goeman's Global test found 4 significant gene sets. Using the KEGG pathway gene sets 13/ 164 investigated gene sets passed the $p < 0.005$ threshold. The LS/KS permutation test found 8 significant gene sets. Goeman's Global test found 6 significant gene sets.

Prognostic miRNA target prediction. The predicted miRNA target genes information in the miRBase Targets database was used to group genes into sets. Enrichment using MirBase Targets led to 36/ 587 miRNA gene sets were significant ($p < 0.005$). The test LS/KS permutation test found 53 significant gene sets. Goeman's Global test found 38 significant gene sets

Prognostic transcription factors targets. Enrichment for transcription factor targets that had been experimentally confirmed revealed 10/88 gene ($p < 0.005$). The LS/KS permutation test found 2 significant gene sets. Goeman's Global test found 8 significant gene sets. Enrichment for computationally predicted transcription factor targets revealed 3/60 gene sets ($p < 0.005$).

Figure 11.20 Frequency plots illustrating the differences in copy number aberrations between lymph node negative and lymph positive specimens

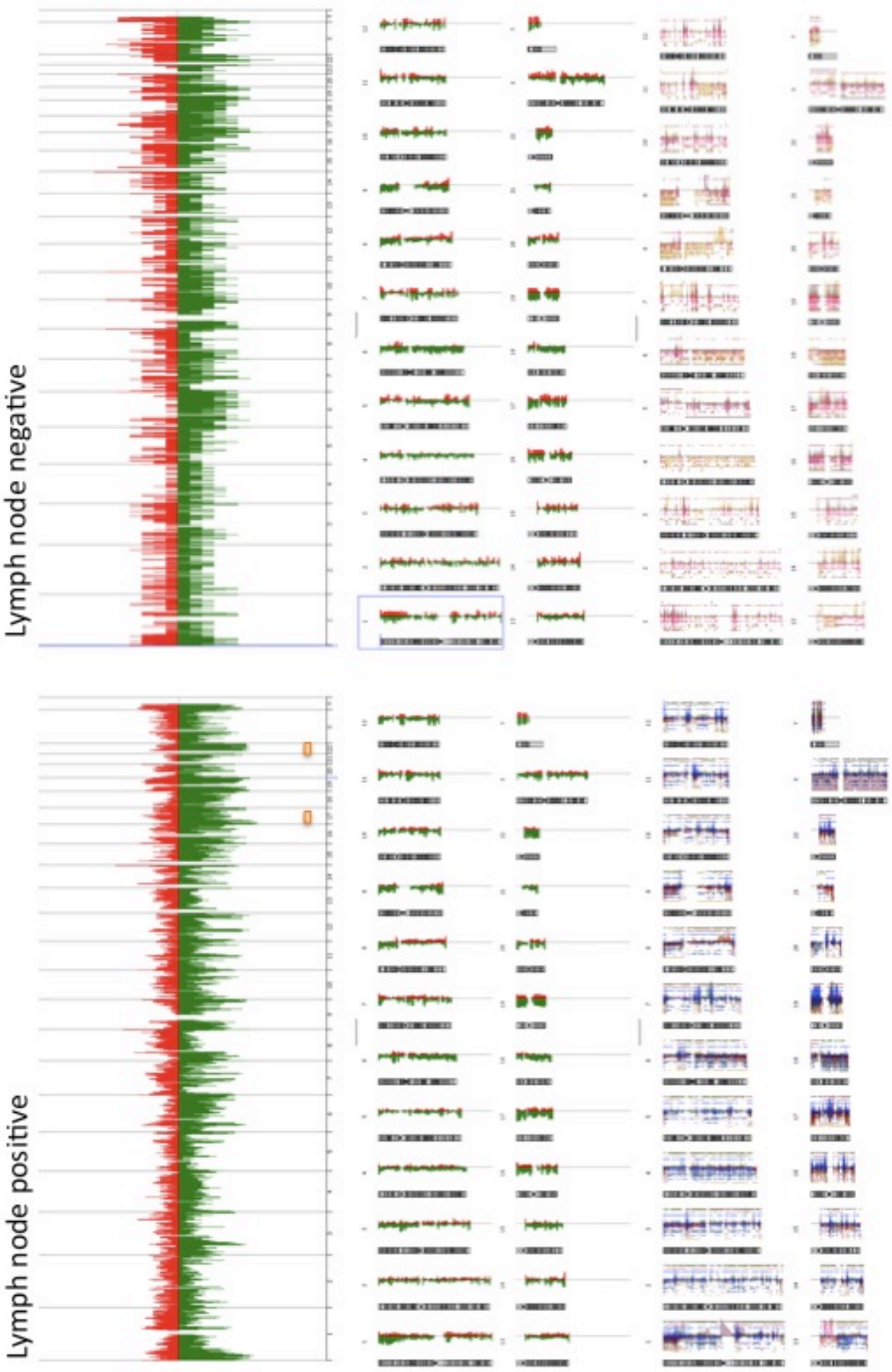

Figure 11.21 Frequency plots illustrating the differences in copy number aberrations between high grade and low grade PDAC

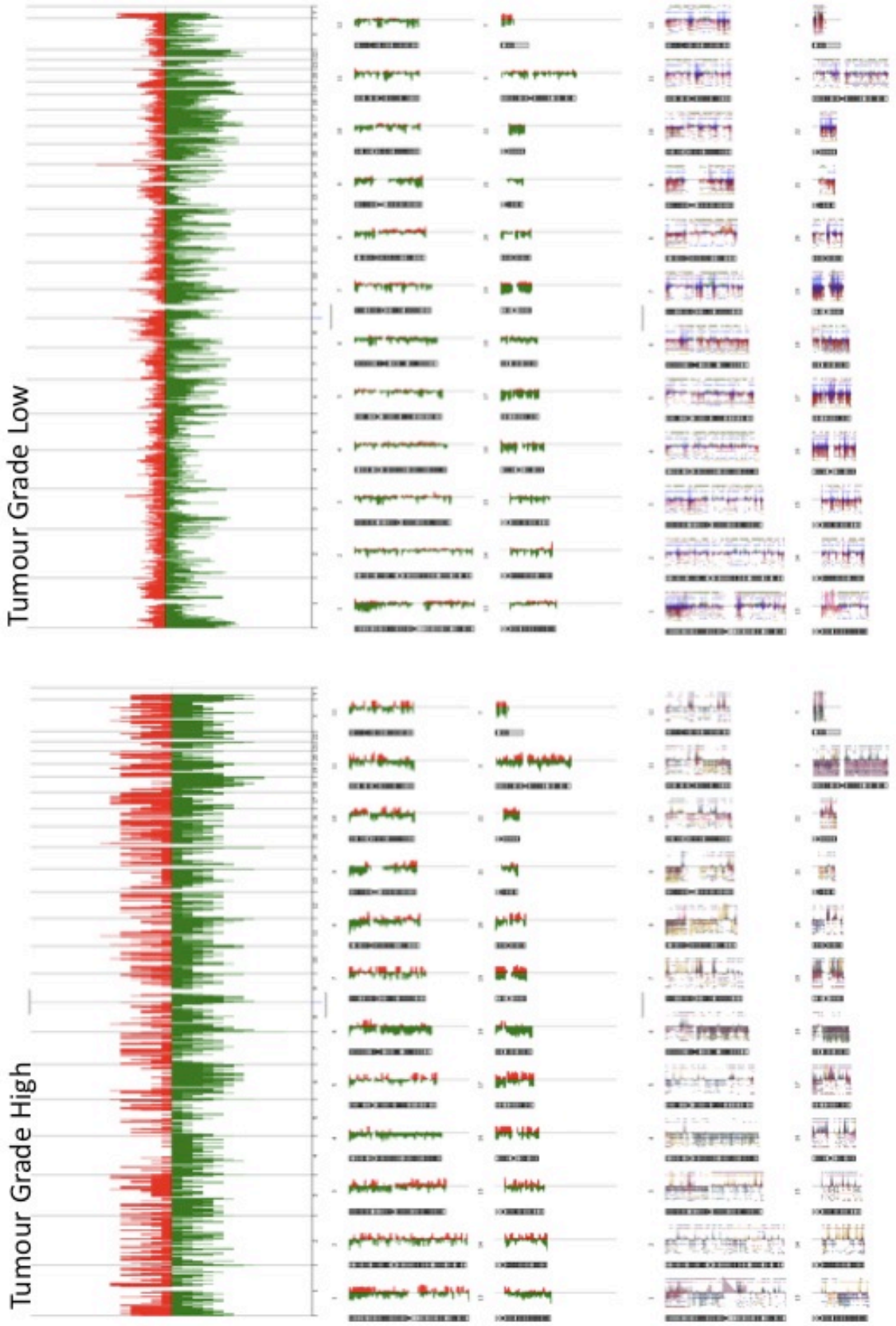

Figure 11.22 Frequency plots illustrating the differences in copy number aberrations between T2 and T3 stage PDACs

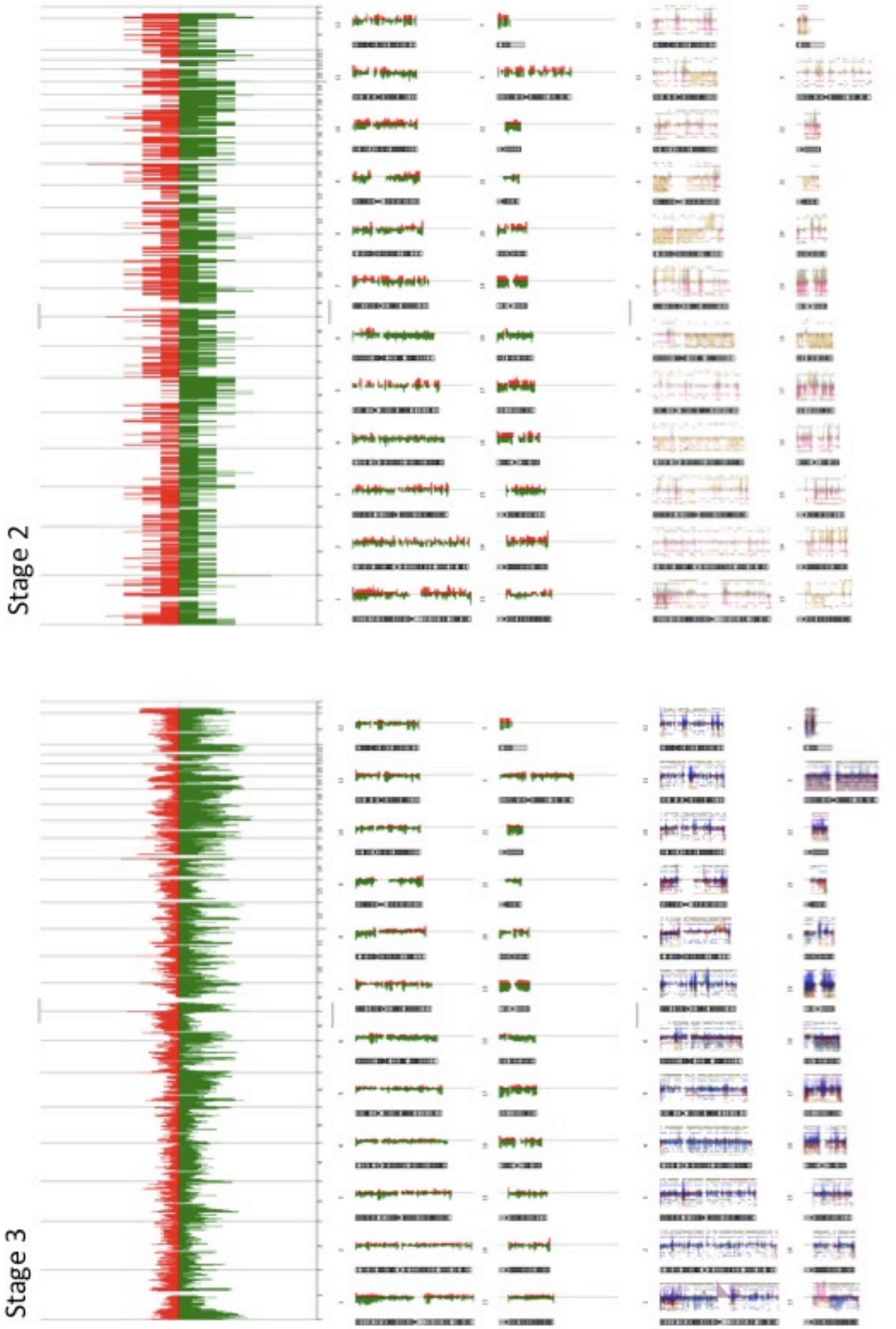

Figure 11.23 Frequency plots illustrating the differences in copy number aberrations between tumours with venous invasion and those without venous invasion

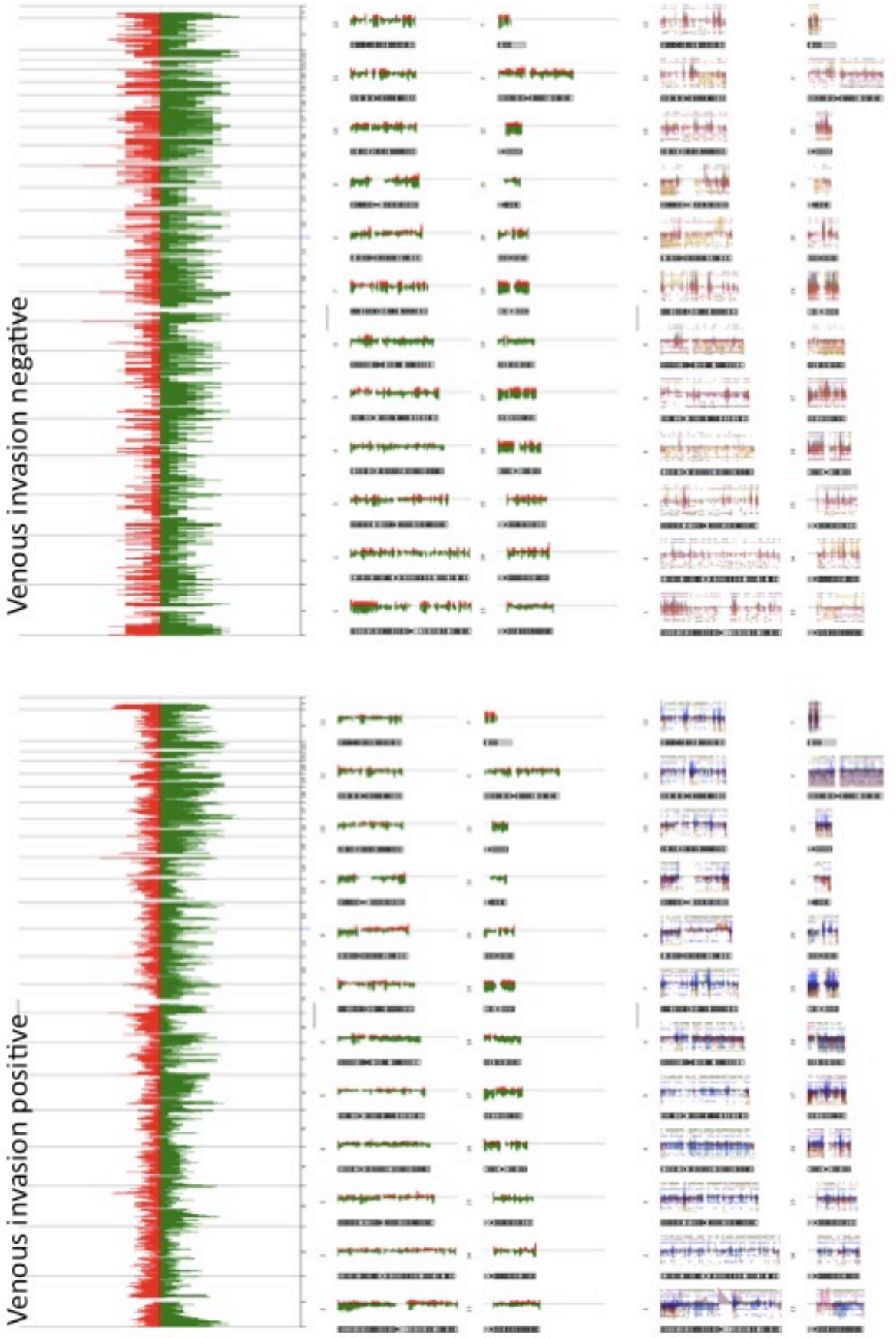

11.7 Appendix 7 - Chapter 9 data: integrative genomics

11.7.1 List of genes with concordant gene expression and copy number

Table 11.36 Correlate analysis list
Supplementary Excel file

Table 11.37 Top 50 genes for which copy number correlated with gene expression

Calculated according to Correlate software analysis method ($p < 0.001$, Spearman's rho correlation coefficient).

	Gene symbol	Chromosome	Correlation Coefficient
1	BU633484	9	0.607
2	DYRK1A	21	0.477
3	USP46	4	0.468
4	AW978428	15	0.466
5	LOC647174	13	0.437
6	LCE3A	1	0.431
7	UNQ6411	9	0.420
8	WNT7B	22	0.416
9	HNF4A	20	0.409
10	TMC2	20	0.408
11	mTOR	1	0.391
12	RTN2	19	0.383
13	GPC5	13	0.379
14	BX455755	22	0.365
15	ABHD2	13	0.360
16	WNT10B	12	0.358
17	SIRT 6	19	0.358
18	C6orf25	6	0.358
19	ARHGEF12	11	0.355
20	AFMID	17	0.346
21	SIRT 2	19	0.346
22	C14orf130	14	0.345
23	C1orf170	1	0.342
24	FBI-1	19	0.341
25	C21orf82	21	0.335
26	NCOR1	17	0.334
27	KIAA0265	7	0.328
28	C10orf49	10	0.327
29	BG951379	10	0.325
30	AF124170	22	0.324
31	NUBPL	14	0.320
32	ZSCAN2	15	0.317
33	NIN	14	0.317
34	GON4L	1	0.315
35	RP11-38O23.2	9	0.308
36	HIST1H4G	6	0.308
37	BC019907	22	0.308
38	MMP24	20	0.302
39	AGPAT4	6	0.302
40	SRFBP1	5	0.300
41	WDR36	5	0.300
42	BE644770	3	0.299
43	FLJ33590	2	0.293
44	WISP3	6	0.292
45	LOC284242	18	0.292
46	FLJ12993	4	0.291
47	ANKRD42	11	0.291
48	CCKAR	4	0.291
49	BVES	6	0.291
50	ROCK1	18	0.290

Table 11.38 Network analysis for genes with concordant gene and copy number expression
Supplementary Excel file

Figure 11.24 Network analysis for genes with concordant copy number

A) *Disease associated networks enrichment (GeneGO analysis).*
B) *Top scoring networks indicate that there is enrichment for autophagy and apoptosis, while HNF4a is an integral component of many networks.*

A

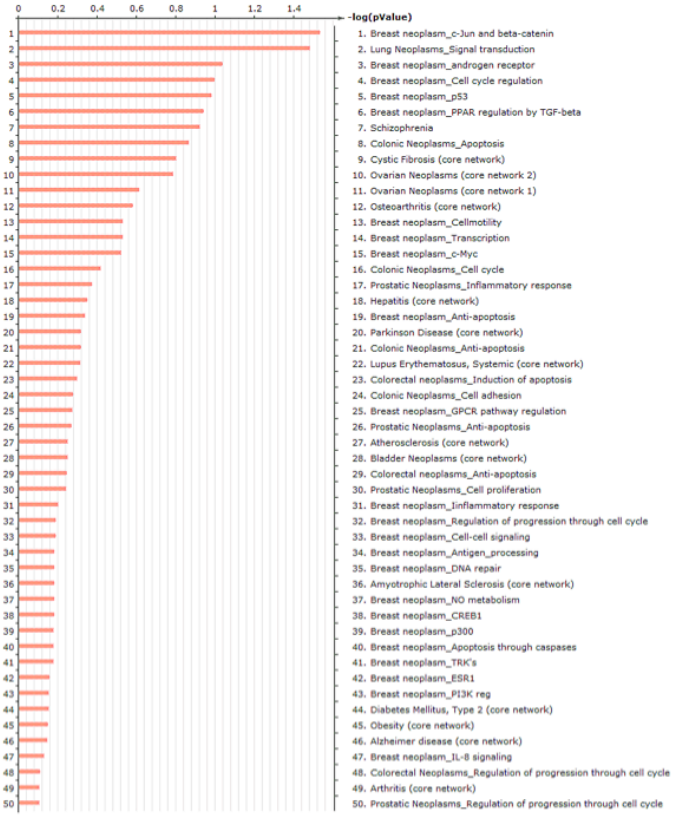

B

No	Network	GO Processes	Total nodes	Root nodes	Pathways	p-Value	zScore	gScore
1	HNF4-alpha, TMPRSS4, AHAP-1, HETTL2B, FAM50B	cAMP biosynthetic process (4.2%: 7.375e-04), regulation of gluconeogenesis (4.2%: 8.231e-04), nucleobase, nucleoside, nucleotide and nucleic acid metabolic process (39.6%: 9.953e-04), activation of protein kinase A activity (4.2%: 1.008e-03), gene expression (35.4%: 1.159e-03)	50	36	0	8.02e-69	63.86	63.86
2	ADHFE1, NRTH, VAPA, Enthoprotin, VAPB1	cellular process (92.7%: 1.223e-06), mitochondrion organization (14.6%: 2.004e-06), protein amino acid glycosylation (12.2%: 6.698e-06), macromolecule glycosylation (12.2%: 6.698e-06), glycosylation (12.2%: 6.698e-06)	50	30	0	8.96e-57	57.36	57.36
3	SSTR5, TFAM, EBAG9, DHAJC12, GPAM	cellular response to hormone stimulus (21.7%: 3.355e-09), cellular response to endogenous stimulus (21.7%: 5.811e-09), gland morphogenesis (15.2%: 6.551e-09), transmembrane receptor protein tyrosine kinase signaling pathway (19.6%: 2.338e-08), response to organic substance (37.0%: 2.493e-08)	50	21	5	1.09e-33	37.40	43.65
4	HGAT2, JAH2, CALB1, HA2A1, PLCL2	vitamin D metabolic process (5.9%: 8.770e-05), immune effector process (11.8%: 5.005e-04), regulation of synaptic transmission (11.8%: 6.513e-04), regulation of transmission of nerve impulse (11.8%: 8.317e-04), steroid metabolic process (11.8%: 1.072e-03)	50	21	0	3.85e-36	41.51	41.51
5	NR2A, hnRNP C, SLC19A2, ActRIIB, RRH2B	response to chemical stimulus (48.9%: 1.826e-08), positive regulation of cellular process (44.4%: 3.751e-07), regulation of cell communication (33.3%: 4.027e-07), regulation of apoptosis (28.9%: 1.042e-06), regulation of programmed cell death (28.9%: 1.181e-06)	50	16	3	8.06e-24	28.67	32.42
6	USP25, RAG1, TGT, TRIP12, Cyclin G1	cellular process (98.0%: 1.404e-10), regulation of apoptosis (34.7%: 9.869e-10), regulation of programmed cell death (34.7%: 1.171e-09), regulation of cell death (34.7%: 1.436e-09), positive regulation of activin receptor signaling pathway (6.1%: 1.130e-08)	50	18	0	2.33e-27	31.65	31.65
7	ROR2, BMP9, NKD2, NPAT, OLIG1	positive regulation of osteoblast differentiation (14.3%: 3.730e-12), regulation of osteoblast differentiation (16.3%: 3.974e-12), BMP signaling pathway (14.3%: 1.964e-11), positive regulation of cellular process (53.1%: 4.940e-11), positive regulation of biological process (55.1%: 6.326e-11)	50	16	2	1.74e-23	28.07	30.57
8	CNBP, NKD2, TOM70, HAPRPE1 (EB1), SWAP-70	positive regulation of cellular process (52.1%: 1.974e-10), cellular component organization (56.2%: 2.331e-10), cellular process (97.9%: 2.395e-10), positive regulation of biological process (52.1%: 1.581e-09), Wnt receptor signaling pathway (16.7%: 5.343e-09)	50	17	0	1.40e-25	30.17	30.17
9	RHO6, UBPY, CEACAM1, SWAP-70, C1orf77	anatomical structure development (56.0%: 1.016e-09), developmental process (58.0%: 1.165e-08), biological regulation (82.0%: 6.085e-08), regulation of cellular process (78.0%: 6.310e-08), regulation of signaling process (28.0%: 6.331e-08)	50	14	0	9.00e-20	24.49	24.49
10	B3GN1, FBI-1 (Pokemon), NPAT, Paraxis, E4F1	cellular macromolecule metabolic process (85.7%: 5.112e-08), developmental process (76.2%: 9.212e-08), macromolecule metabolic process (85.7%: 2.694e-07), protein neddylation (14.3%: 4.531e-07), regulation of transcription (61.9%: 9.121e-07)	50	9	0	6.46e-15	23.90	23.90
11	DLX1, Fc gamma RII alpha, TXNIP (VDUP1), Paraxis, SIGIRR	regulation of transcription from RNA polymerase II promoter (37.8%: 2.017e-11), regulation of macromolecule biosynthetic process (60.0%: 3.944e-11), immune effector process (22.2%: 4.627e-11), regulation of macromolecule metabolic process (64.4%: 5.031e-11), regulation of cellular biosynthetic process (60.0%: 1.524e-10)	51	11	1	7.45e-15	19.76	21.01
12	WNT7B, FOXC2, APH, THP21, SRFBP1	response to organic substance (50.0%: 3.697e-14), response to chemical stimulus (60.9%: 1.624e-13), positive regulation of biological process (60.9%: 9.666e-13), positive regulation of cellular process (56.5%: 7.161e-12), response to stimulus (71.7%: 1.240e-11)	50	12	0	3.13e-16	20.91	20.91
13	RGS6, SIX1, NOXO1, NR2A, TASK	superoxide metabolic process (15.2%: 5.467e-13), superoxide anion generation (13.0%: 1.284e-12), oxygen and reactive oxygen species metabolic process (15.2%: 4.851e-10), cellular process (95.7%: 1.091e-08), respiratory burst (8.7%: 1.091e-07)	50	11	0	1.57e-14	19.12	19.12
14	USP25, PRDX3, PAPP-A, UBPY, SIGIRR	response to organic substance (37.5%: 1.323e-07), innate immune response (15.0%: 3.172e-06), response to stress (40.0%: 6.507e-06), toll-like receptor signaling pathway (7.5%: 1.046e-05), Wnt receptor signaling pathway (12.5%: 1.909e-05)	50	10	0	1.76e-13	18.55	18.55
15	RASSF5, Rhodopsin kinase (GRK1), CREB-H, DPH1 (cat), RAX1.1	sensory perception of light stimulus (24.3%: 3.419e-10), visual perception (24.3%: 3.419e-10), positive regulation of molecular function (32.4%: 2.591e-08), response to stimulus (67.6%: 2.752e-08), regulation of phosphorylation (29.7%: 5.424e-08)	50	9	0	2.50e-12	17.74	17.74
16	GPAM, SLC19A2, PLCD, nAChR alpha-1, RNF4	cellular biosynthetic process (64.3%: 2.848e-04), biosynthetic process (64.3%: 3.538e-04), regulation of centromere complex assembly (7.1%: 6.546e-04), regulation of activation-induced cell death of T cells (7.1%: 6.546e-04), negative regulation of activation-induced cell death of T cells (7.1%: 6.546e-04)	50	7	0	1.16e-10	17.69	17.69
17	ROCK2, ROCK1, DAPK1, PAG, Fc gamma RII alpha	negative regulation of cellular process (53.2%: 7.743e-12), protein amino acid phosphorylation (34.0%: 1.267e-11), biological regulation (91.5%: 1.464e-11), post-translational protein modification (42.6%: 3.684e-11), regulation of apoptosis (38.3%: 4.685e-11)	50	10	0	7.03e-13	17.33	17.33
18	eIF2S1, E4F1, FBI-1 (Pokemon), Rifflylin (RFFL), CNBP	biological regulation (91.7%: 7.100e-12), cellular process (97.9%: 2.355e-10), regulation of metabolic process (64.6%: 6.337e-10), regulation of cellular metabolic process (62.5%: 9.789e-10), regulation of cellular process (83.3%: 1.130e-09)	50	10	0	7.03e-13	17.33	17.33
19	DYRK1a, H1A, SORL1, PGE2R4, hnRNP C	response to external stimulus (34.0%: 1.280e-10), regulation of signaling pathway (34.0%: 8.267e-09), regulation of phosphorylation (27.7%: 8.816e-09), biological regulation (85.1%: 1.071e-08), regulation of phosphorus metabolic process (27.7%: 1.417e-08)	50	10	0	7.03e-13	17.33	17.33
20	VAPB1, IPPK, Rabaptin-5, HLA-H, VAPA	vesicle-mediated transport (63.9%: 4.170e-24), transport (75.0%: 2.816e-15), establishment of localization (75.0%: 3.942e-15), localization (77.8%: 1.031e-14), cellular membrane organization (38.9%: 1.725e-13)	50	9	0	5.18e-12	17.05	17.05

11.7.2 miRNA correlated with regions of copy number aberrations

Supplementary PowerPoint file: contains images cataloguing overlap between CNA and miRNA expression

11.7.3 Gene expression profiles according to miRNA expression

Table 11.39
Supplementary Excel file

A) Gene expression according to miR-21 expression in 43 patients with PDAC.
B) Gene expression according to miR-34a expression in 43 patients with PDAC.